

New Concepts, Catalysts, and Methods in Stereoselective Olefin Metathesis

Author: Rana Kashif Khan

Persistent link: <http://hdl.handle.net/2345/bc-ir:104359>

This work is posted on [eScholarship@BC](#),
Boston College University Libraries.

Boston College Electronic Thesis or Dissertation, 2014

Copyright is held by the author, with all rights reserved, unless otherwise noted.

Boston College
The Graduate School of Arts and Sciences
Department of Chemistry

**NEW CONCEPTS, CATALYSTS, AND METHODS IN
STEREOSELECTIVE OLEFIN METATHESIS**

A dissertation
by
RANA KASHIF KHAN

submitted in partial fulfillment of the requirements
for the degree of
Doctor of Philosophy
August, 2014

© 2014 copyright by RANA KASHIF KHAN

NEW CATALYSTS, CONCEPTS, AND METHODS IN STEREOSELECTIVE OLEFIN METATHESIS

Rana Kashif Khan

Thesis Advisor: Professor Amir H. Hoveyda

Abstract

- **Chapter 1.** *Mechanistic Insights and Factors Influencing Polytopal Rearrangements in Stereogenic-at-Ru Carbenes*
- Herein, the mechanistic elucidation of the stereochemical inversion in stereogenic-at-Ru carbene complexes through olefin metathesis (OM) and non-olefin metathesis (non-OM) based polytopal rearrangements is provided. Our investigations involve the isolation and characterization of previously hypothesized higher-energy (e.g., *endo-anti*) and lower-energy (e.g., *exo-anti*) diastereomers, and their interconversion under thermal and/or acid-catalyzed conditions is demonstrated. Furthermore, our computational efforts highlighting the importance of the anionic ligands, due to their critical role in trans influence, dipolar interactions, and e-e repulsions, in polytopal rearrangements are reported. Finally, the positive influence of H-bonding in OM and non-OM processes is also rationalized.

- (a) Khan, R. K. M.; Zhugralin, A. R.; Torker, S.; O'Brien, R. V.; Lombardi, P. J. and Hoveyda, A. H. “Synthesis, Isolation, Characterization, and Reactivity of High-Energy Stereogenic-at-Ru Carbenes: Stereochemical Inversion Through Olefin Metathesis and Other Pathways,” *J. Am. Chem. Soc.* **2012**, *134*, 12438–12441. (b) Torker, S.; Khan, R. K. M. and Hoveyda, A. H. “The Influence of Anionic Ligands on Stereoisomerism of Ru Carbenes and Their Importance to Efficiency and Selectivity of Catalytic Olefin Metathesis Reactions,” *J. Am. Chem. Soc.* **2014**, *136*, 3439–3455.

▪ ***Chapter 2.*** Highly Z- and Enantioselective Ring-Opening/Cross-Metathesis of Enol Ethers Through Curtin–Hammett Kinetics

- The first instances of Z- and enantioselective Ru-catalyzed olefin metathesis are presented. Ring-opening/cross-metathesis (ROCM) reactions of oxabicyclic alkenes and enol ethers and a phenyl vinyl sulfide are promoted by 0.5–5.0 mol % of enantiomerically pure stereogenic-at-Ru complexes with an aryloxy chelate tethered to the N-heterocyclic carbene. Products are formed efficiently and with exceptional enantioselectivity (up to >98:2 enantiomer ratio). Surprisingly, the enantioselective ROCM reactions proceed with high Z selectivity (up to >98% Z). Moreover, reactions proceed with the opposite sense of enantioselectivity versus aryl olefins, which afford E- isomers exclusively. DFT calculations and deuterium-scrambling experiments, indicating fast interconversion between *endo*- and *exo*-Fischer carbene diastereomers, support a Curtin–Hammett situation. On this basis, models accounting for the stereoselectivity levels and trends are provided. Furthermore, the correlation of Fischer carbene character to the observed chemoselectivity in ROCM with enol ethers is also disclosed. Finally, a general proposal for the substrate-controlled Z selectivity in OM is also discussed.

(a) Khan, R. K. M.; O'Brien, R. V.; Torker, S.; Li, B. and Hoveyda, A. H. “Z- and Enantioselective Ring-Opening Cross-Metathesis with Enol Ethers Catalyzed by Stereogenic-at-Ru Carbenes: Reactivity, Selectivity, and Curtin-Hammett Kinetics,” *J. Am. Chem. Soc.* **2012**, *134*, 12774–12779. (b) Torker, S.; Koh, M. J.; Khan, R. K. M. and Hoveyda, A. H. “Origin of Z selectivity in Olefin Metathesis Reactions of Certain Terminal Alkenes Catalyzed by Typically E-Selective Ru Carbenes,” manuscript submitted.

▪ ***Chapter 3.*** A New Class of Highly Efficient Ru Catalysts for Z-Selective Olefin Metathesis

- Herein, we outline a general design for Z-selective OM, which led to the development of a new class of stereogenic-at-Ru carbene complexes (**Ru4-9**). Furthermore, we demonstrate that the newly developed dithiolate complexes **Ru4b** and **Ru5** efficiently promote high activity and selectivity in ROMP reactions of norbornene and cyclooctene. Notably, the catechothiolate **Ru4b** catalyzes Z-selective ROCM with a broad scope of alkenes involving various functional groups (e.g., alcohols, enol

ethers, vinyl sulfides, amides, heterocycles, and conjugated 1,3-dienes). More importantly, we disclose that the catecholate complex **Ru4a** is kinetically non-selective in OM and readily decomposes in the presence of mildly acidic moieties (e.g., alcohols and CDCl_3). Subsequently, **Ru9** is developed to efficiently promote highly Z-selective CM of a diol cross-partner with a wide range of alkene substrates. Most remarkably, the aforementioned protocol is employed in two natural product syntheses and the OM-based Z-selective cracking of oleic acid, which is unprecedented with existing Ru-carbenes and Mo/W-alkylidenes.

- (a)** Khan, R. K. M.; Torker, S. and Hoveyda, A. H. “Readily Accessible and Easily Modifiable Ru-Based Catalysts for Efficient and Z-Selective Ring-Opening Metathesis Polymerization and Ring-Opening Cross-Metathesis,” *J. Am. Chem. Soc.* **2013**, *135*, 10258–10261. **(b)** Koh, M. J.; Khan, R. K. M.; Torker, S. and Hoveyda, A. H. “Broadly Applicable Z- and Diastereoselective Ring-Opening/Cross-Metathesis Catalyzed By a Dithiolate Ru Complex,” *Angew. Chem., Int. Ed.* **2014**, *53*, 1968–1972. **(c)** Khan, R. K. M. ; Torker, S. and Hoveyda, A. H. “Reactivity and Selectivity Differences Between Catecholate and Catechothiolate Ru Complexes. Implications Regarding Design of Stereoselective Olefin Metathesis Catalysts,” *J. Am. Chem. Soc.* **2014**, *136*, 14337–14340. **(d)** Koh, M. J.; Khan, R. K. M.; Torker, S.; Yu, M.; Mikus, M. S. and Hoveyda, A. H. “Synthesis of High-Value Alcohols, Aldehydes and Acids by Catalytic Z-Selective Cross-Metathesis” manuscript submitted.

In loving memory of Ms. Bushra Nighat (late)



Borrowed from *Selenographia, sive Lunae descriptio*, 1647, by Johannes Hevelius (1611–1687).

First of all, thanks to the almighty Allah for providing me with countless blessings and opportunities. Now, I wish to thank the individuals who have been instrumental in my graduate study.

Although it is the end, rather than the beginning, of a journey that reinvigorates its appreciation, the defining nature of my graduate research described herein was unequivocal at the offset. The culture of excellence, pursuit of scientific curiosity, and the collective drive for solving important problems in the Hoveyda group constantly underscored the significance of my membership. At the helm of such an incredible scientific enterprise, lays the charismatic leadership of Professor Amir H. Hoveyda. Ever since my first encounter with him, I felt a sense of higher purpose to address challenges that spanned beyond the scope of my project. His inspirational personality, ability to instill the desire for excellence, and unwavering support throughout these years have greatly impacted my personal and professional lives alike. One of the most cherished moments of my interactions with him involves an invaluable conversation about the subtleties of nature and paying close attention to details as an experimentalist. His gift of Primo Levi's "*The Periodic Table*," wherein the significance of being a "*militant chemist*" is explained,^a served me very well. Without the appreciation for the aforementioned piece, perhaps I would not have discovered non-olefin metathesis polytopal rearrangements (*cf.* Chapter 1) and Z-selective ring-opening/cross-metathesis through Curtin-Hammett kinetics (*cf.* Chapter 2). In addition to his role as brilliant advisor, his incredible friendship and personal interest in my well-being proved priceless at a number of occasions. In short, none of the work detailed herein and my own intellectual development would have been possible without Professor Hoveyda.

I would also like to mention my deep regard for Professor Olafs Daugulis, who inspired me to pursue a career in Organic Chemistry. His stimulating class lectures and mentorship as an undergraduate research advisor greatly helped in discovering my

^a In the chapter about potassium, Primo Levi reflects on a past incident in which he nearly sets his laboratory on fire. The event unfolds when his inability to find sodium for the purification of benzene leads to the selection of potassium as *suitable* substitute. Later, he ponders the wisdom of the erroneous approximation commonly taught that potassium is "*sodium's twin*" in the following way: "*I believe that every militant chemist can confirm it: that one must mistrust almost-the-same (sodium is almost the same as potassium, but with sodium nothing would have happened), the practically identical, the approximate, the or-even, all surrogates, and all patchwork.*"

passion for Organic Chemistry. Most importantly, his recommendation to join the Hoveyda lab proved crucial for my career development.

I am also especially thankful to Professors Marc L. Snapper and James P. Morken for participating in my independent research proposal and dissertation committees. Their interest in promoting my scientific knowledge through exciting class lectures and cumulative examinations has served me well.

My interaction with Dr. Adil R. Zhugralin and Dr. Robert V. O'Brien is also noteworthy. They not only provided initial experimental training, but also played an important role in my intellectual development. I am deeply indebted to them for the encouragement and support. My close friendships with Dr. Ismail Ibrahim and Dr. Chenbo Wang also helped me grow as a mature scientist. Furthermore, I have a great deal of appreciation for my fruitful collaboration with Dr. Sebastian Torker. His presence served as an indispensable resource in my graduate research endeavor and greatly helped in developing the understanding of important mechanistic principles.

I also thank Ming J. Koh for joining my research project and choosing me as mentor. His experimental contributions have led to the advances in catalyst development and synthetic applications for Z-selective olefin metathesis (*cf.* Chapter 3). Mr. Koh also proofread my thesis, for which I owe many thanks. Furthermore, I wish to acknowledge Thach T. Nguyen, who also proofread my thesis, for choosing me as mentor briefly before my departure. I am excited about his prospects of becoming a successful researcher in the Hoveyda group and wish him the best. Furthermore, my close friendship with Mr. Tyler J. Mann has meant a lot to me. Our conversations about science and beyond during coffee breaks and lunches greatly advanced my desire for scientific inquiry in newly emerging and exciting fields.

The members of my family have been a constant source of love and support over the years. I wish to express the deepest gratitude to my loving parents (Rana Razzaq Khan & Ruqiyya Khan) and affectionate brothers and sister, who have always been great examples and sources of motivation to achieve success. Lastly, I am also thankful to Ms. Shatha Mufti for the wonderful friendship and support.

Table of Contents

Mechanistic Insights and Factors Influencing Polytopal Rearrangements in Stereogenic-at-Ru Carbenes	1
Chapter One	1
1.1 Introduction	1
1.2 Mechanistic Differences Between Stereogenic and Non-Stereogenic-at-Ru Carbenes in Olefin Metathesis	4
1.3 Experimental Evidence for Two Discrete Mechanisms for Polytopal Rearrangement in Ru Carbenes	7
1.3.1 OM-Based Inversions in Stereogenic-at-Ru Carbenes: Isolation and Characterization of High-Energy Diastereomers (<i>endo-anti</i> and <i>endo-anti_F</i>)	7
1.3.2 Non-OM Inversions in Stereogenic-at-Ru Carbenes: Stereoisomerization of High-Energy <i>endo-anti</i> Complex	10
1.4 Computational Rationale for Non-OM Inversion in <i>endo-anti</i>	16
1.4.1 Source of Energetic Difference Between <i>endo-anti</i> and <i>exo-anti</i> Diastereomers	17
1.4.2 PES of Thermally Promoted Non-OM Inversion	18
1.4.3 PES of Acid-Catalyzed Non-OM Inversion: Positive Influence of Proton	21
1.4.4 Critical Factors Associated with Non-OM Transformations	23
1.5 Implications Regarding the Role of Anions on Olefin Metathesis Promoted by Ru Carbenes	27
1.5.1 Effect of Anions on Carbene Orientation	27
1.5.2 Effect of Anions on the Energy Barriers Associated with the Promotion of Olefin Metathesis	29
1.5.3 Influence of H-Bonding on the Rate Acceleration in Olefin Metathesis	30
1.6 Conclusions	32
1.7 Experimental	33
Highly Z- and Enantioselective Ring-Opening/Cross-Metathesis of Enol Ethers Through Curtin-Hammett Kinetics	160
Chapter Two	160
2.1 Introduction	160
2.2 Mechanistic Basis for the Employment of Stereogenic-at-Ru Carbenes to Promote ROCM with Enol Ethers	162

2.3 Development of Z- and Enantioselective ROCM of Enol Ethers	164
2.3.1 Highly Z- and Enantioselective ROCM Involving bve Catalyzed by Stereogenic-at-Ru Carbene (IV)	164
2.3.2 Substrate Scope Investigation of Z-Selective and Enantioselective ROCM with Enol Ethers	166
2.4 Support for Curtin-Hammett Kinetics in Z-Selective and Enantioselective ROCM of Enol Ethers	168
2.4.1 DFT-Guided Investigations	168
2.4.2 Stereochemical Model for Z- and Enantioselective ROCM	171
2.5 Influence of Electronic Attributes of Enol Ether on Chemoselectivity	173
2.6 Rationale for Substrate-Controlled Z Selectivity	175
2.7 Conclusions	177
2.8 Experimental	179
A New Class of Highly Efficient Ru Catalysts for Z-Selective Olefin Metathesis	238
Chapter Three	238
3.1 Introduction	238
3.2 Rationally Designed Ru Carbenes for Z Selectivity in Olefin Metathesis	240
3.2.1 Catalysts for Z Selectivity in Olefin Metathesis	240
3.2.2 Initial Hypothesis for the Development of Z-Selective Ru Catalysts	243
3.2.3 Development of Readily Accessible and Modifiable Catecholate and Catechothiolate Complexes	245
3.3 Ru Catechothiolate as Highly Efficient, Z-Selective, and Group Tolerant Catalyst in Olefin Metathesis	247
3.3.1 Remarkable Efficiency and Z Selectivity in Ring-Opening Metathesis Polymerization (ROMP)	247
3.3.2 Broad Scope Z Selectivity in ROCM	249
3.3.3 DFT Investigation for Stereochemical Model for Z Selectivity	257
3.4 Reactivity and Selectivity Differences Between Catecholate and Catechothiolate Catalysts in Olefin Metathesis	259
3.4.1 Reactivity and Structural Integrity of Diolate vs Dithiolate Complexes	259
3.4.2 Rationale for Kinetic Z Selectivity with Ru Catechothiolate (vs Catecholate) Through Computational Analysis	265

3.5 Simple Access to Biologically Relevant Molecules and Oleochemicals Through Z-Selective Cross-Metathesis Promoted by a Highly Efficient Ru Catalyst	268
3.5.1 Development of a Highly Active and Efficient Ru Catechothiolate for Widely Group Tolerant Z-Selective Cross-Metathesis	269
3.5.2 Applications in Natural Product Synthesis	273
3.5.3 Advantage of Z-Selective CM with Internal Alkenes and its Application to Oleochemicals	275
3.6 Challenges and Opportunities for Future Catalyst Development in Stereoselective Olefin Metathesis	278
3.6.1 Methylidene Longevity Essential for the Development of Ring-Closing Metathesis Catalysts	278
3.6.2 Development of Highly Active Catalysts for Z-Selective OM with Hindered and/or Stabilizing Alkenes	281
3.7 Conclusions	282
3.8 Experimental	284

Mechanistic Insights and Factors Influencing Polytopal Rearrangements in Stereogenic-at-Ru Carbenes

Chapter One

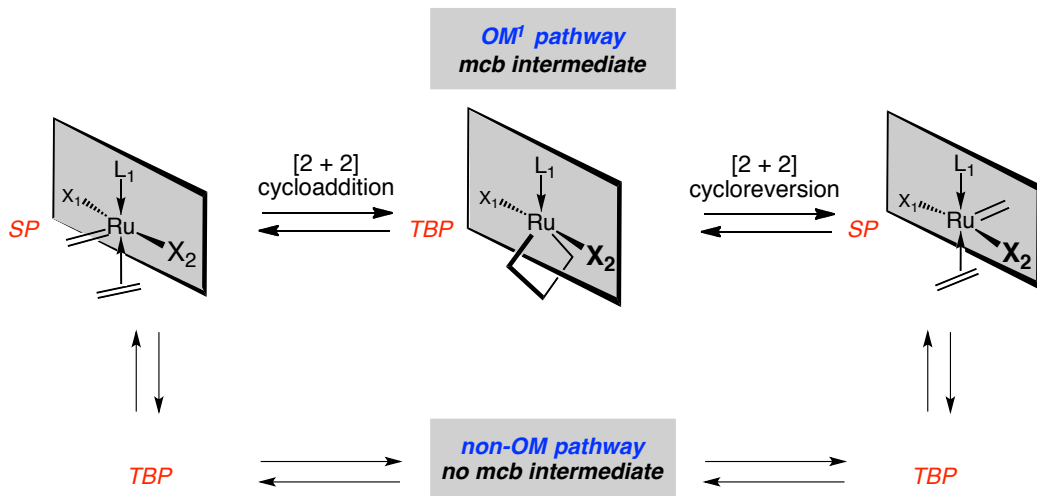
1.1 Introduction

Catalytic olefin metathesis (OM) is one of the hallmarks of a decades long scientific effort that spans across various disciplines,¹ which allows us to efficiently manipulate arguably the most important functional group in organic chemistry: alkenes. In the past decade, swift rise in the number of highly stereoselective catalysts tailored for the promotion of a plethora of important OM transformations is a direct consequence of crucial insights that emerged from mechanistic investigations involving transition metal-based catalysts of both low and high oxidation-state (i.e. Ru^{II} and Mo^{VI}/W^{VI}, respectively).² The core of these mechanistic studies lies in studying the variations in the catalyst architecture during OM. A unique feature of this process is that the M=CR₂ moiety, which represents the catalytically active site of the square pyramidal (SP) olefin π-complex, undergoes a “side change” (e.g., M= Ru, Scheme 1.1-1).³ The route also involves the intermediacy of a trigonal bipyramidal (TBP) metallacyclobutane, which plays a critical role in the overall facility with which this event takes place. Added to this process is the possibility for Ru=CR₂ side-change through a non-OM pathway that completely avoids the intermediacy of metallacyclobutane. In this context, studies regarding the extent to which these pathways of polytopal rearrangements in Ru carbenes are competitive and a collective picture of the factors involved (e.g., influence of anions) are lacking.

(1) *Handbook of Metathesis* (Grubbs, R. H., Ed.), Wiley–VCH, Weinheim, Germany, 2003.

(2) For a comprehensive review regarding the advances in stereoselective olefin metathesis, see: Hoveyda, A. H. *J. Org. Chem.* **2014**, *79*, 4763–4792.

(3) For the mechanism of OM catalyzed by Mo/W-alkylidenes complexes, see: (a) Hoveyda, A. H.; Schrock, R. R. *Angew. Chem. Int. Ed.* **2003**, *42*, 4592–4633. For the mechanism of OM catalyzed by Ru-carbenes, see: (b) Sanford, M. S.; Love, J. A.; Grubbs, R. H. *J. Am. Chem. Soc.* **2001**, *123*, 6543–6554. (c) Adlhart, C.; Chen, P. J. *Am. Chem. Soc.* **2004**, *126*, 3496–3510.

Scheme 1.1-1. Polytopal Rearrangements in Pentavalent Ru Carbenes

¹ Olefin metathesis; X_1 or X_2 = anions; L_1 = neutral ligand; **SP** = square pyramidal; **TBP** = trigonal bipyramidal; **mcb** = metalacyclobutane

In our efforts to gain mechanistic insights, we began with the classification of Ru carbenes employed for catalytic OM into two distinct categories: 1) Non-stereogenic-at-Ru 2) stereogenic-at-Ru (Scheme 1.1-2). The former type can be further divided into achiral (e.g., **I**)⁴ and chiral (e.g., **II**)⁵ complexes depending on the “handedness” or lack thereof in the ligands installed on Ru. In contrast, the stereogenic-at-Ru complexes are chiral irrespective of the chiral (**III–VI**)⁶ or achiral⁷ nature of the ligands. A unique feature of the aforementioned complexes is their remarkable superiority in the promotion of highly efficient and selective OM (vs non-stereogenic-at-Ru carbenes). For example, **III**^{6a} and **IV**,^{6b} which are accessed in a stereoselective manner, have been demonstrated as optimal catalysts for enantioselective ring-opening/cross-metathesis (ROCM). Furthermore, bidentate phosphine complexes (e.g., **V**) promote excellent levels of chemoselectivity in the alternating copolymerization of norbornene and cyclooctene.^{6c,8}

(4) Garber, S. B.; Kingsbury, J. S.; Gray, B. L.; Hoveyda, A. H. *J. Am. Chem. Soc.* **2000**, *122*, 8168–8179.

(5) Funk, T. W.; Berlin, J. M.; Grubbs, R. H. *J. Am. Chem. Soc.* **2006**, *128*, 1840–1846.

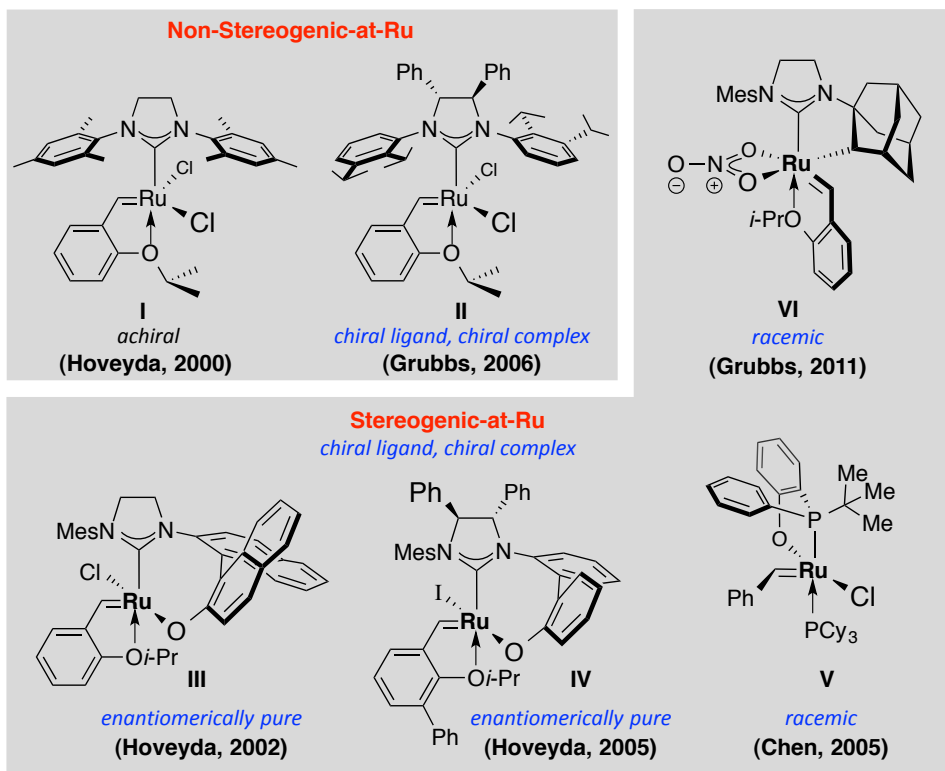
(6) (a) Van Veldhuizen, J. J.; Garber, S. B.; Kingsbury, J. S.; Hoveyda, A. H. *J. Am. Chem. Soc.* **2002**, *124*, 4954–4955. (b) Van Veldhuizen, J. J.; Campbell, J. E.; Giudici, R. E.; Hoveyda, A. H. *J. Am. Chem. Soc.* **2005**, *127*, 6877–6882. (c) Bornand, M.; Chen, P. *Angew. Chem. Int. Ed.* **2005**, *44*, 7909–7911. (d) Keitz, B. K.; Endo, K.; Patel, P. R.; Herbert, M. B.; Grubbs, R. H. *J. Am. Chem. Soc.* **2012**, *134*, 693–699.

(7) For representative examples of stereogenic-at-Ru complexes in which achiral ligands are used, see: (a) Khan, R. K. M.; Torker, S.; Hoveyda, A. H. *J. Am. Chem. Soc.* **2013**, *135*, 10258–10261. (b) Occhipinti, G.; Hansen, F. R.; Törnroos, K. W.; Jensen, V. R. *J. Am. Chem. Soc.* **2013**, *135*, 3331–3334.

(8) Bornand, M.; Torker, S.; Chen, P. *Organometallics* **2007**, *26*, 3585–3596.

The aforementioned transformation is rare with non-stereogenic-at-Ru carbenes.⁹ A bidentate NHC alkyl-chelating complex **VI** is also successfully employed in a wide variety of Z-selective OM reactions.¹⁰

Scheme 1.1-2. Non-Stereogenic and Stereogenic-at- Ru Carbenes for OM



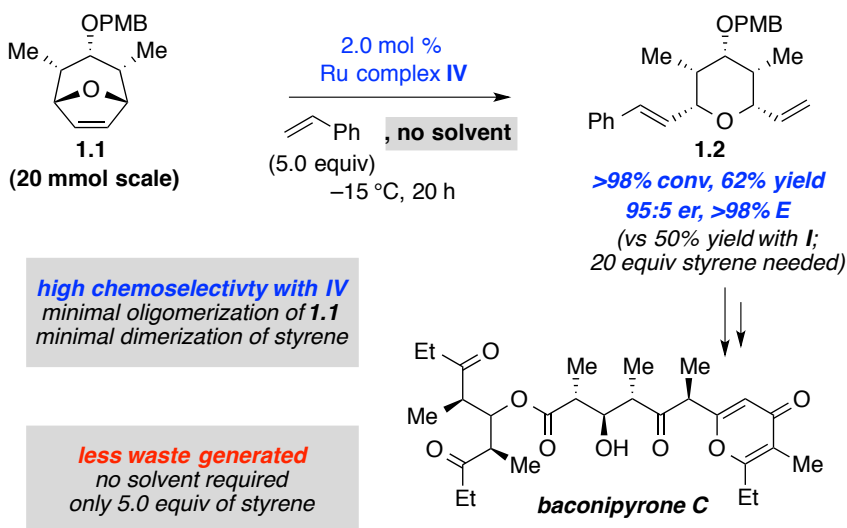
In addition to their success in methodology development, stereogenic-at-Ru complexes have also been demonstrated to play an important role in critical OM steps in natural product synthesis. In this regard, most notable example involves the enantioselective ROCM catalyzed by **IV** in the total synthesis of baconipyrone C (Scheme 1.1-3). In this case, treatment of highly functionalized **1.1** with 2.0 mol% **IV** in the presence of 5.0 equivalents of styrene furnishes **1.2** in unprecedented efficiency (>98% conv., 62% yield) and stereoselectivity (95:5 er and >98% *E*). More importantly, the reaction does not require the use of solvent and low oligomerization of **1.1** and no dimerization of styrene is observed. In contrast, reaction with non-stereogenic-at-Ru **I** provides 50% conversion to the desired **1.2** with 20 equivalents of styrene under

(9) For an example of alternating copolymerization with non-stereogenic-at-Ru complex, see: Vehlow, K.; Wang, D.; Buchmeiser, R.; Blechert, S. *Angew. Chem. Int. Ed.* **2008**, *47*, 2615–2618.

(10) See chapter three for more details.

otherwise similar conditions. Notably, a large excess of styrene (vs 5.0 equiv. with **IV**) is necessary for any appreciable conversion to the desired product as extensive homocoupling side-reaction to form stilbene readily takes place. Additionally, a large amount of the oligomer of **1.1** is also observed, which is the dominant product at lower loadings of styrene (2.0 equiv. or less). The aforementioned complications underlined the lack of chemoselectivity exhibited by non-stereogenic-at-Ru complexes and motivated us to investigate the mechanism of OM promoted by stereogenic-at-Ru carbenes.

Scheme 1.1-3. Advantage of Stereogenic-at-Ru Carbenes in Stereoselective OM



1.2 Mechanistic Differences Between Stereogenic and Non-Stereogenic-at-Ru Carbenes in Olefin Metathesis

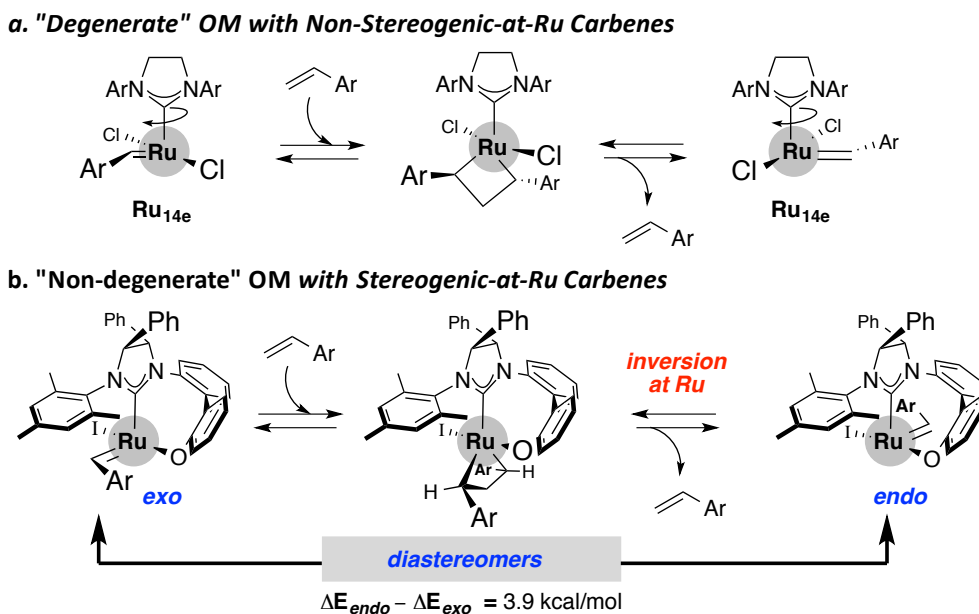
Based on the results listed above, we suspected that the high control of selectivity exhibited by stereogenic-at-Ru catalysts could be due to their distinct mechanism from that of non-stereogenic-at-Ru complexes. For instance, whereas a carbene side-change involving a **Ru_{14e}** complex could be degenerate (Scheme 1.2-1a),¹¹ such process constitutes a stereochemical inversion in stereogenic-at-Ru complex with carbene oriented *outside* the eight-membered azaoxa-Ru ring (hereforth, *exo*) to the corresponding complex with carbene oriented *inside* it (hereforth, *endo*), thereby

(11) For a study involving degenerate processes in OM with non-stereogenic-at-Ru catalysts, see: Keitz, B. K.; Grubbs, R. H. *J. Am. Chem. Soc.* **2011**, *133*, 16277–16284

rendering the overall transformation non-degenerate (Scheme 1.2-1b).¹² The resulting energetically and structurally distinct diastereomers (i.e. *exo* and *endo*, cf. Section 1.4.1) are characterized by their individual reactivity and selectivity profiles.

A brief computational analysis of the two complexes (with Ar= Ph) revealed that the latter diastereomer is approximately 4.0 kcal/mol higher in energy than the former.¹³ The aforementioned result immediately directed us to consider the following: 1) The catalytic cycle of OM promoted by stereogenic-at-Ru complexes involves *two propagating species* (vs one with non-stereogenic-at-Ru catalysts) 2) although the *endo* complex is scarce; it is significantly more reactive than the *exo* 3) high stereocontrol by stereogenic-at-Ru carbenes in OM indicates that only one diastereomer (*exo* or *endo*) is involved in the stereochemistry-determining step 4) high chemoselectivity most likely originates from the differences in reactivity of the two diastereomers (i.e. sequence-selective reactions of *exo* and *endo* with the two alkenes).

Scheme 1.2-1. Stereochemical Inversion Through OM in a Stereogenic-at- Ru Carbene



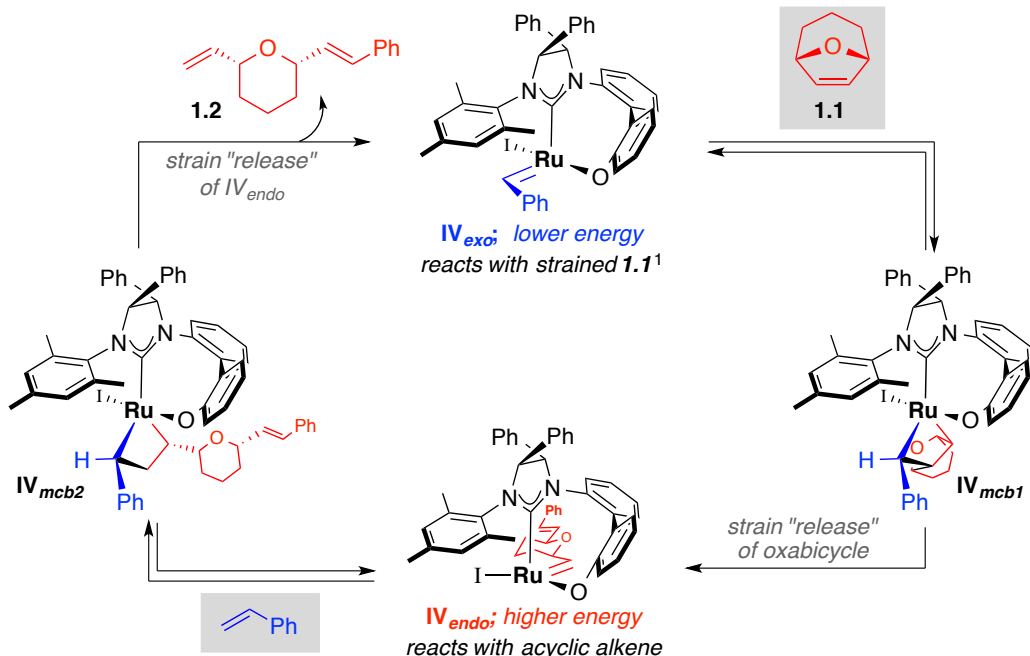
With the above mechanistic nuances in mind, we wished to examine the catalytic cycle for the formation of **1.2** through the ROCM promoted by **IV** (cf. Scheme 1.1-3).

(12) For a study involving the importance of non-degenerate processes in OM with stereogenic-at-metal catalysts, see: Meek, S. J.; Malcolmson, S. J.; Li, B.; Schrock, R. R.; Hoveyda, A. H. *J. Am. Chem. Soc.* **2009**, *131*, 16407–16409.

(13) Zhugralin, A. R. PhD Dissertation, Boston College, **2011**.

We proposed that the lower-energy **IV_{exo}** serves as the resting-state of the catalyst derived from **IV** (Scheme 1.2-2). The predominant diastereomer **IV_{exo}** irreversibly reacts with highly strained oxabicyclic **1.1** to generate the corresponding high-energy **IV_{endo}**. The strain-release of **1.1** (i.e. ~11 kcal/mol)¹⁴ is responsible for overwhelmingly favoring the breakage of metallacyclobutane **IV_{mcb1}** towards **IV_{endo}** (vs the reversion to **IV_{exo}**).

Scheme 1.2-2. Stereochemical Inversion Through OM in a Stereogenic-at- Ru Carbene



¹Substituents in oxabicyclic **1.1** are omitted for clarity. **mcb** = metallacyclobutane; **IV_{exo}** and **IV_{endo}** are derived from parent Ru complex **IV**.

The sterically congested and high-energy carbene in **IV_{endo}** reacts preferentially with less-hindered terminal alkene (i.e. styrene vs 1, 2-disubstituted alkene **1.1**) through the intermediacy of **IV_{mcb2}** to regenerate lower-energy **IV_{exo}** and release the desired alkene **1.2** thereby completing the catalytic cycle.

Overall, the process involves *two propagating species* **IV_{exo}** and **IV_{endo}**, which react in a sequence-selective fashion with **1.1** and styrene, respectively, to promote high chemoselectivity (i.e. minimal dimerization and oligomerization). Additionally, ring-opening step of **1.1** is stereochemistry-determining, which is exclusively promoted by **IV_{exo}** resulting in high stereoselectivity.

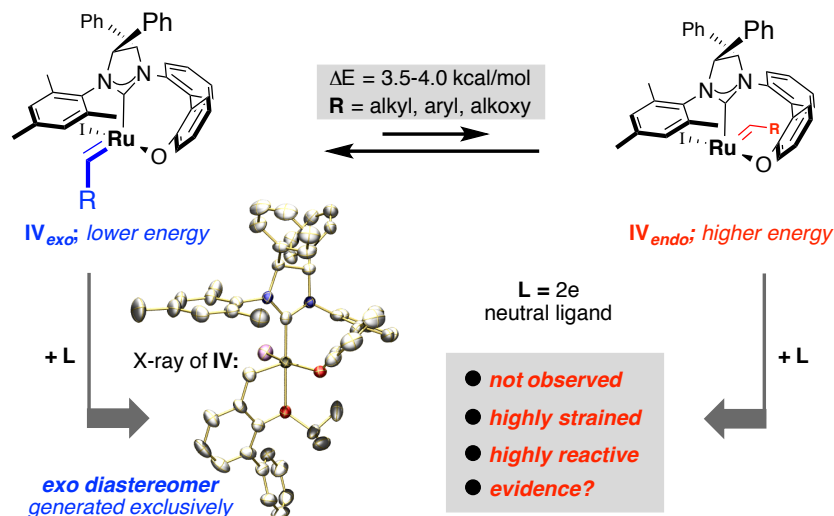
(14) Strain release of a similar oxabicyclic derivative has been computed, see: chapter two for details.

1.3 Experimental Evidence for Two Discrete Mechanisms for Polytopal Rearrangement in Ru Carbenes¹⁵

1.3.1 OM-Based Inversions in Stereogenic-at-Ru Carbenes: Isolation and Characterization of High-Energy Diastereomers (*endo-anti* and *endo-anti_F*)

Although the above proposal provides a plausible rationale for the high efficiency and selectivity promoted by stereogenic-at-Ru complexes in OM, several issues required attention: 1) All protocols to access **IV** result in the exclusive generation of lower-energy *exo*-carbene (see X-ray of **IV**, Scheme 1.3.1-1, *cf.* **IV_{exo}**) 2) no kinetically stable *endo*-type carbenes were reported in the literature,¹⁶ most likely due to its high-energy arising from the orientation of the carbene towards the sterically congested eight-membered azaoxa-Ru-ring, which could substantiate our proposal for the intermediacy of **IV_{endo}** 3) no direct evidence for the OM-based inversion in NHC-containing stereogenic-at-Ru complexes (i.e. *exo* to *endo*) had been reported 4) inversion at Ru stereogenic center through a competitive non-OM pathway could also take place, which could potentially undermine the catalytic fidelity through OM and affect the overall efficiency and selectivity.

Scheme 1.3.1-1. Lack of Evidence for *endo*-Type Carbenes

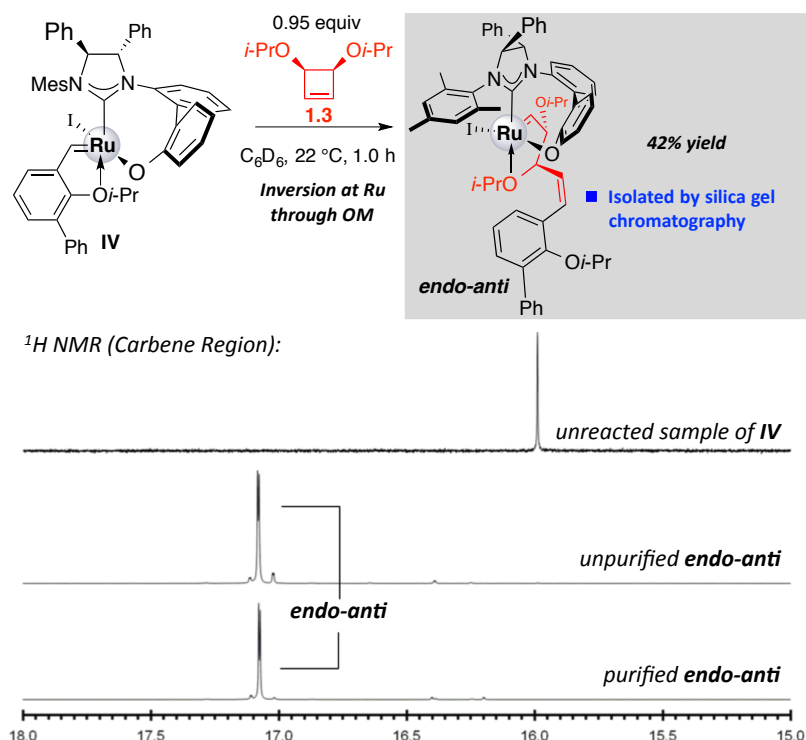


(15) Khan, R. K. M.; Zhugralin, A. R.; Torker, S.; O'Brien, R. V.; Lombardi, P. J.; Hoveyda, A. H. *J. Am. Chem. Soc.* **2012**, *134*, 12438–12441.

(16) Only report of an *endo*-type carbene with a bidentate phosphine, which is thermodynamically stabilized by a C–H agostic interaction, had been isolated and characterized, see: Bornand, M.; Torker, S.; Chen, P. *Organometallics* **2007**, *26*, 3585–3596.

In order to generate a well-defined *endo*-type complex, we chose to probe the reaction of **IV**, which is an *exo*-type complex, with *cis*-3,4-diisopropoxycyclobutene (**1.3**), which was selected as the substrate for two main reasons: the high reactivity of the strained ring ensures facile ring-opening metathesis, and an isopropoxy group, via internal chelation with the Ru center (*cf.* **IV**), would improve stability, and facilitate isolation of the less stable *endo*-type complex.

Scheme 1.3.1-2. Direct Observation of Stereochemical Inversion at Ru

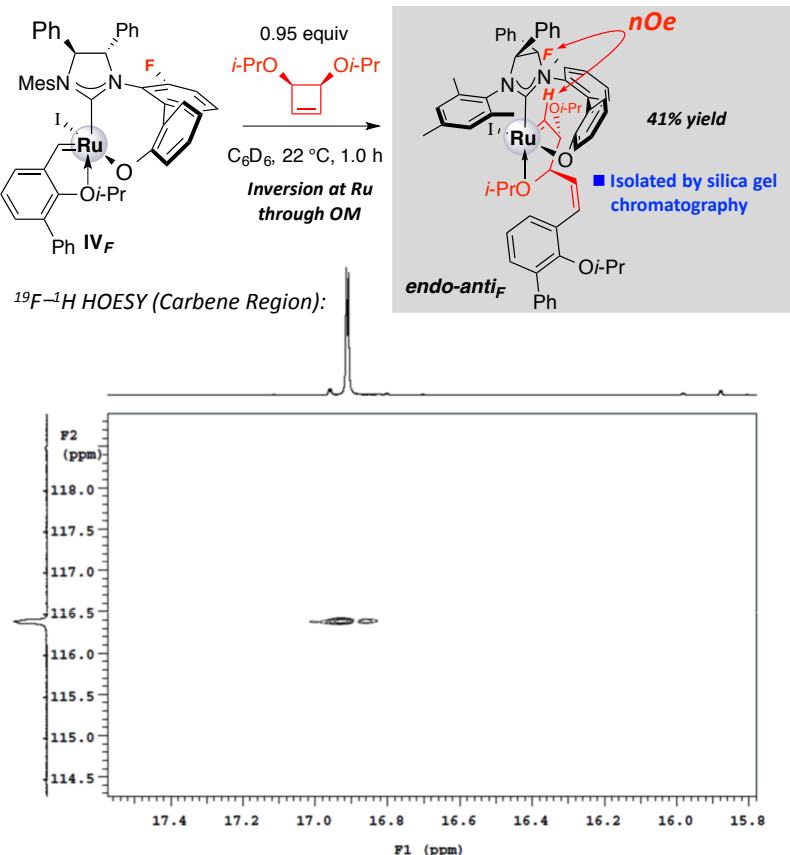


With the hitherto considerations in mind, we began by subjecting **IV** to **1.3** (0.95 equiv) in C_6D_6 at $22\text{ }^\circ\text{C}$. After one hour, the ^1H NMR analysis of the reaction mixture revealed the complete disappearance of **IV** (singlet, 16.0 ppm, Scheme 1.3-2) and generation of a new carbene peak (doublet, 17.07 ppm, Scheme).¹⁷ The downfield shift of the peak is consistent with the formation of an *endo*-type complex, since in an *exo*-type isomer the carbene proton would be relatively upfield due to the anisotropic effect arising from its residence below the π -face of the mesityl moiety (*cf.* **IV**).⁴ Interestingly, not only the newly generated complex **endo-anti** is remarkably stable in solution, but also easily

(17) Computed values of **endo-anti**, **exo-anti**, and **endo-syn** are listed in Table S2 of the experimental section below.

isolated by silica gel chromatography under air (42% yield). Overall, the aforementioned observation is a direct-evidence for the inversion at Ru stereogenic center and the first example of a kinetically stable *endo*-type Ru carbene complex.

Scheme 1.3.1-3. ^{19}F – ^1H Correlation as Supporting Evidence for the *endo*-Carbene



Although the two-dimensional NMR studies were performed to confirm the *endo*-orientation of the *endo-anti*, we decided to synthesize a related *endo-anti_F* complex (Scheme 1.3.1-3) to unambiguously demonstrate this feature. We hypothesized that the *endo*-orientation of the carbene in *endo-anti_F* would place $^{19}\text{F}/\text{N-aryl}$ and $^1\text{H}/\text{carbene}$ in close proximity to each other, rendering the aforementioned feature observable through ^{19}F – ^1H heteronuclear Overhauser effect spectroscopy (HOESY). Similar to the formation of *endo-anti*, reaction of **IV_F** with **1.3** leads to the generation of *endo-anti_F* within one hour, which is also isolable through silica gel chromatography (41% yield, Scheme 1.3.1-3). Consistent with our hypothesis, a strong ^{19}F – ^1H spatial correlation in *endo-anti_F* is observed through the use of HOESY, which confirms the *endo*-orientation of the carbene

in this complex. It is also noteworthy that the similar enhancement is not observed with **IV_F**, which is consistent with the *exo*-orientation of the carbene.

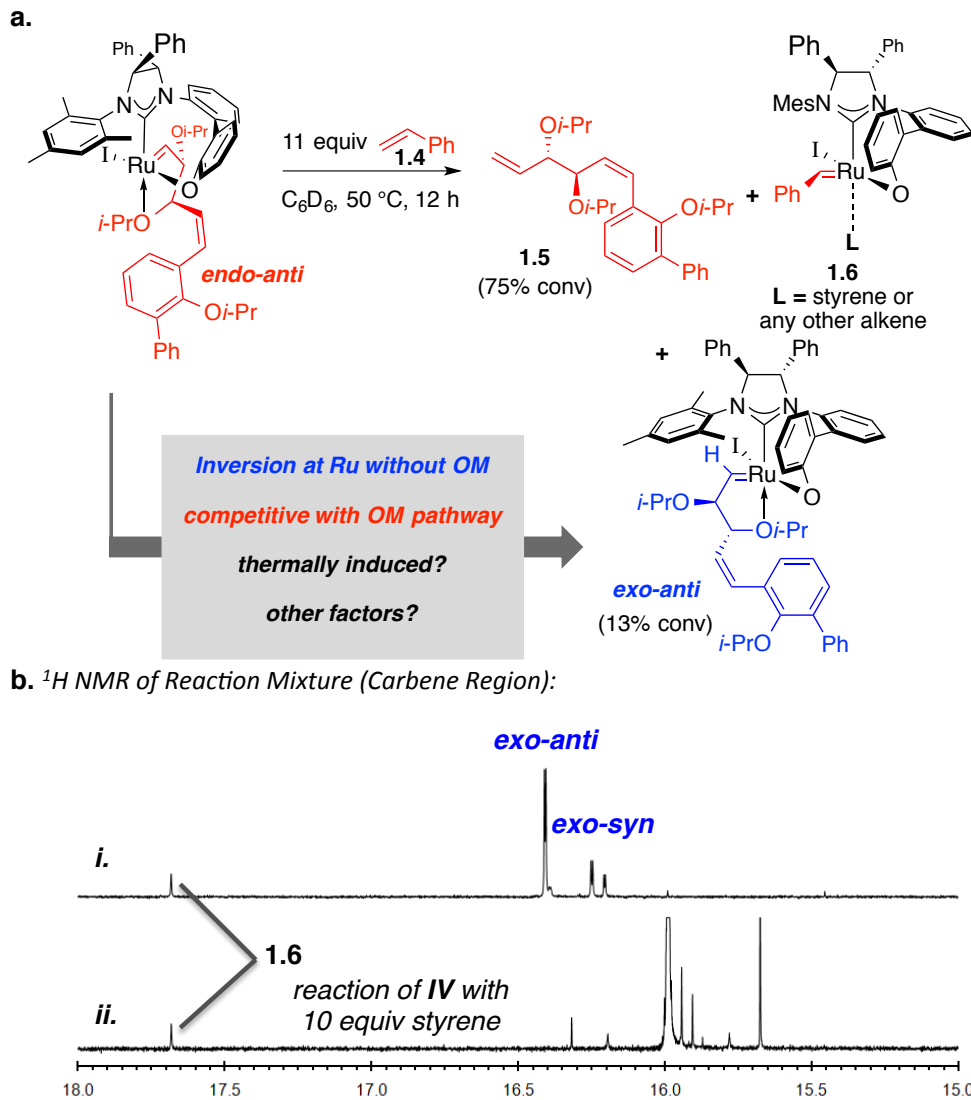
1.3.2 Non-OM Inversions in Stereogenic-at-Ru Carbenes: Stereoisomerization of High-Energy *endo-anti* Complex

With *endo-anti* in hand, the examination of its ability to promote CM with a terminal olefin ensued. Indeed, *endo-anti* reacts (>98% conv.) with 11 equivalents of styrene **1.4** in C₆D₆ at 50 °C within 12 hours to furnish 75% conversion to **1.5** (Scheme 1.3.2.1-1a). The reaction does not proceed to any conversion at 22 °C, which could be due to the lack of initiation at lower temperature. Importantly, the generation of **1.5** represents a stoichiometric ROCM performed in two independent steps (i.e. ROM and CM, respectively) through the intermediacy of *endo-anti*, which is isolated and then resubjected in the reaction. The aforementioned transformation strongly supports our proposed catalytic cycle for ROCM promoted by stereogenic-at-Ru **IV** (*cf.* Scheme 1.2-2). Interestingly, ¹H NMR spectrum of the unpurified reaction mixture reveals a singlet carbene signal at 17.68 ppm and another, with higher intensity, at 16.41 ppm (see **i** in 1.3.2.1-1b). The relatively downfield singlet likely arises from the inversion at Ru to form *exo*-benzylidene **1.6**, which results from the reaction of *endo-anti* with styrene; this is corroborated by the observation that treatment of **IV** with **1.4** led to the appearance of the same signal (see **ii** in 1.3.2.1-1b).

Additional efforts to isolate and characterize **1.6** were not successful, potentially due to its decomposition. Most notably, however, we isolated the Ru complex (generated in 13% conv.) corresponding to the upfield carbene ¹H signal (doublet, 16.41 ppm) through silica gel chromatography, and established its identity as *exo-anti* (i.e. *i*-PrO ligand is chelated trans-to-NHC; carbene ¹H oriented toward Mes).⁴ It is worthy of mention that the latter complex indicates a non-OM based inversion at Ru in *endo-anti*. Not only this is the first example of inversion in a stereogenic-at-Ru carbene without OM, but it also reveals that non-OM pathway is relatively competitive (i.e. 13% *exo-anti*/non-OM vs 75% **1.5**/OM). Given that the catalytic fidelity of stereogenic-at-Ru carbenes is essential for the effective promotion of reactivity and selectivity in OM, the formation of *exo-anti* through non-OM is a significantly complicating factor from a

catalyst development standpoint. For this reason, we decided to further explore the (*endo-anti* to *exo-anti*) transformation in detail.

Scheme 1.3.2-1. Competitive OM and non-OM Based Inversions at Ru

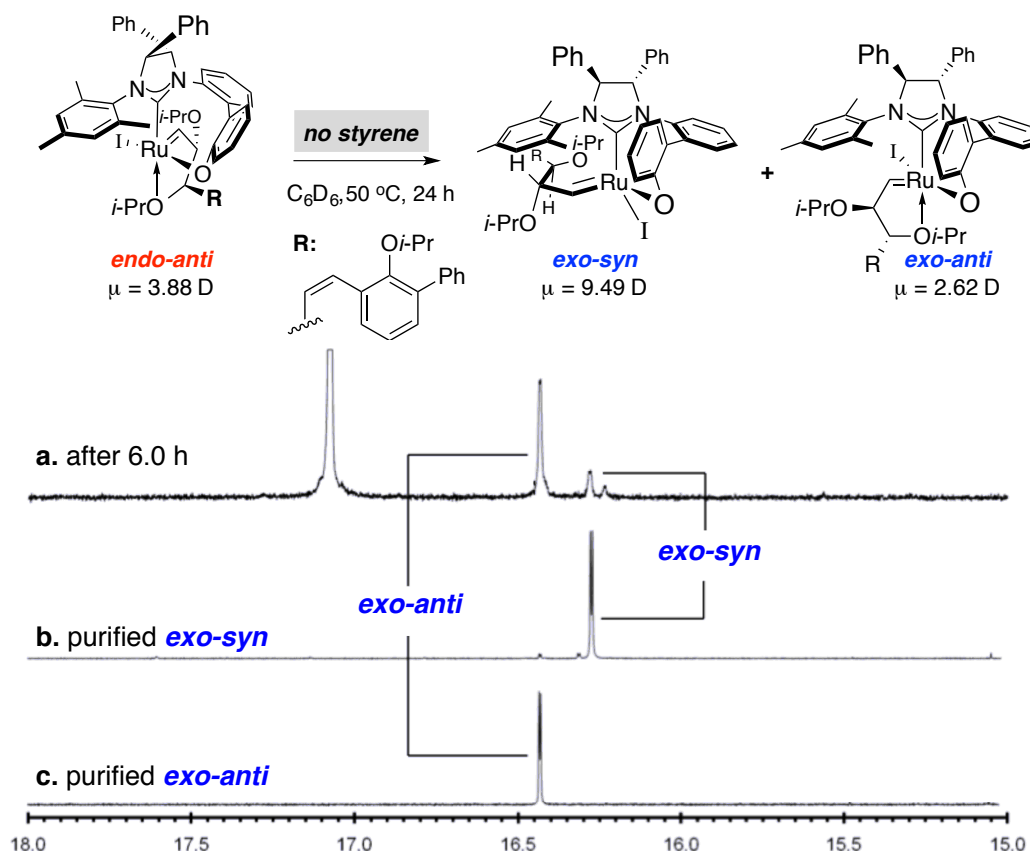


1.3.2.1 Thermally Induced Inversion at Ru Stereogenic Center

At this juncture, we wished to explore the feasibility of the above non-OM transformation in the absence of terminal olefin (**1.4**). Consequently, a solution of *endo-anti* was heated to 50 °C under the conditions shown in Scheme 1.3.2.1-1. After six hours, as shown in the ^1H NMR spectrum (a), two major new carbene peaks appeared: one at 16.41 ppm, corresponding to *exo-anti*, and another at 16.24 ppm. The latter signal appeared transient: an initial burst in intensity was followed by its diminution and then

complete disappearance within 18 hours, with simultaneous increase in the area associated with the signal for *exo-anti*.

Scheme 1.3.2.1-1. Non-OM Inversion at Ru & Isolation of a Critical Intermediate



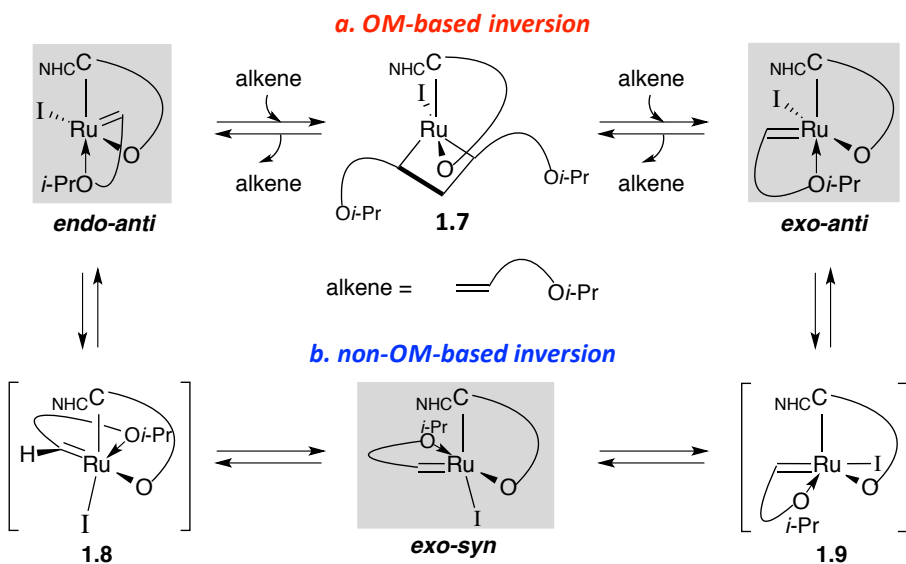
Nevertheless, we isolated and purified the former carbene (i.e. 16.24 ppm, spectrum b) through silica gel chromatography, as it is considerably more polar than the *exo* complexes (i.e. **IV** and *exo-anti*) as well as *endo-anti*. By probing the identity of the relatively fleeting complex by spectroscopic analysis,¹⁸ we established its identity as *exo-syn*, in which the isopropoxy group is chelated syn-to-NHC; the upfield shift of the carbene proton of *exo-syn* relative to *exo-anti* is most likely due to the anisotropic effect induced by the proximal anionic aryloxide ligand.¹⁹ The higher polarity of *exo-syn* probably results from the syn orientation of the iodide and aryloxide anions (vs anti in

(18) See the experimental part of this chapter for details.

(19) For example involving a similar feature exhibited by Ru-based carbene with a syn-to-NHC thioether chelate, see: Ben-Asuly, A.; Tzur, E.; Diesendruck, C. E.; Sigalov, M.; Goldberg, I.; Lemcoff, N. G. *Organometallics* **2008**, *27*, 811–813.

IV, *endo-anti*, and *exo-anti*).²⁰ Consistently, the computed structure of *exo-syn* exhibits a larger dipole moment than the other complexes (9.49 D for *exo-syn* vs 2.76, 3.88, and 2.62 D for **IV**, *endo-anti*, and *exo-anti*, respectively). It is also noteworthy that upon heating pure *exo-syn* for several hours, it transformed to *exo-anti*, showing that the conversion of *endo-anti* to *exo-anti* can proceed via *exo-syn* intermediate. Kinetic studies confirmed that the formation of *exo-anti* is first-order in *endo-anti* and occurs by a unimolecular process.¹⁸

Scheme 1.3.2.1-2. Two Distinct Mechanisms of Polytopal Rearrangements in Ru



Thus far, we have assembled experimental evidence regarding two distinct mechanisms of polytopal rearrangements in Ru carbenes. For instance, as shown in Scheme 1.3.2.1-2a, *endo-anti* can undergo an inversion at Ru through the intermediacy of ruthenacyclobutane **1.7** to give *exo-anti*. Whereas OM involves a sequence of bond formation and breakage events (i.e. cycloaddition and cycloreversion, respectively), a competitive non-OM pathway avoids this scenario altogether through a series of ligand movements through a critical *exo-syn* intermediate, albeit both structures (**1.8** and **1.9**)²¹

(20) Ru complexes with bidentate carbene chelated syn-to-NHC, in which the anions are cis to each other, are more polar than complexes with anti-to-NHC orientation, wherein anions are situated trans to each other. For details, see: (a) Benitez, E.; Goddard, W. A., III. *J. Am. Chem. Soc.* **2005**, *127*, 12218–12219. (b) Correa, A.; Cavallo, L. *J. Am. Chem. Soc.* **2006**, *128*, 13352–13353.

(21) For an observation by Caulton and coworkers that square pyramidal $(\text{Ph}_3\text{P})_3\text{RuCl}_2$ undergoes rapid unimolecular configurational isomerization in solution phase, as determined by the coalescence of ^{31}P NMR peaks of inequivalent basal and apical phosphines at 30 °C, see: Hoffman, P. R.; Caulton, K. G. *J.*

will involve disfavoring interactions due to the trans orientation of the carbene-donor with aryloxide and iodide, respectively (Scheme 1.3.2.1-2b). With these details in mind, we hypothesized that the relative barriers for both pathways will largely depend on the energetic cost (due to donor-donor repulsions, dipolar interactions, and e-e repulsive forces between anions) associated with the formation of **1.7** vs **1.8** and **1.9**.

1.3.2.2 Acid-Catalyzed Inversion at Ru Stereogenic Center

We then set out to assemble support for our proposal regarding non-OM stereoisomerization illustrated in Scheme 1.3.2.1-2. Since *exo-syn* and related complexes **1.8** and **1.9** involve a cis arrangement of anions, we wondered if the use of a Brønsted acid could lead to the partial protonation of aryloxide and/or iodide, which would be beneficial on three counts: 1) H-bonding with the neighboring (syn) heteroatom (in *exo-syn*, **1.8**, and **1.9**) and minimization of e-e repulsions 2) diminution of trans-influence involving aryloxide and iodide with carbene donor in **1.8** and **1.9**, respectively 3) overall stabilization of highly polar intermediates and transition states.

To probe its effect on non-OM, we subjected *endo-anti* to 12 mol% acetic acid (in C₆D₆) at 22 °C. Surprisingly, 68% conversion of *endo-anti* took place to give *exo-syn* within only one hour (vs >98% conv to *exo-anti* in 24 hours by heating, Scheme 1.3.2.1-1); with 1.0 equiv of acetic acid, isomerization was complete in <5 minutes (<2% *exo-anti* in both cases, Scheme 1.3.2.2a). To establish that the aforementioned transformation is not mediated through the oxygen coordination with Ru, various solvents including tetrahydrofuran, acetone, dimethyl sulfoxide and methanol were tested, none of which led to any noticeable conversion. Moreover, whereas trimethylphosphine has been employed to effect inversion in a stereogenic-at-Mo alkylidene through non-OM pathway,²² such transformation is not observed when *endo-anti* is exposed to the same condition.

Unlike the conversion of *endo-anti* to *exo-syn*, the isomerization of the latter

Am. Chem. Soc. **1975**, *97*, 4221–4228. In this study, they point out that in contrast to trigonal bipyramidal systems, where geometries of transition states for Berry pseudorotations are square pyramidal, the transition states and/or associated structures for Berry pseudorotations of square pyramidal complexes are trigonal bipyramidal. Thus, a mechanism of the isomerization of *endo-anti* (square pyramidal) necessitates a distortion to a trigonal bipyramidal geometry, for which we considered the distortions of the aryloxide and iodide ligands in such a fashion that one anion remains orthogonal-to-carbene while the other orients itself trans-to-carbene. Consequently, two new structures **1.8** and **1.9**, which are not observable due to high energy associated with their structural features, are proposed.

(22) Marinescu, S. C.; Schrock, R. R.; Li, B.; Hoveyda, A. H. *J. Am. Chem. Soc.* **2009**, *131*, 58–59.

complex to *exo-anti* is not facilitated by acetic acid. Furthermore, the (*exo-syn* to *exo-anti*) reaction could only be promoted by heat (>98% conv, 50 °C, 25 h, C₆D₆, Scheme 1.3.2.2a). To rationalize these observations, we considered the following scenario: partial protonation of aryloxide (most basic site in *endo-anti*) takes place, which ultimately leads to formation of the corresponding **1.8–H⁺**, wherein severe e–e repulsion due to cis-arrangement of anions (oxide and iodide) is minimized through H⁺ bridge (Scheme 13.2.2b). Additionally, the strongly disfavoring trans influence due to the linear relationship between aryloxide and carbene donor is significantly minimized through reduced e-density on partially protonated aryloxide. Subsequently, an inversion at Ru takes place to give *exo-syn*, which is also stabilized (vs absence of H⁺) due to the positive influence (i.e. minimization in O/I repulsion and reduced dipolar interactions) exerted by acid. In contrast, the added stabilization is less pronounced in **1.9–H⁺** due to the following: although minimization in O/ I repulsion occurs, its influence on reduction of e-density on I, which is a weak H-bond acceptor, is diminutive; consequently, no significant reduction in the trans influence between iodide and carbene donor is effected. As a result of the aforementioned interactions, the barrier associated with **1.9–H⁺** (vs **1.9**) remains unchanged thereby leading to the exclusive generation of *exo-syn*.

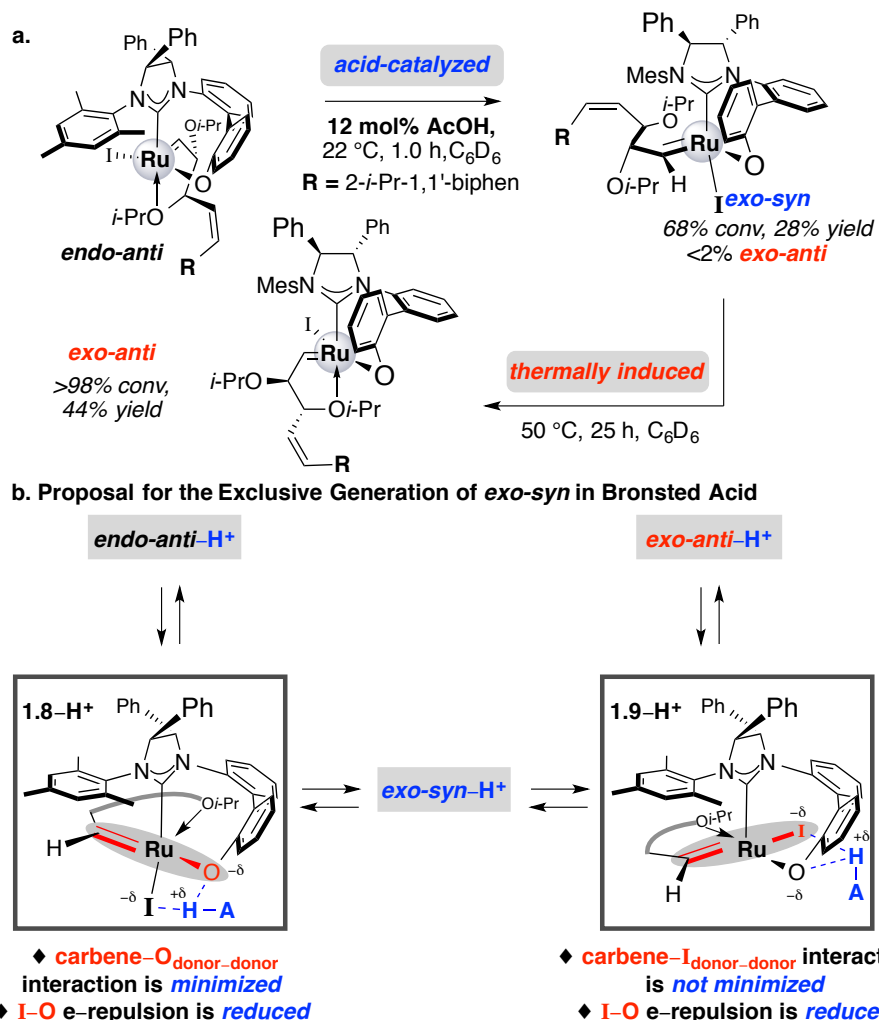
It is noteworthy that in addition to the non-OM mechanism of conversion without bond-breakage, generation of *exo-anti* via *exo-syn* can also occur by O*i*-Pr dissociation/carbene rotation/O*i*-Pr reassociation pathway. In this regard, computational investigations involving quinoline-chelated non-stereogenic-at-Ru carbene complexes have revealed that the aforementioned route and the polytopal rearrangement pathway (*without bond breakage*) might be energetically similar.²³ Nevertheless, it is *less likely* that dechelation/rechelation of O*i*-Pr is facile; otherwise, isolation of *exo-syn* would not be feasible.

Based on the results discussed thus far, it is also important to note that the investigated system involves association of oxygen-chelate (O*i*-Pr) with the Ru center in place of an alkene. It is thus likely that the less structurally rigid complexes with a monodentate NHC and/or a carbene more readily undergo polytopal rearrangements.

(23) Poater, A.; Ragone, F.; Correa, A.; Szadkowska, A.; Barbasiewicz, M.; Grela, K.; Cavallo, L. *Chem.–Eur. J.* **2010**, *16*, 14354–14364.

Furthermore, any knowledge gained regarding the non-OM pathway of carbene isomerization (inversion in stereogenic-at-Ru, *cf.* side-change in non-stereogenic-at-Ru) should also have implications on OM-based polytopal rearrangements.

Scheme 1.3.2.2. Non-OM Stereoisomerization of Ru carbene Catalyzed by Acid



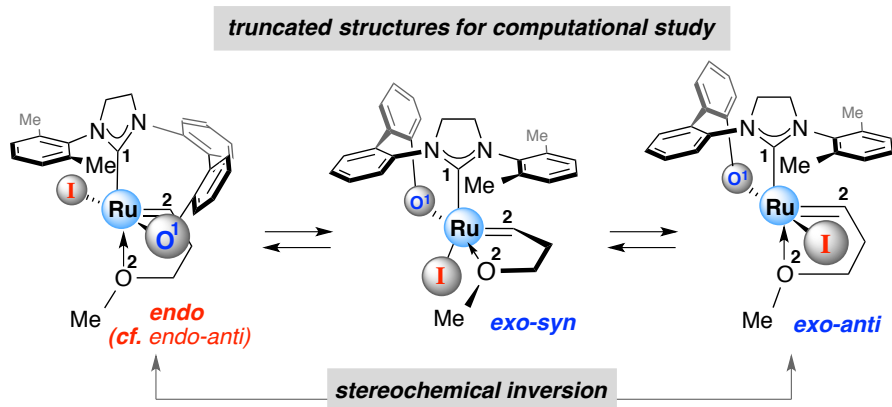
1.4 Computational Rationale for non-OM Inversion in *endo-anti*²⁴

In order to conduct computational analysis, truncated structures of Ru carbenes (i.e. *endo* = *endo-anti*, *exo-syn*, and *exo-anti*) were considered. As shown in Scheme 1.4, the diphenyl substituents at the NHC-backbone, the *p*-methyl substituent of the N-mesityl group, and the side chains of the bidentate alkylidene are omitted to reduce computational

(24) For details regarding the density functional methods, complete description of computed structures, and the related energy diagrams, see the supporting information of: Torker, S.; Khan, R. K. M.; Hoveyda, A. H. *J. Am. Chem. Soc.* **2014**, *136*, 3439–3455.

cost. Additionally, $Oi\text{-Pr}$ is exchanged with OMe to avoid any conformational complexity associated with its rotation. In the discussion below, following nomenclature is used for ligands on Ru: $C^1 = NHC$; $C^2 = \text{metathesis-active carbene}$; $O^1 = \text{aryloxide}$; $O^2 = OMe$; $I = \text{iodide}$. In order to further simplify the *endo* \rightarrow *exo-anti* inversion from reader's perspective, $C^1\text{-Ru-}C^2$ fragment is held at a fixed position, in which C^2 serves as pivot while C^1 undergoes 180° rotation simultaneously with the transposition of the O^1 and I .

Scheme 1.4. Model Systems for the Investigation of Inversion at Ru

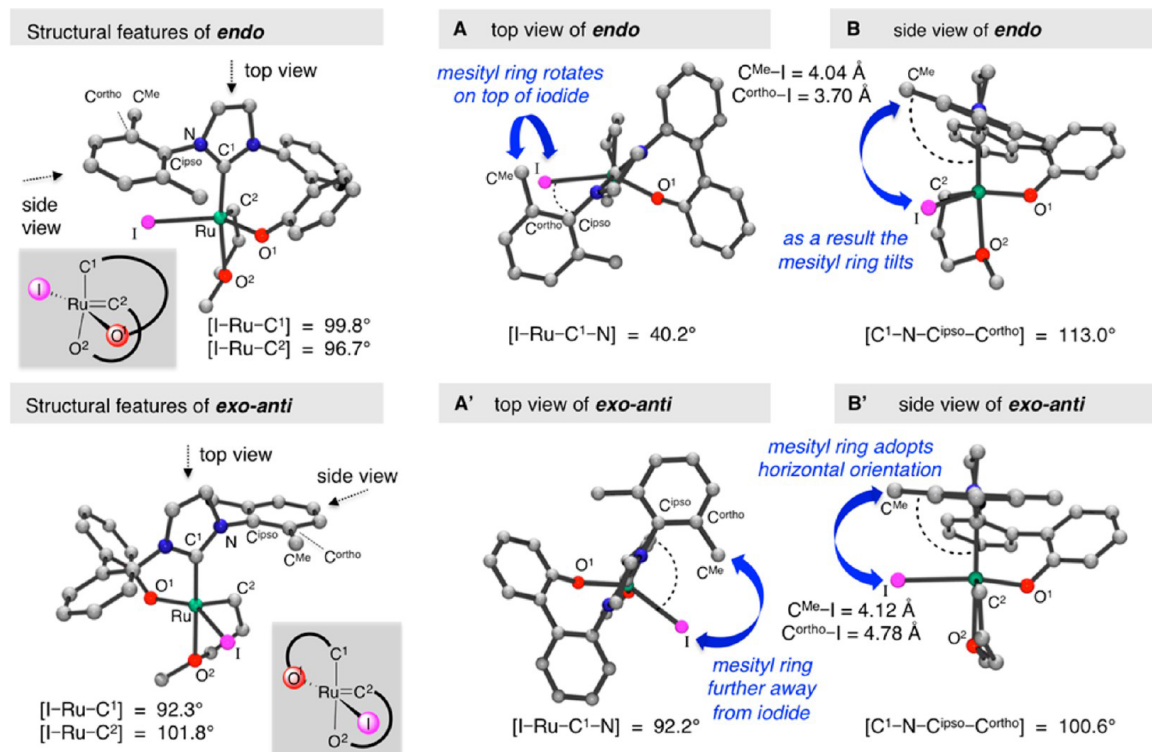


1.4.1 Source of the Energetic Difference Between *endo* and *exo-anti* Diastereomers

First off, we wished to examine the origin of the high-energy (~ 4.0 kcal/mol) associated with the *endo* diastereomer compared with its counterpart (*exo-anti*). In this respect, the computed structures for the two carbenes optimized with BP86 density functional (listed in Scheme 1.4.1) are considered.¹⁸ As illustrated in part A, the 2,6-dimethylphenyl unit of the NHC in the *endo* complex involves ($I\text{-Ru-C}^1\text{-N}$) dihedral angle of 40.2° , which results in its placement above the bulky iodide. In contrast, *exo-anti* involves relatively larger dihedral angle ($I\text{-Ru-C}^1\text{-N}: 92.2^\circ$; part A'). In the former complex, constrained geometry produces steric strain between I and the 2,6-diphenyl ring, as indicated by the reduced $C_{\text{ortho}}\text{-I}$ and $C_{\text{Me}}\text{-I}$ distances (3.70 and 4.04 Å vs 4.78 and 4.12 Å in *exo-anti*); as a consequence, the 2,6-dimethylphenyl substituent is forced to tilt ($C^1\text{-N-C}_{\text{ipso}}\text{-C}_{\text{ortho}}$ dihedral angle of 113.0° vs 100.6° in *exo-anti*, Scheme 1.4.1, parts B and B'). Moreover, the wider $I\text{-Ru-C}^1$ (99.8° in *endo* vs 92.3° in *exo-anti*) and the contracted $I\text{-Ru-C}^2$ angles (96.7° in *endo* vs 101.8° in *exo-anti*) are consistent with there being a more pronounced repulsion between the iodide and 2,6-dimethylphenyl within

the *endo* complex. Overall, the aforementioned feature renders the *endo* higher in energy than the corresponding *exo-anti* diastereomer, which leads to a unique regime in catalytic OM transformations wherein the interplay between the two diastereomers is critical to high efficiency and the promotion of chemo- and stereoselectivity.

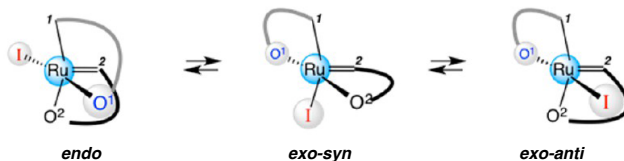
Scheme 1.4.1. Steric Strain as the Main Reason for High-Energy of *endo* (vs *exo-anti*)



1.4.2 PES of Thermally Promoted Non-OM Inversion

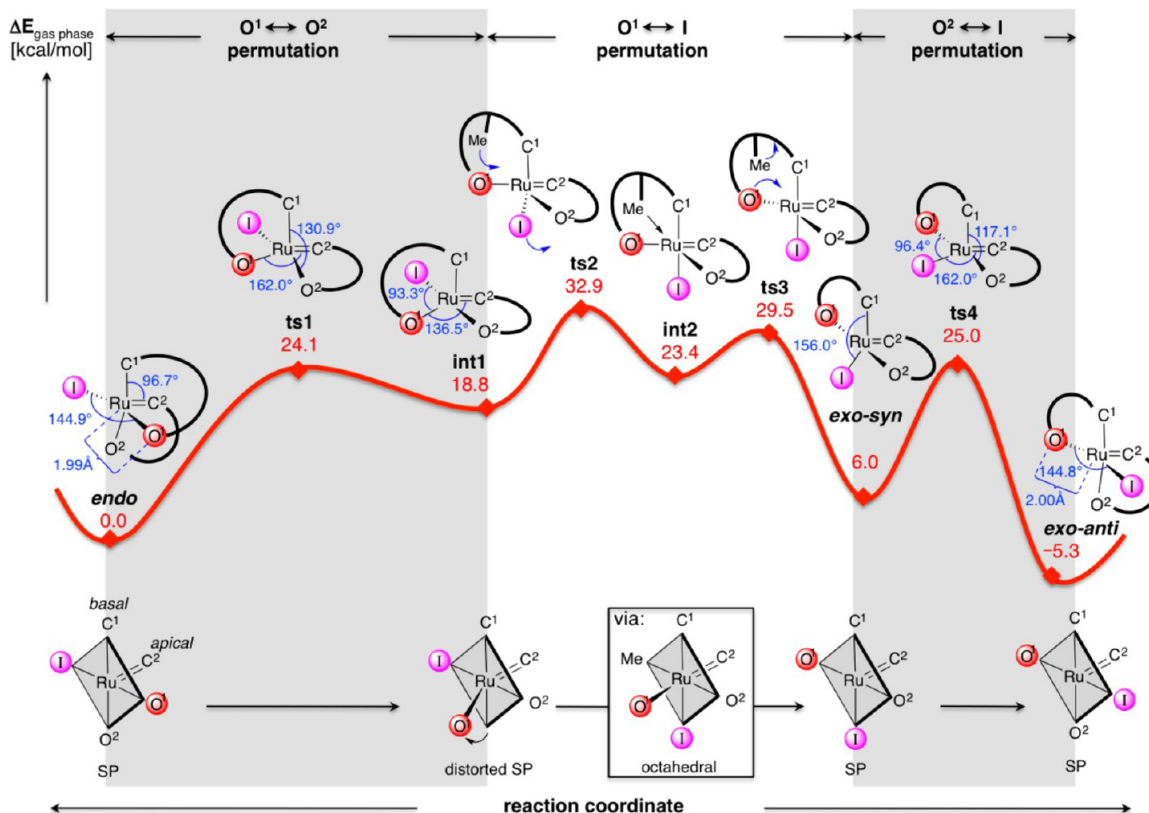
Subsequent to our analysis of the energetic difference between *endo* and *exo-anti* complexes, we investigated the potential energy surface (PES) associated with the thermally promoted non-OM inversion. For the purpose of simplification, structures shown in Scheme 1.4.2-1 are used here forth to discuss the calculated results.

Scheme 1.4.2-1. Simplified Structures of Three Stereoisomers



The computed potential energy surface (PES) in Scheme 1.4.2-2 corresponds to the thermally induced rearrangement of the higher energy, but kinetically stable, *endo* carbene (SP geometry, apical alkylidene C²)²⁵ to the corresponding thermodynamically preferred ($E_{\text{rel}} = -5.3$ kcal/mol) *exo-anti*. As shown, the transformation of *endo* to *exo-syn* ($E_{\text{rel}} = 6.0$ kcal/mol), which is isolable, involves a series of rearrangements that proceed via two additional structures that have not been spectroscopically observed: **int1**, which possesses a distorted SP geometry with the basal O¹ deviated out of plane, and 18e octahedral **int2**, which arises from a C–H/Ru agostic interaction.

Scheme 1.4.2-2. Pathway for Thermally Induced Inversion at Ru (*endo* to *exo-anti*)



Overall, the energetic barrier **ts2** (32.9 kcal/mol), associated with the formation of **int2**, is rate limiting. Furthermore, the final *exo-syn* to *exo-anti* permutation takes place via a **ts4** ($E_{\text{rel}} = 25.0$ kcal/mol). Thus, the complete process consists of three permutations, each leading to an exchange between two basal ligands (bottom graphic,

(25) For a discussion of the geometry of d⁶ ML5 complexes containing either π-accepting or π-donating ligands, see: Riehl, J.-F.; Jean, Y.; Eisenstein, O.; Pelissier, M. *Organometallics* **1992**, *11*, 729–737.

Scheme 1.4.2-2). The outcome of the first rearrangement (*endo* → **ts1** → **int1**) is the interchange of O¹ and O², which is followed by the anionic transposition of O¹ and I to generate *exo-syn* (**int1** → **ts2** → **int2** → **ts3** → *exo-syn*). Subsequently, the swapping of I for O² takes place (*exo-syn* → **ts4** → *exo-anti*).

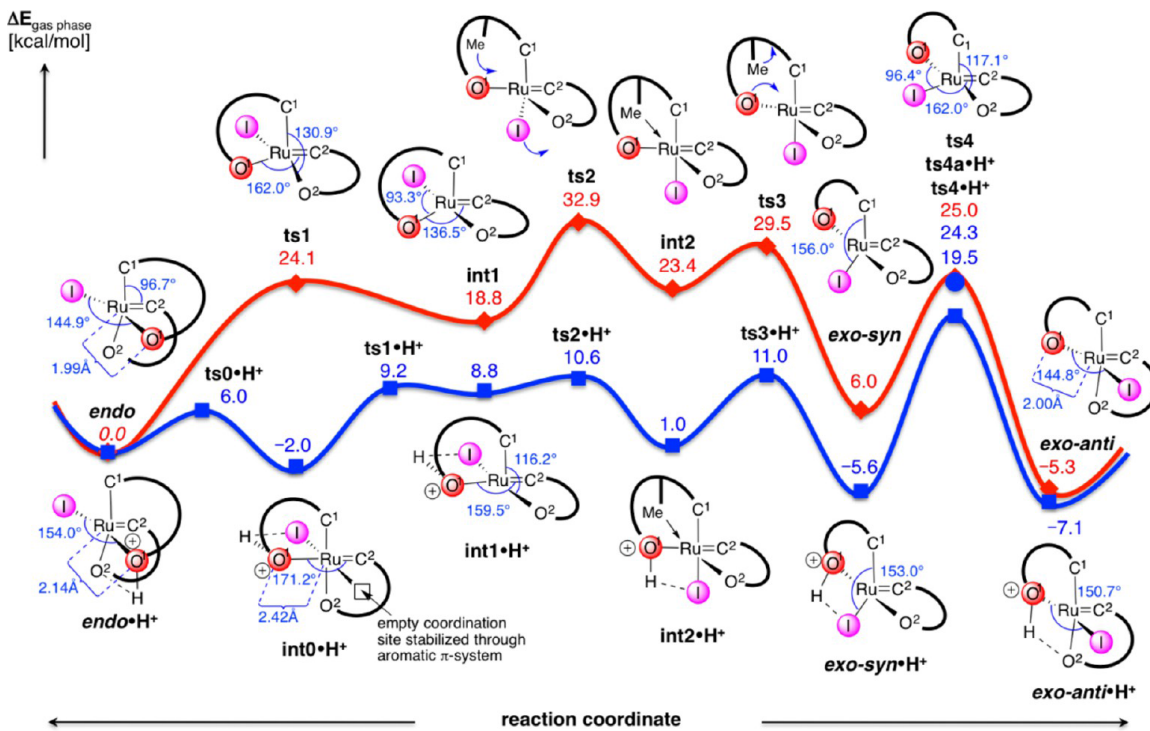
In detail, the rearrangement sequence (from left to right in Scheme 1.4.2-2) begins with the expansion of the O₁–Ru–C₂ angle (i.e. 113.2° in *endo* to 162.0° in **ts1**), which facilitates the rearrangement of O₂ to the coordination site initially occupied by O₁ – as indicated by contraction of the O₂–Ru–C₁ angle (i.e. 171.7° in *endo* to 130.9° in **ts1**). Analysis of the **ts1** reveals a large displacement vector on O₂, whereas O₁ remains static. Subsequently, the O₁–Ru–C₂ angle contracts to 136.5° in **int1**. The distorted SP geometry of this intermediate, which is not spectroscopically observed, can be rationalized by the bidentate nature of the NHC ligand, which prevents complete relaxation to an SP arrangement.

Next, the permutation of O¹ and I proceeds via 18e octahedral **int2**, which is the highest energy intermediate, due to the trans relationship of anions (O¹ and I) with strong donors (C² and C¹, respectively). The expansion of the O¹–Ru–C² in **ts2** causes the iodide to reside trans to C¹; this is facilitated by a C–H/Ru agostic interaction involving a mesityl *o*-methyl group. The distance between the Ru atom and the *o*-methyl in **ts2** decreases from 3.61 Å to 2.49 Å when **int2** is generated. The sterically congested octahedral **int2**, which contains a tridentate, a bidentate, as well as a monodentate ligand, undergoes a dissociative ligand displacement en route to *exo-syn*. The C–H agostic interaction is removed upon movement of O¹, a structural adjustment manifested by the increase in distance between Ru and the carbon atom of the *o*-methyl group to 2.98 Å in **ts3** when the O¹–Ru–C² angle contracts. The structure of *exo-syn* resembles an SP geometry wherein the iodide is distorted out-of-plane (I–Ru–C¹ = 156.0°). The final step is the rearrangement of O¹ and I from a cis orientation in *exo-syn* to the thermodynamically preferred trans alignment in *exo-anti*; the widening of the I–Ru–C² angle in **ts4** makes available a coordination site trans to C¹ that is occupied by O². Complex *exo-anti* is thus generated upon contraction in I–Ru–C² angle.

1.4.3 PES of Acid-Catalyzed Non-OM Inversion: Positive Influence of Proton

To gather insight into the acid catalyzed polytopal rearrangement, we subsequently investigated the potential energy surface of the *endo* complex in gas phase, wherein the aryloxide (O^1) is protonated ($endo \bullet H^+$, blue curve, Scheme 1.4.3-1).

Scheme 1.4.3-1. Acid-Catalyzed Pathway for Stereochemical Inversion

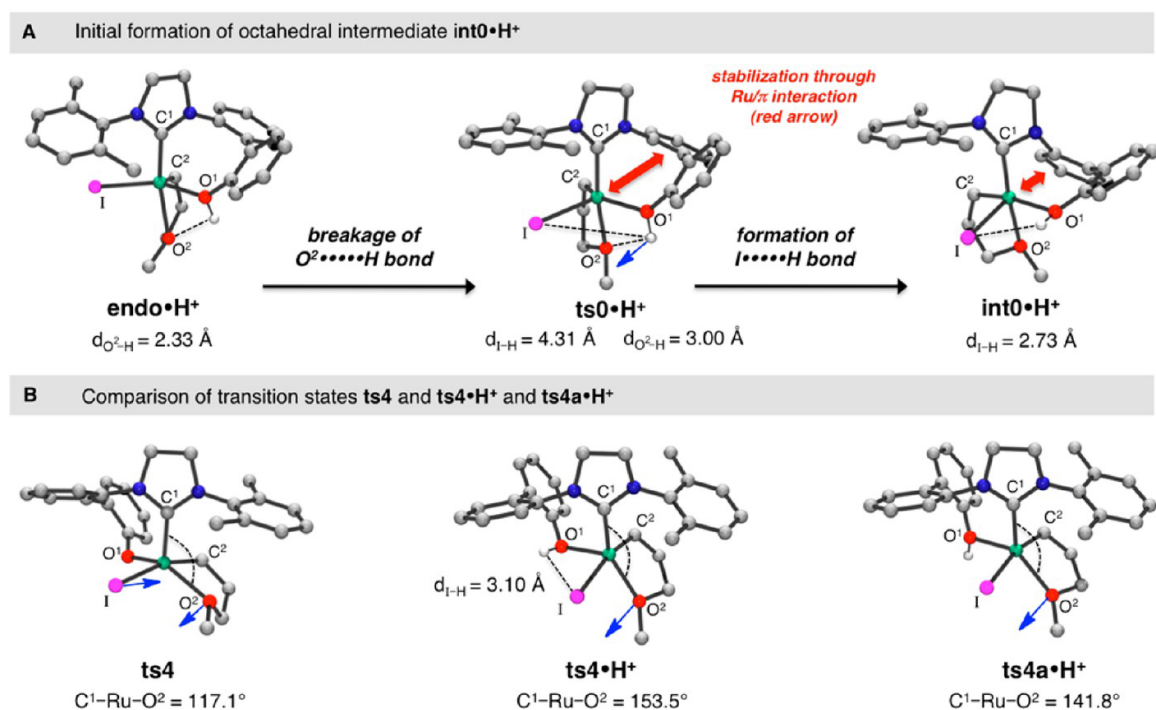


Although the movement of ligands along the reaction coordinate occurs in a similar manner compared to thermally promoted process (red vs blue curve), significantly different structural attributes are evident. The difference results from a strong effect of the proton on the reduction of the barrier associated with the conversion of $endo \bullet H^+ \rightarrow exo\text{-}syn \bullet H^+$ (E_{rel} for $ts2 \bullet H^+ = 10.6$ kcal/mol vs 32.9 kcal/mol for $ts2$). Furthermore, a new intermediate $int0 \bullet H^+$ is located in addition to $int1 \bullet H^+$, and $int2 \bullet H^+$, and there is a change in rate determining step from $ts2$ in the thermally promoted polytopal rearrangement to $ts4 \bullet H^+$ ($E_{rel} = 19.5$ kcal/mol) in the proton-catalyzed process.

Detailed analysis of the acid promoted reaction coordinate (Scheme 1.4.3-1) provides further valuable insights into the effect of the proton on structural attributes of intermediates and transition states. The direct consequence of O^1 protonation is the

significant elongation in Ru–O¹ bond length (i.e. 2.14 Å in *endo*•H⁺ vs 1.99 Å in *endo*). Simultaneously, an additional hydrogen bond O²···H is formed due to the close proximity of the two oxygen ligands (O¹ and O²). This activated intermediate undergoes an initial expansion in the O₁-Ru-C₂ angle from 104.6° to 171.2° at a largely constant O₂-Ru-C₁ angle (169.3° → 168.7°), which leads to the formation of a new octahedral intermediate **int0•H⁺**. The structure associated with the transition state **ts0•H⁺** displays a large displacement vector on the proton that undergoes formation of a new hydrogen bond with the iodide (Scheme 1.4.3-2A). The O₂···H distance is increased from 2.33 Å in *endo*•H⁺ to 3.00 Å in **ts0•H⁺**, whereas the I···H distance is shortened from 4.31 Å in **ts0•H⁺** to 2.73 Å in **int0•H⁺**.

Scheme 1.4.3-2. Noteworthy Features in Acid-Catalyzed Pathway (vs Thermal)



Notably, the empty coordination site, which is situated trans to the iodide, stabilizes due to the π-electron density of the aromatic ring of the biphenyl bridge. Subsequently, the movement of O² trans to the halide generates SP complex **int1•H⁺**. In contrast with the thermally promoted process, in which the **int1** → **int2** rearrangement is associated with a barrier of 14.1 kcal/mol, conversion of **int1•H⁺** to the octahedral

complex **int2•H⁺** requires no more than 1.8 kcal/mol. Complex **ts4•H⁺** ($E_{\text{rel}} = 19.5$ kcal/mol) holds a proton bridge that links anions (i.e. O¹ and I; distance for I···H = 3.10 Å, Scheme 1.4.3-2B), leading to its stabilization relative to the neutral species (**ts4**, $E_{\text{rel}} = 25.0$ kcal/mol). Additionally, we were able to locate transition state structure **ts4a•H⁺** (blue circle in Scheme 1.4.3-1; $E_{\text{rel}} = 24.3$ kcal/mol), which is energetically similar to **ts4** likely because the proton is not associated with the iodide (Scheme 1.4.3-2B, right). The stabilization offered by **ts4•H⁺** appears to be insufficient to allow for conversion of the *exo-syn* to the *exo-anti* complex to be accelerated in the presence of acetic acid.

1.4.4 Critical Factors Associated with non-OM Transformations

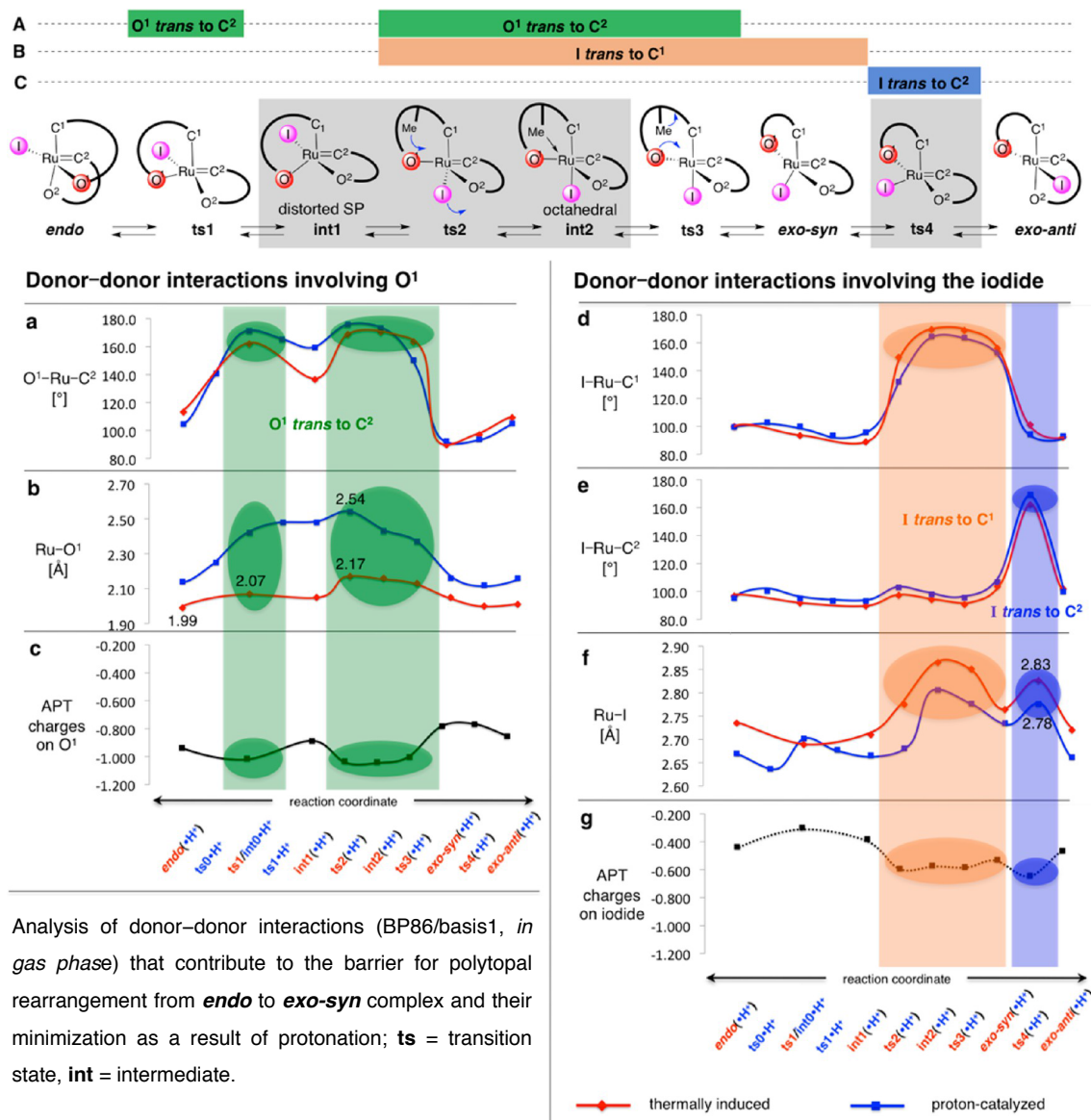
In order to rationalize the experimental results (i.e. unusual kinetic stability of *endo* and the exclusive generation of *exo-syn* in acid), we decided to examine critical factors involved. As discussed earlier (*cf.* Scheme 1.3.2.1-2), we suspected that the destabilizing interactions, due to the trans influence and dipolar effects, arising from the relative orientations of O¹, I, and strongly donating carbenes (C¹ and C²) during the course of polytopal rearrangements play important role. In order to corroborate our proposal, we decided to track the build-up of e-density on anions during the reaction progression (Scheme 1.4.4). In this regard, three critical trans-relationships are identified in thermally promoted rearrangement pathway (Scheme 1.4.4.1, Section 1.4.4.1): (A) O¹ trans to C² in **ts1**, **ts2**, **int2**, and **ts3**; (B) I trans to C¹ in **ts2**, **int2**, **ts3**, and *exo-syn*; and (C) I trans to C² in **ts4**.

1.4.4.1 Donor-Donor Interactions Involving Anions

In order to reveal the critical role of anions, we started with examining the movement of O¹ in various intermediates and transition states. As depicted in graph a, the O¹–Ru–C² angle includes two peak regions corresponding to **ts1** (162.0°) and **int2** (170.6°). Simultaneously, elongation in the Ru–O¹ bond length (1.99 Å in *endo* to 2.07 Å in **ts1** and 2.17 Å in **ts2** to generate **int2** graph b, red curve), indicating trans influence, is noticed. Notably, the examination of the negative charge accumulation on O¹ (i.e. APT charges in graph c) renders the repulsive donor–donor interaction arising from the linearity of O¹ and C² visible. The diminution in the aforementioned destabilizing interaction, due to the protonation of O¹, becomes palpable when **int1** → **int2**

transformation is compared to $\text{int1}\cdot\text{H}^+ \rightarrow \text{int2}\cdot\text{H}^+$. For instance, the distorted geometry of **int1** most likely arises from the minimization in strong trans influence caused by O¹ and C², as illustrated by the deep local minimum in graph a, red curve.

Scheme 1.4.4.1. Destabilizing Trans Influence of Anions as Root Cause for High Barriers



More importantly, the higher barrier associated with **ts2** ($E_{\text{rel}} = 32.9$ kcal/mol), which causes unusual kinetic stability of **endo**, is likely because subsequent rearrangement to generate **int2** necessitates an expansion of the O¹–Ru–C² angle and the overcoming of disfavoring donor–donor repulsions. In contrast, the elongation of the Ru–O¹ bond in **ts2•H⁺** (2.54 Å vs 2.17 Å in **ts2**) resulting from the *protonation of O¹*

translates to a lesser amount of donor–donor repulsion in **int1•H⁺**, leading to its SP geometry (*cf.* shallow minimum in graph a, blue curve) to render **ts2• H⁺** more energetically accessible ($E_{\text{rel}} = 10.6 \text{ kcal/mol}$).

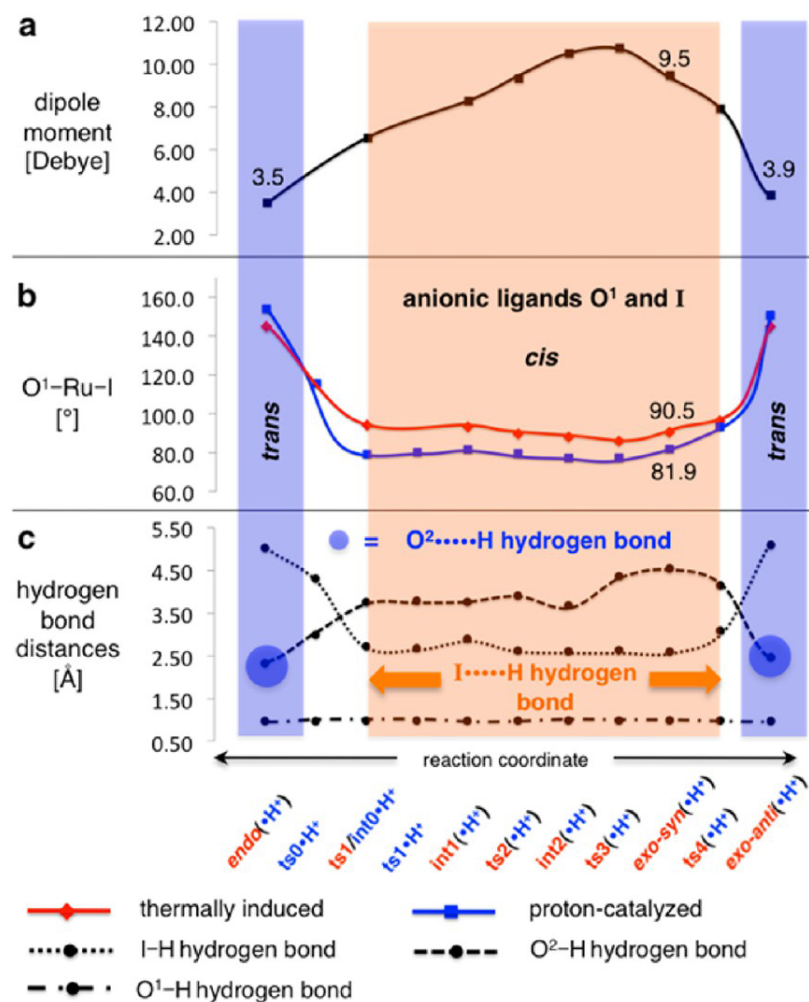
In case of the iodide, it is situated trans to C¹ (see I–Ru–C¹: **ts2**, **int2**, **ts3**, and *exo-syn*, graph d) and C² (see I–Ru–C²: **ts4**, graph e). Notably, the two maxima in graphs d and e correlate with the longer Ru–I bond lengths (see graph f, red curve), and also correspond to the build-up in negative charge on I, which peaks in **ts4** (see graph g). Interestingly, the shortening of the Ru–I bond in **ts4•H⁺** (2.78 Å vs 2.83 Å in **ts4**, *cf.* graph f, blue curve) is observed, which is likely due to enhanced Lewis acidity of Ru in the protonated complex. It is also important to note that unlike the stabilizing influence of a proton on the donor–donor repulsion between O¹ and C¹ in **ts2•H⁺**, the trans influence between the I and C² ligands is *not minimized* in **ts4•H⁺**, which is most likely due to the less H–bond accepting nature of I. Consequently, **ts4•H⁺** emerges as the rate-limiting transition state under acid-catalyzed conditions. Overall, the hitherto mentioned findings provide a clear rationale for the exclusive generation of *exo-syn* in acid-catalyzed process (*cf.* blue curve, Scheme 1.4.3-1), whereas the thermal protocol delivers the lowest energy *exo-anti* complex.

1.4.4.2 Dipolar Effects

In addition to the charge separation and repulsive effects during the course of non-OM inversion at Ru, we envisioned that a sizable dipole moment would also result as a consequence. In this regard, a detailed analysis of the overall dipolar effects was conducted. As shown in Scheme 1.4.4.2, the dipole moment (graph a) can be correlated as a function of the O¹-Ru-I angle (graph b), in which the cis arrangement between O¹ and I leads to the high dipole in *exo-syn* (9.5 Debye), whereas the trans relationship results in the overall dipolar minimization in *endo* and *exo-anti* (3.5 and 3.9 Debye, respectively). In this context, the aforementioned property is the key reason for the high energy of *exo-syn* (6.0 kcal/mol) relative to *endo* (0.0 kcal/mol) and *exo-anti* (-5.3 kcal/mol) in gas phase (*cf.* Figure 1.4.2-2), which seems to be in contrast with the experimental isolation of the former carbene complex. It is noteworthy that the inclusion of solvent effects in the calculations upon a successive increase in polarity (gas phase → benzene → dichloromethane) predicts a stepwise stabilization of the intermediates and

transition states associated with a large dipole moment relative to *endo* and *exo-anti*.²⁶

Scheme 1.4.4.2. Orientation of Anions (i.e. O¹-Ru-I) as Determining Factor



Cumulatively, the abovementioned trend is maximized upon protonation, through which Ru-complex *exo-syn*•H⁺ is preferred by 5.6 kcal/mol relative to *endo*•H⁺ (i.e. an overall reduction of the energy by 11.6 kcal/mol relative to *exo-syn*, cf. Scheme 1.4.3-1), whereas a minimal “solvent effect” is observed in case of the less polar *exo-anti*•H⁺ (1.8 kcal lower in energy than *exo-anti*). Furthermore, the stabilization of dipolar effects is acting in parallel with the reduction of the electron-electron repulsion between the lone

(26) For experimental studies regarding solvent effects on *syn*- vs *anti*-chelate equilibria, see: Ung, T.; Hejl, A.; Grubbs, R. H.; Schrödi, Y. *Organometallics* **2004**, *23*, 5399–5401.

pairs on the anionic ligands (O_1 and I) through the proton, as evident by 10° - 15° smaller O_1 -Ru-I angles, when they are in a *cis* relationship (graph b, blue line, Scheme 1.4.4.2). This is supported by the breakage of the $O^2\cdots H$ hydrogen bond in *endo* and the formation of a hydrogen bond towards the iodide $I\cdots H$ in structures $\text{int0}\bullet\text{H}^+ \rightarrow \text{ts4}\bullet\text{H}^+$ (graph c, Scheme 1.4.4.2). Furthermore, the $O^2\cdots H$ association is re-established in *exo-anti* $\bullet\text{H}^+$ when the $I\cdots H$ interaction is no longer viable.

1.5 Implications Regarding the Role of Anions on Olefin Metathesis Promoted by Ru Carbenes

The results detailed above point to the critical role of anions within a Ru-based carbene complex in determining the facility with which polytopal rearrangements, whether OM-based or otherwise, take place. Our investigations imply that examination of the mechanistic details of catalytic OM reactions or efforts toward designing efficient and stereoselective Ru-based complexes should take into account the influence of anionic ligands on the stability of the associated intermediates and transition states. In this respect, we list illustrative examples and provide rationales that underscore the importance of anions in OM.

1.5.1 Effect of Anions on Carbene Orientation

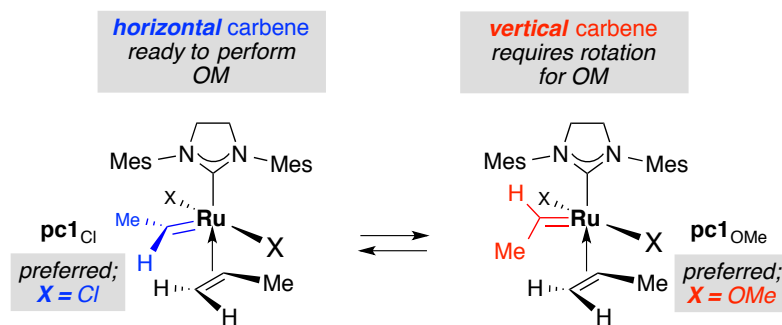
The propensity of Ru carbene to bind alkene, to form a π -complex, is the most basic requirement for OM process to commence.^{3c} In a hypothetical system wherein Ru-ethylidene and propene are considered (Scheme 1.5.1a), the aforementioned complex can acquire two forms,¹⁸ in which one involves the orientation of carbene substituent parallel to the bound olefin (hereforth *horizontal* carbene) and the other engages in a perpendicular arrangement with respect to the alkene (hereforth *vertical* carbene). Notably, the former carbene complex is appropriately aligned to undergo a cycloaddition to form ruthenacyclobutane (*cf.* Scheme 1.1-1),²⁷ rendering the *horizontal* carbene as “active.” In contrast, the *vertical* carbene is not properly aligned to undergo cycloaddition; consequently, the ruthenacyclobutane formation is preceded by the rearrangement of “inactive” *vertical* carbene to its *horizontal* counterpart.

(27) The terms, “active” and “inactive,” have been introduced in the context of olefin metathesis, see: Straub, B. F. *Adv. Synth. Catal.* **2007**, 349, 204–214.

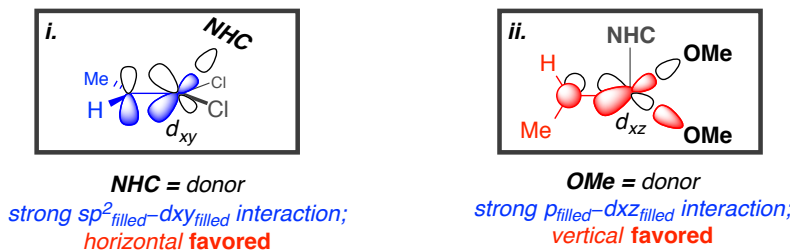
In this context, the computational analysis of the two forms, in which chloride and methoxide anions ($X = \text{Cl}, \text{OMe}$) are considered, revealed that whereas π -complex with Cl ligands is favored for “active” arrangement (pc1_{Cl}), the complex with methoxide anions prefers “inactive” geometry (pc1_{OMe}). The latter insight is consistent with a previous report that alkoxide-containing Ru carbenes are significantly *less active* in OM (vs their Cl counterparts).²⁸ Inspired by initial work by Straub,²⁷ we decided to analyze the critical orbital interactions involving anions and Ru, which could offer additional insight regarding the origins of stark difference in carbene orientation. As depicted in Scheme 1.5.1b, the d_{xy} orbital of Ru in structure *i* is deformed, due to a filled-filled interaction with sp^2 orbital of the NHC, such that the lobes participating in backbonding have higher coefficient (i.e. larger size) thereby resulting in strong preference for *horizontal* carbene.

Scheme 1.5.1. Correlation of Ligand Donorability with Carbene Orientation

a. Influence of Anion on Carbene Orientation (*horizontal* vs *vertical*)



b. Increased π -Backbonding Key for Ru=CHR Orientation



In contrast, a different regime is observed in the presence of methoxide donors. Owing to hard π -donorability of the OMe ligands (vs Cl), two strong filled-filled interactions involving d_{xz} orbital take place (see structure *ii*), resulting in enhanced

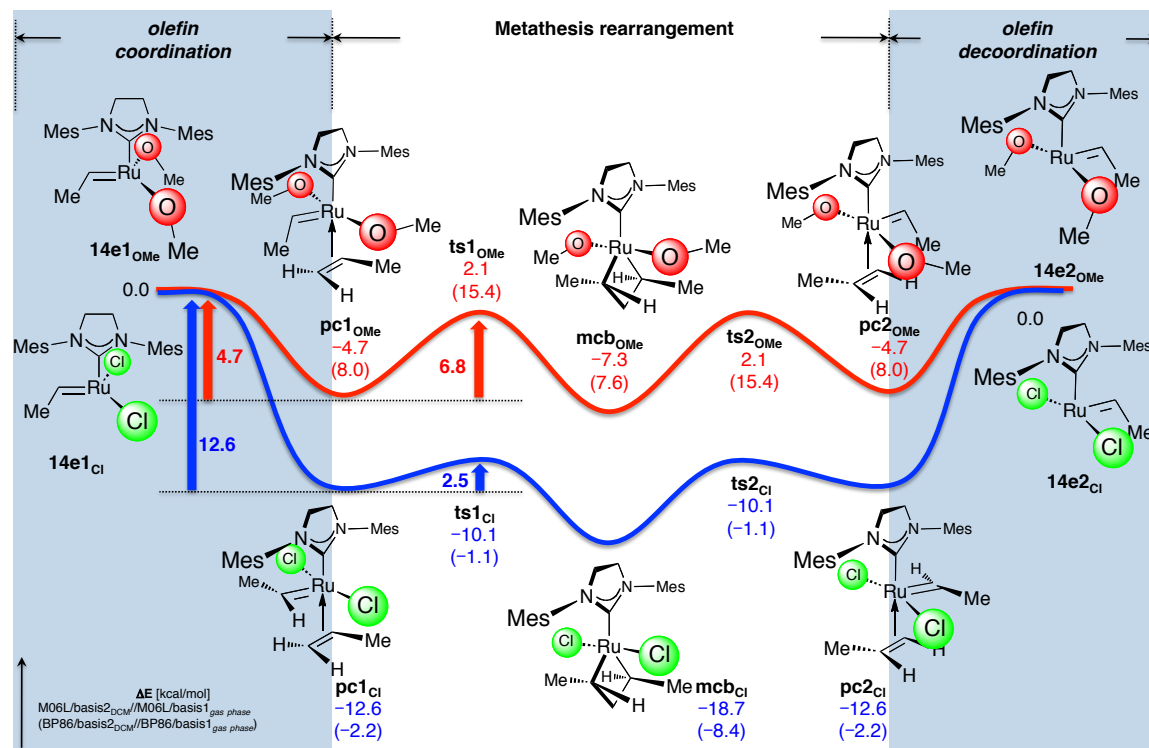
(28) Sanford, M. S.; Henling, L. M.; Day, M. W.; Grubbs, R. H. *Angew. Chem., Int. Ed.* **2000**, *39*, 3451–3453.

backdonation to stabilize *vertical* geometry. Thus, the choice of anions in Ru carbenes plays a critical role in the promotion of OM based polytopal rearrangements just as well as in non-OM.

1.5.2 Effect of Anions on the Energy Barriers Associated with the Promotion of Olefin Metathesis

In order to elucidate further the importance of anionic ligand in OM, we chose to study the side-change process of Ru-ethylidene mediated by propene in dichloromethane (**14e1_X** → **14e2_X**; X = Cl, OMe; Scheme 1.5.2-1). We opted for the electronic energy (ΔE in kcal/mol) as the descriptor since it reflects the individual enthalpic contributions. As shown, the overall process involves the following sequence: 1) Olefin-coordination (**14e1_X** → **pc1_X**, shaded region) 2) OM rearrangement (**pc1_X** → **mcb_X** → **pc2_X**, white region) 3) olefin-decoordination (**pc2_X** → **14e2_X**, shaded region). Herein, the analysis of the barriers associated with the potential energy surfaces indicates that olefin coordination/decoordination as well as OM-based rearrangement are energetically *less favored* with the stronger π -electron donating methoxide ligands.

Scheme 1.5.2. Relationship of Ligand Donorability with OM Activity



Evidently, the initial binding of an alkene to the coordinatively unsaturated Ru-dimethoxide (**14e1_{OMe}**) is favored by 4.7 kcal/mol (red path), affording **pc1_{OMe}**. In comparison, the alkene coordination with dichloride carbene (blue path) is significantly exothermic (-12.6 kcal/mol), which is most likely due to the lower energy LUMO (d_z^2) of **14e1_{Cl}** and increased Lewis acidity at Ru. While therein lies a clear difference between the *horizontal* and *vertical* carbene geometries associated with **pc1_{Cl}** and **pc1_{OMe}**, respectively (*cf.* Section 1.5.1), the relative difference in activation barriers (ΔG^\ddagger = 2.5 kcal/mol vs ΔG^\ddagger = 6.8 kcal/mol) is mainly due to the destabilizing trans influence between two axial OMe donors in **mcb_{OMe}** (vs **mcb_{Cl}**, which involves diminutive chloride donors). The aforementioned stabilizing influence of diminished anionic donorability on the activation barriers for OM, due to minimization of trans influence, is in line with the earlier discussion involving non-OM rearrangements (*cf.* Scheme 1.4.4.1).

1.5.3 Influence of H-Bonding on the Rate Acceleration in Olefin Metathesis

At this juncture, we wished to further extend our understanding to the acceleration in OM with allylic alcohols. For instance, the presence of an allylic substituent in an alkene typically leads to significant attenuation of efficiency in catalytic OM. Such diminished reactivity is mainly due to the steric repulsion imposed by an adjacent secondary alkyl or aryl group or due to electronic deactivation imposed by a heteroatom-based substituent. It is thus anomalous that an allylic alcohol, even as bulky as tertiary substituted, reacts at substantially faster rate and requires lower catalyst loading.²⁹ Moreover, alcohol additives facilitate certain OM processes,³⁰ and the presence of acetic acid has been shown to accelerate RCM of diethyl diallylmalonate.³¹

Recently, our group demonstrated that ROCM of cyclopropene (**1.10**) with an enantioenriched allylic alcohol (**1.11a**; 96:4 *er*) proceeds with high diastereoselectivity (97:3 *dr*; 10:1 *E:Z*) to efficiently generate **1.12** (87% yield) within five minutes in the presence of 0.5 mol% Ru complex **I** (Scheme 1.5.3a). Interestingly, the transformation with methyl protected cross-partner (**1.11b**) furnishes low selectivity (79:21 *dr*; 6:1 *E:Z*)

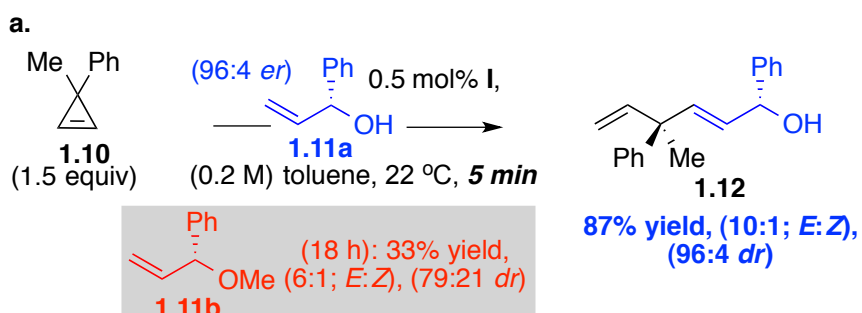
(29) Hoye, T. R.; Zhao, H. *Org. Lett.* **1999**, *1*, 1123–1125.

(30) (a) Forman, G. S.; McConnell, A. E.; Tooze, R. P.; van Rensburg, W. J.; Meyer, W. H.; Kirk, M. M.; Dwyer, C. L.; Serfontein, D. W. *Organometallics* **2005**, *24*, 4528–4542. (b) Schmidt, B.; Staude, L. *J. Org. Chem.* **2009**, *74*, 9237–9240.

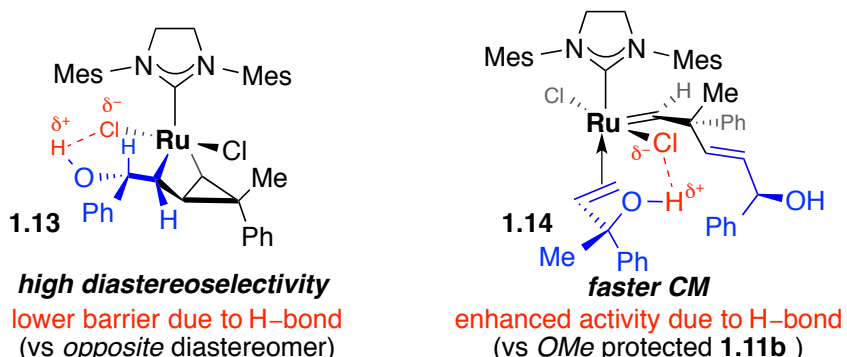
(31) Adjiman, C. S.; Clark, A. J.; Cooper, G.; Taylor, P. C. *Chem. Commun.* **2008**, 2806–2808.

and poor efficiency (33% yield) even after 18 hours under same reaction conditions. Considering the involvement of trans influence and donor-donor repulsions in OM (*cf.* Section 1.5.2) and our results regarding the stabilizing influence of H–bonding on these effects in the context of non-OM polytopal rearrangements (*cf.* Section 1.4.4), we can ascribe the difference in reactivity and selectivity with **1.11a** and **1.11b** to factors listed in Scheme 1.5.3b.

Scheme 1.5.3. Minimization of Trans Influence and e–e Repulsions Through H–Bonding for Faster OM and Higher Selectivity



b. H-bonding for Stereochemical Control and Higher Activity



We proposed that the electrostatic attraction between the chloride and allylic hydroxyl substituent (i.e. H–bonding) in **1.13** takes place, which results in overall stabilization of TBP ruthenacyclobutane intermediate on two counts: 1) Reduction in the trans influence between the two chlorides 2) e–e repulsion between heteroatoms (O[–] and Cl[–]) is minimized through proton bridge. Consequently, the lower energy of **1.3**, which might serve as the reason for the lowering of the barrier for the ROM rearrangement,³² and its structural rigidity translate into high stereochemical control. In contrast, the lack

(32) Formation of a lower energy product (vs reactant) would involve low activation barrier (early-transition state, exothermic) vs generation of a high-energy product (late-transition state, endothermic). See: Hammond, G. S. *J. Am. Chem. Soc.*, **1955**, 77, 334–338.

of stabilization in the presence of OH-protected **1.11b** results in competitive generation of the *opposite* diastereomer. Furthermore, similar stabilization could be operative in the CM process with **1.11a** through **1.14**, which renders the overall ROCM a fast process (vs with **1.11b** as cross-partner).

1.6 Conclusions

The hitherto discussed investigations describe the first instances of the synthesis, isolation, purification (routine silica gel chromatography), and spectroscopic characterization of high-energy *endo-anti* stereogenic-at-Ru carbene intermediate (Scheme 1.3.1-2), which participates in CM (*cf.* Scheme 1.3.2-1) with styrene to validate our proposal for the mechanism of the catalytic ROCM (*cf.* Scheme 1.2-2). Furthermore, we provide experimental evidence showing that an *endo-anti* isomer can undergo thermal or Brønsted acid-catalyzed non-OM polytopal rearrangement (*cf.* Scheme 1.3.2.1-1; Scheme 1.3.2.2), causing conversion to the energetically favored *exo-anti* carbene. Computational analyses (through the use of DFT) reveal that there are two key factors that generate sufficient energy barriers that are responsible for the possibility of isolation and characterization of high-energy, but kinetically stable, intermediates (e.g., *exo-syn*): (1) donor–donor interactions (*cf.* Section 1.4.4.1) that involve the anionic ligands and the strongly electron donating carbene groups and (2) dipolar effects (*cf.* Section 1.4.4.2) arising from the syn relationship between the anionic groups (iodide and aryloxide). We demonstrate that a Brønsted acid lowers barriers to facilitate isomerization, and that the positive influence of a proton source is the result of its ability to diminish the repulsive electronic interactions originating from the anionic ligands. The implications of the present studies regarding a more sophisticated knowledge of the role of anionic units on the efficiency of Ru-catalyzed OM reactions are discussed (Section 1.5). Furthermore, the electronic basis for the increased facility with which allylic alcohols participate in OM processes is presented as well. Finally, these studies shed light on the role of anionic ligands and provide basis for successful design of Ru catalysts for alkene metathesis.

1.7 Experimental

■ **General:** All reactions were carried out in oven-dried (135 °C) or flame-dried glassware under an inert atmosphere of dry N₂ unless otherwise stated. Infrared (IR) spectra were recorded on a Bruker FTIR Alpha (ATR Mode) spectrometer. Bands are characterized as strong (s), medium (m), or weak (w), broad (br). ¹H NMR spectra were recorded on a Varian Unity INOVA 400 (400 MHz), 500 (500 MHz), or 600 (600 MHz) spectrometers. Chemical shifts are reported in ppm from tetramethylsilane with the solvent resonance resulting from incomplete deuteration as the internal reference (CDCl₃: δ 7.26 ppm, C₆D₆: δ 7.16 ppm). ¹⁹F chemical shifts are reported in ppm from C₆F₆ as the internal reference. Data are reported as follows: chemical shift, integration, multiplicity (s = singlet, d = doublet, t = triplet, br = broad, m = multiplet, app = apparent), and coupling constants (Hz). ¹³C NMR spectra were recorded on Varian Unity INOVA 400 (100 MHz) or 500 (125 MHz) spectrometers with complete proton decoupling. Chemical shifts are reported in ppm from tetramethylsilane with the solvent resonance as the internal reference (CDCl₃: δ 77.16 ppm). Peaks arising from ¹³C–¹⁹F coupling are treated as singlets. Circular Dichroism spectra were recorded on Aviv Circular Dichroism Spectrometer (Model 420). High-resolution mass spectrometry was performed on a Micromass LCT ESI-MS (positive mode) at the Boston College and the University of Illinois Mass Spectrometry Facility. Optical rotation values were recorded on a Rudolph Research Analytical Autopol IV polarimeter. Melting points were measured on a Thomas Hoover capillary melting point apparatus and are uncorrected.

■ Reagents:

Acetic Acid was purchased from Fisher Scientific and used as received.

2,2'-Bis(diphenylphosphino)-1,1'-binaphthyl was purchased from Strem and used as received.

Boron tribromide was purchased from Aldrich and used as received.

2-Bromo-6-fluoroaniline was purchased from Fluka and used as received.

2-Bromomesitylene was purchased from Aldrich and passed through basic alumina prior to use.

Benzoyl chloride was purchased from Aldrich and vacuum distilled over calcium hydride prior to use.

cis-3,4-Dichlorocyclobutene was purchased from Aldrich and used as received.

(1S,2S)-1,2-diphenylethane-1,2-diamine was purchased from Ivy Chemicals and used as received.

Hexafluorobenzene was purchased from Cambridge Isotope Laboratories and used as received.

Hydrogen chloride (4M solution in dioxane) was purchased from Aldrich and used as received.

2-Methoxyphenylboronic acid was purchased from Aldrich and used as received.

Potassium iodide was purchased from Strem and used as received.

Sodium hydride was purchased from Aldrich and used as received.

Sodium *tert*-butoxide was purchased from Strem and used as received.

Sodium carbonate was purchased from Aldrich and used as received.

Sodium nitrite was purchased from Aldrich and used as received.

Tetrakis(triphenylphosphine)palladium was purchased from Strem and used as received.

p-Toluenesulfonic acid was purchased from Aldrich and used as received.

Triethyl orthoformate was purchased from Aldrich and distilled from sodium under N₂ atmosphere prior to use.

Tris(dibenzylideneacetone)dipalladium was purchased from Strem and used as received.

Ru-complex IV was prepared by a previously reported literature procedure.^{6b}

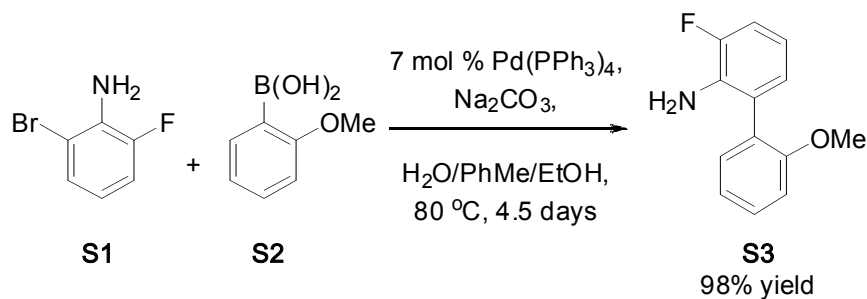
■ Reactions:

3-Fluoro-2'-methoxy-[1,1'-biphenyl]-2-amine (S3, Chart 1). This material was prepared according to modification of a previously reported procedure.³³ In a round-bottom flask equipped with a reflux condenser, Pd(PPh₃)₄ (5.0 g, 4.3 mmol, 0.071 equiv),

(33) Tanabiki, M.; Tsuchiya, K.; Kumanomido, Y.; Matsubara, K.; Motoyama, Y.; Nagashima, H. *Organometallics* **2004**, *23*, 3976–3981.

aniline **S1** (11.6 g, 61.0 mmol, 1.00 equiv), boronic acid **S2** (13.4 g, 88.2 mmol, 1.45 equiv), Na₂CO₃ (100.7 g, 951 mmol, 15.6 equiv), toluene (300 mL), ethanol (90 mL), H₂O (230 mL) were mixed (under N₂ atmosphere). The resulting mixture was allowed to stir at 80 °C for 108 hours. The solution was then allowed to cool to 22 °C and the layers were separated. The aqueous layer was washed with EtOAc (2 x 50 mL), and the combined organic layers were dried over anhydrous MgSO₄, filtered, and concentrated *in vacuo* to give dark brown oil. Purification by silica gel chromatography (10:1 hexanes:EtOAc) gave the desired biaryl **S3** as a colorless oil (13.0 g, 60.0 mmol, 98% yield). **¹H NMR (CDCl₃, 400 MHz):** δ 7.40-7.36 (1H, m), 7.26 (1H, dd, *J* = 7.2, 1.6 Hz), 7.08-6.98 (3H, m), 6.91 (1H, dt, *J* = 7.6, 1.2 Hz), 6.77-6.71 (1H, m), 3.82 (3H, s), 3.77 (2H, br s).

Chart 1. Synthesis of Aniline S3

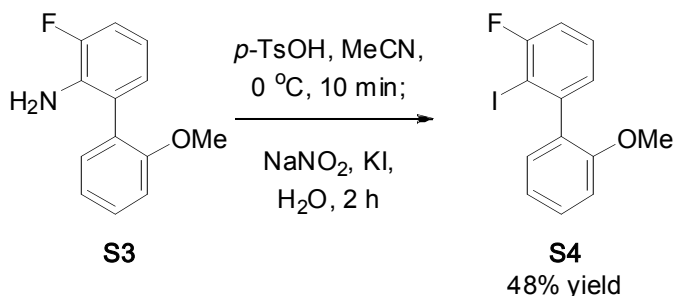


3-Fluoro-2'-methoxy-(1,1'-biphenyl)-2-iodide (S4, Chart 2). This material was prepared according to modification of a previously reported procedure.³⁴ Aniline **S3** (3.50 g, 16.1 mmol, 1.00 equiv), *p*-toluenesulfonic acid monohydrate (9.23 g, 48.5 mmol, 3.01 equiv), and acetonitrile (180 mL) were mixed in a round bottom flask. The solution was cooled to 0 °C, and while being allowed to stir vigorously, a solution of NaNO₂ (2.27 g, 32.9 mmol, 2.04 equiv) and KI (6.9574 g, 41.9 mmol, 2.59 equiv) in H₂O (10 mL) was added in a drop-wise manner. The resulting mixture was allowed to stir at 22 °C for two hours, at which time it was poured into a saturated aqueous solution of Na₂S₂O₃. The layers were separated and the aqueous layer was washed with EtOAc (3x75 mL). The combined organic layers were dried over anhydrous MgSO₄, filtered, and concentrated *in vacuo* to give brown oil. Purification by silica gel chromatography (20:6:1 hexanes:CH₂Cl₂:Et₃N) afforded aryl iodide **S4** as yellow oil (2.51 g, 7.66 mmol, 48%

(34) Krasnokutskaya, E. A.; Semenischeva, N. I.; Filimonov, V. D.; Knochel, P. *Synthesis*, **2007**, 81–84.

yield). **¹H NMR (CDCl₃, 400 MHz):** δ 7.44-7.39 (1H, m), 7.36-7.31 (1H, m), 7.11-7.09 (1H, m), 7.07-7.00 (3H, m), 6.98 (1H, dd, *J* = 8.0, 0.4 Hz), 3.78 (3H, s).

Chart 2. Synthesis of Aryl Iodide S4

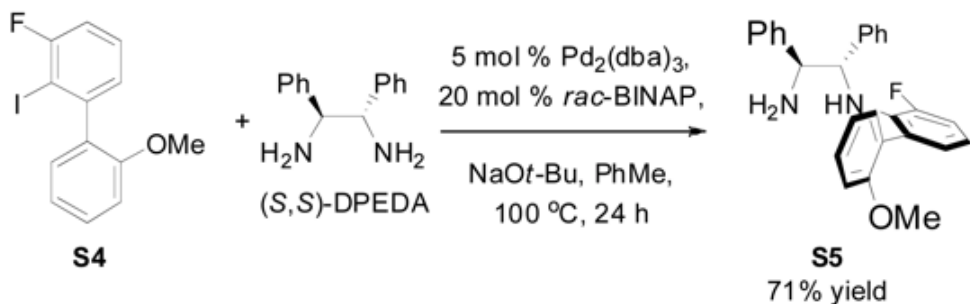


Compounds **S5-S8** were synthesized following modified procedures.^{6b}

(1*S*,2*S*)-*N*-(3-Fluoro-2'-methoxy-(1,1'-biphenyl)-2-yl)-1,2-diphenylethane-1,2-diamine (S5, Chart 3).

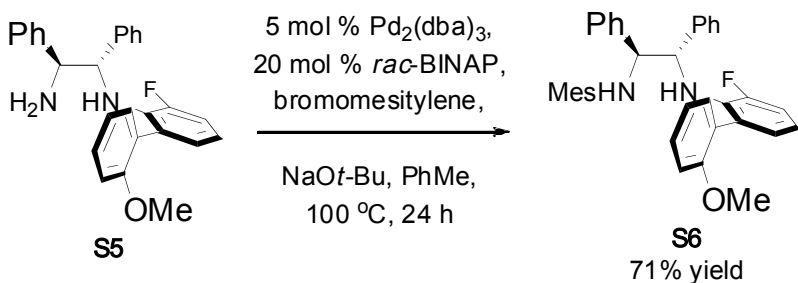
In a round bottom flask equipped with a reflux condenser, Pd₂(dba)₃ (386.0 mg, 0.422 mmol, 0.051 equiv), (*S,S*)-diphenyl-ethylenediamine (2.64 g, 12.5 mmol, 1.50 equiv), iodo-fluoroaryl substrate **S4** (2.72 g, 8.30 mmol, 1.00 equiv), *rac*-binap (1.00 g, 1.61 mmol, 0.194 equiv) and sodium *t*-butoxide (1.95 g, 20.3 mmol, 2.45 equiv) were added (under N₂ atmosphere). Anhydrous toluene (65 mL) was added and the mixture was allowed to stir for 24 hours at 100 °C, after which the mixture was allowed to cool to 22 °C and passed through a short column of silica gel with copious amounts of EtOAc. The solvents were removed *in vacuo* to give brown oil, which was purified by silica gel chromatography (4:1 hexanes:EtOAc) to afford diamine **S5** as a yellow foam (2.41 g, 5.85 mmol, 71% yield). **¹H NMR (CDCl₃, 400 MHz):** δ 7.53-7.44 (1H, m), 7.33-7.27 (2H, m), 7.24-7.22 (4H, m), 7.20-7.10 (4H, m), 7.08-7.02 (2H, m), 6.97-6.85 (3H, m), 6.72-6.61 (1H, m), 5.17-4.85 (1H, m), 4.72-4.67 (1H, m), 4.21-4.12 (1H, m), 3.73-3.72 (3H, s), 1.33 (2H, br s).

Chart 3. Synthesis of Diamine S5

**(1*S*,2*S*)-*N*-(3-Fluoro-2'-methoxy-(1,1'-biphenyl)-2-yl)-*N'*-mesityl-1,2-diphenylethane-1,2-diamine (S6, Chart 4).**

In a round bottom flask equipped with a reflux condenser, $\text{Pd}_2(\text{dba})_3$ (169 mg, 0.184 mmol, 0.053 equiv), diamine **S5** (1.42 g, 3.45 mmol, 1.00 equiv), bromomesitylene (2.12 g, 10.6 mmol, 3.09 equiv), *rac*-binap (451 mg, 0.724 mmol, 0.209 equiv), and sodium *t*-butoxide (853 g, 8.87 mmol, 2.57 equiv) were added (under N_2 atmosphere). Anhydrous toluene (40 mL) was then added and the solution was allowed to stir for 24 hours at 110 °C. The resulting mixture was allowed to cool to 22 °C and passed through a short column of silica gel (EtOAc). The solvents were removed *in vacuo* to give brown oil, which was purified by silica gel chromatography (19:1 hexanes:EtOAc) to furnish diamine **S6** as yellow foam (1.30 g, 2.45 mmol, 71% yield). **1H NMR** (CDCl_3 , 400 MHz): δ 7.39-7.36 (1H, m), 7.20-7.13 (2H, m), 7.08-6.97 (7H, m), 6.92-6.81 (4H, m), 6.75-6.62 (5H, m), 5.05-4.91 (1H, m), 4.58-4.56 (1H, m), 4.31-4.29 (1H, m), 3.71-3.66 (3H, m), 3.59 (1H, br s), 2.13 (3H, s), 1.94-1.92 (6H, s).

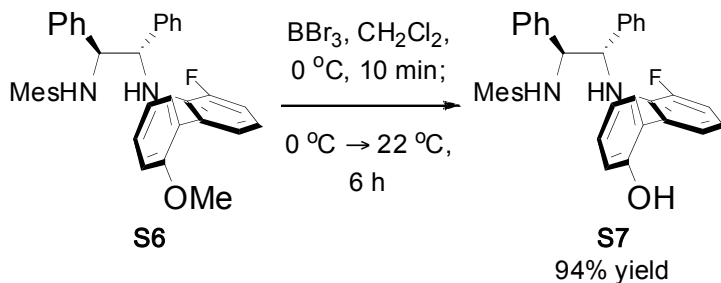
Chart 4. Synthesis of Diamine S6

**3'-Fluoro-2'-((1*S*,2*S*)-2-(mesyliamino)-1,2-diphenylethyl)amino)-(1,1'-biphenyl)-2-ol (S7, Chart 5).**

Diamine **S6** (1.30 g, 2.45 mmol, 1.00 equiv) dissolved in CH_2Cl_2 (50 mL) was added to a round bottom flask cooled to 0 °C. Neat boron tribromide (1.60 mL, 16.9 mmol, 6.91 equiv) was added drop-wise, after which the mixture was allowed to stir

for six hours at 22 °C. At this time, a saturated solution of aqueous sodium bicarbonate was added (~200 mL). The CH₂Cl₂ layer was then separated, and the aqueous layer was washed with EtOAc (2x50 mL). The combined organic layers were dried over anhydrous MgSO₄, filtered, and concentrated *in vacuo* to give brown oil. Purification by silica gel chromatography (19:1 hexanes:EtOAc) delivered diamine S7 (1.19 g, 2.29 mmol, 94% yield). ¹H NMR (CDCl₃, 400 MHz): δ 8.81 (1H, br s), 7.35-7.31 (1H, m), 7.10-6.91 (12H, m), 6.77-6.74 (2H, m), 6.69-6.68 (2H, m), 6.64 (2H, s), 5.11 (1H, br s), 4.58-4.56 (1H, m), 4.47-4.43 (1H, m), 3.50 (1H, br s), 2.12 (3H, s), 2.04 (6H, s).

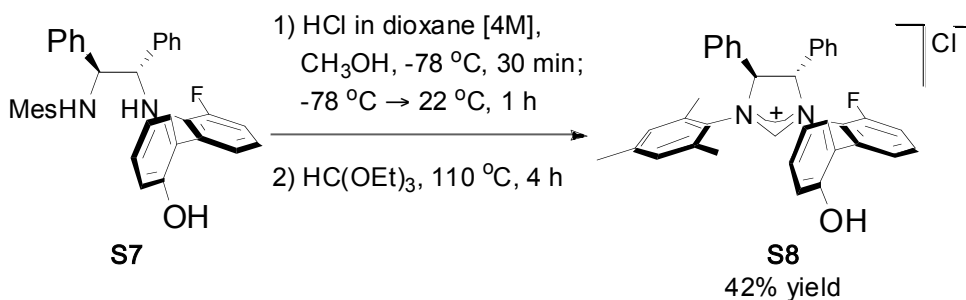
Chart 5. Synthesis of Diamine S7



Imidazolinium salt (S8, Chart 6). Diamine S7 (1.19 g, 2.30 mmol, 1.00 equiv), dissolved in anhydrous methanol (23 mL), was added to a round bottom flask under N₂ atmosphere. The mixture was allowed to cool to -78 °C, after which it was charged with a solution of HCl in dioxane [(4.0 M), 5.00 mL, 20.0 mmol, 8.71 equiv] in a drop-wise manner. The mixture was allowed to stir for 30 min at -78 °C, which led to the formation of a white precipitate. At this point, the mixture was allowed to warm to 22 °C, while being allowed to stir for approximately one hour. The volatiles were removed *in vacuo* to give white powder, which was further washed with Et₂O (20 mL) and pentane (20 mL). The resulting solid was dried under high vacuum for 48 hours; it was then transferred to a round bottom flask containing triethylorthoformate (4.00 mL, 24.1 mmol, 10.5 equiv) and attached to a short-path distillation apparatus. The mixture was allowed to stir for four hours at 110 °C, after which it was allowed to cool to 22 °C, and the remaining triethylorthoformate was removed *in vacuo*. After the addition of Et₂O (2x10 mL) in order to dissolve impurities, the solution was removed through a cannula, affording a white powder consisting of the desired product as an 8.3:1 mixture of two diastereomers (546 mg, 0.970 mmol, 42% yield). **IR (neat, major+minor**

diastereomer): 3034 (w), 2919 (w), 2851 (w), 2705 (w), 2567 (w), 1618 (s), 1600 (s), 1494 (m), 1469 (m), 1446 (m), 1377 (m), 1263 (m), 1218 (m), 1182 (m), 1157 (m), 1119 (m), 1080 (m), 1032 (m), 1003 (m), 923 (m), 899 (m), 854 (m), 795 (m), 758 (s), 727 (s), 698 (s), 639 (m), 631 (m), 553 (w), 516 (w), 453 (w), 407 (w); **¹H NMR (CDCl₃, 400 MHz, major diastereomer):** δ 10.87 (1H, s), 8.87 (1H, s), 7.77-7.75 (1H, m), 7.56-7.52 (1H, m), 7.34-7.32 (5H, m), 7.15-7.09 (7H, m), 6.93 (2H, s), 6.82-6.79 (2H, m), 6.76 (1H, s), 5.42 (1H, d, *J* = 10.4 Hz), 5.31 (1H, d, *J* = 10.8 Hz), 2.55 (3H, s), 2.23 (3H, s), 2.02 (3H, s); **¹³C NMR (CDCl₃, 100 MHz, major+minor diastereomer):** δ 158.96, 158.90, 156.4, 155.2, 140.7, 138.8, 138.2, 134.1, 133.6, 131.6, 131.5, 131.2, 131.0, 130.8, 130.6, 130.2, 129.8, 129.59, 129.56, 129.3, 129.1, 129.0, 128.4, 128.1, 127.94, 127.91, 127.5, 127.4, 123.97, 123.95, 121.1, 120.9, 120.1, 118.8, 115.2, 114.9, 75.7, 71.6, 20.9, 18.7, 18.5; **¹⁹F NMR (CDCl₃, 376 MHZ, major diastereomer):** d -127.4; **HRMS (ESI+):** Calcd for C₃₆H₃₂ON₂F [M-Cl]: 527.2499. Found: 527.2498. [a]_D^{20.0} -203.0 (*c* = 0.66, CDCl₃).

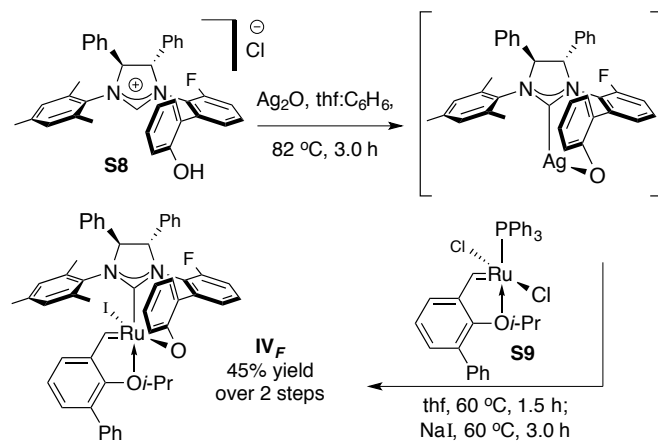
Chart 6. Synthesis of Imidazolinium Salt S8



Synthesis of Fluorine-substituted Ru Complex (IV_F , Chart 7). This complex was prepared based on modified version of a reported procedure.^{6b} Imidazolinium salt **S8** (136 mg, 0.241 mmol, 1.58 equiv), Ag_2O (105 mg, 0.454 mmol, 2.98 equiv), and 4Å molecular sieves were dissolved in a 1:1 mixture of C_6H_6 and thf (12.0 mL) in a round bottom flask. The mixture was allowed to stir for three hours at 82 °C, after which it was passed through a short column of Celite with copious amounts of thf. The volatiles were removed *in vacuo* and the derived Ag^+NHC complex was obtained as brown powder, which was transferred to a different round bottom flask, formerly charged with phosphine-containing achiral Ru complex **S9**^{6b} (100 mg, 0.152 mmol, 1.00 equiv); an additional 12.0 mL of thf was added. The resulting solution was allowed to stir for 1.5

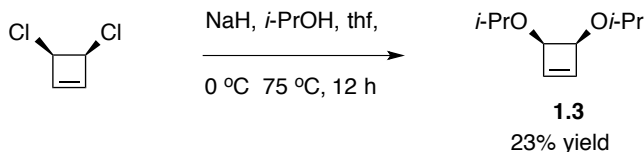
hours at 60 °C, at which time it was allowed to cool to 22 °C. Sodium iodide (516 mg, 3.44 mmol, 22.6 equiv) was then added and the mixture was allowed to stir for three hours at 60 °C. At this point, the solution was allowed to cool to 22 °C and passed through a Celite plug. The volatiles were removed to generate a dark brown solid, which was purified by silica gel chromatography (30% CH₂Cl₂ in pentane) to afford the desired *exo* Ru complex **IV_F** (67.0 mg, 0.068 mmol, 45% yield). **IR (in CH₂Cl₂)**: 3032 (w), 2970 (w), 2919 (w), 2736 (w), 1686 (w), 1604 (w), 1588 (w), 1559 (w), 1484 (w), 1459 (w), 1435 (w), 1422 (w), 1400 (w), 1381 (w), 1371 (w), 1344 (w), 1284 (w), 1264 (w), 1237 (w), 1200 (w), 1176 (w), 1158 (w), 1116 (w), 1102 (m), 1091 (m), 1075 (m), 1029 (s), 1004 (m), 931 (m), 902 (m), 847 (s), 808 (s), 795 (m), 781 (m), 760 (m), 736 (m), 699 (m), 671 (s), 632 (m), 610 (m), 602 (s), 574 (s), 558 (m), 541 (m), 519 (m), 489 (m), 464 (m); **¹H NMR (CDCl₃, 400 MHz)**: δ 15.45 (1H, s), 7.49-7.47 (2H, m), 7.39-7.30 (6H, m), 7.28-7.23 (7H, m), 7.18-7.14 (2H, m), 7.08-7.00 (4H, m), 6.96 (1H, m), 6.93-6.89 (1H, m), 6.83-6.81 (1H, m), 6.79 (1H, m), 6.53 (1H, d, *J* = 8.0 Hz), 6.40 (1H, d, *J* = 7.6 Hz), 5.09 (2H, s), 4.45-4.38 (1H, m), 2.65 (3H, s), 2.32 (3H, s), 1.52 (3H, s), 0.88 (3H, d, *J* = 6.0 Hz), 0.73 (3H, d, *J* = 6.4 Hz); **¹³C NMR (CDCl₃, 100 MHz)**: δ 281.1, 219.4, 170.4, 160.9, 158.3, 149.7, 147.8, 145.4, 139.8, 139.3, 138.5, 137.8, 136.5, 136.3, 135.1, 132.4, 132.3, 131.9, 131.8, 130.7, 130.6, 130.1, 129.8, 129.6, 126.59, 129.4, 129.39, 129.2, 129.1, 128.9, 128.8, 128.7, 128.6, 128.57, 128.4, 128.2, 127.9, 127.7, 127.4, 127.38, 127.3, 126.6, 126.5, 125.5, 123.9, 123.6, 121.1, 117.2, 116.7, 116.4, 78.1, 74.9, 21.3, 20.9, 20.8, 20.4, 19.2; **¹⁹F NMR (CDCl₃, 376 MHz)**: δ -105.4; **HRMS (ESI⁺)**: Calcd for C₅₂H₄₆IFN₂O₂Ru: 978.1632. Found: 978.1641.

Chart 7. Synthesis of Ru Carbene Complex **IV_F**



(3*R*,4*S*)-3,4-Diisopropoxycyclobut-1-ene (1.3**, Chart 8).** 2-Propanol (9.00 mL, 118 mmol, 10.4 equiv), sodium hydride (815 mg, 33.9 mmol, 2.99 equiv) and thf (60 mL) were added to a flame-dried round bottom flask. The resulting solution was allowed to stir for 10 minutes after which it was allowed to cool to 0 °C. *cis*-3,4-Dichlorocyclobutene (1.39 g, 11.3 mmol, 1.00 equiv) was added drop-wise in the course of five minutes, and the resulting mixture was allowed to warm to 22 °C, followed by heating to 75 °C for 12 hours. At this time, the mixture was diluted with water and the organic layer was separated. The aqueous layer was washed with diethyl ether (40 mL x 2), and the combined organic layers were dried over anhydrous MgSO₄, filtered, and concentrated *in vacuo* to give yellow oil. Purification by silica gel chromatography (5% to 10% diethyl ether in hexane) followed by passing through basic alumina afforded product **1.3** (440 mg, 2.59 mmol, 23% yield). **IR (neat):** 3047 (w), 2970 (s), 2931 (w), 2870 (w), 1466 (m), 1375 (s), 1375 (s), 1320 (s), 1296 (m), 1165 (s), 1124 (m), 1104 (s), 1053 (s), 995 (m), 946 (s), 823 (s), 790 (m), 745 (s), 624 (m), 517 (w), 438 (w); **¹H NMR (CDCl₃, 400 MHz):** δ 6.32 (2H, dd, *J* = 1.2, 0.4 Hz), 4.62 (2H, dd, *J* = 0.8, 0.4 Hz), 3.77-3.70 (2H, m), 1.20 (6H, d, *J* = 6.0 Hz), 1.18 (6H, d, *J* = 6.0 Hz); **¹³C NMR (CDCl₃, 100 MHz):** δ 142.4, 80.3, 70.8, 23.1, 22.4; **HRMS (ESI+):** Calcd for C₁₀H₁₉O₂ [M+H]: 171.13850. Found: 171.13787.

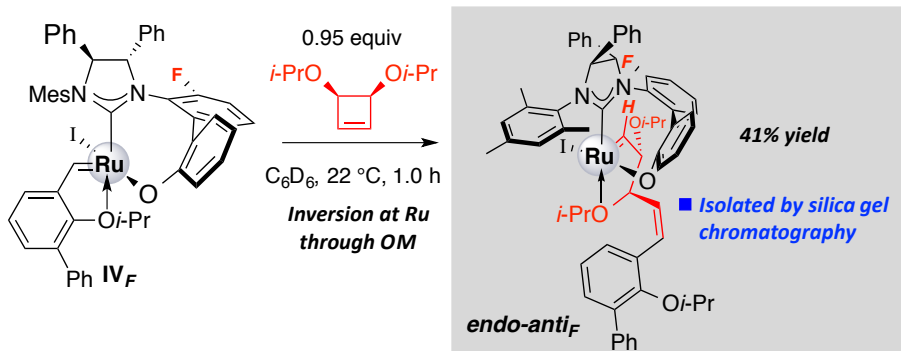
Chart 8. Synthesis of Alkene **1.3**



Synthesis of High-Energy Fluorinated-Diastereomeric Carbene (*endo-anti*_F, Chart 9). Ru carbene **IV_F** (33.5 mg, 0.034 mmol, 1.04 equiv) and cyclobutene **1.3** (5.6 mg, 0.033 mmol, 1.0 equiv) were dissolved in C₆H₆ (1.6 mL) in a 1-dram vial. The mixture was allowed to stir for one hour at 22 °C. The solvent was then removed *in vacuo* to give dark brown solid, which was purified by silica gel chromatography (30% to 60% CH₂Cl₂ in pentane) to furnish complex *endo-anti*_F (15.4 mg, 0.013 mmol, 41% yield). **IR (in CH₂Cl₂):** 3031 (w), 2970 (w), 2924 (w), 1954 (w), 1719 (w), 1687 (w), 1589 (m), 1459 (s), 1433 (m), 1401 (m), 1380 (m), 1344 (m), 1256 (m), 1217 (m), 1177 (m), 1141 (m),

1106 (m), 1079 (m), 1035 (m), 1004 (m), 933 (m), 901 (m), 847 (m), 794 (m), 759 (s), 698 (s), 671 (m), 633 (m), 607 (m), 573 (m); **¹H NMR (CDCl₃, 400 MHz):** δ 16.96 (1H, d, *J* = 2.4 Hz), 7.63 (1H, d, *J* = 6.0 Hz), 7.52-7.49 (3H, m), 7.39-7.28 (4H, m), 7.25-7.21 (2H, m), 7.14-7.09 (2H, m), 7.07-7.00 (10H, m), 6.88-6.85 (1H, m), 6.82 (1H, s), 6.79-6.78 (1H, m), 6.63 (1H, s), 6.22 (2H, d, *J* = 7.2 Hz), 5.64 (1H, dd, *J* = 12.0, 10.0 Hz), 5.19 (1H, d, *J* = 10.4 Hz), 5.00 (1H, dd, *J* = 10.4, 5.6 Hz), 4.85 (1H, d, *J* = 10.4 Hz), 4.18-4.12 (1H, m), 3.78-3.72 (1H, m), 3.71-3.65 (1H, m), 3.17 (1H, dd, *J* = 5.6, 2.4 Hz), 2.59 (3H, s), 2.19 (3H, s), 2.18 (3H, s), 1.59 (3H, d, *J* = 6.0 Hz), 1.15 (3H, d, *J* = 6.4 Hz), 1.04-1.02 (6H, m), 0.98 (3H, d, *J* = 6.0 Hz), 0.77 (3H, d, *J* = 6.0 Hz); **¹³C NMR (CDCl₃, 100 MHz):** δ 214.3, 167.5, 160.2, 158.2, 153.3, 143.4, 139.7, 137.7, 137.6, 137.4, 137.3, 137.1, 136.8, 135.9, 131.2, 130.9, 130.8, 130.7, 130.5, 130.1, 129.8, 129.6, 129.4, 129.3, 129.1, 129.06, 128.7, 128.5, 128.2, 127.9, 127.6, 127.0, 123.8, 123.7, 118.1, 115.0, 114.9, 94.1, 76.5, 76.3, 76.1, 75.6, 73.7, 71.2, 24.5, 23.9, 22.5, 22.2, 21.9, 21.4, 21.3, 20.9, 20.2; **¹⁹F NMR (CDCl₃, 376 MHz):** δ -116.4; **HRMS (ESI+):** Calcd for C₆₂H₆₅IFN₂O₄Ru [M+H]: 1149.3017. Found: 1149.3005.

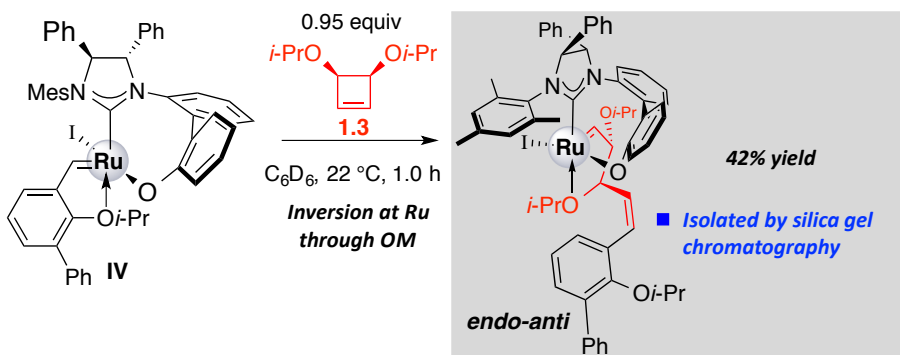
Chart 9. Synthesis of Fluorinated *endo-anti*_F



Synthesis of High-Energy Diastereomeric Carbene (*endo-anti*, Chart 10). Ru-based carbene **IV** (112 mg, 0.117 mmol, 1.05 equiv) and cyclobutene **1.3** (18.9 mg, 0.111 mmol, 1.00 equiv) were dissolved in C₆H₆ (5.0 mL) in a 1-dram vial. The mixture was allowed to stir for one hour at 22 °C; the solvent was then removed *in vacuo* to give dark brown solid, which was purified by silica gel chromatography (30% to 60% CH₂Cl₂ in pentane) to afford Ru complex *endo-anti* (53 mg, 0.047 mmol, 42% yield). **IR (in CH₂Cl₂):** 3060 (w), 3030 (w), 2962 (m), 2921 (m), 2869 (w), 1735 (w), 1601 (w), 1586 (w), 1557 (w), 1494 (w), 1469 (m), 1432 (m), 1399 (m), 1380 (m), 1343 (m), 1273 (m),

1258 (m), 1215 (m), 1176 (m), 1139 (m), 1108 (s), 1060 (m), 1026 (m), 1006 (m), 933 (m), 905 (m), 857 (s), 795 (m), 757 (s), 739 (m), 698 (s), 674 (m), 607 (m), 575 (w), 556 (w), 524 (w); **^1H NMR (CDCl₃, 400 MHz)**: δ 16.82 (1H, d, J = 1.6 Hz), 7.68 (1H, d, J = 7.6 Hz), 7.54-7.52 (1H, m) 7.49-7.47 (2H, m), 7.40-7.39 (4H, m), 7.37-7.31 (3H, m), 7.29-7.27 (2H, m), 7.20-7.14 (2H, m), 7.12-7.08 (1H, m), 7.05-7.03 (2H, m), 7.00 (1H, m), 6.97-6.90 (6H, m), 6.78 (1H, s), 6.62 (1H, s) 6.17 (2H, d, J = 7.6 Hz), 5.70 (1H, dd, J = 12.0, 10.4 Hz), 5.01-4.96 (2H, m), 4.83-4.81 (1H, m), 4.16-4.10 (1H, m), 3.77-3.71 (1H, m), 3.58-3.52 (1H, m), 2.95 (1H, dd, J = 6.4, 1.6 Hz), 2.50 (3H, s), 2.17 (3H, s), 2.11 (3H, s), 1.56 (3H, d, J = 6.0 Hz), 1.08 (3H, d, J = 6.0 Hz), 1.00 (3H, d, J = 6.0 Hz), 0.97-0.95 (6H, m), 0.74 (3H, d, J = 6.4 Hz); **^{13}C NMR (CDCl₃, 100 MHz)**: δ 212.4, 166.97, 153.1, 140.8, 140.5, 140.4, 139.5, 137.8, 137.3, 137.2, 136.9, 136.7, 135.5, 132.3, 131.7, 130.8, 130.7, 130.5, 130.1, 129.9, 129.7, 129.4, 129.3, 128.9, 128.8, 128.8, 128.7, 128.6, 128.3, 128.2, 128.1, 128.0, 127.9, 126.9, 126.8, 126.7, 123.4, 123.2, 117.4, 94.8, 77.2, 76.4, 76.3, 75.4, 75.3, 73.5, 71.1, 24.3, 23.5, 22.3, 21.8, 21.6, 21.3, 21.2, 20.1, 19.9; **HRMS (ESI+)**: Calcd for C₆₂H₆₆IN₂O₄Ru [M+H]: 1131.3129. Found: 1131.3143.

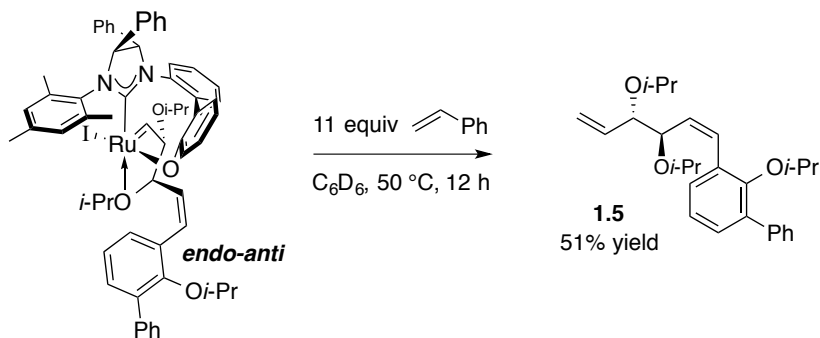
Chart 10. Synthesis of Ru Carbene *endo-anti*



3-((3*R*,4*S*,*Z*)-3,4-Diisopropoxyhexa-1,5-dien-1-yl)-2-isopropoxy-1,1'-biphenyl (1.5, Chart 11). Ru-based complex *endo-anti* (37.2 mg, 0.033 mmol, 1.00 equiv) and styrene (38.2 mg, 0.367 mmol, 11.0 equiv) were dissolved in C₆D₆ (1.1 mL) in a 1-dram vial. The mixture was allowed to stir for 12 hours at 50 °C, after which the solvent was removed *in vacuo* and the resulting colorless oil was purified by silica gel chromatography (10% Et₂O in hexanes) to afford diene 1.5 (6.8 mg, 0.017 mmol, 51% yield) as colorless oil. **IR (in Et₂O)**: 3059 (w), 3023 (w), 2971 (s), 2927 (m), 2872 (w), 1727 (w), 1642 (w), 1601 (w), 1498 (w), 1465 (m), 1452 (m), 1425 (m), 1402 (m), 1380

(s), 1371 (m), 1334 (m), 1261 (m), 1246 (s), 1216 (m), 1174 (m), 1121 (s), 1109 (s), 1066 (s), 1027 (m), 998 (m), 935 (m), 855 (m), 819 (m), 795 (m), 759 (m), 699 (s), 608 (w); **¹H NMR (CDCl₃, 500 MHz):** δ 7.59-7.54 (3H, m), 7.41-7.38 (3H, m), 7.33-7.29 (1H, m), 7.13-7.10 (1H, m), 6.88 (1H, d, *J* = 12.0 Hz), 5.99-5.93 (1H, m), 5.66 (1H, dd, *J* = 12.0, 9.5 Hz), 5.35-5.31 (1H, m), 5.24-5.21 (1H, m), 4.35 (1H, dd, *J* = 10.0, 6.5 Hz), 3.89-3.84 (2H, m), 3.73-3.68 (1H, m), 3.60-3.55 (1H, m), 1.14 (3H, d, *J* = 6.5 Hz), 1.12 (3H, d, *J* = 6.0 Hz), 1.04 (3H, d, *J* = 6.0 Hz), 1.01 (3H, d, *J* = 6.5 Hz), 0.97 (3H, d, *J* = 6.0 Hz), 0.84 (3H, d, *J* = 6.5 Hz); **¹³C NMR(CDCl₃, 125 MHz):** δ 153.4, 139.7, 137.7, 135.9, 131.83, 131.82, 130.4, 130.2, 129.6, 128.9, 128.1, 126.9, 123.3, 116.8, 80.5, 75.6, 75.5, 70.2, 69.7, 23.3, 23.0, 22.4, 22.1, 22.0, 21.9; **HRMS (ESI+):** Calcd for C₂₇H₃₆O₃Na [M+Na]: 431.2562. Found: 431.2548.

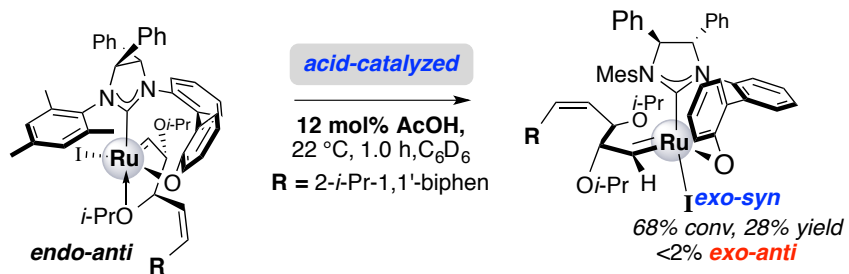
Chart 11. CM of *endo-anti* to form 1.5



Stereoisomerization at Ru (*exo-syn*, Chart 12). Ru-based complex *endo-anti* (20.2 mg, 0.0179 mmol, 1.00 equiv) and acetic acid (0.13 mg, 0.002 mmol, 0.12 equiv) were dissolved in C₆H₆ (0.12 mL) in a 1-dram vial. The mixture was allowed to stir for one hour at 22 °C. The solvent was subsequently removed *in vacuo* to give dark brown solid. Analysis of the ¹H NMR spectrum of the unpurified mixture indicated ~68% conversion. Purification of the solid by silica gel chromatography (100% CH₂Cl₂ to 10% diethyl ether in CH₂Cl₂) afforded the desired Ru complex *exo-syn* (5.6 mg, 0.005 mmol, 28% yield). **IR (in CH₂Cl₂):** 3032 (w), 2970 (w), 2923 (w), 1961 (w), 1758 (w), 1728 (w), 1667 (w), 1637 (w), 1601 (w), 1587 (w), 1495 (w), 1470 (w), 1439 (m), 1380 (m), 1345 (m), 1263 (s), 1236 (m), 1216 (w), 1176 (m), 1155 (m), 1140 (m), 1106 (m), 1061 (m), 1027 (m), 1005 (m), 933 (m), 905 (m), 856 (m), 797 (m), 758 (s), 734 (m), 698 (s), 672 (m), 634 (m), 607 (w), 573 (w), 527 (w), 471 (w); **¹H NMR (CDCl₃, 400 MHz):** δ 15.99 (1H, d, *J*

= 2.4 Hz), 8.21 (1H, dd, J = 8.0, 1.2 Hz), 7.66 (1H, dd, J = 7.6, 1.6 Hz), 7.52-7.48 (3H, m), 7.38-7.35 (3H, m), 7.31-7.28 (2H, m), 7.24-7.21 (5H, m), 7.17-7.13 (5H, m), 7.12-7.08 (1H, m), 7.02 (1H, d, J = 12.4 Hz), 6.96-6.94 (2H, m), 6.91 (1H, m), 6.79 (1H, dt, J = 7.2, 1.2 Hz), 6.69-6.68 (2H, m), 6.53 (1H, dd, J = 8.0, 0.8 Hz), 5.92-5.86 (2H, m), 4.90 (1H, dd, J = 10.4, 6.0 Hz), 4.84 (1H, d, J = 12.0 Hz), 4.04-3.98 (1H, m), 3.78-3.72 (1H, m), 3.50 (1H, dd, J = 6.0, 2.4 Hz), 3.47-3.41 (1H, m), 2.25 (3H, s), 1.88 (3H, s), 1.79 (3H, s), 1.03 (3H, d, J = 6.0 Hz), 0.99 (3H, d, J = 6.4 Hz), 0.96 (3H, d, J = 6.0 Hz), 0.79 (6H, app t, J = 6.4 Hz), 0.74 (3H, d, J = 6.4 Hz); ^{13}C NMR (CDCl_3 , 100 MHz): δ 220.6, 169.5, 153.3, 142.5, 139.8, 139.7, 138.2, 137.5, 137.4, 136.5, 135.8, 135.6, 134.8, 131.8, 131.3, 131.0, 130.9, 130.7, 130.6, 130.57, 130.52, 130.3, 130.1, 129.8, 129.7, 129.6, 129.5, 129.2, 129.16, 128.96, 128.8, 128.5, 128.4, 128.3, 128.2, 128.15, 127.8, 127.0, 123.8, 123.6, 121.6, 116.9, 96.1, 83.9, 75.6, 75.58, 75.3, 74.7, 73.2, 73.0, 70.8, 23.7, 23.4, 23.1, 22.9, 22.5, 22.2, 22.1, 21.9, 21.86, 21.7, 21.2, 20.9, 20.4, 19.0; HRMS (ESI $^+$): Calcd for $\text{C}_{62}\text{H}_{66}\text{IN}_2\text{O}_4\text{Ru}$ [M+H]: 1131.3129. Found: 1131.3160.

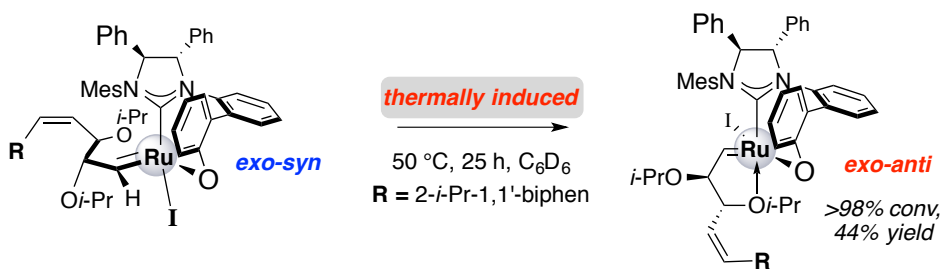
Chart 12. Stereoisomerization of *endo-anti* to *exo-syn*



Synthesis of Low-Energy Carbene Diastereomer (*exo-anti*, Chart 13). Ru-based carbene *exo-syn* (10.9 mg, 0.009 mmol, 1.00 equiv) was dissolved in C_6D_6 (0.50 mL) in a 1-dram vial. The mixture was allowed to stir for 25 hours at 50 °C, after which the solvent was removed *in vacuo* to give dark brown solid. Purification by silica gel chromatography (30% to 80% CH_2Cl_2 in pentane) afforded the Ru complex *exo-anti* (4.8 mg, 0.004 mmol, 44% yield) along with an inseparable decomposition product, which is presumably a precursor to **S10**. IR (in CH_2Cl_2): 3030 (w), 2972 (m), 2918 (w), 1734 (w), 1655 (w), 1602 (w), 1587 (w), 1496 (w), 1465 (w), 1450 (m), 1425 (m), 1402 (m), 1380 (m), 1370 (m), 1343 (m), 1264 (m), 1215 (m), 1176 (m), 1139 (s), 1107 (s), 1074 (m), 1013 (m), 933 (m), 910 (m), 854 (m), 794 (m), 760 (s), 734 (s), 698 (s), 649 (w), 607 (w),

573 (w), 552 (w), 524 (w), 461 (w), 411 (w); **^1H NMR (CDCl₃, 400 MHz):** δ 16.07 (1H, d, J = 1.6 Hz), 7.89 (1H, dd, J = 7.6, 1.6 Hz), 7.60-7.54 (4H, m), 7.52-7.49 (4H, m), 7.39-7.26 (18H, m), 7.25-7.17 (2H, m), 7.14-7.03 (7H, m), 6.89 (1H, s), 6.84 (2H, d, J = 12. Hz), 6.73 (1H, s), 6.55 (1H, d, J = 8.0 Hz), 6.38 (2H, d, J = 7.6 Hz), 5.80 (2H, dd, J = 11.6 Hz, 9.2 Hz), 5.73 (1H, dd, J = 11.6, 10.0 Hz), 5.09 (1H, d, J = 9.2 Hz), 4.96 (1H, dd, J = 9.6, 8.4 Hz), 4.85 (1H, d, J = 9.2 Hz), 4.63 (2H, d, J = 9.2 Hz), 4.33-4.28 (3H, m), 4.04 (2H, d, J = 2.0 Hz), 3.94-3.89 (1H, m), 3.88-3.79 (2H, m), 3.78-3.73 (1H, m), 3.72-3.66 (2H, m), 3.51-3.42 (2H, m), 3.19 (1H, dd, J = 8.4, 2.4 Hz), 2.59 (3H, s), 2.23 (3H, s), 1.52 (3H, s), 1.29-1.23 (12H, m), 1.22-1.19 (3H, m), 1.12 (6H, d, J = 6.0 Hz), 1.09 (6H, d, J = 6.4 Hz), 1.04 (3H, d, J = 6.0 Hz), 1.01 (3H, d, J = 6.0 Hz), 0.97 (3H, d, J = 6.0 Hz), 0.95 (6H, d, J = 6.4 Hz), 0.89 (6H, d, J = 6.4 Hz), 0.771 (3H, d, J = 6.0 Hz), 0.72 (3H, d, J = 6.0 Hz), 0.58 (3H, d, J = 6.0 Hz); **^{13}C NMR (CDCl₃, 100 MHz):** δ 216.7, 170.4, 160.8, 153.6, 153.4, 143.5, 139.8, 139.7, 139.5, 139.4, 138.1, 137.22, 137.17, 136.6, 136.1, 135.9, 135.8, 135.2, 132.1, 132.0, 131.9, 131.2, 131.1, 130.9, 130.8, 130.5, 130.4, 130.2, 129.9, 129.7, 129.3, 129.2, 129.1, 129.0, 128.9, 128.8, 128.5, 128.3, 128.2, 128.16, 127.5, 127.0, 123.5, 123.48, 123.2, 117.1, 99.6, 83.3, 78.0, 76.1, 75.7, 75.6, 74.7, 73.1, 72.7, 71.9, 69.1, 69.08, 45.4, 29.9, 23.5, 23.2, 22.9, 22.8, 22.5, 22.4, 22.3, 22.2, 21.9; **HRMS (ESI⁺):** Calcd for C₆₂H₆₆IN₂O₄Ru [M+H]: 1131.3129. Found: 1131.3141.

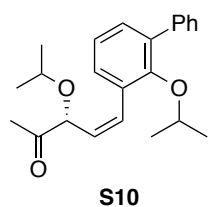
Chart 13. Stereoisomerization of *exo-syn* to *exo-anti*



(R,Z)-3-Isopropoxy-5-(2-isopropoxy-[1,1'-biphenyl]-3-yl)pent-4-en-2-one (S10, Chart 14). A mixture of *exo-anti* and S10 was heated to 60 °C in the presence of 1.0 M acetic acid in C₆H₆ for two hours, resulting in complete decomposition of *exo-anti*. The aforementioned impurity, S10, was then purified through silica gel chromatography (10% diethyl ether in hexanes). **IR (CH₂Cl₂):** 3059 (w), 2972 (m), 2923 (m), 2851 (w), 2074 (s), 1718 (s), 1601 (s), 1498 (m), 1464 (m), 1451 (m), 1424 (m), 1398 (m), 1381 (m),

1370 (m), 1352 (m), 1302 (m), 1260 (m), 1215 (s), 1174 (m), 1140 (m), 1106 (s), 1072 (s), 1027 (m), 933 (s), 855 (w), 794 (w), 761 (s), 699 (s), 664 (s), 626 (w), 608 (w), 565 (w), 536 (w), 464 (w), 410 (w); **¹H NMR (CDCl₃, 500 MHz):** δ 7.57-7.53 (2H, m), 7.46-7.38 (3H, m), 7.34-7.28 (2H, m), 7.10-7.07 (1H, m), 6.98-6.95 (1H, m), 5.58 (1H, dd, *J*=12.0, 9.0 Hz), 4.69 (1H, d, *J*=9.5 Hz), 3.76-3.70 (1H, m), 3.56-3.52 (1H, m), 2.21 (3H, s), 1.06 (3H, d, *J*=6.0 Hz), 1.01 (3H, d, *J*=6.0 Hz), 0.89 (3H, d, *J*=6.0 Hz), 0.81 (3H, d, *J*=6.0 Hz); **¹³C NMR (CDCl₃, 125 MHz):** δ 223.5, 208.9, 136.0, 132.5, 131.3, 131.2, 129.9, 129.5, 128.3, 127.2, 127.0, 123.7, 80.3, 75.8, 70.6, 29.9, 26.9, 26.2, 22.8, 22.4, 22.3, 22.2; **HRMS (ESI+):** Calcd for C₂₃H₂₉O₃ [M+H]: 353.21189. Found: 353.21167.

Chart 13. Identity of compound S10



■ Calculated Geometries and NMR spectra of Complexes *endo-anti*, *exo- anti*, and *exo- syn*, and tetramethylsilane: All geometry optimizations were performed in Gaussian 09 Rev. A1 suite³⁵ employing M06L density functional³⁶ with tight SCF and convergence criteria and an ultrafine integration grid. For atoms H, C, N, O, and Si 6-31G(d) basis sets were employed; basis sets for N, O, and Si were further augmented by sets of diffuse functions [6-31+G(d)].³⁷ For atoms Ru and I Stuttgart-Dresden quasi-relativistic effective core potentials and basis sets were employed (MWB).³⁸ The minimum nature of each stationary point was confirmed by absence of imaginary frequencies. The Cartesian coordinates for fully optimized geometries are listed in Table S3.

NMR shielding tensors were calculated with Gauge-Independent Atomic Orbital method (GIAO) at the same level of theory as described above, except the basis sets employed were 6-311++G(2d,p) for H, C, N, and O, 6-311+G(3d2f) for Si,³⁹ and for Ru and I CEP 121G relativistic effective core potentials and basis sets.^{40a} The basis set for iodide was further augmented by a p and two d polarization functions.^{40b} Solvation by chloroform was modeled by means of an integral equation formalism variant of the polarizable continuum model (IEPCM), which is implemented as the default solvation model in

(35) Gaussian 09, Revision A.1, Frisch, M. J.; Trucks, G. W.; Schlegel, H. B.; Scuseria, G. E.; Robb, M.A.; Cheeseman, J. R.; Scalmani, G.; Barone, V.; Mennucci, B.; Petersson, G. A.; Nakatsuji, H.; Caricato,M.; Li, X.; Hratchian, H. P.; Izmaylov, A. F.; Bloino, J.; Zheng, G.; Sonnenberg, J. L.; Hada, M.; Ehara,M.; Toyota, K.; Fukuda, R.; Hasegawa, J.; Ishida, M.; Nakajima, T.; Honda, Y.; Kitao, O.; Nakai, H.;Vreven, T.; Montgomery, J. A. Jr.; Peralta, J. E.; Ogliaro, F.; Bearpark, M.; Heyd, J. J.; Brothers, E.;Kudin, K. N.; Staroverov, V. N.; Kobayashi, R.; Normand, J.; Raghavachari, K.; Rendell, A.; Burant, J. C.;Iyengar, S. S.; Tomasi, J.; Cossi, M.; Rega, N.; Millam, N. J.; Klene, M.; Knox, J. E.; Cross, J. B.; Bakken,V.; Adamo, C.; Jaramillo, J.; Gomperts, R.; Stratmann, R. E.; Yazev, O.; Austin, A. J.; Cammi, R.;Pomelli, C.; Ochterski, J. W.; Martin, R. L.; Morokuma, K.; Zakrzewski, V. G.; Voth, G. A.; Salvador, P.;Dannenberg, J. J.; Dapprich, S.; Daniels, A. D.; Farkas, O.; Foresman, J. B.; Ortiz, J. V.; Cioslowski, J.;Fox, D. J. Gaussian 09 (Gaussian, Inc., Wallingford CT, 2009).

(36) M06L density functional was recommended for use in computational studies of Ru-catalyzed olefin metathesis: (a) Zhao, Y.; Truhlar, D. G. *J. Chem. Theory Comput.* **2009**, *5*, 324–333. (b) Torker, S.; Merki, D.; Chen, P. *J. Am. Chem. Soc.* **2008**, *130*, 4808-4814. For original disclosure of M06L density functional see: (c) Zhao, Y.; Truhlar, D. G. *J. Chem. Phys.* **2006**, *125*, 194101.

(37) (a) Hehre, W. J.; Fitchfield, R.; Pople, J. A. *J. Chem. Phys.* **1971**, *56*, 2257–2261. (b) Hariharan, P. C.; Pople, J. A. *Theor. Chim. Acta* **1973**, *28*, 213–222. (c) Franel, M. M.; Pietro, W. J.; Hehre, W. J.; Binkley, J. S.; Gordon, M. S.; DeFrees, D. J.; Pople, J. A. *J. Chem. Phys.* **1982**, *77*, 3654–3665.

(38) Ru: (a) Andrae, D.; Häußermann, U.; Dolg, M.; Stoll, H.; Preuß, H. *Theor. Chim. Acta* **1990**, *77*, 123-141. I: (b) Bergner, A.; Dolg, M.; Küchle, W.; Stoll, H.; Preuß, W. *Mol. Phys.* **1993**, *80*, 1431-1441.

(39) (a) Krishnan, R.;Binkley, J. S.; Seeger, R.; Pople, J. A. *J. Chem. Phys.* **1980**, *72*, 650-654. (b) McLean, A. D.; Chandler, G.S. *J. Chem. Phys.* **1980**, *72*, 5639–5648.

(40) (a) Stevens, W. J.; Krauss, M.; Basch, H.; Jasien, P. G. *Can. J. Chem.* **1992**, *70*, 612-630. (b) Labello, N. P.; Ferreira, A. M.; Kurtz, H. A. *J. Comput. Chem.* **2005**, *26*, 1464–1471.

Gaussian 09, with the default scaling factor for atomic radii ($\alpha = 1.1$).⁴¹ All absolute isotropic chemical shifts are listed in Table S1. Chemical shifts of carbene protons in complexes *endo-anti*, *exo-anti*, and *exo-syn* relative to that of protons in tetramethylsilane are reported in Table S2.

Table S1. Isotropic Absolute Chemical Shifts of all Nuclei in Complexes
endo-anti, *exo-anti*, *exo-syn* and in Tetramethylsilane

<i>endo-anti</i>								
#	nucleus	Isotropic shift	#	nucleus	Isotropic shift	#	nucleus	Isotropic shift
1	C	112.05	46	H	24.46	91	H	26.70
2	N	90.61	47	C	62.12	92	C	161.71
3	C	44.13	48	H	25.11	93	H	31.46
4	C	-46.97	49	H	24.70	94	H	31.27
5	Ru	-683.41	50	H	24.65	95	H	31.56
6	N	83.91	51	O	118.13	96	C	163.24
7	C	50.68	52	C	46.09	97	H	29.71
8	C	109.56	53	C	64.35	98	H	31.10
9	H	25.20	54	C	59.41	99	H	30.40
10	H	24.05	55	C	59.90	100	C	57.29
11	C	63.91	56	H	23.79	101	H	26.71
12	C	67.03	57	C	60.21	102	C	58.21
13	C	50.95	58	H	20.83	103	H	25.11
14	C	54.90	59	C	61.81	104	C	59.64
15	C	62.74	60	H	23.81	105	C	36.70
16	H	24.45	61	H	23.49	106	C	62.95
17	H	24.38	62	H	23.91	107	C	57.88
18	C	50.38	63	C	53.44	108	C	67.55
19	C	49.55	64	C	63.81	109	H	24.80
20	C	49.99	65	C	60.96	110	C	60.02
21	C	63.89	66	C	59.29	111	H	24.92
22	C	62.55	67	H	23.72	112	H	24.64
23	C	158.98	68	C	62.44	113	O	217.89
24	C	157.43	69	H	25.18	114	C	107.21
25	H	24.99	70	C	61.99	115	H	28.05

(41) For a review on polarizable continuum model, see: Tomasi, J.; Mennucci, B.; Cammi, R. *Chem. Rev.* **2005**, *105*, 2999-3093 and references therein.

26	H	24.61	71	H	24.17	116	C	162.78
27	C	163.08	72	H	24.56	117	H	31.24
28	H	27.80	73	H	24.40	118	H	30.41
29	H	29.88	74	C	102.72	119	H	30.77
30	H	30.03	75	H	26.21	120	C	163.37
31	H	29.47	76	C	107.96	121	H	30.98
32	H	26.65	77	H	26.71	122	H	30.87
33	H	29.31	78	O	253.76	123	H	31.27
34	H	29.60	79	C	112.53	124	C	50.01
35	H	29.79	80	H	28.17	125	C	62.79
36	H	29.69	81	C	161.99	126	C	61.49
37	C	-132.42	82	H	30.32	127	C	61.50
38	H	15.07	83	H	30.94	128	H	24.59
39	H	23.45	84	H	31.22	129	C	61.67
40	H	24.34	85	C	164.00	130	H	23.72
41	C	59.55	86	H	31.81	131	C	63.42
42	C	22.85	87	H	32.28	132	H	24.28
43	C	55.79	88	H	30.95	133	H	24.33
44	C	68.37	89	O	203.24	134	H	24.46
45	C	72.54	90	C	115.62	135	I	60.58

Table S1 (continued)

<i>exo-anti</i>								
#	nucleus	Isotropic shift	#	nucleus	Isotropic shift	#	nucleus	Isotropic shift
1	C	105.69	46	H	23.93	91	H	27.97
2	N	98.65	47	C	60.23	92	C	160.19
3	C	50.09	48	H	24.87	93	H	30.48
4	C	-46.52	49	H	24.46	94	H	30.85
5	Ru	-761.16	50	H	24.38	95	H	31.04
6	N	87.66	51	O	149.03	96	C	161.88
7	C	51.39	52	C	46.20	97	H	30.31
8	C	104.73	53	C	63.06	98	H	31.16
9	H	25.26	54	C	60.22	99	H	30.78
10	H	25.02	55	C	62.11	100	C	59.02
11	C	60.02	56	H	24.55	101	H	27.26
12	C	53.16	57	C	60.34	102	C	58.44

13	C	45.51	58	H	21.77	103	H	25.31
14	C	57.87	59	C	61.90	104	C	59.45
15	C	63.43	60	H	24.35	105	C	36.19
16	H	24.23	61	H	23.96	106	C	62.28
17	H	24.50	62	H	24.16	107	C	58.43
18	C	51.81	63	C	50.38	108	C	67.71
19	C	49.68	64	C	59.84	109	H	24.70
20	C	50.36	65	C	59.51	110	C	59.94
21	C	58.98	66	C	59.69	111	H	24.85
22	C	61.54	67	H	24.93	112	H	24.60
23	C	158.59	68	C	61.87	113	O	212.24
24	C	162.17	69	H	24.84	114	C	107.13
25	H	24.63	70	C	62.81	115	H	28.17
26	H	24.35	71	H	24.18	116	C	162.80
27	C	161.93	72	H	24.50	117	H	31.26
28	H	29.47	73	H	24.25	118	H	30.70
29	H	30.31	74	C	102.03	119	H	31.05
30	H	32.14	75	H	25.72	120	C	162.81
31	H	28.91	76	C	108.84	121	H	31.19
32	H	25.61	77	H	26.55	122	H	30.94
33	H	28.13	78	O	255.95	123	H	31.60
34	H	29.69	79	C	112.64	124	C	50.03
35	H	29.19	80	H	28.40	125	C	62.99
36	H	29.17	81	C	162.25	126	C	61.95
37	C	-129.83	82	H	30.64	127	C	60.91
38	H	16.24	83	H	31.50	128	H	24.41
39	H	22.87	84	H	31.49	129	C	62.02
40	H	24.31	85	C	163.33	130	H	23.86
41	C	56.77	86	H	31.69	131	C	63.31
42	C	20.19	87	H	31.42	132	H	24.46
43	C	59.87	88	H	30.33	133	H	24.32
44	C	66.74	89	O	203.66	134	H	24.48
45	C	71.86	90	C	117.06	135	I	59.52

Table S1 (continued)

<i>exo-syn</i>								
#	nucleus	Isotropic shift	#	nucleus	Isotropic shift	#	nucleus	Isotropic shift
1	C	107.97	46	H	24.49	91	H	27.54
2	N	98.90	47	C	60.42	92	C	161.83
3	C	56.28	48	H	24.56	93	H	31.68
4	C	-38.47	49	H	24.84	94	H	31.65
5	Ru	-923.29	50	H	24.42	95	H	31.45
6	N	94.19	51	O	254.26	96	C	163.79
7	C	54.65	52	C	46.68	97	H	29.73
8	C	106.92	53	C	61.30	98	H	31.04
9	H	25.32	54	C	61.10	99	H	30.73
10	H	24.93	55	C	61.04	100	C	60.28
11	C	59.13	56	H	24.52	101	H	26.81
12	C	54.45	57	C	61.16	102	C	56.58
13	C	43.78	58	H	22.61	103	H	24.20
14	C	54.61	59	C	62.71	104	C	56.65
15	C	63.88	60	H	24.23	105	C	35.64
16	H	24.67	61	H	23.87	106	C	62.06
17	H	24.61	62	H	24.00	107	C	56.03
18	C	50.56	63	C	52.14	108	C	65.93
19	C	51.54	64	C	60.92	109	H	24.00
20	C	46.66	65	C	59.47	110	C	59.22
21	C	61.65	66	C	59.05	111	H	24.48
22	C	61.89	67	H	25.48	112	H	24.41
23	C	156.55	68	C	62.98	113	O	201.84
24	C	165.22	69	H	25.37	114	C	108.87
25	H	24.68	70	C	61.95	115	H	27.36
26	H	24.39	71	H	24.22	116	C	161.83
27	C	161.98	72	H	24.63	117	H	30.60
28	H	28.15	73	H	24.46	118	H	30.23
29	H	30.07	74	C	103.98	119	H	30.29
30	H	31.58	75	H	25.42	120	C	158.78
31	H	28.91	76	C	106.31	121	H	29.92
32	H	27.97	77	H	25.40	122	H	30.49

33	H	28.49	78	O	268.26	123	H	30.40
34	H	29.29	79	C	108.97	124	C	50.92
35	H	29.78	80	H	28.17	125	C	62.95
36	H	29.19	81	C	156.33	126	C	61.60
37	C	-125.87	82	H	29.68	127	C	60.45
38	H	15.68	83	H	30.04	128	H	24.20
39	H	23.60	84	H	30.86	129	C	61.40
40	H	24.70	85	C	165.52	130	H	23.45
41	C	64.27	86	H	31.47	131	C	62.63
42	C	23.09	87	H	30.40	132	H	24.04
43	C	57.41	88	H	30.46	133	H	24.15
44	C	63.53	89	O	198.44	134	H	24.07
45	C	77.73	90	C	115.94	135	I	59.51

Table S1 (continued)

tetramethylsilane		
#	nucleus	Isotropic shift
1	Si	358.24
2	C	186.94
3	H	32.08
4	H	32.07
5	H	32.08
6	C	187.05
7	H	32.08
8	H	32.07
9	H	32.08
10	C	187.00
11	H	32.08
12	H	32.08
13	H	32.08
14	C	187.03
15	H	32.08
16	H	32.08
17	H	32.08

Table S2. Experimental (CDCl_3) and Calculated ^1H NMR Chemical Shifts of Carbene Protons in Complexes *endo-anti*, *exo-anti*, and *exo-syn* Relative to Tetramethylsilane

Complex	Absolute	Relative	Experimental
	Isotropic Shift	Chemical Shift ^a	Chemical Shift
<i>endo-anti</i>	15.07	17.01	16.82
<i>exo-syn</i>	15.68	16.40	15.99
<i>exo-anti</i>	16.24	15.84	16.07

^aChemical shift relative to protons in tetramethylsilane

Table S3. Geometries of Complex *endo-anti*, *exo-anti*, *exo-syn* and Tetramethylsilane

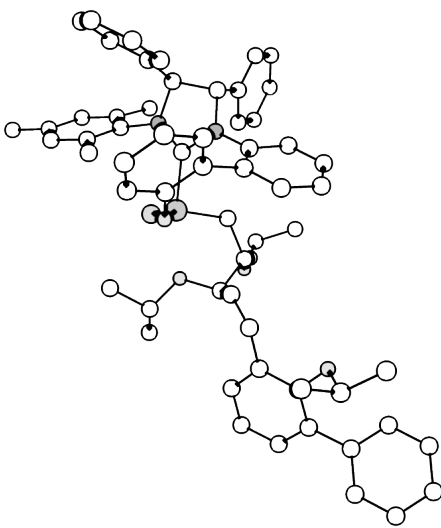
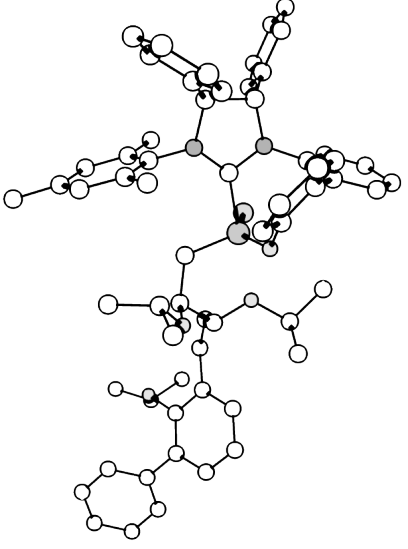
Complex <i>endo-anti</i>						
						
C	3.427026	1.453322	2.202445	H	1.132333	1.123520
N	2.207011	1.297218	1.393519	H	-2.453293	3.326590
C	0.977702	1.895902	1.787441	C	0.702873	3.169750
C	2.400109	0.387315	0.371340	C	0.742384	2.389180
R	0.937564	-0.483691	-0.591701	C	0.998481	4.538387
				H	-0.660870	
				O	-0.973695	-1.428525
				C	-1.340315	-1.749058
				H	-2.176320	-1.080356
				C	-0.147757	-1.441999
				H	0.113478	-0.380077
				H	0.720138	-2.037945
				H	-0.372051	-1.694509
				C	-1.763472	-3.203600
				H	-2.093835	-3.465528
				H	-0.919672	-3.847733
				H	-2.587047	-3.423851
				O	-1.507957	-2.659741
				C	-0.715547	-3.060510
				H	0.339547	-2.807136
				C	-0.845937	-4.564260
				H	-0.526538	-5.012906
				H	-0.222212	-4.969987
				H	-1.886325	-4.855372
				C	-1.156764	-2.376208
				H	-1.029022	-1.286222
				C	-2.213721	-2.586090
				H	-0.564091	-2.739174
				C	-2.603850	0.233633
				H	-1.846553	1.017435
				C	-3.879836	0.594685
						-1.007569

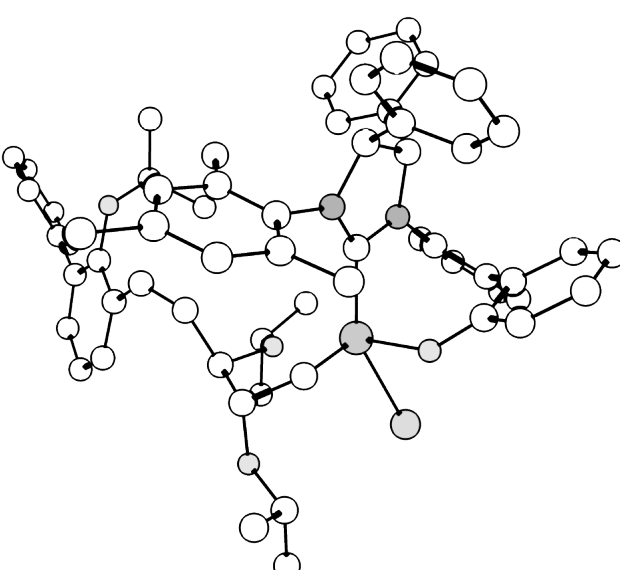
Table S3 (continued)

Complex <i>exo-anti</i>							
							
C	4.849463	-0.584414	-0.603818	H	3.299356	-3.467615	-0.954933
N	3.538893	-0.986431	-0.069543	H	3.315874	-5.383848	2.895134
C	3.406885	-2.159254	0.741345	C	3.536206	-0.751048	2.836586
C	2.546162	-0.071891	-0.272263	C	2.428265	0.135538	2.836415
R							
u	0.760108	-0.534601	0.388972	C	4.680127	-0.424010	3.571386
N	3.109675	1.003461	-0.879413	C	2.553766	1.357787	3.522657
C	2.430012	2.117043	-1.466039	C	4.782598	0.783545	4.257457
C	4.571738	0.852752	-1.105035	H	5.507438	-1.135210	3.587800
H	4.751511	0.911533	-2.189732	C	3.713764	1.678783	4.216198
H	5.579980	-0.566639	0.220157	H	1.702103	2.036513	3.511036
C	3.343872	-4.481891	2.286042	H	5.686060	1.022239	4.815626
C	3.339035	-3.414253	0.129111	H	3.778282	2.631584	4.741043
C	3.447050	-2.054515	2.145874	O	1.255938	-0.224980	2.319327
C	3.417176	-3.235663	2.897714	C	5.355464	-1.496483	-1.692457
C	3.300672	-4.571801	0.897399	C	6.703846	-1.848014	-1.746387
H	3.443940	-3.156426	3.983885	C	4.490555	-1.948613	-2.694259
H	3.233846	-5.540894	0.407520	C	7.186773	-2.636584	-2.788879
C	1.083628	4.270063	-2.658865	H	7.379507	-1.500190	-0.963967
C	1.990477	2.008968	-2.797453	C	4.970349	-2.739013	-3.732529

C	2.232753	3.299695	-0.730708	H	3.427167	-1.705791	-2.633075	H	-8.583862	-0.619540	-4.148791
C	1.559248	4.353595	-1.350539	C	6.321320	-3.082012	-3.783894	H	-8.334585	0.903418	-3.267669
C	1.317922	3.091655	-3.366837	H	8.240490	-2.908377	-2.818793	H	-6.954520	0.075679	-4.022104
C	2.198438	0.754276	-3.584047	H	4.284749	-3.094050	-4.500147	C	-7.109851	-2.246769	-2.461759
C	2.704803	3.464029	0.679587	H	6.696359	-3.702736	-4.595647	H	-6.209365	-2.205638	-3.086991
H	1.387921	5.267727	-0.778934	C	5.353804	1.946629	-0.428312	H	-6.852373	-2.742618	-1.517940
H	0.959236	3.003472	-4.393443	C	5.581932	1.923621	0.950268	H	-7.850580	-2.870199	-2.976383
C	0.333204	5.413105	-3.271957	C	5.790249	3.045072	-1.171067	C	-8.974036	0.472729	0.347687
H	2.798861	2.506428	1.201770	C	6.242814	2.976393	1.572355	C	-10.203514	-0.016607	0.810642
H	2.014689	4.099619	1.249353	H	5.206593	1.095238	1.552449	C	-8.980481	1.598630	-0.489810
H	3.690476	3.948344	0.715817	C	6.446355	4.104864	-0.549466	C	-11.400558	0.590148	0.444091
H	1.791241	0.853521	-4.595499	H	5.602010	3.070229	-2.245485	H	-10.214736	-0.898336	1.451228
H	1.705559	-0.105476	-3.108760	C	6.676526	4.070311	0.824100	C	-10.177299	2.205357	-0.854010
H	3.261346	0.492716	-3.680485	H	6.404286	2.945206	2.648919	H	-8.034414	1.997661	-0.849177
H	0.017877	5.189259	-4.296479	H	6.779706	4.957109	-1.138969	C	-11.392657	1.703250	-0.392322
H	0.940203	6.326955	-3.302203	H	7.191492	4.896388	1.311596	H	-12.343804	0.186935	0.809030
H	-0.567656	5.655254	-2.692510	C	-1.629833	1.078809	0.437874	H	-10.159973	3.082230	-1.499681
C	-0.238192	0.890554	-0.148077	H	-2.247063	1.657186	-0.276413	H	-12.328205	2.178098	-0.682372
H	0.110825	1.701628	-0.803648	C	-2.325723	-0.243691	0.744180	I	0.367513	-2.310868	-1.687618

Table S3 (continued)

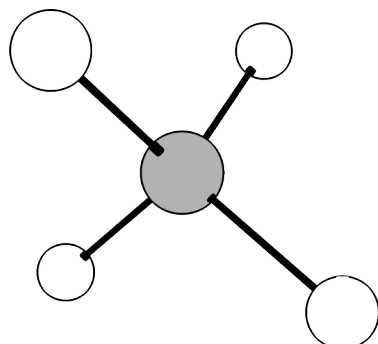
Complex *exo-syn*

												
C -2.075164 -2.701526 -1.121325 H -0.258631 -1.025552 -3.355179						H 2.048146 2.854961 1.109284 O 0.809437 1.814918 -0.170596 C 1.830509 1.960148 -1.191144 H 2.737754 1.492548 -0.772992 C 1.365098 1.181086 -2.391302 H 1.170730 0.136989 -2.115717 H 0.439951 1.612996 -2.794373 H 2.126988 1.195983 -3.180499 C 2.088839 3.423139 -1.487588 H 2.921709 3.516745 -2.195606 H 1.195872 3.887837 -1.920259 H 2.356467 3.984464 -0.584953 O 0.090246 3.987478 1.764543 C -1.114168 4.678036 2.140865 H -1.950795 4.256584 1.557205 C -0.895906 6.111166 1.716491 H -0.670375 6.157352 0.646241 H -1.794180 6.709017 1.906490 H -0.060481 6.557746 2.270231 C -1.398059 4.539916 3.625938 H -1.571893 3.496564 3.920473 H -0.558448 4.925081 4.218696						

N	-1.801073	-1.259984	-1.237063	H	-2.977104	1.335228	-5.705965	H	-2.295837	5.107213	3.897227
C	-2.122170	-0.521791	-2.421077	C	-4.458563	-0.033939	-1.541723	C	1.832267	0.787683	1.746491
C	-1.450912	-0.663964	-0.070414	C	-4.411499	0.565104	-0.250449	H	1.051866	0.139123	2.144522
R											
u	-1.410239	1.344506	-0.187990	C	-5.619520	-0.716778	-1.939103	C	3.087508	0.307059	1.764517
N	-1.419404	-1.618421	0.887039	C	-5.555373	0.414378	0.575642	H	3.203410	-0.709769	2.143736
C	-0.939502	-1.528146	2.230278	C	-6.724579	-0.858739	-1.109352	C	4.337225	0.919391	1.306530
C	-1.913956	-2.940723	0.395480	H	-5.634016	-1.151815	-2.940043	C	5.326226	0.086974	0.738731
H	-1.121555	-3.681713	0.570302	C	-6.681571	-0.271041	0.157820	C	4.615195	2.288192	1.436214
H	-3.114462	-2.886000	-1.434459	H	-5.519471	0.886679	1.556195	C	6.561329	0.603993	0.304176
C	-2.734960	0.799508	-4.789960	H	-7.603218	-1.403862	-1.447357	C	5.808193	2.821507	0.967464
C	-1.204932	-0.503345	-3.475534	H	-7.536744	-0.352423	0.829411	H	3.897298	2.931411	1.940535
C	-3.384584	0.090451	-2.549535	O	-3.434297	1.298064	0.230180	C	6.765837	1.986675	0.404351
C	-3.659439	0.751267	-3.755554	C	-1.143687	-3.537860	-1.961790	H	6.007314	3.885805	1.073267
C	-1.502931	0.163323	-4.656599	C	-1.632426	-4.608476	-2.709230	H	7.722309	2.394737	0.079392
H	-4.623369	1.246531	-3.858080	C	0.231265	-3.278256	-1.965940	O	5.046063	-1.257611	0.654799
H	-0.775474	0.186035	-5.465583	C	-0.763988	-5.413996	-3.443473	C	4.896147	-1.811872	-0.676093
C	0.027579	-1.480905	4.865491	H	-2.703896	-4.810077	-2.715760	H	5.837697	-1.650188	-1.224606
C	0.323814	-2.083738	2.521617	C	1.099826	-4.080637	-2.696492	C	4.679502	-3.292825	-0.479453
C	-1.738983	-0.979507	3.245516	H	0.612828	-2.425393	-1.401036	H	4.654766	-3.805658	-1.447528
C	-1.217929	-0.947422	4.543979	C	0.602992	-5.153373	-3.436828	H	5.487634	-3.728350	0.117527
C	0.779486	-2.056408	3.837826	H	-1.158869	-6.244073	-4.026268	H	3.728111	-3.484730	0.032863
C	1.214332	-2.610773	1.438679	H	2.167828	-3.866895	-2.692506	C	3.761410	-1.132939	-1.413267
C	-3.124388	-0.479933	2.990648	H	1.281619	-5.780452	-4.011947	H	2.828064	-1.198181	-0.836149
H	-1.827653	-0.506512	5.334353	C	-3.140539	-3.376109	1.153585	H	3.977113	-0.071657	-1.582969
H	1.764466	-2.471145	4.059961	C	-4.418522	-2.914917	0.826360	H	3.598496	-1.599009	-2.393228
C	0.556157	-1.434614	6.266741	C	-2.980469	-4.205931	2.267393	C	7.646612	-0.251357	-0.221187
H	-3.229835	-0.013265	2.007132	C	-5.515893	-3.289281	1.596272	C	8.374697	0.148468	-1.350045
H	-3.416949	0.256870	3.748616	H	-4.566984	-2.237338	-0.015185	C	8.002500	-1.453528	0.409212
H	-3.849685	-1.303961	3.042747	C	-4.075714	-4.571918	3.043678	C	9.418134	-0.629659	-1.841482
H	2.206944	-2.854309	1.834194	H	-1.980837	-4.557717	2.529692	H	8.100838	1.073877	-1.856559
H	1.349334	-1.858413	0.648412	C	-5.348183	-4.115766	2.705291	C	9.046550	-2.229057	-0.081426
H	0.827494	-3.516066	0.950898	H	-6.502726	-2.917733	1.325819	H	7.453089	-1.772426	1.292433
H	0.841316	-2.431873	6.624353	H	-3.936345	-5.216554	3.909645	C	9.757134	-1.823178	-1.209858
H	-0.183167	-1.028346	6.964854	H	-6.208573	-4.403973	3.306881	H	9.964529	-0.303908	-2.724987
H	1.454927	-0.808363	6.336178	C	0.112633	2.579948	1.966840	H	9.312410	-3.155265	0.425629
C	-1.162792	1.903346	1.515237	H	0.272584	2.356710	3.042517	H	10.572118	-2.434119	-1.593573
H	-2.034158	1.963234	2.188882	C	1.300109	2.060025	1.176800	I	-1.868544	3.589569	-1.703257

Table S3 (continued)

tetramethylsilane			
Si	0.000035	0.000013	-0.000093
C	1.773448	-0.065515	-0.621825
H	1.816075	-0.076408	-1.715736
H	2.350968	0.800214	-0.281866
H	2.291253	-0.962348	-0.266637
C	-0.832974	1.557978	-0.643969
H	-0.849152	1.582535	-1.738381
H	-1.870160	1.630379	-0.301056
H	-0.314143	2.460628	-0.305387
C	-0.004560	0.018318	1.880167
H	-1.023285	0.056378	2.279348
H	0.473693	-0.876146	2.292245
H	0.532838	0.886496	2.275209
C	-0.935929	-1.510805	-0.614301
H	-0.478964	-2.439519	-0.257556
H	-1.975607	-1.506564	-0.271295
H	-0.953919	-1.555687	-1.708020



■ Kinetic Study of Thermal Isomerization of Complex *endo-anti*:

In a typical experiment, under a dry N₂ atmosphere, complex *endo-anti*.and 9-methylanthracene were dissolved in C₆D₆ to give a solution of desired concentration in *endo-anti*.. The resulting solution was transferred to an oven-dried NMR tube, which was subsequently placed into the NMR probe preheated to 50 °C. Pre-acquisition delay (PAD) ¹H NMR was set up to collect at least 80 spectra of 16 scans each with d1 = 5 sec every 187 sec (a total of 299.8 seconds per spectrum). Concentration of complex *endo-anti*.in each spectrum was estimated from the ratio of ¹H NMR peak areas (complex *endo-anti*./9-methylanthracene). Resulting data was employed to construct ([*endo-anti*.]₀-[*endo-anti*.])/time vs. time plots. Analysis of the linear region of data (2-20% conversion) by means of linear regression gave equations of the type $y = ax + b$, with b intercept being the initial rate. The slope of the linear curve in the ln(b) vs. ln[*endo-anti*.]₀ plot gave the reaction order as shown in Figure SA1.

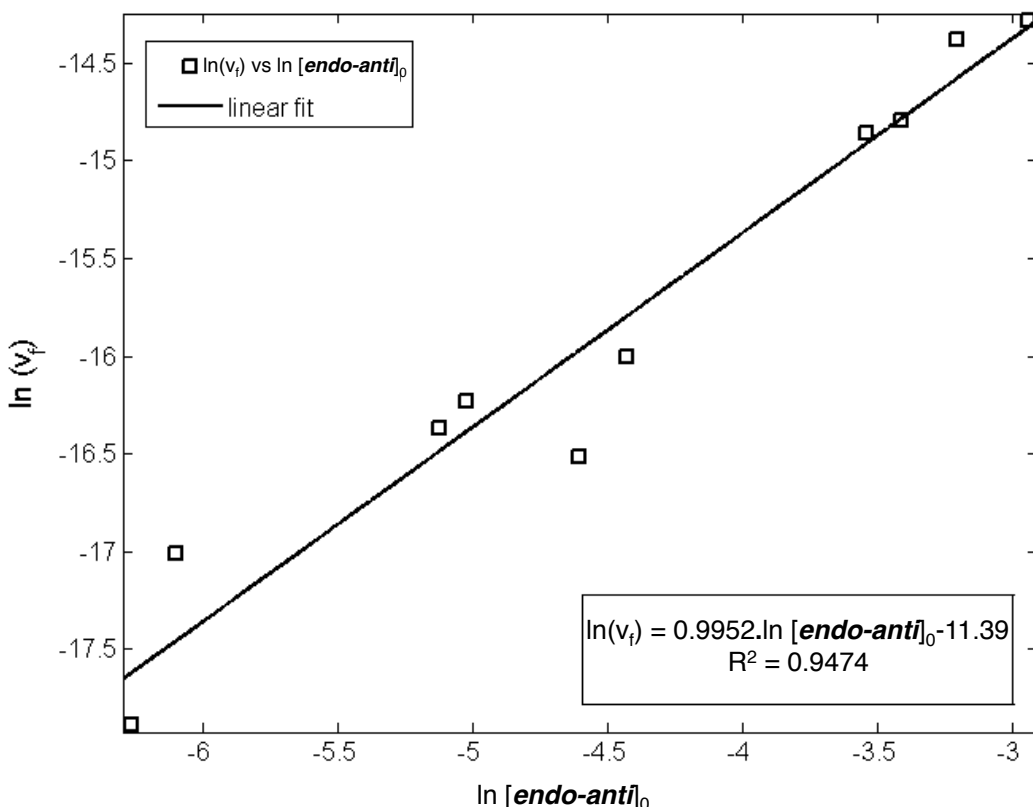


Figure SA1. Initial Rates Plot for Thermal Isomerization of *endo-anti*.

■ Experimental and Calculated Circular Dichroism Spectra of Diene 1.5:

Experimental circular dichroism spectrum for compound **1.5** (solution in dry pentane) was obtained at 22 °C for a wavelength range 200.0-500.0 nm and wavelength step of 1.0 nm, at bandwidth of 1.0 nm, averaging time of 2.00 sec, and settling time of 0.33 sec. For each wavelength an average of 10 scans was taken. The resulting CD spectrum is shown in Figure SA2 (in red).

Circular dichroism spectrum of **1.5** was calculated following the procedure below. Assuming $A_{1,3}$ -strain minimization 15 starting conformers for compound **1.5** were generated. These conformers were optimized at M06/6-311G(d) level of theory in Gaussian 09 Rev.A1 with tight SCF and convergence criteria and ultrafine integration grid. Of the resulting 14 conformers (2 of the initial input geometries converged to give the identical conformer) 9 were selected for further calculations, as the remaining conformers were found to possess relatively high energy compared to the lowest energy conformer ($\Delta H^\circ > 3$ kcal/mol). TD-DFT calculations were carried out to obtain 20 excited states at M06/6-311+G(2d,p) level of theory with ultrafine integration grid. The

solvation by *n*-pentane was modeled by means of an integral equation formalism variant of polarizable continuum model (IEFPCM). The CD spectra for each conformer were constructed according to the following formula:

$$\text{Signal} = \sum_{n=1}^{n=20} R_n e^{-\left[\frac{(x-\lambda_n-\lambda_o)^2}{2\sigma^2}\right]}$$

where, *n* is the number of excited state, R_n is the rotatory strength of the n^{th} excited state, *x* is the wavelength, λ_n is the wavelength of the n^{th} excited state, λ_o is the offset for the calculated λ_n , and σ is the standard deviation of the Gaussian curve. The weighted sum ($\text{Signal}_{\text{total}} = \sum C_m \text{Signal}_m$, where C_m is the weighting coefficient for m^{th} CD spectrum, Signal_m is m^{th} CD spectrum) of the CD spectra for all conformers gave the CD spectrum shown in Figure SA2 (in red). The weights C_m were derived from H° of each conformer, assuming the 9 lowest energy conformers are in equilibrium, and subject to the following constraint: $\sum_m C_m = 1$. The list of rotatory strengths $R(\text{length})$ and the corresponding wavelengths is given in Table S4. The weights C_m and energies H° are listed in Table S5. The list of Cartesian coordinates for all fully optimized conformers along is given in Table S6.

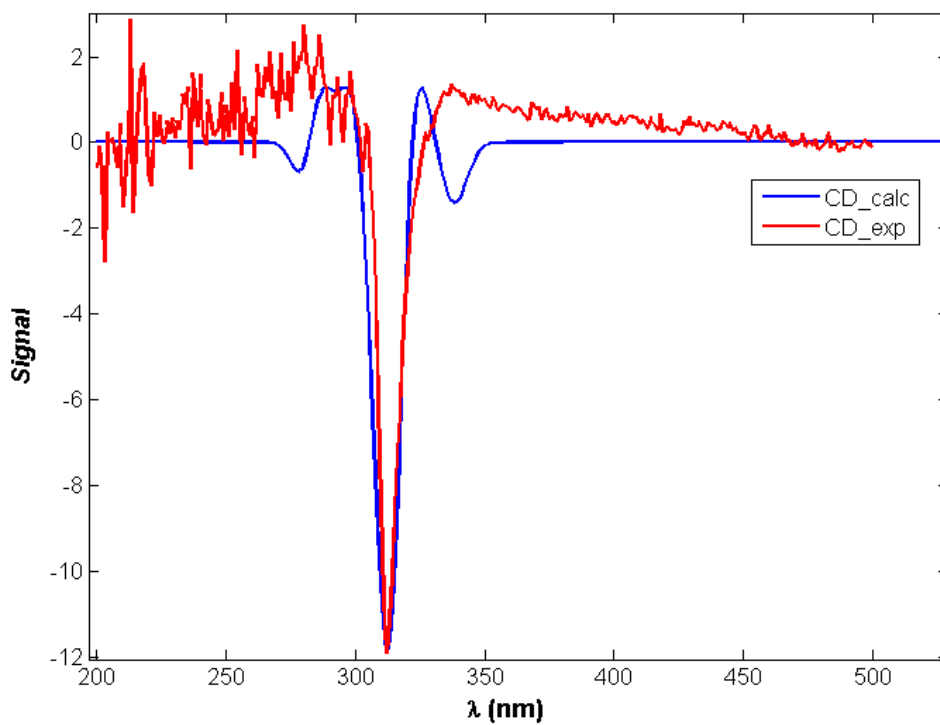


Figure SA2. Experimental and Calculated Circular Dichroism Spectra of Compound 1.5

Table S4. Wavelengths and Rotatory Strengths (R) of 20 Excited States for Each of the 9 Lowest Energy Conformers of Compound 1.5

Compound S16		Compound S17		Compound S18		Compound S19	
λ	R	λ	R	λ	R	λ	R
259.99	-0.4929	280.37	-24.8950	280.13	-27.2238	262.05	-2.0648
250.38	-0.9334	264.57	38.6716	264.32	44.1003	252.65	8.6072
246.61	-5.2860	256.06	-97.1504	255.94	-130.8457	248.75	-1.7062
242.70	1.3266	253.95	-84.6365	253.85	-99.7692	244.15	-0.2559
236.39	34.4355	250.26	-12.1940	250.05	-10.6412	237.55	11.2308
235.49	17.5958	248.57	-5.8712	248.47	-5.3238	236.45	-18.2312
234.74	151.0288	246.63	-31.3258	246.23	-32.2756	235.21	65.8939
233.49	-8.6265	242.33	27.9110	242.32	44.6095	234.70	119.2566
229.37	35.8525	237.67	2.9437	237.62	3.0476	230.78	0.0115
228.68	50.0436	236.78	-2.6645	237.25	-3.7232	230.43	37.0967
228.39	-3.4877	233.69	-2.9832	234.14	-2.5160	229.29	27.2578
226.93	-26.7010	233.19	-1.4407	233.52	-6.3766	228.23	-1.4746
225.74	3.7777	231.87	-5.3164	232.11	-3.6652	226.74	7.4896

221.87	12.8272	230.85	-1.5213	230.78	-2.6610	222.82	14.8837
221.47	-6.5318	228.05	55.3901	226.89	45.7982	222.07	-14.4218
220.27	45.3194	225.77	1.3178	225.89	12.6937	220.98	48.9475
220.00	2.6084	224.67	-3.0695	224.41	-3.4164	220.67	3.8626
219.17	6.1067	224.04	-38.3127	223.87	-40.1320	220.13	1.0173
218.31	26.0212	223.64	0.1993	223.31	-3.7219	219.58	31.0208
217.21	8.0310	221.92	-4.4169	221.94	-9.9273	217.94	6.5487
Compound S21		Compound S22		Compound S25		Compound S26	
λ	R	λ	R	λ	R	λ	R
282.66	-28.2594	280.94	-39.7179	267.83	-0.2351	280.27	-25.1941
265.85	36.7800	264.37	37.2090	255.49	-35.3862	263.64	55.1899
255.40	-110.7487	254.48	-74.6678	248.67	17.8062	253.85	-20.1536
253.29	-60.4150	252.61	-108.9260	246.21	47.8558	252.01	-170.5592
249.28	-19.7857	250.64	-28.3918	240.66	-0.4721	248.40	-19.9380
248.27	-23.7752	247.77	-11.8490	239.50	-1.6552	246.92	-6.4463
246.18	-14.5447	246.27	-29.3708	237.98	29.8371	245.30	-18.7180
239.87	30.7443	241.25	32.2953	237.04	-13.4112	238.56	15.7038
236.34	0.4393	237.58	-1.7843	231.52	-0.9327	236.43	-0.3772
235.15	-2.7080	235.80	-5.1640	230.14	36.6316	235.18	-4.4495
232.89	53.6003	232.81	-4.1733	230.03	5.0584	234.17	40.1496
232.66	5.3473	231.18	4.4050	227.58	3.6446	231.27	-13.5865
230.80	-9.8767	230.48	-10.7771	224.24	14.7036	229.69	-7.8942
230.17	-11.9849	230.14	56.8738	223.80	-2.1286	228.64	7.6706
229.45	0.8683	229.07	-4.6731	223.38	-5.7186	227.94	-1.9425
225.98	8.6135	225.28	-11.1222	222.39	-14.9318	223.89	-14.9394
225.51	-4.7144	224.11	-0.9769	222.09	-3.7433	222.51	2.7137
224.52	6.1066	222.50	8.5929	221.37	-5.2592	221.65	1.9266
223.07	-5.9298	222.15	1.4131	219.98	32.3619	221.07	-14.6077
222.38	-20.9295	221.65	-14.4771	219.65	-4.6789	220.49	-0.3939

Table S4 (continued)

Compound S29	
λ	R
267.27	19.3722
257.30	18.5984
251.24	3.0141
244.02	-11.5772

241.80	15.0929
236.08	-6.2788
234.36	12.5281
232.44	-20.7777
231.29	14.0939
229.58	2.5651
228.52	-52.6331
227.94	31.9247
225.25	21.7648
224.28	62.0719
222.82	38.7509
220.91	-10.4814
220.42	-2.2674
219.50	12.7281
218.82	23.2661
218.32	30.2036

Table S5. Weighting Coefficients (C_m) and Energies of 14 Conformers of the Compound (1.5)

Compound	$\Delta(E+ZPE)$	ΔH	Coefficient
S16	2.22	2.05	2.14E-02
S17	1.05	1.22	8.73E-02
S18	0.00	0.00	6.87E-01
S19	2.14	1.94	2.58E-02
S20	3.39	3.22	0.00E+00
S21	2.70	2.89	5.19E-03
S22	2.44	2.54	9.44E-03
S23	3.76	3.75	0.00E+00
S24	4.90	4.79	0.00E+00
S25	1.00	0.92	1.45E-01
S26	3.17	3.19	3.17E-03
S27	3.94	4.08	0.00E+00
S28	3.90	3.77	0.00E+00
S29	2.30	2.56	9.10E-03

Table S6. Geometries of Fully Optimized Fourteen Conformers of Diene 1.5

Compound S16			Compound S17			Compound S18					
C	-2.956528	1.752936	-1.747813	C	4.785006	0.071899	-1.123143	C	4.833165	0.208185	-1.073899
H	-2.593435	1.068217	-2.519127	H	4.328827	-0.018781	-2.112439	H	5.255107	1.211549	-1.073224
C	-2.414544	1.499202	-0.378572	C	3.860353	-0.180678	0.022517	C	3.907430	-0.097072	0.066362
H	-2.898270	2.188972	0.337763	H	4.384992	0.036681	0.971757	H	4.419786	0.160376	1.013694
C	-2.679488	0.070280	0.090605	C	2.601822	0.681451	-0.034624	C	2.633236	0.753532	0.003702
H	-2.129432	-0.594680	-0.596933	H	2.033866	0.368434	-0.927110	H	2.079439	0.433119	-0.893839
O	-4.070829	-0.130417	-0.002170	O	3.058261	2.009505	-0.173161	O	3.073564	2.090021	-0.129258
C	-4.485440	-1.486555	-0.049214	C	2.062438	2.986494	-0.442445	C	2.069358	3.050987	-0.426795
H	-3.903911	-2.065510	0.692840	H	1.285615	2.933023	0.341706	H	1.280132	2.994171	0.344472
C	-5.943022	-1.497754	0.342719	C	2.767416	4.318654	-0.362235	C	2.753223	4.394131	-0.345634
H	-6.078960	-1.079783	1.344765	H	3.248000	4.442870	0.612796	H	3.225723	4.528493	0.632082
H	-6.521003	-0.885747	-0.359862	H	3.545906	4.378971	-1.132018	H	3.534006	4.467952	-1.112220
H	-6.350617	-2.514404	0.329311	H	2.066178	5.146075	-0.514002	H	2.039529	5.209699	-0.502831
C	-4.270960	-2.067926	-1.433166	C	1.414790	2.776398	-1.797872	C	1.450334	2.818632	-1.791668
H	-4.622652	-3.105030	-1.483537	H	0.734870	3.604280	-2.030204	H	0.779062	3.644889	-2.053081
H	-4.829981	-1.478957	-2.170830	H	2.185217	2.735955	-2.578466	H	2.237412	2.759060	-2.554080
H	-3.215648	-2.065259	-1.728070	H	0.826616	1.852782	-1.851351	H	0.860399	1.896213	-1.841638
O	-1.012771	1.666487	-0.383632	O	3.417130	-1.522220	-0.015727	O	3.501263	-1.440572	0.069541
C	-0.563621	2.970887	-0.041186	C	4.240312	-2.467019	0.653247	C	4.249356	-2.324493	0.894099
H	-1.264033	3.710231	-0.472667	H	5.296979	-2.173952	0.518496	H	5.316397	-2.043695	0.835174
C	0.796787	3.151577	-0.669621	C	4.001270	-3.797751	-0.017305	C	4.059403	-3.708108	0.320493
H	0.740909	3.026274	-1.756481	H	4.274263	-3.754331	-1.076069	H	4.437508	-3.767897	-0.704916
H	1.198805	4.148116	-0.455236	H	4.582287	-4.592934	0.462035	H	4.577776	-4.460662	0.924117
H	1.488034	2.403762	-0.266128	H	2.938782	-4.063759	0.050764	H	2.991484	-3.960171	0.305642
C	-0.506084	3.125758	1.466957	C	3.891039	-2.503751	2.126765	C	3.764934	-2.243737	2.327008
H	-1.495969	3.044072	1.930190	H	4.006316	-1.521752	2.599173	H	3.857676	-1.231974	2.736464
H	0.128189	2.333500	1.882732	H	2.845213	-2.811711	2.251042	H	2.705136	-2.524036	2.373252
H	-0.090207	4.100977	1.747699	H	4.527017	-3.213206	2.668804	H	4.333132	-2.921379	2.974521
C	-2.199853	-0.124968	1.494196	C	1.777161	0.540402	1.206133	C	1.801621	0.611967	1.239598
H	-2.816000	0.368745	2.249842	H	2.252889	0.998311	2.078680	H	2.262090	1.087121	2.111263
C	-1.096223	-0.765231	1.862243	C	0.555952	0.024642	1.360579	C	0.586726	0.080044	1.388517
H	-0.813087	-0.759713	2.916595	H	0.097418	0.120961	2.344844	H	0.116741	0.181428	2.366923
C	-0.207173	-1.485881	0.926578	C	-0.283510	-0.638409	0.356097	C	-0.231042	-0.609456	0.384020
C	1.035828	-0.962082	0.566724	C	-1.673315	-0.435151	0.387408	C	-1.624363	-0.429692	0.397957
C	-0.608325	-2.700608	0.370700	C	0.242934	-1.508898	-0.602470	C	0.320483	-1.481876	-0.558441
C	1.837265	-1.610493	-0.383686	C	-2.521008	-1.069956	-0.530517	C	-2.450820	-1.089649	-0.521437
C	0.202532	-3.383082	-0.520878	C	-0.582714	-2.113557	-1.535859	C	-0.484346	-2.112948	-1.492511
H	-1.573406	-3.113009	0.662094	H	1.307795	-1.729709	-0.583770	H	1.389147	-1.681869	-0.527990
C	1.416826	-2.832600	-0.899742	C	-1.948775	-1.891997	-1.501049	C	-1.854204	-1.914423	-1.475065
H	-0.122153	-4.333623	-0.937573	H	-0.160252	-2.790126	-2.275253	H	-0.042014	-2.790071	-2.219544
H	2.043179	-3.330655	-1.638327	H	-2.604325	-2.399623	-2.206960	H	-2.493178	-2.441585	-2.181808
O	1.443871	0.223429	1.111662	O	-2.185363	0.372301	1.364004	O	-2.160972	0.381073	1.358462

C	2.543215	0.144677	2.035400	C	-2.727554	1.636947	0.949870	C	-2.714575	1.633271	0.922069
H	3.191409	-0.694281	1.736810	H	-3.399786	1.464073	0.093962	H	-3.376621	1.440456	0.062288
C	3.319748	1.432536	1.924836	C	-3.524861	2.149006	2.121377	C	-3.528973	2.151286	2.078989
H	4.158335	1.436813	2.629729	H	-3.964779	3.125819	1.894233	H	-3.979368	3.118944	1.833961
H	3.719769	1.560641	0.913346	H	-4.332817	1.456476	2.377025	H	-4.330195	1.451797	2.336860
H	2.679189	2.292283	2.157482	H	-2.876111	2.260474	2.998323	H	-2.889882	2.283533	2.960117
C	2.013204	-0.104040	3.429770	C	-1.621630	2.581735	0.540009	C	-1.615325	2.584968	0.510432
H	1.326374	0.699605	3.723347	H	-0.958094	2.788479	1.388542	H	-0.957883	2.802223	1.361115
H	1.475351	-1.057069	3.486202	H	-1.018048	2.159943	-0.271392	H	-1.003976	2.162669	-0.294819
H	2.831193	-0.139829	4.158350	H	-2.039529	3.532395	0.188901	H	-2.039267	3.529608	0.150541
C	3.069414	-0.968655	-0.894137	C	-3.990661	-0.909596	-0.482530	C	-3.923178	-0.950175	-0.492682
C	4.321626	-1.556447	-0.734857	C	-4.701582	-0.591866	-1.640385	C	-4.625006	-0.657557	-1.662669
C	2.976709	0.249089	-1.566304	C	-4.701028	-1.088475	0.706309	C	-4.644826	-1.122648	0.690277
C	5.461389	-0.929370	-1.219936	C	-6.080321	-0.443171	-1.611944	C	-6.005845	-0.526646	-1.651627
H	4.399003	-2.507900	-0.209074	H	-4.157417	-0.436241	-2.571002	H	-4.072501	-0.506774	-2.589135
C	4.112393	0.873072	-2.057179	C	-6.078605	-0.941618	0.734198	C	-6.024428	-0.993468	0.700835
H	1.993884	0.696844	-1.701170	H	-4.161444	-1.342696	1.615421	H	-4.112690	-1.357918	1.608814
C	5.359933	0.287831	-1.878297	C	-6.773518	-0.614156	-0.422755	C	-6.710342	-0.690514	-0.468090
H	6.435285	-1.394224	-1.081608	H	-6.615153	-0.186381	-2.523894	H	-6.533357	-0.289047	-2.573025
H	4.022168	1.822786	-2.581151	H	-6.616327	-1.089365	1.668638	H	-6.570740	-1.135782	1.631107
H	6.253615	0.778417	-2.257794	H	-7.854450	-0.496184	-0.396731	H	-7.792897	-0.586068	-0.455960
C	-3.768580	2.751329	-2.056924	C	6.076023	0.333232	-0.994605	C	5.124356	-0.647914	-2.040890
H	-4.135763	3.436332	-1.293148	H	6.536659	0.431404	-0.011869	H	4.693953	-1.646427	-2.057763
H	-4.114490	2.926205	-3.072541	H	6.727977	0.477778	-1.852169	H	5.793984	-0.381897	-2.854194

Table S6 (continued)

Compound S19			Compound S20			Compound S21					
C	-2.914864	2.037181	-1.669159	C	1.404971	-2.043809	-0.245025	C	-3.298705	-2.344085	-0.123863
H	-4.000819	2.040679	-1.755778	H	1.040751	-2.129122	0.780486	H	-2.764453	-2.500518	-1.063711
C	-2.377894	1.645229	-0.323437	C	2.385569	-0.941099	-0.480760	C	-3.674893	-0.924920	0.164926
H	-2.876345	2.267849	0.445079	H	2.623684	-0.886319	-1.557103	H	-4.263483	-0.885221	1.098380
C	-2.716066	0.183684	0.006611	C	1.837534	0.429237	-0.105727	C	-2.470022	-0.011846	0.386816
H	-2.197065	-0.437668	-0.743842	H	0.844593	0.519938	-0.576370	H	-1.846954	-0.475309	1.168744
O	-4.113704	0.065729	-0.136361	O	2.740311	1.363597	-0.670071	O	-3.014312	1.204872	0.858427
C	-4.618792	-1.224439	-0.446790	C	2.318923	2.719567	-0.680095	C	-2.086759	2.199962	1.261897
H	-3.838496	-1.782570	-0.995572	H	1.974918	2.997201	0.332310	H	-1.357336	2.364376	0.448712
C	-4.995526	-1.980880	0.811281	C	3.546528	3.527567	-1.026654	C	-2.901476	3.454590	1.465164
H	-4.130460	-2.140374	1.462657	H	4.345969	3.346419	-0.301919	H	-3.447045	3.710735	0.551780
H	-5.742886	-1.410309	1.376055	H	3.917555	3.240555	-2.017996	H	-3.636867	3.301072	2.264392
H	-5.426094	-2.959724	0.568796	H	3.322668	4.599740	-1.041246	H	-2.264429	4.301311	1.742464
C	-5.807995	-1.010544	-1.354550	C	1.195360	2.955837	-1.671767	C	-1.341711	1.802767	2.522010
H	-6.265198	-1.962278	-1.646575	H	0.913730	4.015254	-1.687627	H	-0.688572	2.617636	2.855740
H	-6.566958	-0.410499	-0.838150	H	1.518068	2.671924	-2.681227	H	-2.054841	1.585941	3.327191
H	-5.510009	-0.472866	-2.260610	H	0.288662	2.390507	-1.428853	H	-0.709566	0.918717	2.379263
O	-0.985491	1.777064	-0.247837	O	3.558498	-1.176706	0.271704	O	-4.426035	-0.418450	-0.916927

C	-0.521714	2.998683	0.315475	C	4.571609	-1.893452	-0.416688	C	-5.834254	-0.531028	-0.776469
H	-1.168691	3.820118	-0.044140	H	4.093665	-2.644363	-1.072821	H	-6.066798	-1.483698	-0.264293
C	0.885310	3.211918	-0.188964	C	5.391408	-2.608006	0.629943	C	-6.408889	-0.569461	-2.171672
H	0.908301	3.261702	-1.283477	H	4.769267	-3.301208	1.204431	H	-6.014341	-1.422583	-2.731866
H	1.305831	4.143792	0.205548	H	6.212869	-3.170187	0.172246	H	-7.501631	-0.641608	-2.146664
H	1.517275	2.379138	0.137232	H	5.822512	-1.880379	1.328042	H	-6.138845	0.345657	-2.712176
C	-0.560741	2.925286	1.829636	C	5.408823	-0.940480	-1.245655	C	-6.371084	0.633878	0.030066
H	-1.582475	2.829532	2.213571	H	4.797956	-0.376914	-1.958546	H	-5.922986	0.681184	1.027814
H	0.004591	2.042983	2.151069	H	5.895506	-0.211629	-0.586477	H	-6.129293	1.574011	-0.480175
H	-0.120178	3.821993	2.281603	H	6.184912	-1.475501	-1.805860	H	-7.459372	0.568316	0.146177
C	-2.268414	-0.164022	1.391532	C	1.731238	0.631248	1.376332	C	-1.687292	0.206334	-0.870784
H	-2.887590	0.273434	2.179339	H	2.643961	0.410073	1.927899	H	-2.257979	0.735181	-1.634772
C	-1.192918	-0.869156	1.724712	C	0.676201	1.121979	2.021297	C	-0.416543	-0.104898	-1.140254
H	-0.945539	-0.971391	2.783426	H	0.761604	1.294943	3.097046	H	-0.026980	0.227921	-2.102046
C	-0.297829	-1.535218	0.754079	C	-0.595643	1.543923	1.395691	C	0.569276	-0.803117	-0.307036
C	0.969511	-1.022773	0.467483	C	-1.470474	0.632763	0.796079	C	1.923438	-0.441028	-0.421573
C	-0.715315	-2.691316	0.095220	C	-0.931511	2.898279	1.384226	C	0.240242	-1.854182	0.554008
C	1.771748	-1.609556	-0.521521	C	-2.615251	1.074034	0.112313	C	2.920235	-1.099265	0.311869
C	0.098868	-3.323292	-0.829966	C	-2.083520	3.343588	0.760195	C	1.209924	-2.484246	1.315075
H	-1.695649	-3.101650	0.333715	H	-0.258207	3.607279	1.864900	H	-0.786060	-2.210541	0.599220
C	1.332365	-2.774650	-1.142637	C	-2.908639	2.435527	0.114763	C	2.536308	-2.106862	1.195823
H	-0.239000	-4.229491	-1.327034	H	-2.325786	4.403585	0.750479	H	0.933467	-3.301925	1.976481
H	1.959350	-3.226152	-1.910012	H	-3.787003	2.782965	-0.426693	H	3.307855	-2.632820	1.755708
O	1.406142	0.090782	1.129594	O	-1.181569	-0.699502	0.845698	O	2.254014	0.543943	-1.307943
C	2.492599	-0.107778	2.049768	C	-1.993624	-1.489715	1.728947	C	2.713291	1.792329	-0.763150
H	3.164157	-0.877675	1.638408	H	-3.037524	-1.144927	1.641667	H	3.492524	1.580109	-0.012689
C	3.239367	1.198705	2.143430	C	-1.900588	-2.915981	1.247655	C	3.318995	2.549257	-1.916477
H	4.063535	1.118403	2.860319	H	-2.528197	-3.569460	1.863039	H	3.687111	3.526657	-1.587168
H	3.655052	1.481329	1.170423	H	-2.228672	-2.997299	0.206376	H	4.155054	1.994170	-2.353211
H	2.572100	2.001031	2.482395	H	-0.867956	-3.280114	1.314180	H	2.566930	2.711153	-2.697879
C	1.953717	-0.572887	3.383919	C	-1.521062	-1.325652	3.155777	C	1.571356	2.536893	-0.111320
H	1.255290	0.168925	3.791090	H	-0.482025	-1.663942	3.252667	H	0.798332	2.779309	-0.850405
H	1.428521	-1.530152	3.290271	H	-1.571137	-0.279186	3.476589	H	1.110137	1.937110	0.680917
H	2.766581	-0.709916	4.106096	H	-2.141656	-1.916306	3.839277	H	1.927373	3.471646	0.336537
C	3.026646	-0.957017	-0.955116	C	-3.480248	0.128623	-0.626031	C	4.354863	-0.779617	0.146332
C	4.255318	-1.608470	-0.878958	C	-4.865687	0.162632	-0.467680	C	5.166741	-0.572401	1.262289
C	2.980853	0.339118	-1.467999	C	-2.932849	-0.798340	-1.515918	C	4.933289	-0.700521	-1.122245
C	5.418827	-0.968695	-1.284076	C	-5.683850	-0.709513	-1.171256	C	6.515570	-0.282224	1.117183
H	4.296098	-2.620449	-0.476780	H	-5.302408	0.870794	0.235423	H	4.724800	-0.617000	2.256731
C	4.140193	0.976260	-1.879041	C	-3.750819	-1.664832	-2.222884	C	6.280974	-0.413348	-1.266581
H	2.015536	0.836854	-1.541957	H	-1.853421	-0.838246	-1.650160	H	4.312146	-0.861950	-1.999846
C	5.364397	0.326230	-1.779829	C	-5.128667	-1.627415	-2.050128	C	7.076512	-0.198672	-0.148442
H	6.374274	-1.483734	-1.209796	H	-6.761620	-0.673578	-1.027687	H	7.129679	-0.113401	1.999082
H	4.087680	1.986744	-2.280116	H	-3.308314	-2.375127	-2.918333	H	6.716706	-0.360225	-2.262216
H	6.276448	0.827593	-2.096249	H	-5.768266	-2.312210	-2.602465	H	8.133104	0.032017	-0.264804
C	-2.152448	2.346444	-2.706418	C	1.002669	-2.885482	-1.185360	C	-3.615522	-3.368515	0.654669

H -1.067503	2.330158	-2.630529	H 1.363035	-2.801238	-2.210722	H -4.162648	-3.223111	1.586037
H -2.580451	2.617774	-3.667749	H 0.297977	-3.689191	-0.983117	H -3.347261	-4.391875	0.404530

Table S6 (continued)

Compound S22			Compound S23			Compound S24		
C 3.397941	-2.378367	-0.445517	C 3.373797	-2.181658	-0.720967	C 1.132461	-1.120686	-1.193078
H 2.964991	-2.760561	-1.373641	H 2.937848	-2.407330	-1.697791	H 0.610608	-0.433789	-1.865006
C 3.705373	-0.911014	-0.437221	C 3.586375	-0.724342	-0.437175	C 2.477663	-0.657404	-0.715534
H 4.260088	-0.669201	-1.362048	H 4.084009	-0.278001	-1.319550	H 3.067193	-0.347113	-1.599954
C 2.442526	-0.044777	-0.498155	C 2.257227	0.028874	-0.268055	C 2.351852	0.588455	0.176756
H 1.788926	-0.449054	-1.288571	H 1.594623	-0.255893	-1.100747	H 1.691698	1.295862	-0.349914
O 2.912026	1.237247	-0.872575	O 2.500328	1.425695	-0.298528	O 3.620549	1.166991	0.409241
C 1.939987	2.248556	-1.078585	C 2.443748	2.016156	-1.585960	C 4.091029	2.062182	-0.581138
H 1.337337	2.364882	-0.160611	H 2.948703	1.352757	-2.315327	H 3.942506	1.617193	-1.584813
C 2.726015	3.514606	-1.322735	C 1.009112	2.235823	-2.024663	C 3.366291	3.394441	-0.516774
H 3.412551	3.705732	-0.492034	H 0.427237	1.305773	-2.021001	H 2.299868	3.306543	-0.750774
H 3.322957	3.418381	-2.237930	H 0.517649	2.939577	-1.342492	H 3.460911	3.815211	0.491997
H 2.061717	4.378234	-1.434274	H 0.967129	2.651678	-3.038030	H 3.797139	4.107975	-1.228452
C 1.020467	1.925006	-2.241125	C 3.203487	3.318014	-1.495534	C 5.571147	2.225358	-0.329449
H 0.358439	2.771800	-2.456529	H 3.198045	3.847467	-2.454498	H 6.026154	2.902613	-1.060105
H 1.613366	1.719859	-3.141498	H 2.738416	3.965557	-0.743084	H 5.732869	2.640320	0.672449
H 0.382543	1.054039	-2.048187	H 4.241830	3.147532	-1.194587	H 6.083620	1.259771	-0.378739
O 4.455423	-0.538564	0.687713	O 4.359019	-0.506198	0.711410	O 3.169274	-1.645189	-0.000641
C 5.854007	-0.415139	0.470158	C 5.758900	-0.407885	0.493881	C 4.038723	-2.455691	-0.776381
H 6.177536	-1.219988	-0.216015	H 6.061435	-1.173953	-0.243570	H 3.552573	-2.676125	-1.744576
C 6.518893	-0.613093	1.810553	C 6.418491	-0.702715	1.819016	C 4.228081	-3.742594	-0.010105
H 6.294013	-1.604368	2.217250	H 6.158886	-1.706319	2.170515	H 3.272498	-4.256246	0.135055
H 7.606233	-0.508647	1.730652	H 7.508675	-0.632028	1.742989	H 4.909672	-4.419882	-0.535842
H 6.154524	0.137219	2.522222	H 6.079110	0.018145	2.572228	H 4.651462	-3.528631	0.978367
C 6.175656	0.939157	-0.129168	C 6.119014	0.972501	-0.018491	C 5.355873	-1.742222	-1.010017
H 5.655816	1.102205	-1.078449	H 5.653227	1.187425	-0.987194	H 5.226335	-0.812291	-1.575513
H 5.848423	1.729490	0.557398	H 5.771882	1.729953	0.694179	H 5.809219	-1.485506	-0.045015
H 7.252843	1.049263	-0.301407	H 7.202874	1.077534	-0.143274	H 6.055396	-2.374538	-1.568943
C 1.731401	0.009439	0.819443	C 1.603419	-0.262649	1.043703	C 1.772718	0.236206	1.508003
H 2.341315	0.455010	1.605119	H 2.213975	0.015653	1.901166	H 2.454917	-0.309159	2.157881
C 0.476507	-0.334677	1.120525	C 0.368835	-0.715390	1.259029	C 0.521085	0.456788	1.895506
H 0.132827	-0.112772	2.130707	H 0.023531	-0.746344	2.292525	H 0.197548	0.056507	2.857441
C -0.543262	-0.932139	0.251223	C -0.630871	-1.121580	0.262279	C -0.487753	1.192457	1.109077
C -1.885577	-0.541313	0.401490	C -1.956775	-0.690548	0.420822	C -1.643261	0.548803	0.656158
C -0.242843	-1.911969	-0.697301	C -0.325465	-1.946141	-0.820727	C -0.300901	2.538500	0.798269
C -2.893482	-1.082746	-0.408561	C -2.952000	-1.043664	-0.498960	C -2.568935	1.221474	-0.156674
C -1.223680	-2.433750	-1.523217	C -1.293638	-2.283521	-1.752876	C -1.233050	3.231600	0.043831
H 0.771161	-2.299758	-0.748475	H 0.679708	-2.354396	-0.902110	H 0.590435	3.038158	1.175968
C -2.534690	-2.011775	-1.385171	C -2.591426	-1.827900	-1.595111	C -2.352170	2.570497	-0.435178
H -0.971541	-3.198151	-2.254367	H -1.042191	-2.929652	-2.590798	H -1.078712	4.283220	-0.186702

H	-3.318022	-2.444973	-2.004840	H	-3.362982	-2.118147	-2.306493	H	-3.063554	3.091649	-1.073963
O	-2.189602	0.334862	1.402776	O	-2.245612	0.063277	1.520631	O	-1.794125	-0.771288	0.962518
C	-2.629489	1.654547	1.043958	C	-2.560780	1.454528	1.330227	C	-2.899171	-1.148814	1.794641
H	-3.421655	1.567847	0.283278	H	-3.524780	1.525533	0.799060	H	-3.813583	-0.659928	1.421650
C	-3.201840	2.249606	2.304192	C	-2.709500	2.014340	2.720522	C	-3.025865	-2.642942	1.641946
H	-3.560797	3.268299	2.124421	H	-2.997966	3.070039	2.686725	H	-3.831174	-3.034336	2.272412
H	-4.037961	1.648022	2.674066	H	-3.473910	1.464090	3.279024	H	-3.237865	-2.911207	0.601758
H	-2.433144	2.288464	3.085100	H	-1.759968	1.930624	3.262998	H	-2.087622	-3.127979	1.937267
C	-1.481660	2.464913	0.488118	C	-1.494537	2.157504	0.523389	C	-2.649529	-0.728628	3.225649
H	-0.670888	2.532076	1.223923	H	-0.505409	2.039753	0.984050	H	-1.761756	-1.235696	3.622643
H	-1.077559	2.017424	-0.426484	H	-1.439920	1.761092	-0.496137	H	-2.496141	0.353597	3.305535
H	-1.813123	3.480827	0.243853	H	-1.721099	3.227448	0.450807	H	-3.503975	-0.990771	3.859743
C	-4.318966	-0.724766	-0.239226	C	-4.355632	-0.612854	-0.328488	C	-3.719207	0.524295	-0.771222
C	-5.081545	-0.346451	-1.344473	C	-5.044750	-0.028546	-1.391029	C	-5.005589	1.056464	-0.685713
C	-4.938514	-0.778968	1.010971	C	-5.020786	-0.778142	0.888909	C	-3.535369	-0.667307	-1.475443
C	-6.422685	-0.020398	-1.207284	C	-6.358217	0.392359	-1.242362	C	-6.081996	0.411798	-1.277604
H	-4.605648	-0.286181	-2.322329	H	-4.531377	0.119767	-2.340139	H	-5.163117	1.978509	-0.127759
C	-6.279215	-0.455465	1.147311	C	-6.332769	-0.359787	1.036171	C	-4.609838	-1.309248	-2.069594
H	-4.358168	-1.076773	1.880836	H	-4.492211	-1.228590	1.725651	H	-2.534197	-1.086546	-1.554983
C	-7.025750	-0.072368	0.040694	C	-7.005444	0.230723	-0.026500	C	-5.887955	-0.774562	-1.969192
H	-6.998085	0.280315	-2.080180	H	-6.875600	0.855998	-2.079590	H	-7.079560	0.837557	-1.193148
H	-6.748248	-0.508825	2.127709	H	-6.837673	-0.497175	1.990146	H	-4.448380	-2.233690	-2.620351
H	-8.076766	0.184616	0.152163	H	-8.034023	0.563340	0.094397	H	-6.730825	-1.281875	-2.433221
C	3.627986	-3.197185	0.568394	C	3.671280	-3.162920	0.116209	C	0.560540	-2.254798	-0.823612
H	4.058809	-2.823863	1.494315	H	4.102573	-2.949790	1.091752	H	1.059917	-2.928427	-0.130803
H	3.391063	-4.256060	0.515804	H	3.491297	-4.204787	-0.133458	H	-0.428909	-2.541601	-1.169299

Table S6 (continued)

Compound S25			Compound S26			Compound S27					
C	3.316566	-0.957403	1.642202	C	-4.559351	0.570435	-1.476179	C	-4.525289	0.582991	-1.690928
H	4.298779	-0.660700	1.271681	H	-5.042254	1.359324	-0.899089	H	-4.149529	0.876640	-2.673346
C	2.193405	-0.767564	0.675234	C	-3.564943	-0.253127	-0.719419	C	-3.586068	-0.245293	-0.864667
H	1.238397	-1.049844	1.147899	H	-3.194936	-1.058095	-1.381882	H	-3.168865	-1.037209	-1.516859
C	2.038551	0.671125	0.194681	C	-2.350009	0.561658	-0.284771	C	-2.389249	0.556275	-0.350566
H	1.192823	0.673132	-0.512550	H	-1.813576	-0.064739	0.444576	H	-1.858685	-0.117246	0.342779
O	3.227196	1.064898	-0.463115	O	-2.792620	1.748505	0.341971	O	-2.869668	1.679443	0.349772
C	3.104340	1.293378	-1.858969	C	-2.059541	2.106668	1.505061	C	-2.066220	2.060080	1.458474
H	2.484132	0.490141	-2.291874	H	-1.019531	1.751353	1.389141	H	-1.033957	1.705272	1.288482
C	2.460723	2.640107	-2.123075	C	-2.051268	3.613353	1.581439	C	-2.057152	3.567911	1.514179
H	1.450388	2.698285	-1.700790	H	-1.578612	4.040297	0.690344	H	-1.639973	3.982915	0.589942
H	3.061915	3.435404	-1.665189	H	-3.078240	3.993977	1.636940	H	-3.080005	3.947258	1.624368
H	2.384000	2.839524	-3.198528	H	-1.508797	3.961871	2.467536	H	-1.462108	3.930026	2.360518
C	4.498500	1.199345	-2.426538	C	-2.686456	1.460296	2.722326	C	-2.621642	1.426047	2.715218
H	4.497393	1.368786	-3.508876	H	-2.127705	1.697903	3.635467	H	-2.018706	1.677304	3.596003
H	5.146129	1.952207	-1.961195	H	-3.715344	1.821522	2.840588	H	-3.646514	1.778106	2.881839
H	4.923148	0.210896	-2.225442	H	-2.732355	0.371477	2.614799	H	-2.660438	0.335755	2.619389

O	2.433318	-1.556519	-0.478717	O	-4.097888	-0.792491	0.469579	O	-4.204815	-0.817555	0.259464
C	1.935516	-2.882526	-0.394322	C	-5.229060	-1.640385	0.341842	C	-4.858011	-2.056228	0.021338
H	1.976688	-3.214244	0.659920	H	-6.032578	-1.095943	-0.185441	H	-5.378951	-2.004659	-0.951553
C	2.847069	-3.756998	-1.219765	C	-5.668485	-1.937288	1.755425	C	-5.873797	-2.226743	1.124423
H	3.868118	-3.732418	-0.826347	H	-5.857419	-1.007632	2.301064	H	-6.598490	-1.406885	1.117928
H	2.498842	-4.795954	-1.228527	H	-6.581228	-2.542350	1.769067	H	-6.417068	-3.171958	1.019488
H	2.873872	-3.396226	-2.255072	H	-4.882175	-2.487175	2.286784	H	-5.371275	-2.225467	2.099003
C	0.501198	-2.912423	-0.882094	C	-4.903325	-2.907351	-0.425168	C	-3.854009	-3.194340	0.006135
H	-0.104703	-2.169384	-0.352919	H	-4.689012	-2.717830	-1.482567	H	-3.132927	-3.104543	-0.814258
H	0.468597	-2.671937	-1.953367	H	-4.028774	-3.398885	0.020862	H	-3.294423	-3.206520	0.950192
H	0.038816	-3.897011	-0.736429	H	-5.744222	-3.608692	-0.386495	H	-4.354371	-4.162465	-0.109984
C	1.796992	1.639853	1.307629	C	-1.454340	0.932942	-1.423333	C	-1.468690	1.022983	-1.436738
H	2.663417	1.800679	1.950801	H	-1.873427	1.700214	-2.076562	H	-1.872080	1.849197	-2.025737
C	0.705186	2.369756	1.521763	C	-0.209632	0.510227	-1.653422	C	-0.212724	0.634150	-1.671862
H	0.744694	3.111665	2.323037	H	0.341544	0.984945	-2.464912	H	0.350803	1.179331	-2.428365
C	-0.543088	2.374932	0.739854	C	0.546044	-0.504999	-0.910665	C	0.536507	-0.424022	-0.986336
C	-1.282450	1.223098	0.448822	C	1.919155	-0.304041	-0.695297	C	1.905704	-0.237133	-0.734305
C	-1.030947	3.602753	0.282269	C	-0.031279	-1.689137	-0.446684	C	-0.049036	-1.630926	-0.598507
C	-2.436611	1.287092	-0.346796	C	2.699177	-1.257682	-0.028914	C	2.667063	-1.223283	-0.093358
C	-2.192498	3.685479	-0.462714	C	0.720203	-2.626245	0.242355	C	0.681965	-2.600803	0.065821
H	-0.467698	4.504466	0.519693	H	-1.079982	-1.891225	-0.656675	H	-1.088532	-1.822424	-0.853988
C	-2.886482	2.527958	-0.783978	C	2.071337	-2.408509	0.448648	C	2.026968	-2.392472	0.318869
H	-2.549217	4.650956	-0.813474	H	0.255973	-3.544360	0.594179	H	0.206653	-3.533850	0.360045
H	-3.779015	2.573183	-1.406030	H	2.675126	-3.161043	0.953027	H	2.618433	-3.166373	0.805267
O	-0.888254	0.009021	0.944305	O	2.478204	0.839374	-1.189132	O	2.479061	0.922420	-1.169081
C	-1.637980	-0.458459	2.082352	C	2.902753	1.831542	-0.239236	C	2.910337	1.869542	-0.176592
H	-2.691962	-0.169708	1.937113	H	3.614639	1.363229	0.460621	H	3.606558	1.363388	0.512133
C	-1.536078	-1.962742	2.097054	C	3.611740	2.887068	-1.047089	C	3.645572	2.942379	-0.936991
H	-2.071512	-2.372216	2.960264	H	3.992791	3.682083	-0.397683	H	4.032994	3.705905	-0.254471
H	-1.965205	-2.396601	1.187691	H	4.454760	2.456821	-1.597130	H	4.487186	2.518700	-1.494184
H	-0.487239	-2.280218	2.171817	H	2.921203	3.335071	-1.771513	H	2.970628	3.428919	-1.651112
C	-1.113698	0.174421	3.351528	C	1.727062	2.382230	0.535806	C	1.734360	2.410359	0.604615
H	-0.064422	-0.099279	3.514888	H	0.984994	2.823889	-0.140946	H	1.003385	2.877456	-0.067259
H	-1.171113	1.267118	3.307646	H	1.230954	1.599255	1.120274	H	1.225863	1.617143	1.163890
H	-1.698429	-0.160061	4.216208	H	2.063070	3.156094	1.235533	H	2.071906	3.162122	1.327187
C	-3.139525	0.048417	-0.748257	C	4.156735	-1.090387	0.157762	C	4.120697	-1.069697	0.131817
C	-4.483083	-0.155466	-0.440700	C	4.733929	-1.313306	1.408005	C	4.668526	-1.329761	1.388097
C	-2.458506	-0.937411	-1.461936	C	4.987745	-0.731577	-0.905627	C	4.975905	-0.683840	-0.902286
C	-5.126885	-1.324244	-0.823755	C	6.101445	-1.175405	1.596241	C	6.031529	-1.199820	1.611114
H	-5.020743	0.607530	0.121557	H	4.093887	-1.578468	2.248348	H	4.008375	-1.616128	2.205658
C	-3.100405	-2.101895	-1.849908	C	6.353993	-0.595929	-0.717648	C	6.337641	-0.556618	-0.679746
H	-1.411493	-0.779485	-1.715740	H	4.551697	-0.557955	-1.886418	H	4.561792	-0.481608	-1.887171
C	-4.436812	-2.301505	-1.526392	C	6.916087	-0.814452	0.533538	C	6.870589	-0.810753	0.577612
H	-6.173803	-1.473104	-0.568173	H	6.531580	-1.345617	2.580901	H	6.439007	-1.398278	2.600089
H	-2.550694	-2.859255	-2.405559	H	6.987968	-0.322174	-1.558438	H	6.991370	-0.261255	-1.497789
H	-4.941080	-3.217715	-1.825403	H	7.988521	-0.704627	0.678138	H	7.939560	-0.706994	0.749731

C	3.168099	-1.474225	2.853488	C	-4.833654	0.392486	-2.759656	C	-5.726910	0.966439	-1.294194
H	2.188040	-1.778985	3.223458	H	-4.347760	-0.393334	-3.338830	H	-6.101093	0.694117	-0.309996
H	4.005495	-1.617939	3.531970	H	-5.538740	1.023198	-3.294987	H	-6.370554	1.575280	-1.922918

Table S6 (continued)

Compound S28				Compound S29			
C	-4.464576	0.510979	-1.472961	C	-2.178515	0.146576	2.162960
H	-4.197798	0.956231	-2.433649	H	-1.896035	-0.815938	2.595112
C	-3.370039	-0.277416	-0.819700	C	-1.858021	0.292134	0.708113
H	-3.009065	-1.028975	-1.548663	H	-0.769402	0.150831	0.596232
C	-2.150832	0.607526	-0.484621	C	-2.507949	-0.813074	-0.149097
H	-1.535996	0.021174	0.219021	H	-2.286389	-0.546604	-1.198394
O	-2.502363	1.855672	0.064827	O	-3.890910	-0.960367	0.052474
C	-3.052521	1.868690	1.381236	C	-4.756429	0.122461	-0.278748
H	-3.848757	1.113516	1.451097	H	-4.481924	1.003587	0.319409
C	-1.993497	1.573371	2.423663	C	-4.687543	0.484541	-1.748424
H	-1.564906	0.571818	2.306649	H	-3.726916	0.936842	-2.015301
H	-1.181246	2.308177	2.357689	H	-4.843907	-0.407526	-2.368543
H	-2.421216	1.627034	3.431458	H	-5.469368	1.211462	-1.996321
C	-3.643286	3.246460	1.553610	C	-6.133263	-0.348426	0.122784
H	-4.099054	3.359952	2.543402	H	-6.881767	0.433832	-0.043612
H	-2.861084	4.007809	1.445171	H	-6.418585	-1.231596	-0.461842
H	-4.407282	3.433602	0.792331	H	-6.146891	-0.623666	1.182052
O	-3.781822	-0.925715	0.360711	O	-2.224953	1.555810	0.203008
C	-4.421217	-2.185162	0.186398	C	-1.162726	2.487447	0.059903
H	-5.082472	-2.132630	-0.696104	H	-0.496479	2.400174	0.939166
C	-5.251158	-2.418119	1.426139	C	-1.791350	3.859453	0.046082
H	-5.998160	-1.628881	1.558510	H	-2.328169	4.056755	0.979445
H	-5.771394	-3.380671	1.378898	H	-1.034684	4.639364	-0.091832
H	-4.604538	-2.421541	2.311739	H	-2.509614	3.930056	-0.780046
C	-3.395228	-3.284738	-0.007294	C	-0.381598	2.212744	-1.209855
H	-2.816820	-3.156548	-0.928598	H	0.028225	1.196971	-1.232420
H	-2.696257	-3.292149	0.838251	H	-1.037992	2.328811	-2.082105
H	-3.878383	-4.266731	-0.064786	H	0.461337	2.906220	-1.318416
C	-1.347206	0.940864	-1.700534	C	-1.916945	-2.153672	0.177388
H	-1.787774	1.713622	-2.332735	H	-2.563457	-2.783912	0.788091
C	-0.134249	0.481209	-1.998951	C	-0.711265	-2.588884	-0.168300
H	0.380065	0.914932	-2.856958	H	-0.392965	-3.571110	0.185823
C	0.626921	-0.529371	-1.249698	C	0.252352	-1.846148	-1.011757
C	1.944933	-0.244692	-0.871346	C	1.305416	-1.133686	-0.429571
C	0.090579	-1.772036	-0.920543	C	0.123587	-1.846049	-2.398548
C	2.725089	-1.186899	-0.189553	C	2.209051	-0.406313	-1.218560
C	0.837431	-2.706302	-0.220927	C	1.032770	-1.168563	-3.194790
H	-0.920768	-2.011548	-1.242681	H	-0.704378	-2.393970	-2.845599
C	2.143152	-2.413440	0.134979	C	2.065053	-0.457817	-2.604845

H	0.407873	-3.675332	0.023401	H	0.924873	-1.176274	-4.276653
H	2.748419	-3.157639	0.649949	H	2.752625	0.118120	-3.222109
O	2.441742	0.982809	-1.196269	O	1.362578	-1.088978	0.934913
C	2.608191	1.918893	-0.114443	C	2.471212	-1.733846	1.581126
H	3.314999	1.483218	0.611853	H	3.402322	-1.411943	1.087209
C	3.224990	3.141568	-0.741164	C	2.452856	-1.239113	3.004133
H	3.424671	3.907913	0.014937	H	3.253934	-1.703224	3.588787
H	4.168642	2.887037	-1.234981	H	2.580407	-0.152751	3.041467
H	2.545384	3.564126	-1.490679	H	1.493319	-1.488305	3.473293
C	1.295273	2.209927	0.578591	C	2.339099	-3.236950	1.485645
H	0.545528	2.595534	-0.122821	H	1.417198	-3.569303	1.978107
H	0.876962	1.313642	1.052015	H	2.317468	-3.574181	0.443135
H	1.448957	2.954891	1.368090	H	3.186839	-3.728932	1.975440
C	4.130281	-0.911965	0.179241	C	3.251627	0.457298	-0.623134
C	4.587151	-1.190560	1.467883	C	4.569844	0.391743	-1.074605
C	5.030298	-0.379713	-0.746965	C	2.935220	1.378973	0.377663
C	5.903080	-0.937339	1.826260	C	5.547767	1.216297	-0.537369
H	3.890533	-1.588321	2.204444	H	4.832392	-0.332250	-1.844645
C	6.345106	-0.129734	-0.389204	C	3.911851	2.203505	0.912918
H	4.687035	-0.156439	-1.753989	H	1.911034	1.442973	0.740327
C	6.786117	-0.404927	0.899026	C	5.222320	2.123730	0.459720
H	6.238199	-1.152630	2.838620	H	6.571871	1.144262	-0.897112
H	7.034543	0.280777	-1.123953	H	3.646834	2.918870	1.688628
H	7.817735	-0.203235	1.178754	H	5.987881	2.769854	0.883252
C	-5.675078	0.700797	-0.973864	C	-2.736562	1.080515	2.915791
H	-5.963443	0.278279	-0.013625	H	-3.026408	2.040939	2.494944
H	-6.421830	1.290637	-1.497765	H	-2.934097	0.920585	3.972153

■ X-ray Crystal Structure of Ru Complex IV:

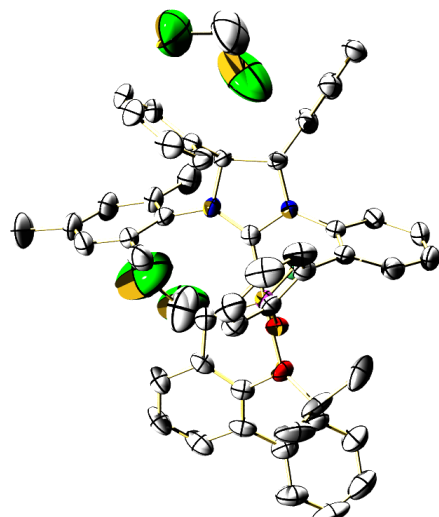


Table S7. Crystal Data and Structure Refinement for **IV**

Identification code	IV
Empirical formula	C ₅₄ H ₅₁ C ₁₄ I N ₂ O ₂ Ru
Formula weight	1129.74
Temperature	193(2) K
Wavelength	0.71073 Å
Crystal system	Monoclinic
Space group	P2(1)
Unit cell dimensions	a = 12.6693(18) Å α= 90°. b = 15.589(2) Å β= 90.318(2)°. c = 12.7899(18) Å γ = 90°.
Volume	2526.0(6) Å ³
Z	2
Density (calculated)	1.485 Mg/m ³
Absorption coefficient	1.175 mm ⁻¹
F(000)	1140
Crystal size	0.10 x 0.10 x 0.05 mm ³
Theta range for data collection:	1.59 to 28.38°.
Index ranges	-14<=h<=16, -20<=k<=16, -15<=l<=17
Reflections collected	19260
Independent reflections	10888 [R(int) = 0.0274]
Completeness to theta = 28.38°	99.7 %
Absorption correction	Empirical
Max. and min. transmission	0.9436 and 0.8916
Refinement method	Full-matrix least-squares on F ²
Data / restraints / parameters	10888 / 1 / 582
Goodness-of-fit on F ²	1.044
Final R indices [I>2sigma(I)]	R1 = 0.0504, wR2 = 0.1223
R indices (all data)	R1 = 0.0641, wR2 = 0.1328

Absolute structure parameter	0.02(2)
Largest diff. peak and hole	1.020 and -0.777 e. \AA^{-3}

Table S8. Atomic Coordinates ($\times 10^4$) and Equivalent Isotropic Displacement Parameters ($\text{\AA}^2 \times 10^3$) for **IV**. U(eq) is Defined as 1/3 of the Trace of the Orthogonalized U^{ij} Tensor

	x	y	z	U(eq)
Cl(3S)	4770(5)	8596(5)	283(6)	243(3)
C(29)	10597(4)	7823(4)	3716(5)	40(1)
Ru(1)	8077(1)	8785(1)	2800(1)	31(1)
I(2)	6182(1)	8762(1)	3667(1)	49(1)
C(103)	8186(4)	7533(4)	2825(4)	31(1)
O(2)	7914(3)	10229(3)	2831(3)	40(1)
C(27)	7642(4)	6932(4)	1080(4)	36(1)
O(1)	9607(3)	8950(2)	2908(3)	36(1)
N(2)	8049(3)	6890(3)	2136(3)	31(1)
C(2)	8172(4)	6029(3)	2603(4)	29(1)
C(9)	8198(4)	5191(4)	5204(4)	39(1)
C(17)	9738(6)	8344(4)	6440(5)	59(2)
C(10)	7788(4)	5800(3)	4551(4)	32(1)
C(19)	8232(5)	7743(4)	5524(4)	43(1)
C(3)	8489(4)	6238(3)	3745(4)	31(1)
C(18)	8668(6)	8121(5)	6411(4)	52(2)
C(14)	6732(4)	6008(4)	4629(4)	42(1)
C(22)	8316(5)	7034(4)	236(4)	40(1)
C(23)	7903(6)	7025(5)	-762(5)	53(2)
C(16)	10330(6)	8226(4)	5573(5)	53(2)
C(15)	9916(5)	7879(4)	4654(4)	38(1)

C(5)	8580(6)	4822(4)	1377(4)	49(2)
C(33)	7457(4)	9849(4)	1145(4)	39(1)
C(13)	6106(5)	5592(5)	5338(5)	49(2)
C(35)	7511(4)	10513(4)	1884(5)	37(1)
C(12)	6526(5)	4977(5)	5991(4)	49(2)
C(28)	5805(5)	6745(6)	1801(5)	60(2)
C(4)	8944(4)	5459(3)	2017(4)	36(1)
C(38)	6324(5)	11754(5)	3374(5)	51(2)
C(21)	9472(5)	7179(5)	391(5)	60(2)
C(36)	7125(4)	11324(4)	1695(5)	45(1)
C(34)	8677(5)	10822(5)	3393(7)	62(2)
N(1)	8429(3)	7173(3)	3763(3)	30(1)
C(20)	8855(5)	7631(4)	4637(4)	36(1)
C(30)	10385(4)	8361(4)	2863(4)	36(1)
C(31)	11083(5)	8372(4)	2023(5)	47(1)
C(24)	6825(6)	6904(5)	-953(5)	59(2)
C(8)	10715(6)	5062(5)	1558(6)	60(2)
C(6)	9292(7)	4315(4)	839(5)	59(2)
C(26)	6548(5)	6823(4)	926(4)	44(1)
C(32)	7693(4)	8979(4)	1439(4)	40(1)
C(11)	7565(5)	4784(4)	5928(5)	50(2)
C(25)	6180(6)	6827(5)	-108(5)	55(2)
C(37)	6923(4)	11967(4)	2513(5)	46(1)
C(7)	10352(6)	4432(5)	943(6)	60(2)
C(42)	7123(5)	10068(5)	119(5)	50(2)
C(44)	6831(5)	11507(5)	654(5)	55(2)
C(43)	6842(6)	10908(5)	-106(5)	58(2)
C(49)	7004(6)	13396(5)	3202(8)	78(3)
C(45)	10030(5)	5573(4)	2117(5)	47(1)
C(48)	7265(6)	12815(5)	2426(7)	64(2)
C(47)	11933(6)	7851(5)	2011(6)	65(2)

C(46)	11511(5)	7312(5)	3674(6)	57(2)
C(53)	12155(5)	7328(6)	2866(8)	71(2)
C(51)	6094(6)	12344(5)	4142(6)	64(2)
C(54)	8797(6)	10378(6)	4472(6)	71(2)
C(50)	6457(7)	13175(6)	4055(8)	71(2)
C(52)	6393(8)	6852(8)	-2076(6)	95(3)
C(55)	9652(6)	10947(5)	2767(8)	82(3)
Cl(2S)	3625(5)	5485(5)	3596(4)	226(3)
Cl(1S)	4430(7)	4246(4)	2202(4)	237(3)
C(124)	4443(9)	9489(10)	985(11)	133(5)
C(123)	4244(14)	4519(11)	3471(11)	164(7)
Cl(4S)	3197(4)	9693(3)	998(5)	179(2)

Table S9. Bond Lengths [Å] and Angles [°] for **IV**

Cl(3S)-C(124)	1.709(14)
C(29)-C(30)	1.400(8)
C(29)-C(46)	1.407(9)
C(29)-C(15)	1.484(8)
Ru(1)-C(32)	1.830(6)
Ru(1)-C(103)	1.957(6)
Ru(1)-O(1)	1.960(3)
Ru(1)-O(2)	2.261(4)
Ru(1)-I(2)	2.6504(5)
C(103)-N(2)	1.346(7)
C(103)-N(1)	1.358(7)
O(2)-C(35)	1.384(7)
O(2)-C(34)	1.517(7)
C(27)-C(22)	1.390(7)
C(27)-C(26)	1.409(8)

C(27)-N(2)	1.444(7)
O(1)-C(30)	1.348(7)
N(2)-C(2)	1.476(7)
C(2)-C(4)	1.522(7)
C(2)-C(3)	1.548(7)
C(2)-H(2)	1.0000
C(9)-C(10)	1.366(8)
C(9)-C(11)	1.382(8)
C(9)-H(9)	0.9500
C(17)-C(16)	1.355(10)
C(17)-C(18)	1.400(10)
C(17)-H(17)	0.9500
C(10)-C(14)	1.381(7)
C(10)-C(3)	1.525(7)
C(19)-C(18)	1.390(8)
C(19)-C(20)	1.396(8)
C(19)-H(19)	0.9500
C(3)-N(1)	1.460(7)
C(3)-H(3)	1.0000
C(18)-H(18)	0.9500
C(14)-C(13)	1.372(8)
C(14)-H(14)	0.9500
C(22)-C(23)	1.377(8)
C(22)-C(21)	1.494(9)
C(23)-C(24)	1.399(10)
C(23)-H(23)	0.9500
C(16)-C(15)	1.394(8)
C(16)-H(16)	0.9500
C(15)-C(20)	1.398(8)
C(5)-C(4)	1.365(8)
C(5)-C(6)	1.385(10)

C(5)-H(5) 0.9500
C(33)-C(35) 1.403(9)
C(33)-C(42) 1.417(8)
C(33)-C(32) 1.439(8)
C(13)-C(12) 1.377(10)
C(13)-H(13) 0.9500
C(35)-C(36) 1.376(8)
C(12)-C(11) 1.352(9)
C(12)-H(12) 0.9500
C(28)-C(26) 1.472(9)
C(28)-H(28A) 0.9800
C(28)-H(28B) 0.9800
C(28)-H(28C) 0.9800
C(4)-C(45) 1.393(8)
C(38)-C(51) 1.378(10)
C(38)-C(37) 1.382(9)
C(38)-H(38) 0.9500
C(21)-H(21A) 0.9800
C(21)-H(21B) 0.9800
C(21)-H(21C) 0.9800
C(36)-C(44) 1.410(9)
C(36)-C(37) 1.472(9)
C(34)-C(55) 1.489(12)
C(34)-C(54) 1.551(12)
C(34)-H(34) 1.0000
N(1)-C(20) 1.430(7)
C(30)-C(31) 1.396(8)
C(31)-C(47) 1.350(10)
C(31)-H(31) 0.9500
C(24)-C(25) 1.364(10)
C(24)-C(52) 1.536(9)

C(8)-C(7)	1.339(10)
C(8)-C(45)	1.380(9)
C(8)-H(8)	0.9500
C(6)-C(7)	1.362(11)
C(6)-H(6)	0.9500
C(26)-C(25)	1.400(8)
C(32)-H(32)	0.9500
C(11)-H(11)	0.9500
C(25)-H(25)	0.9500
C(37)-C(48)	1.395(9)
C(7)-H(7)	0.9500
C(42)-C(43)	1.388(10)
C(42)-H(42)	0.9500
C(44)-C(43)	1.347(11)
C(44)-H(44)	0.9500
C(43)-H(43)	0.9500
C(49)-C(50)	1.341(12)
C(49)-C(48)	1.385(12)
C(49)-H(49)	0.9500
C(45)-H(45)	0.9500
C(48)-H(48)	0.9500
C(47)-C(53)	1.391(12)
C(47)-H(47)	0.9500
C(46)-C(53)	1.322(11)
C(46)-H(46)	0.9500
C(53)-H(53)	0.9500
C(51)-C(50)	1.380(12)
C(51)-H(51)	0.9500
C(54)-H(54A)	0.9800
C(54)-H(54B)	0.9800
C(54)-H(54C)	0.9800

C(50)-H(50)	0.9500
C(52)-H(52A)	0.9800
C(52)-H(52B)	0.9800
C(52)-H(52C)	0.9800
C(55)-H(55A)	0.9800
C(55)-H(55B)	0.9800
C(55)-H(55C)	0.9800
Cl(2S)-C(123)	1.706(17)
Cl(1S)-C(123)	1.696(16)
C(124)-Cl(4S)	1.610(12)
C(124)-H(12A)	0.9900
C(124)-H(12B)	0.9900
C(123)-H(12C)	0.9900
C(123)-H(12D)	0.9900
C(30)-C(29)-C(46)	117.7(6)
C(30)-C(29)-C(15)	119.0(5)
C(46)-C(29)-C(15)	123.1(6)
C(32)-Ru(1)-C(103)	101.5(2)
C(32)-Ru(1)-O(1)	107.7(2)
C(103)-Ru(1)-O(1)	93.46(18)
C(32)-Ru(1)-O(2)	80.1(2)
C(103)-Ru(1)-O(2)	177.69(17)
O(1)-Ru(1)-O(2)	87.64(15)
C(32)-Ru(1)-I(2)	99.41(16)
C(103)-Ru(1)-I(2)	92.50(15)
O(1)-Ru(1)-I(2)	150.47(11)
O(2)-Ru(1)-I(2)	85.56(11)
N(2)-C(103)-N(1)	107.4(5)
N(2)-C(103)-Ru(1)	136.4(4)
N(1)-C(103)-Ru(1)	116.2(4)
C(35)-O(2)-C(34)	116.7(5)

C(35)-O(2)-Ru(1)	109.7(3)
C(34)-O(2)-Ru(1)	123.9(3)
C(22)-C(27)-C(26)	120.9(5)
C(22)-C(27)-N(2)	120.9(5)
C(26)-C(27)-N(2)	118.2(5)
C(30)-O(1)-Ru(1)	129.1(3)
C(103)-N(2)-C(27)	128.5(5)
C(103)-N(2)-C(2)	113.5(4)
C(27)-N(2)-C(2)	117.1(4)
N(2)-C(2)-C(4)	113.5(4)
N(2)-C(2)-C(3)	102.5(4)
C(4)-C(2)-C(3)	115.1(4)
N(2)-C(2)-H(2)	108.5
C(4)-C(2)-H(2)	108.5
C(3)-C(2)-H(2)	108.5
C(10)-C(9)-C(11)	120.6(5)
C(10)-C(9)-H(9)	119.7
C(11)-C(9)-H(9)	119.7
C(16)-C(17)-C(18)	118.9(6)
C(16)-C(17)-H(17)	120.5
C(18)-C(17)-H(17)	120.5
C(9)-C(10)-C(14)	119.0(5)
C(9)-C(10)-C(3)	120.2(5)
C(14)-C(10)-C(3)	120.8(5)
C(18)-C(19)-C(20)	119.5(6)
C(18)-C(19)-H(19)	120.3
C(20)-C(19)-H(19)	120.3
N(1)-C(3)-C(10)	114.0(4)
N(1)-C(3)-C(2)	102.2(4)
C(10)-C(3)-C(2)	113.2(4)
N(1)-C(3)-H(3)	109.1

C(10)-C(3)-H(3)	109.1
C(2)-C(3)-H(3)	109.1
C(19)-C(18)-C(17)	120.5(6)
C(19)-C(18)-H(18)	119.7
C(17)-C(18)-H(18)	119.7
C(13)-C(14)-C(10)	120.0(6)
C(13)-C(14)-H(14)	120.0
C(10)-C(14)-H(14)	120.0
C(23)-C(22)-C(27)	119.1(6)
C(23)-C(22)-C(21)	119.5(6)
C(27)-C(22)-C(21)	121.4(5)
C(22)-C(23)-C(24)	122.0(6)
C(22)-C(23)-H(23)	119.0
C(24)-C(23)-H(23)	119.0
C(17)-C(16)-C(15)	122.5(6)
C(17)-C(16)-H(16)	118.8
C(15)-C(16)-H(16)	118.8
C(16)-C(15)-C(20)	118.4(6)
C(16)-C(15)-C(29)	119.1(5)
C(20)-C(15)-C(29)	122.3(5)
C(4)-C(5)-C(6)	119.6(6)
C(4)-C(5)-H(5)	120.2
C(6)-C(5)-H(5)	120.2
C(35)-C(33)-C(42)	117.4(6)
C(35)-C(33)-C(32)	120.6(5)
C(42)-C(33)-C(32)	122.0(6)
C(14)-C(13)-C(12)	120.5(6)
C(14)-C(13)-H(13)	119.8
C(12)-C(13)-H(13)	119.8
C(36)-C(35)-O(2)	125.2(6)
C(36)-C(35)-C(33)	122.9(6)

O(2)-C(35)-C(33)	111.7(5)
C(11)-C(12)-C(13)	119.5(6)
C(11)-C(12)-H(12)	120.3
C(13)-C(12)-H(12)	120.3
C(26)-C(28)-H(28A)	109.5
C(26)-C(28)-H(28B)	109.5
H(28A)-C(28)-H(28B)	109.5
C(26)-C(28)-H(28C)	109.5
H(28A)-C(28)-H(28C)	109.5
H(28B)-C(28)-H(28C)	109.5
C(5)-C(4)-C(45)	118.5(5)
C(5)-C(4)-C(2)	120.3(5)
C(45)-C(4)-C(2)	121.1(5)
C(51)-C(38)-C(37)	121.9(7)
C(51)-C(38)-H(38)	119.1
C(37)-C(38)-H(38)	119.1
C(22)-C(21)-H(21A)	109.5
C(22)-C(21)-H(21B)	109.5
H(21A)-C(21)-H(21B)	109.5
C(22)-C(21)-H(21C)	109.5
H(21A)-C(21)-H(21C)	109.5
H(21B)-C(21)-H(21C)	109.5
C(35)-C(36)-C(44)	116.3(6)
C(35)-C(36)-C(37)	124.4(6)
C(44)-C(36)-C(37)	119.2(6)
C(55)-C(34)-O(2)	110.7(6)
C(55)-C(34)-C(54)	117.4(6)
O(2)-C(34)-C(54)	102.0(6)
C(55)-C(34)-H(34)	108.8
O(2)-C(34)-H(34)	108.8
C(54)-C(34)-H(34)	108.8

C(103)-N(1)-C(20)	124.6(5)
C(103)-N(1)-C(3)	114.2(4)
C(20)-N(1)-C(3)	119.4(4)
C(19)-C(20)-C(15)	120.1(5)
C(19)-C(20)-N(1)	119.0(5)
C(15)-C(20)-N(1)	120.5(5)
O(1)-C(30)-C(31)	119.4(5)
O(1)-C(30)-C(29)	120.8(5)
C(31)-C(30)-C(29)	119.1(5)
C(47)-C(31)-C(30)	120.7(7)
C(47)-C(31)-H(31)	119.6
C(30)-C(31)-H(31)	119.6
C(25)-C(24)-C(23)	117.5(6)
C(25)-C(24)-C(52)	121.6(7)
C(23)-C(24)-C(52)	120.9(7)
C(7)-C(8)-C(45)	120.9(7)
C(7)-C(8)-H(8)	119.6
C(45)-C(8)-H(8)	119.6
C(7)-C(6)-C(5)	121.3(6)
C(7)-C(6)-H(6)	119.3
C(5)-C(6)-H(6)	119.3
C(25)-C(26)-C(27)	117.0(6)
C(25)-C(26)-C(28)	120.5(6)
C(27)-C(26)-C(28)	122.4(5)
C(33)-C(32)-Ru(1)	117.3(4)
C(33)-C(32)-H(32)	121.3
Ru(1)-C(32)-H(32)	121.3
C(12)-C(11)-C(9)	120.4(6)
C(12)-C(11)-H(11)	119.8
C(9)-C(11)-H(11)	119.8
C(24)-C(25)-C(26)	123.4(6)

C(24)-C(25)-H(25)	118.3
C(26)-C(25)-H(25)	118.3
C(38)-C(37)-C(48)	117.6(7)
C(38)-C(37)-C(36)	120.1(6)
C(48)-C(37)-C(36)	122.2(7)
C(8)-C(7)-C(6)	119.4(6)
C(8)-C(7)-H(7)	120.3
C(6)-C(7)-H(7)	120.3
C(43)-C(42)-C(33)	119.6(7)
C(43)-C(42)-H(42)	120.2
C(33)-C(42)-H(42)	120.2
C(43)-C(44)-C(36)	122.6(6)
C(43)-C(44)-H(44)	118.7
C(36)-C(44)-H(44)	118.7
C(44)-C(43)-C(42)	120.5(6)
C(44)-C(43)-H(43)	119.7
C(42)-C(43)-H(43)	119.7
C(50)-C(49)-C(48)	122.7(8)
C(50)-C(49)-H(49)	118.6
C(48)-C(49)-H(49)	118.6
C(8)-C(45)-C(4)	120.2(6)
C(8)-C(45)-H(45)	119.9
C(4)-C(45)-H(45)	119.9
C(49)-C(48)-C(37)	119.2(8)
C(49)-C(48)-H(48)	120.4
C(37)-C(48)-H(48)	120.4
C(31)-C(47)-C(53)	120.1(7)
C(31)-C(47)-H(47)	119.9
C(53)-C(47)-H(47)	119.9
C(53)-C(46)-C(29)	122.1(7)
C(53)-C(46)-H(46)	119.0

C(29)-C(46)-H(46)	118.9
C(46)-C(53)-C(47)	120.1(7)
C(46)-C(53)-H(53)	119.9
C(47)-C(53)-H(53)	119.9
C(38)-C(51)-C(50)	119.7(8)
C(38)-C(51)-H(51)	120.1
C(50)-C(51)-H(51)	120.1
C(34)-C(54)-H(54A)	109.5
C(34)-C(54)-H(54B)	109.5
H(54A)-C(54)-H(54B)	109.5
C(34)-C(54)-H(54C)	109.5
H(54A)-C(54)-H(54C)	109.5
H(54B)-C(54)-H(54C)	109.5
C(49)-C(50)-C(51)	118.8(8)
C(49)-C(50)-H(50)	120.6
C(51)-C(50)-H(50)	120.6
C(24)-C(52)-H(52A)	109.5
C(24)-C(52)-H(52B)	109.5
H(52A)-C(52)-H(52B)	109.5
C(24)-C(52)-H(52C)	109.5
H(52A)-C(52)-H(52C)	109.5
H(52B)-C(52)-H(52C)	109.5
C(34)-C(55)-H(55A)	109.5
C(34)-C(55)-H(55B)	109.5
H(55A)-C(55)-H(55B)	109.5
C(34)-C(55)-H(55C)	109.5
H(55A)-C(55)-H(55C)	109.5
H(55B)-C(55)-H(55C)	109.5
Cl(4S)-C(124)-Cl(3S)	114.0(8)
Cl(4S)-C(124)-H(12A)	108.7
Cl(3S)-C(124)-H(12A)	108.8

Cl(4S)-C(124)-H(12B)	108.7
Cl(3S)-C(124)-H(12B)	108.7
H(12A)-C(124)-H(12B)	107.6
Cl(1S)-C(123)-Cl(2S)	112.1(8)
Cl(1S)-C(123)-H(12C)	109.2
Cl(2S)-C(123)-H(12C)	109.2
Cl(1S)-C(123)-H(12D)	109.2
Cl(2S)-C(123)-H(12D)	109.2
H(12C)-C(123)-H(12D)	107.9

Symmetry transformations used to generate equivalent atoms:

Table S10. Anisotropic Displacement Parameters ($\text{\AA}^2 \times 10^3$) for **IV**. The Anisotropic Displacement Factor Exponent Takes the Form: $-2\mathbf{p}^2[\ h^2 \mathbf{a}^*{}^2 \mathbf{U}^{11} + \dots + 2 \mathbf{h} \mathbf{k} \mathbf{a}^* \mathbf{b}^* \mathbf{U}^{12}]$

	U11	U22	U33	U23	U13	U12
Cl(3S)	226(5)	178(6)	326(7)	-90(5)	122(5)	-14(4)
C(29)	37(3)	36(3)	45(3)	0(2)	-7(2)	-7(2)
Ru(1)	31(1)	29(1)	31(1)	0(1)	-2(1)	1(1)
I(2)	38(1)	56(1)	52(1)	-9(1)	8(1)	3(1)
C(103)	22(2)	38(3)	31(3)	0(2)	3(2)	-2(2)
O(2)	38(2)	35(2)	46(2)	-2(2)	-14(2)	-1(2)
C(27)	43(3)	29(3)	34(3)	-2(2)	-2(2)	2(2)
O(1)	35(2)	29(3)	43(2)	4(1)	-5(1)	-3(1)
N(2)	33(2)	32(2)	28(2)	-5(2)	-4(2)	-2(2)
C(2)	33(2)	26(3)	29(2)	-2(2)	3(2)	-3(2)
C(9)	36(3)	38(3)	43(3)	6(2)	-7(2)	-2(2)
C(17)	93(5)	47(4)	37(3)	-2(3)	-22(3)	-11(4)

C(10)	37(3)	28(3)	32(3)	-4(2)	7(2)	-1(2)
C(19)	59(4)	36(3)	35(3)	1(2)	6(3)	-1(3)
C(3)	32(2)	27(3)	34(3)	-1(2)	4(2)	0(2)
C(18)	81(5)	46(4)	28(3)	-1(2)	1(3)	-3(3)
C(14)	36(3)	52(4)	39(3)	4(3)	5(2)	9(3)
C(22)	53(3)	36(3)	30(3)	0(2)	4(2)	-3(3)
C(23)	78(5)	51(4)	30(3)	3(3)	7(3)	2(3)
C(16)	68(4)	43(4)	47(4)	9(3)	-20(3)	-13(3)
C(15)	49(3)	30(3)	35(3)	4(2)	-4(2)	-4(2)
C(5)	72(4)	45(4)	30(3)	-5(2)	7(3)	-9(3)
C(33)	30(2)	43(3)	43(3)	12(2)	0(2)	6(2)
C(13)	40(3)	61(4)	46(3)	-6(3)	11(3)	-2(3)
C(35)	27(2)	37(3)	46(3)	5(2)	0(2)	1(2)
C(12)	60(4)	58(4)	30(3)	2(3)	8(3)	-20(3)
C(28)	39(3)	82(6)	59(4)	-14(4)	-6(3)	-2(3)
C(4)	49(3)	26(3)	33(3)	3(2)	12(2)	0(2)
C(38)	52(3)	43(4)	58(4)	1(3)	-7(3)	-10(3)
C(21)	59(4)	70(5)	51(4)	10(3)	11(3)	-11(3)
C(36)	34(3)	40(3)	61(4)	12(3)	8(3)	-1(2)
C(34)	53(4)	31(4)	102(6)	-20(4)	-39(4)	9(3)
N(1)	35(2)	30(2)	24(2)	1(2)	-1(2)	-5(2)
C(20)	52(3)	25(3)	31(3)	3(2)	-3(2)	-2(2)
C(30)	32(3)	36(3)	40(3)	-6(2)	-6(2)	-8(2)
C(31)	38(3)	47(4)	55(4)	-6(3)	7(3)	-9(3)
C(24)	84(5)	59(5)	35(3)	-7(3)	-19(3)	-4(4)
C(8)	61(4)	55(5)	63(4)	-1(3)	26(3)	9(3)
C(6)	99(6)	41(4)	38(3)	-16(3)	11(3)	-6(4)
C(26)	43(3)	51(4)	37(3)	-8(3)	-5(2)	-1(3)
C(32)	39(3)	43(4)	39(3)	-1(2)	-1(2)	5(2)
C(11)	56(4)	46(4)	49(4)	15(3)	-4(3)	-13(3)
C(25)	53(4)	66(5)	45(4)	-8(3)	-17(3)	-3(3)

C(37) 33(3) 37(3) 67(4) 2(3) -9(3) 8(2)
 C(7) 82(5) 45(4) 53(4) -11(3) 25(4) 11(4)
 C(42) 52(4) 61(4) 37(3) 10(3) 4(3) 16(3)
 C(44) 50(4) 58(4) 58(4) 23(3) 13(3) 21(3)
 C(43) 62(4) 69(5) 43(4) 23(3) 3(3) 20(4)
 C(49) 67(5) 26(4) 141(9) -3(4) -26(6) 3(3)
 C(45) 52(3) 36(3) 52(4) -1(3) 15(3) 0(3)
 C(48) 60(4) 41(4) 92(6) 16(4) -14(4) -4(3)
 C(47) 60(4) 59(5) 77(5) -12(4) 20(4) -3(4)
 C(46) 41(3) 43(4) 86(5) 7(3) -5(3) 0(3)
 C(53) 39(4) 60(5) 115(7) -4(5) 19(4) 12(3)
 C(51) 64(4) 55(5) 73(5) -18(4) 2(4) 7(4)
 C(54) 64(4) 71(6) 78(5) -35(4) -37(4) 27(4)
 C(50) 70(5) 50(4) 93(6) -23(4) -27(5) 11(4)
 C(52) 132(8) 110(8) 43(4) -1(4) -36(5) -14(7)
 C(55) 57(4) 49(5) 139(8) 24(5) -31(5) -22(4)
 Cl(2S) 213(5) 258(7) 207(5) 98(5) 48(4) 139(5)
 Cl(1S) 396(9) 173(5) 139(4) 12(3) -111(5) 29(5)
 C(124) 107(9) 167(15) 125(10) -44(10)-5(8) 30(9)
 C(123) 210(16) 170(17) 113(10) 33(10)-48(11) 56(13)
 Cl(4S) 142(3) 143(4) 251(6) 5(4) 22(3) -16(3)

Table S11. Hydrogen Coordinates ($\times 10^4$) and Isotropic Displacement Parameters ($\text{\AA}^2 \times 10^3$) for **IV**

x	y	z	U(eq)
H(2)	7467	5742	2606
H(9)	8924	5046	5161

H(17)	10045	8576	7059	71
H(19)	7516	7563	5521	52
H(3)	9238	6059	3865	37
H(18)	8237	8228	7002	62
H(14)	6439	6440	4191	51
H(23)	8364	7103	-1338	63
H(16)	11053	8385	5592	63
H(5)	7843	4726	1302	59
H(13)	5376	5729	5379	59
H(12)	6091	4690	6482	59
H(28A)5082	6824	1542	90	
H(28B)5965	7184	2327	90	
H(28C)5873	6175	2117	90	
H(38)	6063	11186	3438	61
H(21A)9822	6630	527	90	
H(21B)9584	7564	988	90	
H(21C)9769	7440	-239	90	
H(34)	8328	11392	3494	74
H(31)	10958	8751	1454	56
H(8)	11454	5160	1611	72
H(6)	9035	3877	388	71
H(32)	7651	8524	947	48
H(11)	7861	4367	6385	61
H(25)	5442	6774	-228	66
H(7)	10831	4069	582	72
H(42)	7092	9641	-411	60
H(44)	6617	12073	482	66
H(43)	6655	11063	-801	69
H(49)	7221	13976	3126	94
H(45)	10300	6004	2570	56
H(48)	7672	12991	1842	77

H(47)	12381	7841	1418	78
H(46)	11669	6944	4245	68
H(53)	12772	6981	2868	85
H(51)	5686	12178	4730	77
H(54A)9164	9829	4386	107	
H(54B)8097	10276	4769	107	
H(54C)9205	10748	4944	107	
H(50)	6323	13583	4590	86
H(52A)5672	6624	-2066	143	
H(52B)6843	6472	-2491	143	
H(52C)6389	7426	-2388	143	
H(55A)9897	10391	2505	122	
H(55B)10202	11205	3207	122	
H(55C)9499	11328	2175	122	
H(12A)4692	9414	1714	160	
H(12B)4818	9989	688	160	
H(12C)4937	4544	3832	197	
H(12D)3816	4070	3816	197	

Table S12. Torsion Angles [°] for IV

C(32)-Ru(1)-C(103)-N(2)	-0.2(6)
O(1)-Ru(1)-C(103)-N(2)	-109.0(5)
O(2)-Ru(1)-C(103)-N(2)	133(4)
I(2)-Ru(1)-C(103)-N(2)	100.0(5)
C(32)-Ru(1)-C(103)-N(1)	-177.7(4)
O(1)-Ru(1)-C(103)-N(1)	73.5(4)
O(2)-Ru(1)-C(103)-N(1)	-45(5)
I(2)-Ru(1)-C(103)-N(1)	-77.6(4)
C(32)-Ru(1)-O(2)-C(35)	6.3(4)
C(103)-Ru(1)-O(2)-C(35)	-127(4)

O(1)-Ru(1)-O(2)-C(35)	114.7(4)
I(2)-Ru(1)-O(2)-C(35)	-94.1(3)
C(32)-Ru(1)-O(2)-C(34)	-138.4(5)
C(103)-Ru(1)-O(2)-C(34)	89(4)
O(1)-Ru(1)-O(2)-C(34)	-30.0(5)
I(2)-Ru(1)-O(2)-C(34)	121.3(5)
C(32)-Ru(1)-O(1)-C(30)	-95.6(4)
C(103)-Ru(1)-O(1)-C(30)	7.6(4)
O(2)-Ru(1)-O(1)-C(30)	-174.4(4)
I(2)-Ru(1)-O(1)-C(30)	108.9(4)
N(1)-C(103)-N(2)-C(27)	170.5(5)
Ru(1)-C(103)-N(2)-C(27)	-7.2(9)
N(1)-C(103)-N(2)-C(2)	1.5(6)
Ru(1)-C(103)-N(2)-C(2)	-176.1(4)
C(22)-C(27)-N(2)-C(103)	92.3(7)
C(26)-C(27)-N(2)-C(103)	-90.9(7)
C(22)-C(27)-N(2)-C(2)	-99.1(6)
C(26)-C(27)-N(2)-C(2)	77.8(6)
C(103)-N(2)-C(2)-C(4)	-128.1(5)
C(27)-N(2)-C(2)-C(4)	61.6(6)
C(103)-N(2)-C(2)-C(3)	-3.3(5)
C(27)-N(2)-C(2)-C(3)	-173.6(4)
C(11)-C(9)-C(10)-C(14)	0.5(9)
C(11)-C(9)-C(10)-C(3)	-179.3(5)
C(9)-C(10)-C(3)-N(1)	-129.3(5)
C(14)-C(10)-C(3)-N(1)	51.0(7)
C(9)-C(10)-C(3)-C(2)	114.4(6)
C(14)-C(10)-C(3)-C(2)	-65.3(7)
N(2)-C(2)-C(3)-N(1)	3.5(5)
C(4)-C(2)-C(3)-N(1)	127.2(4)
N(2)-C(2)-C(3)-C(10)	126.5(4)

C(4)-C(2)-C(3)-C(10)	-109.8(5)
C(20)-C(19)-C(18)-C(17)	-3.6(10)
C(16)-C(17)-C(18)-C(19)	3.2(10)
C(9)-C(10)-C(14)-C(13)	-1.5(9)
C(3)-C(10)-C(14)-C(13)	178.2(5)
C(26)-C(27)-C(22)-C(23)	-0.3(9)
N(2)-C(27)-C(22)-C(23)	176.5(6)
C(26)-C(27)-C(22)-C(21)	177.9(6)
N(2)-C(27)-C(22)-C(21)	-5.3(9)
C(27)-C(22)-C(23)-C(24)	-0.9(10)
C(21)-C(22)-C(23)-C(24)	-179.1(7)
C(18)-C(17)-C(16)-C(15)	-0.8(11)
C(17)-C(16)-C(15)-C(20)	-1.2(9)
C(17)-C(16)-C(15)-C(29)	175.9(6)
C(30)-C(29)-C(15)-C(16)	-109.8(6)
C(46)-C(29)-C(15)-C(16)	64.1(8)
C(30)-C(29)-C(15)-C(20)	67.2(8)
C(46)-C(29)-C(15)-C(20)	-118.9(7)
C(10)-C(14)-C(13)-C(12)	1.3(10)
C(34)-O(2)-C(35)-C(36)	-45.5(8)
Ru(1)-O(2)-C(35)-C(36)	167.0(5)
C(34)-O(2)-C(35)-C(33)	139.6(5)
Ru(1)-O(2)-C(35)-C(33)	-7.9(6)
C(42)-C(33)-C(35)-C(36)	8.9(8)
C(32)-C(33)-C(35)-C(36)	-168.6(5)
C(42)-C(33)-C(35)-O(2)	-176.0(5)
C(32)-C(33)-C(35)-O(2)	6.4(7)
C(14)-C(13)-C(12)-C(11)	-0.1(10)
C(6)-C(5)-C(4)-C(45)	-0.6(9)
C(6)-C(5)-C(4)-C(2)	179.2(6)
N(2)-C(2)-C(4)-C(5)	-103.3(6)

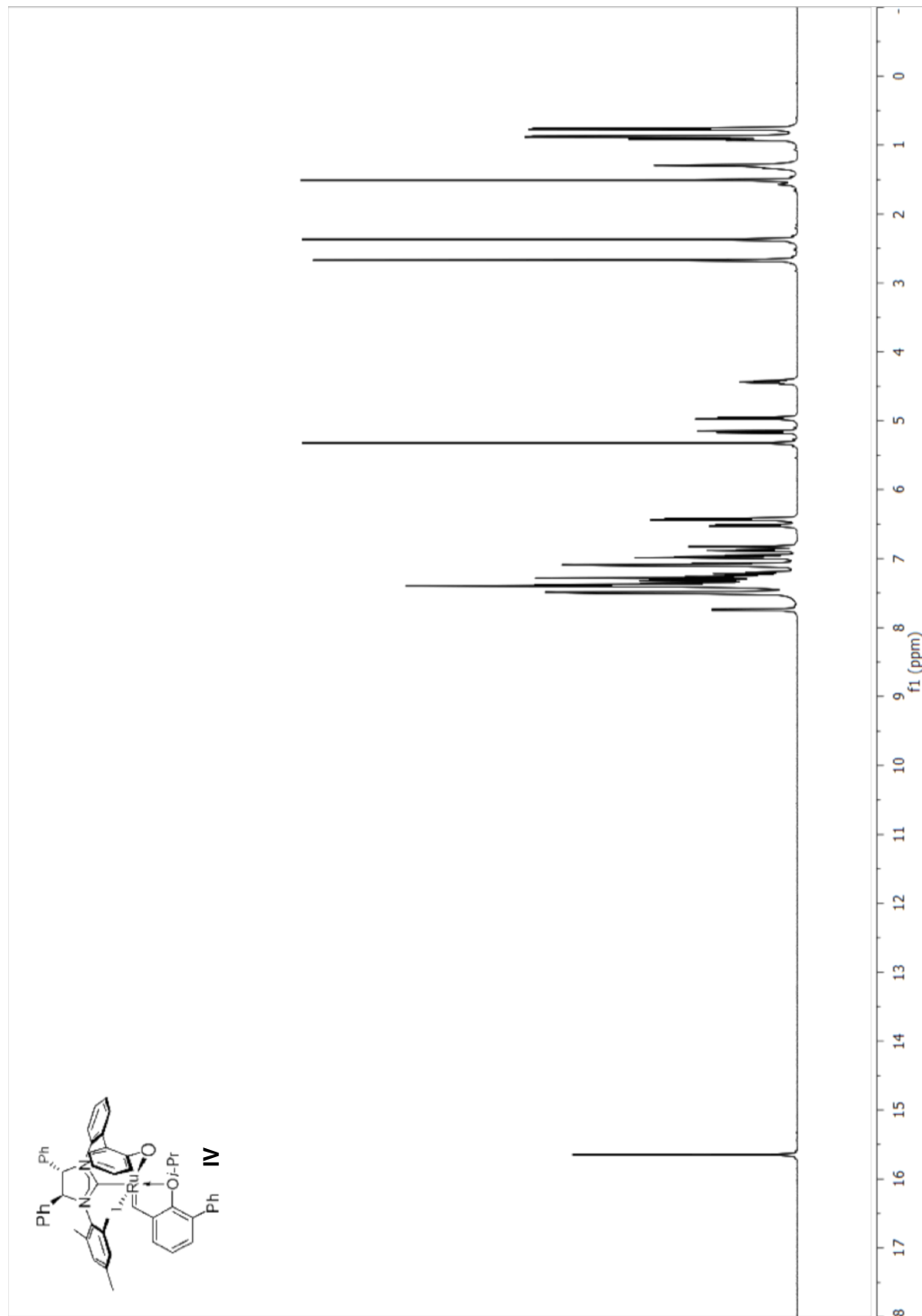
C(3)-C(2)-C(4)-C(5)	139.0(5)
N(2)-C(2)-C(4)-C(45)	76.5(6)
C(3)-C(2)-C(4)-C(45)	-41.2(7)
O(2)-C(35)-C(36)-C(44)	175.0(5)
C(33)-C(35)-C(36)-C(44)	-10.6(8)
O(2)-C(35)-C(36)-C(37)	-10.4(9)
C(33)-C(35)-C(36)-C(37)	164.0(6)
C(35)-O(2)-C(34)-C(55)	-63.8(7)
Ru(1)-O(2)-C(34)-C(55)	78.6(7)
C(35)-O(2)-C(34)-C(54)	170.6(5)
Ru(1)-O(2)-C(34)-C(54)	-47.0(7)
N(2)-C(103)-N(1)-C(20)	165.6(5)
Ru(1)-C(103)-N(1)-C(20)	-16.1(7)
N(2)-C(103)-N(1)-C(3)	1.1(6)
Ru(1)-C(103)-N(1)-C(3)	179.3(3)
C(10)-C(3)-N(1)-C(103)	-125.6(5)
C(2)-C(3)-N(1)-C(103)	-3.0(5)
C(10)-C(3)-N(1)-C(20)	69.0(6)
C(2)-C(3)-N(1)-C(20)	-168.4(4)
C(18)-C(19)-C(20)-C(15)	1.5(9)
C(18)-C(19)-C(20)-N(1)	174.4(6)
C(16)-C(15)-C(20)-C(19)	0.8(9)
C(29)-C(15)-C(20)-C(19)	-176.2(5)
C(16)-C(15)-C(20)-N(1)	-172.0(5)
C(29)-C(15)-C(20)-N(1)	11.0(8)
C(103)-N(1)-C(20)-C(19)	111.5(6)
C(3)-N(1)-C(20)-C(19)	-84.7(6)
C(103)-N(1)-C(20)-C(15)	-75.6(7)
C(3)-N(1)-C(20)-C(15)	88.2(6)
Ru(1)-O(1)-C(30)-C(31)	113.4(5)
Ru(1)-O(1)-C(30)-C(29)	-76.1(6)

C(46)-C(29)-C(30)-O(1)	-171.0(5)
C(15)-C(29)-C(30)-O(1)	3.2(8)
C(46)-C(29)-C(30)-C(31)	-0.5(8)
C(15)-C(29)-C(30)-C(31)	173.7(5)
O(1)-C(30)-C(31)-C(47)	173.0(6)
C(29)-C(30)-C(31)-C(47)	2.3(9)
C(22)-C(23)-C(24)-C(25)	2.5(11)
C(22)-C(23)-C(24)-C(52)	-176.9(8)
C(4)-C(5)-C(6)-C(7)	0.7(11)
C(22)-C(27)-C(26)-C(25)	-0.3(9)
N(2)-C(27)-C(26)-C(25)	-177.1(6)
C(22)-C(27)-C(26)-C(28)	-177.7(6)
N(2)-C(27)-C(26)-C(28)	5.4(9)
C(35)-C(33)-C(32)-Ru(1)	-0.7(7)
C(42)-C(33)-C(32)-Ru(1)	-178.2(4)
C(103)-Ru(1)-C(32)-C(33)	175.3(4)
O(1)-Ru(1)-C(32)-C(33)	-87.3(4)
O(2)-Ru(1)-C(32)-C(33)	-3.0(4)
I(2)-Ru(1)-C(32)-C(33)	80.8(4)
C(13)-C(12)-C(11)-C(9)	-1.0(10)
C(10)-C(9)-C(11)-C(12)	0.8(10)
C(23)-C(24)-C(25)-C(26)	-3.1(12)
C(52)-C(24)-C(25)-C(26)	176.3(8)
C(27)-C(26)-C(25)-C(24)	2.0(11)
C(28)-C(26)-C(25)-C(24)	179.5(7)
C(51)-C(38)-C(37)-C(48)	-2.0(10)
C(51)-C(38)-C(37)-C(36)	-178.3(6)
C(35)-C(36)-C(37)-C(38)	-51.3(8)
C(44)-C(36)-C(37)-C(38)	123.2(6)
C(35)-C(36)-C(37)-C(48)	132.6(7)
C(44)-C(36)-C(37)-C(48)	-52.9(8)

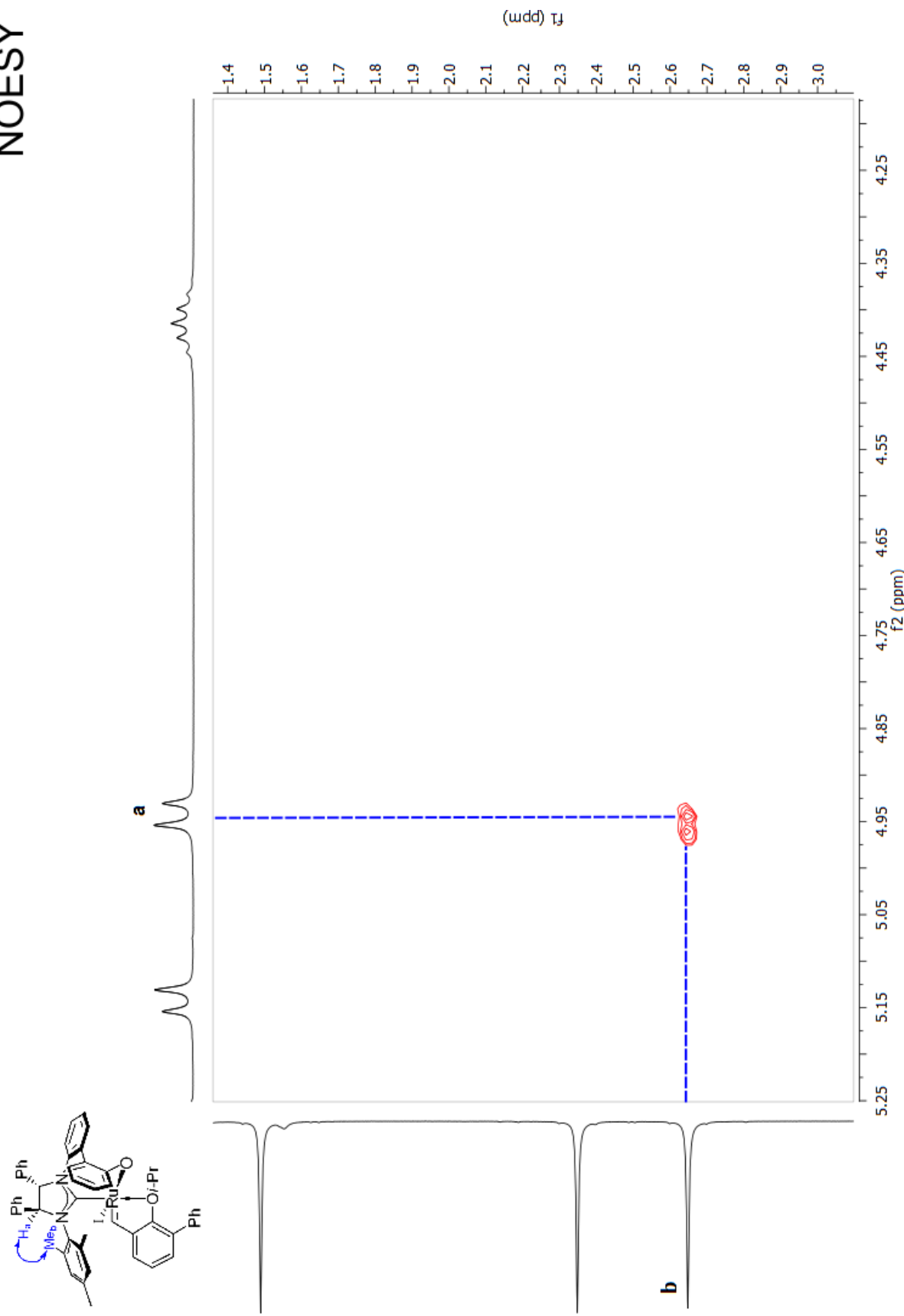
C(45)-C(8)-C(7)-C(6)	2.4(12)
C(5)-C(6)-C(7)-C(8)	-1.6(11)
C(35)-C(33)-C(42)-C(43)	-1.6(9)
C(32)-C(33)-C(42)-C(43)	176.0(6)
C(35)-C(36)-C(44)-C(43)	5.2(9)
C(37)-C(36)-C(44)-C(43)	-169.7(6)
C(36)-C(44)-C(43)-C(42)	1.7(11)
C(33)-C(42)-C(43)-C(44)	-3.5(10)
C(7)-C(8)-C(45)-C(4)	-2.4(11)
C(5)-C(4)-C(45)-C(8)	1.5(9)
C(2)-C(4)-C(45)-C(8)	-178.4(6)
C(50)-C(49)-C(48)-C(37)	1.9(11)
C(38)-C(37)-C(48)-C(49)	0.8(9)
C(36)-C(37)-C(48)-C(49)	176.9(6)
C(30)-C(31)-C(47)-C(53)	-3.5(11)
C(30)-C(29)-C(46)-C(53)	-0.1(10)
C(15)-C(29)-C(46)-C(53)	-174.1(7)
C(29)-C(46)-C(53)-C(47)	-1.0(12)
C(31)-C(47)-C(53)-C(46)	2.9(12)
C(37)-C(38)-C(51)-C(50)	0.7(11)
C(48)-C(49)-C(50)-C(51)	-3.3(12)
C(38)-C(51)-C(50)-C(49)	2.0(12)

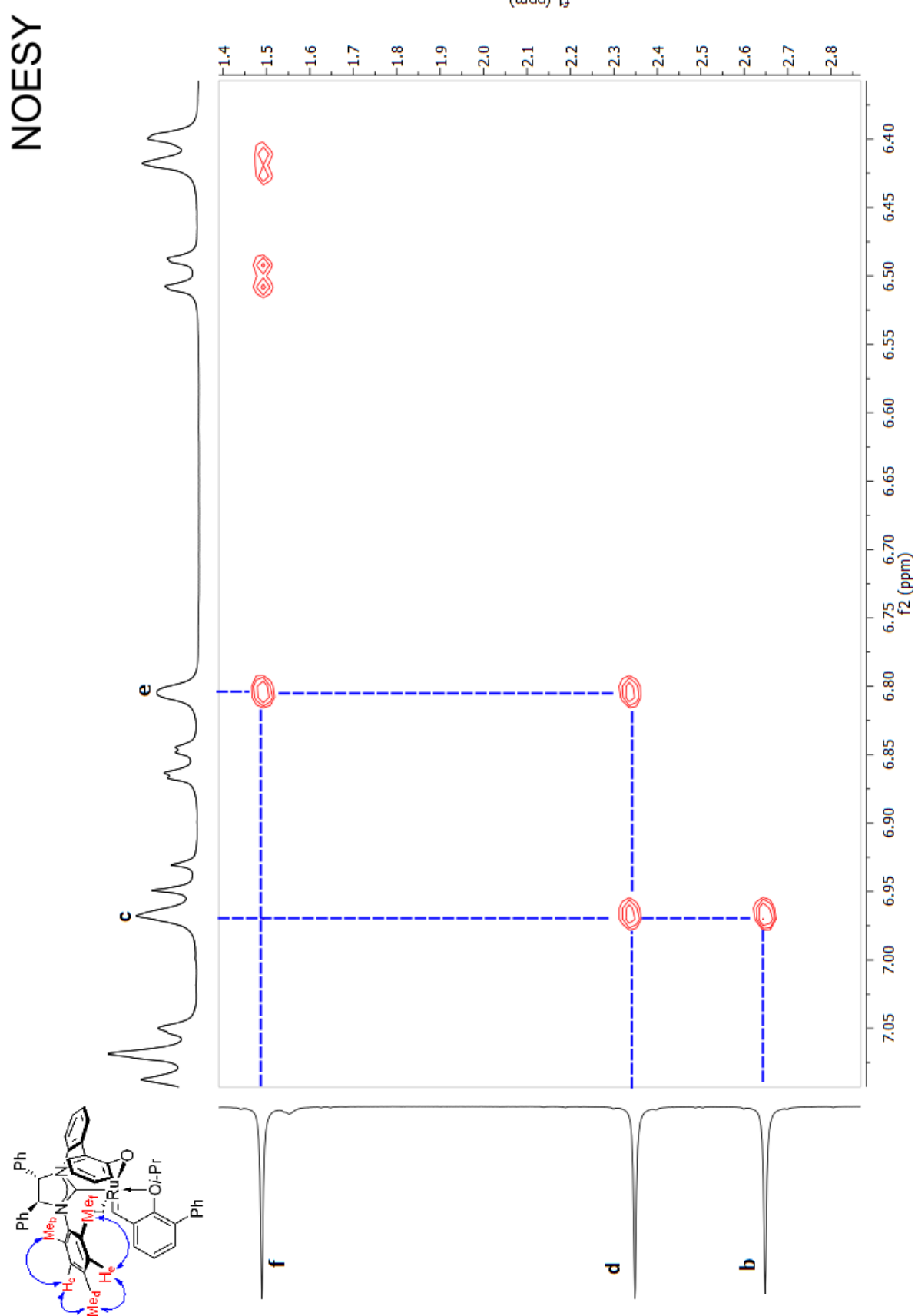
Symmetry transformations used to generate equivalent atoms.

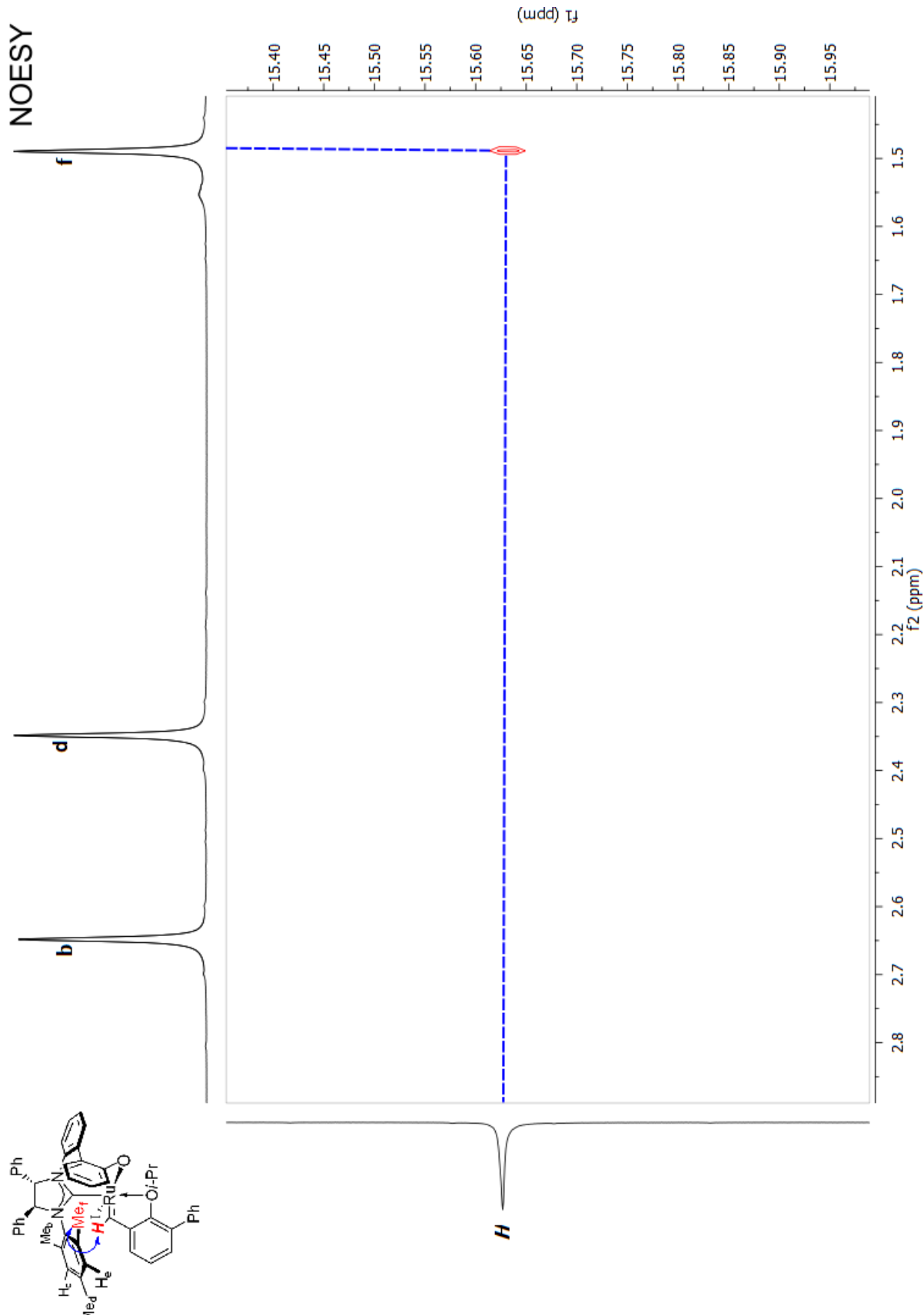
■ NMR Spectra for Complex IV:



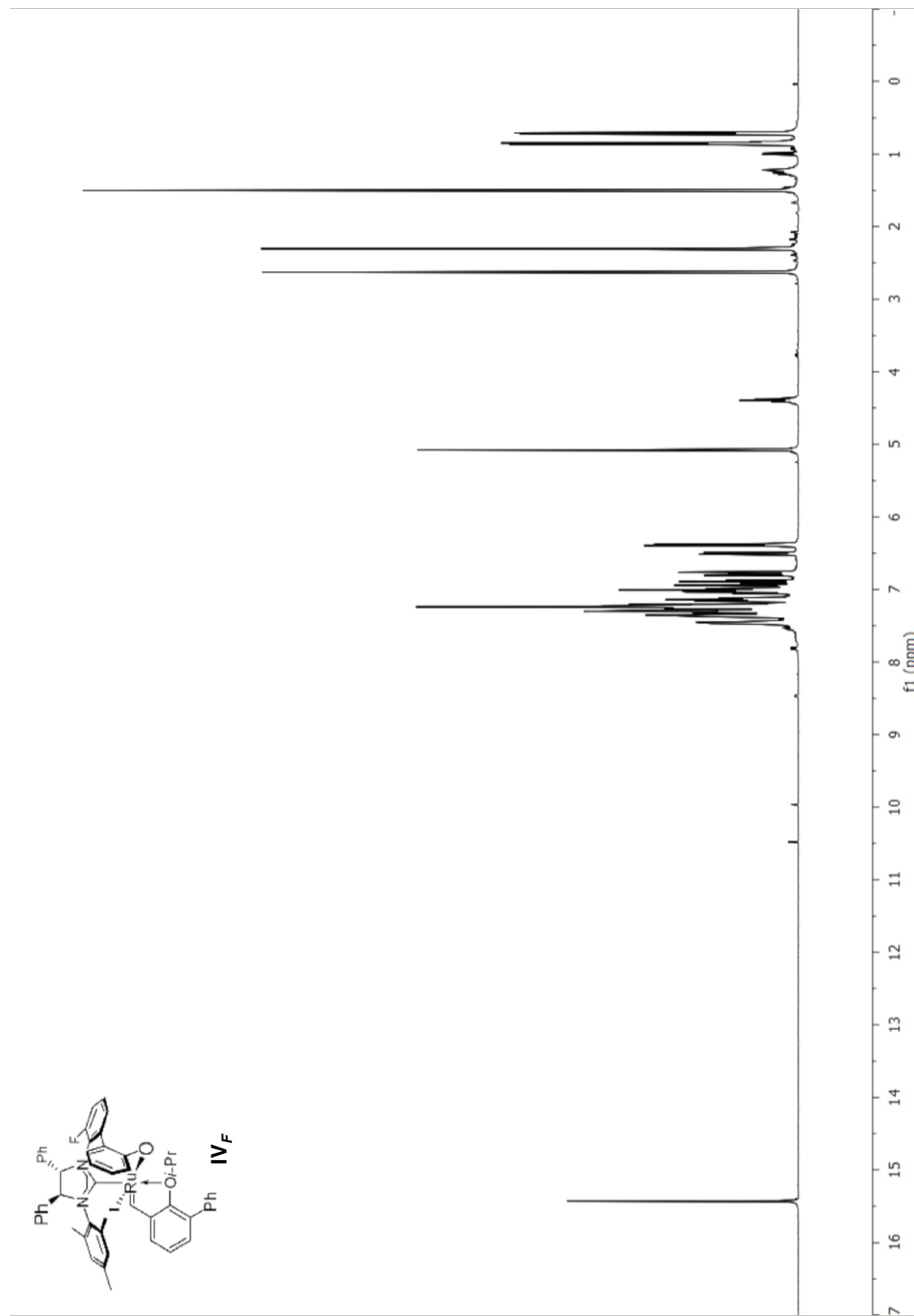
NOESY

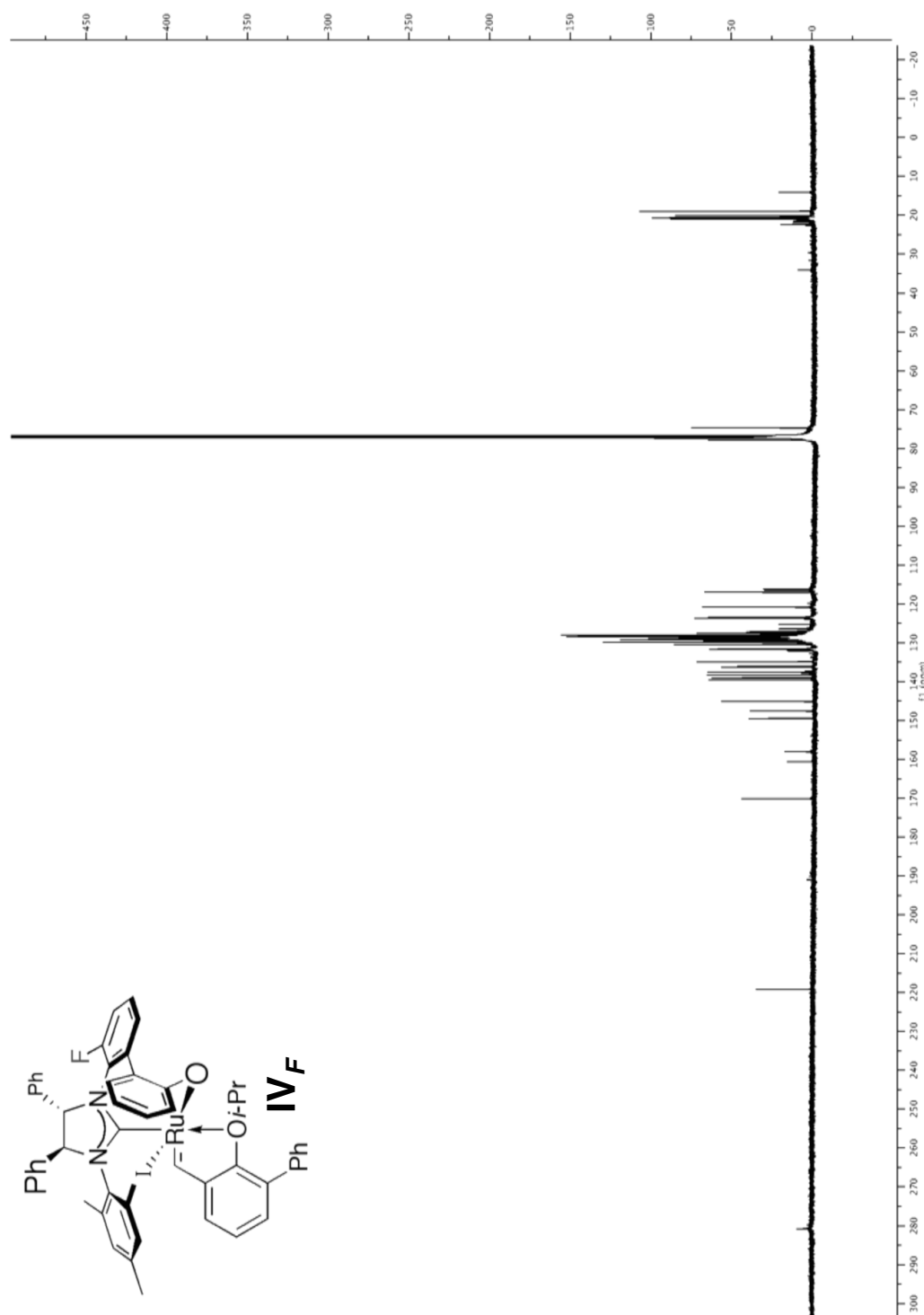




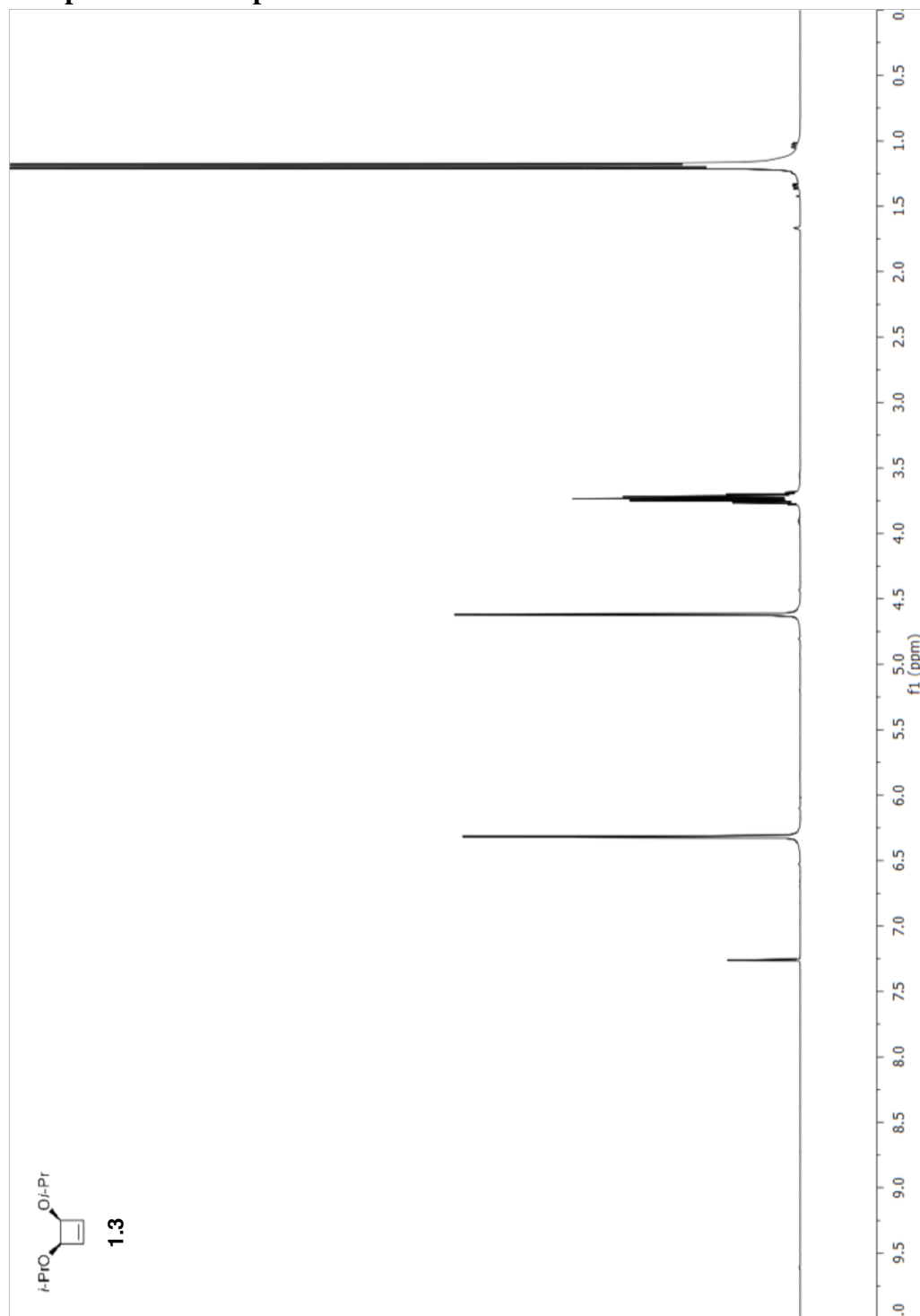


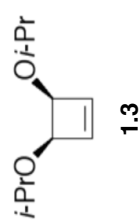
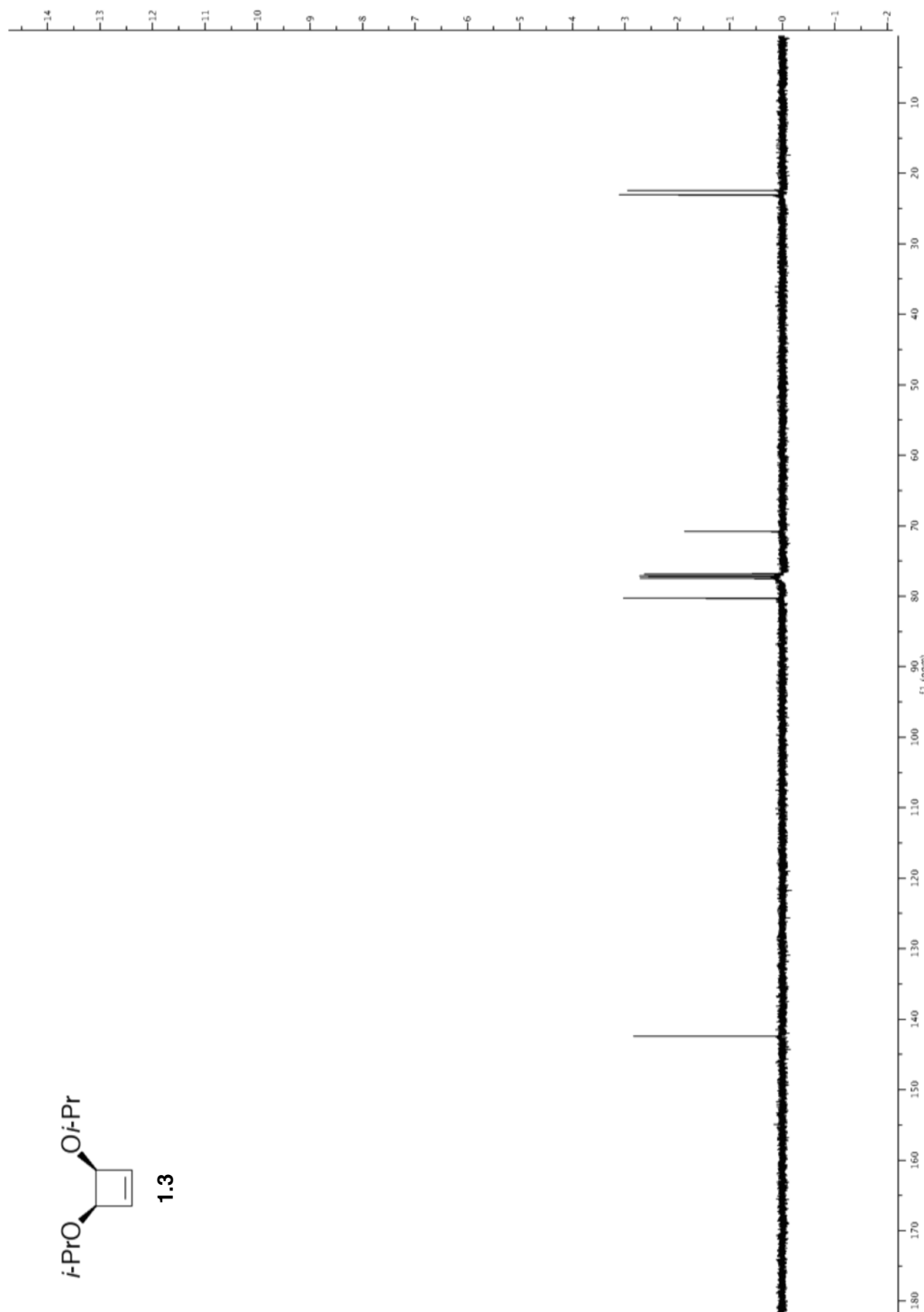
■ NMR Spectra for Complex IV_F:



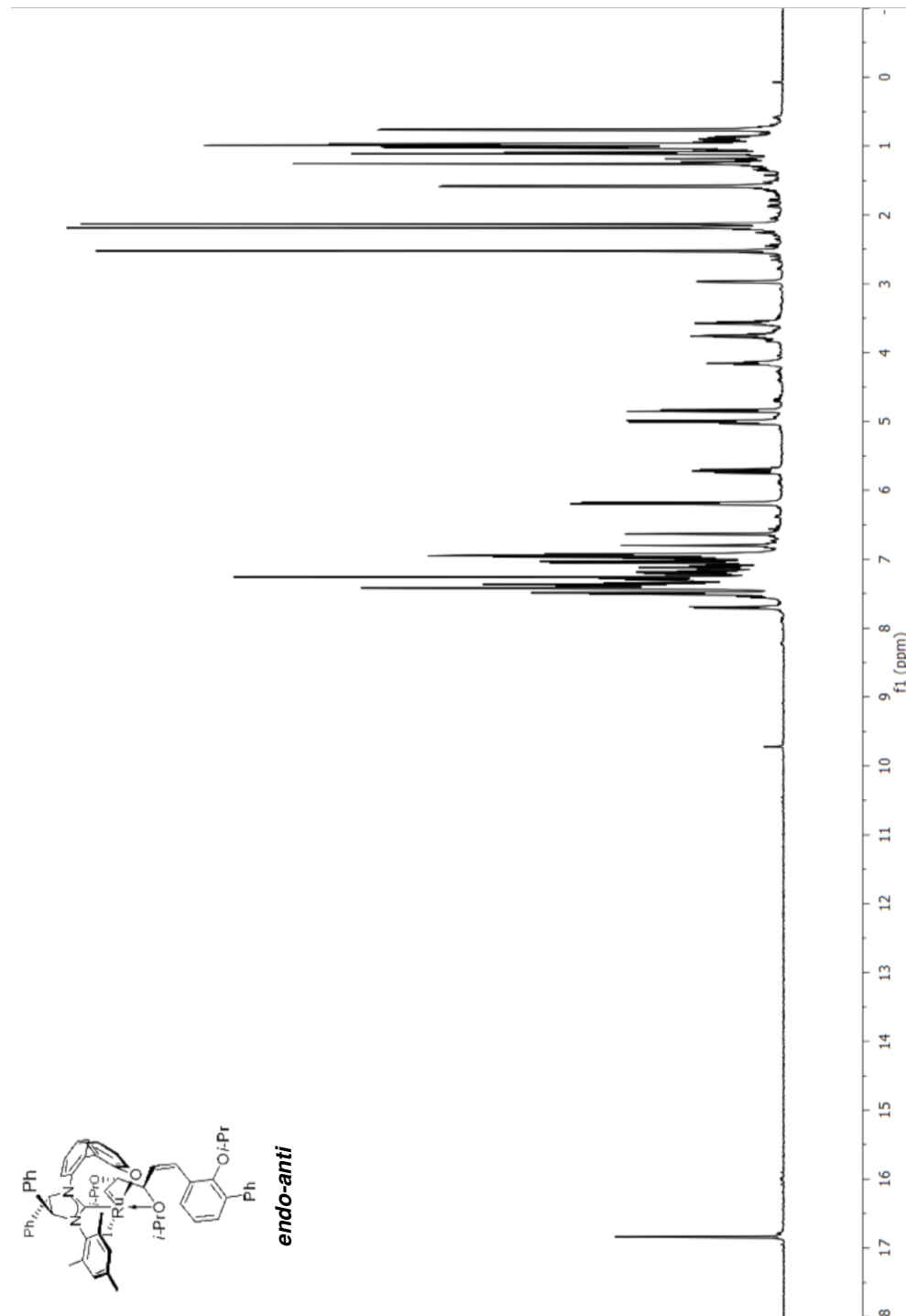


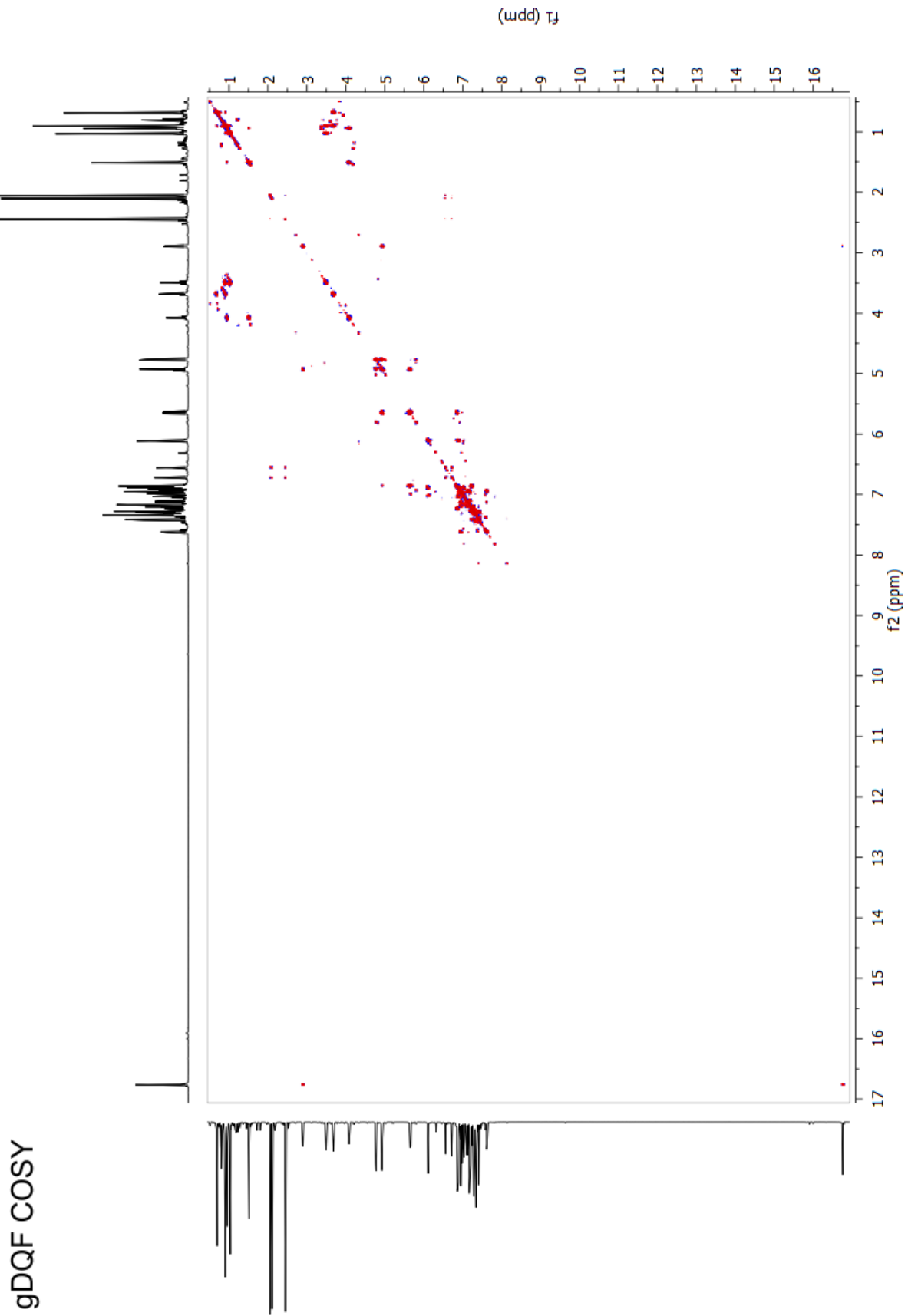
■ NMR Spectra for Compound 1.3:

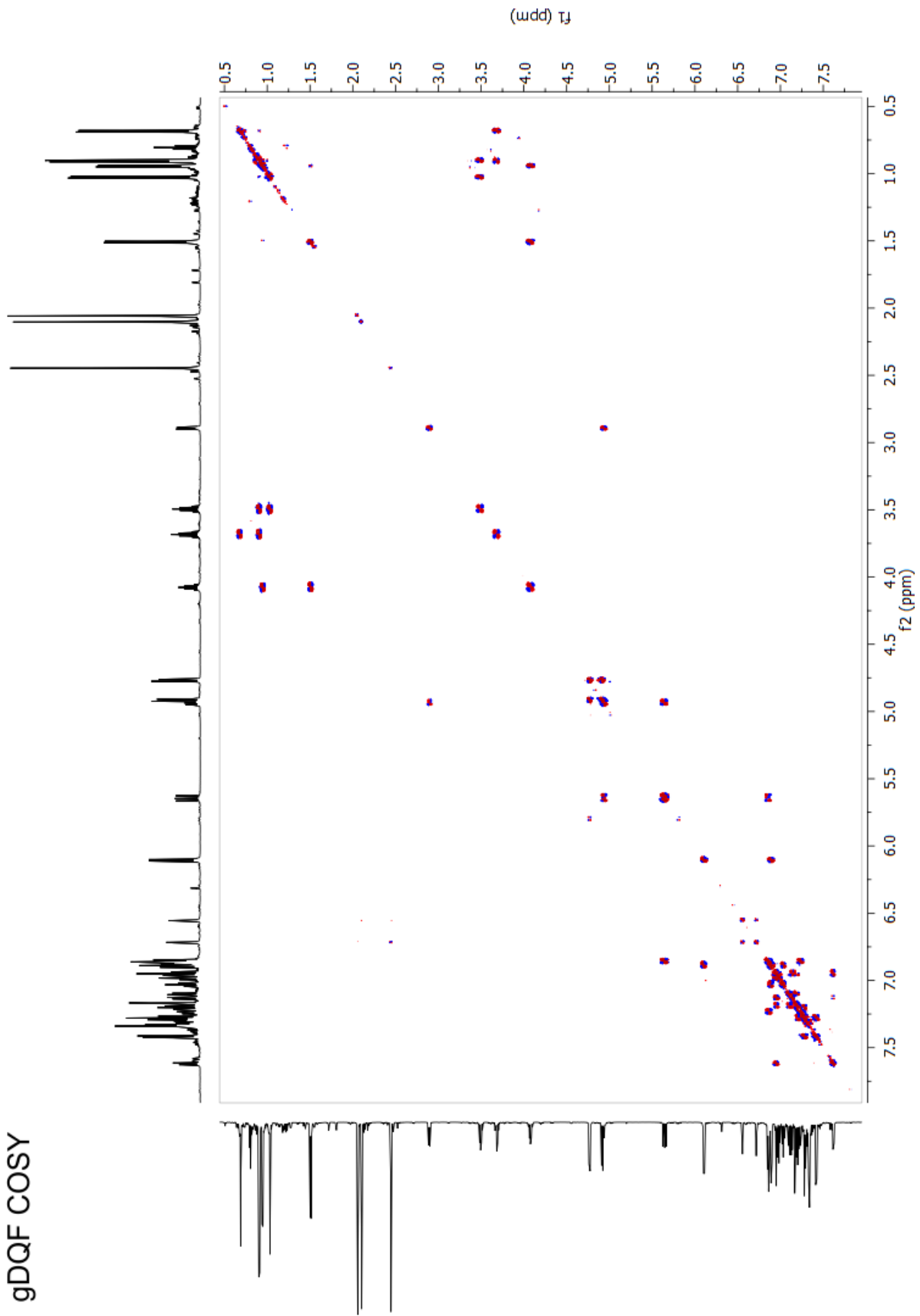


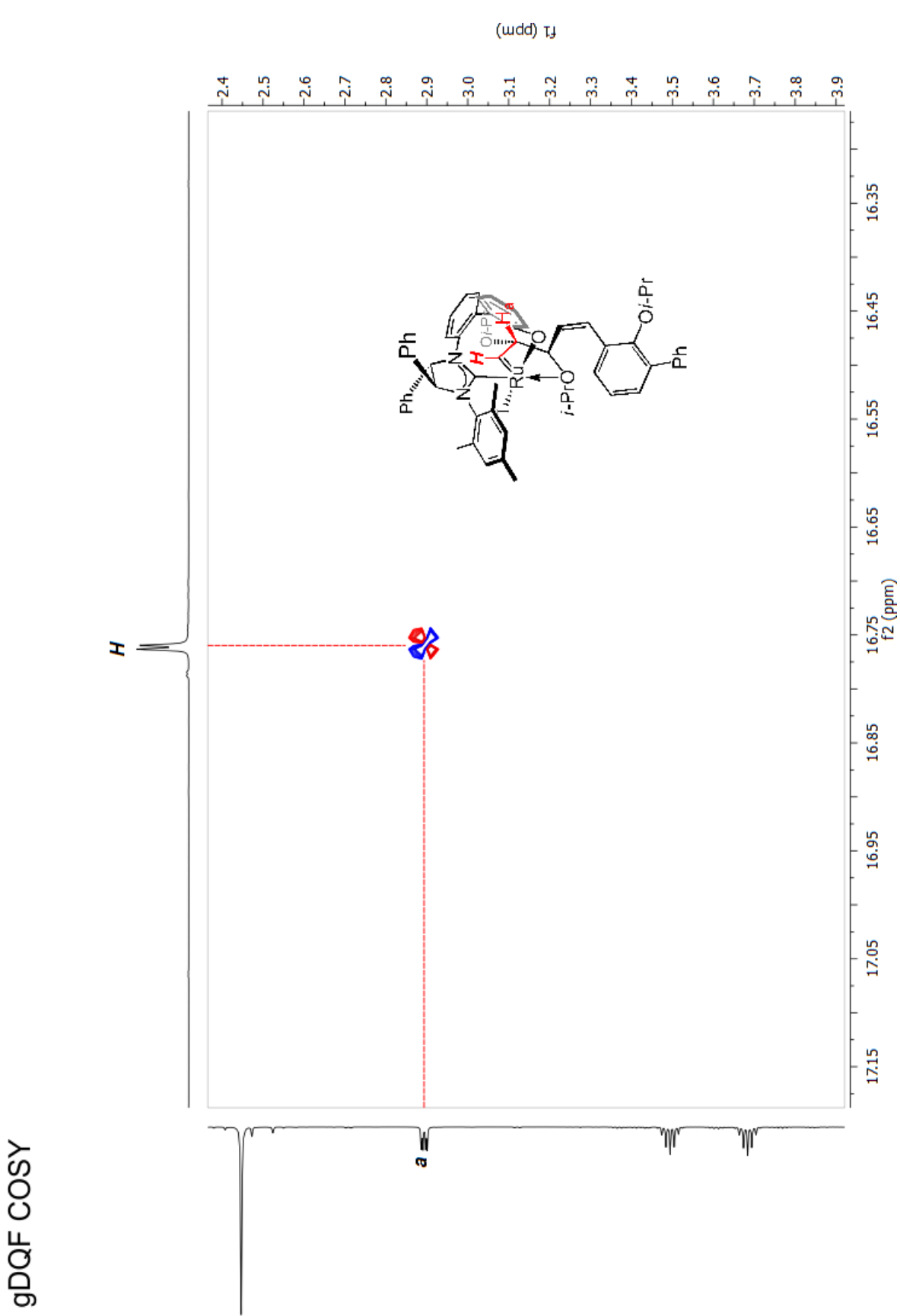


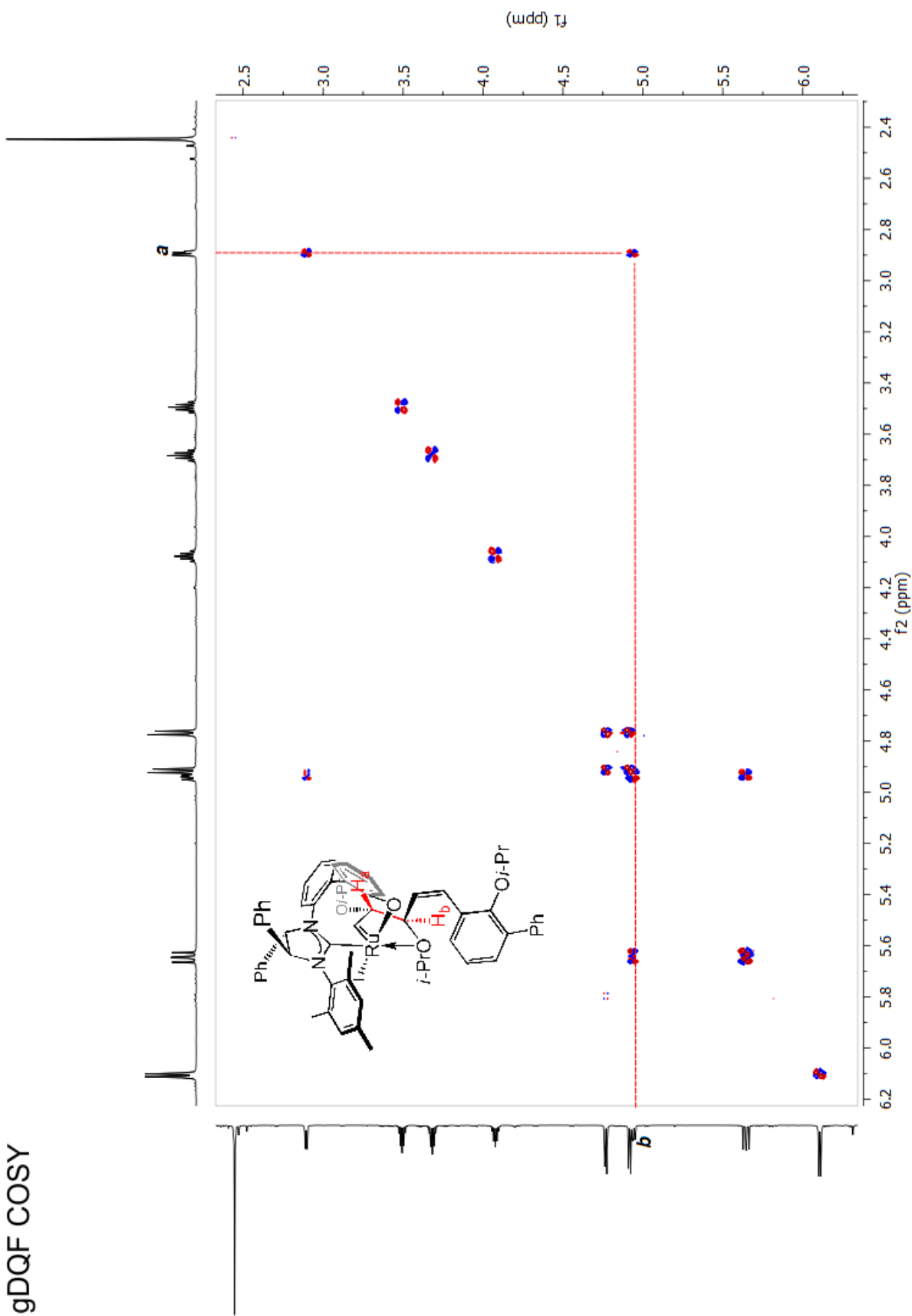
■ NMR Spectra for Complex *endo-anti*:

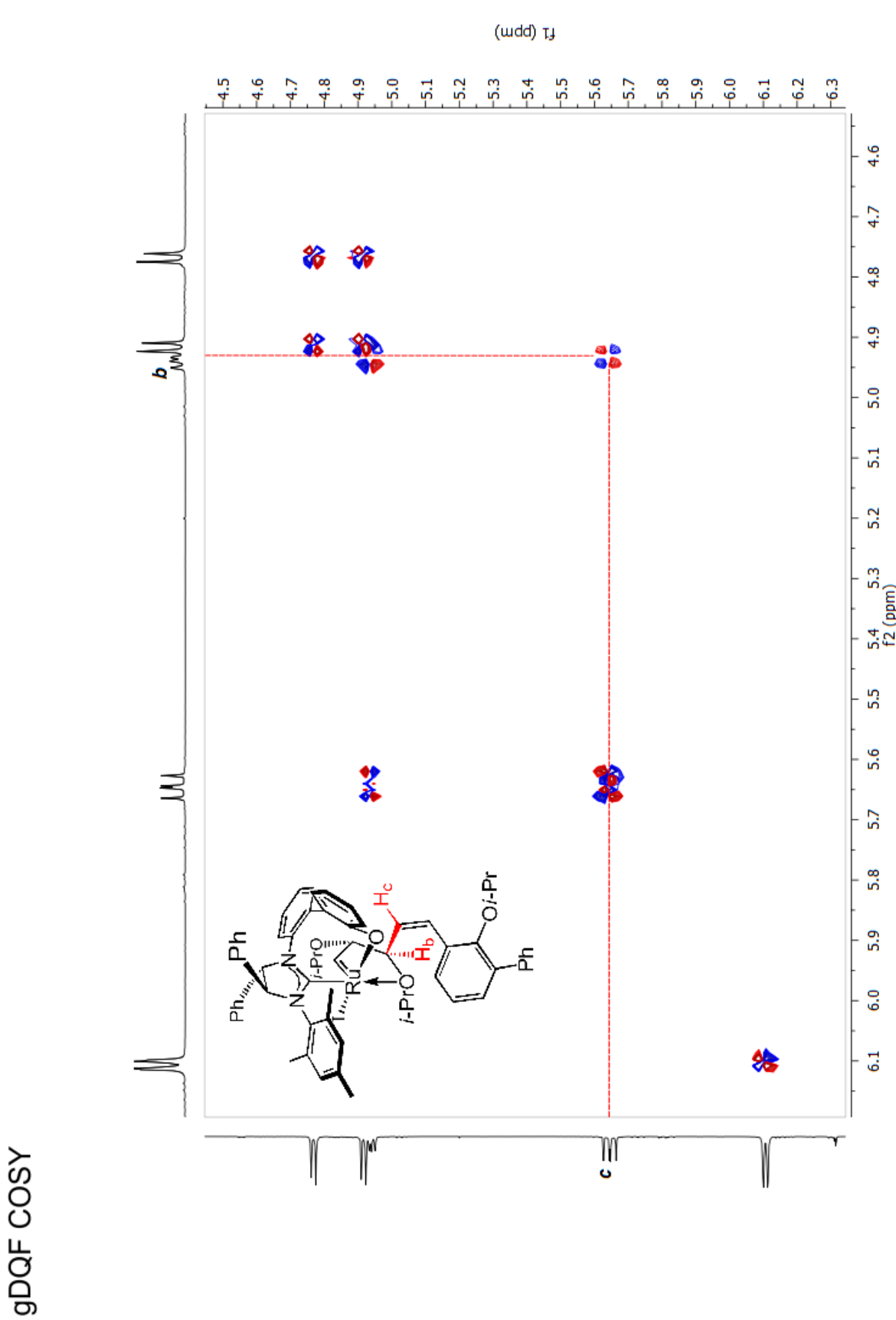


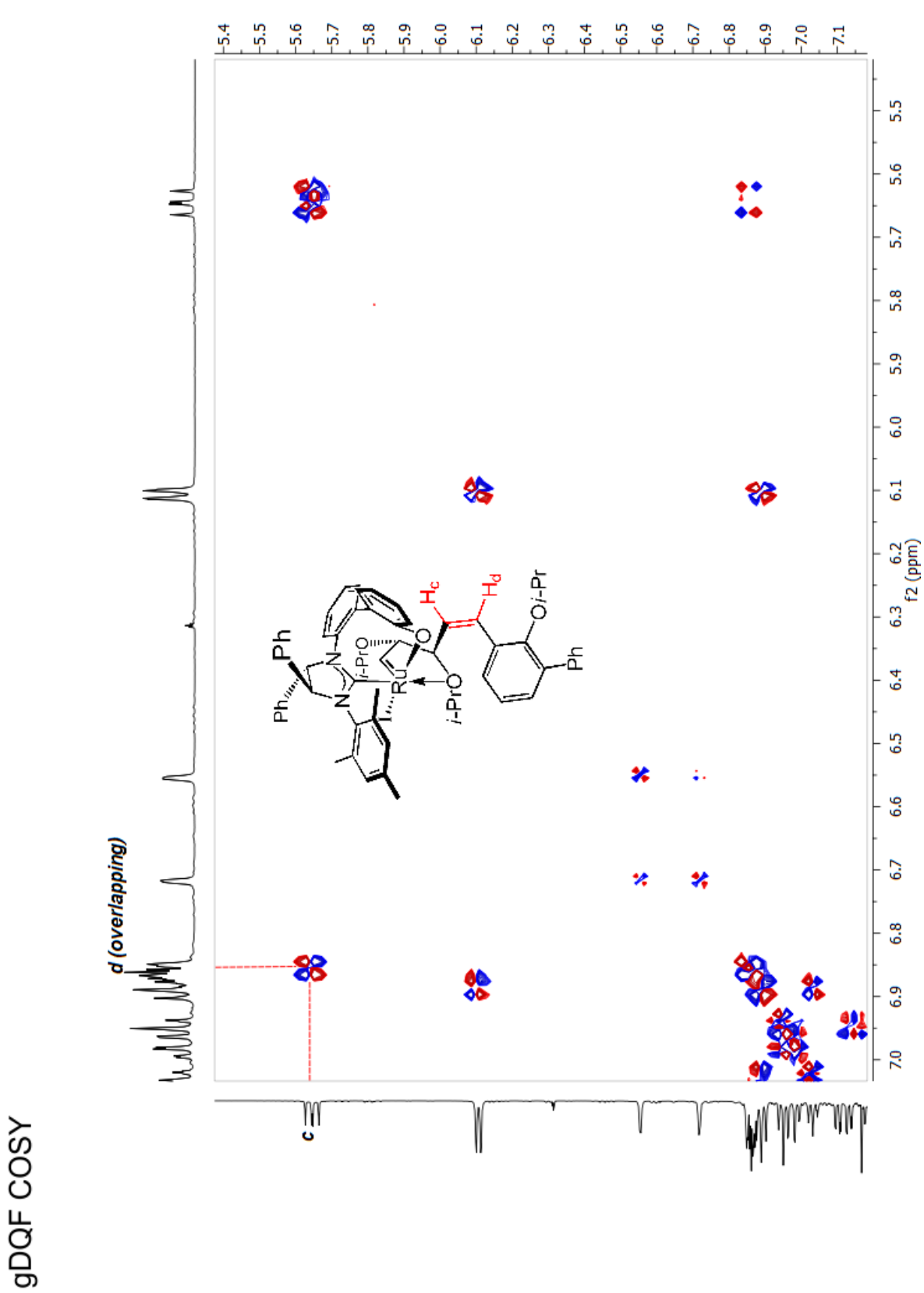


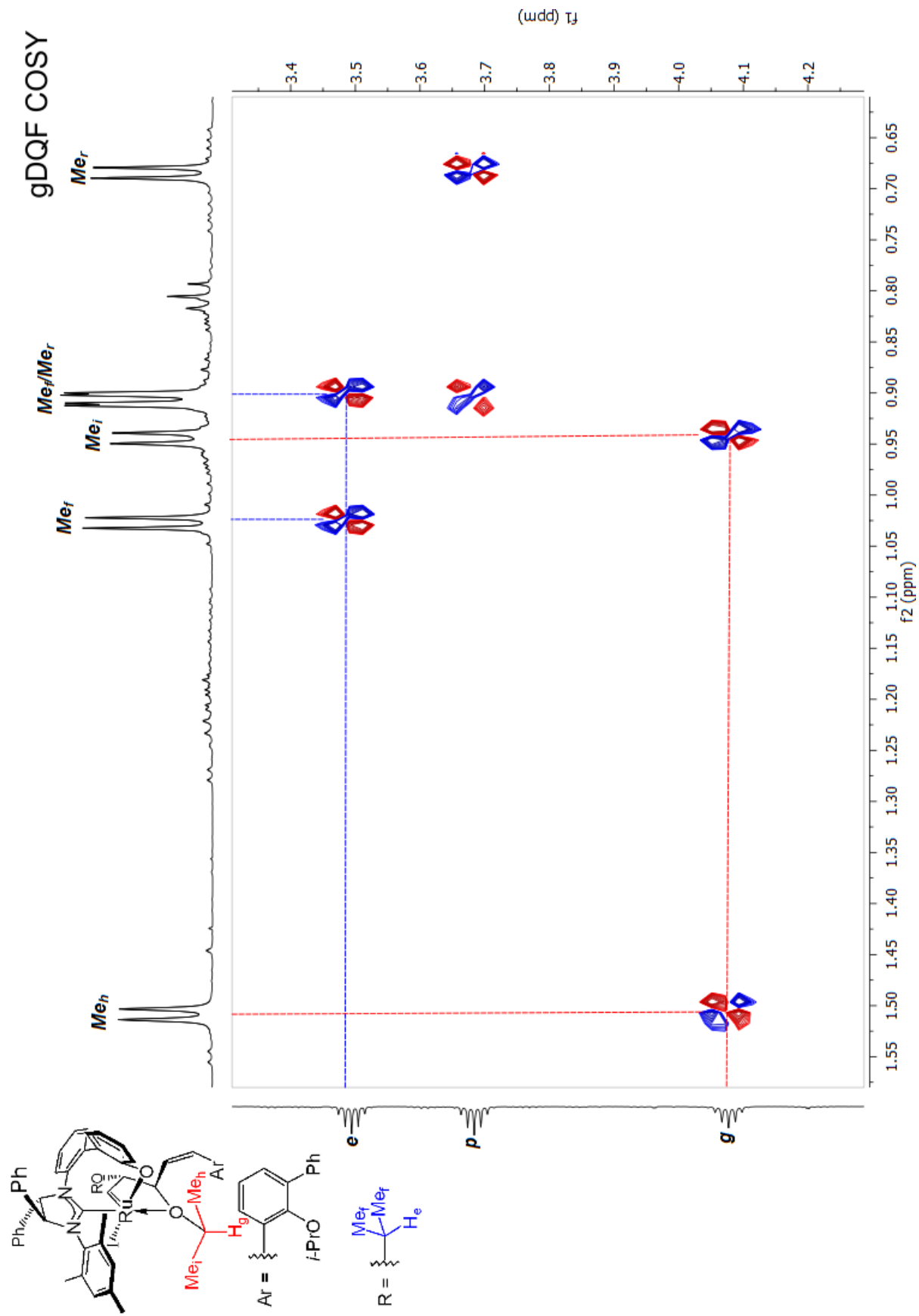


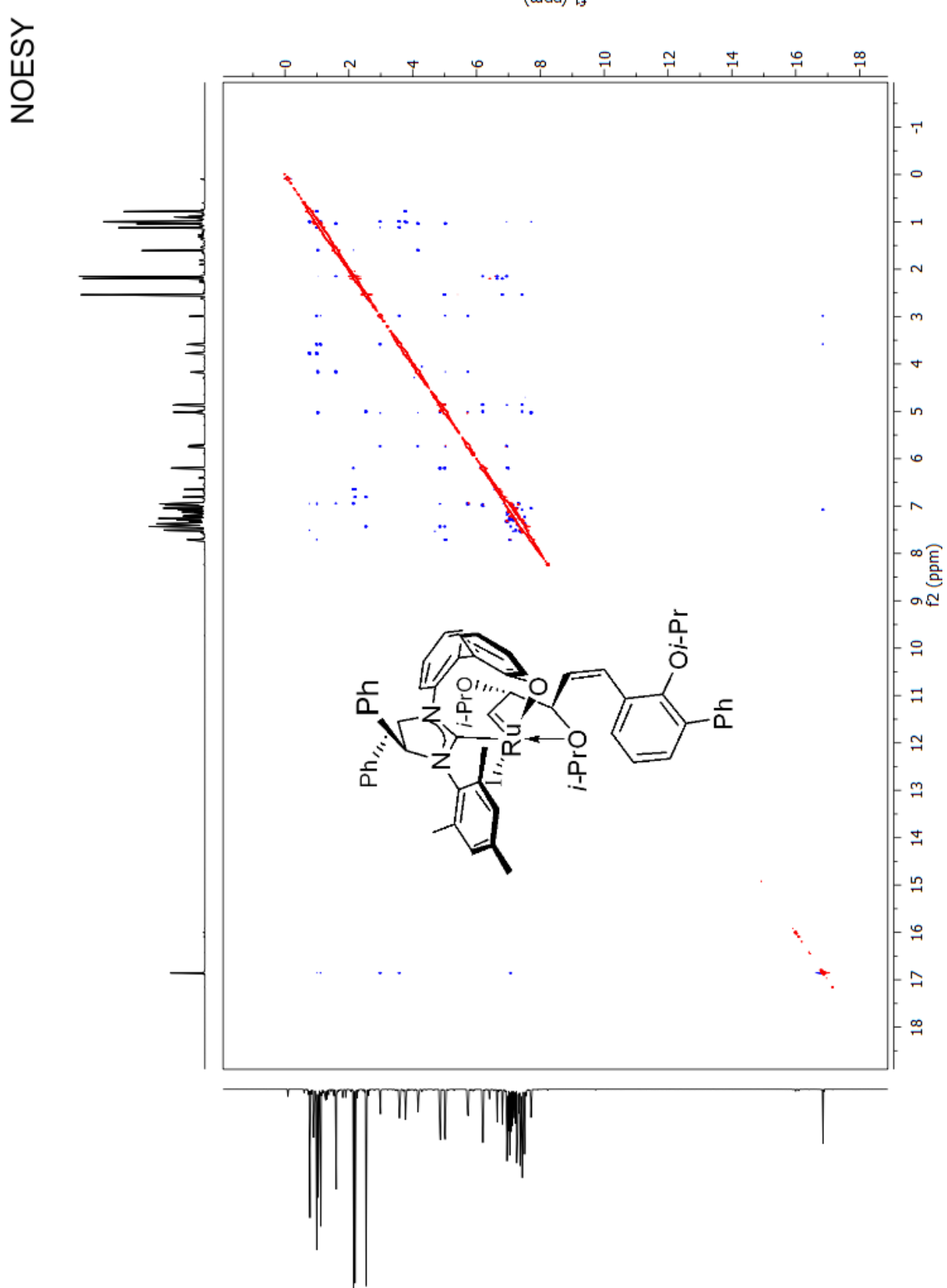


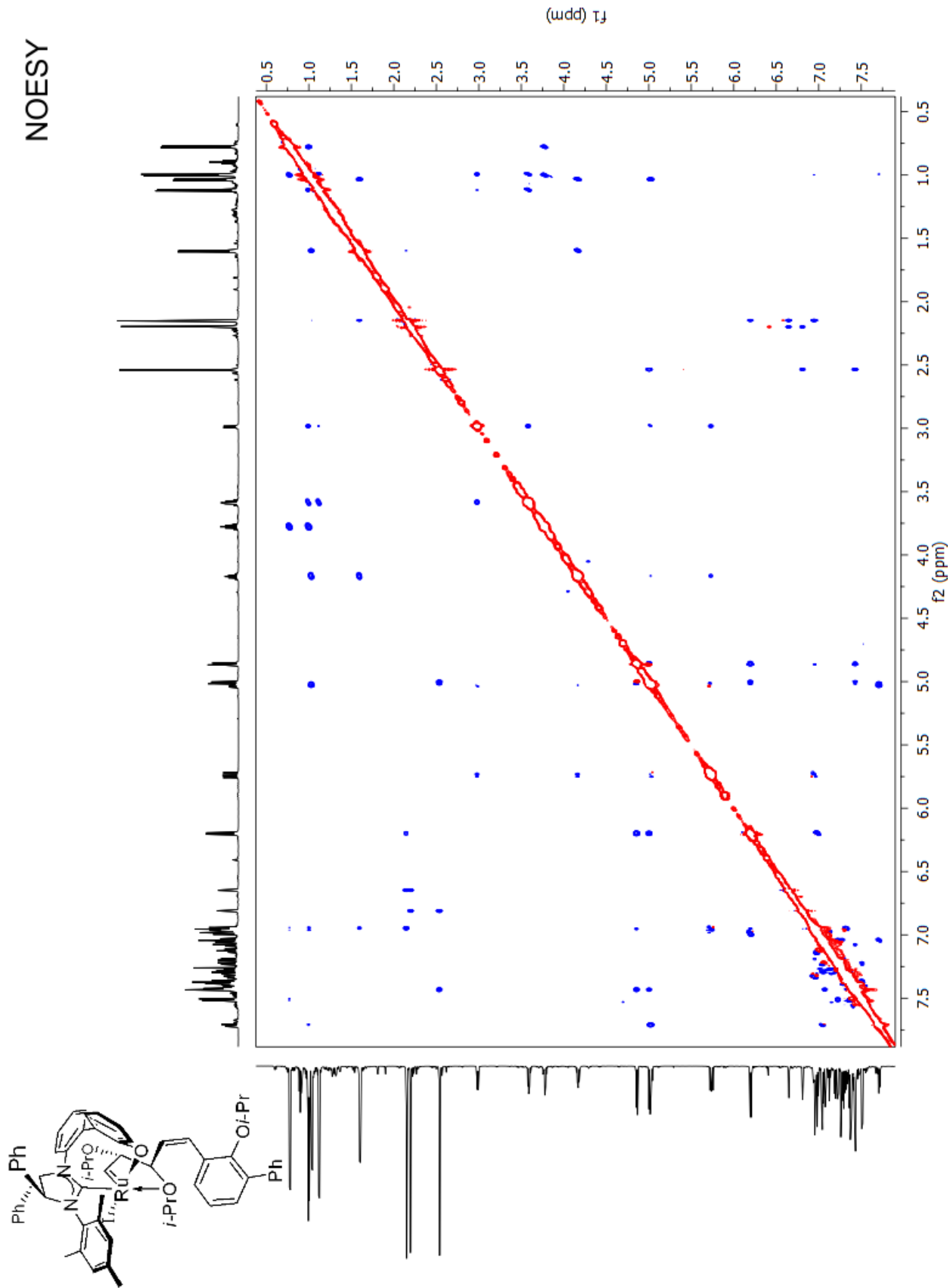


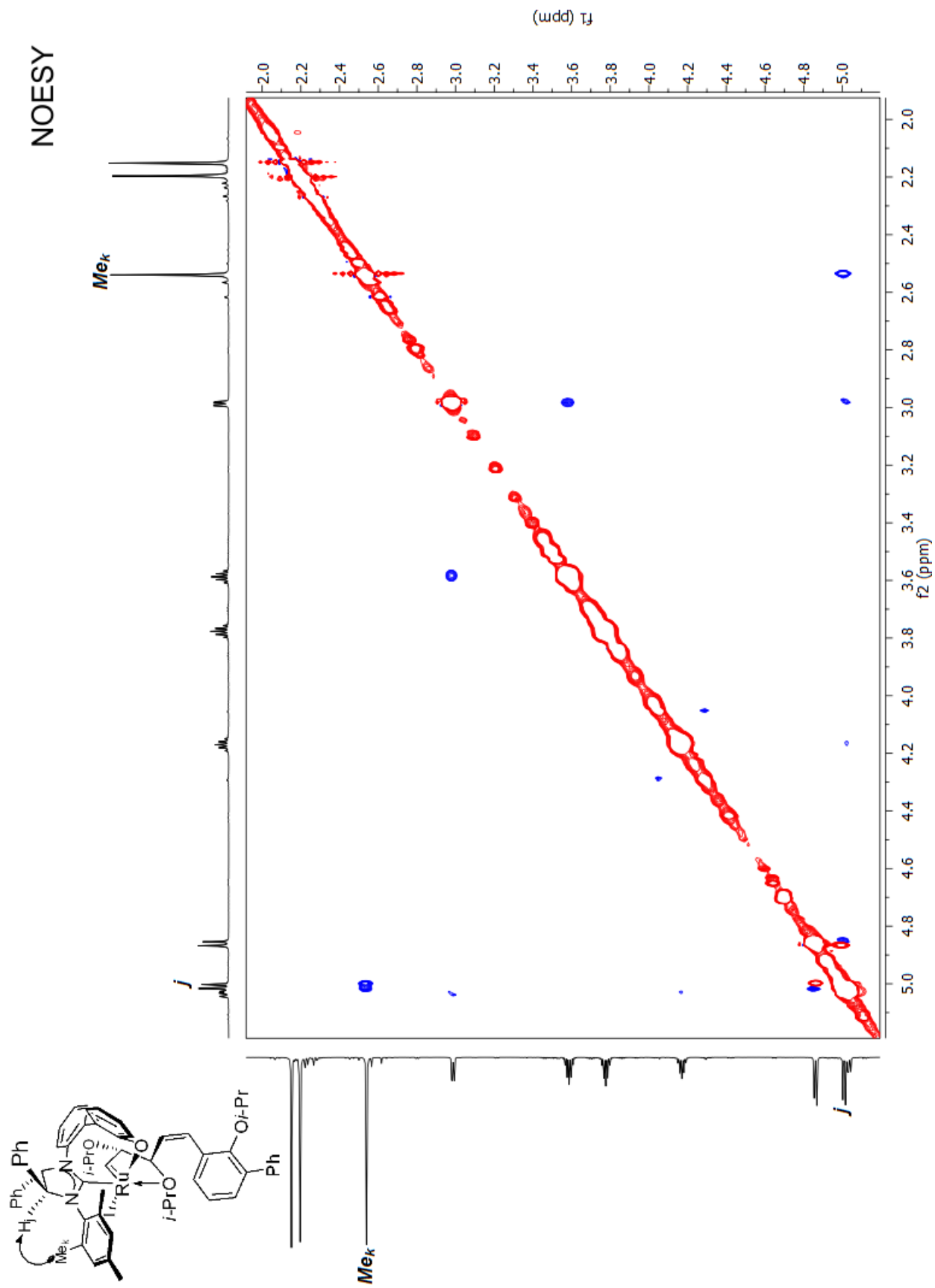


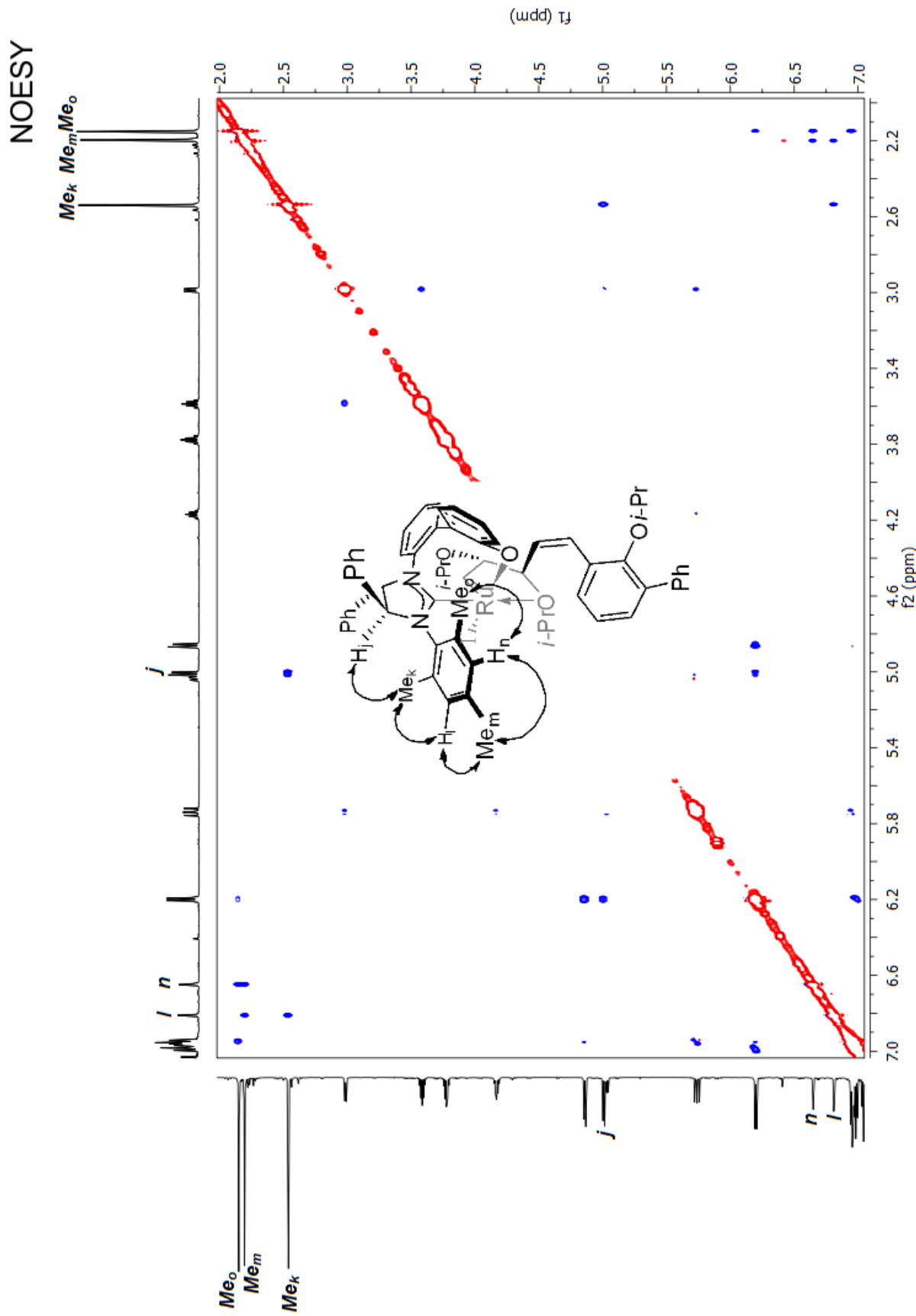


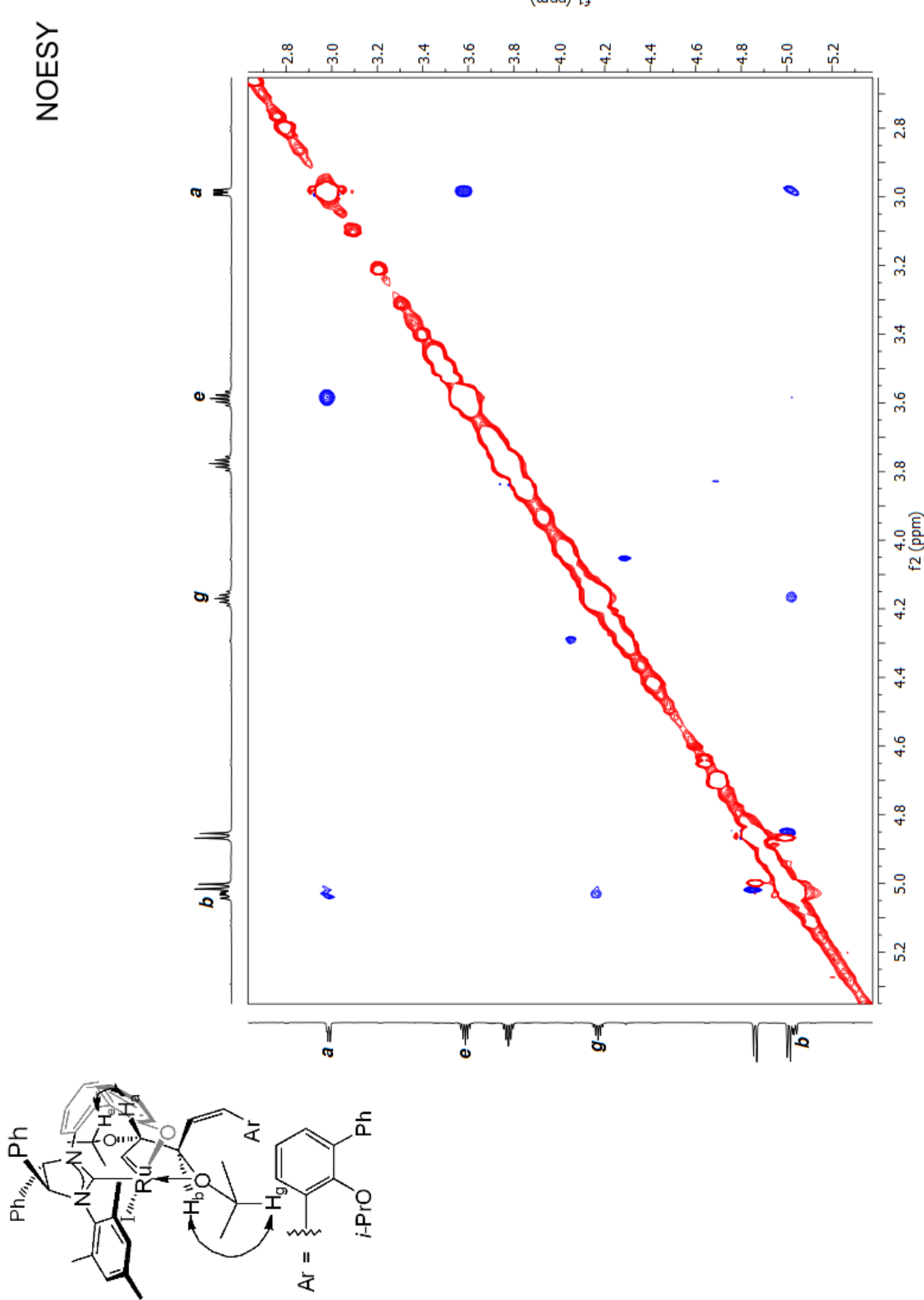


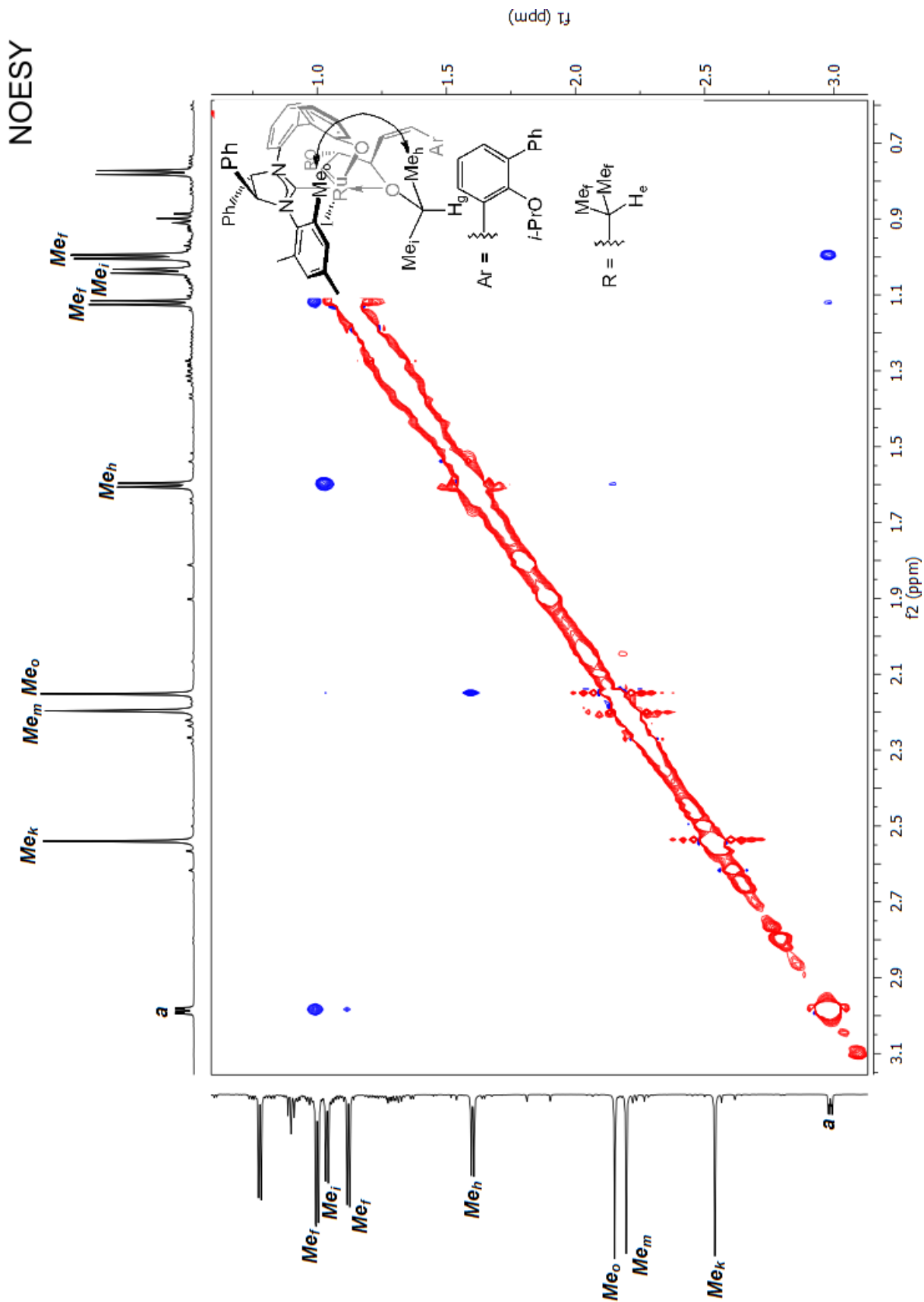


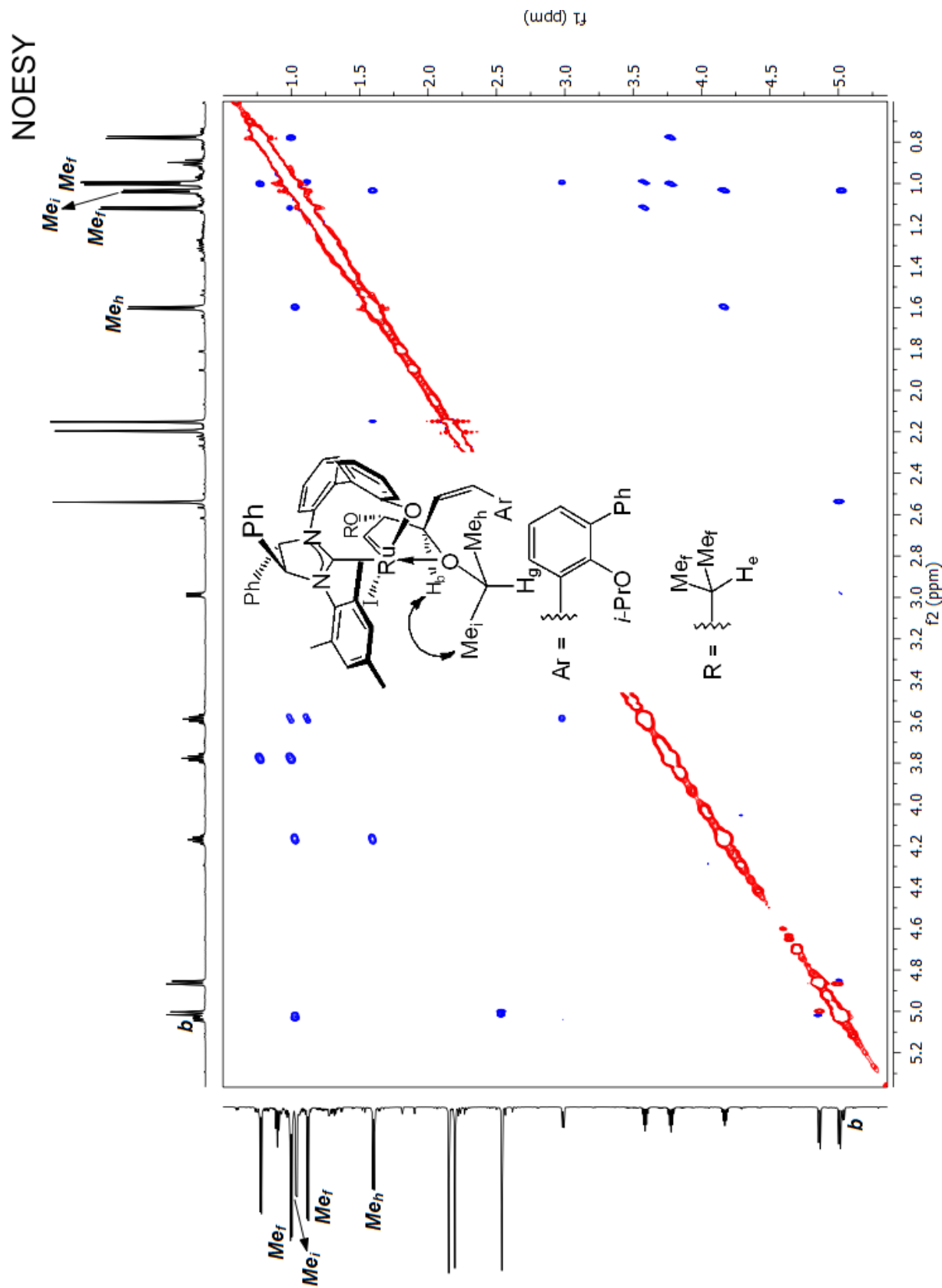




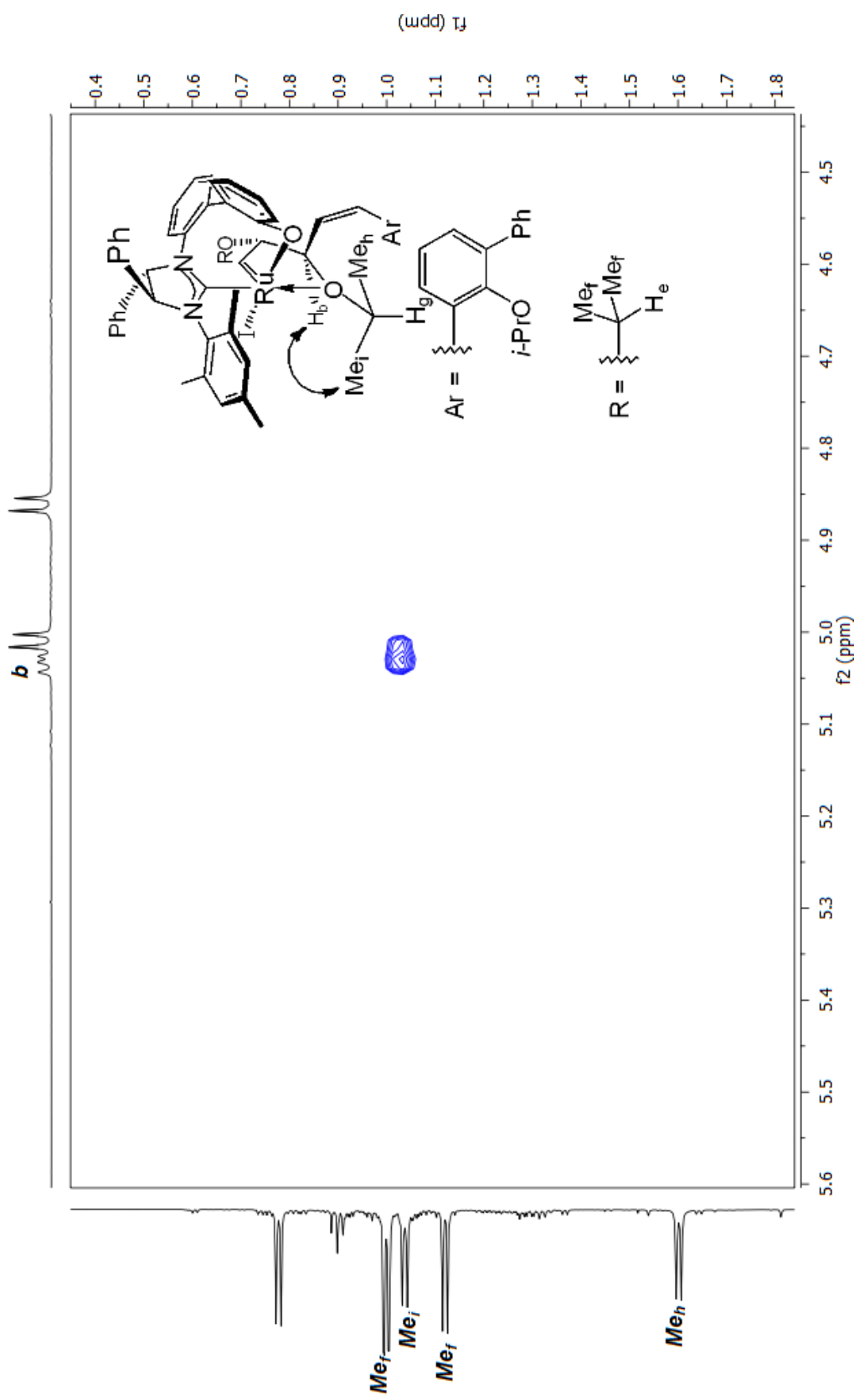


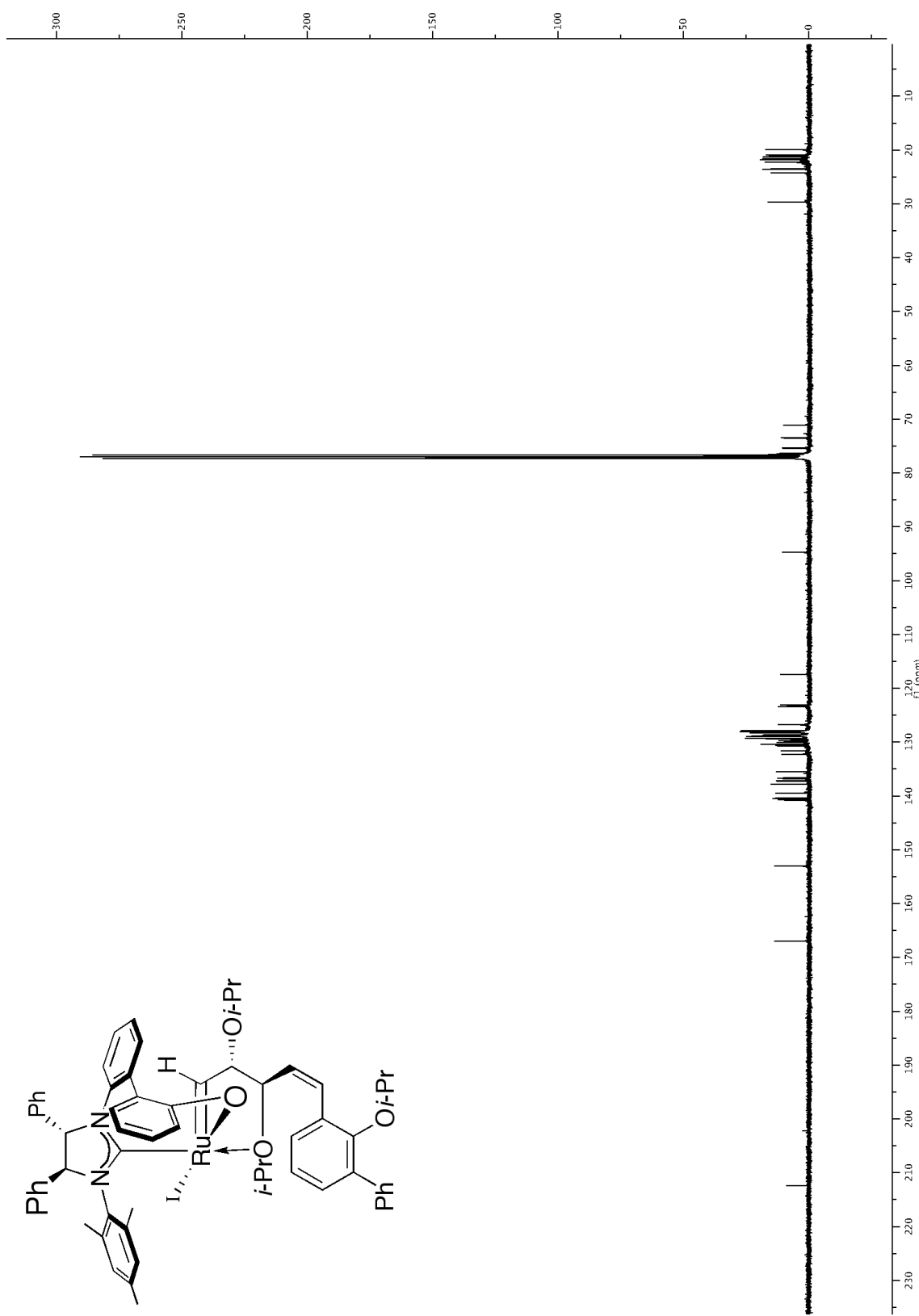




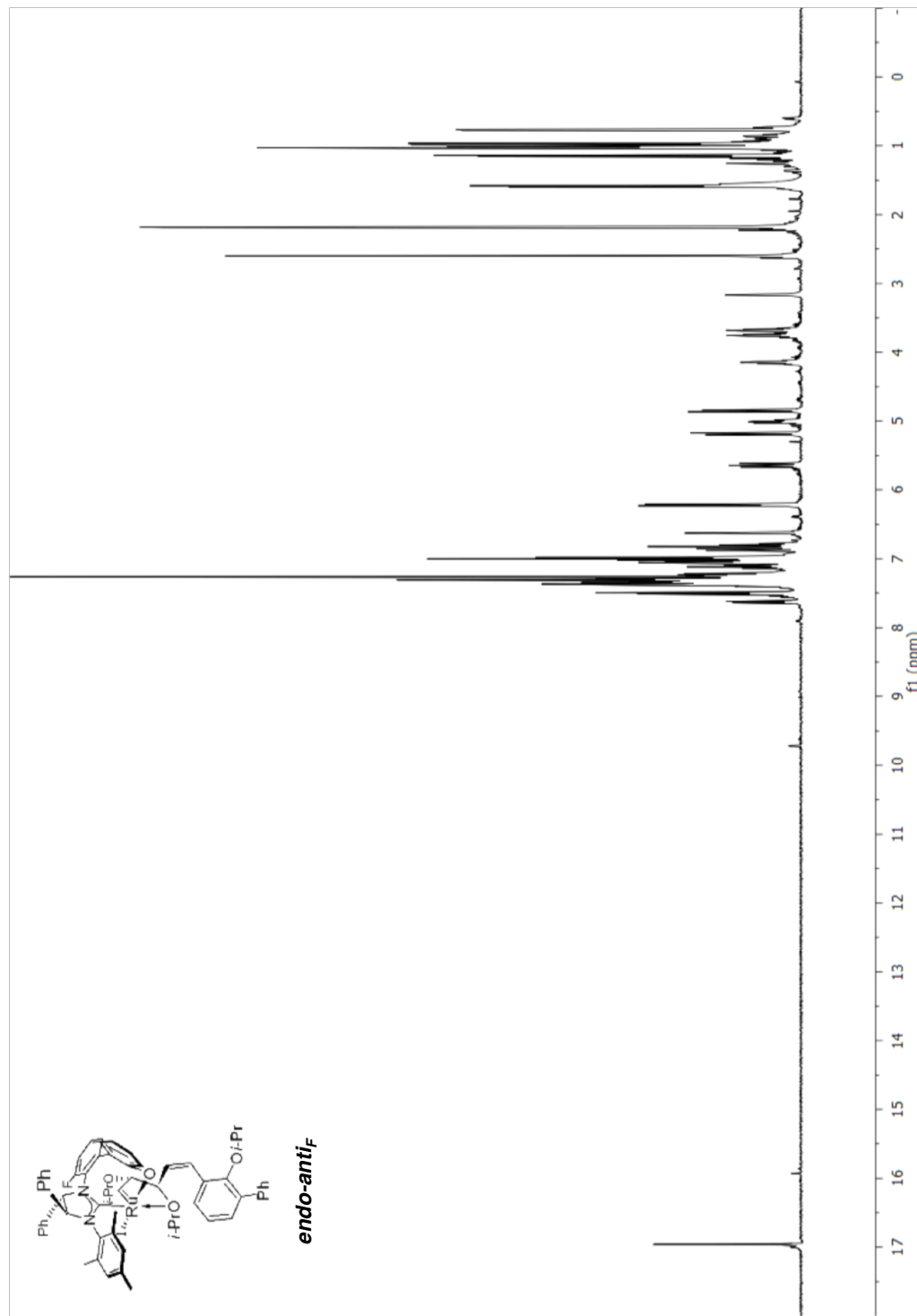


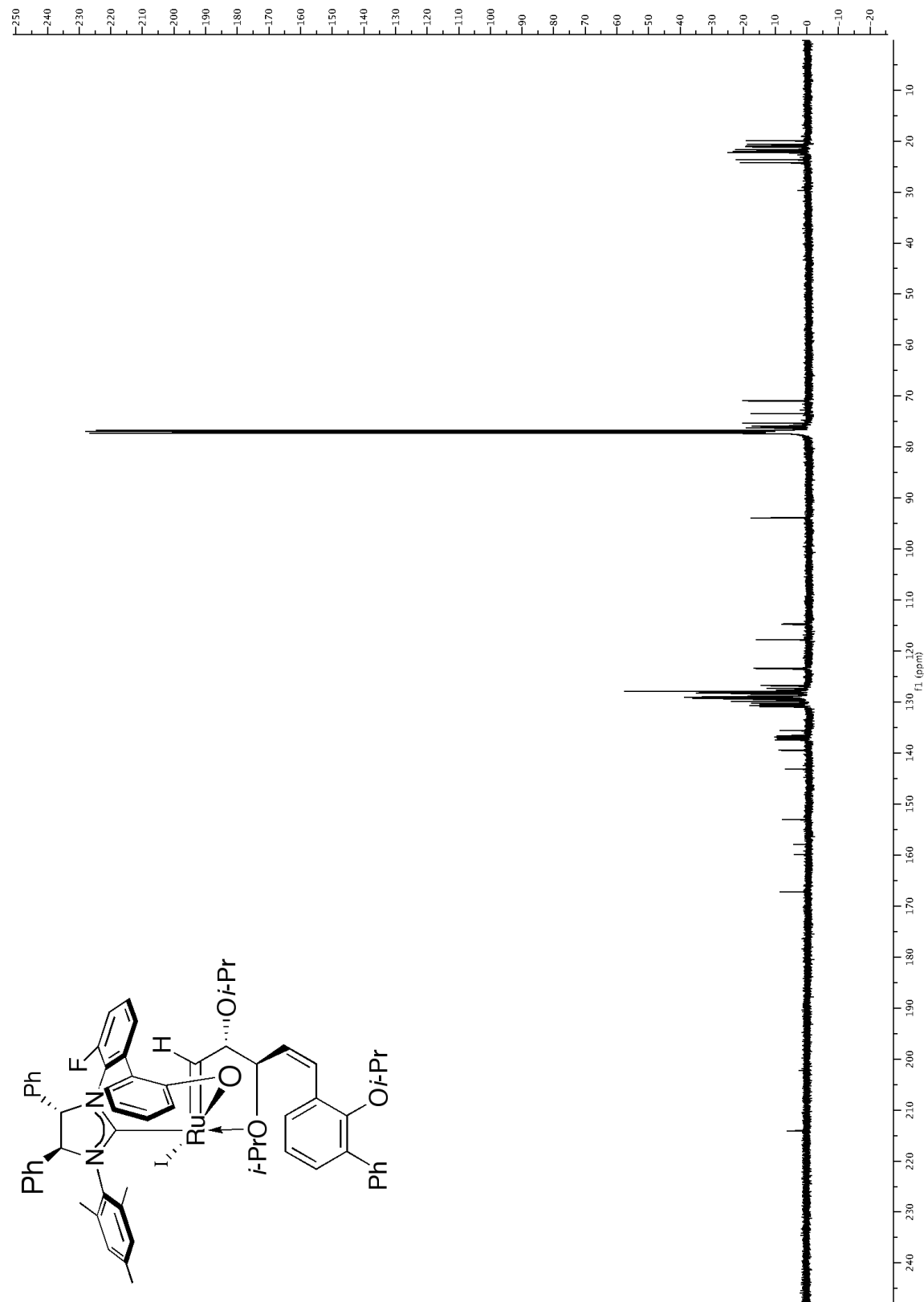
NOESY



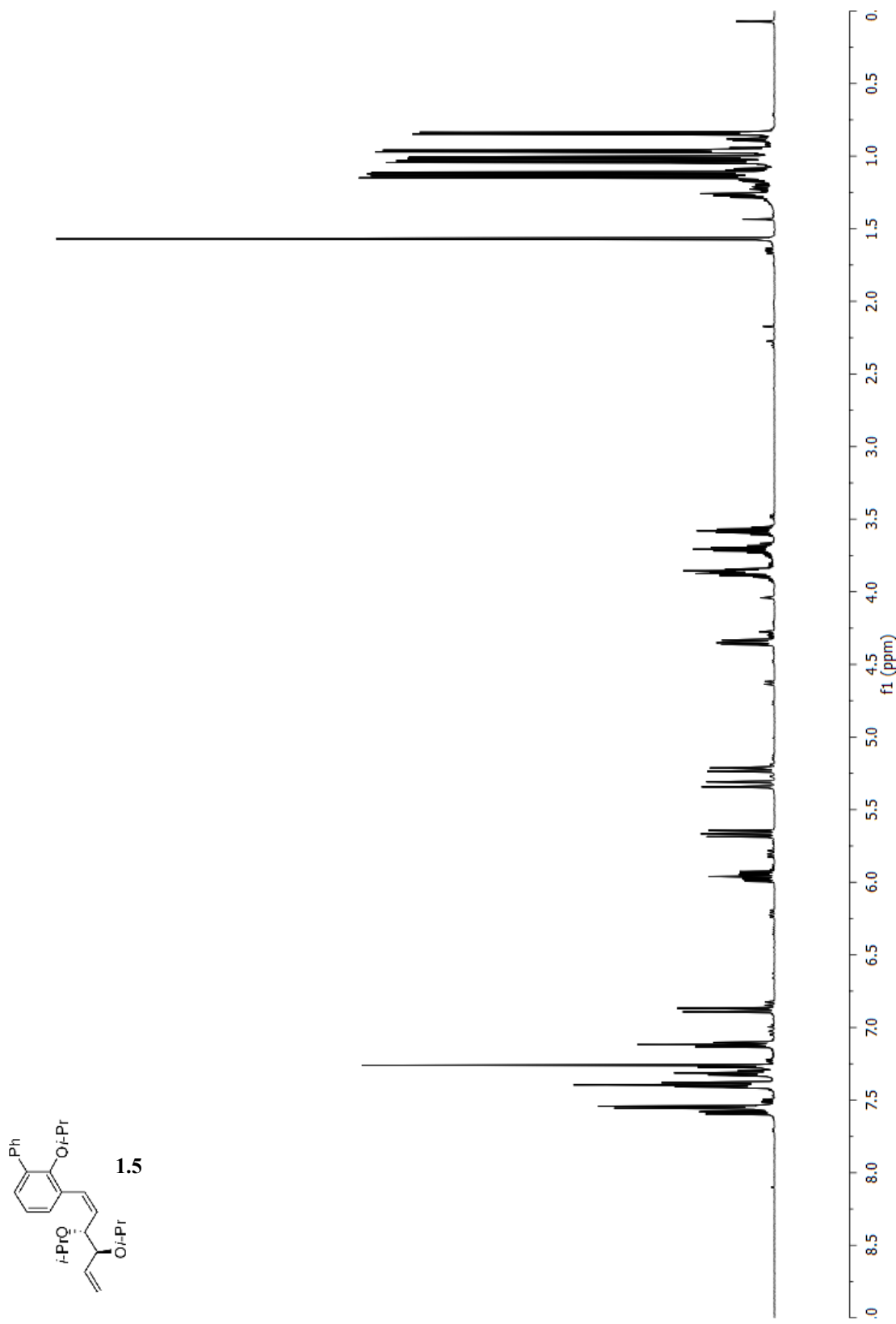


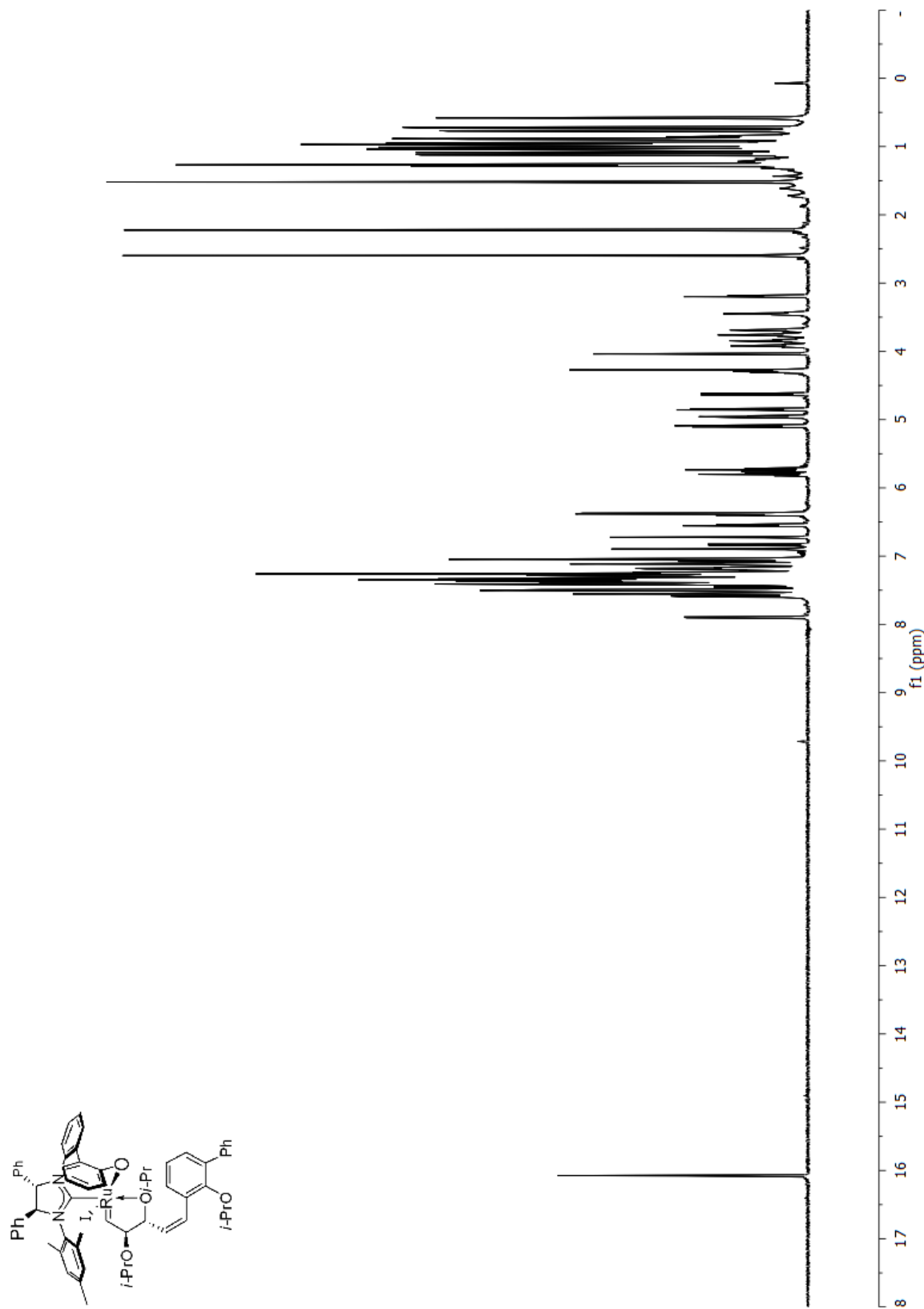
■ NMR Spectra for Complex *endo-anti*_F:

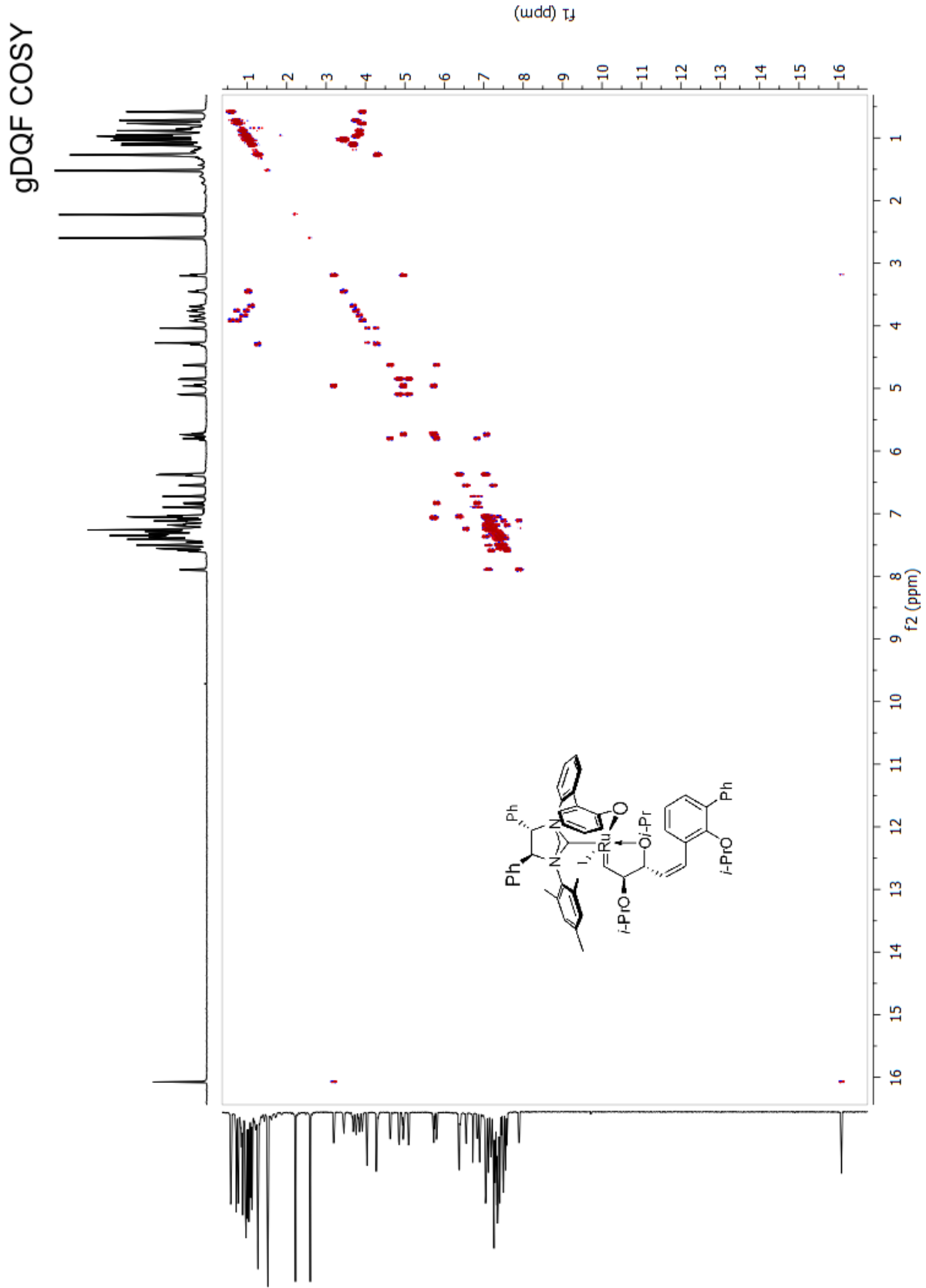


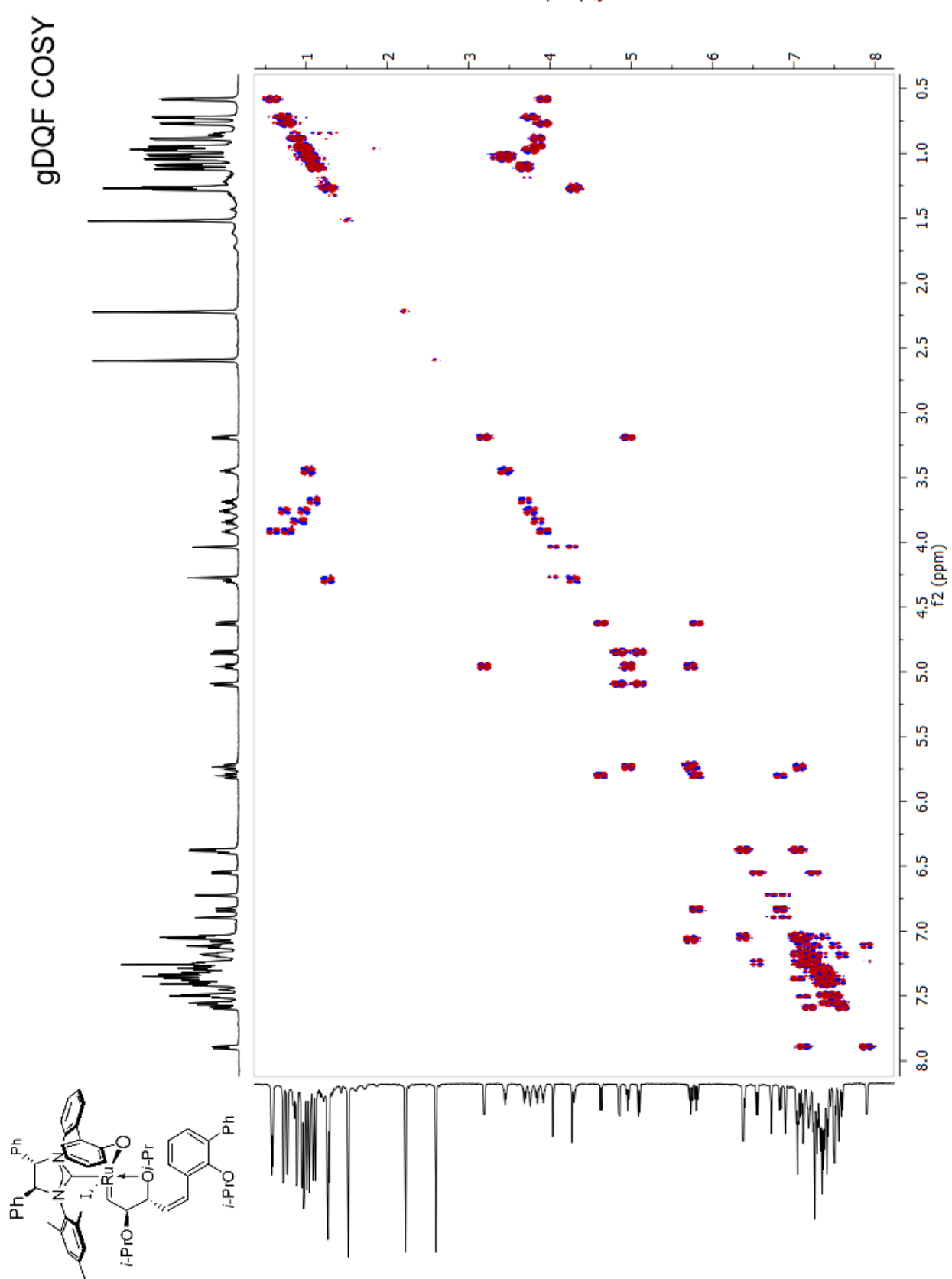


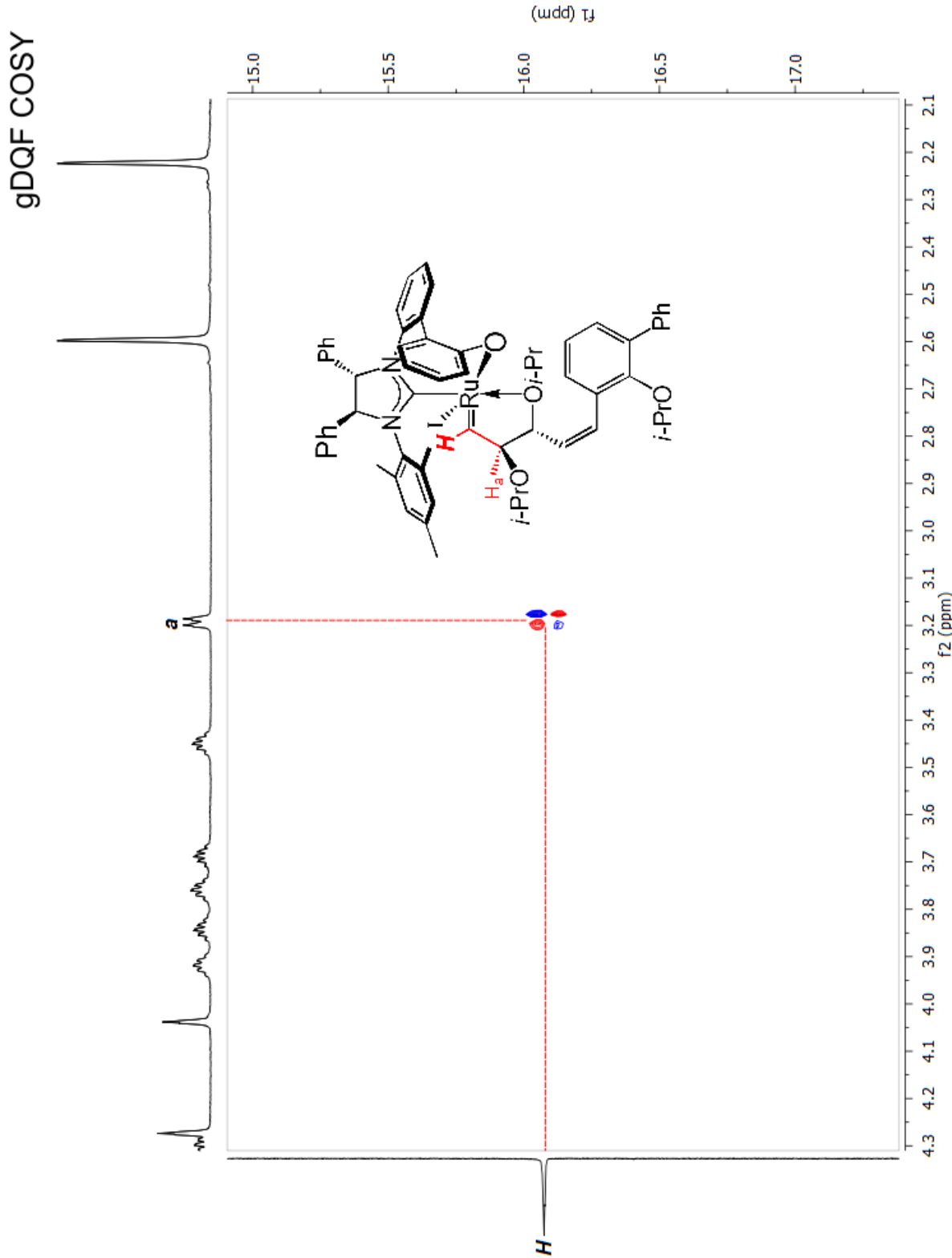
■ NMR Spectra for Compound 1.5



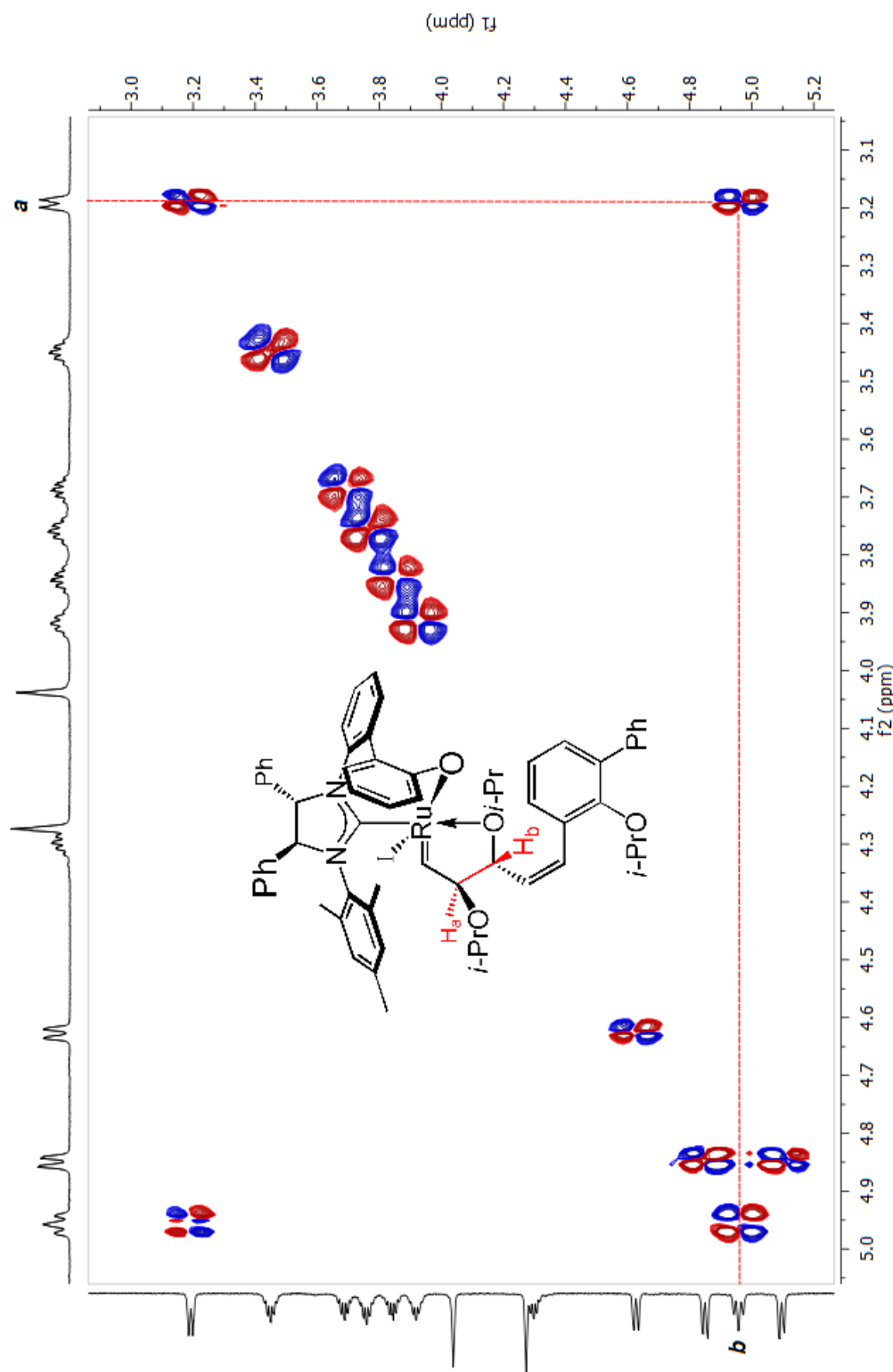
■ NMR Spectra for Complex *exo-anti*:



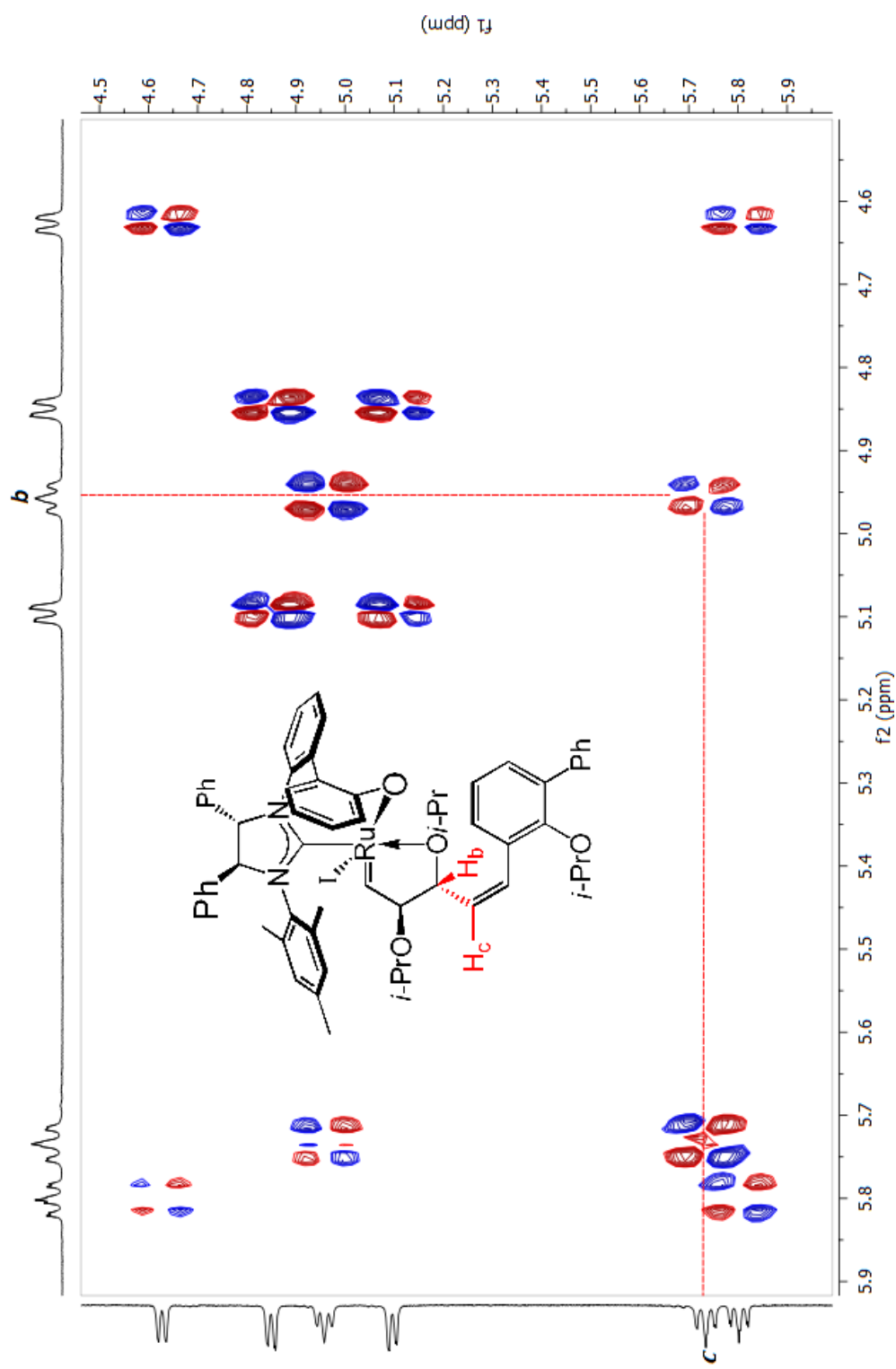


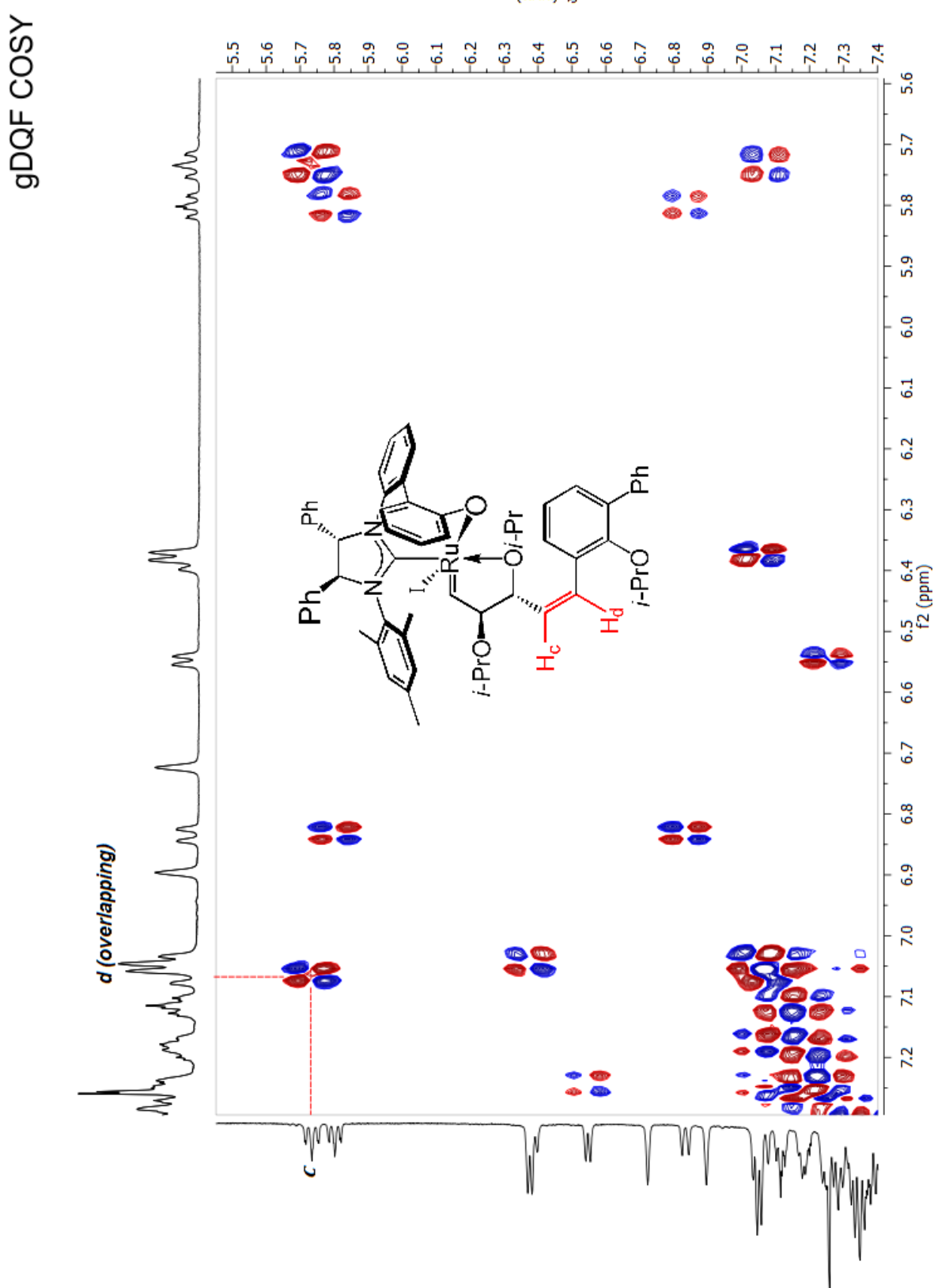


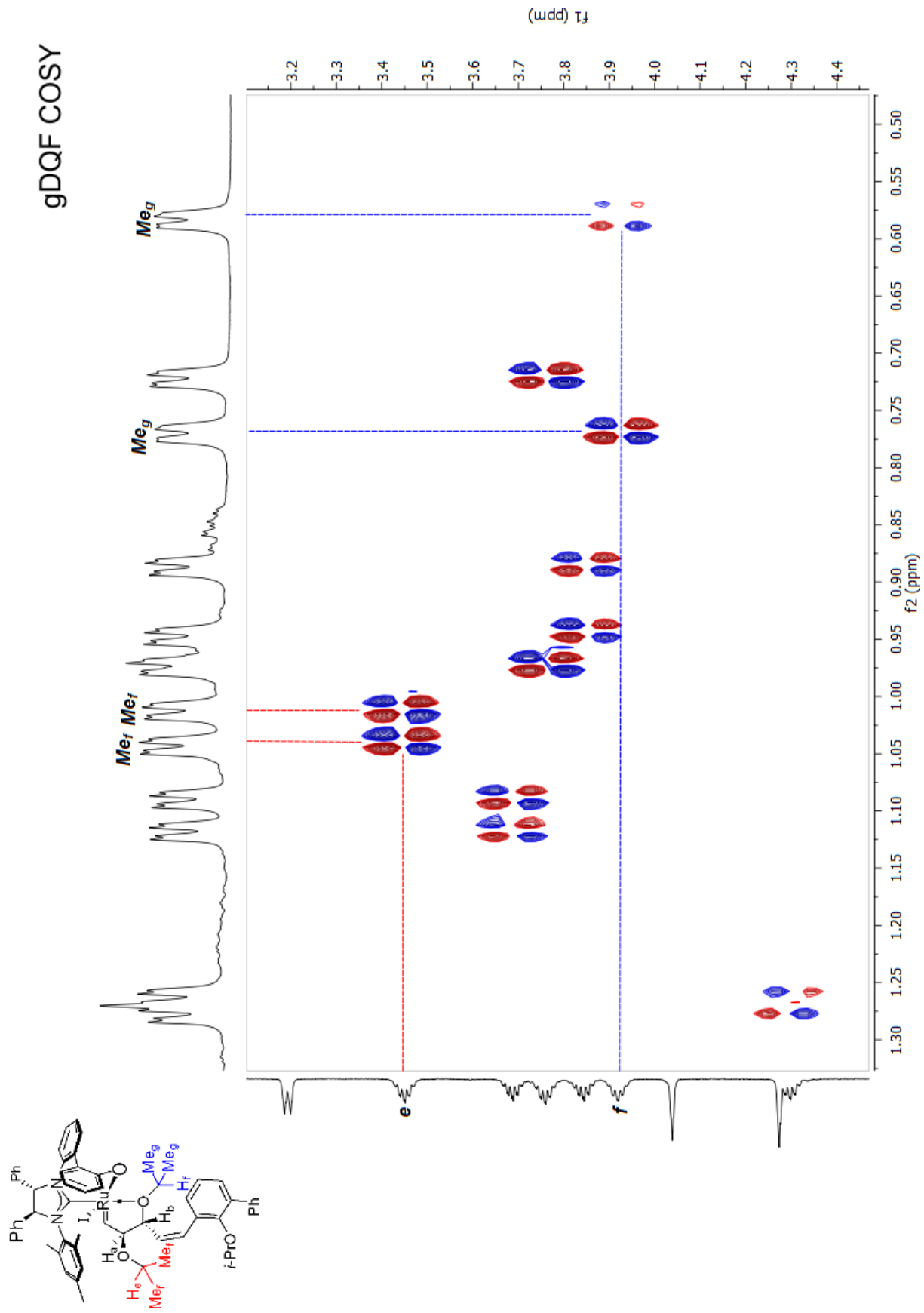
gDQF COSY

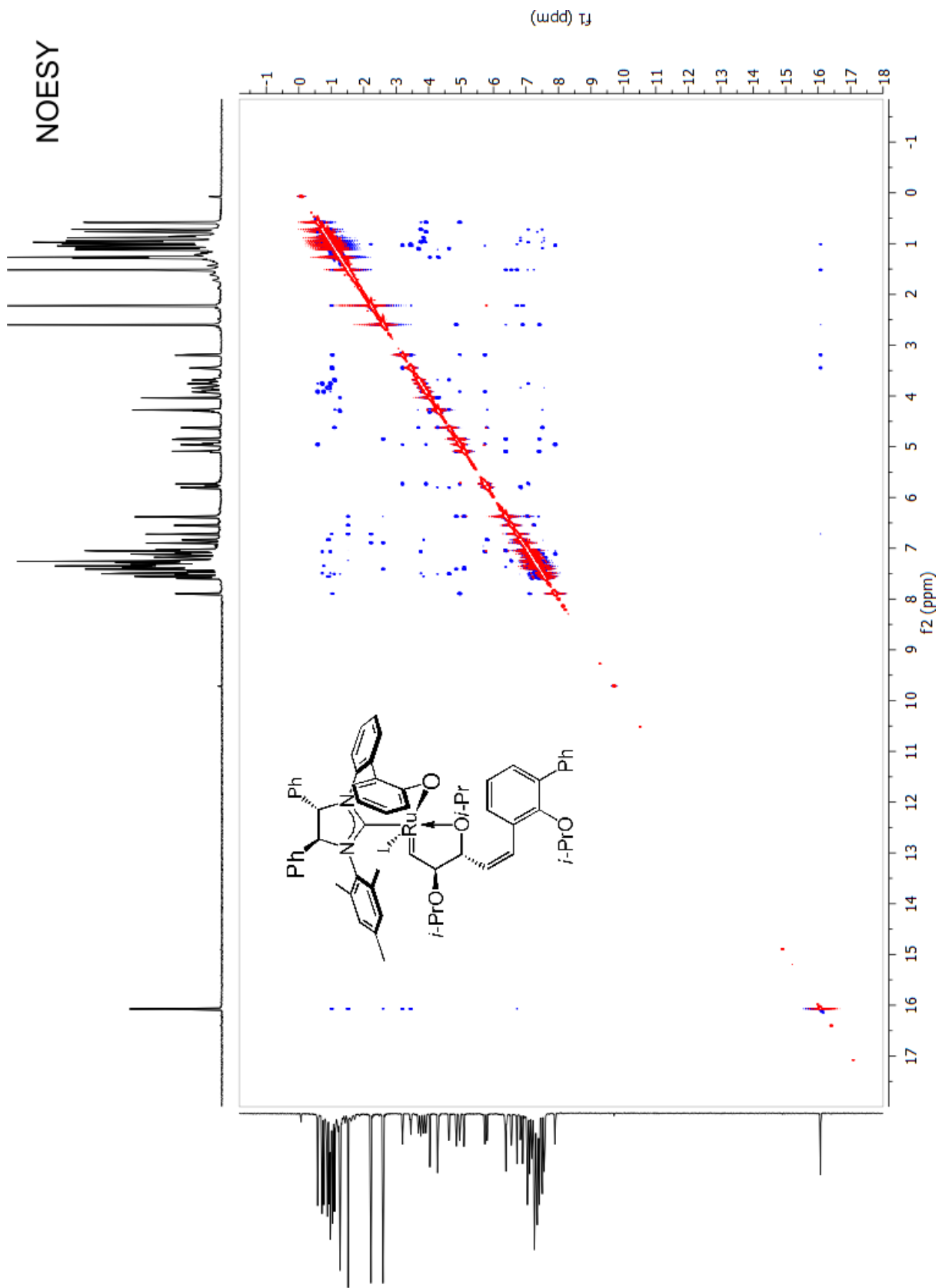


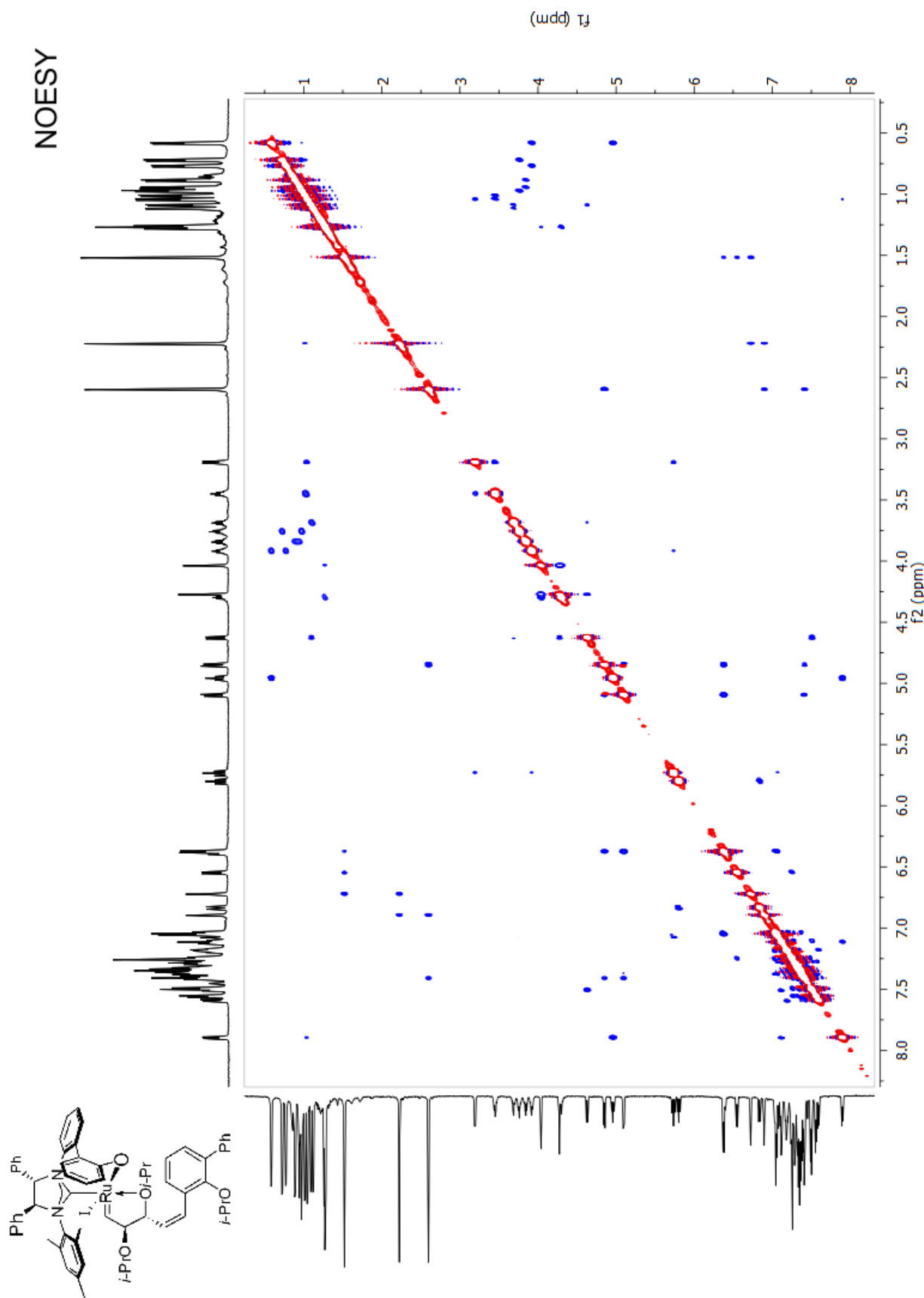
gDQF COSY

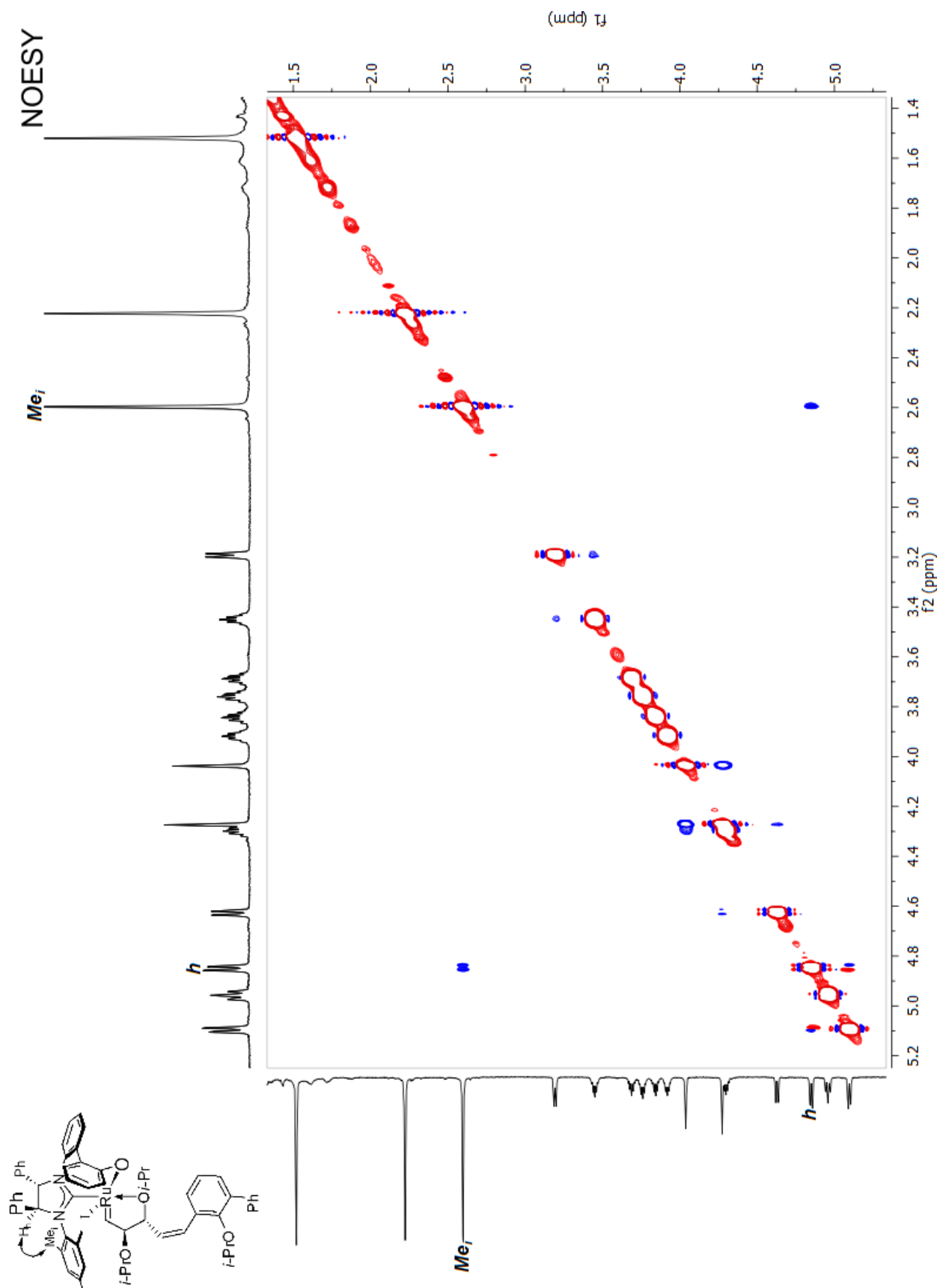


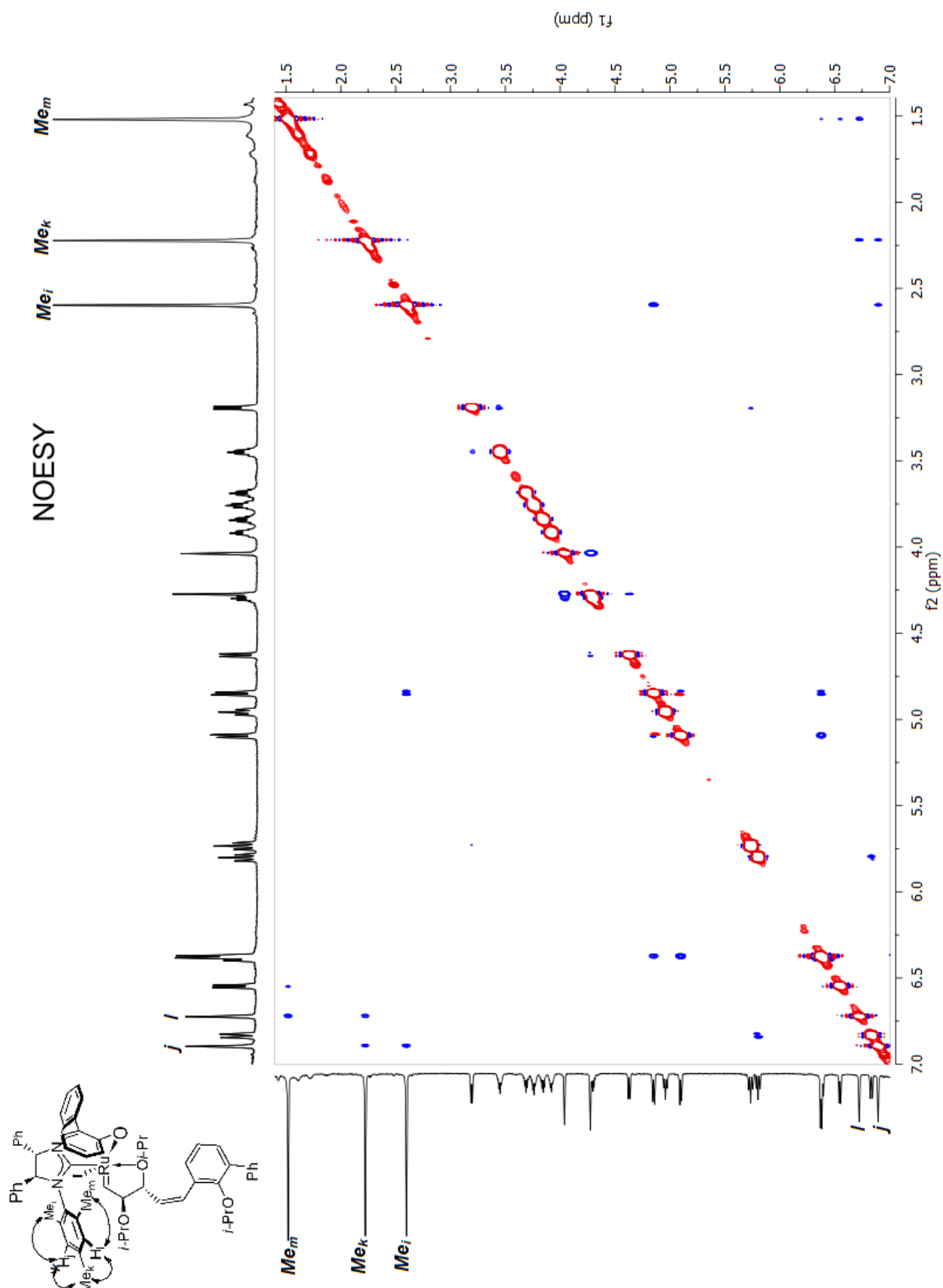


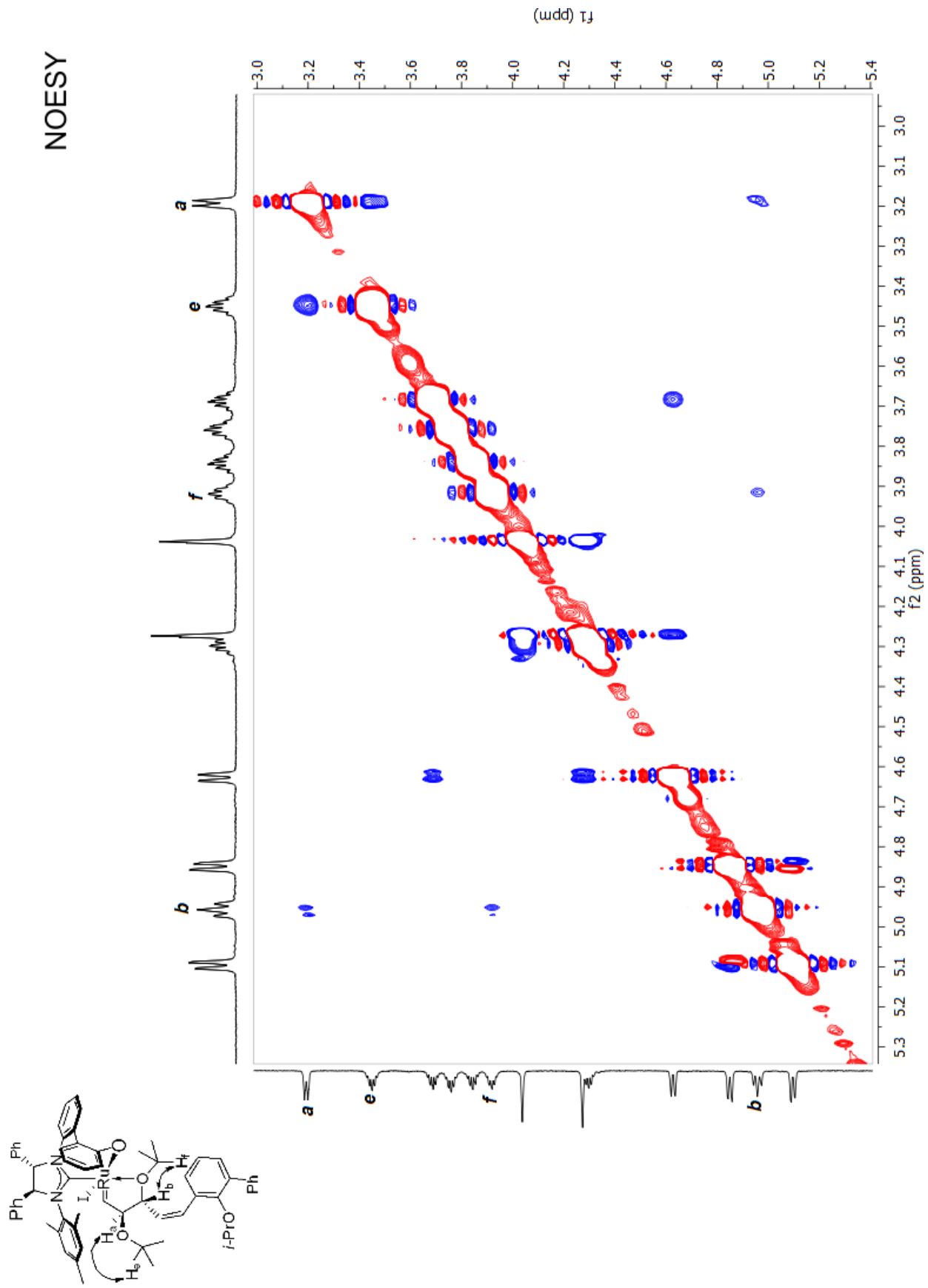


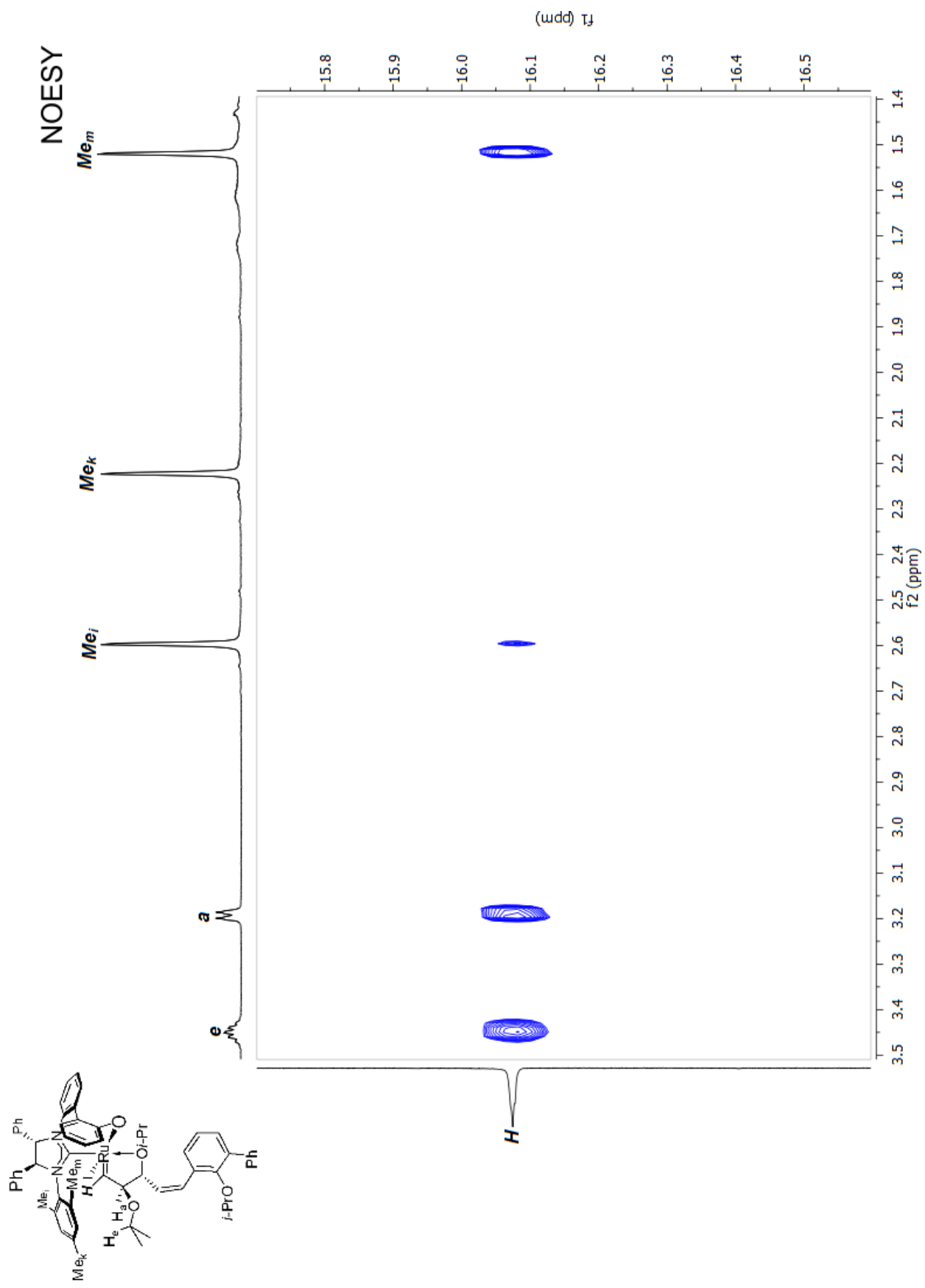


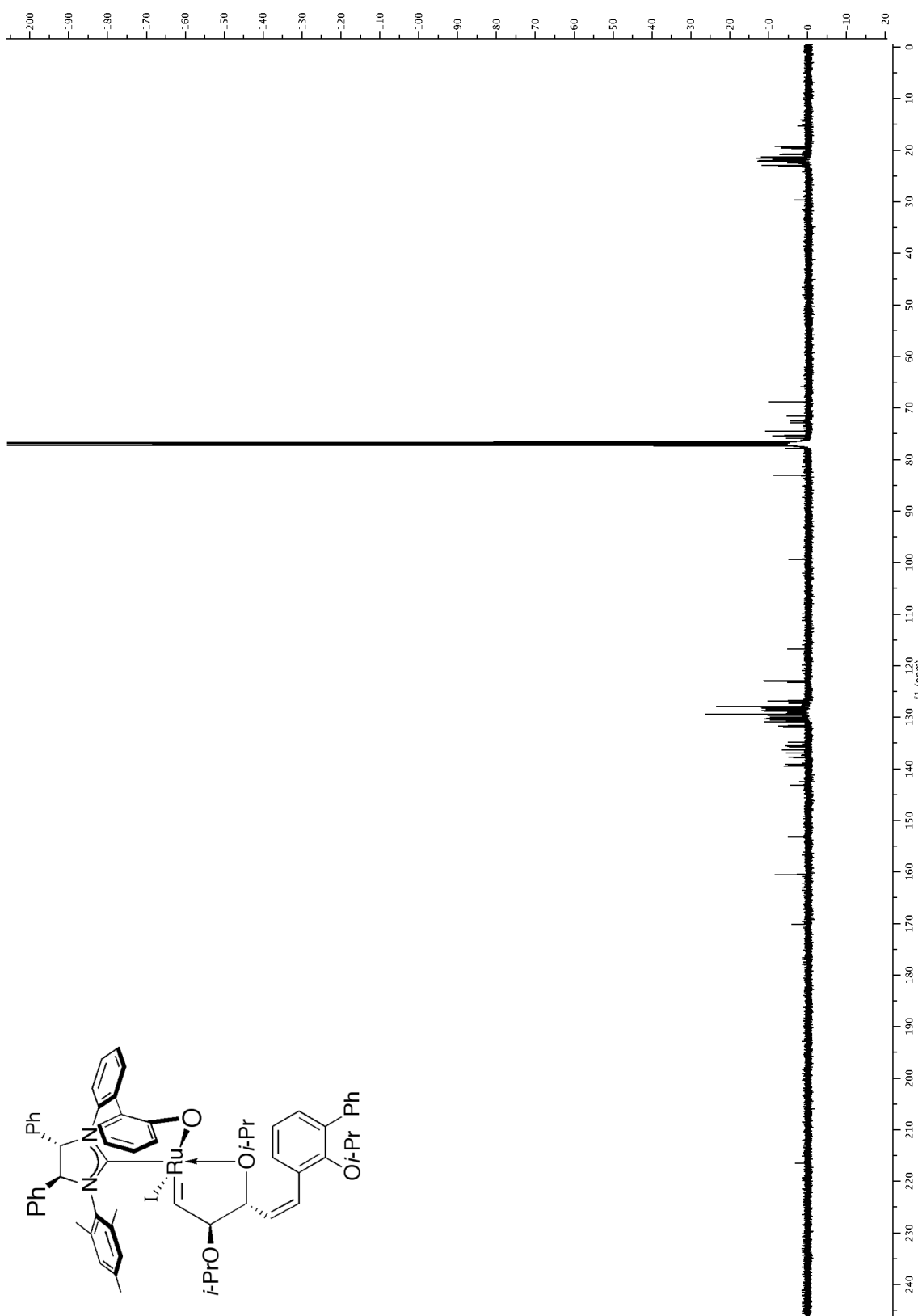


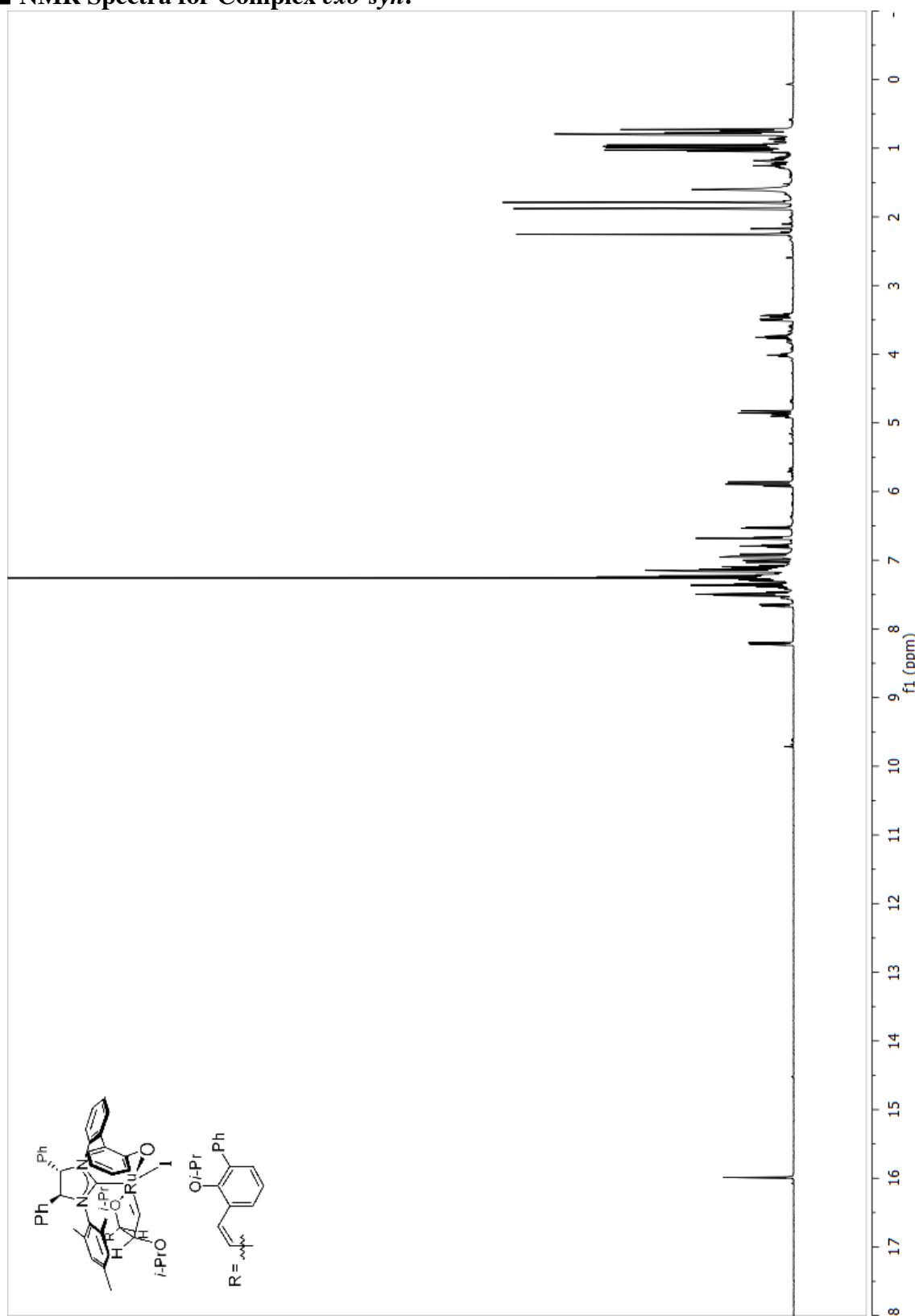


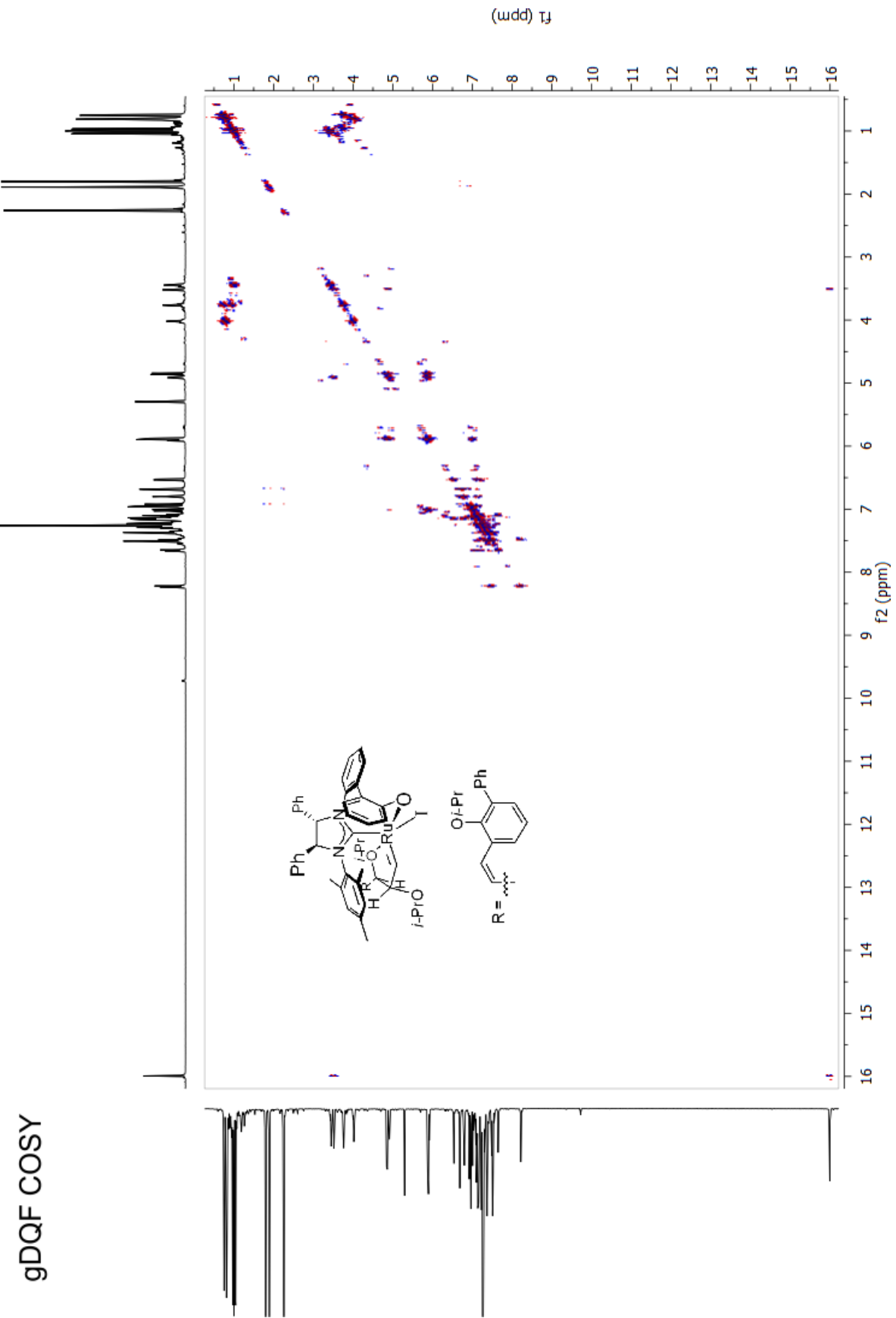


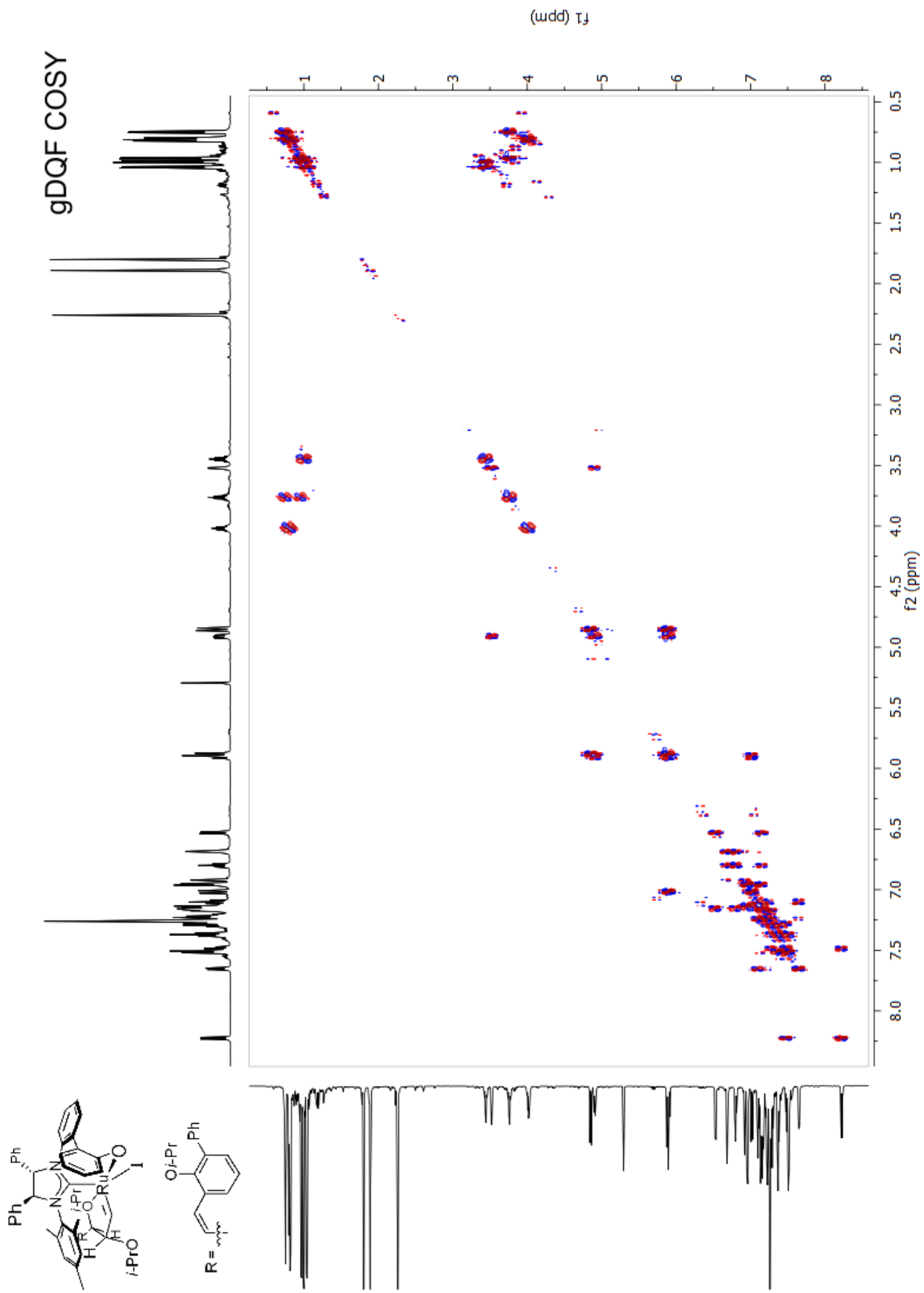




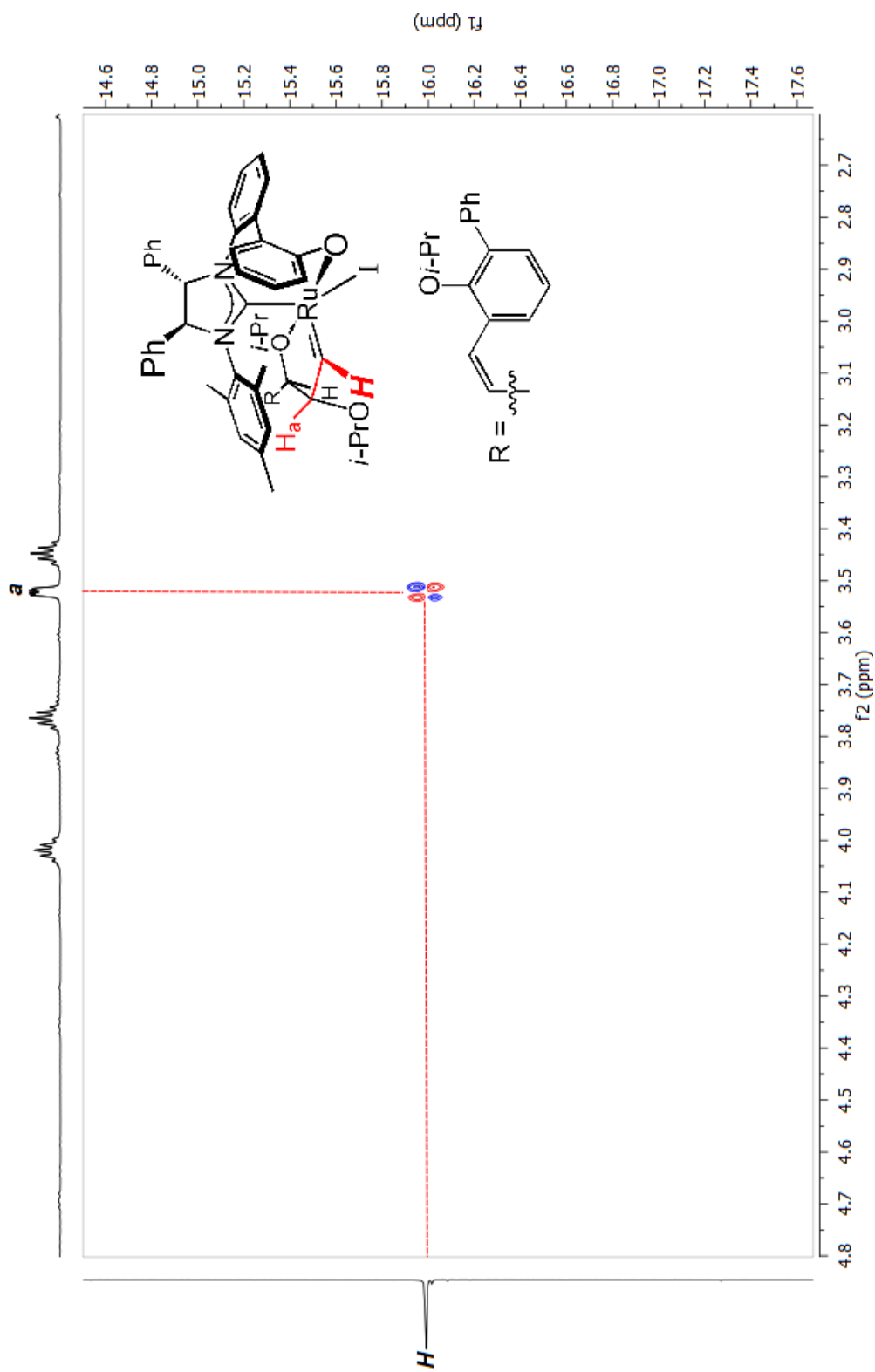


■ NMR Spectra for Complex *exo-syn*:

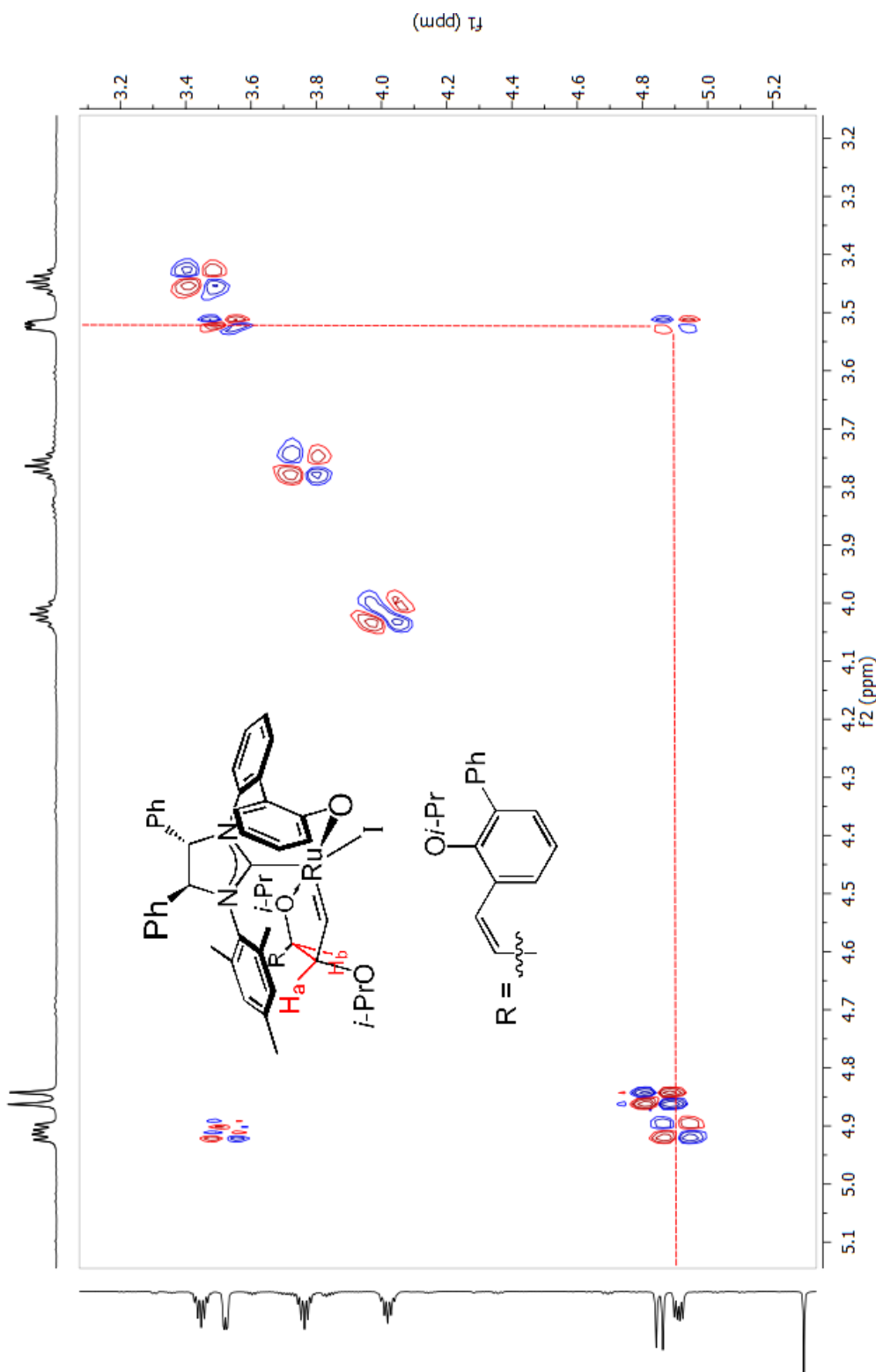




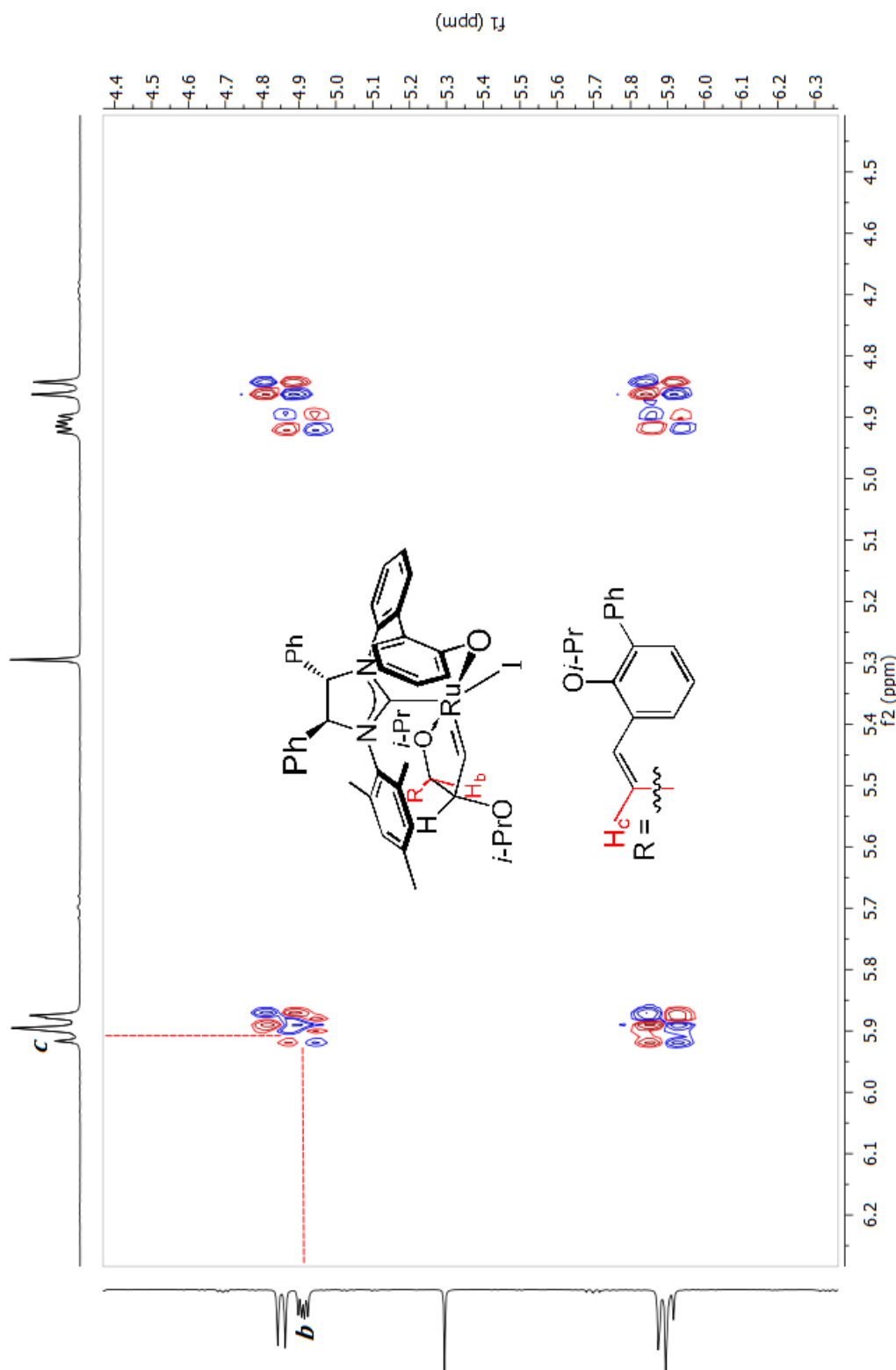
gDQF COSY

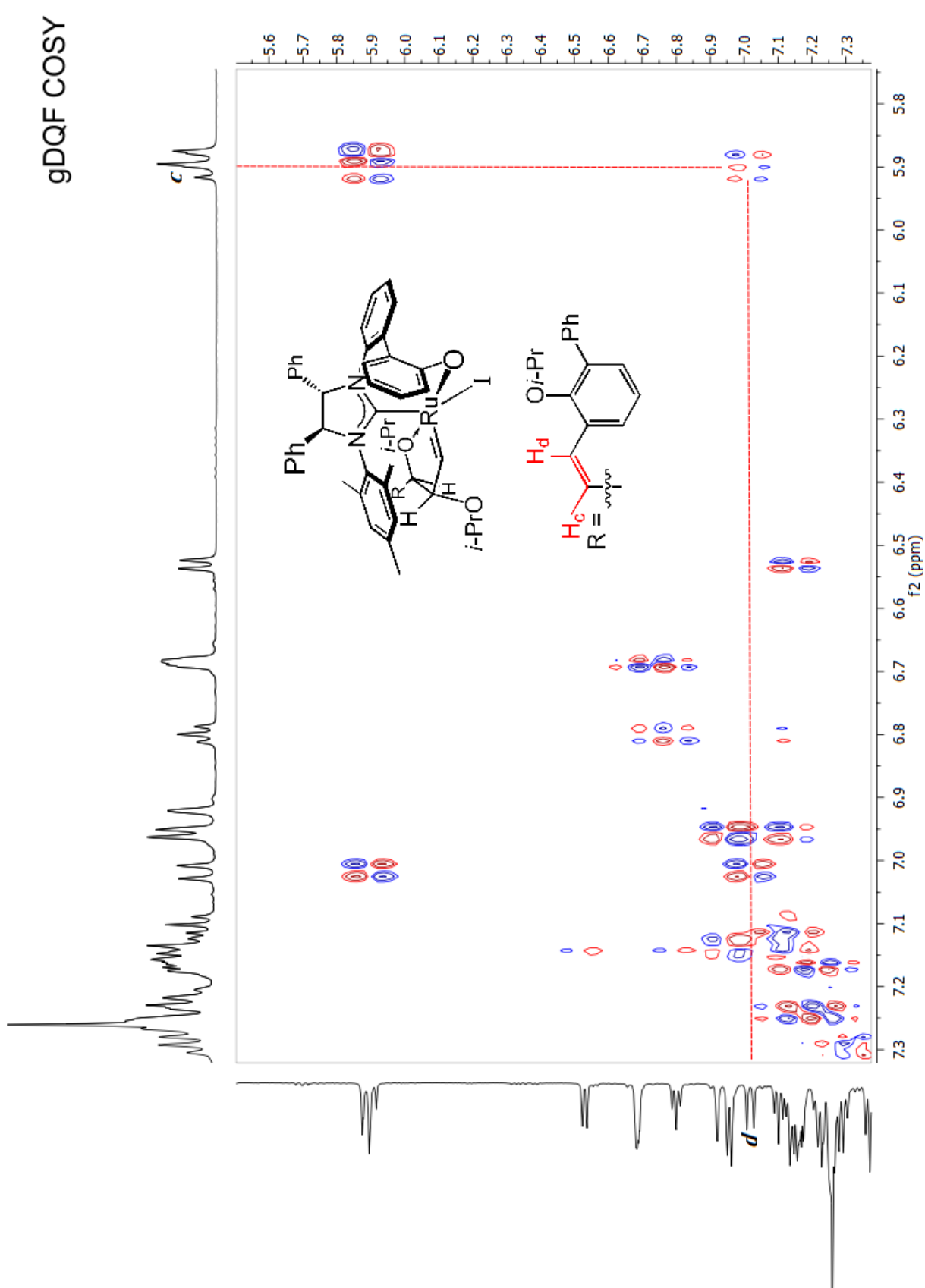


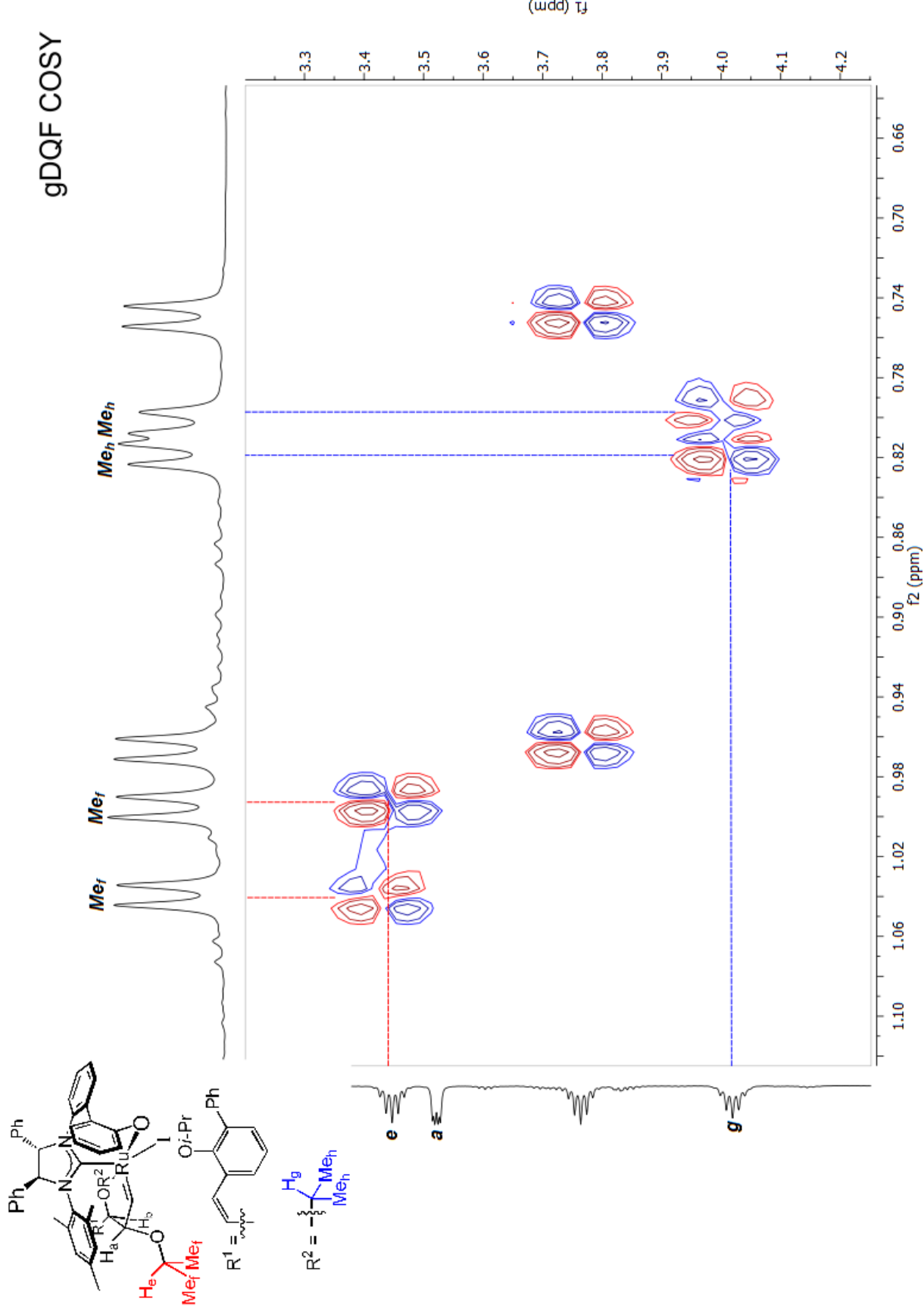
gDQF COSY

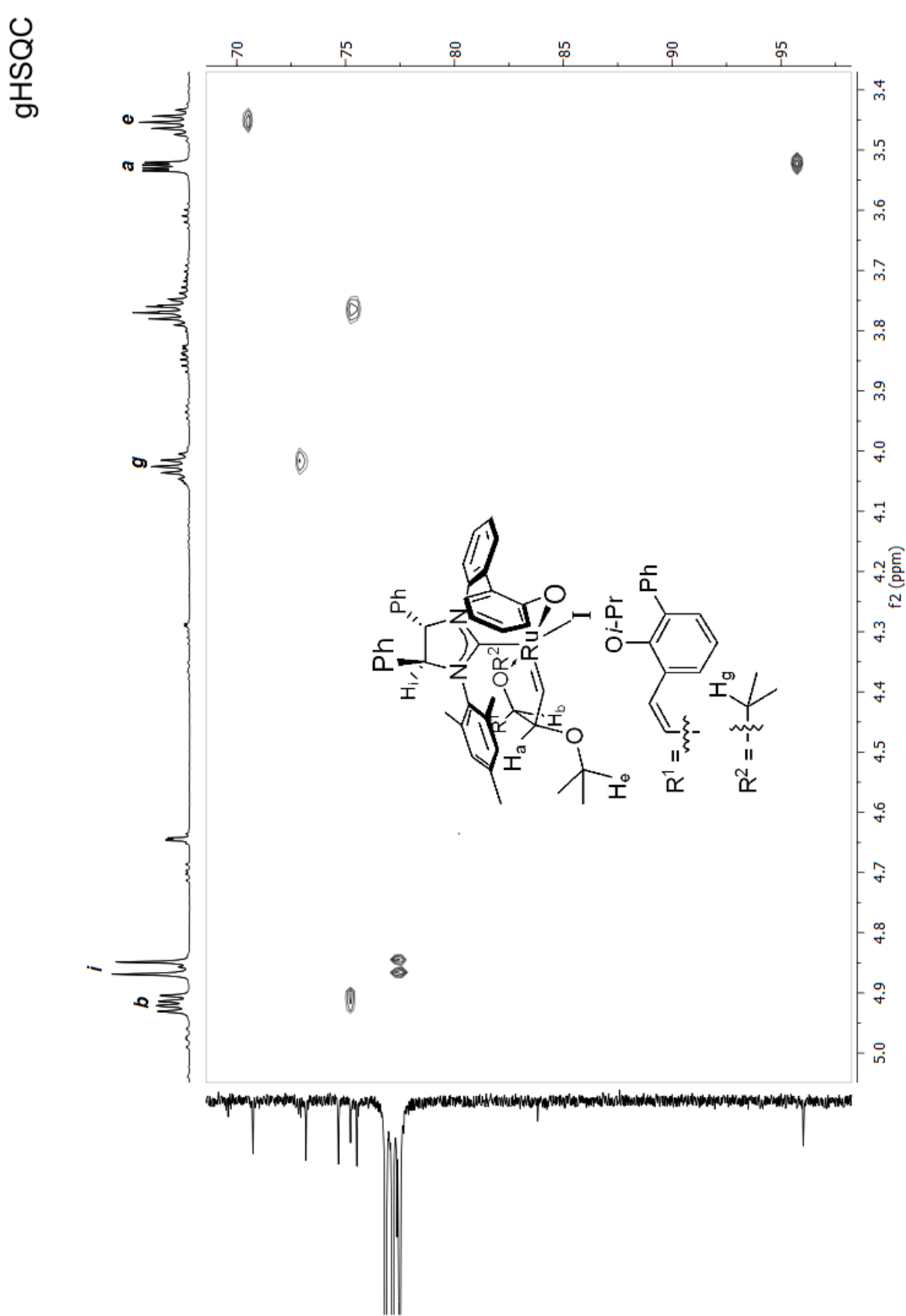


gDQF COSY

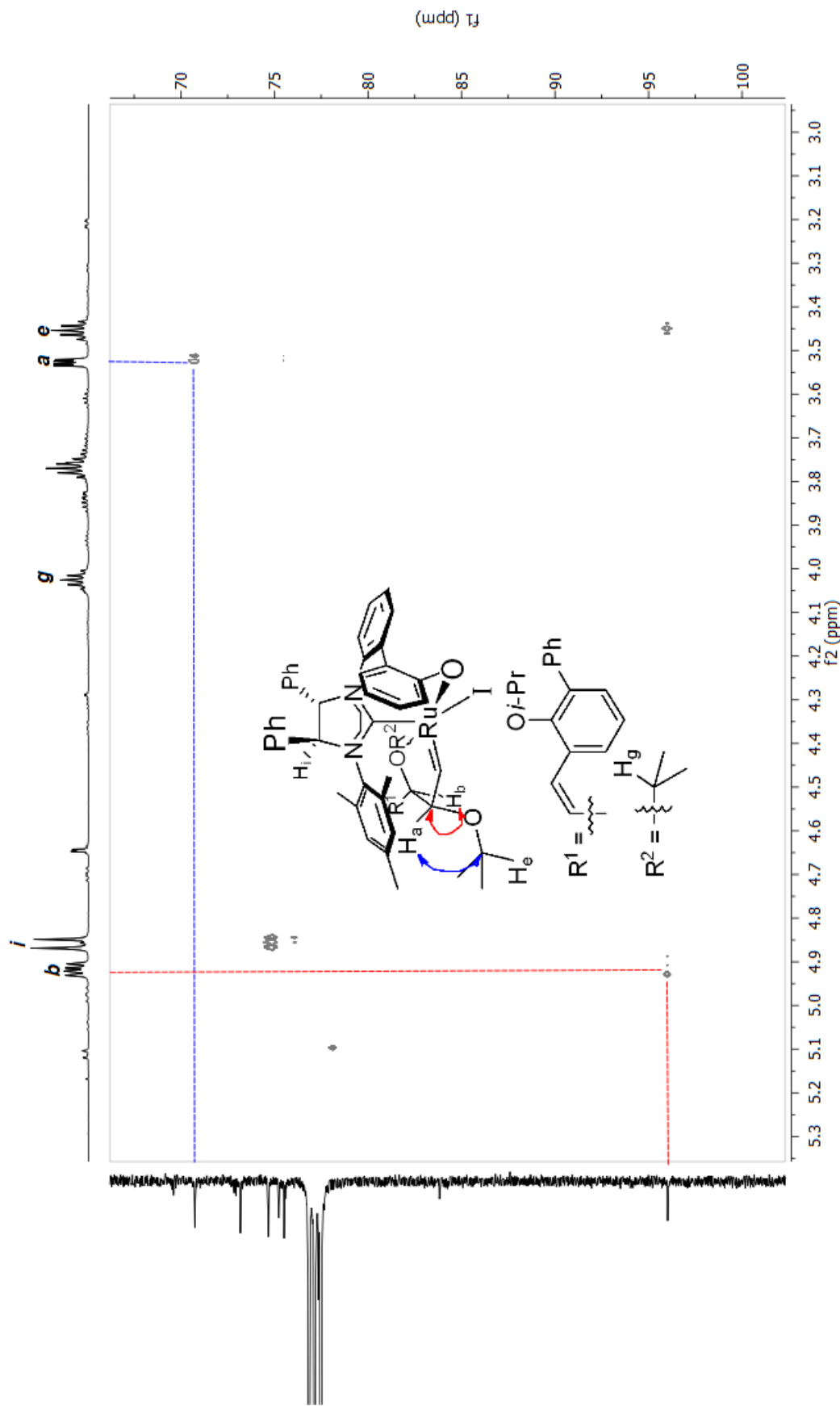


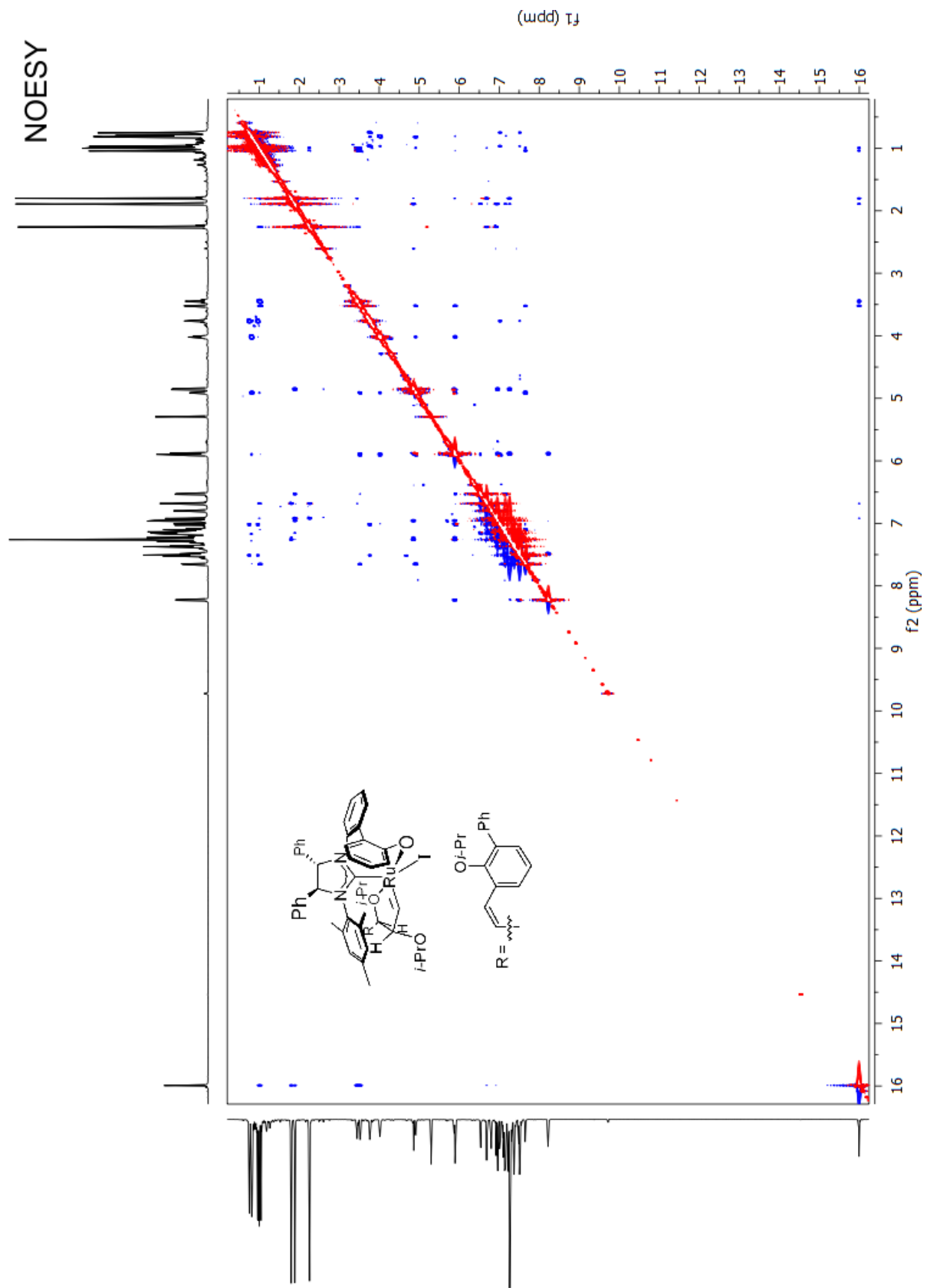


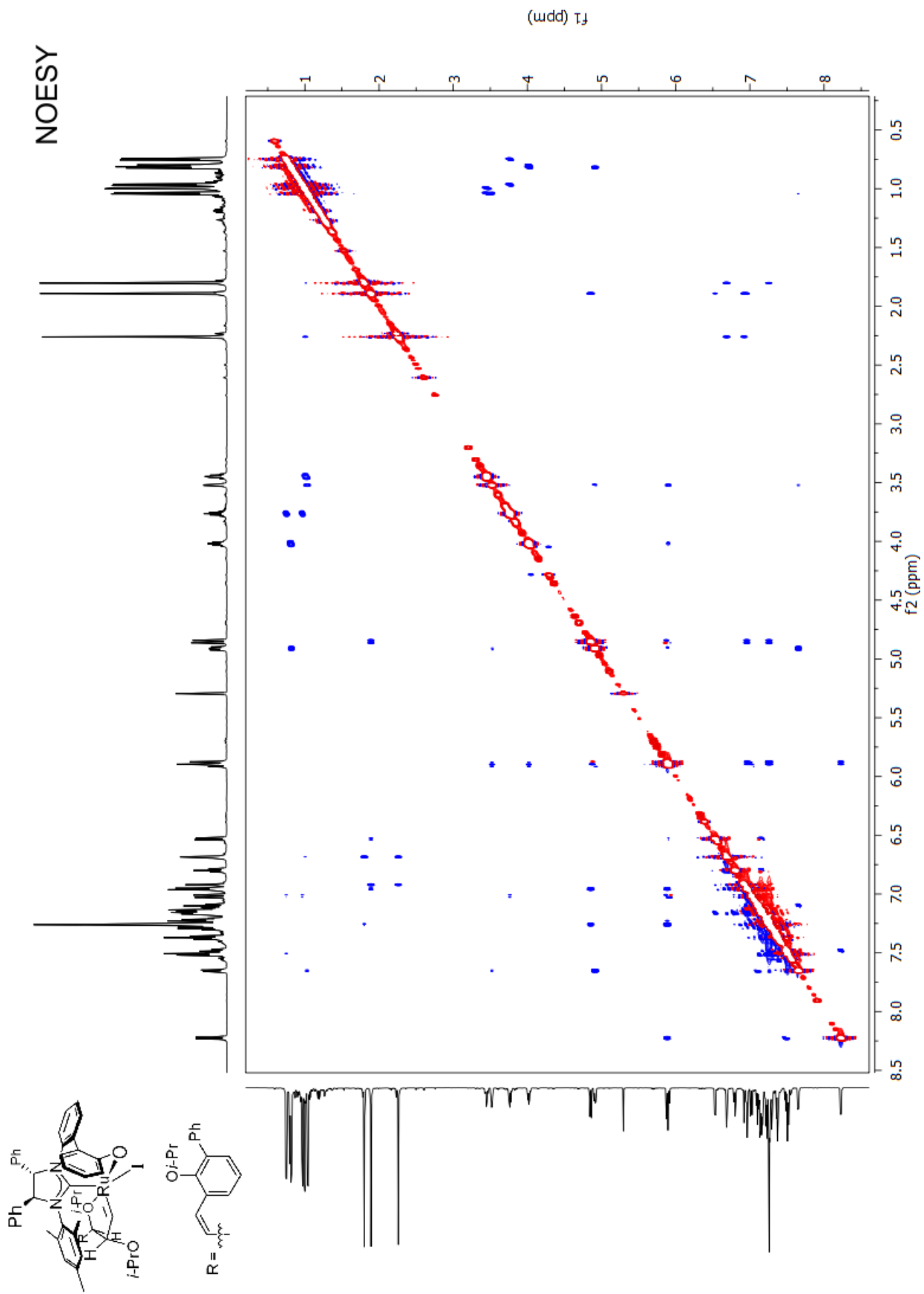


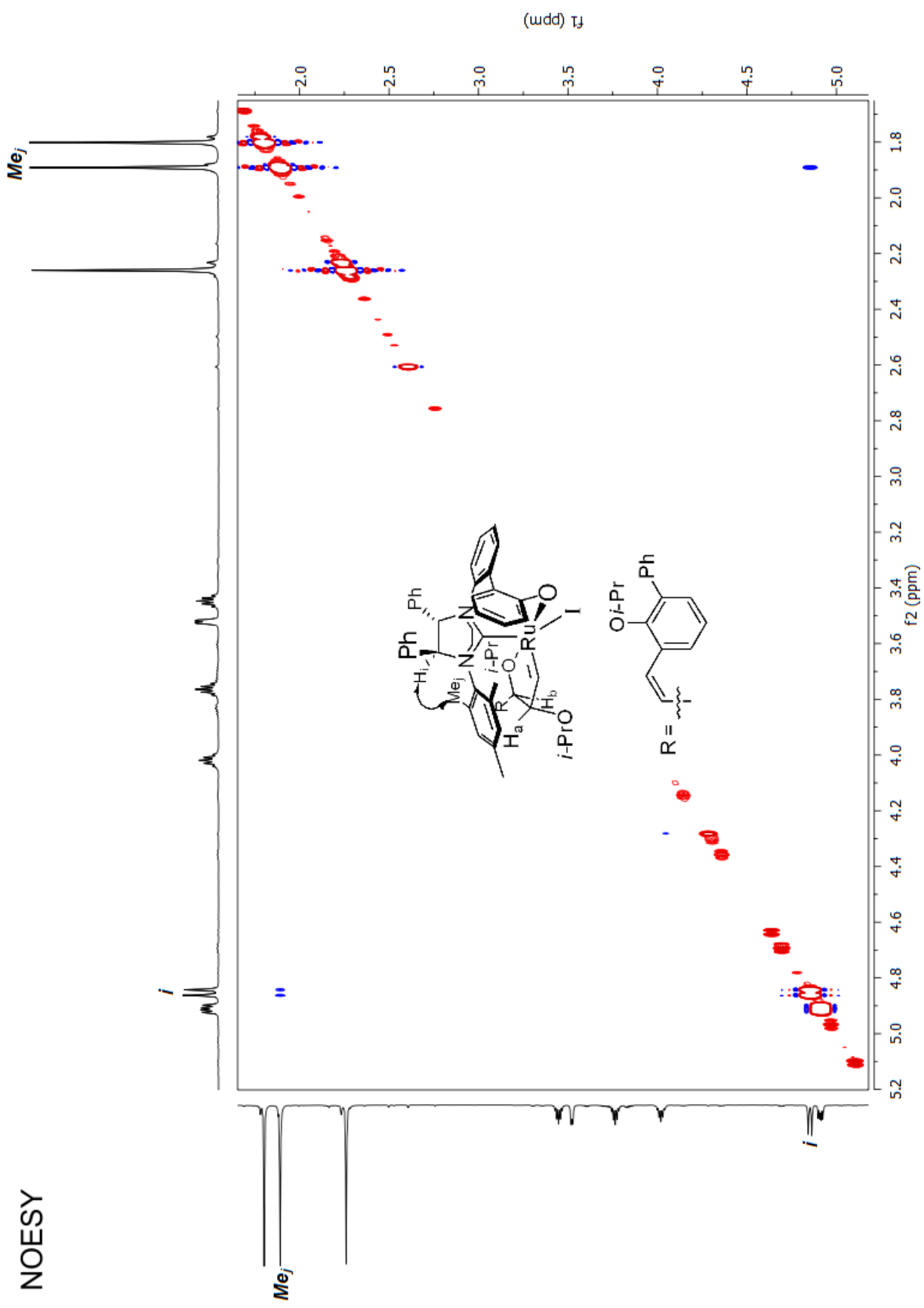


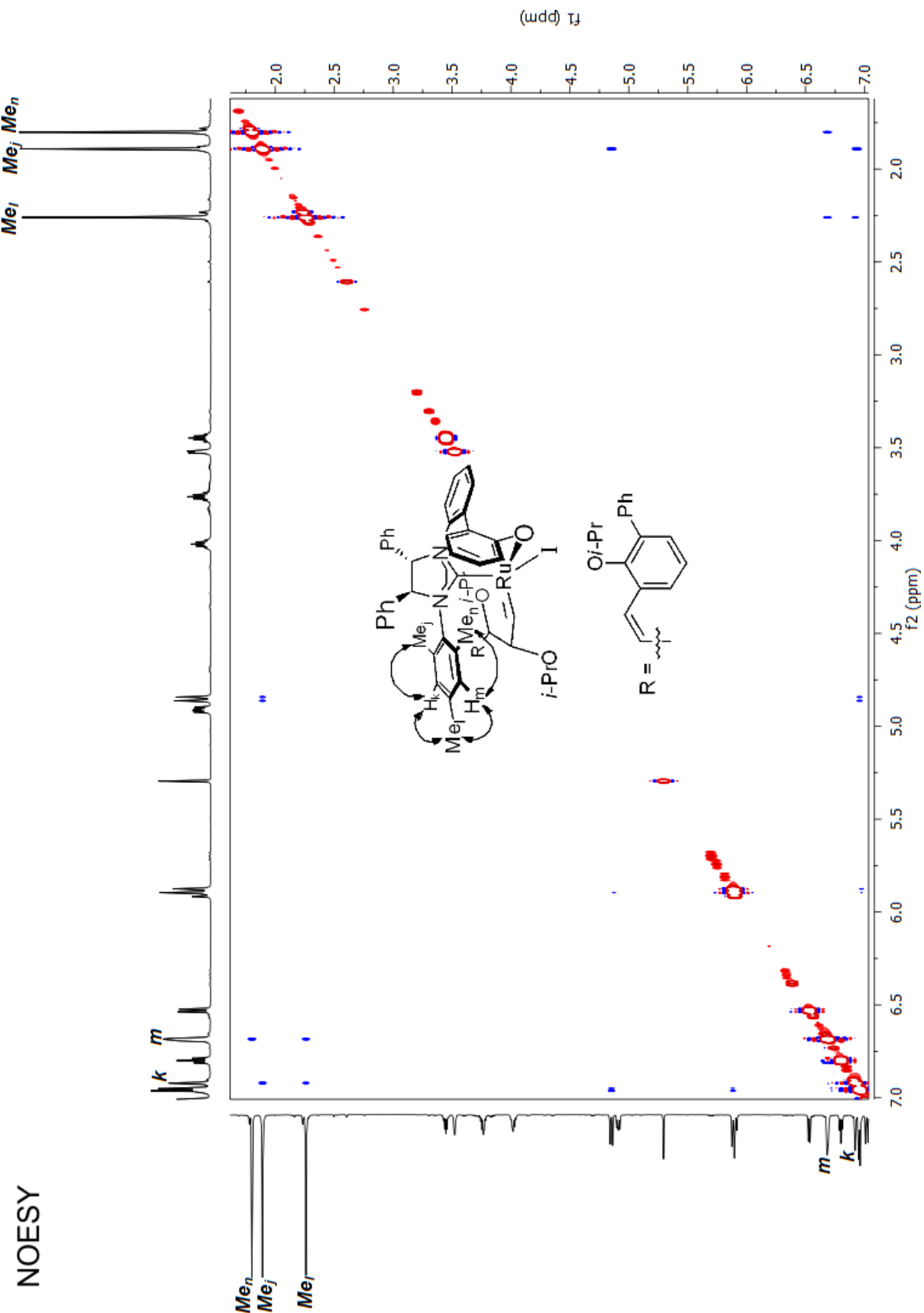
gHMBC

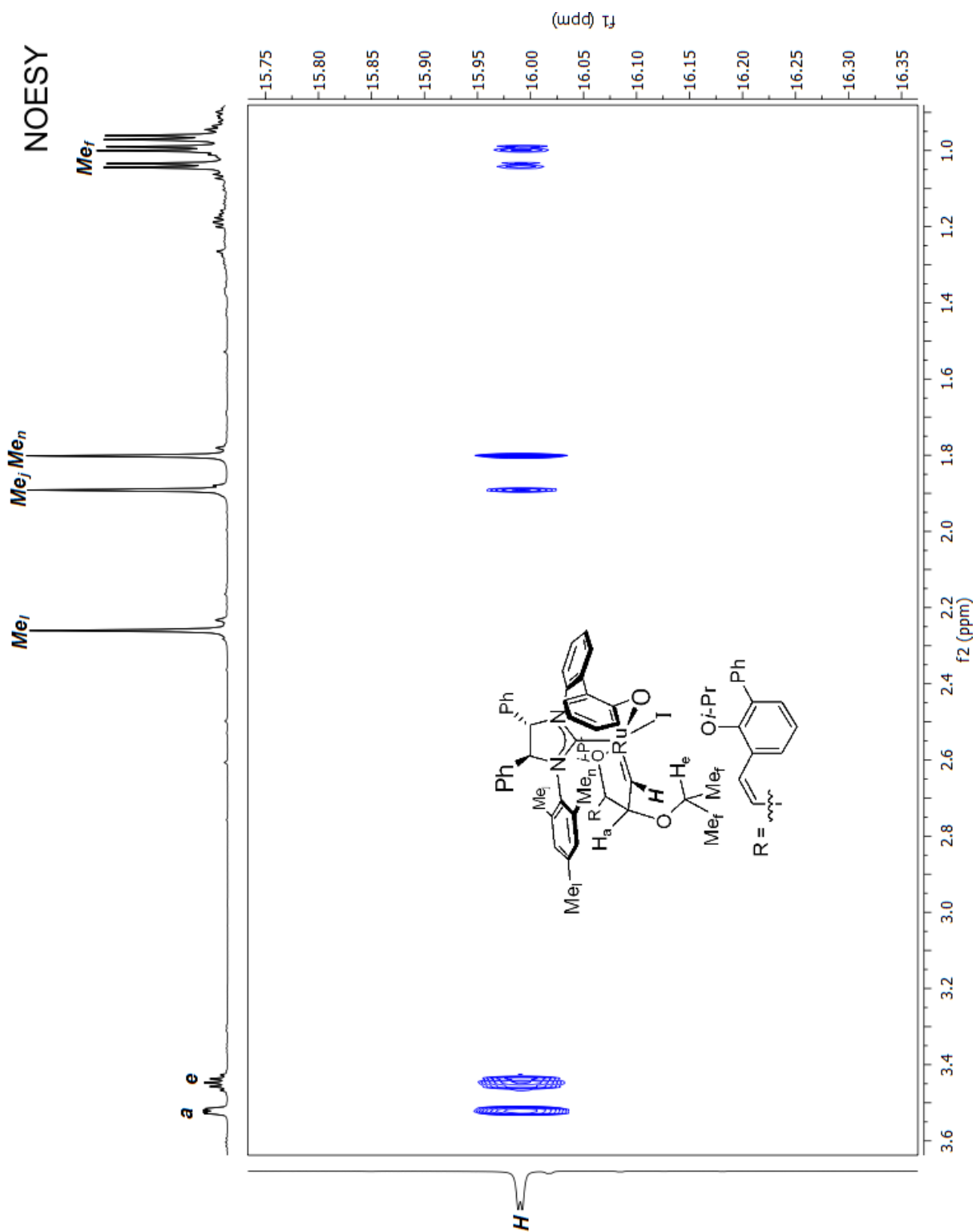


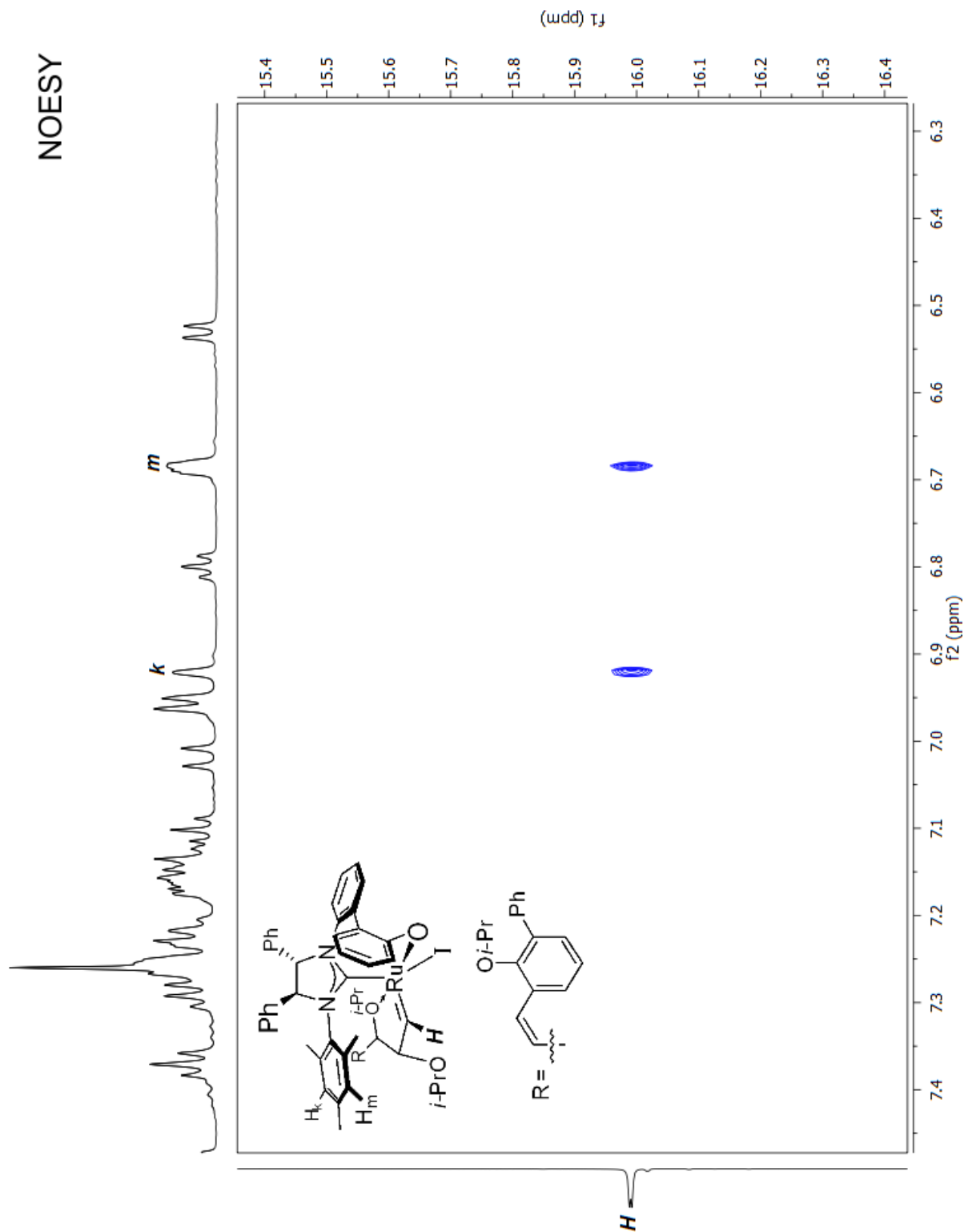


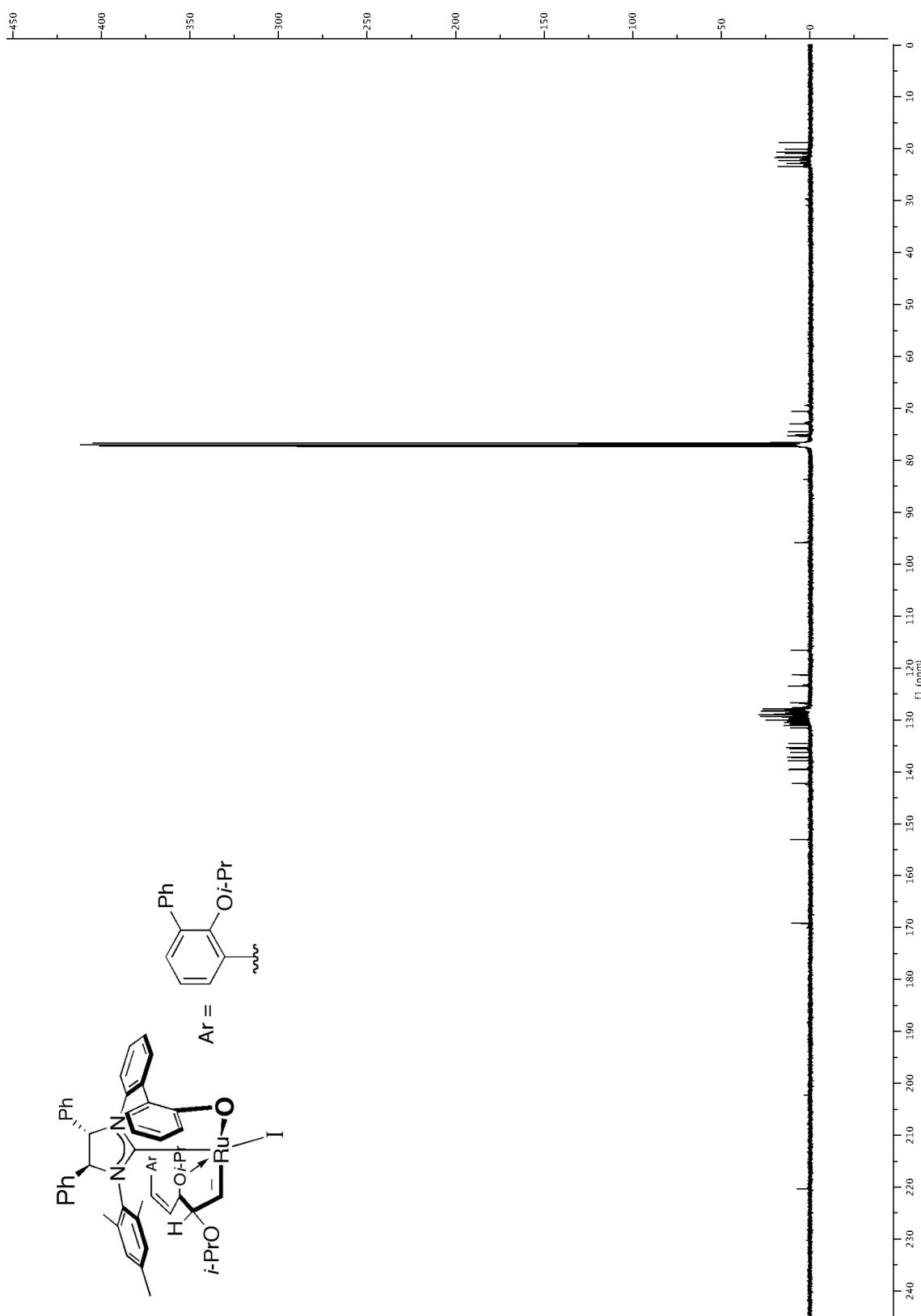




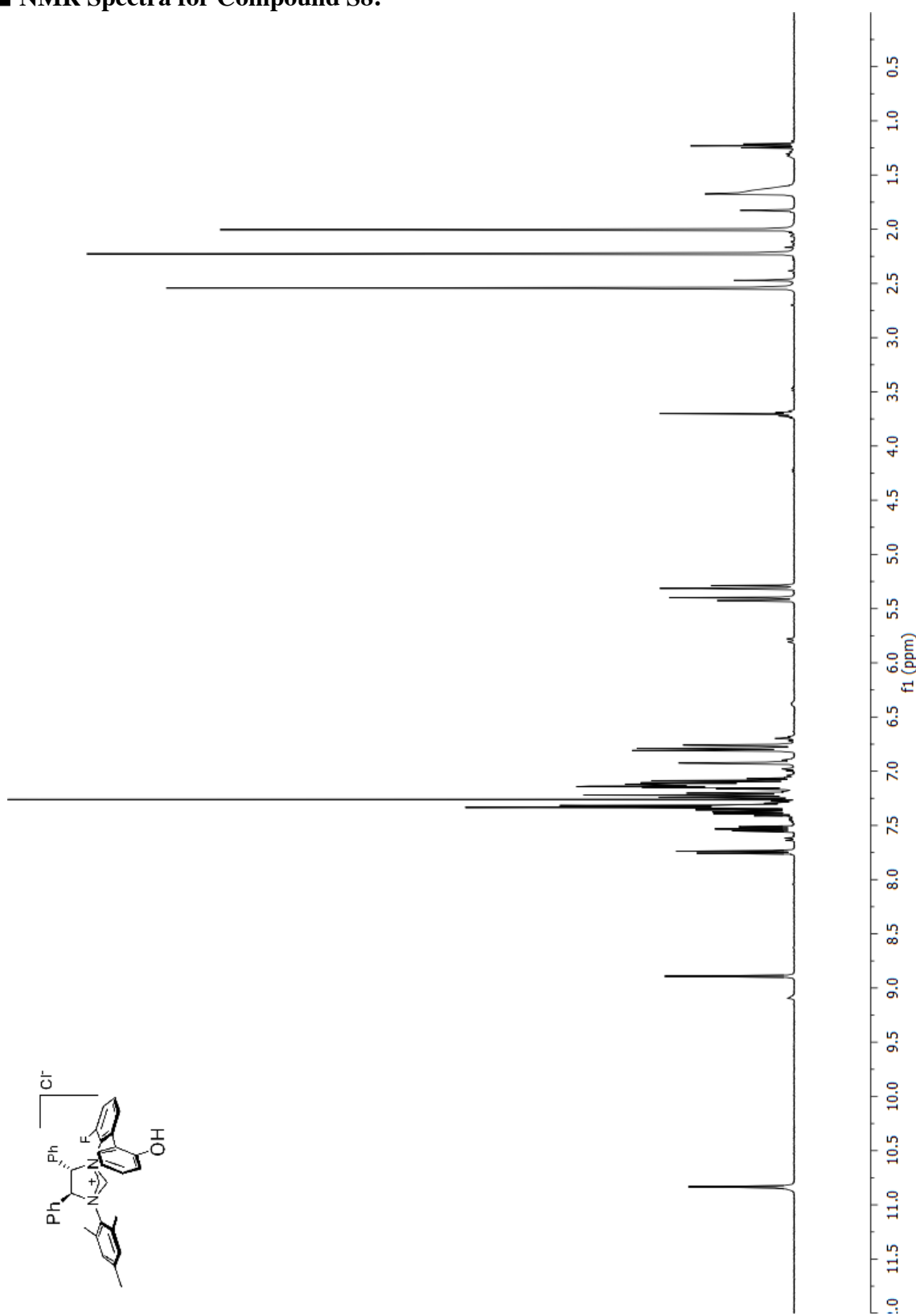




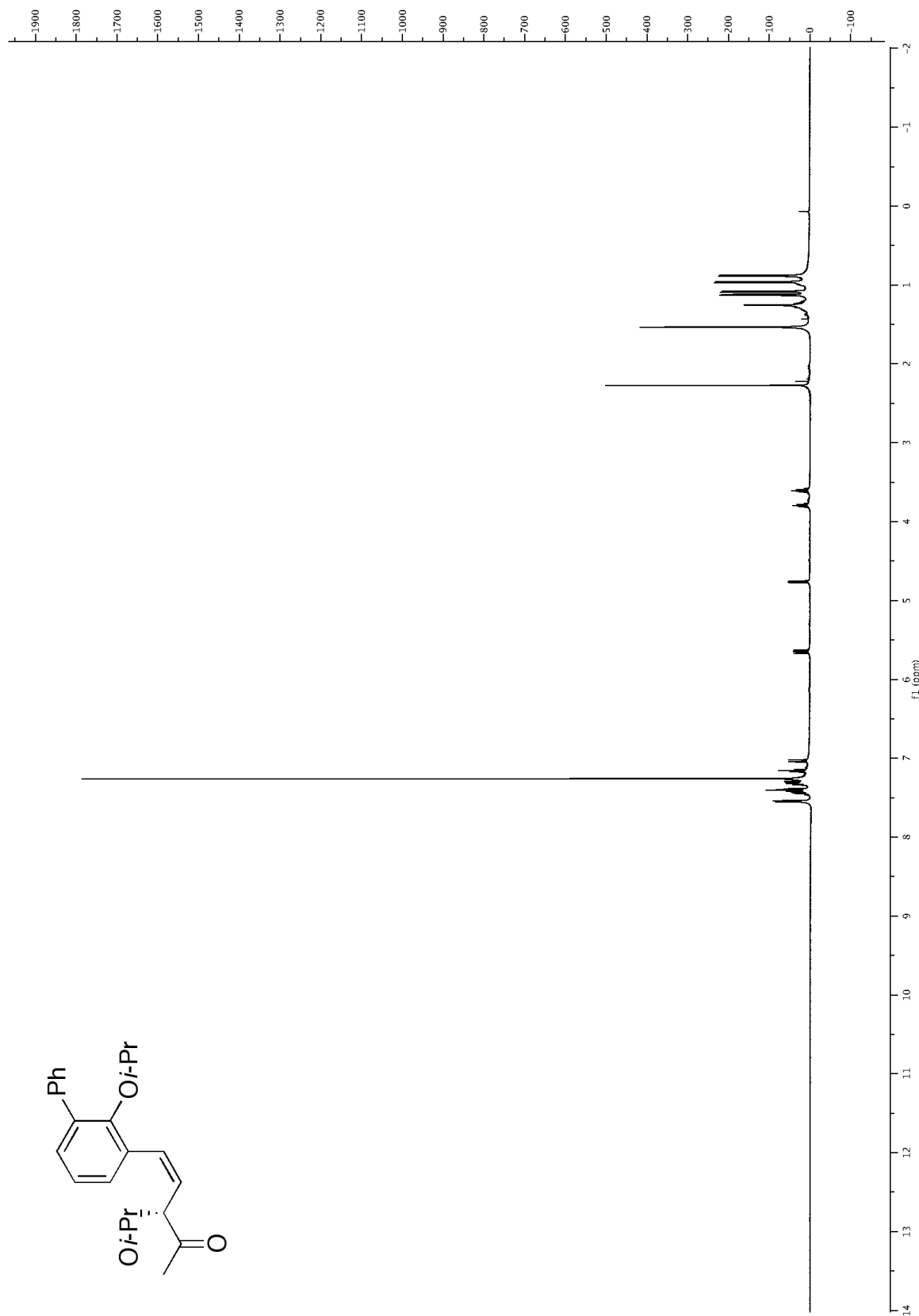


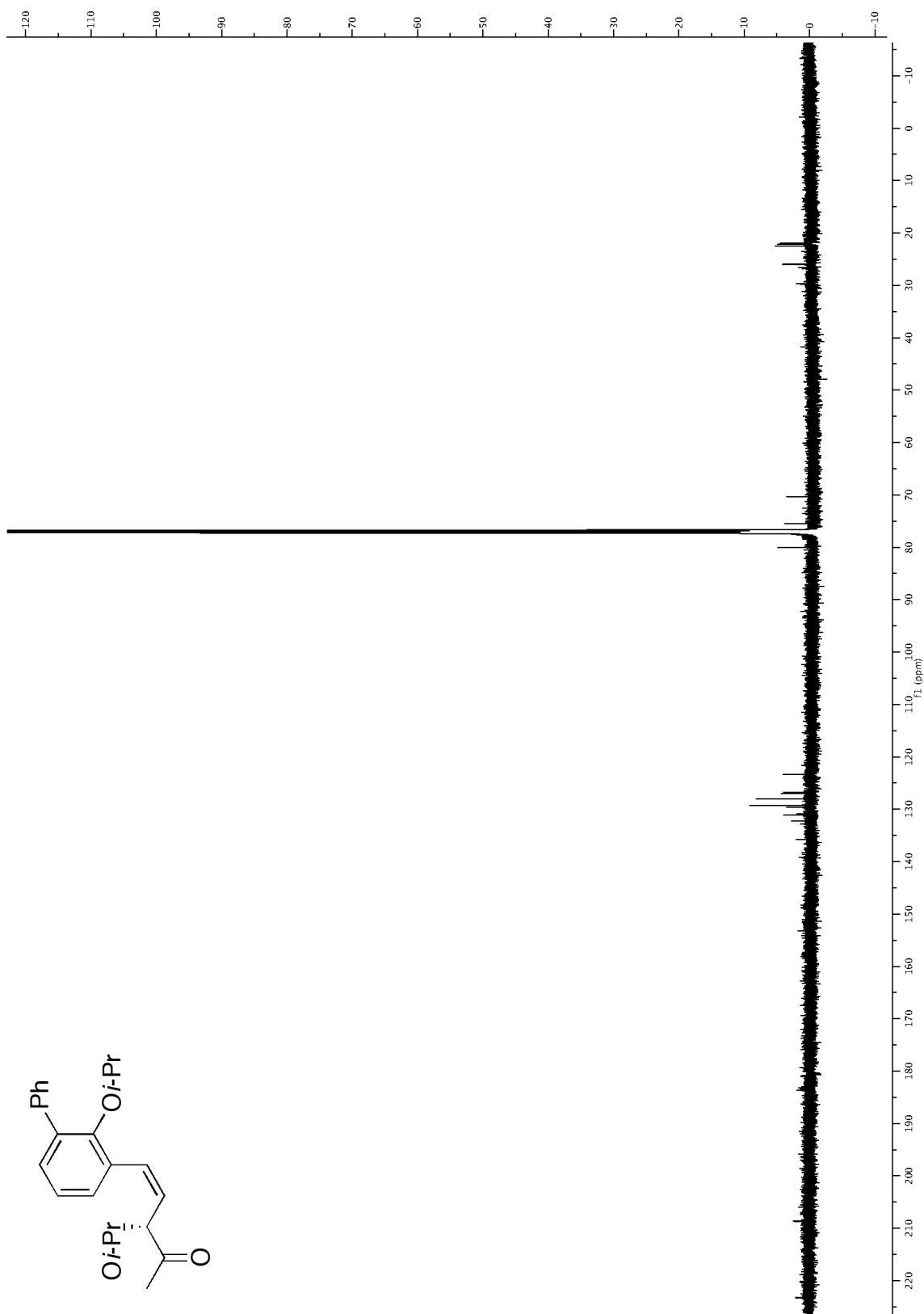


■ NMR Spectra for Compound S8:



■ NMR Spectra for Compound S10:





Highly Z- and Enantioselective Ring-Opening/Cross-Metathesis of Enol Ethers Through Curtin-Hammett Kinetics

Chapter Two

2.1 Introduction

A decade ago, research in our laboratories led to the development of stereogenic-at-Ru complexes that contained ligands involving a bidentate N-heterocyclic carbene with an aryloxide bridge (*cf.* **III** and **IV** in Chapter 1). Since then, we have demonstrated that these diastereo- and enantiomerically pure Ru carbenes, similar to various chiral Mo-based diolates,¹ promote ring-opening/cross-metathesis (ROCM) with high enantioselectivity; however, transformations involve predominantly aryl-substituted alkenes with lower energy *E* product isomers being formed exclusively.² Under their regime, inversions in stereogenic-at-Ru carbenes occur upon each olefin metathesis (OM) event, rendering the presence of two diastereomeric propagating species possible in a productive catalytic cycle (*cf.* *endo* and *exo*, Scheme 1.2-2). After our initial investigations that encompassed the isolation and characterization of the two diastereomeric forms and the appreciation of their energetic differences that directed us to study their stereoisomerization through OM and non-OM pathways (*cf.* Chapter 1), we wished to explore the utility of these carbenes in catalyzing synthetically useful but challenging OM transformations. In this context, we were attracted towards the employment of stereogenic-at-Ru carbenes to efficiently promote highly stereoselective ROCM involving enol ether cross-partners. To the best of our knowledge, there were no examples of highly *E*- or *Z*-selective and/or enantioselective Ru-catalyzed OM transformations involving enol ethers in the literature.

(1) (a) La, D. S.; Ford, J. G.; Sattely, E. S.; Bonitatebus, P. J.; Schrock, R. R.; Hoveyda, A. H. *J. Am. Chem. Soc.* **1999**, *121*, 11603–11604. (b) La, D. S.; Sattely, E. S.; Ford, J. G.; Schrock, R. R.; Hoveyda, A. H. *J. Am. Chem. Soc.* **2001**, *123*, 7767–7778. (c) Cortez, G. A.; Schrock, R. R.; Hoveyda, A. H. *Angew. Chem., Int. Ed.* **2007**, *46*, 4534–4538. For a comparison of Mo- and Ru-based enantioselective ROCM processes, see: (d) Cortez, G. A.; Baxter, C. A.; Schrock, R. R.; Hoveyda, A. H. *Org. Lett.* **2007**, *9*, 2871–2874.

(2) For a representative example, see: Van Veldhuizen, J. J.; Gillingham, D. G.; Garber, S. B.; Kataoka, O.; Hoveyda, A. H. *J. Am. Chem. Soc.* **2003**, *125*, 12502–12508.

Although the commercially available Ru carbenes had been employed as catalysts in ROCM transformations with enol ethers, the reactions suffered from either low efficiency or selectivity (Scheme 2.1A). For instance, Ozawa and coworkers first showed that ROCM of norbornene with phenylvinyl ether in the presence of 2.0 mol% Ru carbene **VII** leads to only 17% yield of **2.1**,³ albeit Z-alkene is favored.⁴ In this case, the main reason for low catalytic activity is the formation of O-substituted Fischer-type carbene (Scheme 2.1A.i),⁵ which is highly stabilized due to resonance (i.e. π -conjugation of O-lone pair with the carbene p-orbital which participates in backbonding with Ru d_{π} -orbital; *cf.* d_{xy} in *horizontal* or d_{xz} in *vertical* orientation, Scheme 1.5.1). Next, although the high activity is achieved through the use of more active second generation carbene **I** (*cf.* Scheme 1.1-2, Chapter 1) to generate **2.2** in 94% yield, relatively similar amounts of *E* and *Z* isomers are observed. The lack of *Z* selectivity (vs with **VII** to give **2.1**) could originate from post-OM based isomerization of kinetically generated *Z* to the corresponding lower energy *E*-isomer of **2.2** (Scheme 2.1A.ii). In contrast with low activity of Ru-carbenes, stereogenic-at-Mo monoaryloxide monopyrrolide (MAP) alkylidenes have been demonstrated to efficiently promote highly *Z*- and enantioselective ROCM with enol ethers.⁶ For example, ROCM of **2.3** with 5.0 equiv of butylvinyl ether (bve) in the presence of 0.15 mol% MAP complex proceeds within 10 minutes to generate **2.4** with unprecedented selectivity (>98% *Z*; 99:1 *er*) and efficiency (76% yield). Notably, unlike the attenuated activity with low oxidation-state Ru Fischer carbenes, no diminution in reactivity is observed with high oxidation-state Mo-alkoxylidenes, which is most likely due to the lack of resonance stabilization.

With the aforementioned details in mind, we argued that the development of highly efficient and stereoselective Ru-catalyzed ROCM involving enol ethers would entail two main advantages: 1) It would provide an opportunity to develop more active

(3) Katayama, H.; Urushima, H.; Nishioka, T.; Wada, C.; Nagao, M.; Ozawa, F. *Angew. Chem., Int. Ed.* **2000**, *39*, 4513–4515.

(4) We believe that the *Z* selectivity is *kinetically* favored in this process. For details, see: Section 2.6 for substrate-based *Z* selectivity.

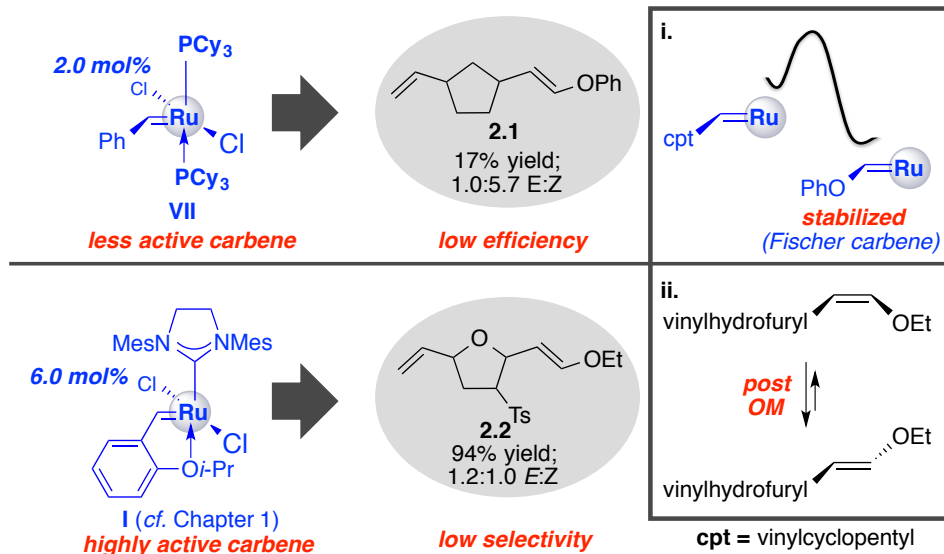
(5) Enol ethers are typically utilized to terminate OM transformations due to their “irreversible” formation of the Fischer-type carbenes or in studies regarding catalyst initiation. See: Maynard, H. D.; Okada, S. Y.; Grubbs, R. H. *Macromolecules* **2000**, *33*, 6239–6248.

(6) For Mo-catalyzed enantioselective ROCM with enol ethers, see: Yu, M.; Ibrahim, I.; Hasegawa, M.; Schrock, R. R.; Hoveyda, A. H. *J. Am. Chem. Soc.* **2012**, *134*, 2788–2799.

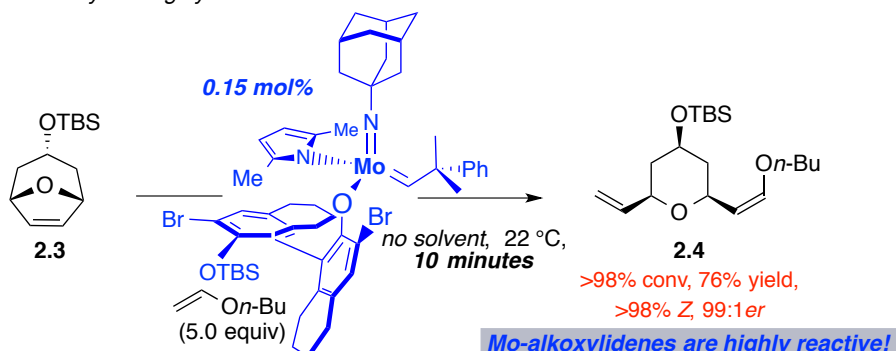
low oxidation-state Ru catalysts that could tolerate alcohols and a broad range of electrophilic moieties (vs Mo-catalysts), rendering them useful in organic synthesis 2) The transformations catalyzed by stereogenic-at-Ru Fischer carbenes could offer mechanistic insights distinct from reactions involving aryl- or alkyl-substituted alkenes.

Scheme 2.1. Comparison of Ru-Carbenes and Mo-Alkyldenes in ROCM of Enol Ethers

A. Ru-Catalyzed Olefin Metathesis with Enol Ether Cross Partners



B. Mo-Catalyzed Highly Efficient and Stereoselective Olefin Metathesis with Enol Ethers

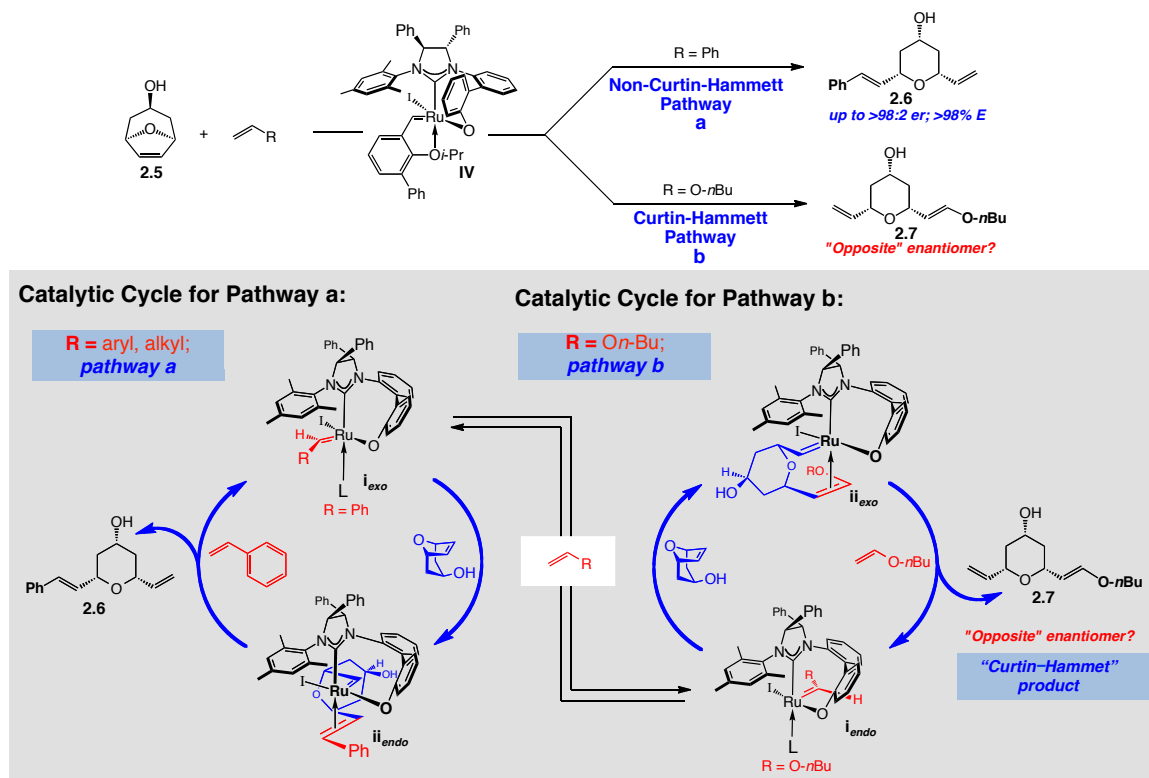


Our investigation initiated by considering the catalytic cycle of ROCM involving styrene and oxabicycle **2.5** promoted by stereogenic-at-Ru carbene **IV**, which affords **2.6** in high selectivity (>98% *E* and >98% *er*).⁷ As shown below (*pathway a*, Scheme 2.2),

(7) Van Veldhuizen, J. J.; Campbell, J. E.; Giudici, R. E.; Hoveyda, A. H. *J. Am. Chem. Soc.* **2005**, *127*, 6877–6882.

benzylidene **i_{exo}** (i.e. preferred state of the catalyst) is reactive enough to promote ring-opening metathesis (ROM) with strained oxabicyclic (2.5) to afford the higher energy alkylidene **ii_{endo}**. The latter species subsequently reacts with styrene to complete the catalytic cycle and product (2.6) is furnished. However, in the presence of enol ether cross-partner, which would generate stabilized Fischer carbene **i_{exo}** (wherein R = On-Bu), we became concerned with the feasibility of ROM with 2.5 through *pathway a*. We reasoned that the aforementioned reaction would incur a high-activation barrier due to the loss of stability on two counts: a) Transformation of lower energy **i_{exo}** to higher energy **ii_{endo}** (*cf.* Scheme 1.2-1, Chapter 1) b) ROM of Fischer carbene to generate non-resonance stabilized **ii_{endo}** carbene.

Scheme 2.2. Advantage of Curtin–Hammett Pathway for ROCM with Enol Ethers



Alternatively, we considered the viability of ROM involving Fischer-type carbene through *pathway b*. According to this proposal, if fast equilibration between two diastereomeric Fischer carbenes (**i_{exo}** and **i_{endo}**) is achieved, then the reaction could proceed through the participation of the more-active but less-abundant **i_{endo}** (i.e. Curtin–Hammett situation). Furthermore, the formation of lower-energy **ii_{exo}** (vs **ii_{endo}**,

pathway a) would involve a lower-activation barrier, rendering the ROM facile. Subsequently, **ii_{exo}** could react with bve to regenerate resonance-stabilized **i_{endo}** and afford the ROCM product (**2.7**). Additionally, computational efforts corroborated our considerations, indicating that **i_{exo}–i_{endo}** interconversion of heteroatom-substituted carbenes is less energetically demanding than the other steps in the catalytic cycle, and that Curtin–Hammett kinetics might be operative (see below for details). It is also noteworthy that the absolute stereochemistry of the Curtin–Hammett kinetics product (**2.7**) would be *opposite* to the one obtained through *pathway a* (i.e. **2.6**, stereochemistry-determining ROM is promoted by **i_{exo}** vs **i_{endo}** in *pathway b*), given that the same mode of oxabicyclic alkene addition takes place. Furthermore, we anticipated high *E*-selectivity, as all previous ROCM reactions with this class of chiral Ru catalysts had uniformly afforded the lower energy disubstituted alkene isomer exclusively.⁷

2.3 Development of *Z*- and Enantioselective ROCM of Enol Ethers⁸

2.3.1 Highly *Z*- and Enantioselective ROCM Involving bve Catalyzed by Stereogenic-at-Ru Carbene (IV)

We began our investigation by subjecting oxabicycle **2.5** to bve and 5.0 mol % **IV** (Scheme 2.3.1a). The desired process took place readily indeed, affording **2.8a** in 80% yield and >98:2 *er*. We established that the sense of enantioselectivity is *opposite* to that found in reactions with aryl olefins.⁷ Furthermore, and unexpectedly, we discovered that the *Z* enol ether is generated predominantly (95% *Z*-**28a**). As further demonstrated in Scheme 2.3-1, the Ru-catalyzed ROCM can be performed with as low as 0.5 mol % **IV** to afford **28a** in 60% yield, 95% *Z* selectivity, and >98:2 *er*. In stark contrast, in the recently disclosed version of the process catalyzed by MAP complex (Scheme 2.1B), a uniform sense of enantioselectivity is observed regardless of whether an aryl olefin⁹ or an enol ether⁶ is used as the cross partner. In other words, unlike stereogenic-at-Ru carbenes such as those derived from **IV**, the same stereogenic-at-Mo alkylidene diastereomer is

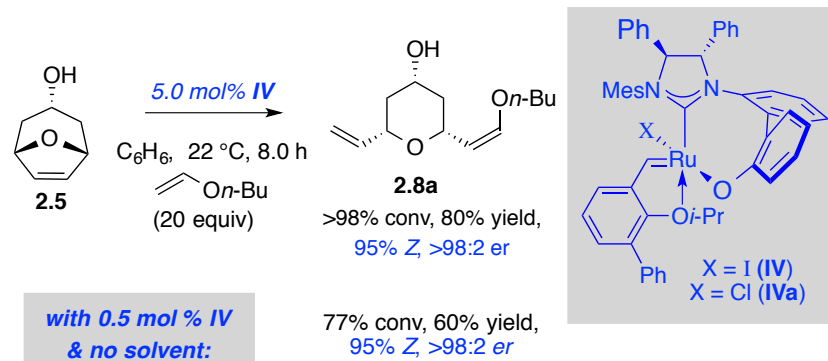
(8) Khan, R. K. M.; O'Brien, R. V.; Torker, S.; Li, B.; Hoveyda, A. H. *J. Am. Chem. Soc.* **2012**, *134*, 12774–12779.

(9) For ROCM reactions with aryl olefin catalyzed by MAP alkylidenes, see: Ibrahem, I.; Yu, M.; Schrock, R. R.; Hoveyda, A. H. *J. Am. Chem. Soc.* **2009**, *131*, 3844–3845.

probably involved in the stereochemistry-determining stage of the transformation. More importantly, the Mo-catalyzed ROCM reactions do not tolerate the presence of an unprotected alcohol, rendering the development of the Ru-catalyzed protocol synthetically attractive.

Scheme 2.3.1. Efficient and Z-Selective ROCM of Enol Ethers with IV

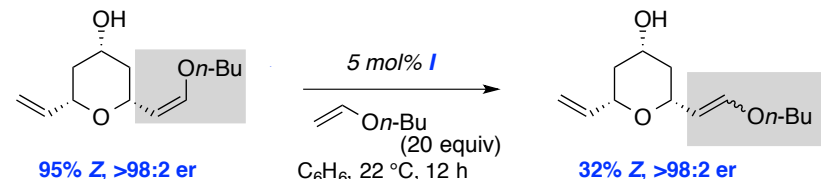
a. Highly Z- and Enantioselective ROCM with Stereogenic-at-Ru Carbenes



b. Low Efficiency with Non-Stereogenic-at-Ru Complexes

IVa	VII	I
85% conv, 58% yield, 92% Z, 97:3 er	7% conv, yield nd, 82% Z	79% conv, 41% yield, 77% E

c. Post-OM Isomerization Possible for Low Z-Selectivity with I



Next, studying the outcome of reactions with different Ru carbenes ensued (Scheme 2.3.1b). Interestingly, the catalytic ROCM with chloride analogue **IVa** furnishes **28a** in lower yield, Z - and enantioselectivity than when Ru iodide **IV** is employed (58% vs 80% yield, 97:3 vs >98:2 er, 92% vs 95% Z with **IVa** and **IV**, respectively). Potentially, the lower efficiency and selectivity with **IVa** could be due to more facile competitive non-OM isomerization with Cl (vs strongly donating iodide-containing **IV**; cf. Section 1.4, Chapter 1) that result in out-of-sequence events. In the spectrum of non-stereogenic-at-Ru carbenes, achiral Ru phosphine **VII** is far less effective in generating **28a** (7% conv), the ROCM product is formed with 82% Z selectivity. Reaction with phosphine-free **I** is relatively less facile (79% conv, 41% yield) than with **IV** or **IVa**, in

spite of being a more active and less conformationally constrained¹⁰ Ru-dichloride; the major product is obtained with 77% *E*. As noted earlier (*cf.* Scheme 2.1A.ii), we set out to establish if **I** could promote post-OM based isomerization of *Z* to the thermodynamically favored *E*-isomer. Upon treatment of 95% *Z* **2.8a** with 5 mol% **I** in the presence of bve (20 equiv), lowering of *Z*-content to 32% is indeed observed within 12 hours at 22 °C (Scheme 2.3.1c). The stereoisomerization of ROCM product indicates that reaction with enol ethers catalyzed by **I**, similar to **VII**, could be kinetically *Z*-selective. However, more insights could not be obtained as the analysis of *Z*-content in product at 10% and 20% conversion consistently showed 77% *E*-selectivity. Nonetheless, the aforementioned observations point to a principal attribute of any *Z*-selective olefin metathesis process: catalysts must efficiently promote ROCM without being too active to engender significant erosion of kinetic selectivity.

2.3.2 Substrate Scope Investigation of *Z*-Selective and Enantioselective ROCM with Enol Ethers

Subsequently, we analyzed the influence of alterations in the structure of the enol ether cross-partners. For instance, the catalytic ROCM with the more sterically demanding cyclohexylvinyl ether affords **28b** in 64% yield, 98% *Z* selectivity (vs **28a** in 95% *Z*), and >98:2 er (entry 1, Table 2.3.2). With an aryl-substituted vinyl ether (entry 2), **28c** is obtained with the same *Z* selectivity as **28a** and in 97:3 *er*. The findings in entries 3–4 illustrate that pyrans with an electron-withdrawing trifluoromethyl (**28d**) or a chloroethyl ether substituent (**28e**) can also be accessed with high *Z* and enantioselectivity (94% & 95% *Z* and 96% & >98% *er* for **28d** and **28e**, respectively). In comparison with the results promoted by **IV**, all reactions with carbene **I** involved lower efficiency (highest: 59% yield) and *Z* selectivity (highest: 43%). Furthermore, we also investigated the reaction of cyclic olefin **2.5** with an S-substituted alkene, a member of a family of cross partners formerly shown to behave similarly to enol ethers in Ru-catalyzed olefin

(10) Since in an OM reaction the structure of the intermediate complex undergoes stereochemical inversion (detectable only with stereogenic-at-metal complexes), higher structural rigidity in species that contain a bidentate ligand can raise the barrier to such interconversions, leading to diminution of catalytic activity. For a more detailed discussion, see: Hoveyda, A. H.; Malcolmson, S. J.; Meek, S. J.; Zhugralin, A. R. *Angew. Chem., Int. Ed.* **2010**, *49*, 34–44.

metathesis.¹¹ Vinyl sulfide **2.9** is obtained in 67% yield, 96:4 *er*, and with 91% *Z* selectivity. As indicated by the X-ray structure of **2.9**, the ROCM proceeds with the same sense of enantioselectivity as enol ethers—*opposite* to what is observed with aryl olefins. Consistent with the aforementioned significance of post-OM isomerization, when the reaction to generate **2.9** is analyzed after 75% conversion (14 h), complete *Z* selectivity is detected (>98% vs 91% at >98% conv in 24 h). The stereogenic-at-Ru complex therefore appears to possess some ability—albeit minimal—to promote *Z*-to-*E* stereoisomerization. *It is also worth noting that the control experiments indicate that the high E-selectivity in ROCM reactions with aryl olefins is not due to the facile post-OM stereoisomerization of the products.* For example, subjection of a mixture of oxabicycle **2.5** and styrene (20 equiv) to 0.1 mol % **IV** at 22 °C leads to 63% conversion after 30 min and the desired product exclusively as the *E*-isomer (<2% *Z* based on ¹H NMR analysis).

Table 2.3.2. Stereochemical Variations in Cross Partner Alkenes

2.8b–e

entry	R	with chiral IV			with achiral I	
		conv (%); yield (%)	<i>Z:E</i>	<i>er</i>	conv (%); yield (%)	<i>Z:E</i>
1	Cy	b	>98; 64	98:2	>98:2	>98; 58
2	PMP	c	>98; 67	95:5	97: 3	>98; 41
3	CH ₂ CF ₃	d	>98; 65	94:6	96:4	>98; 59
4	(CH ₂) ₂ Cl	e	>98; 63	95:5	>98:2	>98; 31

2.9

98% conv, 67% yield,
91% *Z*, 96:4 *er*

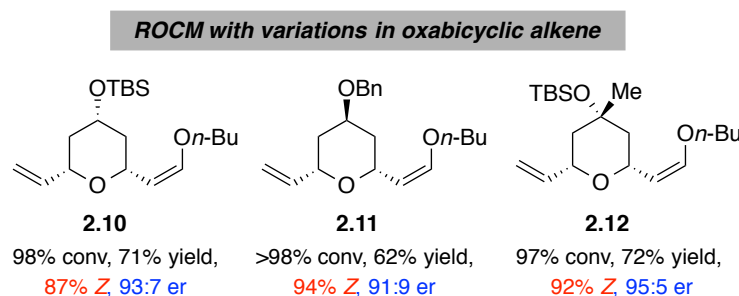
X-ray

We then turned our attention to investigating the structural modifications in cyclic alkene substrates (Scheme 2.3.2). In this respect, we found that TBS-protected diene **2.10**

(11) For relative reactivity of O- and S-substituted Fischer-type carbenes, see: (a) Louie, J.; Grubbs, R. H. *Organometallics* **2002**, *21*, 2153–2164. (b) Katayama, H.; Urushima, H.; Ozawa, F. *Chem. Lett.* **1999**, 369–370.

is generated in lower efficiency and selectivity than unprotected **2.8a** (71% yield vs 80% yield, 87% *Z* vs 95% *Z*, and 93:7 *er* vs >98:2 *er* with **2.10** and **2.8a**, respectively), showing that not only the alcohol groups are tolerated in this methodology, but they could also have a positive influence on overall reaction efficiency. Reaction of bve with *exo*-oxabicyclic benzyl-protected alkene also proceeds to form **2.11** with 94% *Z* and 91:9 *er* in 64% yield after purification. More impressively, diene **2.12**, involving a TBS-protected tertiary ether unit, is obtained in 72% yield with 92% *Z* and 95:5 *er*. Overall, the above examples indicate that the catalytic protocol can be applied to *Z*- and enantioselective synthesis of a range broad range of trisubstituted pyrans.

Scheme 2.3.2. Other Notable Examples



2.4 Support for Curtin-Hammett Kinetics in *Z*-Selective and Enantioselective ROCM of Enol Ethers

In order to provide support for our assertion that the high efficiency and selectivity of **IV** in the above ROCM is due to the establishment of a Curtin–Hammett situation, we set out to conduct a computational investigation.

2.4.1 DFT-Guided Investigations

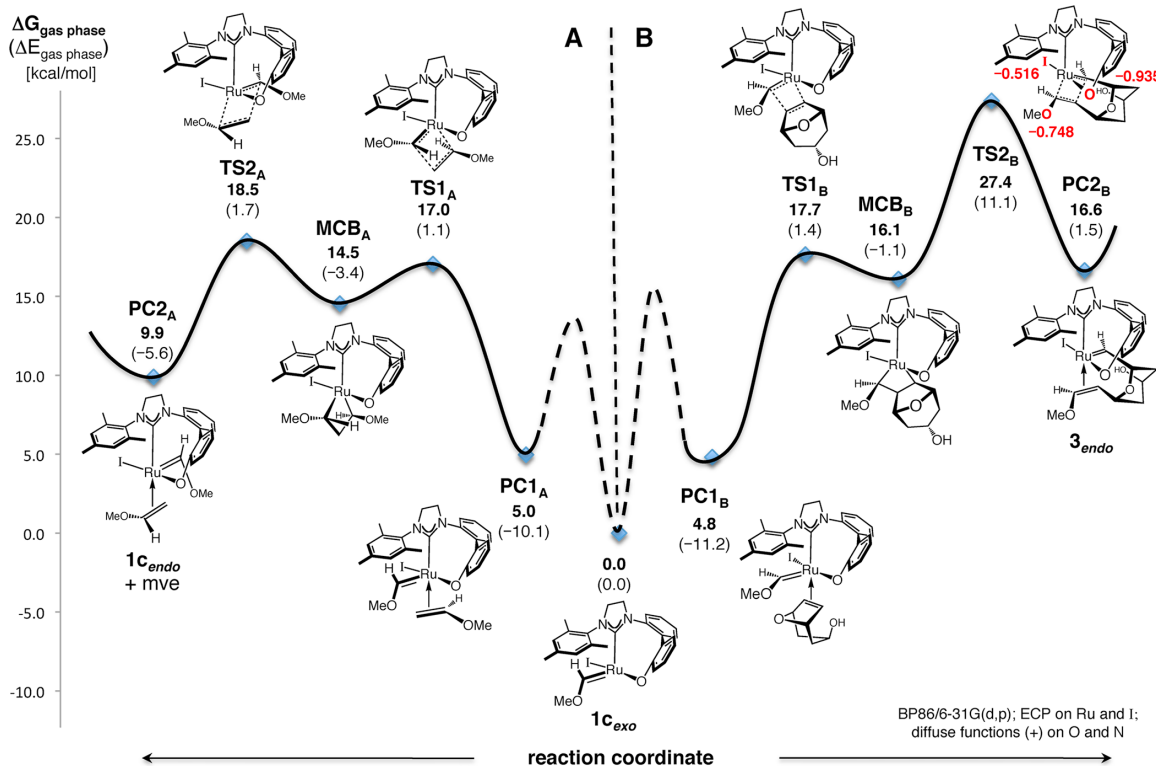
In order to minimize the computational cost, the phenyl groups of the NHC moiety were omitted.¹² As shown, the relative difference in energy between the two diastereomeric 14-electron carbenes of the truncated model system ($\Delta E = 4.1$ and 4.2 kcal/mol for G = Ph and OMe, respectively) proves to be only slightly larger compared to the real system presented in Scheme 2.2. Hence, we saw it fit to consider the model Ru complex as an appropriate approximation for further computational analysis (Scheme

(12) See experimental section for more details.

2.4.1).

The potential energy surfaces depicted in Scheme 2.4.1, calculated for the reaction of the *exo* Fischer carbene **1c_{exo}** with either methyl vinyl ether or oxabicycle **2.5**, indicate that *exo–endo* interconversion of heteroatom-substituted carbenes is energetically less demanding than the other steps in the catalytic cycle, and that Curtin–Hammett kinetics can be operative.¹² Specifically, the low barrier ($\text{TS2}_A = 18.5 \text{ kcal/mol}$; TS = transition state) to access the higher energy *endo* Fischer carbene **1c_{endo}** (PC2_A ; PC = π -complex) through nonproductive OM supports *fast equilibration* between the two diastereomeric carbenes, a requirement for Curtin–Hammett situation. In contrast, the barrier for the productive ROM step involving the cyclic alkene **2.5** through the lower energy Fischer carbene **1c_{exo}** to generate the product with the observed Z-alkene stereochemistry [via intermediate **3_{endo}** (PC2_B)] is found to be higher ($\text{TS2}_B = 27.4 \text{ kcal/mol}$).

Scheme 2.4.1-1. Support for Nonproductive OM to Promote Curtin–Hammett Kinetics

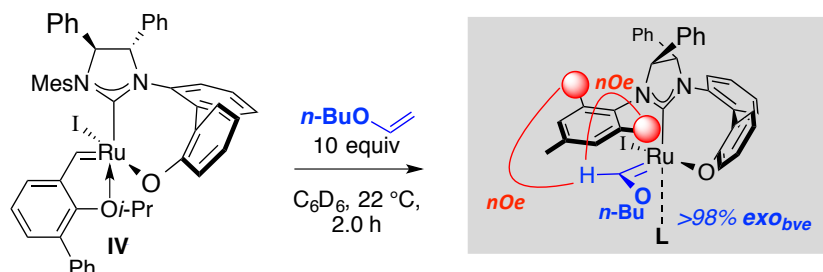


Scheme 2.4.1-1. Computed energy barriers (ΔG in kcal/mol; bold values) for nonproductive OM reactions of methylvinyl ether (A, $\mathbf{1c}_{\text{exo}}$ to $\mathbf{1c}_{\text{endo}} + \text{mve}$) and productive ROM of the *exo* carbene derived from the same enol ether with oxabicyclic alkene **2.5** (B, $\mathbf{1c}_{\text{exo}}$ to $\mathbf{3}_{\text{endo}}$; non-Curtin–Hammett pathway). ΔE values (gas phase) are provided in parentheses. mve = methylvinyl ether; PC = π -complex, TS = transition state; MCB = metallacyclobutane.

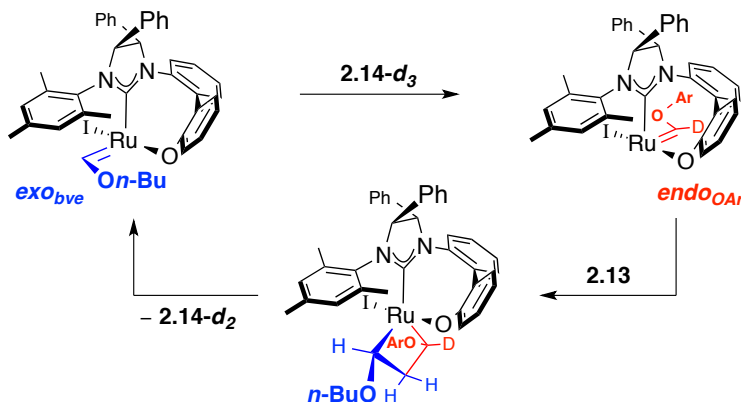
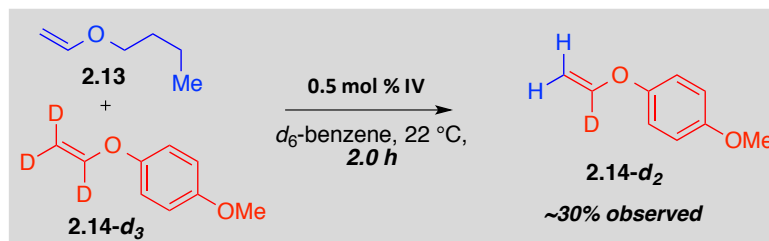
To explore the role of the diastereomeric carbenes yet further, we probed the identity of the complex formed by reaction of **IV** with bve. As forecasted by theory (*cf.* Scheme 2.4.1-1), two-dimensional spectroscopic analysis (*n*Oe)¹² indicates the exclusive presence of low-energy *exo* carbene (>98% to *exo_{bve}*; Scheme 2.4.1-2a).¹³ The latter complex likely forms via the higher energy *endo* species (*endo_{bve}*), which participates in stereoisomerization by nonproductive cross-metathesis with another molecule of bve (*cf.* interconversion represented in section A, Scheme 2.4.1-1).

Scheme 2.4.1-2. Evidence for the Facile Nonproductive OM Involving Enol Ethers

a. Predominance of "exo" Carbene in Solution



b. Nonproductive OM is Facile



Furthermore, the abovementioned scenario is validated by facile deuterium scrambling experiment (Scheme 2.4.1-2b), in which the subjection of bve **2.13** and d₃-*p* –

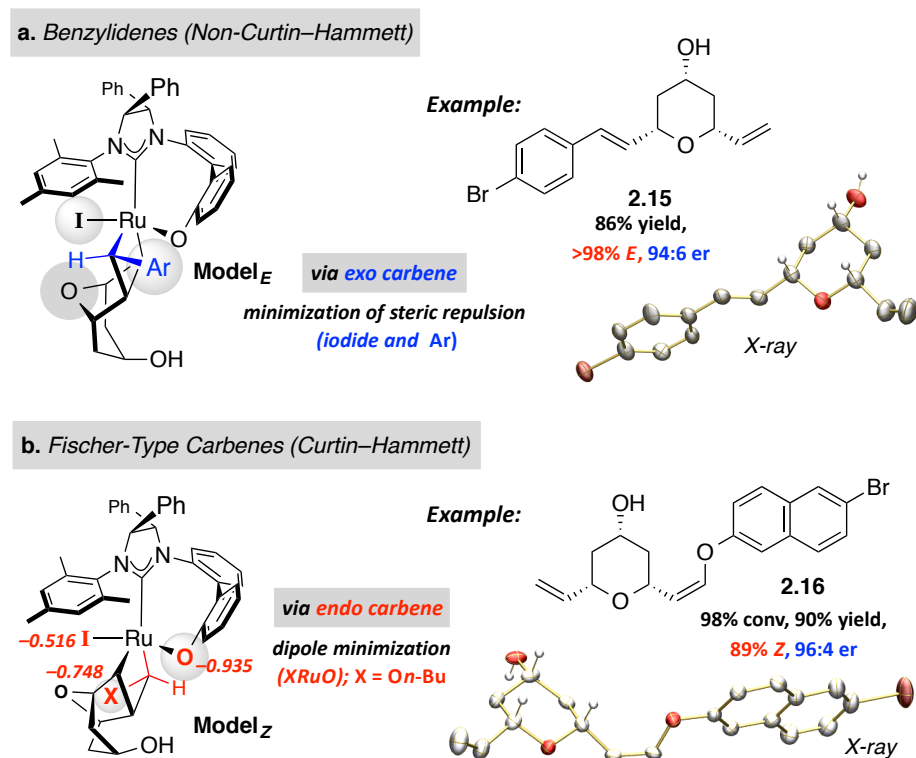
(13) This observation underscores the importance of the isolation and characterization of *endo-anti* (*cf.* Scheme 1.3.1-2, Chapter 1).

methoxyphenylvinyl ether **2.14-d₃** to 0.5 mol % **IV** (C_6D_6 , 22 °C, 2.0 h) leads to 30% of monodeutero-*p*-methoxyphenylvinyl ether **2.14-d₂**.¹² The generation of the latter compound can be rationalized, for instance, by the reaction of *exo_{bve}* with **2.14-d₃** to generate *endo_{OAr}*, which then participates in OM with **2.13** to furnish **2.14-d₂** and regenerate *exo_{bve}*. Overall, the aforementioned experiments lend credence to the notion that nonproductive OM with enol ethers is relatively fast and Curtin–Hammett kinetics can be applied to the present class of transformations.

2.4.2 Stereochemical Model for Z- and Enantioselective ROCM

Preliminary rationales for the observed *Z*- and enantioselectivities are presented through the metallacyclobutanes illustrated in Scheme 2.4.2.

Scheme 2.4.2. Stereochemical Rationalization for the Observed Selectivity Through Curtin–Hammett and Other pathways



With aryl alkenes, the stereochemical identity of which has been rigorously established through chemical correlation as well as X-ray crystallography (e.g., **2.15** in Scheme 2.4.2a),¹² *exo* benzylidenes are likely sufficiently reactive (vs Fischer-type carbenes) to serve as intermediates in ROCM, leading to metallacyclobutane shown in

Model_E, in which unfavorable propinquity between the large aryl group, the iodide ligand, and the oxabicycle moiety is avoided.

With enol ethers, transformations can occur via ruthenacyclobutane in **Model_Z**, which originates from the higher energy *endo* carbene (“Curtin–Hammett pathway”). The pyran product bearing *Z* enol ether is thus generated with the *opposite* sense of enantioselectivity versus aryl olefins (*cf.* **Model_E**), which is confirmed by chemical correlation as well as the X-ray data of **2.16**.¹² In **Model_Z**, the heteroatomic substituent (e.g., On-Bu from bve) prefers to be anti to the Ru-bound oxygen in order to *minimize the dipole* (*cf.* Section 1.4.4.2 in Chapter 1). For instance, analysis of the atomic polar tensor (APT) charges for **Model_Z** shows that e-density on the opposing O-atoms belonging to Ru-aryloxide and Fischer carbene (Ru=CHO_n-Bu) is -0.935 and -0.748, respectively. In contrast, **TS2_B** involves the syn-orientation of the two O-atoms, rendering the ROM pathway less favorable. Furthermore, since the enol ether substituent is relatively small (vs Ar), steric repulsion between such a unit and the iodide ligand in **Model_Z** would incur little energetic cost. In the case of the phenylvinyl sulfide, similar to enol ethers, ROCM also proceeds via the *endo* carbene through **Model_Z**.

The stronger influence of sterics in reactions with styrene is supported in that enol ether **28a** is only slightly higher in energy than its *E* isomer (0.34 kcal/mol), while aryl-substituted *E*-alkene (*cf.* **2.6**, Ar = Ph, Scheme 2.2) is preferred by 2.8 kcal/mol.¹² The high *E* selectivity in ROCM of aryl olefins likely arises from a pathway that is preferred due to factors that reflect the favorability of the corresponding trans products. In contrast, enol ether *Z* selectivity is largely *catalyst-induced*, as demonstrated by the influence of variation in ligands on overall selectivity of the reaction (*cf.* Scheme 2.3.1b).

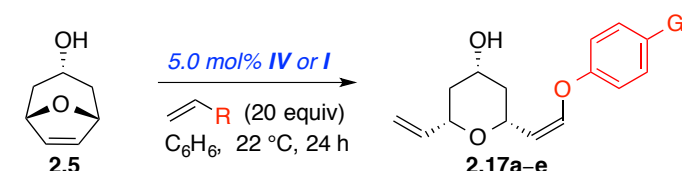
The models in Scheme 2.4.2 also account for a number of other findings. For instance, the lower *er* in ROCM with Ru chloride **IVa** (vs iodide **IV**) can be attributed to the competing influence of dipole minimization between the C–O of the enol ether substituent and the Ru–Cl bond (vs Ru–OAr). Similarly, the higher electron density at the oxygen atom of the more electron-rich enol ether with cyclohexylvinyl ether (*cf.* **2.8b**, entry 1, Table 2.3.2) leads to higher *Z:E* than when bve is used, in spite of its larger size (steric repulsion with the iodide ligand). Furthermore, the more sterically demanding and diminished electron density at the oxygen substituent of the (aryloxy)vinyl ether (**28c**,

entry 2, Table 2.3.2) might be counter-balanced by the electron-donating *p*-methoxy group, resulting in a similar *Z* selectivity as observed with bve. Currently, in-depth computational investigations are underway to provide the mechanistic basis for the stereoselectivity difference as well as the overall rate-limiting step in this useful transformation.

2.5 Influence of Electronic Attributes of Enol Ether on Chemoselectivity

At this juncture, we wished to elucidate the extent to which the reactivity of the propagating Fischer carbene is critical in the promotion of high chemoselectivity (e.g., minimal oligomerization of strained oxabicyclic substrates is observed in most examples with **IV**). In this respect, we hypothesized that the preference for either the formation (resulting from CM step involving **ii_{exo}**) or disappearance (resulting from ROM of **i_{endo}**) of the Fischer carbenes must be dictated by the overall energy stabilization gained through the mesomeric effect of RO-substituent (i.e. Fischer carbene character).¹⁴

Table 2.5. Change in Selectivity with Electronic Variations in Enol Ethers



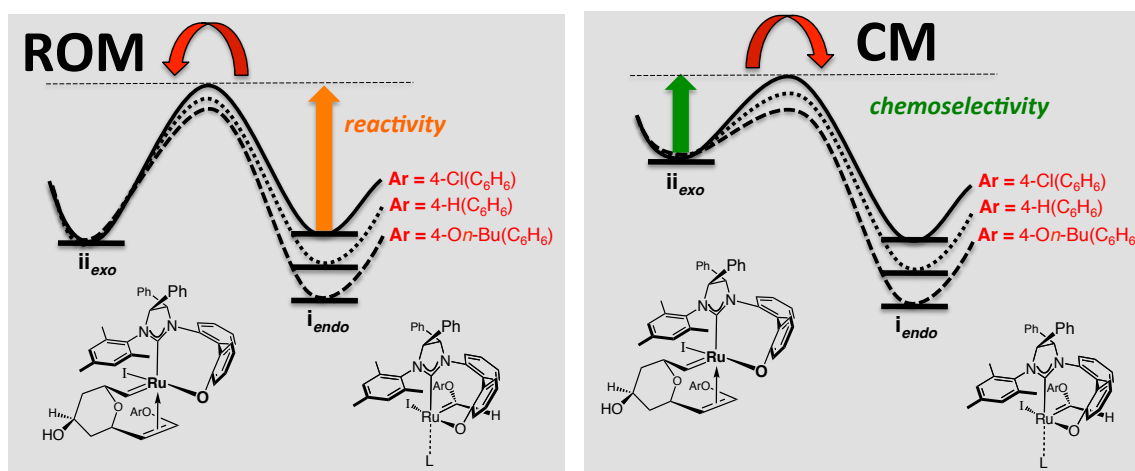
entry	G	with IV				with I	
		conv (%)	yield (%)	chemoselectivity yield/conv	<i>Z/E</i> (%)	<i>er</i> (%)	conv; yield (%); (<i>Z/E</i>)
1	On-Bu	66; 64	0.97		92:8	97:3	>98; 57; (40:60)
2	Et	74; 69	0.93		91:9	97:3	>98; 57; (45:55)
3	H	82; 74	0.90		93:7	96:4	>98; 69; (45:45)
4	Br	90; 79	0.88		93:7	95:5	>98; 59; (42:58)
5	Cl	93; 75	0.81		93:7	96:4	>98; 61; (43:57)

To gain insight and correlate the chemoselectivity (i.e. ROCM-product-yield/oxabicycle-conversion) as function of carbene reactivity/stability, we devised an

(14) For a comprehensive study regarding the rate of carbene formation with respect to the e-donorability of the alkene reactant, see: Lane, D. R.; Beavers, C. M.; Olmstead, M. M.; Schore, N. E. *Organometallics* **2009**, 28, 6789–6797.

investigation involving the ROCM of **2.5** with phenylvinyl ethers containing *p*-substituents of varying e-donorability (On-Bu, Et, H, Br, Cl as **a**, **b**, **c**, **d**, **e**, respectively, Table 2.5). As listed above, the reaction to generate **2.17a** proceeds with remarkable chemoselectivity (0.97), however, only 66% conversion of **2.5** is detected after 24 hours (entry 1). With relatively less e-donating ethyl-substituted phenylvinyl ether, whereas slightly lower chemoselectivity (0.93) is observed to give **2.17b**, 74% conversion of **2.5** takes place (entry 2). In a similar fashion, 0.90 chemoselectivity is promoted in the reaction to form H-substituted **2.17c** (82% conv. of **2.5**, entry 3). Most remarkably, halogen-substituted least e-rich phenylvinyl ethers, shown in entries 4-5, gave lowest chemoselectivities (Br = 0.88 and Cl = 0.81) and highest conversions of **2.5** (Br = 90% and Cl = 093%). It is noteworthy that the Z- and enantioselectivities remain largely unaffected in all cases, mainly because the productive reaction pathway involves the intermediacy of a Fischer carbene (*cf.* Curtin-Hammett kinetics, Section 2.4).

Scheme 2.5. Proposal for Reactivity and Chemoselectivity Correlation of Fischer Carbenes in ROCM



To rationalize the results above, we decided to consider the influence of carbene stabilization on two fronts: 1) The intrinsic barrier associated with the formation of non-resonance stabilized **ii_{exo}** (Scheme 2.5) is affected by the relative energy of the Fischer carbene **i_{endo}**, thereby influencing the “reactivity” of the latter species in ROM 2) The preference for the regeneration of **i_{endo}** through CM of **ii_{exo}** (vs anomalous oligomeric ROM with **2.5**) determines overall chemoselectivity observed in the reaction. For instance, with Ar = 4-On-Bu(C₆H₅), the resulting **i_{endo}** carbene is lower in energy [vs Ar =

$4\text{-Cl}(\text{C}_6\text{H}_6)$], which results in *slower* ROM due to higher barrier for the formation of **ii_{exo}** [66% conv, entry 1 vs 93% conv, entry 5, Table 2.5]. In the subsequent CM step, the strong preference for the generation of the lower in energy Ar = 4-On-Bu(C_6H_6)-derived **i_{endo}** plays a critical role in the promotion of high chemoselectivity. In contrast, relatively lower preference for the generation of the Cl-substituted **i_{endo}** is responsible for the competitive oligomerization sequence (i.e. ROM with **2.5**), rendering the ROCM transformation less chemoselective.

2.6 Rationale for Substrate-Controlled *Z* Selectivity

Based on the higher *Z*-content with non-stereogenic-at-Ru **VII** (*cf.* Scheme 2.1A and Scheme 2.3.1b) and the ability of **I** to promote *Z*-to-*E* stereoisomerization through post-OM (*cf.* Scheme 2.3.1c), we propose that the dichloride Ru carbenes are likely kinetically *Z*-selective in ROCM with enol ethers. Furthermore, we suggest that the inherent preference for the *Z* selectivity could be tied to the smaller size of the heteroatomic-substituent (vs aryl or alkyl) of the olefin. In fact, there are a few examples of *Z* selectivity in CM with heteroatom-substituted alkenes in the literature.¹⁵ With C-substituted alkenes, the most notable instances of *Z*-selective metathesis involve substrates with sp-hybridized (-CN or -yne)^{16,17} substituent. In all cases, the reason for high *Z* selectivity is not explained. To the best of our knowledge, the only instance of a proposed model for *Z* selectivity involves ROCM with aliphatic alkene substrate, in which Snapper and coworkers rationalized the kinetic preference for the *Z*-alkene by considering a syn-to- PCy_3 ruthenacyclobutane pathway.¹⁸

In order to provide a general model for *Z* selectivity in OM with alkenes of diminutive size (i.e. nitrile, yne, heteroatomic-substituents), herein we consider a representative CM listed in Scheme 2.6a.^{16b} In this particular example, aliphatic alkene **2.18** reacts with acrylonitrile in the presence of 5.0 mol% **I** to give 81% yield of **2.19** in

(15) For *Z*-selective Ru-catalyzed cross-metathesis between vinyl sulfides and 1,2-dichloroethylene, see: (a) Macnaughtan, M. L.; Gray, J. B.; Gerlach, D. L.; Johnson, M. J. A.; Kampf, J. W. *Organometallics* **2009**, *28*, 2880–2887. (b) Sashuk, V.; Samojlowicz, C.; Szadkowska, A.; Grela, K. *Chem. Commun.* **2008**, 2468–2470.

(16) For representative examples, see: (a) Miao, X.; Dixneuf, P. H.; Fischmeister, C.; Bruneau, C. *Green Chem.*, **2011**, *13*, 2258–2271. (b) Randl, S.; Gessler, S.; Wakamatsu, H.; Blechert, S. *Synlett* **2001**, *3*, 430–432.

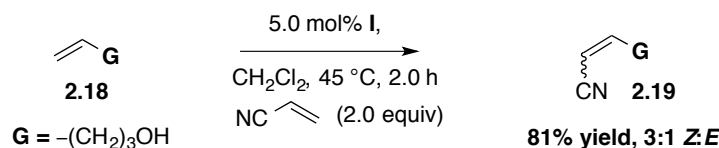
(17) Hansen, E. C.; Lee, D. *Org Lett.* **2004**, *6*, 2035–2038.

(18) Tallarico, J. A.; Randall, M. L.; Snapper, M. L. *Tetrahedron* **1997**, *53*, 16511–16520.

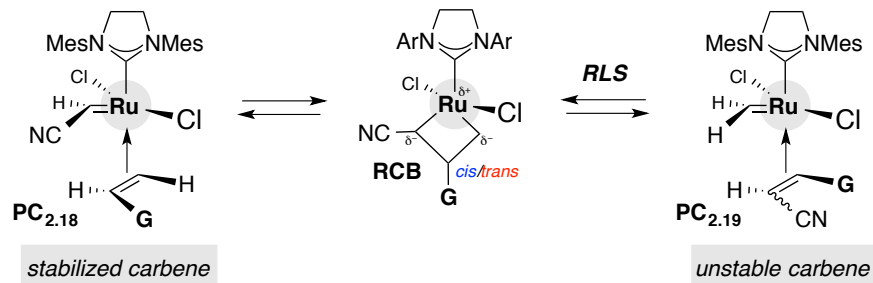
3:1 (*Z/E*) ratio. Since the productive CM pathway must include α/β -substituted ruthenacyclobutane, we propose the intermediacy of the **RCB** for two main reasons (Scheme 2.6b): 1) e-withdrawing effect of the CN unit lowers the overall energy of the ruthenacyclobutane by stabilizing negative charge accumulated at the α -position due to the polarized Ru^{IV}–C _{α} bond 2) The steric clash between the larger substituent **G** (vs CN) and the bulky Ru center is minimal at β -position (vs α). More importantly, we propose that the cycloreversion of **RCB** to form **2.19** (*E* or *Z*) could be *rate limiting*, as this step would necessitate the formation of unstable and higher energy methylidene **PC_{2.19}** (vs stabilized and lower energy **PC_{2.18}**), thereby raising the barrier for productive breakage.

Scheme 2.6. General Model for Substrate Controlled *Z*-Selectivity in Ru Catalyzed OM

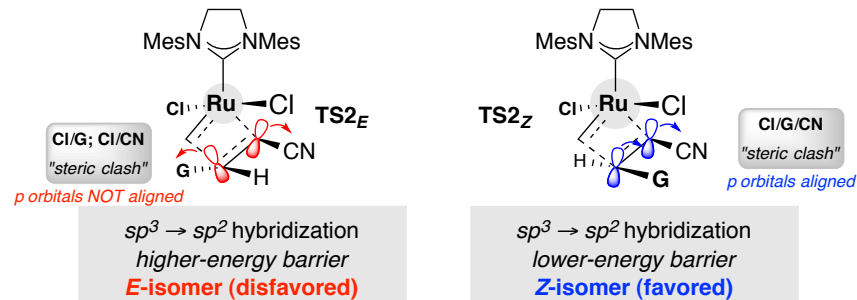
a. Representative Example of Substrate-Based *Z*-Selectivity in OM



b. Productive Cycloreversion of **RCB** is Likely Turnover Limiting



c. Orbital Alignment in **TS2_Z** Could Favor *Z*-Alkene



Based on the above scenario, a close examination of the transition states (**TS2_E** and **TS2_Z**) could offer a possible reason for the preference of the *Z*-isomer in rate-limiting

cycloreversion (Scheme 2.6c).¹⁹ As shown in **TS2_E**, the two axial Cl anions exert steric pressure on CN and **G**, which could result in an improper alignment of the two p-orbitals, rendering the establishment of the sp² hybridization (i.e., productive cycloreversion) energetically costly. In contrast, although the steric clash of axial Cl with CN and **G** in **TS2_Z** would also be energetically taxing, the proper alignment of the p-orbitals would likely render the process favorable. Overall, the hitherto considerations provide a plausible rationale for the promotion of substrate-controlled Z selectivity in a variety of OM transformations.

2.7 Conclusions

The ROCM results presented herein involve the first instances of Z- and enantioselective OM catalyzed by Ru-based complexes. The reactions involve a broad range of oxabicyclic alkenes and enol ether or phenylvinyl sulfide cross-partners, and promoted with as low as 0.5 mol % of enantiomerically pure stereogenic-at-Ru complex **IV**. The products are formed efficiently and with exceptional Z- (up to 98%) and enantioselectivity (>98:2 *er*). Most notably, based on the absolute stereochemistry of the ROCM products, computational investigations, and deuterium-labeling studies, we reveal that the mechanism of the enol ether reaction involves a Curtin-Hammett pathway, which is distinct from the mechanism with aryl alkene cross-partners (*cf.* Section 2.4). Moreover, the results of these studies are also relevant to the recently reported Z- and enantioselective transformations.²⁰

Additionally, for the first time, we have provided a plausible mechanistic rationale for substrate-controlled Z selectivity (*cf.* Scheme 2.6) in OM, which remains largely unaddressed in the literature. In this respect, we propose that the productive cycloreversion step (*cf.* **TS2**, Scheme 2.6) is rate limiting, and the lower barrier of **TS2_Z** (vs **TS2_E**) renders the formation of the Z-alkene favorable in OM. Thus, in this chapter, we have outlined new principles that not only play an important role in the development

(19) Currently, a detailed computational investigation is underway to explain the substrate-controlled Z selectivity. However, preliminary results with M06 density functional have indicated that **TS2_Z** is lower in energy (vs **TS2_E**) and the productive cycloreversion is turnover limiting.

(20) (a) Hartung, J.; Grubbs, R. H. *Angew. Chem. Int. Ed.* **2014**, *126*, 1–5. (b) J. Hartung, J.; Grubbs, R. H. *J. Am. Chem. Soc.* **2013**, *135*, 10183–10185.

of new OM methodologies, but also help us understand previous observations that lack explanation.

2.8 Experimental

■ **General:** Unless otherwise noted, all reactions were performed with distilled and degassed solvents under an atmosphere of dry N₂ in oven- (135 °C) or flame-dried glassware with standard dry box or vacuum line techniques. Infrared (IR) spectra were recorded on a Bruker FTIR Alpha (ATR Mode) spectrometer, ν_{max} in cm⁻¹. Bands are characterized as broad (br), strong (s), medium (m), or weak (w). ¹H NMR spectra were recorded on a Varian Unity INOVA 400 (400 MHz) spectrometer. Chemical shifts are reported in ppm from tetramethylsilane with the solvent resonance resulting from incomplete deuterium incorporation as the internal standard (CDCl₃: δ 7.26 ppm, C₆D₆: δ 7.16 ppm). Data are reported as follows: chemical shift, integration, multiplicity (s = singlet, d = doublet, q = quartet, br = broad, m = multiplet), and coupling constants (Hz). ¹³C NMR spectra were recorded on a Varian Unity INOVA 400 (100 MHz) spectrometer with complete proton decoupling. Chemical shifts are reported in ppm from tetramethylsilane with the solvent resonance as the internal standard (CDCl₃: δ 77.16 ppm). 1D-nOe NMR spectrum was recorded on a Varian Unity INOVA 500 (500MHz) spectrometer High-resolution mass spectrometry was performed on a Micromass LCT ESI-MS and JEOL Accu TOF Dart (positive mode) at the Boston College Mass Spectrometry Facility. Z:E ratios of ROCM products were determined by analysis of ¹H NMR spectra. Enantiomeric ratios were determined by HPLC (Chiral Technologies Chiraldex OD-H, AS-H, and AD-H columns) in comparison with authentic racemic materials. Optical rotations were measured on a Rudolph Research Analytical Autopol IV Polarimeter.

Solvents: Solvents were purged with Ar and purified under a positive pressure of dry Ar by a modified Innovative Technologies purification system. Benzene (Aldrich) was passed successively through activated copper and alumina columns. All work-up and purification procedures were carried out with reagent grade solvents (purchased from Fisher) under bench-top conditions.

Ru-based Complexes: Enantiomerically pure Ru-carbene complexes **IV** and **IVa** were synthesized by following a previously reported procedure.²¹ Achiral Ru-carbene complexes **I** and **VII** were obtained from Materia, Inc. and purified by silica gel chromatography or by recrystallization (dichloromethane/pentane) prior to use.

■ Reagents:

d₆-Benzene was purchased from Cambridge Isotope Laboratories and distilled from Na into activated 4 Å molecular sieves prior to use.

n-Butyl vinyl ether was purchased from Acros and distilled from CaH₂ prior to use.

t-butyldimethylsilyl chloride was purchased from Oakwood and used as received.

t-butyldimethylsilyl trifluoromethanesulfonate was purchased from Aldrich and used as received.

Benzoic anhydride was purchased from Acros Organics.

d-Chloroform was purchased from Cambridge Isotope Laboratories and passed through basic alumina then stored in activated 4 Å molecular sieves prior to use.

2-Chloroethyl vinyl ether was purchased from Aldrich and used as received.

Cyclohexyl vinyl ether was purchased from Aldrich and distilled from CaH₂ prior to use.

Dimethylaminopyridine (DMAP) was purchased from Advanced ChemTech.

Imidazole was purchased from Aldrich and used as received.

2,6-lutidine was purchased from Aldrich and used as received.

Methylolithium was purchased as a 1.6 M solution in diethyl ether from Aldrich and titrated before use (1,10-phenanthroline, *sec*-butanol in C₆H₆).

para-Methoxyphenyl vinyl ether was prepared according to previously published procedures and distilled under vacuum from CaH₂ prior to use.²² Deuterated analogue (**d₃-b**) was prepared from d₄-1,2-dibromoethane.

Phenyl vinyl sulfide was purchased from Aldrich and distilled from CaH₂ prior to use.

Triethylamine trihydrofluoride was purchased from Aldrich and used as received.

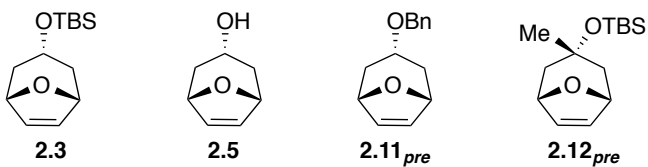
(21) Van Veldhuizen, J. J.; Campbell, J. E.; Giudici, R. E.; Hoveyda, A. H. *J. Am. Chem. Soc.*, **2005**, *127*, 6877–6882.

(22) Solinas, M.; Gladiali, S.; Marchetti, M. *J. Mol. Catal. A: Chem.* **2005**, *226*, 141–147.

2, 2, 2-Trifluoroethyl vinyl ether was purchased from Aldrich and distilled from CaH₂ prior to use.

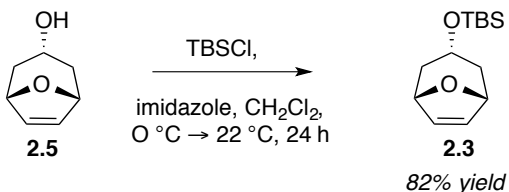
■ Synthesis of Oxabicycle Substrates:

Chart 1. Oxabicyclic Alkenes for ROCM Reactions



Oxabicyclic alkenes (**2.5** and **2.11** precursor) were prepared by following previously reported procedures in the literature (Chart 1).²³

Chart 2. Synthesis of Oxabicycle 2.3

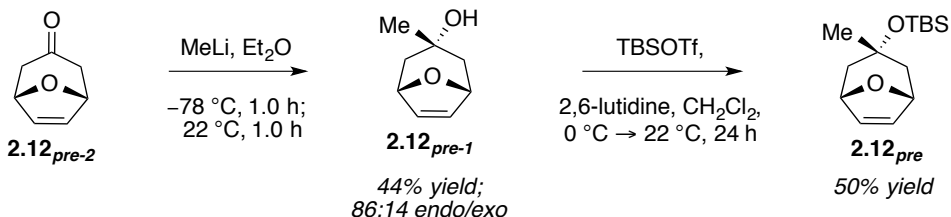


tert-Butyldimethyl((1*R*,3*S*,5*S*)-8-oxabicyclo[3.2.1]oct-6-en-3-yloxy)silane (2.3**, Chart 2):** An oven-dried 50 mL round bottom flask equipped with a magnetic stir bar was charged with 506 mg (4.02 mol, 1.00 equiv) oxabicycle alcohol **2.5**,²³ and 603 mg (4.00 mmol, 1.00 equiv) imidazole, and the flask was purged under N₂. Anhydrous CH₂Cl₂ (6 mL) was added and the resulting mixture was cooled to 0 °C. A separate 25 mL round bottom flask was charged with 745 mg (11.0 mmol, 2.72 equiv) TBSCl, and the flask was purged under N₂. The TBSCl was dissolved in anhydrous CH₂Cl₂ (6 mL) and the resulting solution was transferred to the flask containing the oxabicycle and imidazole. The mixture was allowed to stir as it slowly warmed to 22 °C over 24 h. The reaction was quenched in water, the organic layer was separated, and the aqueous layer was washed in CH₂Cl₂ (5 x 10 mL). The organic layers were pooled, dried with MgSO₄, filtered, and concentrated *in vacuo*, affording a yellow oil. Purification by silica gel chromatography

(23) For oxabicycle ketone synthesis, see: (a) Sendelbach, S.; Schwetzler-Raschke, R.; Radl, A.; Kaiser, R.; Henle, G. H.; Korfant, H.; Reiner, S.; Fohlisch, B. *J. Org. Chem.* **1999**, *64*, 3398-3408. For oxabicycle ketone reductions, see: (b) Dunkel, R.; Mentzel, M.; Hoffmann, H. M. R. *Tetrahedron*, **1997**, *53*, 14929-14936.

(10% EtOAc/hexanes eluent) delivered 790 mg (3.29 mmol, 82% yield) oxabicycle **2.3** as a clear, colorless oil. **IR (neat)**: 3080 (w), 2929 (m), 2856 (w), 1602 (w), 1472 (w), 1463 (w), 1419 (w), 1375 (w), 1360 (w), 1346 (w), 1276 (m), 1253 (w), 1227 (w), 1172 (w), 1112 (w), 1070 (s), 1038 (m), 1023 (m), 1000 (w), 962 (w), 939 (w), 907 (w), 873 (s), 834 (s), 789 (s), 771 (w), 735 (w), 699 (s), 676 (w), 645 (w), 570 (w), 493 (w), 452 (w), 401 (w); **¹H NMR (400 MHz, CDCl₃)**: δ 6.22 (2H, s), 4.66 (2H, d, *J* = 4 Hz), 4.04 (1H, apparent tt, *J* = 5, 1.2 Hz), 2.15 (2H, apparent dt, *J* = 14.6, 4.2 Hz), 1.49 (2H, dd, *J* = 14.6, 1.2 Hz), 0.85 (9H, s), -0.04 (6H, s); **¹³C NMR (100 MHz, CDCl₃)**: δ 133.9, 78.0, 64.7, 36.3, 25.9, 18.0, -4.8; **HRMS (ESI⁺) [M]⁺** calcd for C₁₃H₂₅O₂Si: 241.1624, found: 241.1624.

Chart 3. Synthesis of Oxabicycle **2.12_{pre}-1**



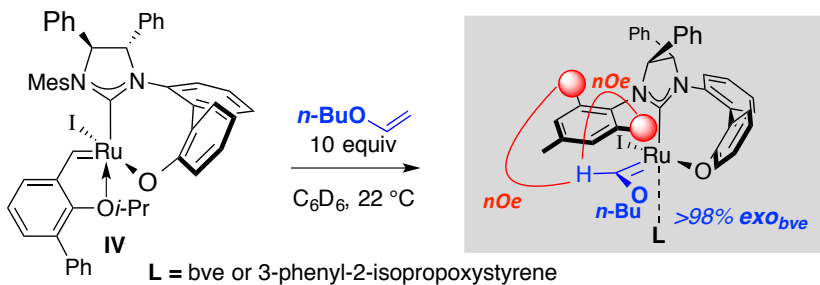
(1*R*,3*S*,5*S*)-3-Methyl-8-oxabicyclo[3.2.1]oct-6-en-3-ol (2.12_{pre-1}**, Chart 3):** An oven-dried 25 mL round bottom flask equipped with a magnetic stir bar was charged with 411 mg (3.31 mmol, 1.00 equiv) oxabicycle ketone **2.12_{pre-2}**,²³ and the flask was purged under N₂. Anhydrous Et₂O (3 mL) was added and the mixture was stirred vigorously as it was cooled to -78 °C. A solution of 1.26 M MeLi in Et₂O (2.80 mL, 3.48 mmol, 1.05 equiv) was added drop-wise over five minutes to the ketone solution, and the resulting mixture was stirred for one hour at -78 °C. The mixture was then allowed to warm to 22 °C as it was stirred for an additional one hour. The reaction was quenched by addition of 5 mL saturated aqueous ammonium chloride, organic layer was separated, and the aqueous layer was washed in dichloromethane (5 x 10 mL). Organic layers were pooled, dried with MgSO₄, filtered, and concentrated *in vacuo*, affording a red oil. Analysis of the 400 MHz ¹H NMR revealed a 92:8 mixture of *endo* and *exo* tertiary alcohols (*endo* isomer is predominant). Purification by silica gel chromatography (4:1:1 hexanes:EtOAc:CH₂Cl₂ eluent) afforded 204 mg (1.46 mmol, 44% yield) oxabicycle **2.12_{pre-1}** as yellow oil (86:14

endo:exo). The spectral data for this compound were identical to those reported in the literature.²⁴

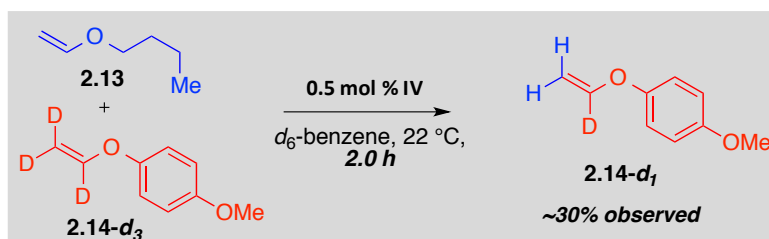
tert-Butyldimethyl(((1*R*,3*S*,5*S*)-3-methyl-8-oxabicyclo[3.2.1]oct-6-en-3-yl)oxy)silane (2.12_{pre}, Chart 3): An oven-dried 25 mL round bottom flask equipped with a magnetic stir bar was charged with 204 mg (1.46 mol, 1.00 equiv) oxabicycle alcohol **2.12_{pre-1}**, and 407 mg (3.80 mmol, 2.60 equiv) imidazole, and the flask was purged under N₂. Anhydrous CH₂Cl₂ (5 mL) was added, the resulting mixture was cooled to 0 °C, and 440 µL TBSOTf (1.91 mmol, 1.31 equiv) was then added. The mixture was allowed to stir as it slowly warmed to 22 °C over 24 h. The reaction was quenched in saturated aqueous NaHCO₃, the organic layer was separated, and the aqueous layer was washed in CH₂Cl₂ (5 x 10 mL). The organic layers were pooled, dried with MgSO₄, filtered, and concentrated *in vacuo*, affording yellow oil. Purification by silica gel chromatography (5% EtOAc/hexanes eluent) delivered 185 mg (0.727 mmol, 50% yield) oxabicycle **2.12_{pre}** as yellow oil. **IR (neat):** 3083 (w), 2931 (m), 2855 (w), 1472 (w), 1462 (w), 1418 (w), 1387 (w), 1374 (w), 1358 (w), 1348 (w), 1307 (w), 1281 (w), 1250 (s), 1204 (w), 1168 (w), 1141 (w), 1103 (s), 1092 (w), 1051 (w), 1028 (s), 1004 (w), 980 (w), 948 (w), 907 (w), 872 (m), 824 (s), 811 (w), 769 (s), 702 (s), 681 (m), 634 (w), 618 (w), 566 (w), 484 (m), 470 (w); **¹H NMR (400 MHz, CDCl₃):** δ 6.15 (2H, s), 4.69 (2H, d, *J* = 4 Hz), 1.92 (2H, dd, *J* = 14.6, 4.2 Hz), 1.66 (2H, d, *J* = 14 Hz), 1.19 (3H, s), 0.83 (9H, s), 0.03 (6H, s); **¹³C NMR (100 MHz, CDCl₃):** δ 133.3, 78.0, 71.6, 42.1, 35.0, 26.1, 18.3, -1.5; **HRMS (ESI⁺) [M]⁺** calcd for C₁₄H₂₇O₂Si: 255.1780, found: 255.1792.

(24) Buchs, P.; Ganter, C. *Helv. Chimica Acta* **1980**, *63*, 1420-1424.

■ Synthesis of Ru-Based Fischer Carbene and Evidence for Nonproductive Metathesis:

Chart 4. Synthesis of *exo_{bve}*

Synthesis of Ru-Based Fischer Carbene (*exo_{bve}*, Chart 4): In an N₂-filled glove box, butyl vinyl ether (11.7 mg, 0.117 mmol, 10.2 equiv) dissolved in C₆D₆ (600 μL) was added to a 4 mL vial charged with a magnetic stir bar and Ru complex **IV** (10.9 mg, 0.0114 mmol, 1.00 equiv) by syringe. The vial was capped and the mixture was allowed to stir for 22 h, at which time it was transferred to an NMR tube (screw cap) by a pipette. The NMR tube was capped and sealed with Teflon tape. Please note that for in situ-generated Fischer-type carbene complex *exo_{bve}*, only the new diagnostic signal of the Fischer type carbene proton is listed (see below for further spectral information). ¹H NMR (500 MHz, C₆D₆): δ 14.03 (1H, s).

Chart 5. Deuterium Scrambling in Enol Ethers Promoted by **IV**

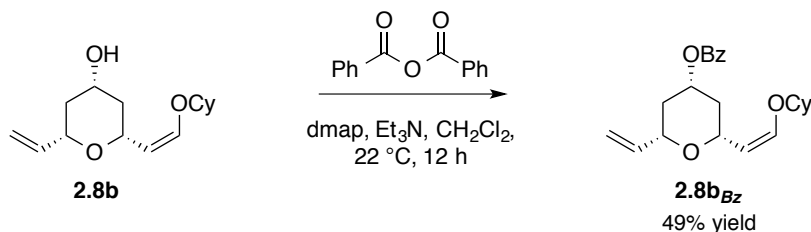
Evidence for Nonproductive Metathesis by Deuterium Scrambling (Chart 5): In an N₂-filled glove box, a 4 mL vial with a magnetic stir bar was charged with **2.14-d₃** (60.6 mg, 0.396 mmol, 1.00 equiv) and **2.13** (39.6 mg, 0.396 mmol, 1.00 equiv). The mixture was dissolved in benzene (200 μL), and added to a 4 mL vial with **IV** (1.9 mg, 2.0 mmol, 0.50 mol %) by syringe. The vial was capped and the reaction mixture was allowed to stir for two hours, after which the solvent, and **2.13** were removed by vacuum, furnishing a mixture of **2.14-d₃** and **2.14-d₁**. The H/D exchange to generate **2.14-d₁** was found to be

30% by 400 MHz ^1H NMR analysis. HRMS (ESI $^+$) [M+H] $^+$ calcd for **2.14-d₁** ($\text{C}_9\text{H}_{10}\text{DO}_2$): 152.0822, found: 152.0824.

■ Procedures for Synthesis and Spectra of Z- and Enantioselective Ru-catalyzed Ring-Opening/Cross-Metathesis (ROCM) Reactions:

General Procedure for Z- and Enantioselective ROCM: In an N_2 -filled glovebox, an oven-dried 4 mL vial equipped with a magnetic stir bar was charged with 0.5-5 mol % of the Ru complex **IV** and the cross partner alkene (20 equiv). The resulting mixture was allowed to stir for 30 minutes and then added by syringe to a solution of the cyclic alkene (1.0 equiv) in C_6H_6 (or neat) in a 4 mL vial. The resulting solution was allowed to stir for 8-24 hours at 22 °C. The reaction was then quenched by addition of wet diethyl ether and concentrated *in vacuo* (percent conversion determined by 400 MHz ^1H NMR analysis). Purification was performed by silica gel chromatography. Enantiomeric purity of the product was determined by HPLC analysis.

Chart 6. Representative Benzoylation of Oxabicyclic Alcohols



Representative Procedure for the Conversion of Alcohol to Benzoyl Ester (Chart 6):

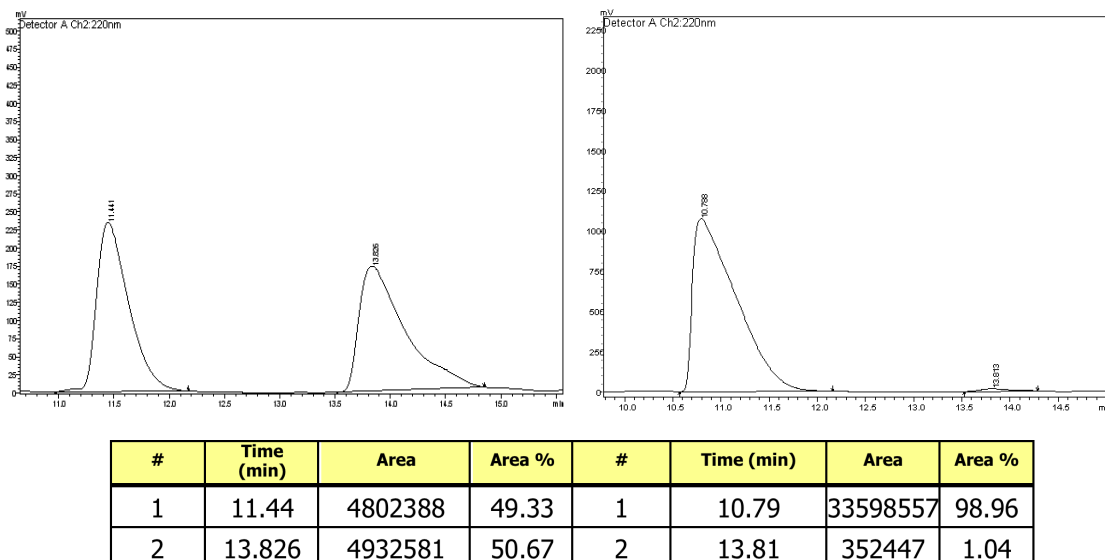
To a 4 mL vial charged with a magnetic stir bar and the enantiomerically enriched **2.8b** (26.3 mg, 0.104 mmol), a mixture of benzoic anhydride (47.0 mg, 0.209 mmol, 2.0 equiv), 4-dimethylaminopyridine (3.8 mg, 0.031 mmol, 0.30 equiv), and triethylamine (100 μL, 0.717 mmol, 6.9 equiv) was dissolved in CH_2Cl_2 (1.3 mL). The resulting mixture was allowed to stir for 12 hours at 22 °C, after which the solvents were removed *in vacuo* and the residue was purified by silica gel chromatography (10% diethyl ether in hexanes) affording **2.8b_{Bz}** as colorless oil (18.3 mg, 0.0513 mmol, 49% yield).

■ Z-Selective and Enantioselective Ring-Opening/Cross-Metathesis (ROCM):²⁵

(25) For ^1H and ^{13}C spectra of all ROCM products, see: Khan, R. K. M.; O'Brien, R. V.; Torker, S.; Li, B.; Hoveyda, A. H. *J. Am. Chem. Soc.* **2012**, *134*, 12774–12779.

(2*R*,4*S*,6*S*)-2-((*Z*)-2-Butoxyvinyl)-6-vinyltetrahydro-2*H*-pyran-4-ol (2.8a). Following the general procedure, *n*-butylvinyl ether (240 mg, 2.40 mmol, 20.2 equiv) was added to **IV** (5.6 mg, 5.8 mmol, 5.0 mol %) and allowed to stir for 30 minutes. The mixture was transferred by syringe to a solution of oxabicycle **2.5** (15.0 mg, 0.119 mmol, 1.00 equiv) in C₆H₆ (600 μL) and allowed to stir for eight hours. Analysis of the 400 MHz ¹H NMR spectrum revealed >98% conv of **2.5**, and product **2.8a** was obtained as a 95:5 mixture of *Z/E* isomers. The resulting brown oil was purified by silica gel chromatography (10-40% diethyl ether in hexanes) to afford **2.8a** (21.6 mg, 0.0954 mmol, 80% yield) as colorless oil (>98:2 e. r., 98% *Z*). The spectral data for this compound were identical to those reported in the literature.²⁶ [α]_D²⁰ −13.1 (c = 1.66, CH₂Cl₂) for an enantiomerically enriched sample of >98:2. The enantiomeric purity was determined by HPLC (Chart 7) analysis in comparison with authentic racemic material [OD-H column, 98:2 hexanes:*i*-PrOH, 1.0 mL/min, 220 nm; *Z*-isomer: t_r (major enantiomer) = 10.79 min, t_r (minor enantiomer) = 13.81 min].

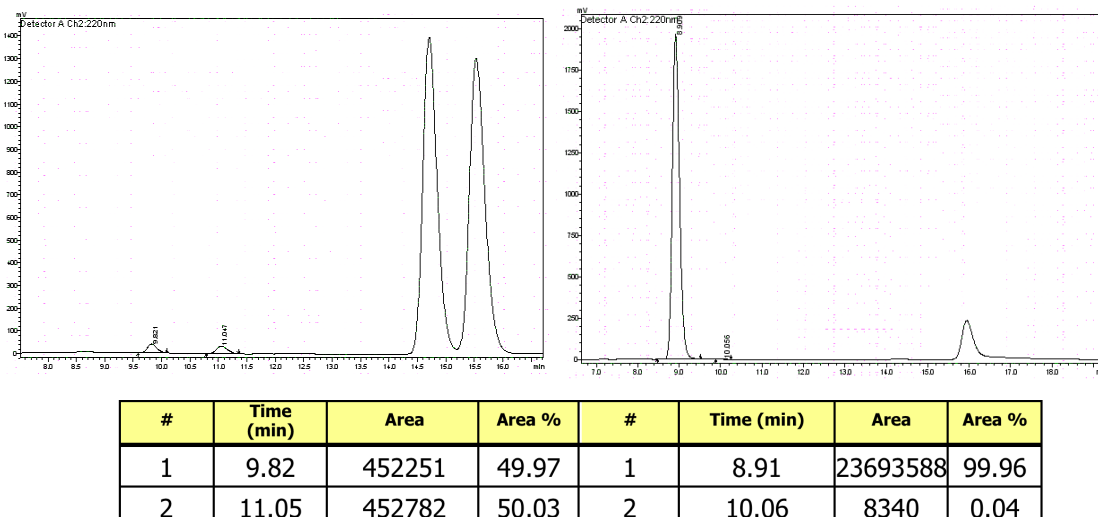
Chart 7. HPLC Traces for Racemic (left) and Enantiomerically Pure 2.8a (right)



(2*R*,4*S*,6*S*)-2-((*Z*)-2-(Cyclohexyloxy)vinyl)-6-vinyltetrahydro-2*H*-pyran-4-ol (2.8b). Following the general procedure, cyclohexylvinyl ether (301 mg, 2.39 mmol, 20.1 equiv) was added to **IV** (5.7 mg, 5.7 mmol, 5.0 mol %) and allowed to stir for 30 minutes. The

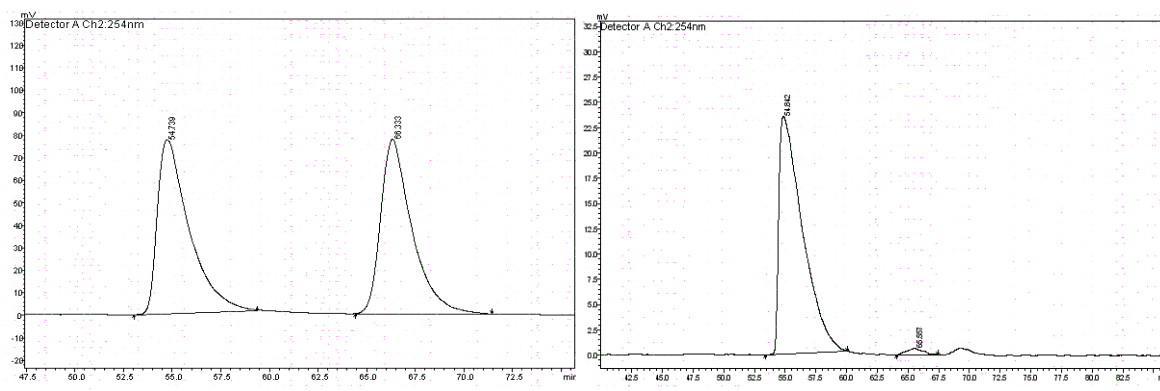
(26) Yu, M.; Ibrahim, I.; Hasegawa, M.; Schrock, R. R.; Hoveyda, A. H. *J. Am. Chem. Soc.* **2012**, *134*, 2788–2799.

mixture was transferred by syringe to a solution of oxabicycle **2.5** (15.0 mg, 0.119 mmol, 1.00 equiv) in C₆H₆ (600 µL) and allowed to stir for 24 hours. Analysis of the 400 MHz ¹H NMR spectrum revealed >98% conv of **2.5**, and product **2.8b** was obtained as a 98:2 mixture of Z/E isomers. The resulting brown oil was purified by silica gel chromatography (0-40% diethyl ether in hexanes) to afford **2.8b** (19.3 mg, 0.0765 mmol, 64.0% yield) as colorless oil (>98:2 e. r., 93% Z). **IR (neat)**: 3414 (br), 2933 (s), 2857 (s), 1666 (s), 1449 (s), 1424 (m), 1367 (s), 1265 (s), 1229 (m), 1163 (m), 1061 (m), 1024 (m), 987 (m), 925 (s), 888 (s), 861 (s), 822 (m), 733 (s), 703 (s), 671 (s), 606 (m), 484 (m); **¹H NMR (400 MHz, CDCl₃)**: δ 6.55 (*E*-isomer, 1H, d, *J* = 12 Hz), 5.97 (1H, dd, *J* = 6.4, 0.8 Hz), 5.83 (1H, ddd, *J* = 17.6, 10.4, 5.6 Hz), 5.18 (1H, apparent dt, *J* = 16, 1.6 Hz), 5.05 (1H, apparent dt, *J* = 10.8, 1.4 Hz), 4.42 (1H, dd, *J* = 8.0, 6.4 Hz), 4.36–4.31 (1H, m), 3.86–3.81 (2H, m), 3.57–3.52 (1H, m), 1.98–1.92 (2H, m), 1.78–1.75 (2H, m), 1.68–1.64 (2H, m), 1.45–1.43 (2H, m), 1.38–1.33 (2H, m), 1.26–1.16 (4H, m); **¹³C NMR (100 MHz, CDCl₃)**: δ 144.9, 138.7, 115.5, 107.2, 80.1, 76.3, 70.5, 68.3, 41.6, 40.8, 32.5, 25.7, 23.8; **HRMS (ESI⁺) [M-OH]⁺** calcd for C₁₅H₂₃O₂: 235.1698, found: 235.1687; $[\alpha]_D^{20} -24.2$ (*c* = 1.48, CH₂Cl₂) for an enantiomerically enriched sample of >98:2. Enantiomeric purity was determined by HPLC (Chart 8) analysis of the benzoyl derivative of **2.8b_{Bz}** (synthesized according to the benzoylation procedure listed above) in comparison with authentic racemic material: **¹H NMR (400 MHz, CDCl₃)**: δ 8.05–8.03 (2H, m), 7.57–7.51 (2H, m), 7.46–7.42 (1H, m), 6.07 (1H, d, *J* = 5.6 Hz), 5.95–5.87 (1H, m), 5.31–5.24 (overlapping, 1H, dd, *J* = 17.2, 1.2 Hz; overlapping 1H, m), 5.13 (1H, dd, *J* = 10.4, 1.2 Hz), 4.58–4.48 (2H, m), 4.08–4.03 (1H, m), 3.65–3.59 (1H, m), 2.21–2.14 (2H, m), 1.85–1.75 (2H, m), 1.75–1.72 (2H, m), 1.59–1.38 (5H, m), 1.32–1.26 (4H, m); AD-H column, 98:2 hexanes:*i*-PrOH, 0.5 mL/min, 220 nm; *Z*-isomer: t_r (major enantiomer) = 8.91 min, t_r (minor enantiomer) = 10.06 min].

Chart 8. HPLC Traces for Racemic (left) and Enantiomerically Pure 2.8b (right)

(2*R*,4*S*,6*S*)-2-((*Z*)-2-(4-Methoxyphenoxy)vinyl)-6-vinyltetrahydro-2*H*-pyran-4-ol

(2.8c). Following the general procedure, *p*-methoxyphenylvinyl ether (182 mg, 1.21 mmol, 10.1 equiv) was added to **IV** (5.6 mg, 5.8 mmol, 5.0 mol %) and allowed to stir for 30 minutes. The mixture was transferred by syringe to a solution of oxabicycle **2.5** (15.1 mg, 0.120 mmol, 1.00 equiv) in C₆H₆ (600 μL) and allowed to stir for 24 hours. Analysis of the 400 MHz ¹H NMR spectrum revealed >98% conv of **2.5**, and product **2.8c** was obtained as a 95:5 mixture of *Z/E* isomers. The resulting brown oil was purified by silica gel chromatography (10–40% diethyl ether in hexanes) to afford **2.8c** (21.0 mg, 0.0807 mmol, 67.0% yield) as colorless oil (98:2 e. r., >98% *Z*). The spectral data for this compound were identical to those reported in the literature.²⁶ [α]_D²⁰ –8.0 (c = 1.5, CH₂Cl₂) for an enantiomerically enriched sample of 98:2. Enantiomeric purity was determined by HPLC (Chart 9) analysis in comparison with authentic racemic material (OD-H column, 97:3 hexanes:*i*-PrOH, 1.0 mL/min, 254 nm); *Z*-isomer: t_r (major enantiomer) = 54.84 min, t_r (minor enantiomer) = 65.56 min.

Chart 9. HPLC Traces for Racemic (left) and Enantiomerically Pure 2.8c (right)

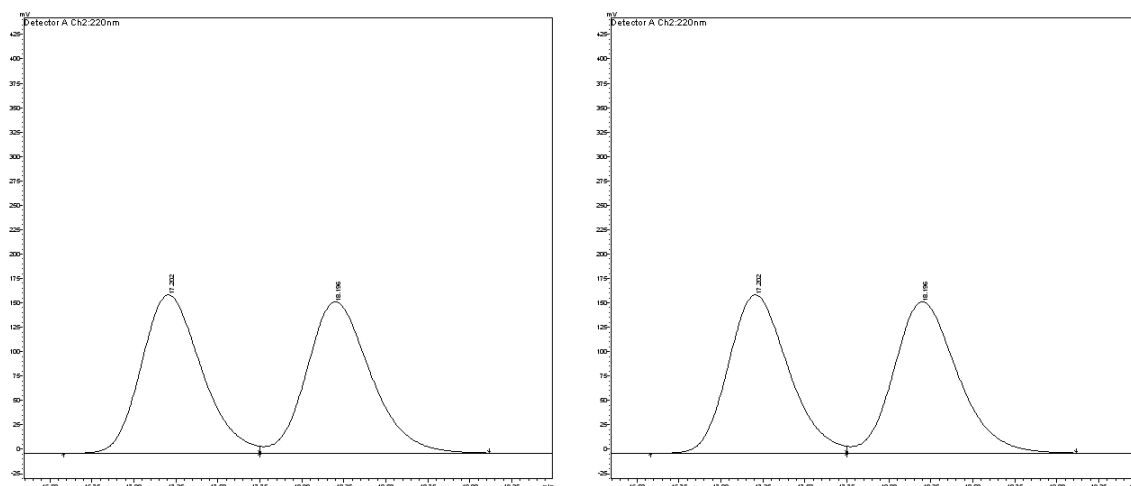
#	Time (min)	Area	Area %	#	Time (min)	Area	Area %
1	54.74	8856339	50.61	1	54.84	3145557	98.22
2	66.33	77615	49.39	2	65.56	57016	1.78

(2*R*,4*S*,6*S*)-2-((*Z*)-2-(2,2,2-Trifluoroethoxy)vinyl)-6-vinyltetrahydro-2*H*-pyran-4-ol (2.8d).

Following the general procedure, trifluoromethylvinyl ether (180 mg, 1.43 mmol, 20.0 equiv) was added to **IV** (3.4 mg, 3.5 mmol, 5.0 mol %) and allowed to stir for one minute. The mixture was transferred by syringe to a solution of oxabicycle **2.5** (9.0 mg, 0.071 mmol, 1.0 equiv) in C₆H₆ (360 μL) and allowed to stir for 24 hours. Analysis of the 400 MHz ¹H NMR spectrum revealed >98% conv of **2.5**, and product **2.8d** was obtained as a 94:6 mixture of *Z/E* isomers. The resulting brown oil was purified by silica gel chromatography (10% diethyl ether in hexanes-100% diethyl ether) to afford **2.8d** (12 mg, 0.046 mmol, 65% yield) as colorless oil (96:4 e. r., 93% *Z*). **IR (neat):** 3375 (br), 2946 (m), 2849 (m), 1675 (s), 1421 (s), 1362 (s), 1317 (s), 1279 (s), 1225 (s), 1160 (s), 1125 (s), 1063 (s), 986 (s), 958 (s), 929 (s), 883 (s), 852 (s), 831 (s), 728 (s), 657 (s), 608 (s); **¹H NMR (400 MHz, CDCl₃):** δ 6.54 (*E* isomer, 1H, d, *J* = 12 Hz), 5.97 (1H, dd, *J* = 6.4, 1.6 Hz), 5.87 (1H, m) 5.26 (1H, dd, *J* = 17.2, 1.4 Hz), 5.13 (1H, dd, *J* = 10.6, 1.2 Hz), 4.72–4.68 (1H, dd, *J* = 17.2, 1.4 Hz), 4.40 (1H, apparent t, *J* = 10 Hz), 4.08–3.99 (2H, m), 3.90–3.88 (2H, m), 2.03–2.00 (2H, m), 1.58 (1H, br s), 1.32–1.18 (2H, m); **¹³C NMR (100 MHz, CDCl₃):** δ 145.8, 144.0, 139.2, 137.6, 123.4 (q, *J* = 279 Hz), 117.3, 115.7, 114.2, 111.4, 109.8, 70.6, 68.7, 41.2, 40.8, 39.9, 39.4; **¹⁹F NMR (376 MHz, CDCl₃):** δ -74.70; **HRMS (ESI⁺) [M+NH₄]⁺** calcd for C₁₁H₁₉O₃F₃N: 270.1317, found: 270.1323; [a]_D²⁰ -9.1 (c = 0.65, CH₂Cl₂) for an enantiomerically enriched sample of 96:4.

Enantiomeric purity was determined by HPLC (Chart 10) analysis of the benzoyl derivative of **2.8d_{Bz}** (synthesized according to the benzoylation procedure above) in comparison with authentic racemic material: **¹H NMR (400 MHz, CDCl₃)**: δ 8.04 (2H, m), 7.56 (1H, m), 7.44 (2H, m), 6.00 (1H, d, *J* = 6 Hz), 5.90 (1H, m), 5.32-5.22 (overlapping, 1H, apparent dt, *J* = 17.2, 1.4 Hz; overlapping 1H, m), 5.15 (1H, apparent dt, *J* = 10.4, 1.2 Hz), 4.72 (1H, dd, *J* = 7.8, 6.2 Hz), 4.58-4.53 (1H, m), 4.15-4.04 (3H, m), 2.23-2.14 (2H, m), 1.60-1.48 (2H, m); AD-H column, 98:2 hexanes:*i*-PrOH, 0.5 mL/min, 220 nm; Z-isomer: *t*_r (minor enantiomer) = 17.17 min, *t*_r (major enantiomer) = 18.02 min].

Chart 10. HPLC Traces for Racemic (left) and Enantiomerically Pure **2.8d (right)**



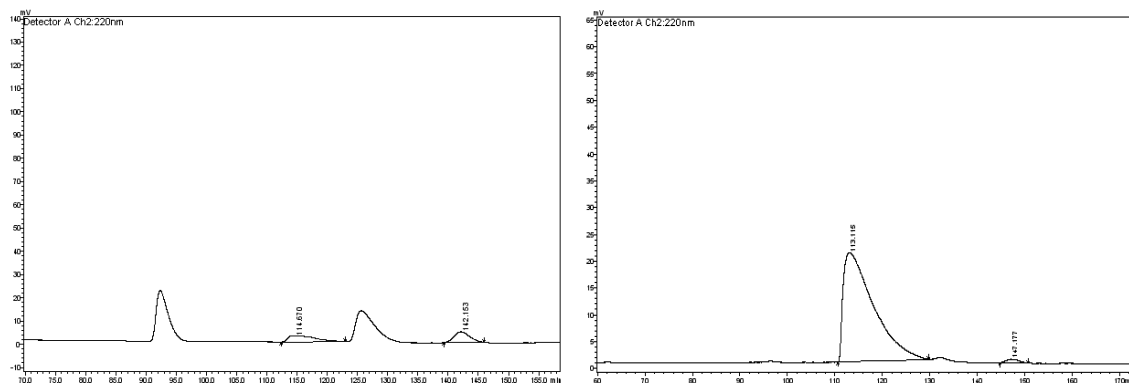
#	Time (min)	Area	Area %	#	Time (min)	Area	Area %
1	17.01	6818140	50.11	1	17.17	4053065	3.54
2	18.05	6787808	49.89	2	18.02	110396416	96.46

(2*R*,4*S*,6*S*)-2-((*Z*)-2-(2-Chloroethoxy)vinyl)-6-vinyltetrahydro-2*H*-pyran-4-ol (2.8e**).**

Following the general procedure, chloroethylvinyl ether (119 mg, 1.11 mmol, 19.5 equiv) was added to **IV** (2.7 mg, 2.8 mmol, 5.0 mol %) and allowed to stir for one minute. The mixture was transferred by syringe to a solution of oxabicyclic **2.5** (7.2 mg, 0.057 mmol, 1.0 equiv) in C₆H₆ (600 μL) and allowed to stir for 24 hours. Analysis of the 400 MHz **¹H NMR** spectrum revealed >98% conv of **2.5**, and product **2.8e** was obtained as a 95:5 mixture of *Z/E* isomers. The resulting brown oil was purified by silica gel chromatography (20-70% diethyl ether in hexanes) to afford **2.8e** (8.4 mg, 0.036 mmol,

63% yield) as colorless oil (>98:2 e. r., 96% Z). **IR (neat)**: 3376 (br), 2941 (m), 2918 (m), 2849 (m), 1669 (s), 1449 (m), 1426 (s), 1361 (s), 1303 (s), 1266 (s), 1222 (s), 1104 (s), 1059 (s), 989 (s), 926 (s), 882 (s), 850 (m), 752 (s), 707 (s), 666 (s), 607 (s), 479 (m), 420 (m); **¹H NMR (400 MHz, CDCl₃)**: δ 5.99 (dd, *J* = 6.4, 1.2 Hz, 1H), 5.89 (ddd, *J* = 17.6, 10.8, 6 Hz, 1H), 5.26 (apparent dt, *J* = 17.2, 1.6 Hz, 1H), 5.12 (apparent dt, *J* = 10.4, 1.6 Hz, 1H), 4.59 (dd, *J* = 8.0, 6.4 Hz, 1H), 4.37–4.38 (m, 1H), 4.05–3.94 (m, 2H), 3.93–3.89 (m, 2H), 3.64 (t, *J* = 6.4 Hz, 2H), 2.05–1.99 (m, 2H), 1.33–1.24 (m, 3H); **¹³C NMR (100 MHz, CDCl₃)**: δ 145.5, 138.6, 115.7, 108.9, 76.3, 72.4, 70.1, 68.2, 42.4, 41.4, 40.8; **HRMS (ESI⁺) [M+NH₄]⁺** calcd for C₁₁H₂₁O₃ClN: 250.1210, found: 250.1220; [a]_D²⁰ −15.1 (*c* = 0.646, CH₂Cl₂) for an enantiomerically enriched sample of >98:2. Enantiomeric purity was determined by HPLC (Chart 11) analysis in comparison with authentic racemic material [AS-H column, 98:2 hexanes:*i*-PrOH, 0.5 mL/min, 220 nm; Z-isomer: t_r (major enantiomer) = 113.12 min, t_r (minor enantiomer) = 147.18 min].

Chart 11. HPLC Traces for Racemic (left) and Enantiomerically Pure 2.8e (right)



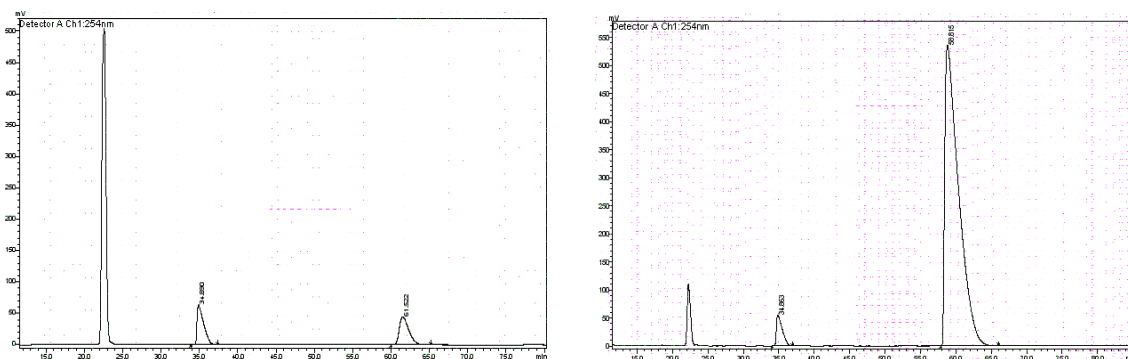
#	Time (min)	Area	Area %	#	Time (min)	Area	Area %
1	114.67	830649	50.26	1	113.12	9046220	98.69
2	142.15	822117	49.74	2	147.18	120012	1.31

(2*S*,4*R*,6*R*)-2-((*Z*)-2-(Phenylthio)vinyl)-6-vinyltetrahydro-2*H*-pyran-4-ol (2.9).

Following the general procedure, phenylvinyl sulfide (326 mg, 2.39 mmol, 20.1 equiv) was added to **IV** (5.8 mg, 6.0 μmol, 5.0 mol %) and allowed to stir for five minutes. The mixture was transferred by syringe to a solution of oxabicycle **2.5** (15.0 mg, 0.0589 mmol, 1.00 equiv) in C₆H₆ (600 μL) and allowed to stir for 24 hours. Analysis of the 400 MHz ¹H NMR spectrum revealed 98% conv of **2.5**, and product **2.9** was obtained as a 91:9 mixture of *Z/E* isomers. The resulting brown oil was purified by silica gel

chromatography (10–40% diethyl ether in hexanes) to afford **2.9** (21.5 mg, 0.0819 mmol, 69% yield) as colorless oil (96:4 e. r., 91% Z). **IR (neat):** 3355 (br), 3075 (m), 3016 (m), 2941 (s), 2917 (s), 2848 (m), 1647 (s), 1613 (s), 1585 (s), 1479 (s), 1439 (s), 1426 (s), 1358 (s), 1295 (s), 1265 (s), 1227 (s), 1167 (s), 1147 (s), 1063 (s), 1024 (s), 987 (s), 925 (s), 882 (s), 852 (s), 773 (s), 737 (s), 688 (s), 647 (s), 470 (s), 423 (s), 400 (s); **¹H NMR (400 MHz, CDCl₃):** δ 7.37–7.29 (4H, m), 7.26–7.21 (1H, m), 6.32 (1H, dd, *J* = 9.6, 1.2 Hz), 5.95–5.87 (overlapping 1H, m), 5.85 (overlapping 1H, dd, *J* = 9.6, 7.4 Hz), 5.31 (1H, apparent dt, *J* = 17.6, 1.2 Hz), 5.16 (1H, apparent dt, *J* = 10.8, 1.2 Hz), 4.41–4.36 (1H, m), 3.98–3.91 (2H, m), 2.08–2.02 (2H, m), 1.42–1.26 (2H, m); **¹³C NMR (100 MHz, CDCl₃):** δ 138.2, 135.8, 131.8, 129.6, 129.3, 127.0, 125.6, 115.9, 76.4, 73.5, 68.0, 40.7, 40.4; **HRMS (ESI+):** [M+NH₄]⁺ calcd for C₁₅H₂₂O₂SN: 280.1371, found: 280.1373; [α]_D²⁰+88.1 (*c* = 0.661, CH₂Cl₂) for an enantiomerically enriched sample of 96:4. Enantiomeric purity was determined by HPLC (Chart 12) analysis in comparison with authentic racemic material [AD-H column, 95:5 hexanes:*i*-PrOH, 0.5 mL/min, 220 nm; Z-isomer: t_r (minor enantiomer) = 34.86 min, t_r (major enantiomer) = 58.82 min].

Chart 12. HPLC Traces for Racemic (left) and Enantiomerically Pure 2.9 (right)

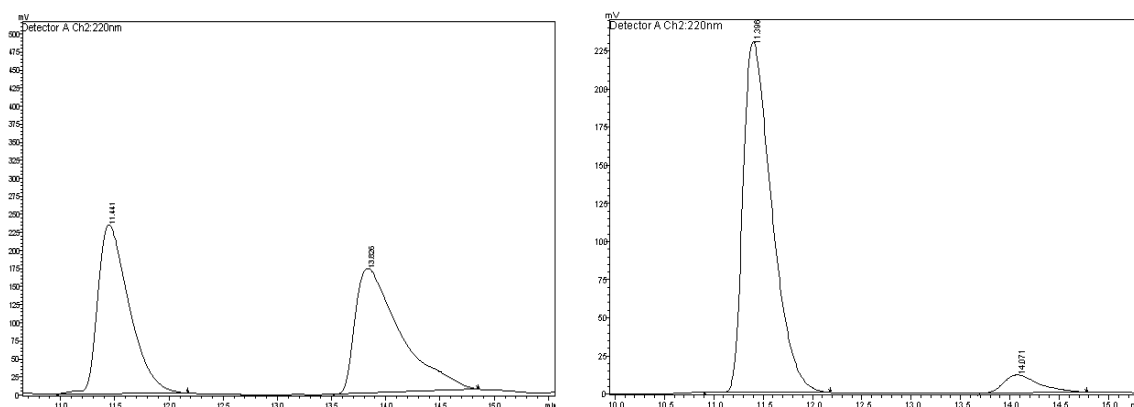


#	Time (min)	Area	Area %	#	Time (min)	Area	Area %
1	34.89	3728581	49.57	1	34.86	3168042	4.18
2	61.52	3794026	50.43	2	58.82	72680485	95.82

(2*R*,4*S*,6*S*)-2-(*Z*)-2-Butoxyvinyl)-6-vinyltetrahydro-2*H*-pyran-4-yl)oxy)(*tert*-butyl)-dimethyl-silane (2.10). Following the general procedure, *n*-butylvinyl ether (130 mg, 1.30 mmol, 20.2 equiv) was added to **IV** (3.1 mg, 3.2 mmol, 5.0 mol %) and allowed to stir for 30 minutes. The mixture was transferred by syringe to a solution of TBS-protected oxabicyclic alcohol **2.3** (15.5 mg, 0.0645 mmol, 1.00 equiv) in C₆H₆ (350 μL)

and allowed to stir for 24 hours. Analysis of the 400 MHz ^1H NMR spectrum revealed >98% conv of **2.3**, and product **2.10** was obtained as a 87:13 mixture of *Z/E* isomers. The resulting brown oil was purified by silica gel chromatography (0-40% diethyl ether in hexanes) to afford **2.10** (10.4 mg, 0.0459 mmol, 71% yield) as colorless oil (94:6 e. r., 92% *Z*). The spectral data for this compound were identical to those reported in the literature.²⁶ $[\alpha]_D^{20} -1.9$ ($c = 0.44$, CH_2Cl_2) for an enantiomerically enriched sample of 94:6. Enantiomeric purity was determined by HPLC (Chart 13) analysis of the corresponding alcohol (after removal of the silyl group)²⁶ in comparison with authentic racemic material [OD-H column, 99:1 hexanes:*i*-PrOH, 0.5 mL/min, 220 nm; *Z*-isomer: t_r (major enantiomer) = 14.07 min, t_r (minor enantiomer) = 11.39 min].

Chart 13. HPLC Traces for Racemic (left) and Enantiomerically Pure **2.10 (right)**



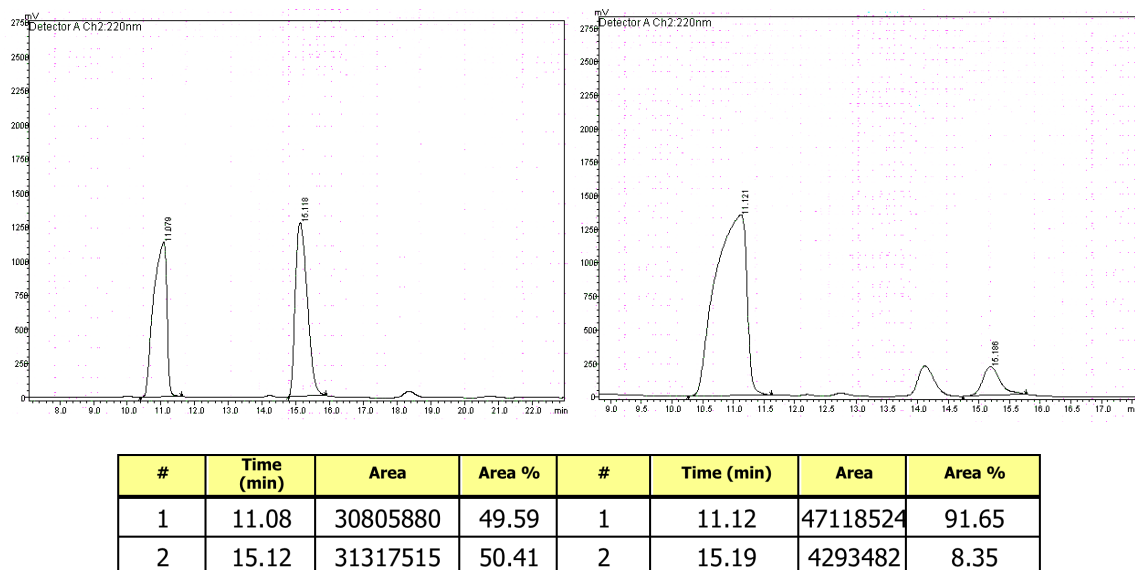
#	Time (min)	Area	Area %	#	Time (min)	Area	Area %
1	11.44	4802388	49.33	1	11.39	4665675	94.03
2	13.826	4932581	50.67	2	14.07	4951171	5.97

(2*S*,4*S*,6*R*)-4-(Benzylxy)-2-((*Z*)-2-butoxyvinyl)-6-vinyltetrahydro-2*H*-pyran (2.11).

Following the general procedure, *n*-butylvinyl ether (92.6 mg, 0.925 mmol, 20.0 equiv) was added to **IV** (2.2 mg, 2.3 mmol, 5.0 mol %) and allowed to stir for 30 minutes. The mixture was transferred by syringe to a vial containing the oxabicyclic **2.11_{pre}** (10.0 mg, 0.0462 mmol, 1.00 equiv) and allowed to stir for 24 hours. Analysis of the 400 MHz ^1H NMR spectrum revealed >98% conv of **2.11_{pre}**, and product **2.11** was obtained as a 94:6 mixture of *Z/E* isomers. The resulting brown oil was purified by silica gel chromatography (10% ethyl acetate in hexanes) to afford **2.11** (9.1 mg, 0.029 mmol, 62% yield) as colorless oil (92:8 e. r., 94% *Z*). The spectral data for this compound were

identical to those reported in the literature.²⁶ $[\alpha]_D^{20} -26.3$ ($c = 0.662$, CH_2Cl_2) for an enantiomerically enriched sample of 92:8. Enantiomeric purity was determined by HPLC (Chart 14) analysis in comparison with authentic racemic material [OD-H column, 99.5:0.5 hexanes:*i*-PrOH, 0.5 mL/min, 220 nm; Z-isomer: t_r (major enantiomer) = 11.12 min, t_r (minor enantiomer) = 15.19 min].

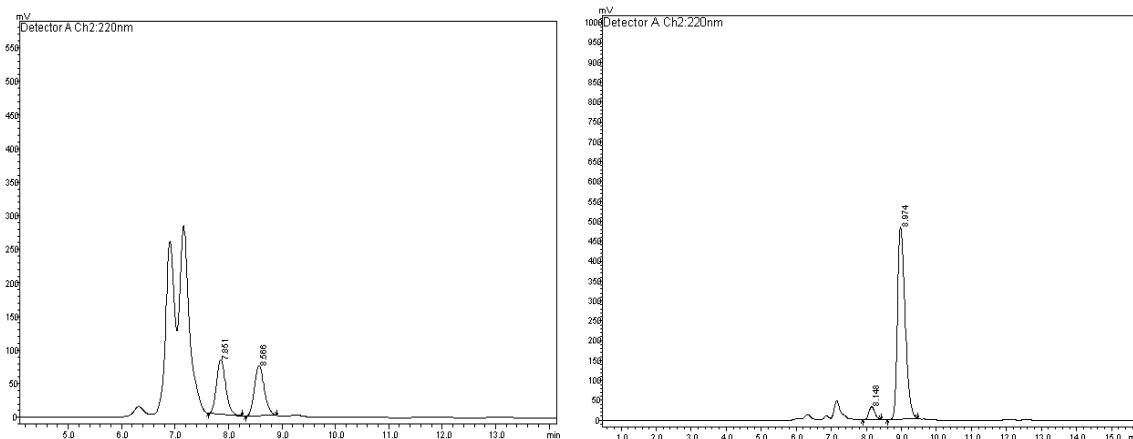
Chart 14. HPLC Traces for Racemic (left) and Enantiomerically Pure 2.11 (right)



(2*R*,4*S*,6*S*)-2-(*Z*)-2-Butoxyvinyl)-4-methyl-6-vinyltetrahydro-2*H*-pyran-4-yl)oxy)(*tert*-butyl)- dimethylsilane (2.12). Following the general procedure, *n*-butylvinyl ether (119 mg, 1.19 mmol, 20.0 equiv) was added to **IV** (2.8 mg, 2.9 mmol, 5.0 mol %) and allowed to stir for 30 minutes. The mixture was transferred by syringe to a solution of oxabicycle **2.12_{pre}** (15.0 mg, 0.0589 mmol, 1.00 equiv) in C_6H_6 (300 μL) and allowed to stir for 24 hours. Analysis of the 400 MHz ^1H NMR spectrum revealed 97% conv of **2.12_{pre}**, and product **2.12** was obtained as a 92:8 mixture of *Z/E* isomers. The resulting brown oil was purified by silica gel chromatography (2% diethyl ether in hexanes) to afford **2.12** (15.1 mg, 0.0426 mmol, 72% yield) as colorless oil (95:5 e. r., 92% *Z*). **IR (neat):** 2956 (s), 2929 (s), 2857 (s), 1669 (s), 1472 (s), 1463 (s), 1409 (s), 1376 (s), 1351 (s), 1301 (s), 1278 (s), 1252 (s), 1152.3 (s), 1152 (s), 1105 (s), 1074 (s), 1045 (s), 1006 (s), 988 (s), 922 (s), 890 (s), 835 (s), 800 (s), 773 (s), 734 (s), 663 (s); **^1H NMR (400 MHz, CDCl_3):** δ 6.55 (*E*-isomer, 1H, d, $J = 12$ Hz), 5.96 (1H, dd, $J = 6.0, 0.8$ Hz), 5.85 (1H, ddd, $J = 17.6, 10.8, 6.0$ Hz), 5.23 (1H, apparent dt, $J = 17.2, 1.6$ Hz), 5.08 (1H,

apparent dt, $J = 10.4, 1.2$ Hz), 4.47–4.36 (2H, m), 3.92–3.87 (1H, m), 3.77–3.71 (2H, m), 1.70–1.63 (3H, m), 1.61–1.56 (2H, m), 1.54–1.44 (3H, m), 1.43–1.34 (overlapping 3H, s; overlapping, 2H, m), 0.93 (3H, t, $J = 8$ Hz), 0.85 (9H, s), 0.085 (6H, s); ^{13}C NMR (100 MHz, CDCl_3): δ 146.2, 139.2, 115.1, 107.6, 75.8, 72.5, 71.8, 69.6, 46.9, 46.5, 31.9, 26.6, 25.9, 19.1, 18.0, 13.9, –1.7; HRMS (ESI $^+$) [M+Na] $^+$ calcd for $\text{C}_{20}\text{H}_{38}\text{O}_3\text{SiNa}$: 377.2488, found: 377.2471; $[a]_D^{20} +10.5$ ($c = 1.15$, CH_2Cl_2) for an enantiomerically enriched sample of 95:5. Enantiomeric purity was determined by HPLC (Chart 15) analysis in comparison with authentic racemic material [OD-H column, 99.9:0.1 hexanes:*i*-PrOH, 0.5 mL/min, 220 nm; Z-isomer: t_r (minor enantiomer) = 8.15 min, t_r (major enantiomer) = 8.97 min].

Chart 15. HPLC Traces for Racemic (left) and Enantiomerically Pure 2.12 (right)

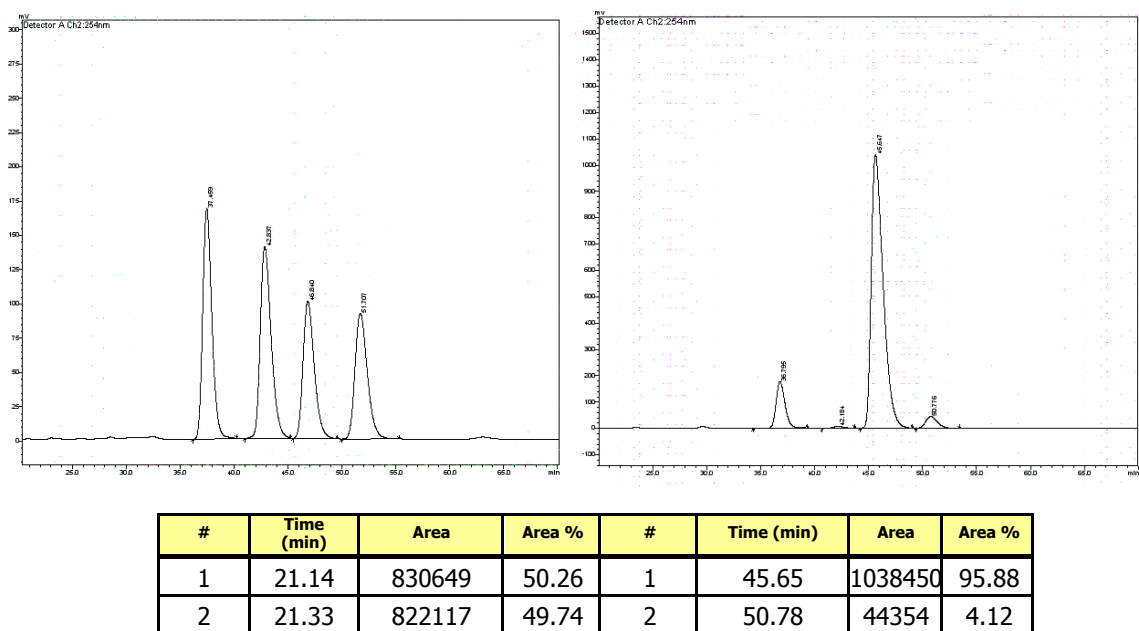


#	Time (min)	Area	Area %	#	Time (min)	Area	Area %
1	7.85	973986	50.21	1	8.15	346036	4.52
2	8.57	965720	49.79	2	8.97	7303709	95.48

(2*S*,4*R*,6*R*)-2-((*E*)-4-bromostyryl)-6-vinyltetrahydro-2*H*-pyran-4-ol (2.15). The compound was accessed through a previously reported procedure.²¹

(2*R*,4*S*,6*S*)-2-((*Z*)-2-((6-Bromonaphthalen-2-yl)oxy)vinyl)-6-vinyltetrahydro-2*H*-pyran-4-ol (2.16). Following the general procedure, 2-bromo-6-(vinyloxy)naphthalene (198 mg, 0.793 mmol, 10.0 equiv) and **IV** (3.8 mg, 4.0 mmol, 5.0 mol %) in C_6H_6 (500 μL) were allowed to stir for 20 min. The mixture was transferred by syringe to a solution of oxabicycle **2.5** (10.0 mg, 0.079 mmol, 1.0 equiv) in C_6H_6 (300 μL) and allowed to stir for 24 hours. Analysis of the 400 MHz ^1H NMR spectrum revealed >98% conv of **2.5**,

and product **2.16** was obtained as a 89:11 mixture of *Z/E* isomers. The resulting brown oil was purified by silica gel chromatography (17–33% ethyl acetate in hexanes) to afford **2.16** (26.7 mg, 0.071 mmol, 90% yield) as white solid (96:4 e. r., 89% *Z*). **IR (neat)**: 3367 (br), 2942 (w), 2919 (w), 2852 (w), 1673 (m), 1626 (m), 1589 (s), 1500 (s), 1361 (m), 1255 (s), 1201 (s), 1161 (m), 1063 (s), 1016 (m), 912 (m), 879 (m), 801 (w), 473 (w); **¹H NMR (400 MHz, CDCl₃)**: δ 7.95 (d, *J* = 2.0 Hz, 1H), 7.70 (d, *J* = 8.8 Hz, 1H), 7.61 (d, *J* = 8.8 Hz, 1H), 7.53 (dd, *J* = 8.8, 2.0 Hz, 1H), 7.28 (d, *J* = 2.4 Hz, 1H), 7.24 (dd, *J* = 8.8, 2.8 Hz, 1H), 6.51 (dd, *J* = 6.0, 1.2 Hz, 1H), 5.91 (ddd, *J* = 17.2, 10.4, 5.6 Hz, 1H), 5.29 (apparent dt, *J* = 17.2, 1.2 Hz, 1H), 5.15 (apparent dt, *J* = 10.4, 1.2 Hz, 1H), 5.07 (dd, *J* = 8.0, 6.0 Hz, 1H), 4.61–4.55 (m, 1H), 4.00–3.92 (m, 2H), 2.15–2.02 (m, 2H), 1.64 (br s, 1H), 1.44–1.29 (m, 2H); **¹³C NMR (100 MHz, CDCl₃)**: δ 155.3, 140.9, 138.3, 132.8, 131.1, 130.2, 129.9, 129.0, 128.8, 119.6, 118.4, 115.7, 114.0, 111.0, 76.3, 70.1, 68.0, 41.2, 40.7; **HRMS (ESI⁺) [M]⁺** calcd for C₁₉H₁₉⁷⁹Br₁O₃: 374.05176, found: 374.04995; [a]_D²⁰ 2.735 (*c* = 0.585, CH₂Cl₂) for an enantiomerically enriched sample of 96:4. Enantiomeric purity was determined by HPLC (Chart 16) analysis in comparison with authentic racemic material [AD-H column, 95:5 hexanes:*i*-PrOH, 0.5 mL/min, 254 nm; *Z*-isomer: t_r (major enantiomer) = 45.65 min, t_r (minor enantiomer) = 50.78 min].

Chart 16. HPLC Traces for Racemic (left) and Enantiomerically Pure 2.16 (right)

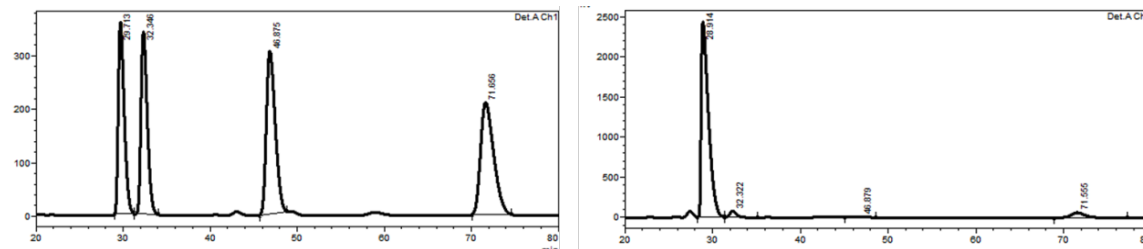
(2*R*,4*S*,6*S*)-2-((*Z*)-2-(4-butoxyphenoxy)vinyl)-6-vinyltetrahydro-2*H*-pyran-4-ol

(2.17a). Following the general procedure, a solution of **IV** (5.6 mg, 5.8 μ mol, 5.0 mol %) in benzene (600 μ L) was transferred by syringe to a vial containing oxabicyclic alkene **2.5** (15.0 mg, 0.119 mmol, 1.00 equiv) and enol ether (457 mg, 2.38 mmol, 20.0 equiv). The resulting mixture was allowed to stir for 12 hours at 22 °C. Analysis of the unpurified mixture revealed 66% conv of the substrate, and the ROCM product was obtained in 92:08 Z/E ratio. The resulting brown oil was purified by silica gel chromatography (10% Et₂O in hexanes to 50% Et₂O in hexanes) to afford product **2.17a** (24.3 mg, 0.0763 mmol, 64% yield) as colorless oil; **IR** (CH₂Cl₂): 3383 (br), 2936 (w), 2871 (w), 1674 (w), 1502 (s), 826 (m); **¹H NMR** (400 MHz, CDCl₃): Z-isomer (major): δ 6.95–6.88 (2H, m), 6.86–6.79 (2H, m), 6.31 (1H, dd, J = 6.2, 1.0 Hz),²⁷ 5.90 (1H, ddd, J = 17.3, 10.6, 5.7 Hz), 5.28 (1H, dt, J = 17.3, 1.4 Hz), 5.14 (1H, dt, J = 10.6, 1.3 Hz), 4.87 (1H, dd, J = 8.0, 6.2 Hz), 4.54 (1H, dddd, J = 11.2, 8.0, 2.0, 1.0 Hz), 3.97–3.89 (4H, m), 2.10 (1H, ddt, J = 12.3, 4.4, 2.1 Hz), 2.03 (1H, ddt, J = 12.3, 4.3, 2.1 Hz), 1.79–1.70 (2H, m), 1.53–1.43 (2H, m), 1.43–1.24 (3H, m), 0.97 (3H, t, J = 7.4 Hz); **¹³C NMR** (100 MHz, CDCl₃): δ 155.1, 151.1, 142.4, 138.2, 117.7, 115.5, 115.3, 111.5, 76.1, 70.0, 68.2, 67.9, 41.1, 40.5, 31.3, 19.2, 13.8; **HRMS** [M+H]⁺ calcd for C₁₉H₂₆O₄: 318.1831, found:

(27) Coupling constant (J = 6.2 Hz) for the signal at 6.31 ppm is indicative of **2.17a**.

318.1847. $[\alpha]_D^{20} +12.8$ ($c = 0.48$, CHCl_3) for an enantiomerically enriched sample of 97:03. Enantiomeric purity was determined by HPLC (Chart 17) analysis in comparison with authentic racemic material (Daicel Chiralpak OD-H column, 97:3 hexanes:*i*-PrOH, 0.5 mL/min, 220 nm).

Chart 17. HPLC Traces for Racemic (left) and Enantiomerically Pure 2.17a (right)



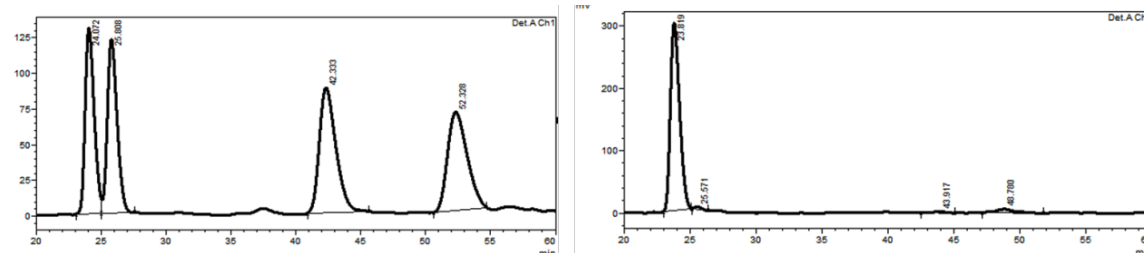
Peak #	Retention time (min)	Area	Area %	Peak #	Retention time (min)	Area	Area %
1	29.71	17032013	21.93	1	28.91	140649946	94.39
2	32.35	22706960	22.10	2	32.32	3844804	3.05
3	46.88	21599199	27.81	3	46.88	408209	0.20
4	71.66	21881097	28.17	4	71.56	6309277	2.37

(2*R*,4*S*,6*S*)-2-((Z)-2-(4-ethylphenoxy)vinyl)-6-vinyltetrahydro-2*H*-pyran-4-ol (2.17b). Following the general procedure, a solution of **IV** (5.6 mg, 5.8 μmol , 5.0 mol %) in benzene (600 μL) was transferred by syringe to a vial containing oxabicyclic alkene **2.5** (15.0 mg, 0.119 mmol, 1.00 equiv) and enol ether (352 mg, 2.38 mmol, 20.0 equiv). The resulting mixture was allowed to stir for 12 hours at 22 °C. Analysis of the unpurified mixture revealed 74% conv of the substrate, and the ROCM product was obtained in 91:09 *Z/E* ratio. The resulting brown oil was purified by silica gel chromatography (10% Et_2O in hexanes to 50% Et_2O in hexanes) to afford product **2.17b** (22.5 mg, 0.0820 mmol, 69% yield) as colorless oil; **IR (CH₂Cl₂)**: 3375 (br), 2962 (w), 2920 (w), 2850 (w), 1674 (m), 1606 (w), 1506(s), 925 (m), 829 (m); **¹H NMR (400 MHz, CDCl₃)**: Z-isomer (major): δ 7.14 (2H, d, *J*=8.7 Hz), 6.92 (2H, d, *J*=8.6 Hz), 6.37 (1H, dd, *J*=6.2, 1.1 Hz),²⁸ 5.90 (1H, ddd, *J*=17.3, 10.6, 5.7 Hz), 5.28 (1H, dt, *J*=17.3, 1.4 Hz), 5.14 (1H, dt, *J*=10.6, 1.3 Hz), 4.92 (1H, dd, *J*=8.0, 6.2 Hz), 4.64–4.44 (1H, m), 4.01–3.86 (2H, m), 2.61 (2H, q, *J*=7.6 Hz), 2.10 (1H, ddt, *J*=12.2, 4.2, 2.0 Hz), 2.03 (1H, ddt, *J*=12.3, 4.3, 2.0 Hz), 1.41–1.25 (3H, m), 1.21 (3H, t, *J*=7.6 Hz); **¹³C NMR (100 MHz, CDCl₃)**: δ 155.2, 141.7, 139.0, 138.2, 128.9, 116.5, 115.5, 112.2, 76.1, 70.0, 67.9, 41.1,

(28) Coupling constant (*J*=6.2 Hz) for the signal at 6.37 ppm is indicative of **2.17b**.

40.5, 28.0, 15.7; **HRMS** $[\text{M}+\text{H}]^+$ calcd for $\text{C}_{17}\text{H}_{21}\text{O}_3$: 273.1491, found: 273.1491. $[\alpha]_D^{20}$ - 55.4 ($c = 0.36$, CHCl_3) for an enantiomerically enriched sample of 97:03. Enantiomeric purity was determined by HPLC (Chart 18) analysis in comparison with authentic racemic material (Daicel Chiralpak OD-H column, 97:3 hexanes:*i*-PrOH, 0.5 mL/min, 220 nm).

Chart 18. HPLC Traces for Racemic (left) and Enantiomerically Pure 2.17b (right)



Peak #	Retention time (min)	Area	Area %	Peak #	Retention time (min)	Area	Area %
1	24.07	6279887	22.76	1	23.82	300587	96.03
2	25.81	6354881	23.03	2	25.57	4483	1.43
3	42.33	7756172	28.11	3	43.92	1915	0.61
4	52.33	7200278	26.10	4	48.78	6017	1.92

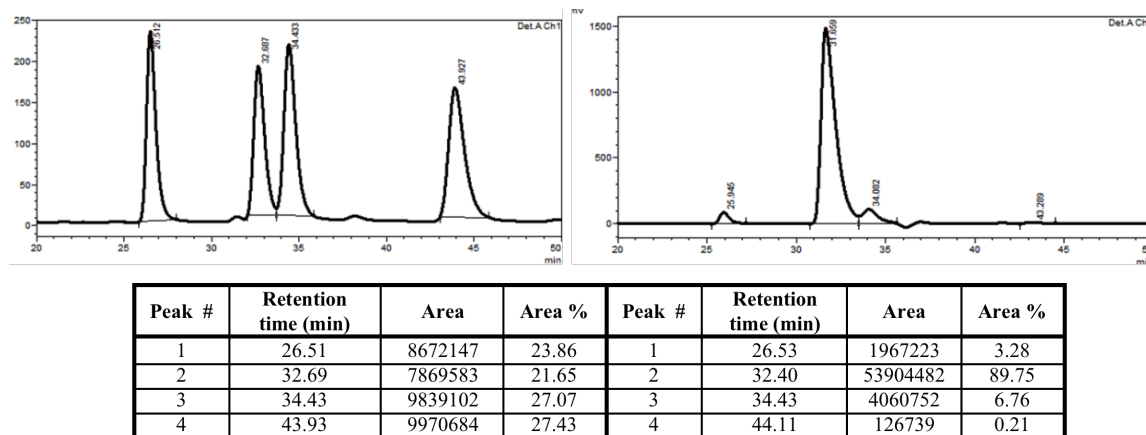
(2*R*,4*S*,6*S*)-2-((*Z*)-2-phenoxyvinyl)-6-vinyltetrahydro-2*H*-pyran-4-ol (2.17c).

Following the general procedure, a solution of **IV** (5.6 mg, 5.8 μmol , 5.0 mol %) in benzene (600 μL) was transferred by syringe to a vial containing oxabicyclic alkene **2.5** (15.0 mg, 0.119 mmol, 1.00 equiv) and enol ether (286 mg, 2.38 mmol, 20.0 equiv). The resulting mixture was allowed to stir for 12 hours at 22 °C. Analysis of the unpurified mixture revealed 82% conv of the substrate, and the ROCM product was obtained in 93:07 *Z/E* ratio. The resulting brown oil was purified by silica gel chromatography (10% Et_2O in hexanes to 50% Et_2O in hexanes) to afford product **2.17c** (21.7 mg, 0.0881 mmol, 74% yield) as colorless oil; **IR** (CH_2Cl_2): 3368 (br), 2942 (w), 2919 (w), 2850 (w), 1675 (m), 1594 (m), 1489 (s), 927 (m); **$^1\text{H NMR}$ (400 MHz, CDCl_3)**: *Z*-isomer (major): δ 7.36–7.28 (2H, m), 7.11–7.04 (1H, m), 7.03–6.97 (2H, m), 6.40 (1H, dd, $J = 6.2, 1.0$ Hz),²⁹ 5.90 (1H, ddd, $J = 17.2, 10.5, 5.7$ Hz), 5.28 (1H, dt, $J = 17.3, 1.4$ Hz), 5.14 (1H, dt, $J = 10.6, 1.3$ Hz), 4.96 (1H, dd, $J = 8.0, 6.2$ Hz), 4.62–4.50 (1H, m), 4.02–3.87 (2H, m), 2.10 (1H, ddt, $J = 12.3, 4.4, 2.1$ Hz), 2.03 (1H, ddt, $J = 12.4, 4.3, 2.0$ Hz), 1.45–1.23 (3H,

(29) Coupling constant ($J = 6.2$ Hz) for the signal at 6.40 ppm is indicative of **2.17c**.

m); **^{13}C NMR (100 MHz, CDCl_3):** δ 157.1, 141.2, 138.2, 129.6, 123.1, 116.6, 115.5, 112.7, 76.1, 70.0, 67.9, 41.1, 40.5; **HRMS [M+H] $^+$** calcd for $\text{C}_{15}\text{H}_{17}\text{O}_3$: 245.1178, found: 245.1174. $[\alpha]_{D}^{20} +104.0$ ($c = 0.48$, CHCl_3) for an enantiomerically enriched sample of 96:04. Enantiomeric purity was determined by HPLC (Chart 19) analysis in comparison with authentic racemic material (Daicel Chiralpak OJ-H column, 95:5 hexanes:*i*-PrOH, 0.5 mL/min, 220 nm).

Chart 19. HPLC Traces for Racemic (left) and Enantiomerically Pure 2.17c (right)



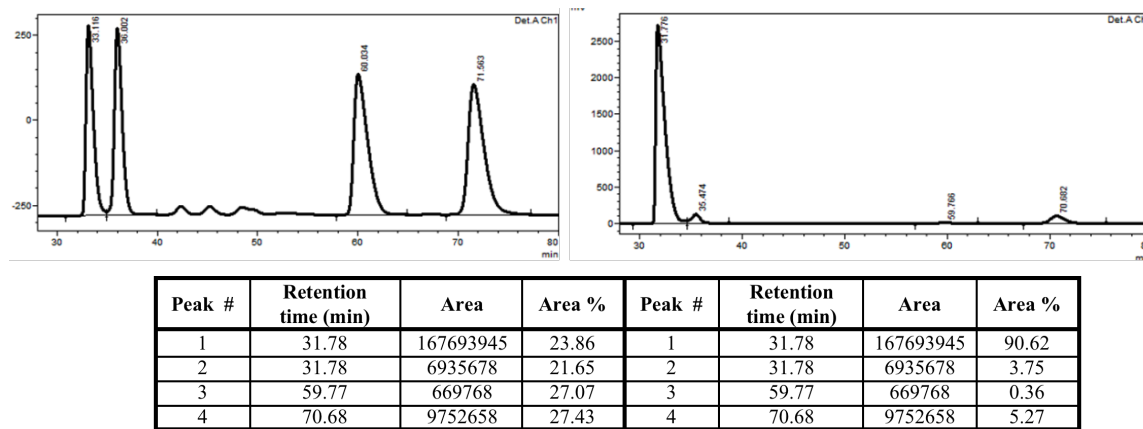
(2*R*,4*S*,6*S*)-2-((*Z*)-2-(4-bromophenoxy)vinyl)-6-vinyltetrahydro-2*H*-pyran-4-ol (2.17d).

Following the general procedure, a solution of **IV** (5.6 mg, 5.8 μmol , 5.0 mol %) in benzene (600 μL) was transferred by syringe to a vial containing oxabicyclic alkene **2.5** (15.0 mg, 0.119 mmol, 1.00 equiv) and enol ether (473 mg, 2.38 mmol, 20.0 equiv). The resulting mixture was allowed to stir for 12 hours at 22 °C. Analysis of the unpurified mixture revealed 90% conv of the substrate, and the ROCM product was obtained in 93:07 *Z/E* ratio. The resulting brown oil was purified by silica gel chromatography (10% Et_2O in hexanes to 60% Et_2O in hexanes) to afford product **2.17d** (30.6 mg, 0.0941 mmol, 79% yield) as colorless oil; **IR (CH₂Cl₂):** 3376 (br), 2918 (w), 2849 (w), 1674 (m), 1585 (m), 1483 (s), 924 (m), 820 (m); **^1H NMR (400 MHz, CDCl_3):** *Z*-isomer (major): δ 7.45–7.38 (2H, m), 6.91–6.85 (2H, m), 6.33 (1H, dd, $J = 6.2, 1.0$ Hz),³⁰ 5.89 (1H, ddd, $J = 17.3, 10.6, 5.7$ Hz), 5.28 (1H, dt, $J = 17.3, 1.4$ Hz), 5.14 (1H, dt, $J = 10.6, 1.3$ Hz), 4.99 (1H, dd, $J = 8.0, 6.2$ Hz), 4.58–4.41 (1H, m), 4.00–3.82 (2H, m),

(30) Coupling constant ($J = 6.2$ Hz) for the signal at 6.33 ppm is indicative of **2.17d**.

2.11–2.00 (2H, m), 1.41–1.24 (3H, m); **¹³C NMR (100 MHz, CDCl₃)**: δ 156.1, 140.7, 138.1, 132.5, 118.3, 115.6, 115.5, 113.6, 76.1, 69.9, 67.8, 41.0, 40.6; **HRMS [M+Na]⁺** found for C₁₅H₁₇O₃NaBr: 347.0247. [α]_D²⁰ +69.9 (c = 1.0, CHCl₃) for an enantiomerically enriched sample of 96:04. Enantiomeric purity was determined by HPLC (Chart 20) analysis in comparison with authentic racemic material (Daicel Chiralpak OD-H column, 97:3 hexanes:*i*-PrOH, 0.5 mL/min, 220 nm).

Chart 20. HPLC Traces for Racemic (left) and Enantiomerically Pure 2.17d (right)



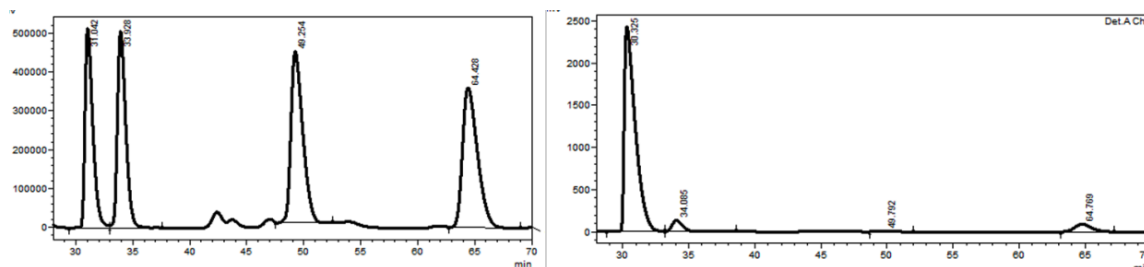
(2*R*,4*S*,6*S*)-2-((Z)-2-(4-chlorophenoxy)vinyl)-6-vinyltetrahydro-2*H*-pyran-4-ol

(2.17e). Following the general procedure, a solution of **IV** (5.6 mg, 5.8 μmol, 5.0 mol %) in benzene (600 μL) was transferred by syringe to a vial containing oxabicyclic alkene **2.5** (15.0 mg, 0.119 mmol, 1.00 equiv) and enol ether (368 mg, 2.38 mmol, 20.0 equiv). The resulting mixture was allowed to stir for 12 hours at 22 °C. Analysis of the unpurified mixture revealed 93% conv of the substrate, and the ROCM product was obtained in 93:07 Z/E ratio. The resulting brown oil was purified by silica gel chromatography (10% Et₂O in hexanes to 60% Et₂O in hexanes) to afford product **2.17e** (25.0 mg, 0.0890 mmol, 75% yield) as colorless oil; **IR (CH₂Cl₂)**: 3374 (br), 2942 (w), 2918 (w), 2949 (w) 1675 (m), 1592 (m), 1486 (s), 926 (m), 823 (m); **¹H NMR (400 MHz, CDCl₃)**: Z-isomer (major): δ 7.33–7.23 (2H, m), 6.98–6.89 (2H, m), 6.33 (1H, d, *J* = 6.2 Hz), ³¹ 5.89 (1H, ddd, *J* = 16.2, 10.5, 5.7 Hz), 5.28 (1H, dt, *J* = 17.3, 1.4 Hz), 5.14 (1H, dt, *J* = 10.6, 1.3 Hz), 4.98 (1H, dd, *J* = 7.9, 6.3 Hz), 4.57–4.46 (1H, m), 4.01–3.83 (2H, m), 2.14–1.98 (2H, m), 1.41–1.22 (3H, m); **¹³C NMR (100 MHz, CDCl₃)**: δ 155.6,

(31) Coupling constant (*J* = 6.2 Hz) for the signal at 6.33 ppm is indicative of **2.17e**.

140.9, 138.1, 129.6, 128.1, 117.8, 115.6, 113.4, 76.1, 69.9, 67.8, 41.0, 40.5; **HRMS** $[\text{M}+\text{Na}]^+$ found for $\text{C}_{15}\text{H}_{17}\text{O}_3\text{NaCl}$: 303.0749. $[\alpha]_D^{20} +103.2$ ($c = 0.58$, CHCl_3) for an enantiomerically enriched sample of 95:05. Enantiomeric purity was determined by HPLC (Chart 21) analysis in comparison with authentic racemic material (Daicel Chiralpak OD-H column, 97:3 hexanes:*i*-PrOH, 0.5 mL/min, 220 nm).

Chart 21. HPLC Traces for Racemic (left) and Enantiomerically Pure 2.17e (right)

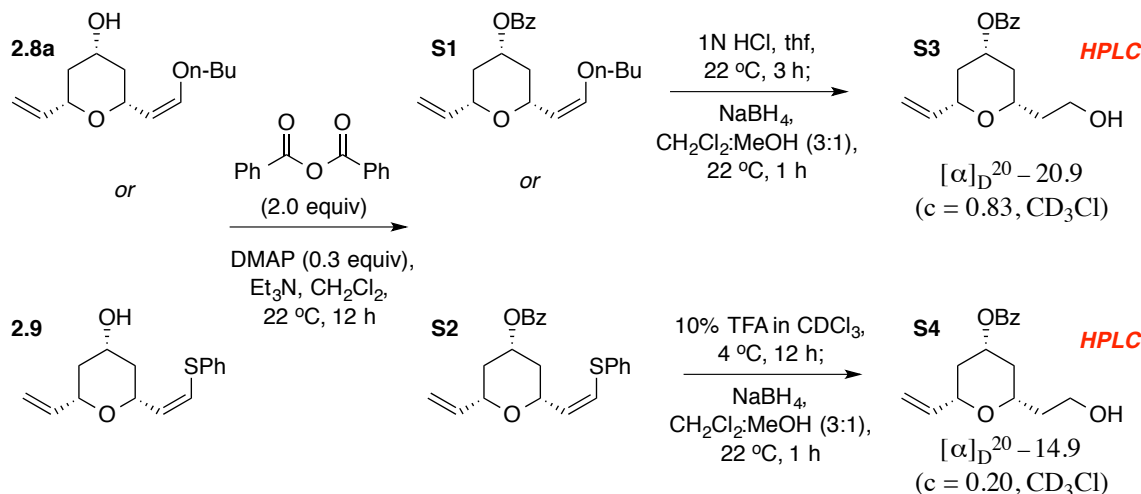


Peak #	Retention time (min)	Area	Area %	Peak #	Retention time (min)	Area	Area %
1	31.04	24494013	21.40	1	30.33	140839691	89.77
2	33.93	25722642	22.47	2	34.09	7572864	4.83
3	49.25	31561739	27.57	3	49.79	541771	0.35
4	64.43	32688385	28.56	4	64.77	7929359	5.05

■ Stereochemical Determination of the ROCM products:

I. Relative stereochemical identity of **2.8a** and **2.9** via chemical correlation:

Chart 22. Chemical Correlation between **2.8a** and **2.9**

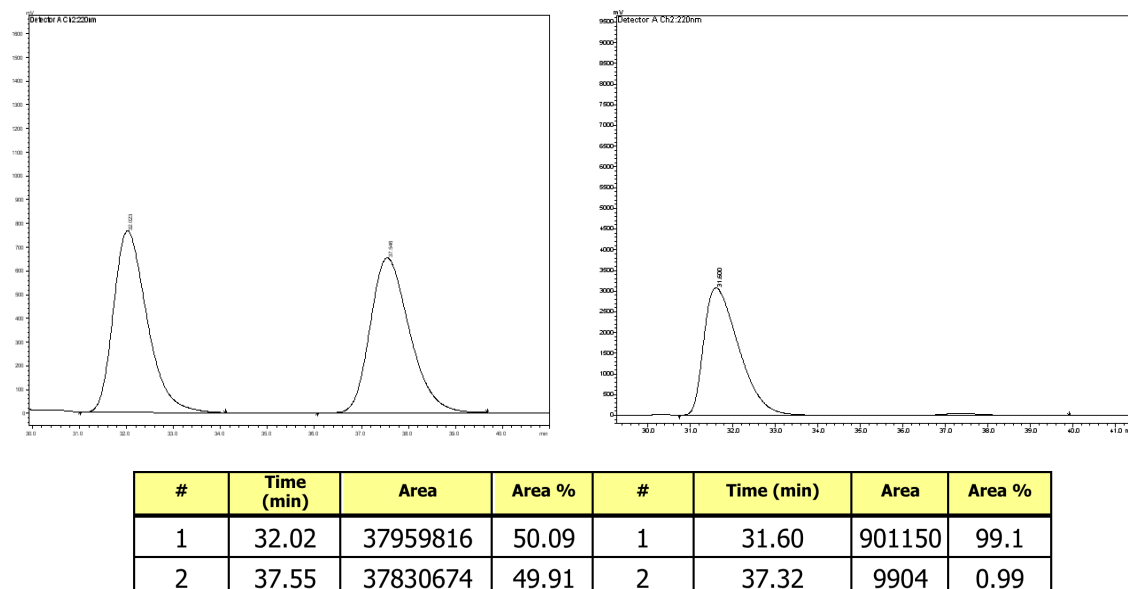


A. Procedure for the Synthesis of **S3**:

Pyran **2.8a** (>98:2 er, 98% Z, 18.7 mg, 0.0826 mmol) was converted to the corresponding benzoyl ester **S1** (>98% conv) following the aforementioned procedure. The unpurified **S1** was dissolved in anhydrous tetrahydrofuran (1.6 mL), and 1N HCl (0.330 mL) was added to this solution. The reaction mixture was allowed to stir for three hours at 22 °C, after which the product was washed with saturated aqueous NaHCO₃ and washed with EtOAc (3x25 mL). The combined organic layers were dried over anhydrous MgSO₄, filtered, and concentrated *in vacuo*. The corresponding aldehyde intermediate was dissolved in (3:1) CH₂Cl₂:MeOH (1.6 mL) and NaBH₄ (31 mg) was added. The resulting mixture was allowed to stir for one hour at 22 °C, after which water (0.5 mL) was added. The resulting alcohol was washed with CH₂Cl₂ (3x10 mL). The combined organic layers were dried over anhydrous MgSO₄, filtered, and concentrated *in vacuo* providing colorless oil. Purification by silica gel chromatography (40-80% diethyl ether in hexanes) afforded **S3** (13 mg, 0.047 mmol, 57% yield). ¹H NMR (400 MHz, CDCl₃): δ 8.04-8.01 (2H, m), 7.58-7.54 (m, 1H), 7.46-7.41 (2H, m), 5.91-5.82 (1H, m), 5.29-5.13 (3H, m), 4.05-4.00 (1H, m), 3.84-3.76 (3H, m), 2.54 (1H, s), 2.23-2.17 (1H, m), 2.14-2.09 (1H, m), 1.93-1.76 (2H, m), 1.61-1.48 (2H, m); ¹³C NMR (100 MHz, CDCl₃):

δ 165.8, 137.5, 132.9, 130.2, 129.5, 128.3, 115.5, 76.1, 75.6, 70.4, 61.0, 37.8, 37.1, 36.9; $[\alpha]_D^{20} -20.9$ ($c = 0.833$, CD_3Cl) for an enantiomerically enriched sample of 99:1. The absolute stereochemical identity of ROCM product was determined by HPLC (Chart 23) analysis of the enantiomerically enriched sample with authentic racemic material [AD-H column, 95:5 hexanes:*i*-PrOH, 0.5 mL/min, 220 nm, t_r (major enantiomer) 31.60 = min, t_r (minor enantiomer) = 37.32 min].

Chart 23. Synthesis of S3

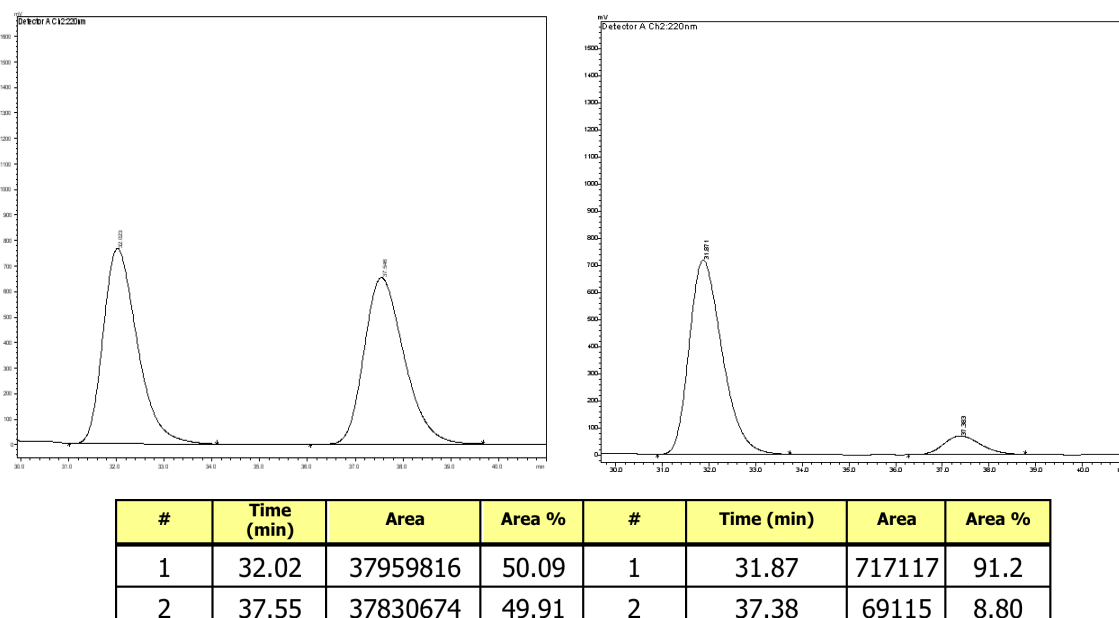


B. Procedure for the Synthesis of S4:

Pyran **2.9** (96:4 er, 91% *Z*, 5.5 mg, 0.021 mmol) was converted to the benzoyl ester **S2** (>98% conv) following the aforementioned procedure. The purified **S2** (9.0 mg, 0.025 mmol) was dissolved in a solution of 10% trifluoroacetic acid in $CDCl_3$ (500 μ L), and allowed to stir for 12 hours at 4 °C. The product was washed with saturated aqueous $NaHCO_3$ and washed with EtOAc (3x25 mL). The combined organic layers were dried over anhydrous $MgSO_4$, filtered, and concentrated *in vacuo*. The desired aldehyde was dissolved in (3:1) CH_2Cl_2 :MeOH (800 mL) and $NaBH_4$ (100 mg) was added. The resulting mixture was allowed to stir for one hour at 22 °C, after which water (0.5 mL) was added. The resulting alcohol was washed in CH_2Cl_2 (3x10 mL). The combined organic layers were dried over anhydrous $MgSO_4$, filtered, and concentrated *in vacuo*, providing colorless oil. Purification by silica gel chromatography (40-80% diethyl ether

in hexanes) afforded **S3** (3.0 mg, 0.011 mmol, 44% yield). The spectral data for **S4** were identical to **S3**; $[\alpha]_D^{20} -14.9$ ($c = 0.20$, CDCl_3) for an enantiomerically enriched sample of 91:9. The absolute stereochemical identity of ROCM product was determined by HPLC (Chart 24) analysis of the enantiomerically enriched sample with authentic racemic material [AD-H column, 95/5 hexanes/*i*-PrOH, 0.5 mL/min, 220 nm, t_r (major enantiomer) = 31.87 min, t_r (minor enantiomer) = 37.38 min].

Chart 24. Synthesis of S4



II. Absolute stereochemical identity of 2.15, 2.16 and 2.9 through the use of X-ray Crystallography:

■ X-ray Crystal Structure for ROCM Product 2.15:

Chart 25. X-ray Structure of 2.15

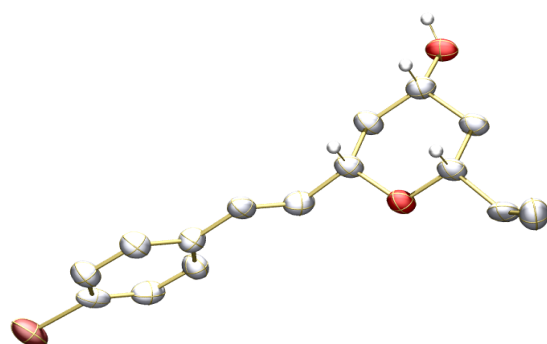


Table 1. Crystal Data and Structure Refinement for **2.15**

Identification code	<chem>C15H17BrO2</chem>	
Empirical formula	<chem>C15H17BrO2</chem>	
Formula weight	309.20	
Temperature	100(2) K	
Wavelength	1.54178 Å	
Crystal system	Orthorhombic	
Space group	P2(1)2(1)2(1)	
Unit cell dimensions	$a = 4.6190(2)$ Å	$\alpha = 90^\circ$
	$b = 18.6734(6)$ Å	$\beta = 90^\circ$
	$c = 35.2274(10)$ Å	$\gamma = 90^\circ$
Volume	3038.45(19) Å ³	
Z	8	
Density (calculated)	1.352 Mg/m ³	
Absorption coefficient	3.625 mm ⁻¹	
F(000)	1264	
Crystal size	0.13 x 0.02 x 0.02 mm ³	
Theta range for data collection	2.51 to 66.50°	
Index ranges	-5≤h≤5, 0≤k≤22, 0≤l≤41	
Reflections collected	5243	
Independent reflections	5243 [R(int) = 0.0505]	
Completeness to theta = 66.50°	98.4 %	
Absorption correction	Semi-empirical from equivalents	
Max. and min. transmission	0.9310 and 0.6501	
Refinement method	Full-matrix least-squares on F ²	
Data / restraints / parameters	5243 / 2 / 331	
Goodness-of-fit on F ²	1.023	
Final R indices [I>2sigma(I)]	R1 = 0.0377, wR2 = 0.0831	
R indices (all data)	R1 = 0.0459, wR2 = 0.0860	
Absolute structure parameter	-0.07(2)	
Extinction coefficient	na	

Largest diff. peak and hole 0.420 and -0.255 e. \AA^{-3}

Table 2. Atomic Coordinates ($\times 10^4$) and Equivalent Isotropic Displacement Parameters ($\text{\AA}^2 \times 10^3$) for **2.15**. U(eq) is Defined as 1/3 of the Trace of the Orthogonalized U_{ij}^{ij} Tensor

	x	y	z	U(eq)
Br(1)	-5225(1)	7368(1)	1748(1)	43(1)
O(1)	5504(5)	7581(1)	3933(1)	24(1)
O(2)	9943(6)	5650(1)	4102(1)	31(1)
C(1)	7729(10)	8505(2)	4735(1)	37(1)
C(2)	6343(9)	7980(2)	4563(1)	29(1)
C(3)	7568(7)	7565(2)	4240(1)	25(1)
C(4)	6636(8)	7233(2)	3600(1)	23(1)
C(5)	7308(8)	6446(2)	3678(1)	25(1)
C(6)	9368(8)	6380(2)	4010(1)	25(1)
C(7)	8204(8)	6796(2)	4351(1)	26(1)
C(8)	4496(7)	7381(2)	3287(1)	25(1)
C(9)	3330(8)	6892(2)	3057(1)	24(1)
C(10)	1242(8)	7027(2)	2750(1)	27(1)
C(11)	353(9)	7718(2)	2649(1)	30(1)
C(12)	-1590(9)	7817(2)	2355(1)	34(1)
C(13)	-2681(8)	7231(2)	2168(1)	32(1)
C(14)	-1902(9)	6543(2)	2264(1)	37(1)
C(15)	79(9)	6445(2)	2557(1)	32(1)
Br(2)	1310(1)	5416(1)	7038(1)	44(1)
O(3)	10268(6)	3514(1)	4959(1)	28(1)
O(4)	14970(7)	5089(2)	4381(1)	38(1)
C(16)	9496(10)	2633(2)	4090(1)	40(1)
C(17)	10002(10)	2719(2)	4450(1)	35(1)

C(18)	11865(10)	3279(2)	4632(1)	32(1)
C(19)	11813(9)	4020(2)	5190(1)	30(1)
C(20)	12613(8)	4674(2)	4958(1)	30(1)
C(21)	14291(8)	4469(2)	4610(1)	36(1)
C(22)	12666(9)	3910(2)	4377(1)	30(1)
C(23)	9915(10)	4144(2)	5527(1)	30(1)
C(24)	9253(8)	4775(2)	5676(1)	31(1)
C(25)	7368(9)	4917(2)	6004(1)	30(1)
C(26)	6020(9)	4367(2)	6210(1)	34(1)
C(27)	4212(9)	4518(2)	6512(1)	34(1)
C(28)	3697(10)	5222(2)	6607(1)	33(1)
C(29)	4964(11)	5771(2)	6414(1)	40(1)
C(30)	6820(9)	5614(2)	6112(1)	34(1)

Table 3. Bond Lengths [Å] and Angles [°] for **2.15**

Br(1)-C(13)	1.907(4)
O(1)-C(4)	1.440(4)
O(1)-C(3)	1.442(4)
O(2)-C(6)	1.425(4)
O(2)-H(2O)	0.828(19)
C(1)-C(2)	1.318(5)
C(1)-H(1A)	0.9500
C(1)-H(1B)	0.9500
C(2)-C(3)	1.488(5)
C(2)-H(2)	0.9500
C(3)-C(7)	1.517(5)
C(3)-H(3)	1.0000
C(4)-C(8)	1.505(5)
C(4)-C(5)	1.526(4)
C(4)-H(4)	1.0000

C(5)-C(6)	1.514(5)
C(5)-H(5A)	0.9900
C(5)-H(5B)	0.9900
C(6)-C(7)	1.528(5)
C(6)-H(6)	1.0000
C(7)-H(7A)	0.9900
C(7)-H(7B)	0.9900
C(8)-C(9)	1.334(5)
C(8)-H(8)	0.9500
C(9)-C(10)	1.473(5)
C(9)-H(9)	0.9500
C(10)-C(15)	1.390(5)
C(10)-C(11)	1.399(5)
C(11)-C(12)	1.383(5)
C(11)-H(11)	0.9500
C(12)-C(13)	1.374(5)
C(12)-H(12)	0.9500
C(13)-C(14)	1.377(6)
C(14)-C(15)	1.391(6)
C(14)-H(14)	0.9500
C(15)-H(15)	0.9500
Br(2)-C(28)	1.911(4)
O(3)-C(18)	1.437(5)
O(3)-C(19)	1.437(4)
O(4)-C(21)	1.445(4)
O(4)-H(4O)	0.813(19)
C(16)-C(17)	1.301(5)
C(16)-H(16A)	0.9500
C(16)-H(16B)	0.9500
C(17)-C(18)	1.498(6)
C(17)-H(17)	0.9500

C(18)-C(22)	1.526(5)
C(18)-H(18)	1.0000
C(19)-C(23)	1.495(5)
C(19)-C(20)	1.514(5)
C(19)-H(19)	1.0000
C(20)-C(21)	1.501(6)
C(20)-H(20A)	0.9900
C(20)-H(20B)	0.9900
C(21)-C(22)	1.525(6)
C(21)-H(21)	1.0000
C(22)-H(22A)	0.9900
C(22)-H(22B)	0.9900
C(23)-C(24)	1.325(5)
C(23)-H(23)	0.9500
C(24)-C(25)	1.472(6)
C(24)-H(24)	0.9500
C(25)-C(30)	1.379(6)
C(25)-C(26)	1.403(5)
C(26)-C(27)	1.382(6)
C(26)-H(26)	0.9500
C(27)-C(28)	1.377(5)
C(27)-H(27)	0.9500
C(28)-C(29)	1.363(6)
C(29)-C(30)	1.396(6)
C(29)-H(29)	0.9500
C(30)-H(30)	0.9500
C(4)-O(1)-C(3)	111.2(3)
C(6)-O(2)-H(2O)	109(3)
C(2)-C(1)-H(1A)	120.0
C(2)-C(1)-H(1B)	120.0
H(1A)-C(1)-H(1B)	120.0

C(1)-C(2)-C(3)	123.7(4)
C(1)-C(2)-H(2)	118.2
C(3)-C(2)-H(2)	118.2
O(1)-C(3)-C(2)	108.1(3)
O(1)-C(3)-C(7)	109.9(3)
C(2)-C(3)-C(7)	111.7(3)
O(1)-C(3)-H(3)	109.0
C(2)-C(3)-H(3)	109.0
C(7)-C(3)-H(3)	109.0
O(1)-C(4)-C(8)	105.9(3)
O(1)-C(4)-C(5)	111.2(3)
C(8)-C(4)-C(5)	116.2(3)
O(1)-C(4)-H(4)	107.7
C(8)-C(4)-H(4)	107.7
C(5)-C(4)-H(4)	107.7
C(6)-C(5)-C(4)	110.2(3)
C(6)-C(5)-H(5A)	109.6
C(4)-C(5)-H(5A)	109.6
C(6)-C(5)-H(5B)	109.6
C(4)-C(5)-H(5B)	109.6
H(5A)-C(5)-H(5B)	108.1
O(2)-C(6)-C(5)	111.8(3)
O(2)-C(6)-C(7)	111.9(3)
C(5)-C(6)-C(7)	110.2(3)
O(2)-C(6)-H(6)	107.6
C(5)-C(6)-H(6)	107.6
C(7)-C(6)-H(6)	107.6
C(3)-C(7)-C(6)	110.3(3)
C(3)-C(7)-H(7A)	109.6
C(6)-C(7)-H(7A)	109.6
C(3)-C(7)-H(7B)	109.6

C(6)-C(7)-H(7B)	109.6
H(7A)-C(7)-H(7B)	108.1
C(9)-C(8)-C(4)	125.6(3)
C(9)-C(8)-H(8)	117.2
C(4)-C(8)-H(8)	117.2
C(8)-C(9)-C(10)	126.4(3)
C(8)-C(9)-H(9)	116.8
C(10)-C(9)-H(9)	116.8
C(15)-C(10)-C(11)	119.0(4)
C(15)-C(10)-C(9)	118.5(4)
C(11)-C(10)-C(9)	122.4(3)
C(12)-C(11)-C(10)	120.2(4)
C(12)-C(11)-H(11)	119.9
C(10)-C(11)-H(11)	119.9
C(13)-C(12)-C(11)	119.4(4)
C(13)-C(12)-H(12)	120.3
C(11)-C(12)-H(12)	120.3
C(12)-C(13)-C(14)	122.0(4)
C(12)-C(13)-Br(1)	119.4(3)
C(14)-C(13)-Br(1)	118.5(3)
C(13)-C(14)-C(15)	118.6(4)
C(13)-C(14)-H(14)	120.7
C(15)-C(14)-H(14)	120.7
C(10)-C(15)-C(14)	120.8(4)
C(10)-C(15)-H(15)	119.6
C(14)-C(15)-H(15)	119.6
C(18)-O(3)-C(19)	113.6(3)
C(21)-O(4)-H(4O)	108(3)
C(17)-C(16)-H(16A)	120.0
C(17)-C(16)-H(16B)	120.0
H(16A)-C(16)-H(16B)	120.0

C(16)-C(17)-C(18)	127.3(4)
C(16)-C(17)-H(17)	116.3
C(18)-C(17)-H(17)	116.3
O(3)-C(18)-C(17)	105.1(3)
O(3)-C(18)-C(22)	111.1(3)
C(17)-C(18)-C(22)	115.3(3)
O(3)-C(18)-H(18)	108.4
C(17)-C(18)-H(18)	108.4
C(22)-C(18)-H(18)	108.4
O(3)-C(19)-C(23)	105.1(3)
O(3)-C(19)-C(20)	110.3(3)
C(23)-C(19)-C(20)	116.5(3)
O(3)-C(19)-H(19)	108.2
C(23)-C(19)-H(19)	108.2
C(20)-C(19)-H(19)	108.2
C(21)-C(20)-C(19)	111.1(3)
C(21)-C(20)-H(20A)	109.4
C(19)-C(20)-H(20A)	109.4
C(21)-C(20)-H(20B)	109.4
C(19)-C(20)-H(20B)	109.4
H(20A)-C(20)-H(20B)	108.0
O(4)-C(21)-C(20)	111.4(3)
O(4)-C(21)-C(22)	110.7(3)
C(20)-C(21)-C(22)	111.1(3)
O(4)-C(21)-H(21)	107.8
C(20)-C(21)-H(21)	107.8
C(22)-C(21)-H(21)	107.8
C(21)-C(22)-C(18)	109.4(3)
C(21)-C(22)-H(22A)	109.8
C(18)-C(22)-H(22A)	109.8
C(21)-C(22)-H(22B)	109.8

C(18)-C(22)-H(22B)	109.8
H(22A)-C(22)-H(22B)	108.2
C(24)-C(23)-C(19)	125.9(4)
C(24)-C(23)-H(23)	117.1
C(19)-C(23)-H(23)	117.1
C(23)-C(24)-C(25)	127.3(4)
C(23)-C(24)-H(24)	116.3
C(25)-C(24)-H(24)	116.3
C(30)-C(25)-C(26)	117.9(4)
C(30)-C(25)-C(24)	119.7(4)
C(26)-C(25)-C(24)	122.4(4)
C(27)-C(26)-C(25)	121.1(4)
C(27)-C(26)-H(26)	119.5
C(25)-C(26)-H(26)	119.5
C(28)-C(27)-C(26)	119.1(4)
C(28)-C(27)-H(27)	120.4
C(26)-C(27)-H(27)	120.4
C(29)-C(28)-C(27)	121.5(4)
C(29)-C(28)-Br(2)	120.1(3)
C(27)-C(28)-Br(2)	118.3(3)
C(28)-C(29)-C(30)	119.1(4)
C(28)-C(29)-H(29)	120.4
C(30)-C(29)-H(29)	120.4
C(25)-C(30)-C(29)	121.4(4)
C(25)-C(30)-H(30)	119.3
C(29)-C(30)-H(30)	119.3

Symmetry transformations used to generate equivalent atoms:

Table 4. Anisotropic Displacement Parameters ($\text{\AA}^2 \times 10^3$) for **2.15**. The Anisotropic

Displacement Factor Exponent Takes the Form: $-2\pi^2 [h^2 a^* 2U^{11} + \dots + 2 h k a^* b^* U^{12}]$

	U ¹¹	U ²²	U ³³	U ²³	U ¹³	U ¹²
Br(1)	30(1)	71(1)	28(1)	0(1)	-5(1)	-7(1)
O(1)	22(1)	24(1)	24(1)	1(1)	-1(1)	0(1)
O(2)	24(1)	23(1)	45(2)	9(1)	2(1)	3(1)
C(1)	48(3)	30(2)	33(2)	0(2)	12(2)	3(2)
C(2)	30(2)	28(2)	28(2)	5(2)	-1(2)	2(2)
C(3)	20(2)	28(2)	29(2)	4(2)	-1(1)	4(2)
C(4)	19(2)	20(2)	31(2)	4(2)	2(2)	1(2)
C(5)	22(2)	21(2)	33(2)	1(2)	4(2)	3(2)
C(6)	20(2)	22(2)	33(2)	4(2)	2(2)	3(2)
C(7)	24(2)	26(2)	29(2)	3(2)	-4(2)	2(2)
C(8)	20(2)	24(2)	30(2)	4(2)	5(2)	4(2)
C(9)	20(2)	21(2)	32(2)	0(2)	4(2)	3(2)
C(10)	21(2)	34(2)	27(2)	-6(2)	8(2)	2(2)
C(11)	30(2)	30(2)	29(2)	0(2)	0(2)	4(2)
C(12)	32(2)	36(2)	32(2)	0(2)	-6(2)	2(2)
C(13)	22(2)	54(3)	19(2)	2(2)	-2(1)	-2(2)
C(14)	25(2)	50(3)	36(2)	-6(2)	7(2)	-7(2)
C(15)	26(2)	35(2)	33(2)	-1(2)	5(2)	0(2)
Br(2)	50(1)	44(1)	38(1)	0(1)	0(1)	0(1)
O(3)	31(1)	25(1)	28(1)	3(1)	-4(1)	-3(1)
O(4)	24(1)	37(2)	55(2)	22(1)	-3(2)	-1(1)
C(16)	47(3)	33(2)	41(2)	5(2)	0(2)	5(2)
C(17)	51(2)	22(2)	31(2)	2(2)	3(2)	5(2)
C(18)	40(2)	24(2)	30(2)	6(2)	-2(2)	4(2)
C(19)	31(2)	23(2)	37(2)	2(2)	-9(2)	-4(2)
C(20)	24(2)	25(2)	41(2)	6(2)	-9(2)	1(2)

C(21)	24(2)	31(2)	52(3)	18(2)	-5(2)	0(2)
C(22)	29(2)	29(2)	33(2)	10(2)	1(2)	8(2)
C(23)	37(2)	20(2)	34(2)	5(2)	-12(2)	-4(2)
C(24)	28(2)	26(2)	39(2)	9(2)	-10(2)	-6(2)
C(25)	33(2)	26(2)	32(2)	4(2)	-14(2)	-2(2)
C(26)	39(2)	24(2)	39(2)	-1(2)	-9(2)	1(2)
C(27)	38(2)	28(2)	36(2)	4(2)	-10(2)	-6(2)
C(28)	36(2)	36(2)	28(2)	0(2)	-6(2)	1(2)
C(29)	43(2)	34(2)	45(2)	1(2)	-9(2)	1(2)
C(30)	39(2)	28(2)	36(2)	8(2)	-8(2)	-3(2)

Table 5. Hydrogen coordinates ($\times 10^4$) and isotropic displacement parameters ($\text{\AA}^2 \times 10^3$) for **2.15**

	x	y	z	U(eq)
H(2O)	8450(60)	5470(20)	4189(12)	46
H(1A)	9619	8636	4654	44
H(1B)	6838	8752	4940	44
H(2)	4457	7861	4649	34
H(3)	9404	7798	4154	30
H(4)	8495	7475	3531	28
H(5A)	5491	6186	3734	30
H(5B)	8191	6227	3449	30
H(6)	11243	6605	3934	30
H(7A)	6412	6565	4445	31
H(7B)	9650	6788	4558	31
H(8)	3927	7865	3251	30
H(9)	3904	6409	3096	29
H(11)	1087	8120	2783	36

H(12)	-2165	8287	2283	40
H(14)	-2700	6144	2134	44
H(15)	644	5973	2626	38
H(4O)	13460(70)	5260(20)	4302(13)	57
H(16A)	10354	2948	3910	48
H(16B)	8269	2257	4006	48
H(17)	9088	2389	4617	42
H(18)	13693	3046	4721	38
H(19)	13642	3788	5279	36
H(20A)	10829	4931	4883	36
H(20B)	13792	5003	5116	36
H(21)	16159	4251	4695	43
H(22A)	13899	3743	4165	36
H(22B)	10890	4125	4269	36
H(23)	9110	3733	5646	36
H(24)	10091	5182	5557	37
H(26)	6355	3882	6140	41
H(27)	3335	4141	6652	41
H(29)	4588	6253	6483	48
H(30)	7724	5995	5979	41

Table 6. Torsion angles [°] for **2.15**

C(4)-O(1)-C(3)-C(2)	175.7(3)
C(4)-O(1)-C(3)-C(7)	-62.0(3)
C(1)-C(2)-C(3)-O(1)	-127.2(4)
C(1)-C(2)-C(3)-C(7)	111.6(4)
C(3)-O(1)-C(4)-C(8)	-171.7(3)
C(3)-O(1)-C(4)-C(5)	61.1(4)
O(1)-C(4)-C(5)-C(6)	-55.9(4)

C(8)-C(4)-C(5)-C(6)	-177.2(3)
C(4)-C(5)-C(6)-O(2)	177.4(3)
C(4)-C(5)-C(6)-C(7)	52.3(4)
O(1)-C(3)-C(7)-C(6)	58.2(4)
C(2)-C(3)-C(7)-C(6)	178.2(3)
O(2)-C(6)-C(7)-C(3)	-179.0(3)
C(5)-C(6)-C(7)-C(3)	-53.9(4)
O(1)-C(4)-C(8)-C(9)	-129.5(3)
C(5)-C(4)-C(8)-C(9)	-5.4(5)
C(4)-C(8)-C(9)-C(10)	-179.8(3)
C(8)-C(9)-C(10)-C(15)	-175.0(4)
C(8)-C(9)-C(10)-C(11)	3.8(6)
C(15)-C(10)-C(11)-C(12)	-1.9(6)
C(9)-C(10)-C(11)-C(12)	179.3(4)
C(10)-C(11)-C(12)-C(13)	1.3(6)
C(11)-C(12)-C(13)-C(14)	0.1(6)
C(11)-C(12)-C(13)-Br(1)	-177.2(3)
C(12)-C(13)-C(14)-C(15)	-0.8(6)
Br(1)-C(13)-C(14)-C(15)	176.5(3)
C(11)-C(10)-C(15)-C(14)	1.1(6)
C(9)-C(10)-C(15)-C(14)	180.0(4)
C(13)-C(14)-C(15)-C(10)	0.2(6)
C(19)-O(3)-C(18)-C(17)	175.6(3)
C(19)-O(3)-C(18)-C(22)	-59.1(4)
C(16)-C(17)-C(18)-O(3)	137.9(4)
C(16)-C(17)-C(18)-C(22)	15.3(7)
C(18)-O(3)-C(19)-C(23)	-175.2(3)
C(18)-O(3)-C(19)-C(20)	58.5(4)
O(3)-C(19)-C(20)-C(21)	-55.2(4)
C(23)-C(19)-C(20)-C(21)	-174.9(3)
C(19)-C(20)-C(21)-O(4)	177.9(3)

C(19)-C(20)-C(21)-C(22)	53.9(4)
O(4)-C(21)-C(22)-C(18)	-177.5(3)
C(20)-C(21)-C(22)-C(18)	-53.1(4)
O(3)-C(18)-C(22)-C(21)	54.8(4)
C(17)-C(18)-C(22)-C(21)	174.3(3)
O(3)-C(19)-C(23)-C(24)	-133.8(4)
C(20)-C(19)-C(23)-C(24)	-11.4(6)
C(19)-C(23)-C(24)-C(25)	179.2(4)
C(23)-C(24)-C(25)-C(30)	-177.4(4)
C(23)-C(24)-C(25)-C(26)	0.8(6)
C(30)-C(25)-C(26)-C(27)	-0.3(6)
C(24)-C(25)-C(26)-C(27)	-178.6(4)
C(25)-C(26)-C(27)-C(28)	1.1(6)
C(26)-C(27)-C(28)-C(29)	-1.0(6)
C(26)-C(27)-C(28)-Br(2)	-177.6(3)
C(27)-C(28)-C(29)-C(30)	0.1(7)
Br(2)-C(28)-C(29)-C(30)	176.7(3)
C(26)-C(25)-C(30)-C(29)	-0.6(6)
C(24)-C(25)-C(30)-C(29)	177.7(4)
C(28)-C(29)-C(30)-C(25)	0.7(6)

Symmetry transformations used to generate equivalent atoms:

Table 7. Hydrogen bonds for **2.15** [Å and °]

D-H...A	d(D-H)	d(H...A)	d(D...A)	<(DHA)
O(2)-H(2O)...O(4)#1	0.828(19)	1.88(2)	2.710(4)	178(5)
O(4)-H(4O)...O(2)	0.813(19)	1.92(2)	2.731(4)	178(5)

Symmetry transformations used to generate equivalent atoms:

#1 x-1,y,z

■ X-ray Crystal Structure for ROCM Product 2.16:

Chart 26. X-ray Structure of 2.16

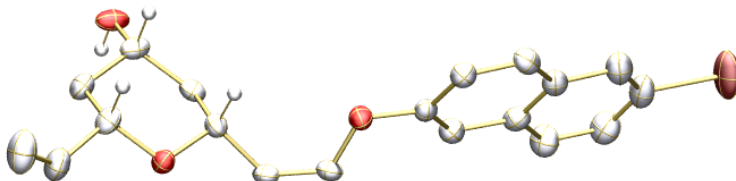


Table 1. Crystal Data and Structure Refinement for 2.16

Identification code	$\text{C}_{19}\text{H}_{19}\text{BrO}_3$		
Empirical formula	$\text{C}_{19}\text{H}_{19}\text{BrO}_3$		
Formula weight	375.25		
Temperature	100(2) K		
Wavelength	1.54178 Å		
Crystal system	Monoclinic		
Space group	C 2		
Unit cell dimensions	$a = 23.6367(8)$ Å	$\alpha = 90^\circ$	
	$b = 4.8124(2)$ Å	$\beta = 118.196(3)^\circ$	
	$c = 16.9657(6)$ Å	$\gamma = 90^\circ$	
Volume	$1700.83(11)$ Å ³		
Z	4		
Density (calculated)	1.465 Mg/m ³		
Absorption coefficient	3.394 mm ⁻¹		
F(000)	768		
Crystal size	0.07 x 0.05 x 0.02 mm ³		
Theta range for data collection	3.86 to 66.63°		
Index ranges	-27≤h≤27, -5≤k≤5, -20≤l≤19		
Reflections collected	9872		
Independent reflections	2865 [R(int) = 0.0485]		
Completeness to theta = 66.63°	98.1 %		
Absorption correction	Semi-empirical from equivalents		
Max. and min. transmission	0.9352 and 0.7971		

Refinement method	Full-matrix least-squares on F^2
Data / restraints / parameters	2865 / 2 / 211
Goodness-of-fit on F^2	1.045
Final R indices [$I > 2\sigma(I)$]	$R_1 = 0.0331$, $wR_2 = 0.0702$
R indices (all data)	$R_1 = 0.0409$, $wR_2 = 0.0736$
Absolute structure parameter	0.01(2)
Extinction coefficient	na
Largest diff. peak and hole	0.272 and -0.343 e. \AA^{-3}

Table 2. Atomic coordinates ($\times 10^4$) and Equivalent Isotropic Displacement Parameters ($\text{\AA}^2 \times 10^3$) for **2.16**. $U(\text{eq})$ is Defined as 1/3 of the Trace of the Orthogonalized U^{ij} Tensor

	x	y	z	$U(\text{eq})$
Br(1)	6934(1)	5926(2)	6818(1)	65(1)
O(1)	5614(1)	11138(6)	12877(1)	25(1)
O(2)	7178(1)	6416(5)	14705(1)	34(1)
O(3)	5816(1)	8581(5)	10687(1)	28(1)
C(1)	4631(2)	10427(12)	13881(2)	51(1)
C(2)	5127(1)	11265(11)	13803(2)	38(1)
C(3)	5514(2)	9526(7)	13515(2)	29(1)
C(4)	5970(1)	9663(6)	12516(2)	25(1)
C(5)	6626(1)	8764(7)	13265(2)	26(1)
C(6)	6562(2)	7105(6)	13979(2)	30(1)
C(7)	6158(2)	8700(8)	14305(2)	30(1)
C(8)	6040(1)	11644(6)	11892(2)	28(1)
C(9)	5990(1)	11147(8)	11096(2)	27(1)
C(10)	5949(1)	8076(7)	9987(2)	25(1)
C(11)	6443(2)	9261(7)	9911(2)	29(1)

C(12)	6554(2)	8528(8)	9185(2)	31(1)
C(13)	7049(2)	9790(8)	9061(2)	40(1)
C(14)	7162(2)	9023(9)	8370(2)	42(1)
C(15)	6780(2)	6941(8)	7785(2)	41(1)
C(16)	6296(1)	5670(11)	7870(2)	38(1)
C(17)	6169(1)	6491(8)	8572(2)	29(1)
C(18)	5658(1)	5303(7)	8680(2)	30(1)
C(19)	5548(1)	6093(9)	9363(2)	27(1)

Table 3. Bond Lengths [Å] and Angles [°] for **2.16**

Br(1)-C(15)	1.906(3)
O(1)-C(3)	1.439(4)
O(1)-C(4)	1.440(4)
O(2)-C(6)	1.433(4)
O(2)-H(2O)	0.825(19)
O(3)-C(9)	1.380(5)
O(3)-C(10)	1.385(3)
C(1)-C(2)	1.305(5)
C(1)-H(1A)	0.9500
C(1)-H(1B)	0.9500
C(2)-C(3)	1.482(5)
C(2)-H(2A)	0.9500
C(3)-C(7)	1.530(4)
C(3)-H(3A)	1.0000
C(4)-C(8)	1.491(4)
C(4)-C(5)	1.531(4)
C(4)-H(4A)	1.0000
C(5)-C(6)	1.518(4)
C(5)-H(5A)	0.9900
C(5)-H(5B)	0.9900
C(6)-C(7)	1.519(4)

C(6)-H(6A)	1.0000
C(7)-H(7A)	0.9900
C(7)-H(7B)	0.9900
C(8)-C(9)	1.320(4)
C(8)-H(8A)	0.9500
C(9)-H(9A)	0.9500
C(10)-C(11)	1.361(4)
C(10)-C(19)	1.407(5)
C(11)-C(12)	1.419(4)
C(11)-H(11A)	0.9500
C(12)-C(17)	1.406(5)
C(12)-C(13)	1.418(5)
C(13)-C(14)	1.371(5)
C(13)-H(13A)	0.9500
C(14)-C(15)	1.399(5)
C(14)-H(14A)	0.9500
C(15)-C(16)	1.363(5)
C(16)-C(17)	1.414(4)
C(16)-H(16A)	0.9500
C(17)-C(18)	1.425(4)
C(18)-C(19)	1.356(4)
C(18)-H(18A)	0.9500
C(19)-H(19A)	0.9500
C(3)-O(1)-C(4)	113.0(3)
C(6)-O(2)-H(2O)	107(4)
C(9)-O(3)-C(10)	117.0(2)
C(2)-C(1)-H(1A)	120.0
C(2)-C(1)-H(1B)	120.0
H(1A)-C(1)-H(1B)	120.0
C(1)-C(2)-C(3)	125.7(5)
C(1)-C(2)-H(2A)	117.2

C(3)-C(2)-H(2A)	117.2
O(1)-C(3)-C(2)	106.9(3)
O(1)-C(3)-C(7)	110.5(2)
C(2)-C(3)-C(7)	111.8(3)
O(1)-C(3)-H(3A)	109.2
C(2)-C(3)-H(3A)	109.2
C(7)-C(3)-H(3A)	109.2
O(1)-C(4)-C(8)	105.7(2)
O(1)-C(4)-C(5)	110.7(2)
C(8)-C(4)-C(5)	111.2(2)
O(1)-C(4)-H(4A)	109.7
C(8)-C(4)-H(4A)	109.7
C(5)-C(4)-H(4A)	109.7
C(6)-C(5)-C(4)	111.5(2)
C(6)-C(5)-H(5A)	109.3
C(4)-C(5)-H(5A)	109.3
C(6)-C(5)-H(5B)	109.3
C(4)-C(5)-H(5B)	109.3
H(5A)-C(5)-H(5B)	108.0
O(2)-C(6)-C(5)	111.3(3)
O(2)-C(6)-C(7)	111.2(3)
C(5)-C(6)-C(7)	110.0(3)
O(2)-C(6)-H(6A)	108.0
C(5)-C(6)-H(6A)	108.0
C(7)-C(6)-H(6A)	108.0
C(6)-C(7)-C(3)	110.4(3)
C(6)-C(7)-H(7A)	109.6
C(3)-C(7)-H(7A)	109.6
C(6)-C(7)-H(7B)	109.6
C(3)-C(7)-H(7B)	109.6
H(7A)-C(7)-H(7B)	108.1

C(9)-C(8)-C(4)	128.7(3)
C(9)-C(8)-H(8A)	115.7
C(4)-C(8)-H(8A)	115.7
C(8)-C(9)-O(3)	122.5(3)
C(8)-C(9)-H(9A)	118.8
O(3)-C(9)-H(9A)	118.8
C(11)-C(10)-O(3)	124.1(3)
C(11)-C(10)-C(19)	121.0(3)
O(3)-C(10)-C(19)	114.9(3)
C(10)-C(11)-C(12)	119.9(3)
C(10)-C(11)-H(11A)	120.1
C(12)-C(11)-H(11A)	120.1
C(17)-C(12)-C(13)	118.7(3)
C(17)-C(12)-C(11)	119.6(3)
C(13)-C(12)-C(11)	121.7(3)
C(14)-C(13)-C(12)	121.3(4)
C(14)-C(13)-H(13A)	119.4
C(12)-C(13)-H(13A)	119.4
C(13)-C(14)-C(15)	118.6(3)
C(13)-C(14)-H(14A)	120.7
C(15)-C(14)-H(14A)	120.7
C(16)-C(15)-C(14)	122.6(3)
C(16)-C(15)-Br(1)	119.2(3)
C(14)-C(15)-Br(1)	118.2(3)
C(15)-C(16)-C(17)	119.0(4)
C(15)-C(16)-H(16A)	120.5
C(17)-C(16)-H(16A)	120.5
C(12)-C(17)-C(16)	119.8(3)
C(12)-C(17)-C(18)	118.4(3)
C(16)-C(17)-C(18)	121.7(3)
C(19)-C(18)-C(17)	120.9(3)

C(19)-C(18)-H(18A)	119.5
C(17)-C(18)-H(18A)	119.5
C(18)-C(19)-C(10)	120.1(3)
C(18)-C(19)-H(19A)	120.0
C(10)-C(19)-H(19A)	120.0

Symmetry transformations used to generate equivalent atoms:

Table 4. Anisotropic Displacement Parameters ($\text{\AA}^2 \times 10^3$) for **2.16**. The Anisotropic Displacement Factor Exponent Takes the Form: $-2\pi^2 [h^2 a^*{}^2 U^{11} + \dots + 2 h k a^* b^* U^{12}]$

	U ¹¹	U ²²	U ³³	U ²³	U ¹³	U ¹²
Br(1)	44(1)	116(1)	45(1)	-6(1)	30(1)	17(1)
O(1)	23(1)	28(1)	26(1)	4(1)	13(1)	3(1)
O(2)	27(1)	22(1)	37(1)	1(1)	2(1)	-1(1)
O(3)	34(1)	25(1)	30(1)	-2(1)	19(1)	-5(1)
C(1)	34(2)	81(3)	39(2)	2(2)	19(1)	-2(2)
C(2)	35(2)	51(2)	33(1)	7(2)	19(1)	3(2)
C(3)	25(2)	33(2)	29(2)	5(1)	12(1)	-5(1)
C(4)	26(2)	25(2)	26(2)	-3(1)	13(1)	-2(1)
C(5)	24(2)	22(2)	31(2)	-6(1)	12(1)	-1(1)
C(6)	25(2)	23(2)	30(2)	3(1)	4(1)	-2(1)
C(7)	32(2)	32(2)	27(2)	5(1)	14(1)	-2(2)
C(8)	30(2)	19(2)	34(2)	1(1)	16(1)	1(1)
C(9)	28(1)	20(2)	34(1)	-1(2)	15(1)	1(2)
C(10)	25(2)	26(2)	24(2)	4(1)	12(1)	7(1)
C(11)	25(2)	31(2)	29(2)	-1(1)	11(1)	1(1)
C(12)	25(2)	33(2)	36(2)	7(2)	16(1)	7(2)
C(13)	29(2)	52(3)	44(2)	1(2)	20(2)	2(2)

C(14)	28(2)	58(3)	47(2)	8(2)	22(2)	8(2)
C(15)	32(2)	61(3)	33(2)	9(2)	19(1)	21(2)
C(16)	27(1)	54(2)	31(1)	1(2)	11(1)	12(2)
C(17)	20(1)	36(2)	27(1)	3(2)	8(1)	10(1)
C(18)	25(1)	31(2)	28(1)	-4(1)	6(1)	2(1)
C(19)	22(1)	30(2)	28(1)	2(2)	10(1)	1(2)

Table 5. Hydrogen coordinates ($\times 10^4$) and isotropic displacement parameters ($\text{\AA}^2 \times 10^3$) for **2.16**

	x	y	z	U(eq)
H(2O)	7360(20)	7900(60)	14930(30)	51
H(1A)	4490	8555	13748	61
H(1B)	4410	11690	14071	61
H(2A)	5251	13153	13943	46
H(3A)	5267	7809	13217	35
H(4A)	5723	7994	12178	30
H(5A)	6847	7620	13008	32
H(5B)	6893	10432	13540	32
H(6A)	6334	5331	13702	36
H(7A)	6391	10389	14628	36
H(7B)	6082	7530	14726	36
H(8A)	6132	13512	12093	33
H(9A)	6077	12611	10793	32
H(11A)	6713	10578	10342	35
H(13A)	7307	11194	9465	49
H(14A)	7492	9886	8290	51
H(16A)	6047	4253	7463	46
H(18A)	5390	3938	8268	37

H(19A)	5201	5306	9420
--------	------	------	------

Table 6. Torsion Angles [°] for **2.16**

C(4)-O(1)-C(3)-C(2)	-178.2(2)
C(4)-O(1)-C(3)-C(7)	60.0(3)
C(1)-C(2)-C(3)-O(1)	134.9(3)
C(1)-C(2)-C(3)-C(7)	-104.1(4)
C(3)-O(1)-C(4)-C(8)	-178.8(2)
C(3)-O(1)-C(4)-C(5)	-58.4(3)
O(1)-C(4)-C(5)-C(6)	54.2(3)
C(8)-C(4)-C(5)-C(6)	171.4(3)
C(4)-C(5)-C(6)-O(2)	-176.4(2)
C(4)-C(5)-C(6)-C(7)	-52.6(3)
O(2)-C(6)-C(7)-C(3)	177.5(3)
C(5)-C(6)-C(7)-C(3)	53.7(3)
O(1)-C(3)-C(7)-C(6)	-57.0(4)
C(2)-C(3)-C(7)-C(6)	-175.8(3)
O(1)-C(4)-C(8)-C(9)	-139.0(3)
C(5)-C(4)-C(8)-C(9)	100.8(4)
C(4)-C(8)-C(9)-O(3)	4.4(5)
C(10)-O(3)-C(9)-C(8)	-162.7(3)
C(9)-O(3)-C(10)-C(11)	28.8(4)
C(9)-O(3)-C(10)-C(19)	-154.3(3)
O(3)-C(10)-C(11)-C(12)	177.6(3)
C(19)-C(10)-C(11)-C(12)	0.9(5)
C(10)-C(11)-C(12)-C(17)	-2.7(5)
C(10)-C(11)-C(12)-C(13)	177.6(3)
C(17)-C(12)-C(13)-C(14)	-1.2(5)
C(11)-C(12)-C(13)-C(14)	178.5(3)
C(12)-C(13)-C(14)-C(15)	-0.3(5)

C(13)-C(14)-C(15)-C(16)	0.7(5)
C(13)-C(14)-C(15)-Br(1)	179.2(3)
C(14)-C(15)-C(16)-C(17)	0.4(6)
Br(1)-C(15)-C(16)-C(17)	-178.0(3)
C(13)-C(12)-C(17)-C(16)	2.4(5)
C(11)-C(12)-C(17)-C(16)	-177.4(3)
C(13)-C(12)-C(17)-C(18)	-177.7(3)
C(11)-C(12)-C(17)-C(18)	2.6(4)
C(15)-C(16)-C(17)-C(12)	-2.0(5)
C(15)-C(16)-C(17)-C(18)	178.1(3)
C(12)-C(17)-C(18)-C(19)	-0.7(5)
C(16)-C(17)-C(18)-C(19)	179.2(3)
C(17)-C(18)-C(19)-C(10)	-1.1(5)
C(11)-C(10)-C(19)-C(18)	1.0(5)
O(3)-C(10)-C(19)-C(18)	-175.9(3)

Symmetry transformations used to generate equivalent atoms:

Table 7. Hydrogen Bonds for **2.16** [Å and °]

D-H...A	d(D-H)	d(H...A)	d(D...A)	<(DHA)
O(2)-H(2O)...O(2)#1	0.825(19)	1.95(2)	2.769(2)	170(5)

Symmetry transformations used to generate equivalent atoms:

#1 -x+3/2,y+1/2,-z+3

■ X-ray Crystal Structure for ROCM Product 2.9:

Chart 27. X-ray Structure of 2.9

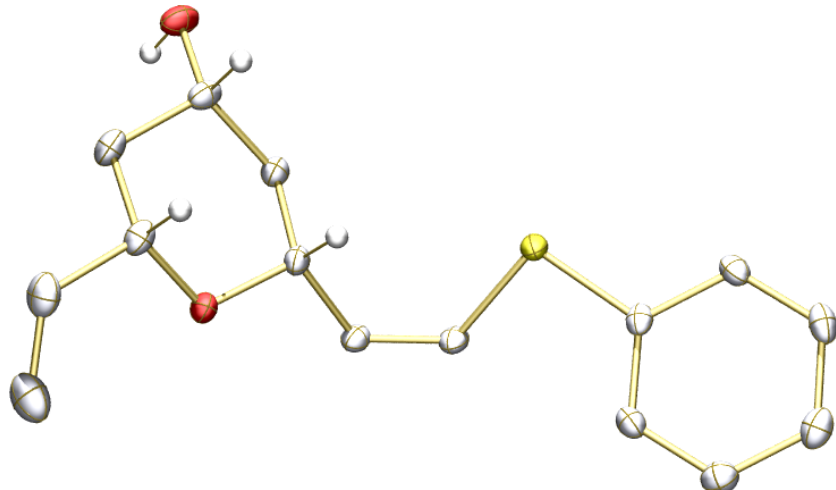


Table 1. Crystal Data and Structure Refinement for 2.9

Identification code	$C_{15}H_{18}O_2S$		
Empirical formula	$C_{15}H_{18}O_2S$		
Formula weight	262.35		
Temperature	100(2) K		
Wavelength	0.71073 Å		
Crystal system	Monoclinic		
Space group	P 2(1)		
Unit cell dimensions	$a = 7.6609(4)$ Å	$\alpha = 90^\circ$	
	$b = 5.2659(3)$ Å	$\beta = 97.885(3)^\circ$	
	$c = 17.4520(8)$ Å	$\gamma = 90^\circ$	
Volume	$697.38(6)$ Å ³		
Z	2		
Density (calculated)	1.249 Mg/m ³		
Absorption coefficient	0.224 mm ⁻¹		
F(000)	280		
Crystal size	0.20 x 0.05 x 0.03 mm ³		
Theta range for data collection	2.36 to 28.31°		

Index ranges	-10<=h<=10, -7<=k<=6, -23<=l<=23
Reflections collected	11243
Independent reflections	3377 [R(int) = 0.0292]
Completeness to theta = 28.31°	99.7 %
Absorption correction	Semi-empirical from equivalents
Max. and min. transmission	0.9933 and 0.9566
Refinement method	Full-matrix least-squares on F ²
Data / restraints / parameters	3377 / 2 / 166
Goodness-of-fit on F ²	1.041
Final R indices [I>2sigma(I)]	R1 = 0.0271, wR2 = 0.0661
R indices (all data)	R1 = 0.0305, wR2 = 0.0679
Absolute structure parameter	0.01(5)
Extinction coefficient	na
Largest diff. peak and hole	0.285 and -0.170 e.Å ⁻³

Table 2. Atomic Coordinates (x 10⁴) and Equivalent Isotropic Displacement Parameters (Å² x 10³) for **2.9**. U(eq) is Defined as one third of the trace of the Orthogonalized U^{ij} Tensor

	x	y	z	U(eq)
S(1)	2891(1)	3070(1)	6495(1)	17(1)
O(1)	7390(1)	-241(2)	8088(1)	17(1)
O(2)	5411(2)	4416(2)	9715(1)	24(1)
C(1)	10762(2)	-2174(4)	8432(1)	33(1)
C(2)	10351(2)	1(3)	8726(1)	25(1)
C(3)	8638(2)	1385(3)	8532(1)	19(1)
C(4)	5793(2)	1089(3)	7818(1)	15(1)
C(5)	4926(2)	2071(3)	8499(1)	18(1)
C(6)	6193(2)	3702(3)	9041(1)	19(1)

C(7)	7924(2)	2308(3)	9258(1)	21(1)
C(8)	4617(2)	-734(3)	7334(1)	17(1)
C(9)	3381(2)	-92(3)	6756(1)	17(1)
C(10)	2602(2)	2897(3)	5471(1)	15(1)
C(11)	1591(2)	4793(3)	5064(1)	18(1)
C(12)	1384(2)	4804(3)	4262(1)	20(1)
C(13)	2128(2)	2915(4)	3861(1)	22(1)
C(14)	3119(2)	1013(3)	4267(1)	21(1)
C(15)	3380(2)	1014(3)	5072(1)	17(1)

Table 3. Bond Lengths [Å] and Angles [°] for **2.9**

S(1)-C(9)	1.7536(15)
S(1)-C(10)	1.7729(12)
O(1)-C(3)	1.4301(17)
O(1)-C(4)	1.4326(16)
O(2)-C(6)	1.4401(16)
C(1)-C(2)	1.311(3)
C(2)-C(3)	1.498(2)
C(3)-C(7)	1.5264(19)
C(4)-C(8)	1.4955(18)
C(4)-C(5)	1.5285(18)
C(5)-C(6)	1.5245(19)
C(6)-C(7)	1.517(2)
C(8)-C(9)	1.3288(19)
C(10)-C(15)	1.391(2)
C(10)-C(11)	1.3963(19)
C(11)-C(12)	1.3867(19)
C(12)-C(13)	1.383(2)
C(13)-C(14)	1.391(2)
C(14)-C(15)	1.3918(19)

C(9)-S(1)-C(10)	101.87(7)
C(3)-O(1)-C(4)	111.31(11)
C(1)-C(2)-C(3)	125.94(14)
O(1)-C(3)-C(2)	109.30(12)
O(1)-C(3)-C(7)	110.55(11)
C(2)-C(3)-C(7)	111.76(12)
O(1)-C(4)-C(8)	107.05(11)
O(1)-C(4)-C(5)	110.60(10)
C(8)-C(4)-C(5)	111.33(11)
C(6)-C(5)-C(4)	111.48(11)
O(2)-C(6)-C(7)	111.71(11)
O(2)-C(6)-C(5)	110.70(11)
C(7)-C(6)-C(5)	110.01(11)
C(6)-C(7)-C(3)	110.37(11)
C(9)-C(8)-C(4)	125.19(13)
C(8)-C(9)-S(1)	122.92(11)
C(15)-C(10)-C(11)	120.04(12)
C(15)-C(10)-S(1)	122.56(11)
C(11)-C(10)-S(1)	117.38(11)
C(12)-C(11)-C(10)	119.67(13)
C(13)-C(12)-C(11)	120.65(13)
C(12)-C(13)-C(14)	119.59(12)
C(13)-C(14)-C(15)	120.45(13)
C(10)-C(15)-C(14)	119.57(12)

Symmetry transformations used to generate equivalent atoms:

Table 4. Anisotropic Displacement Parameters ($\text{\AA}^2 \times 10^3$) for **2.9**. The Anisotropic Displacement Factor Exponent Takes the Form: $-2\pi^2 [h^2 a^*{}^2 U^{11} + \dots + 2 h k a^* b^* U^{12}]$

	U ¹¹	U ²²	U ³³	U ²³	U ¹³	U ¹²
S(1)	20(1)	13(1)	16(1)	-1(1)	-3(1)	1(1)
O(1)	16(1)	19(1)	16(1)	-2(1)	-1(1)	0(1)
O(2)	35(1)	22(1)	17(1)	-3(1)	8(1)	-1(1)
C(1)	19(1)	35(1)	44(1)	5(1)	2(1)	1(1)
C(2)	16(1)	35(1)	25(1)	2(1)	1(1)	-2(1)
C(3)	18(1)	22(1)	16(1)	0(1)	1(1)	-5(1)
C(4)	17(1)	16(1)	13(1)	1(1)	0(1)	0(1)
C(5)	18(1)	19(1)	15(1)	0(1)	1(1)	0(1)
C(6)	25(1)	18(1)	14(1)	-2(1)	4(1)	-3(1)
C(7)	22(1)	26(1)	15(1)	-2(1)	-1(1)	-4(1)
C(8)	21(1)	13(1)	15(1)	0(1)	2(1)	-2(1)
C(9)	21(1)	14(1)	17(1)	-2(1)	0(1)	-3(1)
C(10)	15(1)	15(1)	16(1)	1(1)	-2(1)	-4(1)
C(11)	16(1)	13(1)	23(1)	1(1)	0(1)	0(1)
C(12)	16(1)	20(1)	23(1)	7(1)	-3(1)	-2(1)
C(13)	19(1)	28(1)	18(1)	2(1)	1(1)	-6(1)
C(14)	19(1)	23(1)	22(1)	-3(1)	5(1)	-1(1)
C(15)	15(1)	15(1)	21(1)	2(1)	0(1)	1(1)

Table 5. Hydrogen Coordinates ($\times 10^4$) and Isotropic Displacement Parameters ($\text{\AA}^2 \times 10^3$) for **2.9**

	x	y	z	U(eq)
H(2O)	5270(30)	3030(30)	9928(11)	36
H(1A)	9937	-3014	8061	40
H(1B)	11886	-2912	8590	40
H(2)	11218	770	9095	30
H(3)	8841	2898	8209	23
H(4)	6065	2556	7490	18
H(5A)	3873	3087	8300	21
H(5B)	4534	612	8789	21
H(6)	6437	5288	8759	23
H(7A)	7740	838	9592	26
H(7B)	8791	3458	9553	26
H(8)	4766	-2491	7449	20
H(9)	2733	-1405	6472	21
H(11)	1048	6069	5335	21
H(12)	725	6121	3986	24
H(13)	1964	2918	3312	26
H(14)	3620	-297	3993	25
H(15)	4084	-261	5348	21

Table 6. Torsion Angles [°] for 2.9

C(4)-O(1)-C(3)-C(2)	-173.68(11)
C(4)-O(1)-C(3)-C(7)	62.89(14)
C(1)-C(2)-C(3)-O(1)	10.8(2)
C(1)-C(2)-C(3)-C(7)	133.52(17)
C(3)-O(1)-C(4)-C(8)	177.52(10)
C(3)-O(1)-C(4)-C(5)	-61.03(14)
O(1)-C(4)-C(5)-C(6)	54.95(15)
C(8)-C(4)-C(5)-C(6)	173.83(11)
C(4)-C(5)-C(6)-O(2)	-174.71(11)
C(4)-C(5)-C(6)-C(7)	-50.76(15)
O(2)-C(6)-C(7)-C(3)	175.26(11)
C(5)-C(6)-C(7)-C(3)	51.90(15)
O(1)-C(3)-C(7)-C(6)	-58.09(15)
C(2)-C(3)-C(7)-C(6)	179.93(12)
O(1)-C(4)-C(8)-C(9)	-152.50(13)
C(5)-C(4)-C(8)-C(9)	86.51(17)
C(4)-C(8)-C(9)-S(1)	-2.3(2)
C(10)-S(1)-C(9)-C(8)	138.73(12)
C(9)-S(1)-C(10)-C(15)	-24.88(13)
C(9)-S(1)-C(10)-C(11)	157.11(11)
C(15)-C(10)-C(11)-C(12)	-0.7(2)
S(1)-C(10)-C(11)-C(12)	177.37(10)
C(10)-C(11)-C(12)-C(13)	1.8(2)
C(11)-C(12)-C(13)-C(14)	-1.1(2)
C(12)-C(13)-C(14)-C(15)	-0.7(2)
C(11)-C(10)-C(15)-C(14)	-1.1(2)
S(1)-C(10)-C(15)-C(14)	-179.04(11)
C(13)-C(14)-C(15)-C(10)	1.8(2)

Symmetry transformations used to generate equivalent atoms:

Table 7. Hydrogen bonds for **2.9** [Å and °]

D-H...A	d(D-H)	d(H...A)	d(D...A)	<(DHA)
O(2)-H(2O)...O(2)#1	0.831(16)	2.093(16)	2.9143(9)	170(2)

Symmetry transformations used to generate equivalent atoms:

#1 -x+1,y-1/2,-z+2

A New Class of Highly Efficient Ru Catalysts for Z-Selective Olefin Metathesis

Chapter Three

3.1 Introduction

Development of methods to construct C=C bonds in geometrically selective manner is of utmost importance in chemical synthesis. Of this goal, particularly challenging is the fabrication of sterically congested Z-alkenes. Although over the years several strategies have been developed to furnish alkenes of *cis* configuration (Scheme 3.1-1),^{1,2} many of the protocols suffer from significant complicating factors: 1) limited scope of substrates 2) control of selectivity (e.g., over reduction in hydrogenation of alkynes and C=C migration in alkene-isomerization strategy) 3) difficulty to access substrate (e.g., alkyne synthesis and access to functionalized precursors for cross-coupling) 4) waste generation (e.g., lack of atom economy with Wittig and cross-coupling methodologies). In comparison, olefin metathesis (OM) has emerged as an indispensable approach to access functionalized olefins in high stereoselectivity with relative ease.³ Not only this strategy circumvents the need to construct highly elaborate substrates, the ubiquitous nature of alkenes renders it highly applicable in a plethora of synthetic schemes.⁴ Additionally, OM offers an opportunity to develop methods with

(1) For a review of strategies to access Z-alkenes, see: Siau, W.-Y.; Zhang, Y.; Zhao, Y. *Top. Curr. Chem.* **2012**, *327*, 33.

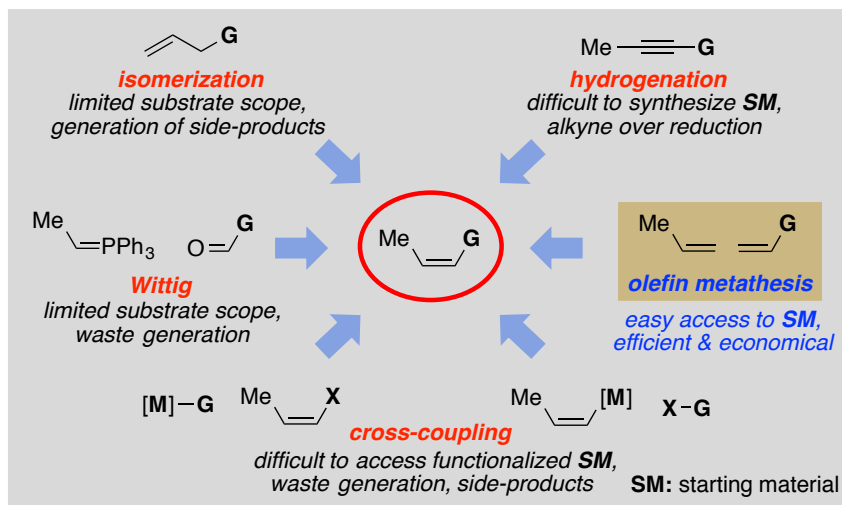
(2) For an initial report on partial hydrogenation of alkynes, see: (a) Lindlar, H. *Helv. Chim. Acta* **1952**, *35*, 446–450. For a representative report concerning stereoselectivity in Wittig reaction, see: (b) Bergelson, L. D.; Shemyakin, M. M. *Tetrahedron* **1963**, *19*, 149–159. For representative reports regarding Z-selective alkene isomerization, see: (a) Chen, C.; Dugan, T. R.; Brennessel, W. W.; Weix, D. J.; Holland, P. L. *J. Am. Chem. Soc.* **2014**, *136*, 945–955. (b) Zhuo, L.-G.; Yao, Z.-K.; Yu, Z.-X. *Org. Lett.* **2013**, *15*, 4634–4637. For a recently developed hydroboration protocol, see: Ely, R. J.; Morken, J. P. *J. Am. Chem. Soc.* **2010**, *132*, 2534–2535.

(3) For comprehensive review regarding the advances in stereoselective olefin metathesis, see: (a) Hoveyda, A. H. *J. Org. Chem.* **2014**, *79*, 4763–4792. For related reviews, see: (b) “Catalyst-Controlled Stereoselective Olefin Metathesis Reactions,” Hoveyda, A. H.; Khan, R. K. M.; Torker, S.; Malcolmson, S. J.; in *Handbook of Olefin Metathesis*; Grubbs, R. H.; O’Leary, D. Eds; VCH–Wiley, **2014**, in press. (c) Hoveyda, A. H.; Zhugralin, A. R. *Nature* **2007**, *450*, 243–251.

(4) (a) *Metathesis in Natural Product Synthesis: Strategies, Substrates and Catalysts*; Cossy, J.;

high atom economy and minimal generation of waste. In this context, recent advances in Z-selective OM have highlighted its importance as a viable strategy to easily access molecules of biological and synthetic importance.⁵

Scheme 3.1-1. Notable Strategies to Form Z-Alkenes



While the main challenge in OM deals with the catalyst-controlled stereoselective generation of single alkene isomer (*E* or *Z*), its inherent reversible nature also offers opportunity for loss in kinetic selectivity. The aforementioned issue is more pronounced in cases wherein the high energy *Z*-alkene is desired. Therefore, a competent catalyst must be capable of delivering *Z* selectivity versus the formation of lower energy *E*-isomer, which is generated in most instances.⁶ Additionally, reversion to the starting reagents must remain at minimal level. Even with *Z*-selective catalyst in hand, the generation of undesired homocoupled-products could also take place (i). Another impediment is that while sufficient promotion of reaction efficiency must be exhibited, high catalytic activity could also engender significant erosion of *Z* selectivity through post-OM isomerization (ii).⁷ The aforementioned issue poses a significant challenge during the late stage of OM

Arseniyadis, S.; Meyer, C.; Grubbs, R. H. Eds.; Wiley–VCH, Weinheim, Germany, 2010. (b) Fürstner, A. *Angew. Chem. Int. Ed.* 2014, DOI: 10.1002/anie.201402719.

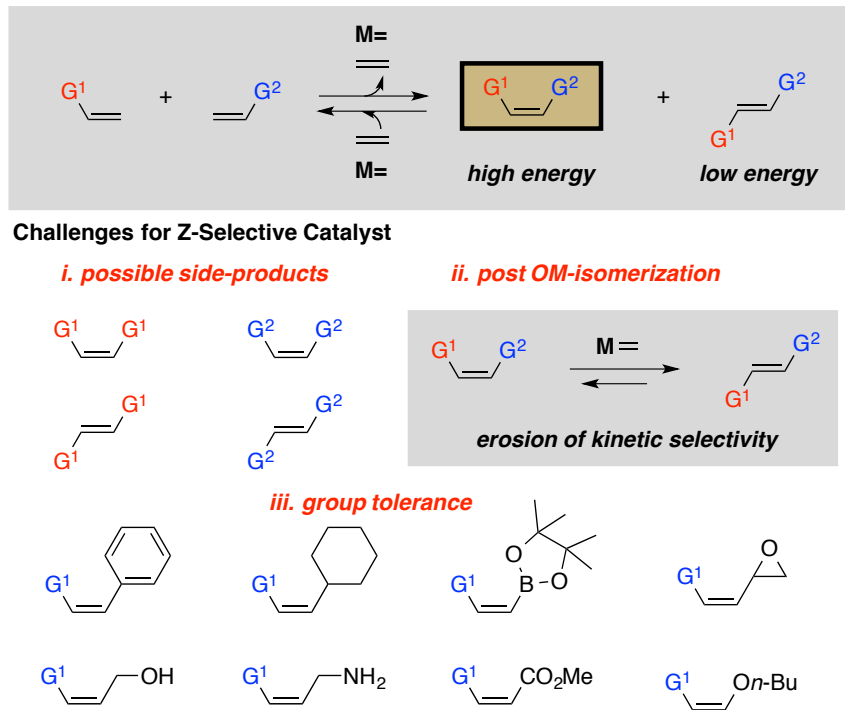
(5) Fürstner, A. *Science* 2013, 341, 1357–1344.

(6) Anderson, D. R.; Ung, T.; Mkrtumyan, G.; Bertrand, G.; Grubbs, R. H., Schrödi, Y. *Organometallics* 2008, 27, 563–566.

(7) For the importance of interplay between kinetic *Z* selectivity and post-metathesis isomerization, see: (a) Meek, S. J.; O'Brien, R. V.; Llaveria, J.; Schrock, R. R.; Hoveyda, A. H. *Nature* 2011, 471, 461–466. (b) Yu, M.; Wang, C.; Kyle, A. F.; Jakubec, P.; Dixon, D. J.; Schrock, R. R.; Hoveyda, A. H. *Nature* 2011, 479, 88–93. (c) Ritter, T.; Hejl, A.; Wenzel, A. G.; Funk, T. W.; Grubbs, R. H. *Organometallics* 2006, 25,

and makes the development of efficient and *Z*-selective transformations an uphill task. It is also noteworthy that functional group tolerance is of utmost importance for broader implications in organic synthesis (iii).

Scheme 3.1-2. Challenges for a Competent *Z*-Selective Catalyst



3.2 Rationally Designed Ru Carbenes for *Z* Selectivity in Olefin Metathesis

3.2.1 Catalysts for *Z* Selectivity in Olefin Metathesis

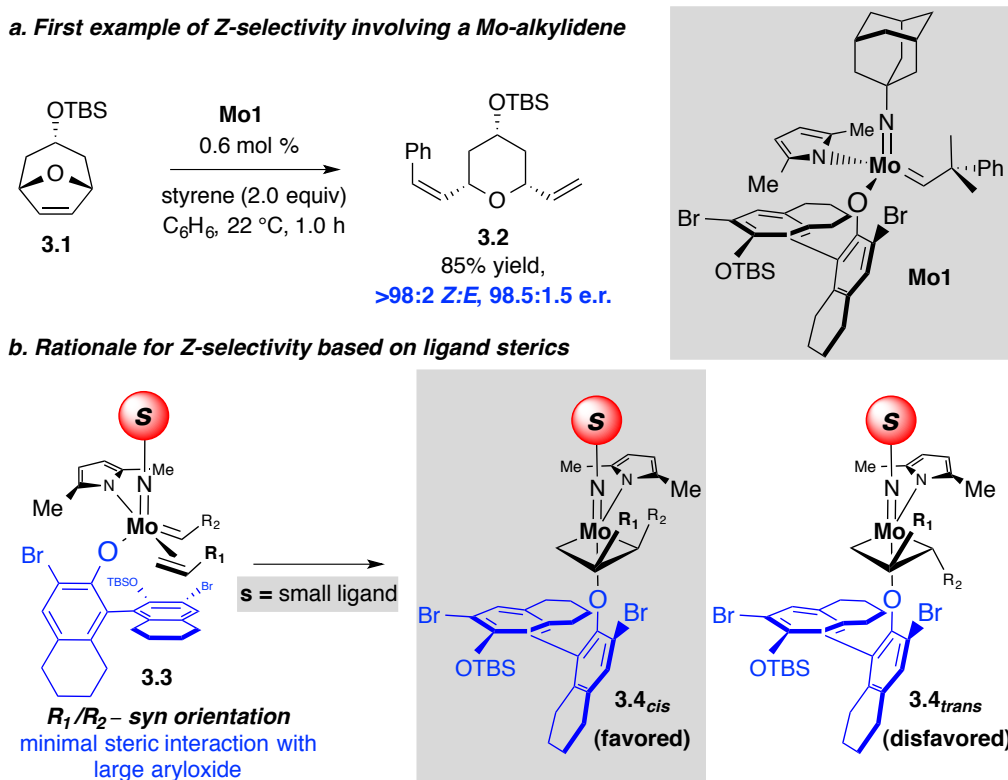
The earliest advance in this field emerged from the employment of high-oxidation-state Mo- and W-alkylidenes that contained a combination of monodentate aryloxide and pyrrolide (MAP) ligands as catalysts. In 2009, first instance of highly *Z*- and enantioselective ROCM involving an oxabicyclic alkene **3.1** with styrene was reported (Scheme 3.2.1-1a). As low as 0.6 mol% **Mo1** furnished **3.2** in 85% yield and unprecedented selectivity (>98% *Z*, >98% er).^{8a} The transformation involves the olefin

5740–5745.

(8) For representative examples of Mo catalysts for *Z*-selective OM, see: (a) Ibrahim, I.; Yu, M.; Schrock, R. R.; Hoveyda, A. H. *J. Am. Chem. Soc.* **2009**, *131*, 3844–3845. (b) Meek, S. J.; O'Brien, R. V.; Llaveria, J.; Schrock, R. R.; Hoveyda, A. H. *Nature* **2011**, *471*, 461–466. (c) Kiesewetter, E. T.; O'Brien, R. V.; Yu, E. C.; Meek, S. J.; Schrock, R. R.; Hoveyda, A. H. *J. Am. Chem. Soc.* **2013**, *135*, 6026–6029. (d) Flook, M.; Jiang, A. J.; Schrock, R. R.; Müller, P.; Hoveyda, A. H. *J. Am. Chem. Soc.* **2009**, *131*, 7962–7963. For

approach trans to the strong pyrrolide donor due to its ability to stabilize the empty coordination-site for ligation, which engenders the formation of **3.3** (Scheme 3.2.1-1b). The high *Z* selectivity originates from the size differential between the aryloxide (large) and imido (small) ligands, which renders the generation of **3.4_{cis}**, in which R₁ and R₂ point *away* from aryloxide to minimize steric interaction, as favored. The aforementioned design principle was further used to develop various Mo-^{8b-d} and W-alkylidenes^{8e,f} as efficient and *Z*-selective catalysts to access a wide range of useful molecules.

Scheme 3.2.1-1. Monoaryloxide Pyrrolide Mo-Alkylidene for *Z*-Selective OM

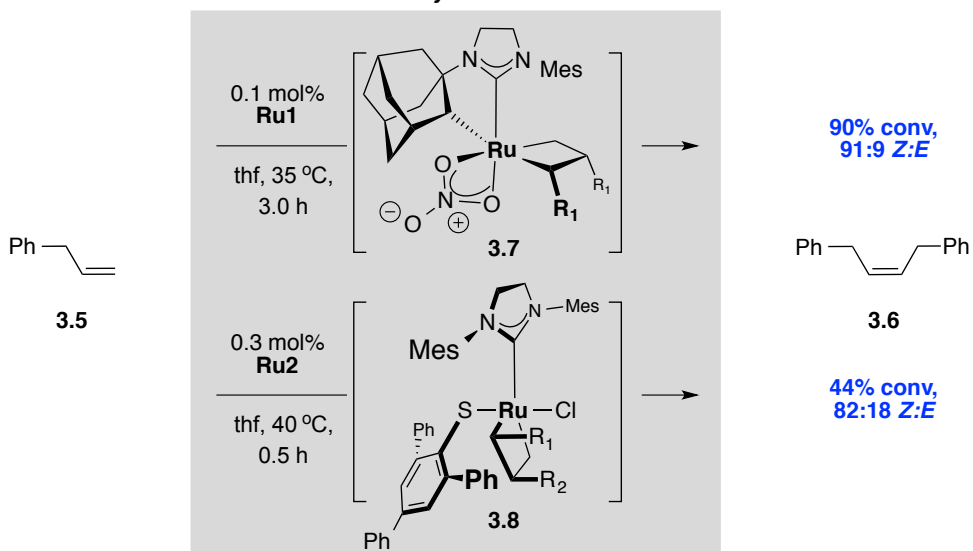
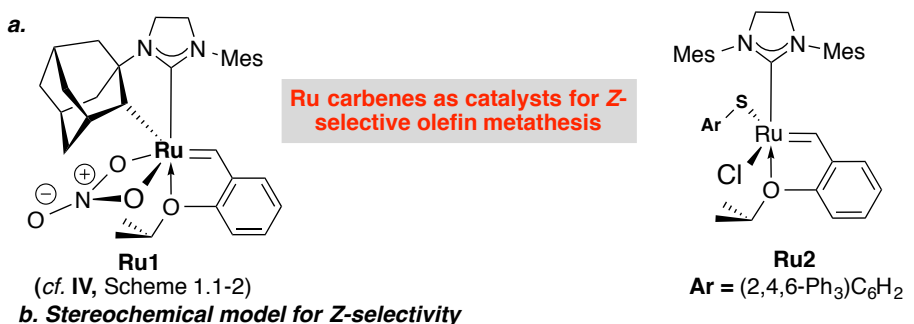


Success of Mo- and W-MAP complexes as *Z*-selective catalysts has subsequently inspired several efforts to develop low oxidation-state Ru carbenes as viable catalysts. The impetus for such investigations is rooted in the complementary nature of Ru carbenes (vs Mo/W-alkylidenes) that could significantly enhance the impact of *Z*-selective OM in synthetic processes. After initial investigation involving a bidentate P-containing Ru

representative examples of W catalysts for *Z*-selective OM, see: (e) Jiang, A. J.; Zhao, Y.; Schrock, R. R.; Hoveyda, A. H. *J. Am. Chem. Soc.* **2009**, *131*, 16630–16631. (f) Marinescu, S. C.; Schrock, R. R.; Müller, P.; Takase, M. K.; Hoveyda, A. H. *Organometallics* **2011**, *30*, 1780–1782.

carbene for ROMP,⁹ bidentate NHC-containing carbene **Ru 1**^{10a} and related analogues¹¹ are reported to promote *Z*-selective OM (Scheme 3.2.1-2a).

Scheme 3.2.1-2. Ru-Carbenes for *Z*-Selective OM



For instance, 90% conv of allylbenzene to generate **3.6** is achieved with 91% preference for the *Z*-isomer (Scheme 3.2.1-2b). The source of high *Z* selectivity lies in preference for the formation of ruthenacyclobutane *syn* to the large NHC (**3.7**), which results in *cis* orientation of R₁ and R₂ in order to minimize steric interaction with the

(9) As high as 51% *Z* selectivity in copolymerization of norbornene with cyclooctene has been reported: Torker, S.; Müller, A.; Chen, P. *Angew. Chem. Int. Ed.* **2010**, *49*, 3762–3766.

(10) (a) Keitz, B. K.; Endo, K.; Patel, P. R.; Herbert, M. B.; Grubbs, R. H. *J. Am. Chem. Soc.* **2012**, *134*, 693–699. For application in cross-metathesis, see: (b) Herbert, M. B.; Marx, V. M.; Pederson, R. L.; Grubbs, R. H. *Angew. Chem. Int. Ed.* **2013**, *52*, 310–314. For application in ring-closing metathesis, see: (c) Marx, V. M.; Herbert, M. B.; Keitz, B. K.; Grubbs, R. H. *J. Am. Chem. Soc.* **2013**, *135*, 94–97. For application in ring-opening/cross-metathesis, see: (d) Hartung, J.; Grubbs, R. H. *Angew. Chem. Int. Ed.* **2014**, *53*, 3885–3888.

(11) (a) Endo, K.; Grubbs, R. H. *J. Am. Chem. Soc.* **2011**, *133*, 8525–8527. (b) Keitz, B. K.; Endo, K.; Herbert, M. B.; Grubbs, R. H. *J. Am. Chem. Soc.* **2011**, *133*, 9686–9688. (c) Rosebrugh, L. E.; Herbert, M. B.; Marx, V. M.; Keitz, B. K.; Grubbs, R. H. *J. Am. Chem. Soc.* **2013**, *135*, 1276–1279.

bulky NHC.¹² Although **Ru1** has been shown to be effective in several methodologies,^{10b-d} limitations regarding the substrate-scope for use in organic synthesis remain.¹³

More recently, **Ru2** is also shown to homocouple allylbenzene *Z*-selectively at moderate conversion (82% *Z*; 44% conv).^{14a} In this case, the stereochemical outcome is rationalized by considering the intermediacy of **3.8**, in which R₁ and R₂ orient *cis* to each other in order to avoid steric interaction with the large thiolate. A major limitation of this class of catalysts is associated with the generation of large amounts of *E*-isomer at higher conversions (e.g. only 45% *Z* is observed at >98% conv for **3.6**, presumably due to post OM)⁷ and the use of additives^{14b} at the expense of diminished catalytic activity.

3.2.2 Initial Hypothesis for the Development of *Z*-Selective Ru Catalysts

Based on the limitations associated with the abovementioned Ru carbenes, development of highly efficient and *Z*-selective catalysts with broad group tolerance is critical for synthetic applications. In this regard, we wished to implement the design principles that emerged from investigations concerning *Z*-selective Mo/W-alkylidenes (**3.9**, Scheme 3.2.2a) to a new ligand framework involving Ru-carbenes. In particular, we hypothesized that high *Z* selectivity could be attained if the ruthenacyclobutane intermediate involves axial moieties that significantly differ in size (i.e. *large L* and *small s*) to favor the *cis* orientation of substituents away from **L** (e.g. **3.10**). In case of commonly used Ru dichloride carbenes, **3.11_{syn}** (Scheme 3.2.2b) would contain the appropriate ligand arrangement (*cf.* **3.10**) to deliver *Z* selectivity. However, its intermediacy is largely disfavored due to several reasons: electron-electron repulsion between Cl ligands (*syn* to each other),¹⁵ high dipole moment,^{16,17} and steric repulsion

(12) Liu, P.; Xu, X.; Dong, X.; Keitz, B. K.; Herbert, M. B.; Grubbs, R. H.; Houk, K. N. *J. Am. Chem. Soc.* **2012**, *134*, 1464–1467.

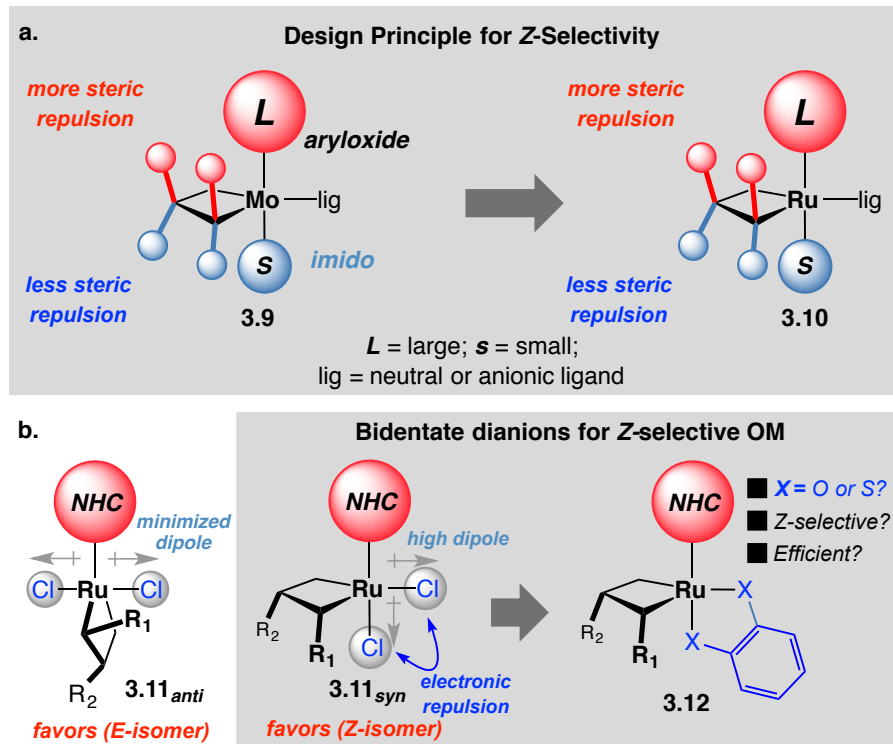
(13) Lack of activity is observed with sterically hindered alkenes: (a) 30 mol% **Ru1**, introduced in three portions, is shown to deliver 32% yield of cross-metathesis of a functionalized vinyl epoxide: (b) Chong, W.; Carlson, J. S.; Bedke, D. K.; Vanderwal, C. D. *Angew. Chem., Int. Ed.* **2013**, *52*, 10052–10055. In many instances, protection of alcohols is required: (c) Hartung, J.; Grubbs, R. H. *J. Am. Chem. Soc.* **2013**, *135*, 10183–10185.

(14) (a) Occhipinti, G.; Hansen, F. R.; Törnroos, K. W.; Jensen, V. R. *J. Am. Chem. Soc.* **2013**, *135*, 3331–3334. (b) Higher selectivity is observed in the presence of 1,8-bis(dimethylamino)naphthalene as an additive.

(15) Syn arrangement in dichlororuthenium complexes has been observed, which likely arises from donor strength of the chelating units. For example: (a) Ung, T.; Hejl, A.; Grubbs, R. H.; Schrodi, Y. *Organometallics* **2004**, *23*, 5399–5401. (b) Slugovc, C.; Perner, B.; Stelzer, F.; Mereiter, K. *Organometallics* **2004**, *23*, 3622–3626. (c) Barbasiewicz, M.; Szadkowska, A.; Bujok, R.; Grela, K.

between the NHC and ruthenacycle substituents. Consequently, OM proceeds through **3.11_{anti}**,¹⁸ in which the unbiased stereoelectronic nature of the axial Cl ligands leads to the trans-orientation of R₁ and R₂ thereby resulting in the predominant generation of the *E*-isomer).

Scheme 3.2.2. Rational Design of New Ru Catalysts for Z-Selective OM



Organometallics **2006**, *25*, 3599–3604. (d) Diesendruck, C. E.; Tzur, E.; Ben-Asuly, A.; Goldberg, I.; Straub, B. F.; Lemcoff, N. G. *Inorg. Chem.* **2009**, *48*, 10819–10825. (e) Tzur, E.; Szadkowska, A.; Ben-Asuly, A.; Makal, A.; Goldberg, I.; Wozniak, K.; Grela, K.; Lemcoff, N. G. *Chem.–Eur. J.* **2010**, *16*, 8726–8737. For a study involving syn/anti isomerization, see: (f) Poater, A.; Ragone, F.; Correa, A.; Szadkowska, A.; Barbasiewicz, M.; Grela, K.; Cavallo, L. *Chem.–Eur. J.* **2010**, *16*, 14354–14364.

(16) Polar solvents have been proposed to stabilize the high dipole moment of syn alkene–NHC complexes and the related metallacyclobutanes. See: (a) Benitez, D.; Goddard, W. A., III. *J. Am. Chem. Soc.* **2005**, *127*, 12218–12219. (b) Correa, A.; Cavallo, L. *J. Am. Chem. Soc.* **2006**, *128*, 13352–13353.

(17) For the significance of minimizing donor–donor interactions in Ru-catalyzed olefin metathesis, see: Khan, R. K. M.; Zhugralin, A. R.; Torker, S.; O'Brien, R. V.; Lombardi, P. J.; Hoveyda, A. H. *J. Am. Chem. Soc.* **2012**, *134*, 12438–12441.

(18) Mechanistic investigations regarding favored reaction pathways through computations have been explored: (a) Vyboishchikov, S. F.; Bühl, M.; Thiel, W. *Chem.–Eur. J.* **2002**, *8*, 3962–3964. (b) Adlhart, C.; Chen, P. *J. Am. Chem. Soc.* **2004**, *126*, 3496–3510. (c) Straub, B. F. *Adv. Synth. Catal.* **2007**, *349*, 204–214. (d) Benitez, D.; Tkatchouk, E.; Goddard, W. A., III. *Chem. Commun.* **2008**, 6194–6196. For reports involving spectroscopic evidence: (e) van der Eide, E. F.; Romero, P. E.; Piers, W. E. *J. Am. Chem. Soc.* **2008**, *130*, 4485–4491. (f) Wenzel, A. G.; Blake, G.; VanderVelde, D. G.; Grubbs, R. H. *J. Am. Chem. Soc.* **2011**, *133*, 6429–6439.

In order to favor the formation of **3.11_{syn}**-like intermediate, we envisioned the replacement of chlorides with a bidentate dianion as represented in **3.12**, which might provide the steric environment necessary for the promotion of Z-selective OM. More notably, the anti-to-NHC approach of the olefin in this arrangement, to generate **3.11_{anti}**-like intermediate, would not be feasible because the ligation site would already be occupied by a heteroatom. Alternatively, the anti-to-NHC association of the alkene would require the dianions to adopt a syn-to-NHC arrangement leading to severe filled-filled interactions involving Ru^{II} d_{xy}-orbital (*cf.* Scheme 1.5.1b.ii, Chapter 1).

3.2.3 Development of Readily Accessible and Modifiable Catecholate and Catechothiolate Complexes¹⁹

Although the exchange of chlorides with catecholates has been reported in the literature, the transformation involves the use of highly toxic thallium salts and relatively sensitive dipyridyl-Ru carbene precursors.²⁰ In order to devise a practical synthetic route, we envisaged the use of commercially available **Ru3**²¹ and disodium salts of catecholate and dithiolates (**3.13**, X₂= O₂; **3.14** and **3.15**, X₂= S₂; Scheme 3.2.3a). Indeed, the reaction proceeds readily (22 °C, thf, 3.0 h) to give complex **Ru4a** in 65% yield after purification; dithiolates **Ru4b** and **Ru5** are thus obtained in 61% and 82% yields, respectively.

The high polarity of **Ru4a**, **Ru4b** and **Ru5** (7.9, 7.7, 17.3 Debye) renders them easier to purify from any trace impurities of highly active and *E*-selective parent complex **Ru3** (2.0 Debye). As evident from the X-ray structures of **Ru4a** and **Ru4b**, the isopropoxy ligand is chelated syn-to-NHC, in a similar way as the approach of an alkene is envisioned to take place during the course of OM (Scheme 3.2.3b). Furthermore, another important feature entails the avoidance of trans-influence between the strongly donating NHC and anionic ligand (O or S) as seen by the significant deviation from linearity of the C–Ru–O₁ (149.2°) and C–Ru–S (143.4°) angles. Due to the stronger σ-

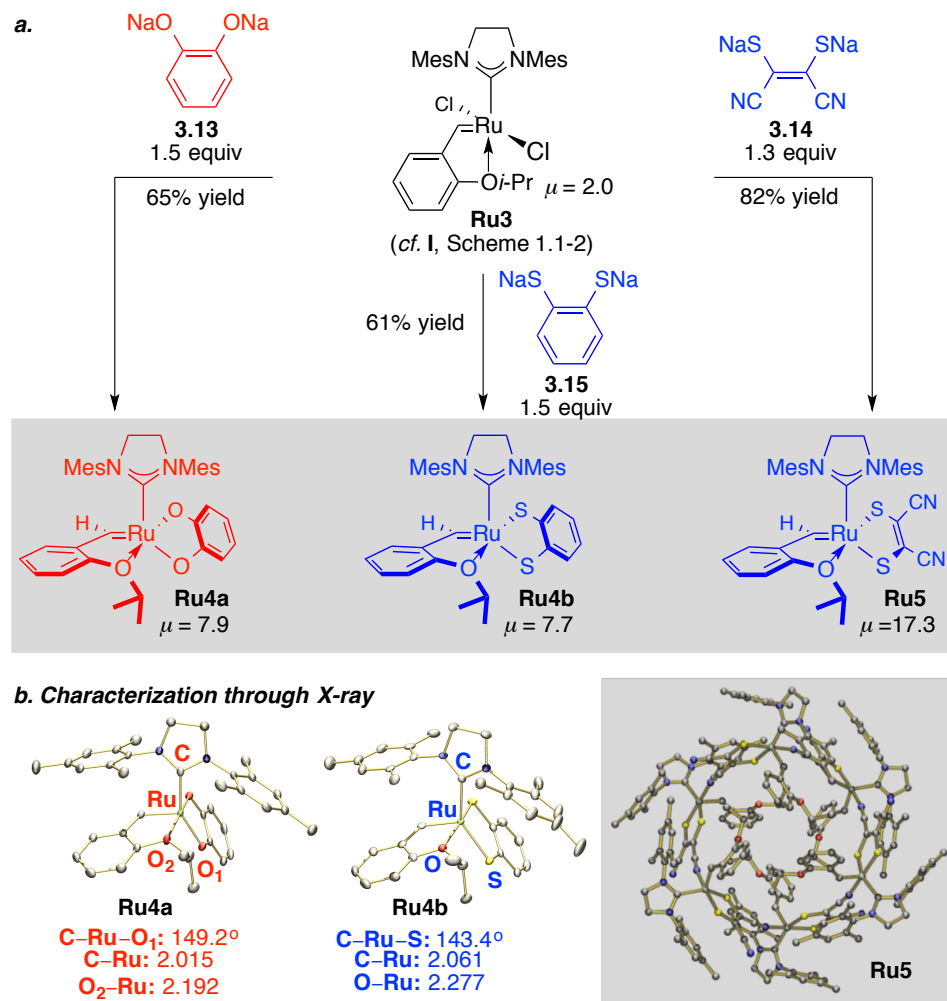
(19) Khan, R. K. M.; Torker, S.; Hoveyda, A. H. *J. Am. Chem. Soc.* **2013**, *135*, 10258–10261.

(20) (a) Monfette, S.; Fogg, D. E. *Organometallics* **2006**, *25*, 1940–1944. (b) Monfette, S.; Silva, J. A. D.; Gorelsky, S. I.; Dalgarno, S. J.; dos Santos, E. N.; Araujo, M. H.; Fogg, D. E. *Can. J. Chem.* **2009**, *87*, 361–367.

(21) Garber, S. B.; Kingsbury, J. S.; Gray, B. L.; Hoveyda, A. H. *J. Am. Chem. Soc.* **2000**, *122*, 8168–8179.

donation of S (vs O), the C–Ru and O–Ru bonds are longer in **Ru4b** (vs C–Ru and O₂–Ru in **Ru4a**).

Scheme 3.2.3. Synthesis and Characterization of New Ru Complexes for Z-Selective OM



More notably, a cyclohexameric-Ru complex arising from the participation of the CN-groups in intermolecular chelation is observed. The aforementioned attribute provides an insight into the potential ability of **Ru5** to protect the catalytically active species (*after initiation*).

3.3 Ru Catechothiolate as Highly Efficient, Z-Selective, and Group Tolerant Catalyst in Olefin Metathesis

3.3.1 Remarkable Efficiency and Z Selectivity in Ring-Opening Metathesis Polymerization (ROMP)

An important application of catalytic OM pertains to the construction of organic materials through ring-opening metathesis polymerization (ROMP).²² Synthesis of polymers through highly stereoregular ROMP can provide access to materials that exhibit specific properties due to their respective tacticities (e.g., atactic, isotactic, and syndiotactic) and olefinic geometries (cis or trans). In this context, recent developments have shown that alterations in the architecture of the catalyst (Mo/W²³ or Ru²⁴) have a direct impact on the promotion of high Z selectivity in ROMP.

In order to test the performance and selectivity of newly developed complexes **Ru4a-b** and **Ru5** as catalysts, polymerization of norbornene **3.16** was investigated (Table 3.3.1). Indeed, the reaction takes place readily in the presence of 0.1 mol% of **Ru4a** at 22 °C in dichloromethane (96% yield of **3.17** after 1 h), albeit with low Z selectivity (58%, entry 1). In contrast, the S-containing analogues **Ru4b** and **Ru5** promote the transformation in similar yield but with remarkably high and unprecedented Z selectivity (>98%, entries 2 and 3). It is also noteworthy that rigorous purification of norbornene monomer is not required. The high stereoregularity of polynorbornene **3.17** produced from **Ru4b** or **Ru5** (vs **Ru4a**) is highlighted by comparison of the ¹³C NMR spectra (olefinic region, Table 3.3.1). Moreover, the stark difference in selectivity promoted by **Ru4a** and **Ru4b** is topic of a later discussion (see Section 3.4), which provides a critical insight that the origin of low Z selectivity with the latter complex is of kinetic nature.

A similar trend in Z content is observed in ROMP polymer **3.19** obtained from less-strained 1,5-cyclooctadiene: **3.18** (72% with **Ru4a** whereas >98% Z with **Ru4b** and **Ru5** entries 4-6), albeit with the requirement for extended reaction times (24 h). In order

(22) For representative reviews, see: (a) Sutthasupa, S.; Shiotsuki, M; Sanda, F. *Polymer Journal* **2010**, *42*, 905–915. (b) Buchmeiser, M. R. *Chem. Rev.* **2000**, *100*, 1565–1604. (c) Xia, Y.; Kornfield, J. A.; Grubbs, R. H. *Macromolecules* **2009**, *42*, 3761–3766.

(23) For a review on latest developments in stereoselective ROMP promoted by Mo/W-alkylidenes, see: Schrock, R. R. *Dalton Trans.* **2011**, *40*, 7484–7495.

(24) (a) Keitz, B. K.; Fedorov, A.; Grubbs, R. H. *J. Am. Chem. Soc.* **2012**, *134*, 2040–2043. (b) Rosebrugh, L. E.; Marx, V. M.; Keitz, B. K.; Grubbs, R. H. *J. Am. Chem. Soc.* **2013**, *135*, 10032–10035.

to gain further insight into the activity levels that can be promoted by **Ru5**, polymerizations with reduced catalyst loadings were performed (entries 7–10). With as little as 0.002 mol % **Ru5**, **3.17** was generated with a TON of 43 000 in 1 h (entry 8). More remarkably, TON of 3500 is achieved for ROMP of 1,5-cyclooctadiene after 24 h at 0.01 mol% loading of **Ru5** (entry 9), which increases to 5,400 after 48 h (entry 10), underscoring the longevity of the catalytically active species. These findings compare favorably with the *Z* selectivities (e.g., 88% *Z* for **3.17** and 96% *Z* for **3.19**) and TONs (e.g., 38 in 72 h for **3.19**) reported recently for the same ROMP process catalyzed by **Ru1**.^{24a}

The above findings not only highlight that **Ru4b** and **Ru5** are more effective in the promotion of *Z*-selective ROMP compared with **Ru1**, but also the observed efficiency and selectivity is comparable to the performance of Mo-based MAP catalysts.^{8d}.

Table 3.3.1. Highly *Z*-Selective ROMP Catalyzed by Stereogenic-at-Ru Carbenes

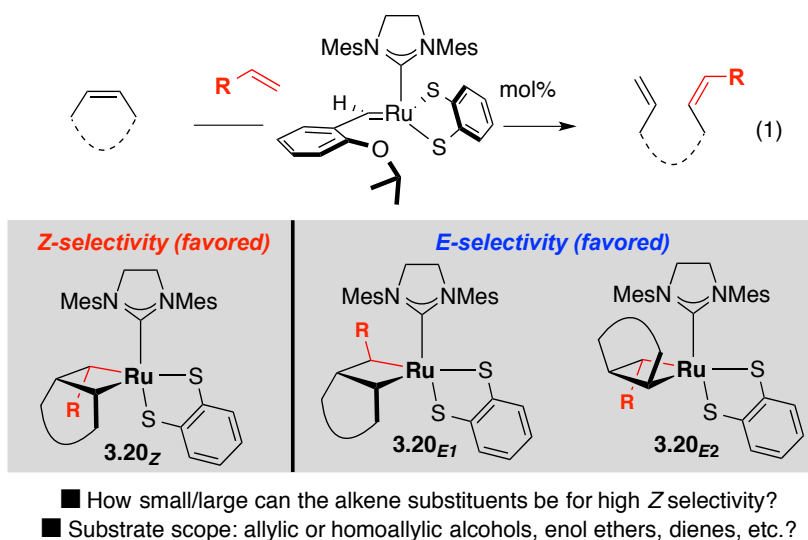
entry	monomer	complex; mol %	time (h); yield ^b	<i>ZE</i> ^b	TON
1	3.16	Ru4a ; 0.1	1.0; 96	58:42	960
2	3.16	Ru4b ; 0.1	1.0; 93	>98:2	930
3	3.16	Ru5 ; 0.1	1.0; 90	>98:2	900
4	3.18^c	Ru4a ; 0.1	24; 88	72:38	880
5	3.18^c	Ru4b ; 0.1	24; 75	>98:2	750
6	3.18^c	Ru5 ; 0.1	24; 75	>98:2	750
7	3.16^c	Ru5 ; 0.01	1.0; 92	>98:2	9,200
8	3.16^c	Ru5 ; 0.002	1.0; 86	>98:2	43,000
9	3.18^c	Ru5 ; 0.01	24; 35	>98:2	3,500
10	3.18^c	Ru5 ; 0.01	48; 54	>98:2	5,400

^aSee the Supporting Information for experimental details. ^bDetermined by ¹H NMR analysis of the purified products. ^cThe substrate was passed through a short column of basic alumina before use.

3.3.2 Broad Scope *Z* Selectivity in ROCM²⁵

Ring-opening/cross-metathesis (ROCM) involving two stereoelectronically-differentiated alkenes (i.e. cyclic and terminal) is a useful strategy to construct highly elaborate olefin products. In literature, a wide variety of synthetic strategies have emerged that employ ROCM as key step.²⁶ More recently, highly *Z*-selective examples of ROCM catalyzed by Mo-alkylidenes were reported.^{8a} However, the inherent basic nature of Mo/W-alkylidenes renders them intolerant towards alcohols, consequently requiring the installation of appropriate protection groups on alkenes. A similar trend is also observed in many cases reported with **Ru1**.^{13c} Although we have demonstrated that Ru-catalyzed ROCM of O- and S-substituted alkenes could be achieved with high *Z*- and enantioselectivity in the presence of alcohols, the same catalysts could only promote *E*-selectivity with other types of alkene cross partners.²⁷

Scheme 3.3.2. *Z*-Selective ROCM with Ru Dithiolates as Catalysts



In light of the hitherto mentioned findings with Ru dithiolates (i.e. high *Z* selectivity and efficiency in ROMP, Section 3.3.1), we wished to investigate their effectiveness in ROCM involving a wide variety of synthetically useful alkenes (e.g., allylic and homoallylic alcohols, aryl and heteroaryl alkenes, enol ethers, 1,3-dienes, etc.).

(25) Koh, M. J.; Khan, R. K. M.; Torker, S.; Hoveyda, A. H. *Angew. Chem., Int. Ed.* **2014**, *53*, 1968–1972.

(26) For brief introduction, see: Grela, K. *Angew. Chem. Int. Ed.* **2008**, *47*, 5504–5507.

(27) Khan, R. K. M.; O'Brien, R. V.; Torker, S.; Li, B.; Hoveyda, A. H. *J. Am. Chem. Soc.* **2012**, *134*, 12774–12779.

Furthermore, ROCM with alkenes of various steric sizes could also shed light on the scenario depicted in **3.20_Z** (Scheme 3.3.2), in which all substituents point *away* from the large NHC to minimize steric interaction thereby promoting high *Z* selectivity (vs **3.20_{E1}** and **3.20_{E2}**, which lead to the corresponding *E*-isomer).

3.3.2.1 Reactions Involving Sterically Bulky Cross Partners

The investigation began with the ROCM of **3.16** with styrene in the presence of 1 mol% **Ru4b**, which readily furnishes **3.21a** (97% *Z*-isomer) in 75% yield (entry 1, Table 3.3.2.1). *The remarkably high Z selectivity underlines the efficient kinetic control of the catalyst that results in disfavoring the corresponding E-isomer, which is 2.9 kcal/mol lower in energy* (see experimental section).

Table 3.3.2.1. Z-Selective and Efficient ROCM of Hindered Alkenes Catalyzed by Ru

entry ^a	substrate	G	time (h)	product	conv (%); ^b yield (%)	<i>ZE</i> ^b
1 ^c		a C ₆ H ₅	1.0		>98; 75	97:3
2		b Cy	2.0		>98; 59	>98:2
3		a C ₆ H ₅	1.0		>98; 85	98:2
4		b m-FC ₆ H ₄	1.0		>98; 81	98:2
5		c p-MeOC ₆ H ₄	1.0		>98; 93	96:4
6		d Cy	8.0		88; 62	>98:2
7 ^d		C ₆ H ₅	12		94; 67	93:7
8 ^d		C ₆ H ₅	2.0		>98; 69	>98:2

^aSee experimental section for details. ^bDetermined by ¹H NMR analysis of the unpurified products.

^cReaction with 1 mol% **Ru5** gives 29% yield of **3.21a**. ^d3 mol% and 2 mol% **Ru4b** for entries 7 and 8, respectively.

In comparison with **Ru4b**, reaction with 1 mol% **Ru5** gives rise to 29% yield of **3.21a**, albeit with >98% *Z*-content. The low reaction efficiency with **Ru5** could be due to the relative instability of Ru-methylidene that is competitively generated as a result of

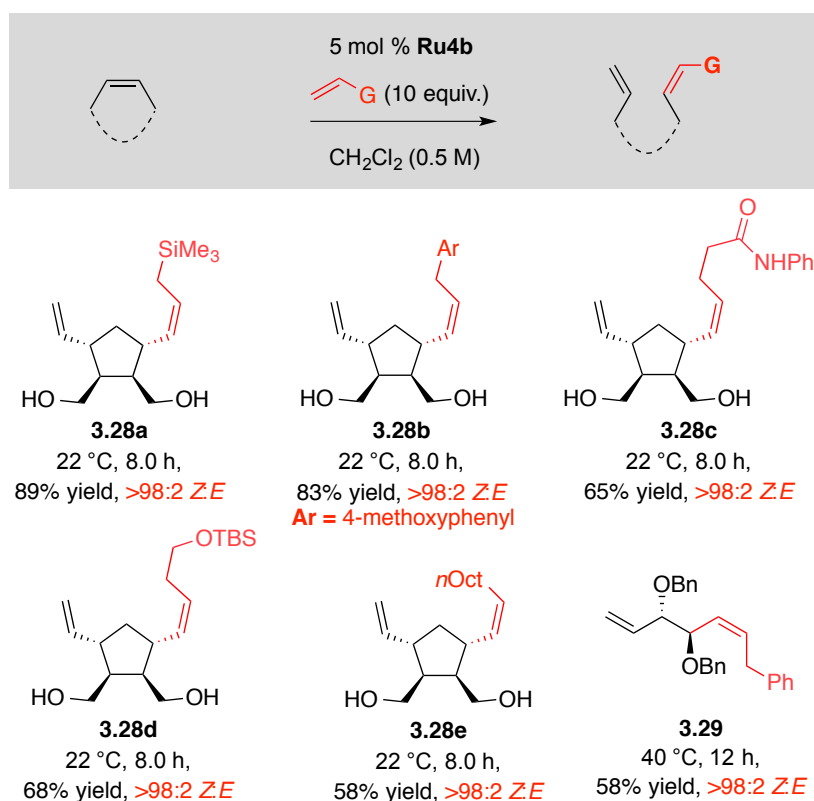
homocoupling of terminal alkene as side reaction. Furthermore, ROCM with sterically bulkier and less reactive vinyl cyclohexane cross partner also proceeds with >98% *Z* selectivity and 59% yield of **3.21b** (entry 2). More importantly, catechothiolate **Ru4b** is fully tolerant of alcohols, as evidenced by the efficient ROCM involving a diol substrate **3.22**, which proceeds readily with styrene to give **3.23a** in 85% yield and 98% *Z* (entry 3). The reaction also readily takes place with electron-deficient 3-fluorostyrene (98% *Z*; 81% yield of **3.23b**, entry 4), electron-rich 4-methoxystyrene (96% *Z*; 93% yield of **3.23c**, entry 5), and vinyl cyclohexane (>98% *Z*; 62% yield, entry 6).

In addition to norbornene and related derivatives, ROCM of cyclobutene **3.24** with styrene also proceeds to give 67% yield of **3.25** (93% *Z*) with 3 mol% **Ru4b** (40 °C, 12 h, entry 7). The elevated temperature (vs 22 °C) and catalyst loading (vs 1.0 mol %) required in this case might be a consequence of intramolecular chelation of the Ru center with the benzyloxy group, which would decrease the catalyst activity (*cf.* Scheme 1.3.2-1, Chapter 1). Most remarkably, synthesis of sterically congested **3.27** involving a quaternary carbon center at the allylic position is achieved through ROCM involving styrene cross partner (69% yield and >98% *Z*, entry 8).

3.3.2.2 Reactions With Less Hindered Cross Partners

Although highly efficient transformations with hindered olefins demonstrate ideal catalytic activity, there are distinct issues associated with reactions involving less sterically imposing substrates: 1) Unhindered cross partners could undergo more facile homocoupling to generate the potentially unstable Ru-methylidene that might rapidly decompose 2) ROCM products with more diminutive substrates would be relatively exposed and susceptible to post-OM isomerization.⁷ In order to investigate the variation in efficiency and selectivity as function of steric hindrance of the cross partner, we selected terminal alkenes of different sizes (Scheme 3.3.2.2). With cross partners involving bulky groups situated at β -position (i.e. allyl trimethylsilane and allyl 4-methoxybenzene), the ROCM proceeds to give **3.28a** and **3.28b** with high *Z* (>98%) and exceptional yields (89% and 83%, respectively). Although the reactions with terminal alkenes involving a substituent at γ -site also proceed with >98% *Z* selectivity to give **3.28c** and **3.28d**, the relatively lower efficiency (65% and 68%, respectively) could result from the generation of unstable Ru-methylidene due to competitive homocoupling.

Scheme 3.3.2.2. Z-selective ROCM of Less Hindered Alkenes



Consistent with the aforementioned hypothesis, ROCM involving the least hindered 1-decene generated **3.28e** in 58% yield and >98% *Z*. Another comparison involves ROCM of cyclobutene **3.24** with allylbenzene, which affords 58% yield (vs 67% with more-hindered styrene, entry 7, Table 3.3.2-1). These studies led to two important findings: 1) The preference for **3.20z** (*cf.* Scheme 3.3.2-1) remains despite the diminishing size of the terminal alkene partners 2) homocoupling of unhindered alkenes poses a serious complication that affects the catalyst longevity and overall reaction efficiency.

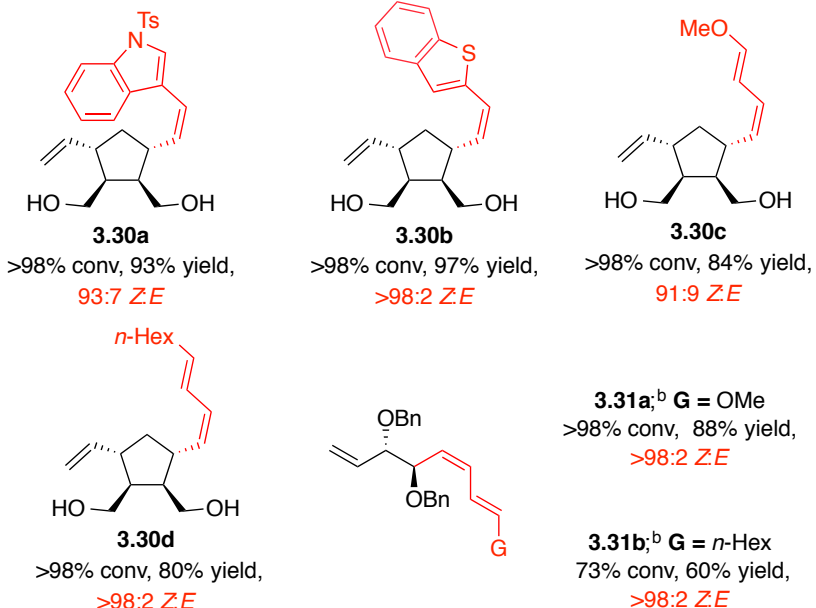
3.3.2.3 Scope With Conjugated Alkenes

After exploring the effect of sterics on selectivity, we set out to examine the reaction scope with different conjugated terminal alkenes. Our study began with considering carbon-substituted conjugated alkenes listed below (Scheme 3.3.2.3a). In this respect, synthesis of *Z*-alkene heteroaryls **3.30a** and **3.30b** readily takes place with impressive efficiency and selectivity (93% yield, 93% *Z* and 97% yield, >98% *Z*, respectively) within 2 h at ambient temperature. These results further encouraged us to

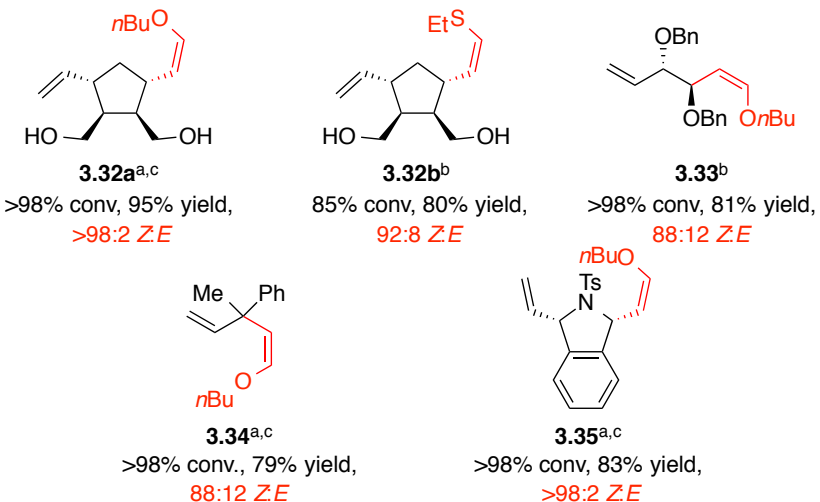
explore reactions with 1,3-dienes as cross partners, the *Z*-selective examples of which are scarce.²⁸ As shown, the transformations proceed with considerable facility and at least 80% isolation yield and >98% *Z* is observed in most examples (**3.30c-d** and **3.31a-b**).

Scheme 3.3.2.3. High *Z* selectivity with Conjugated Olefins

a. ROCM with C-substituted conjugated olefins^a



b. ROCM with O- and S-substituted conjugated olefins



^aReaction is run for 2.0 h at 22 °C. ^bReaction is run for 12 h at 40 °C. ^c2 mol% loading of **Ru4b**.

(28) For the only examples of *Z*-selective OM with 1,3-dienes: Townsend, E. M.; Schrock, R. R.; Hoveyda, A. H. *J. Am. Chem. Soc.* **2012**, *134*, 11334–11337.

Subsequently, ROCM with O- and S-substituted alkenes, which is known to be sluggish (see chapter two), was considered. The only report of Ru-catalyzed Z-selective ROCM with such alkenes is promoted by a stereogenic-at-Ru carbene bearing a bidentate NHC ligand, which promotes the desired reaction through a Curtin-Hammett pathway.²⁷ However, the ability of the iodo-aryloxide Ru complex to catalyze Z-selective ROCM processes is limited (i.e. *E*-selectivity with aryl or aliphatic olefins). In comparison, **Ru4b** is just as effective in Z-selective ROCM with enol and thienol ethers as it is with aryl- and alkyl-substituted alkenes (Scheme 3.3.2.3b). For instance, reactions of *n*-butylvinyl ether (bve) and phenylvinyl sulfide with diol **3.22** to afford **3.32a** and **3.32b** are robust (95% and 80% yields, respectively) and favor the *Z*-isomer (>98% and 92%, respectively). Moreover, reactions with elaborate cyclic alkenes with different strain energies and functional groups were also investigated. In these instances, ROCM reactions proceeded to generate products (**3.33-3.35**) with remarkable selectivity (i.e. 88-98% *Z*) and efficiency (up to 83% yield).

3.3.2.4 Positive Influence of H-Bonding on Reactivity and Selectivity

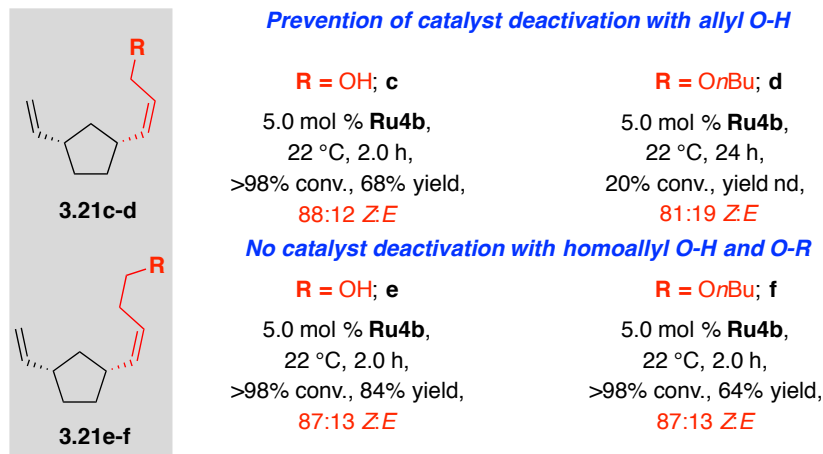
Considering the robust nature of **Ru4b** in the presence of alcohols shown in the examples listed thus far, we turned our attention towards exploiting allylic and homoallylic alcohols as viable cross partner in this methodology. It is noteworthy that metathesis reactions involving allyl alcohol are generally associated with various complications regarding catalyst decomposition and/or generation of undesired products.²⁹ Gratifyingly, the reaction of norbornene with allyl alcohol in the presence of 5 mol% **Ru4b** readily takes place (2 h, ambient temperature) and 68% of the desired product **3.21c** is isolated with 88% *Z* content (Scheme 3.3.2.4a).

For qualitative assessment of the efficiency of reaction with allyl alcohol, ROCM with the corresponding *n*-butyl protected derivative was performed. Interestingly, only 20% conversion takes place to generate **3.21d** after 24 hours. Most remarkably, such a difference in reactivity does not apply to homoallyl alcohol and its alkyl ether (**3.31e** and **3.21f**). Bearing in mind the efficiency of reactions with linear alkenes (*cf.* Scheme

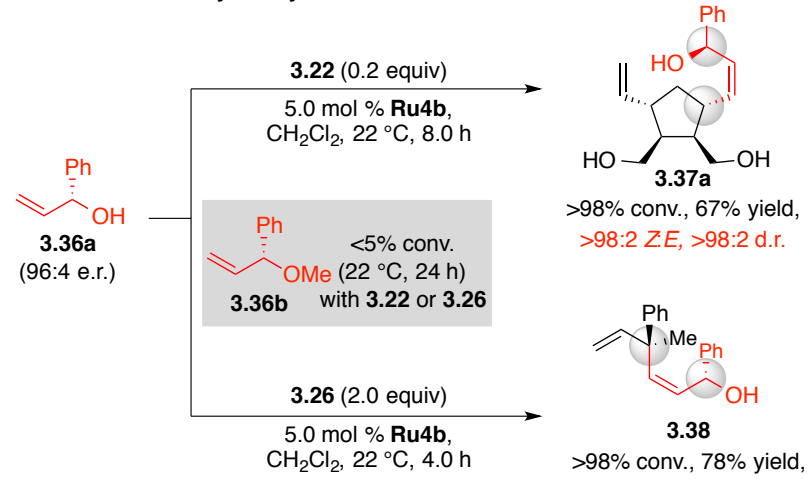
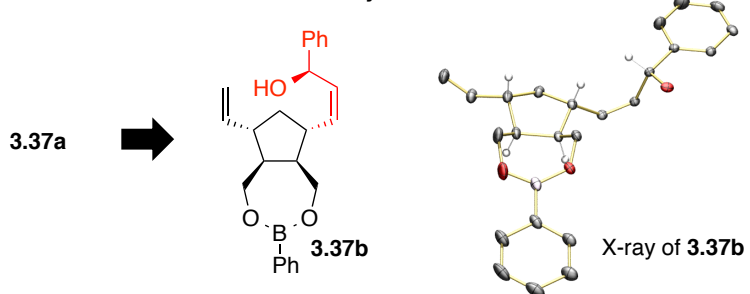
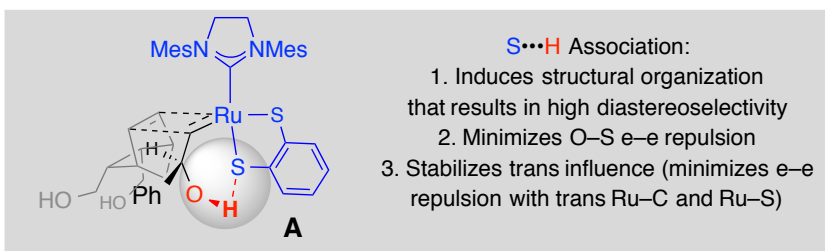
(29) Olefin metathesis with allyl alcohol can lead to catalyst decomposition, see: (a) Werner, H.; Grünwald, C.; Stürer, W.; Wolf, J. *Organometallics* **2003**, *22*, 1558–1560. Olefin metathesis products of allylic alcohols can also undergo undesirable alkene isomerization/ketone formation, see: (b) Schmidt, B.; Hauke, S. *Org. Biomol. Chem.* **2013**, *11*, 4194–4206.

3.3.2.2), it appears that insertion of an alkoxy substituent at the allylic position induces an unfavorable effect pertaining to catalyst deactivation, one that is no longer present when a hydroxyl group is used (i.e. allyl alcohol). The aforementioned positive influence of the allylic alcohol on catalyst activity could likely originate from the H–bonding that takes place between the hydroxyl group and the S-dianions (*cf.* Section 1.5.3, Chapter 1).

Scheme 3.3.2.4a. Enhancement of Activity in the Presence of Allyl Alcohol



In order to gain further insight, we examined the ROCM of an enantiomerically enriched 2° allylic alcohol **3.36a** (96:4 er), since the facility with which the relatively bulky *Z*-alkene is generated could further validate the positive impact of the –OH group. Furthermore, the extent of the promotion of diastereoselectivity could provide crucial information regarding the nature of the positive influence of allylic alcohol substituent. Consistent with our observation with allyl alcohol, the subjection of **3.36a** and **3.22** (5:1) in the presence of 5.0 mol % **Ru4a** leads to complete disappearance of the starting material (8 hours, 22 °C, Scheme 3.3.2.4b-1), affording triol **3.37a** in 67% yield as a single diastereomer (>98:2 *Z:E* and >98:2 d.r.). The stereochemical identity of the major isomer was established by the X-ray structure of the corresponding phenylboronate derivative **3.37b** (Scheme 3.3.2.4b-2). When **3.36a** is treated with cyclopropene **3.26** (1:2), under the same conditions, the desired *cis* alkene **3.38** is obtained in 78% yield, 91% *Z* selectivity, and 93:7 d.r. Most notably, as before, there is no noticeable conversion after 24 hours (22 °C) when the methyl ether **3.36b** is used as cross partner in transformations with **3.22** or **3.26**.

Scheme 3.3.2.4b. Highly Z- and Diastereoselective ROCM Involving 2° Allylic Alcohol**1. Enhanced activity of allylic alcohols in Z- and diastereoselective ROCM****2. Proof of absolute stereochemistry for 3.37a****3. H-bonding leads to high diastereoselectivity**

The above observations are similar to our previous results with Ru-dichloride catalyst that showed higher activity and diastereoselectivity in ROCM with allylic alcohols (vs their protected variants). In that particular case, the electrostatic attraction (H-bonding) between the hydroxyl unit and the halides was put forth as the principal reason for the rate acceleration and structural organization that translates to elevated d.r.

values (Chapter 1). Thus, it is hypothesized that similar principles are likely operative with Ru complex containing S-based dianions (Scheme 3.3.2.4b-3).³⁰

The structural organization provided by H-bonding translates into a high degree of diastereofacial differentiation. Such interaction could also stabilize the ruthenacyclobutane **A** and the corresponding transition state for its formation by minimizing the trans influence that arises from the presence of the NHC and sulfide donors anti to each other. Moreover, the proton bridge dispenses with the electron–electron repulsion that otherwise exists between the heteroatom-containing carbene substituent derived from an allylic oxygen and the nearby sulfide leading to a slow rate of ROCM. These observations point to important electronic interactions involving an anionic sulfur ligand, particularly one positioned opposite to a donor ligand (e.g., an NHC). Overall, catechothiolate **Ru4a** takes advantage of the proximal alcohol substituent in alkenes, and high activity and selectivity is promoted.

3.3.3 DFT Investigation for Stereochemical Model for Z Selectivity

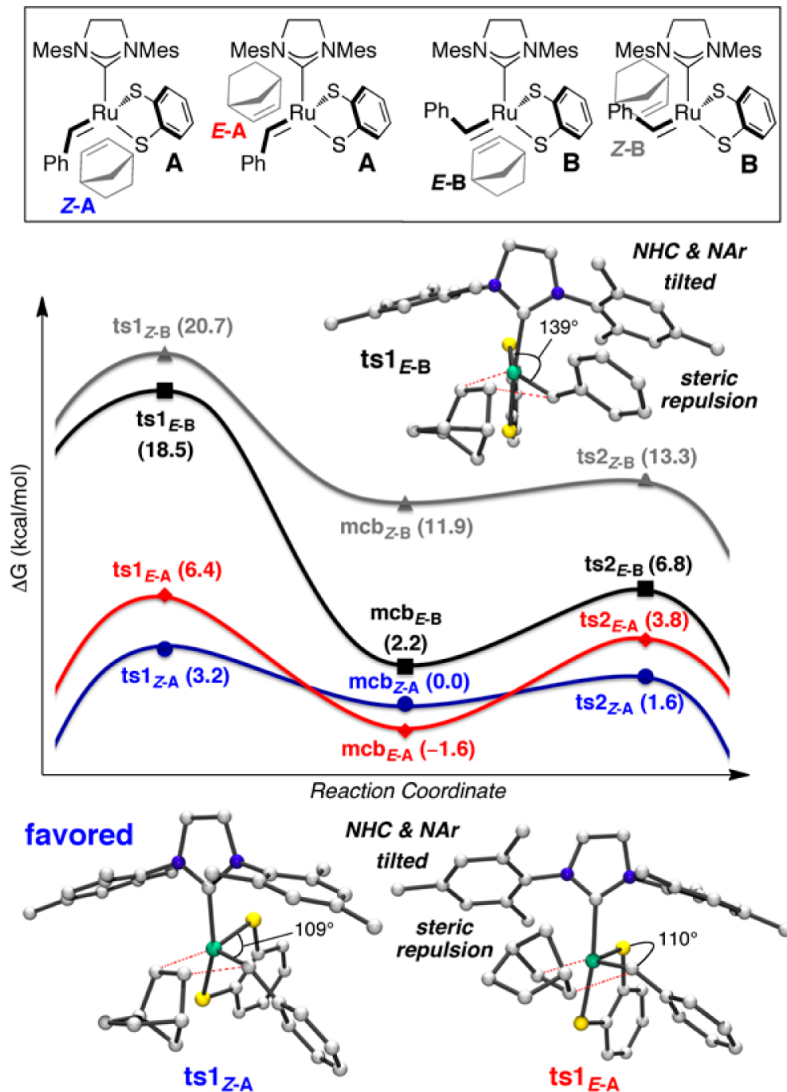
To gain insight regarding the origin of *Z* selectivity with **Ru4b**, ROCM of norbornene and styrene was considered for a detailed computational analysis. As shown in Scheme 3.3.3, free energy surfaces of four possible modes of norbornene addition leading to the formation of both alkene isomers were computed (*Z*-**A**, *E*-**A** and *Z*-**B**, *E*-**B**). The analysis of calculations reveals that formation of ruthenacyclobutane (**mcb**) is the rate-limiting step, which is likely due to the sterically demanding nature of its syn-to-NHC orientation.

Furthermore, the transition states (**ts1_{Z-B}** and **ts1_{E-B}**) associated with the formation of **mcb_{Z-B}** and **mcb_{E-B}**, respectively, are highly disfavored due to steric repulsion between the benzylidene and the large NHC ligand, which forces the heterocyclic moiety and the mesityl plane to undergo a tilt (*cf.* **ts1_{E-B}**). The latter effect is manifested in bending of benzylidene to give S–Ru–C angle of 139° in **ts1_{E-B}** (vs 109° and 110° in

(30) For studies on H-bonding interactions with S-containing functional groups, see: a) Wennmohs, F.; Staemmler, V.; Schindler, M. *J. Chem. Phys.* **2003**, *119*, 3208–3218; b) Tsogoeva, S. B.; Yalalov, D. A.; Hateley, M. J.; Weckbecker, C.; Hutchmacher, K. *Eur. J. Org. Chem.* **2005**, 4995–5000; c) Schreiner, E.; Nair, N. N.; Pollet, R.; Staemmler, V.; Marx, D. *Proc. Nat. Acad. Sci.* **2007**, *104*, 20725–20730; d) Zhou, P.; Tian, F.; Lv, F.; Z. Shang, *Proteins* **2008**, *76*, 151–163.

ts1_{Z-A} and **ts1_{E-A}**, respectively). More importantly, comparison of the lower in energy modes of addition clearly shows that **ts1_{Z-A}** (3.2 kcal/mol), which leads to the Z alkene, is favored over **ts1_{E-A}** (6.4 kcal/mol). Overall, the hitherto mentioned results point towards the validity of our initial hypothesis for the development of Z-selective OM catalyst (*cf.* Scheme 3.2.2-1).

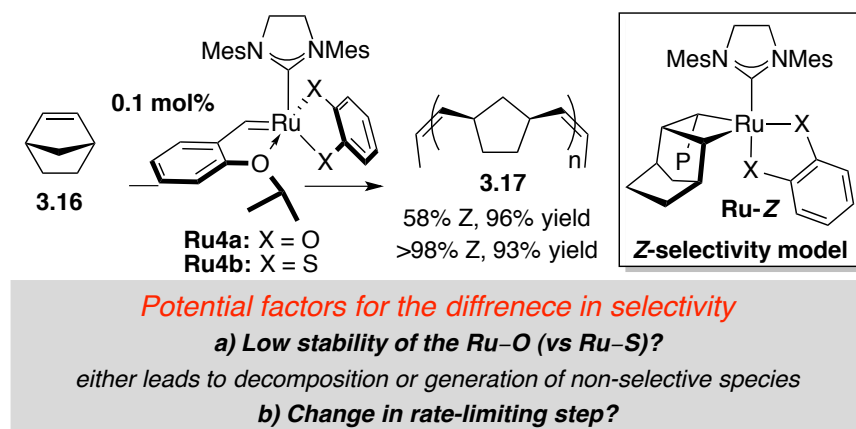
Scheme 3.3.3. Z-Selectivity Model Based on Computational Analysis



3.4 Reactivity and Selectivity Differences Between Catecholate and Catechothiolate Catalysts in Olefin Metathesis³¹

Ever since the disclosure of high Z selectivity with **Ru4b** and lack thereof with **Ru4a** in OM (Scheme 3.4 and Section 3.3.1), we reasoned that the general scheme for *cis* alkene formation, which is largely based on steric environment, solely should not function as a reliable design template. Other factors such as the distinct electronic attributes (donorability, hard/soft anionic character and orbital overlap) of oxygen and sulfur, which would affect the relative strengths of Ru-O and Ru-S bonds, must also play a critical role in the promotion of Z selectivity.

Scheme 3.4. Difference in Selectivity Promoted by Ru4a and Ru4b



In order to put forth a plausible rationale, we set out to investigate the stability of **Ru4a** and **Ru4b** under various conditions. Additionally, a computational investigation was performed to probe whether the observed selectivity has kinetic origins that arise due to a change in rate-limiting step.

3.4.1 Reactivity and Structural Integrity of Diolate vs Dithiolate Complexes

In order to shed light onto the factors that cause the stark difference in selectivity for **Ru4a** and **Ru4b**, we initiated our investigation by studying their reactivity and structural robustness differences in the presence of various conditions listed below.

(31) Khan, R. K. M.; Torker, S.; Hoveyda, A. H. *J. Am. Chem. Soc.* **2014** *136*, 14337–14340.

3.4.1.1 Stability in the Presence of Alkenes with Alcohol Substituents

First off, we suspected that the disparity in selectivity could be resulting from differences in lability of Ru–O vs Ru–S bonds. A slight slippage of the catecholate in the ruthenacyclobutane intermediate (**Ru-Z**, Scheme 3.4; *cf.* **mcb_{Z-A}**, Scheme 3.3.3) would be detrimental in effective promotion of *Z* selectivity. Moreover, **Ru4a** could be prone to decomposition in the presence of various functional groups to complexes that readily catalyze non-selective OM. On this basis, we decided to evaluate the performance of **Ru4a** and **Ru4b** in ROCM with alcohol-containing alkenes.

Table 3.4.1.1. Reactivity Comparison of Ru4a and Ru4b in Z-Selective ROCM

entry	product	G	Ru mol%	with Ru4a conv (%); ^a <i>Z:E</i> ^b	with Ru4b conv (%); ^a <i>Z:E</i> ^b
1		g C ₆ H ₅	5.0	>98; 55:45	>98; 97:3
2		h CH ₂ OH	5.0	<2; na	>98; 88:12
3		i CH ₂ CH ₂ OH	5.0	<2; na	>98; 87:13
4		a C ₆ H ₅	1.0	<2; na	>98; 97:3
5		b C ₆ H ₁₁	1.0	<2; na	88; >98:2

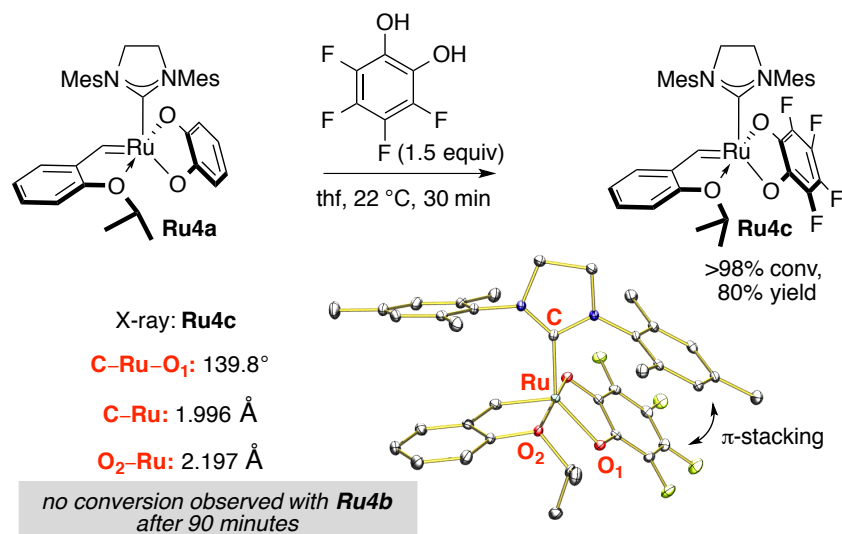
^aSee experimental section for details. ^bDetermined by ¹H NMR analysis of the unpurified products.

As shown in Table 3.4.1.1, while transformation promoted by **Ru4a** is efficient with styrene (entry 1), albeit with poor *Z* selectivity, there is no noticeable conversion when alcohol containing cross partners are used (entries 2 and 3). A similar trend emerges with a cyclic alkene bearing two alcohol units (entries 4 and 5). In contrast, **Ru4b** efficiently promotes highly *Z*-selective reactions in all cases. The above examples with **Ru4a** (entries 2–5) indicate that exchange of the catecholate with alcohol units (alcoholysis) likely leads to the inhibition of catalyst activity, which would be consistent

with a previous report that demonstrates the lability of oxygen-based ligands involving a Ru–carbene under protic environment.³²

Most notably, treatment of **Ru4a** with tetrafluorocatechol readily leads to its full conversion within 30 minutes at 22 °C (>98% conv, 80% yield of **Ru4c**, Scheme 3.4.1.1). The mentioned outcome validates the proposal that O-anions in Ru carbene complex readily exchange with hydroxyl groups. To our surprise, the C–Ru–O¹ angle is considerably more contracted in **Ru4c** as compared to **Ru4a** (139.8° vs 149.2°), despite the presumably reduced trans influence between NHC donor (C) and aryloxide anion (O¹). The latter feature potentially originates from the π-stacking interaction between the electron deficient tetrafluorocatecholate and the mesityl ring of the NHC.

Scheme 3.4.1.1. Facile Exchange of Catecholate in Ru4a Through Alcoholysis



Moreover, NHC donor is strongly coordinated to the relatively more Lewis acidic Ru center in **Ru4c** as represented by the shorter 1.996 Å length of C–Ru (vs 2.015 Å in **Ru4a**). As a consequence of the close proximity of the large NHC (i.e. shorter C–Ru length and tilt due to π-stacking) to the 2-isopropoxy chelating unit, the O₂–Ru length is slightly longer in **Ru4c** (2.197 Å vs 2.192 Å in **Ru4a**). In contrast with **Ru4a**, exposure of catechothiolate **Ru4b** to tetrafluorocatechol under the same condition does not lead to

(32) For example involving the alcoholysis of oxygen-based anion in Ru complex, see: Sanford, M. S.; Henling, L. M.; Day, M. W.; Grubbs, R. H. *Angew. Chem., Int. Ed.* **2000**, *39*, 3451–3453.

any conversion even after 90 min. This finding provides a clear rationale for facile reactions with **Ru4b** (listed in Table 3.4.1.1).

3.4.1.2 Non-Innocent Character of Chlorinated Solvents

At this juncture, we were faced with studying further the constitutional stability of catecholate and catechiolate complexes in commonly used chlorinated solvents. The motivation for this investigation came from previous reports in which Fogg and coworkers have shown that ROMP promoted by Ru bisaryloxides³³ and a closely related catecholate³⁴ are considerably efficient but non-stereoselective in the presence of chloroform as solvent. It was surmised that a ligand exchange with chlorinated solvents such as CHCl₃ or CH₂Cl₂ would potentially give rise to a highly active dichloro-Ru carbene, which might account for the stereoselectivity differences noted above. In line with our hypothesis, ROMP of **3.16** in the presence of **Ru3** and **Ru4a** in CHCl₃ proceeds with nearly identical stereoselectivities (~55:45 Z:E and ~58:42 Z:E). This proposal is further supported by a report by Grubbs and coworkers that involves decomposition of a Ru complex containing two carboxylic ester ligands to the corresponding dichloride upon exposure to dichloromethane.³⁵ Although the said study does not include any discussion regarding the cause or implications on olefin metathesis, the observation clearly indicates the potential for generation of an entirely different catalytically active species other than the precatalyst entrusted with promoting efficient and stereoselective reaction.

Most unexpectedly, we discovered that the addition of catecholate **Ru4a** to CDCl₃, which is freshly passed through basic alumina to neutralize acidic residues, leads to complete disappearance of the initial carbene signal at δ 16.03 within 15 minutes at ambient temperature (Scheme 3.4.1.2-1a). The transient carbene (δ 16.68, Scheme 3.4.1.2-1c), the exact identity of which is unknown and currently the subject of ongoing investigations, subsequently converts to Ru dichloride **Ru3**²¹ (δ 16.51, Scheme 3.4.1.2-1d) in 12 hours, which is easily isolated in 48% yield after silica gel chromatography.

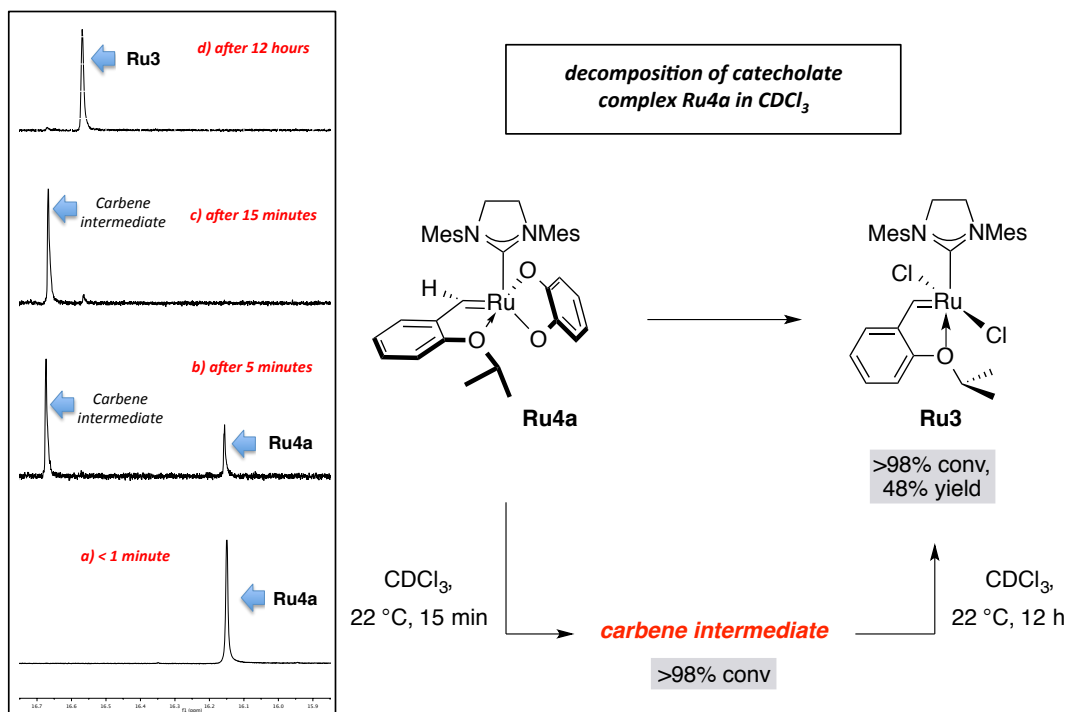
(33) Conrad, J. C.; Amoroso, D.; Czechura, P.; Yap, G. P. A.; Fogg, D. E. *Organometallics* **2003**, *22*, 3634–3636.

(34) (a) Monfette, S.; Fogg, D. E. *Organometallics* **2006**, *25*, 1940–1944. (b) Monfette, S.; Camm, K. D.; Gorelsky, S. I.; Fogg, D. E. *Organometallics* **2009**, *28*, 944–946.

(35) (a) Herbert, M. B.; Lan, Y.; Keitz, B. K.; Liu, P.; Endo, K.; Day, M. W.; Houk, K. N.; Grubbs, R. H. *J. Am. Chem. Soc.* **2012**, *134*, 7861–7866. For reactions of Ru(II) complexes with CH₂Cl₂, see: (b) Oliván, M.; Caulton, K. G. *Inorg. Chem.* **1999**, *38*, 566–570.

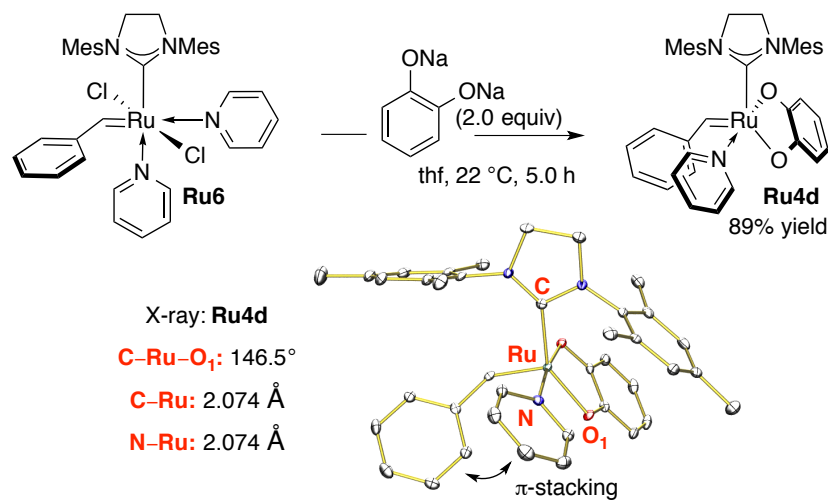
The aforementioned transformation casts serious doubts over the viability of $\text{CHCl}_3/\text{CDCl}_3^{33,34}$ as a solvent of choice in selective OM promoted by Ru bisaryl- and alkyloxides.

Scheme 3.4.1.2-1. Stepwise Conversion of Ru4a to Ru3 Mediated by CDCl_3



At this stage, we decided to study the change in Lewis acidity at Ru and/or the strength of the chelating unit on complex stability. In this respect, comparison of **Ru4a**

Scheme 3.4.1.2-2. Preparation of Pyridine Adduct of Catecholate Ru4d



with the more Lewis acidic **Ru4c** and the strongly coordinating pyridine adduct **Ru4d** was proposed. The latter complex is easily accessed through the reaction of **Ru6** with 2.0 equivalents of disodium catecholate at 22 °C within 5.0 h (Scheme 3.4.1.2-2). Consistent with the strongly coordinating nature of pyridine, the X-ray of **Ru4d** reveals that N–Ru bond (2.074 Å) is significantly shorter than the chelation bonds involving 2-isopropoxy units in **Ru4a** and **Ru4c** (O₂–Ru: 2.192 Å and O₂–Ru: 2.197 Å, respectively).

Table 3.4.1.2. Stability of Catecholates (Ru4a**, **Ru4c**, and **Ru4d**) in Chlorinated Solvents**

Ru carbene complexes		CDCl ₃ or CD ₂ Cl ₂		conversion products (mainly transient carbene intermediate and Ru3) ^a	
		with CDCl ₃		with CD ₂ Cl ₂	
entry	Ru complex	temp (°C); time	conv (%) ^b	temp (°C); time	conv (%) ^b
1	Ru4a	22; 10 min	97	50; 24 h	82
2	Ru4c	22; 10 min	16	50; 24 h	29
3	Ru4d	22; 12 h	11	50; 24 h	20

^aSee experimental section for details. ^bDetermined by ¹H NMR analysis of the reaction mixture.

With **Ru4d** in hand, solution-phase stabilities of all catecholate Ru complexes in CDCl₃ and CD₂Cl₂ were assessed through ¹H NMR spectroscopy (table 3.4.1.2). In comparison with 97% conversion of **Ru4a** in CDCl₃ at 22 °C, only 16% of **Ru4c** is consumed (entries 1-2). The slower rate of decomposition with the latter complex could be due to relatively stronger coordination of the 2-isopropoxy chelate with the electron-deficient Ru, which leads to enhancement in stability (vs fast formation of the unstable 14e complex in **Ru4a** which results from 2-isopropoxy decoordination).³⁶ More notably, only 11% degradation of **Ru4d** takes place after 12 h (entry 3). This observation further gives credence to our proposal that stability of the 16e complex disfavors decomposition in CDCl₃. Decomposition in CD₂Cl₂ demanded elevated temperatures, conditions under which Ru catecholates have been used to promote OM;^{34b} specifically, 82% conv of **Ru4a** was observed at 50 °C, affording 27% **Ru3** (<2% conv at 22 °C). Furthermore, degradation of **Ru4c** and **Ru4d** also takes place (29% and 20%, respectively). The

(36) The significance of the loss of a coordinating ligand to Kharasch-type reactions with chloroform has indeed been documented; see: (a) Simal, F.; Włodarczak, L.; Demonceau, A. Noels, A. F. *Eur. J. Org. Chem.* **2001**, 2689–2695. For Kharasch reaction in the presence of a dichloro-Ru carbene, see: (b) Tallarico, J. A.; Malnick, L., M.; Snapper, M. L. *J. Org. Chem.* **1999**, 64, 344–345.

spectroscopic analysis of catechothiolate **Ru4b** sample in CDCl_3 (22 °C) or CD_2Cl_2 (50 °C) indicates decomposition as well (~50% in CDCl_3 , 1.0 h, 22 °C; <10% in CD_2Cl_2 , 24 h, 50 °C) but dichloride **Ru3** is not detectable (with 400 MHz NMR spectrometer). Currently, studies are underway to investigate the mechanisms of such decompositions.

With regards to **Ru4a** as catalyst in OM, lack of stereoselectivity is observed (*cf.* entry 1, Table 3.3.1) even when adverse conditions for the formation of **Ru3** are avoided altogether (i.e. no **Ru3** is formed in CD_2Cl_2 at 22 °C). More importantly, ROMP of norbornene in thf, wherein the conversion of **Ru4a** to **Ru3** is impossible, also proceeds with minimal stereoselectivity (~55:45 Z:E). These observations in turn indicate the potentially kinetic origins of selectivity with catecholate and catechothiolate catalysts.

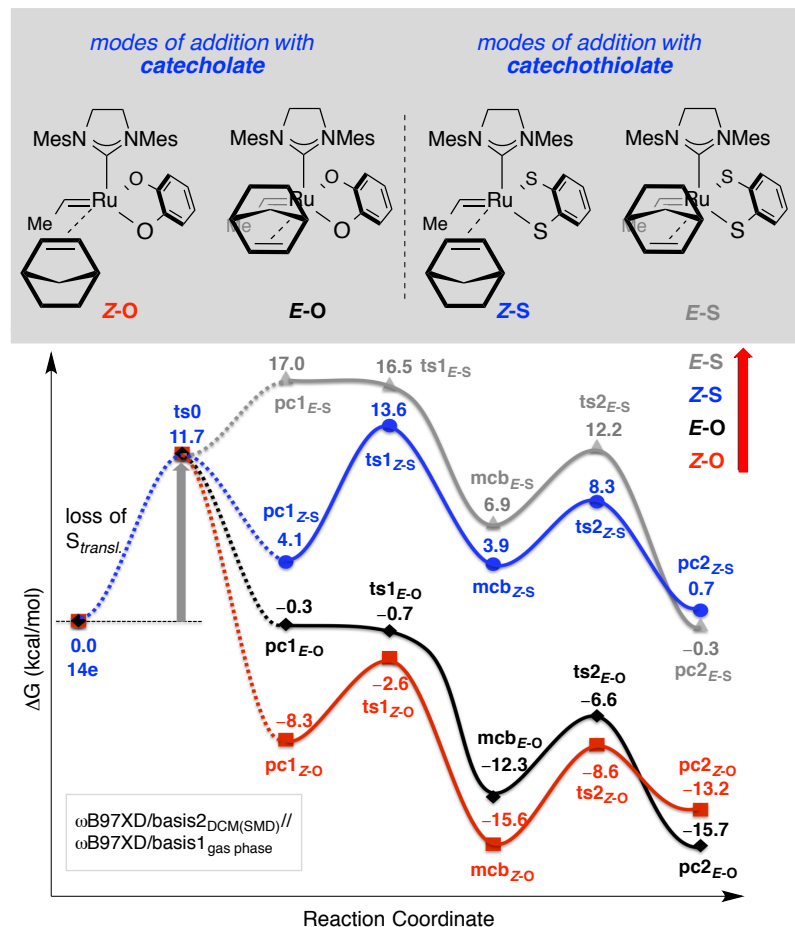
3.4.2 Rationale for Kinetic Z Selectivity with Ru Catechothiolate (vs Catecholate) Through Computational Analysis

While the abovementioned results clearly indicate the lack of stability with Ru–O (vs Ru–S), computational studies³⁷ were conducted to uncover the factors that lead to the observed selectivity with catecholate and catechothiolate in OM. In this respect, comparison of the calculated Gibbs free energy surfaces of metatheses involving norbornene **3.16** (up and down approach) and ethylidene derived from **Ru4a** and **Ru4b** was performed (Scheme 3.4.2-1). The study reveals that transformation promoted by the former complex is kinetically not Z-selective. What is more, irrespective of the nature of the bidentate dianion, the pathways leading to the Z isomer are lower in energy (**Z-O** and **Z-S** for catecholate and catechothiolate, respectively) indicating that **mcb_{Z-O}** and **mcb_{Z-S}** posses the sterics necessary for the generation of cis-alkene. However, the difference in stereoselectivity is manifested due to the change in rate-limiting steps involving these pathways (i.e. **ts0** for catecholate and **ts1** for catechothiolate). Detailed analysis of the energy diagram provides details for the aforementioned change. Whereas the norbornene coordination with **Ru4a**-derived ethylidene is endergonic (4.1 kcal/mol, **pc1_{Z-S}**) in **Z-S** pathway, it is exergonic in case of **Ru4b**-derived ethylidene (**pc1_{Z-O}**, -8.3 kcal/mol). The difference in relative energies of the corresponding ruthenacycles is even larger, placing

(37) DFT computations are performed with Gaussian 09 at: $\omega\text{B97XD}/\text{basis2}_{\text{DCM}(\text{SMD})}/\omega\text{B97XD}/\text{basis1}_{\text{gas-phase}}$ level of theory.

mcb_{Z-O} significantly below the unsaturated 14e intermediate (-15.6 kcal/mol). Such energetic characteristics overwhelmingly suggest a change in stereochemistry-determining step. While **ts1** shows the preference for **Z-S** (13.6 kcal/mol vs 16.5 kcal/mol in **E-S**) with catecholate, leading to the generation of Z-alkenes, the stereochemical differentiation with catecholate through formation of a metal–olefin complex (**ts0**) is less effective, thus rendering **Z-O** and **E-O** equally likely. This electronic effect overrides the proper steric environment for the formation of Z-olefins with **Ru4a**, which is reflected by the difference between **ts1_{Z-O}** and **ts1_{E-O}** (-2.6 vs -0.7 kcal/mol).

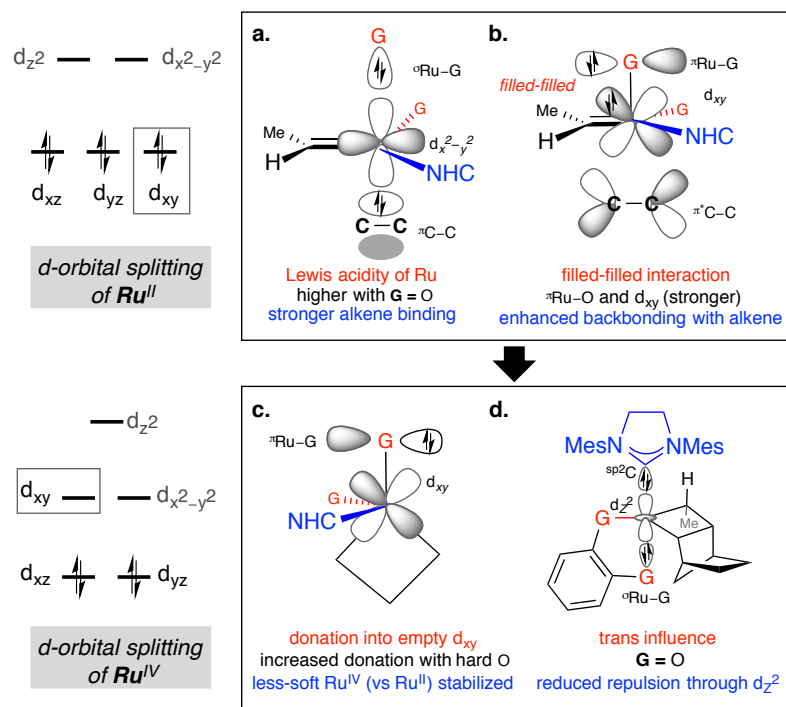
Scheme 3.4.2-1. DFT Based Rationale for (Ru4a and Ru4b) Selectivity



The high affinity for 14e Ru catecholate to bind olefin (vs 14e Ru catechothiolate) to form the square pyramidal π -complex comprises of two salient features: 1) weaker σ -donorability of O-based dianions renders the Ru^{II} center more Lewis acidic (Scheme

3.4.2-2a) and favors coordination with the 2e donor alkene 2) filled-filled interactions³⁸ between hard O and Ru-d_{xy} orbital result in increased backdonation into the π^* orbital of the alkene for preferred association (Scheme 3.4.2-2b). Furthermore, the stabilizing effect of oxygen is even more pronounced in Ru^{IV} metallacyclobutane of trigonal bipyramidal (TBP) geometry (i.e. **mcb_{Z-O}**: -15.6 kcal/mol vs **mcb_{Z-S}**: 3.9 kcal/mol, Scheme 3.4.2-1). Presumably, stronger π -donation of oxygen into empty Ru-d_{xy} orbital effectively stabilizes the higher Ru oxidation state (Scheme 3.4.2-2c). Added to this influence is the diminution of trans influence between the strong NHC σ -donor and weaker σ -donating O in the axial plane, which also lowers the energy of O-based ruthenacycle (Scheme 3.4.2-2d).

Scheme 3.4.2-2. Operative Electronics Effects for Selectivity Differences



The abovementioned results, in conjunction with the utility of **Ru4b** in promoting a wide range of OM transformations, point towards the potential for thiolate-based dianions as optimal ligands for future catalyst development.

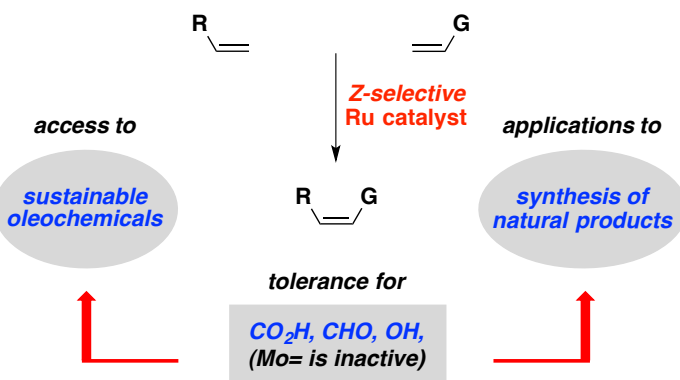
(38) For reports dealing with the stronger π -donor ability of O vs S ligands, see: (a) Huang, J.; Li, C.; Nolan, S. P.; Petersen, J. L. *Organometallics* **1998**, *17*, 3516–3521. (b) Chisholm, M.; Davidson, E. R.; Huffman, J. C.; Quinlan, K. B. *J. Am. Chem. Soc.* **2001**, *123*, 9652–9664.

3.5 Simple Access to Biologically Relevant Molecules and Oleochemicals Through Z-Selective Cross-Metathesis Promoted by a Highly Efficient Ru Catalyst

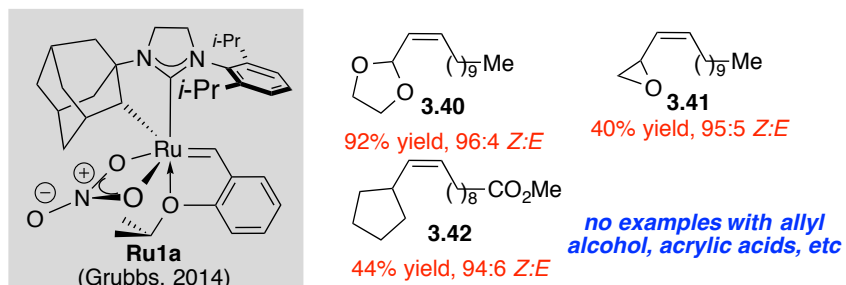
One of the hallmarks of the Ru-carbenes (vs their Mo/W-alkylidene counterparts) is their ability to tolerate air and moisture.³⁹ More notably, alkenes with various protic functional groups (e.g., alcohols and acids)⁴⁰ are used in efficient olefin metathesis protocols. In particular, the alcohol substitutions are shown to increase the catalytic activity of Ru-carbenes in many instances.⁴¹

Scheme 3.5. Advantages and Limitations Associated with Z-Selective CM with Ru

a. Advantages of Z-selective cross-metathesis with Ru carbenes



b. State-of-the-art in Ru catalyzed Z-selective cross-metathesis



(39) For examples of olefin metathesis in aqueous medium, see: (a) Binder, J. B.; Blank, J. J.; Raines, R. T. *Org. Lett.* **2007**, *9*, 4885–4888. For examples involving thin layer chromatography technique, see: (b) Cabrera, J.; Padilla, R.; Dehn, R.; Deuerlein, S.; Gulajski, L.; Chomiszczak, E.; Teles, J. H.; Limbach, M.; Grela, K. *Adv. Synth. Catal.* **2012**, *354*, 1043–1051.

(40) For cross-metathesis of acrylic acid with a highly functionalized alkene involving alcohol substituents, see: Meng, X.; Matson, J. B.; Edgar, K. J. *Biomacromolecules*, **2014**, *15*, 177–187.

(41) For the positive influence of alcohols on Ru-catalyzed olefin metathesis, see: (a) Hoveyda, A. H.; Lombardi, P. J.; O'Brien, R. V.; Zhugralin, A. R. *J. Am. Chem. Soc.* **2009**, *131*, 8378–8379. (b) Hoye, T. R.; Zhao, H. *Org. Lett.* **1999**, *1*, 1123–1125.

In this context, development of efficient and highly *Z*-selective Ru-based catalysts will provide synthetic chemists with an invaluable opportunity to access various natural products of biological importance.^{3a} Moreover, advances in this area will also result in *Z*-selective generation of oleochemicals, which are largely limited to non-stereoselective olefin metathesis.⁴² Although a new class of Ru-based catalysts (e.g., **Ru7**) has been employed to effect *Z*-selective cross-metathesis (CM), these transformations lack the use of functionalizable cross partners such as allylic alcohols (e.g., installation of protecting group is required; **3.40** and **3.41**, Scheme 3.5).⁴³ Additionally, this class of catalysts is highly sensitive to slight variations in sterics of alkene substrate (e.g., 44% yield of **3.42** with bulky vinyl cyclopentane). In light of these observations, the aforementioned class of catalysts does not seem to exhibit similar characteristics as known with the traditionally used Ru-carbenes in OM,^{39,40} which significantly undermine their advantage over highly versatile and robust *Z*-selective Mo/W-catalysts.^{7a-b, 8}

3.5.1 Development of a Highly Active and Efficient Ru Catechothiolate for Widely Group Tolerant *Z*-Selective Cross-Metathesis

Based on the abovementioned observations, we set out to develop a highly *Z*-selective and functional group tolerant CM protocol. Instantly, we were reminded of the high efficiency of **Ru4b** in promoting *Z*-selective ROCM with various alcohols (Section 3.4.1.1), which prompted us to explore its viability in CM to access cis-disubstituted allyl alcohol derivatives. For this purpose, the inexpensive cis-2-butene-1,4-diol was selected as a feasible cross partner.

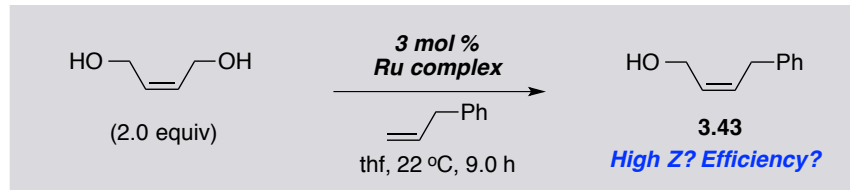
Our studies began with a comparison of **Ru4b**, **Ru5**, and commercially available **Ru1** in CM of allylbenzene with cis-2-butene-1,4-diol to generate **3.43** with high efficiency and *Z* selectivity (Scheme 3.5.1-1a). As shown below, reaction with **Ru1** proceeds to 70% conversion of allylbenzene with 2.0 equivalents of diol to generate **3.43** in 91% *Z*-content within nine hours (thf, 22 °C). While dithiolate **Ru5** does not lead to any conversion to the desired alkene under the same conditions, **Ru4b** promotes 50%

(42) Mol, J. C. *Green Chemistry* **2002**, *4*, 5–13.

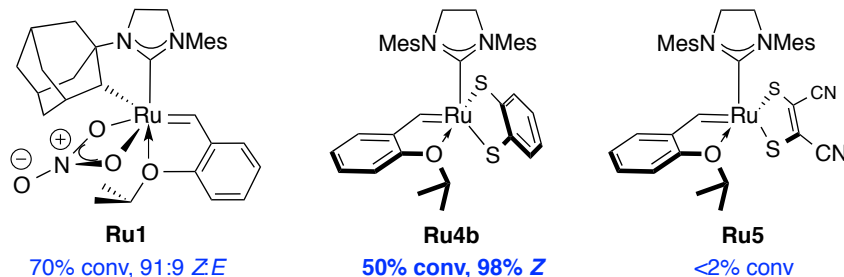
(43) For examples of Ru catalyzed *Z*-selective cross-metathesis with allylic-substituted alkenes, see: Quigley, B. L.; Grubbs, R. H. *Chem. Sci.*, **2014**, *5*, 501–506.

conversion with exclusive generation of the Z-isomer, which is desirable (vs 91% Z with **Ru1**) in cases where separation of the two isomers (*E* and *Z*) is challenging.

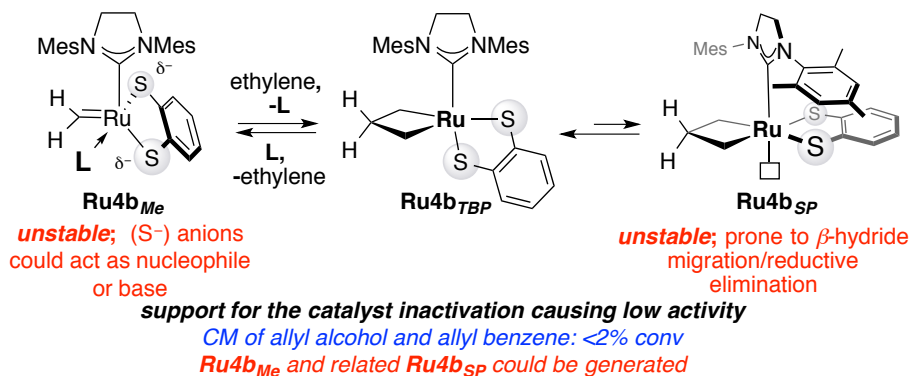
Scheme 3.5.1-1. Z-Selective CM for Functionalized Allyl Alcohol Derivatives



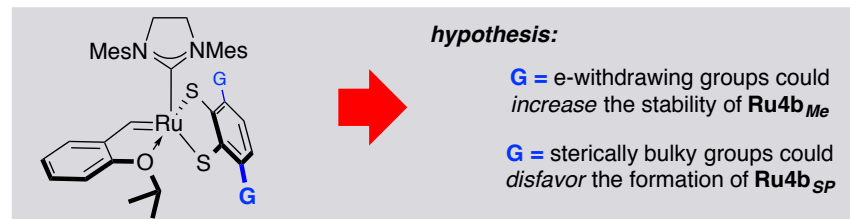
a. Initial screen with Ru carbenes for Z-selective OM



b. Rationale for low activity of dithiolate carbenes



c. Proposal for more active complexes

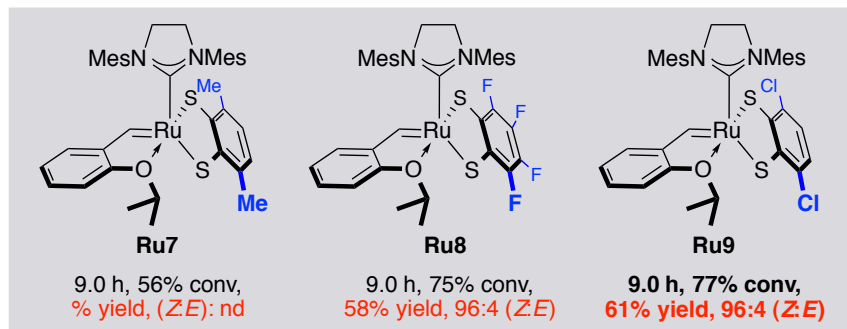


In order to rationalize the relatively lower activity of **Ru4b**, we considered the scenario depicted in Scheme 3.5.1-1b, in which the generation of two unstable complexes (**Ru4b_{Me}** and **Ru4b_{SP}**) derived from side-reactions leads to the decomposition of the

catalytically active species.⁴⁴ In **Ru4b_{Me}**, which results from the homocoupling side-reactions involving allylbenzene and/or allyl alcohol generated at higher conversions, the S-anions could pose two problems that lead to catalytic inactivity: 1) S⁻ adds to the unhindered and electrophilic carbon of the (Ru=C) carbene followed by further decomposition^{35a} 2) deprotonation of carbene ¹H leading to the formation of a carbyne.³³

Another pathway of decomposition could involve the conversion of **Ru4b_{Me}** to form the corresponding **Ru4b_{TBP}**, which then rearranges to **Ru4b_{SP}** isomer that allows for the β-hydride elimination due to an empty coordination site available syn-to-ruthenacyclobutane followed by reductive elimination. It is also noteworthy that only 28% conversion to **3.43** is observed in the presence of less coordinating CH₂Cl₂ (vs thf; 50% conv). The mentioned result indicates the added catalyst stability provided by thf through strong coordination with Ru-methylidene, which disfavors its decomposition. In support for our proposal that implicates the instability of methylidene and/or its **Ru4b_{SP}** derivative for low catalytic activity, the reaction involving allylbenzene and allyl alcohol in the presence of 5 mol% **Ru4b** leads to <2% conversion. In the decomposition scenarios mentioned thus far, the stereoelectronics of S-dianion (i.e. high e-density of S in **Ru4b_{Me}** and small steric size that permits **Ru4b_{TBP}** → **Ru4b_{SP}** rearrangement) allow for the structural variations in Ru-catalyst that lead to decomposition. In order to enhance the catalyst longevity, we proposed the installation of **G** substituents with sizable and e-withdrawing groups that could render the nuances listed in Scheme 3.5.1-1b less effective.

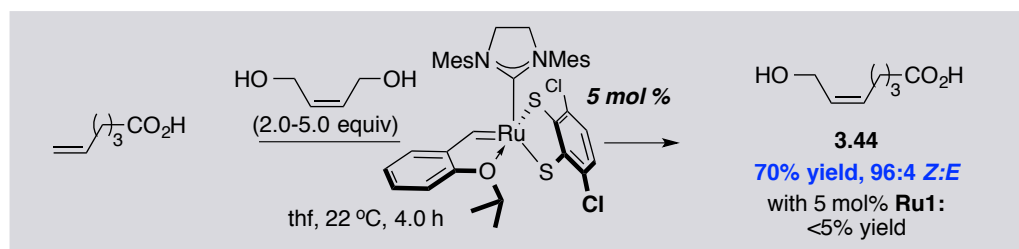
Scheme 3.5.1-2. Highly Efficient and Z-Selective Catalyst for CM



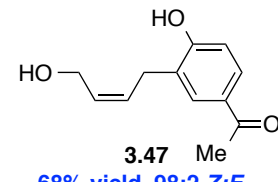
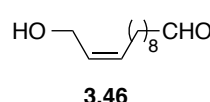
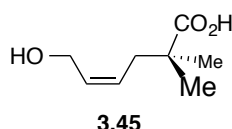
(44) For examples of catalyst deactivation either through the addition of a nucleophile to methylidene or through the formation of unsubstituted ruthenacyclobutane, see: *J. Am. Chem. Soc.* **2007**, *129*, 7961-7968.

To test our hypothesis, we developed⁴⁵ **Ru7**, **Ru8**, and **Ru9** and explored their activity in CM (Scheme 3.5.1-2). As shown, no appreciable change in efficiency (56% conv) takes place with **Ru7** after 9.0 hours, in which the two methyl units are situated at 2,5-positions (vs hydrogen in **Ru4b**; 50% conv, 9.0 h, Scheme 3.5.1-2). Interestingly, the fluorinated analogue **Ru8** leads to 75% conversion under these conditions, which is consistent with our proposal that less e-rich S-dianions could enhance the catalyst lifetime. Most remarkably, reaction with **Ru9**, made from a commercially available dithiol precursor, involving Cl groups at 3,6-positions displays considerable activity (77% conv, 61% yield, 9.0 h). Similar to **Ru8**, we attribute the increased efficiency with **Ru9** to the catalyst longevity that is caused by two-pronged effect of Cl (i.e. large steric size and e-withdrawing ability). Moreover, participation of Cl substituents in intermolecular chelation involving two or more Ru centers (*cf.* cyclohexameric **Ru5**, Scheme 3.2.3) could also offer added stability.

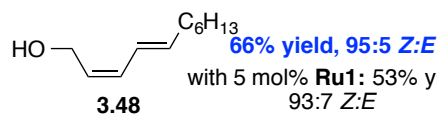
Scheme 3.5.1-3. Comparison for High Group Tolerance with Ru9 and Ru1



Other notable examples:



with 5 mol% **Ru1**: <5% yield



With competent and easily accessible **Ru9** in hand, we decided to investigate the scope of its utility with alkenes involving various functional groups. Outstandingly, CM with 5 mol% **Ru9** proceeds to form **3.44**, which involves a carboxylic acid at the

(45) See experimental section for details.

terminus, in 70% yield and 96% *Z* selectivity (thf, 22 °C, 4.0 h, Scheme 3.5.1-3). In contrast, **Ru1** displays lack of activity. The aforementioned observation indicates the potential for decomposition of the catalyst through protonation of the alkyl chelate (Ru-C) in the presence of protic groups. Our assertion is further confirmed in the generation of **3.45**, in which <5% conversion is observed with **Ru1** whereas 61% yield and 98% preference for the *Z*-isomer is obtained with **Ru9**. It is also noteworthy that the abovementioned transformation is not possible with the high oxidation-state Mo/W-alkylidene counterparts used for *Z*-selective CM. Clearly, **Ru9** provides a unique opportunity in organic synthesis for the facile construction of *Z*-alkenes with acid derivatives through the use of OM. Furthermore, the superiority of **Ru9** (vs **Ru1**) persists in the formation of aldehyde **3.46** (i.e. 80% vs 30% yield and 94% vs 87% *Z*) and ketone **3.47** (68% vs 50% yield and 98% vs 82% *Z*). CM to generate diene **3.48** also proceeds with relative efficiency and selectivity (66% yield and 95% *Z*). Importantly, the reaction with sterically congested styrene to form **3.49** shows sluggishness in efficiency (42% yield with **Ru9**). However, the depreciation in efficiency is even starker with **Ru1**, which gives 35% yield and poor selectivity (72% *Z*). In order to address the issue of lower activity with bulky olefins, efforts are underway to develop highly efficient catalysts. Overall, the results listed in Scheme 3.5.1-3 clearly demonstrate the unrivaled functional group tolerance of **Ru9** and render its employment favorable in a variety of *Z*-selective CM transformations.

3.5.2 Applications in Natural Product Synthesis

To demonstrate the value of the above listed protocols in the context of organic synthesis, we decided to construct functionalized alkenes for biologically relevant targets. Towards this goal, we began by showing that the exposure of 5 mol% **Ru9** to cis-2-butene-1,4-diol and 1-dodecene gives rise to the desired alkene **3.50** in 72% yield with 96% *Z* (thf, 22 °C, 4.0 h, Scheme 3.5.2a). Previously, the olefin product has been

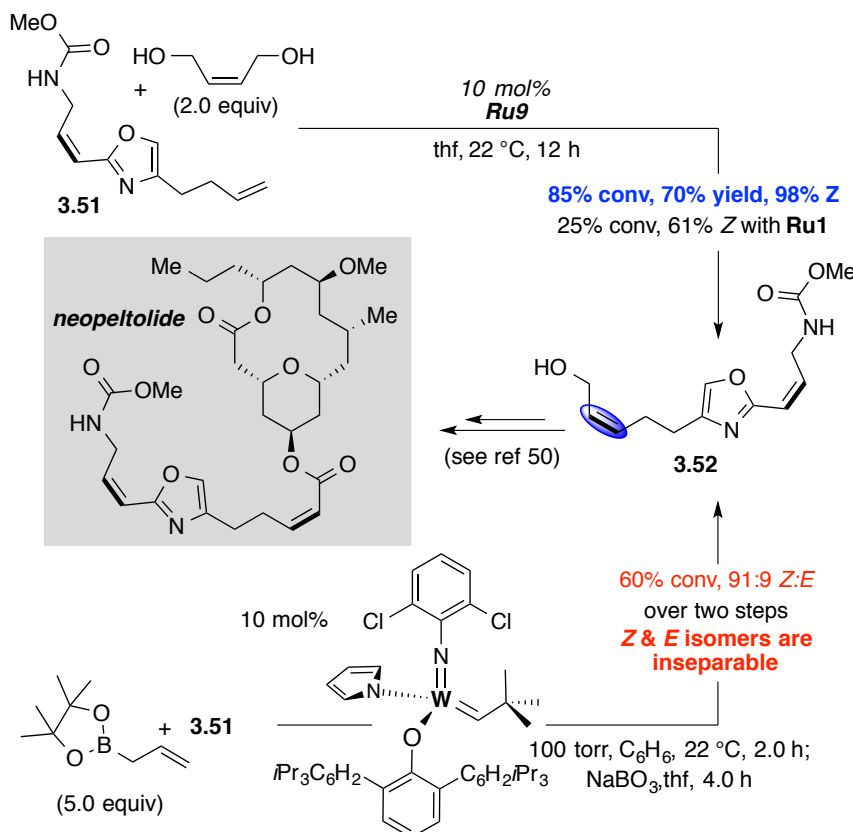
elaborated in three steps⁴⁶ to form (+)-Disparlure, a female sex pheromone of gypsy moth *Porthetria dispar* (L.).⁴⁷

Scheme 3.5.2. Synthetic Applications of Ru-Catalyzed Z-Selective CM

a. Synthesis of a female insect sex pheromone:



b. Synthesis of an anti tumor agent:



We then turned our attention towards the application of **Ru9** catalyzed Z-selective CM in the synthesis of a potent anti tumor agent (+)-neopeltolide.⁴⁸ Our group has

(46) (a) Rossiter, B. E.; Katsuki, T.; Sharpless, K. B. *J. Am. Chem. Soc.* **1981**, *103*, 464–465. For a related report, also see: (b) Wang, Z.; Zheng, J.; Huang, P. *Chin. J. Chem.* **2012**, *30*, 23–28.

(47) This class of gypsy moth has been implicated as a potent despoiler of forests, see: Bierl, B. A.; Beroza, M.; Collier, C. W. *Science* **1970**, *170*, 87.

(48) Wright, A. E.; Botelho, J. C.; Guzman, E.; Harmody, D.; Linley, P.; McCarthy, P. J.; Pitts, T. P.; Pomponi, S. A.; Reed, J. K. *J. Nat. Prod.* **2007**, *70*, 412–416.

recently shown that the side-chain **3.52**, which is also present in leucascandrolide A,⁴⁹ can be accessed through Z-selective CM of **3.51** with allyl pinacolatoborane in the presence of 10 mol% of Mo-alkylidene followed by oxidation (Scheme 3.5.2b).⁵⁰ Although the moderate conversion of 60% is attained to access **3.52** in 91:9 Z:E ratio, the two isomers are essentially inseparable. In contrast, we demonstrate that 10 mol% **Ru9** readily promotes the conversion of **3.51** with cis-2-butene-1,4-diol (thf, 22 °C, 12 h) to **3.52** (85% conv) with high Z selectivity (98%). More importantly, the cis-geometry of the internal alkene originally present in **3.51** remains intact.

The above transformation provides two noteworthy advantages over the Mo-catalyzed process; not only the indirect conversion of boronate-to-alcohol is avoided, the generation of high Z-content circumvents the need for laborious separation of the alkene isomers. Furthermore, the inability of **Ru1** as viable complex to catalyze Z-selective CM is underlined as it promotes 25% conversion and 61% Z selectivity of **3.52** under the same conditions with cis-2-butene-1,4-diol.

3.5.3 Advantage of Z-Selective CM with Internal Alkenes and its Application to Oleochemicals

The hitherto presented results motivated us to extend the utility of our strategy to internal alkenes. The prime reason for such study is associated with its inherent advantage compared with CM involving terminal alkenes: For instance, although the CM involving two RHC=CH₂ units allows us to readily construct complex alkenes, this strategy involves the generation of at least an equivalent of ethylene molecule for each equivalent of the target olefin (Scheme 3.5.3-1a). Furthermore, whereas the formation of the disubstituted alkene of cis/trans-geometry is the point of exhibition in all methodology reports describing such transformations, generation of ethylene as waste is rarely acknowledged. The venue of mention for the latter species is largely limited to the matters of mechanistic significance.⁵¹ Moreover, ethylene is implicated in the

(49) D'Ambrosio, M.; Guerriero, A.; Debitus, C.; Pietra, F. *Helv. Chim. Acta* **1996**, 79, 51–60.

(50) Yu, M.; Hoveyda, A. H. *Angew. Chem. Int. Ed.* (manuscript submitted for publication).

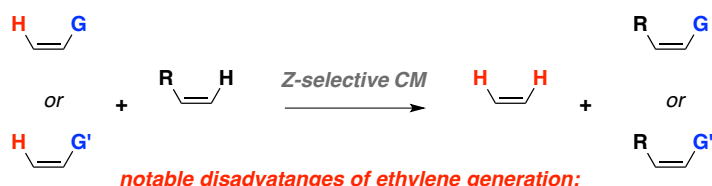
(51) For the role of ethylene in establishment of a Curtin-Hammet situation that gives rise to highly enantioselective ring-closing metathesis, see: Meek, S. J.; Malcolmson, S. J.; Li, B.; Schrock, R. R.; Hoveyda, A. H. *J. Am. Chem. Soc.* **2009**, 131, 16407–16409.

decomposition pathways involving low oxidation-state Ru-carbenes⁵² as well as high oxidation-state Mo/W-alkylidenes.⁵³ In the context of Z-selective CM, its presence is detrimental to the promotion of high stereoselectivity and most efficient protocols include its removal during the course of reaction.^{7a}

On the other hand, development of efficient CM involving two internal alkenes not only avoids the wasteful generation of H₂C=CH₂, but also constitutes a synthetic equivalent of two separate reactions involving terminal alkenes (Scheme 3.5.3-1b). However, a caveat associated with the proposed strategy to be of significance in synthesis is the ready access to disubstituted alkene substrates. In this regard, we identified oleic acid and its derivatives as ideal substrates to access highly valuable alkene targets. Although the metathesis-based functionalization of renewable oleic acid related alkenes is highly lucrative and represents an active area of research,⁵⁴ many methods involve harsh conditions and suffer from lack of efficiency and stereoselectivity (*E/Z*).⁵⁵

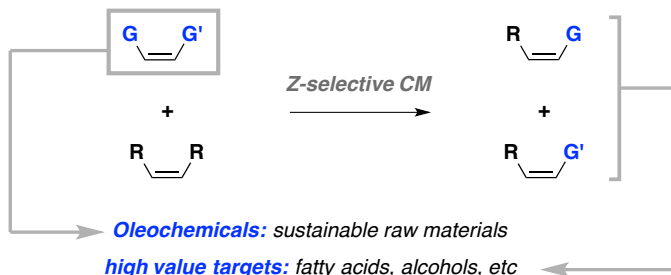
Scheme 3.5.3-1. Advantageous Z-Selective CM of Internal Alkenes

a. Issue with CM involving terminal alkenes:



- 1) carbon waste 2) detrimental to catalyst longevity 3) undermines Z-selectivity

b. Opportunity for efficient and waste-free CM with internal alkenes:



(52) (a) Reference 44. (b) Ulman, M.; Grubbs, R. H. *J. Org. Chem.* **1999**, *64*, 7202–7207.

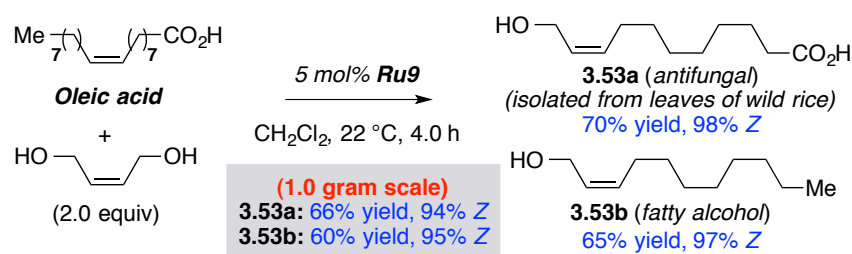
(53) Schrock, R. R. *Chem. Rev.* **2009**, *109*, 3211–3226.

(54) (a) Biermann, U.; Bornscheuer, U.; Meier, M. A. R.; Metzger, J. O.; Schäfer, H. J. *Angew. Chem. Int. Ed.* **2011**, *50*, 3854 – 3871. (b) Behr, A.; Westfachtel, A.; Gomes, J. P. *Chem. Eng. Technol.* **2008**, *31*, 700–714. (c) Behr, A.; Gomes, J. P. *Eur. J. Lipid Sci. Technol.* **2010**, *112*, 31–50. (d) Mol, J. C. *Green Chem.*, **2002**, *4*, 5–13.

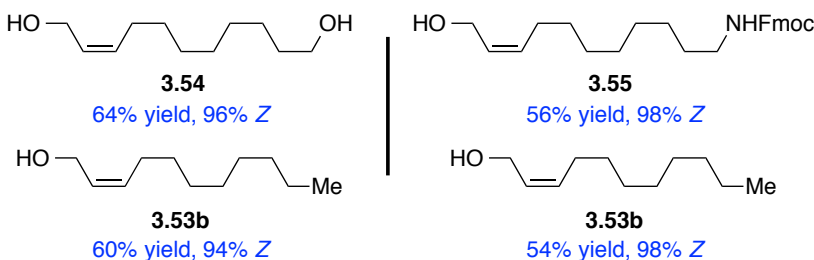
(55) For representative examples requiring 50 °C and the use of PhSiCl₃ (up to 100 equiv. with respect to the catalyst) to give low efficiency, see: Behr, A.; Gomes, J. P. *Beilstein J. Org. Chem.* **2011**, *7*, 1–8. Additionally, there are no known stereoselective metathesis protocols involving oleochemicals.

Keeping in mind the ability of **Ru9** to tolerate acids (Scheme 3.5.1-3), our study commenced with the examination of CM involving oleic acid. We were pleased to find that the treatment of substrate with cis-2-butene-1,4-diol (2.0 equiv) and 5 mol% **Ru9** readily promotes highly efficient and Z-selective formation of **3.53a** (98% Z, 70% yield) and **3.53b** (97% Z, 65% yield) at ambient temperature. The simultaneous generation of the former molecule, which is a naturally occurring antifungal agent,⁵⁶ and the latter fatty alcohol from a renewable alkene source demonstrates the overwhelming value of our strategy. Another notable feature of this protocol is the absence of symmetric alkenes resulting from the self-metathesis of oleic acid,⁵⁵ which could potentially undermine the overall reaction efficiency. From a mechanistic view, it is also important to point out that CH₂Cl₂ is the optimal solvent (vs 65% conv of oleic acid in thf). The relatively lower conversion in strongly coordinating thf is likely due to the slower rate of reaction (i.e. thf competes with the olefin coordination). Moreover, thf is not necessary for catalyst stability since the CM of internal alkenes precludes the possibility for the unstable Ru-methylidene generation (vs cases with terminal alkenes, *cf.* Scheme 3.5.1-3). The robust nature of this reaction is further highlighted as 1.0 gram-scale variant readily furnishes **3.53a** (94% Z, 66% yield) and **3.53b** (95% Z, 60% yield).

Scheme 3.5.3-2. Advantageous Z-Selective CM of Internal Alkenes



Other examples:



(56) Suzuki, Y.; Kurita, O.; Kono, Y.; Hyakutake, H.; Sakurai, A. *Biosci. Biotech. Biochem.* **1995**, *59*, 2049–2051.

In addition to the above result with oleic acid, CM of a related alcohol also proceeds with high *Z* selectivity (94–96%) to give **3.54** and **3.53b** in 64% and 60% yields, respectively. Furthermore, 98% *Z* and moderate efficiency is observed for **3.55** and **3.53b** (56% and 54% yields, respectively), which results from the CM involving a protected fatty amine variant. Overall, the transformations noted in this section offer a glimpse into the feasibility of *Z*-selective CM with internal alkenes that are readily available as substrates to access incredibly valuable molecules. Moreover, these transformations are unaccompanied with wasteful generation of ethylene as well as complicating factors associated with it. On this basis, we hereby reiterate that efforts are ongoing to investigate *Z*-selective CM involving other useful substrates (i.e. homo- or hetero-disubstituted alkenes).

3.6 Challenges and Opportunities for Future Catalyst Development in Stereoselective Olefin Metathesis

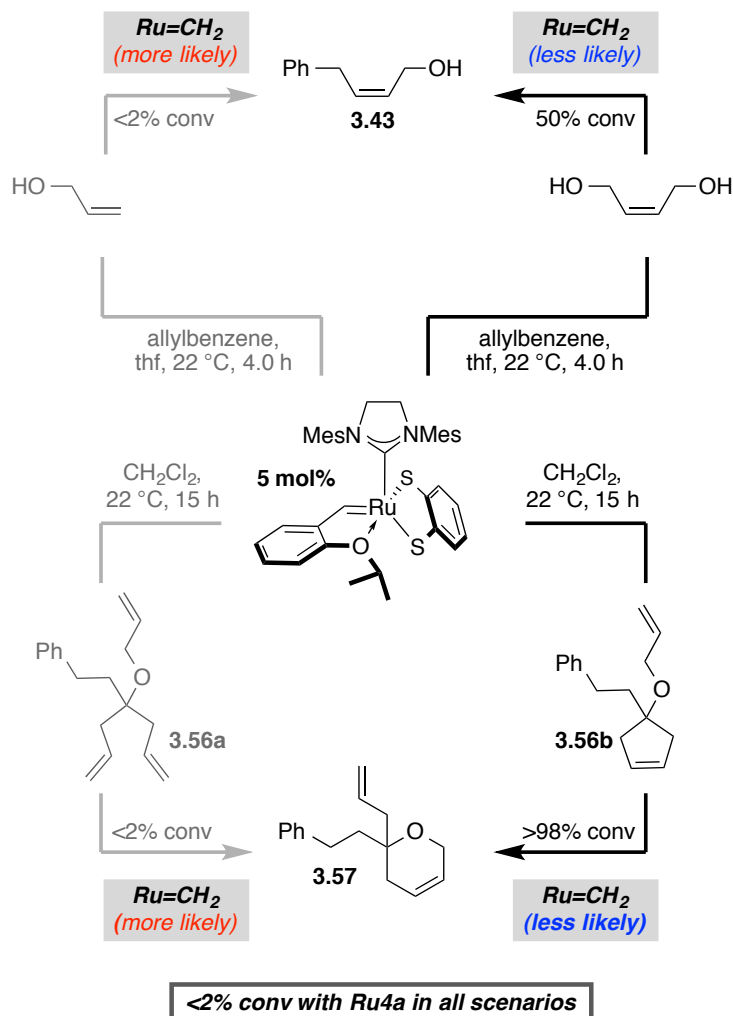
As demonstrated above, the overall catalytic competence of a Ru complex in OM involves various factors that relate to longevity and reactivity. Owing to their high potential for structural modularity (e.g., changes in NHC, dianion, and initiator ligands), the catechothiolate class of Ru carbenes serves as an ideal scaffold to develop optimal *Z*-selective catalysts.

3.6.1 Methylidene Longevity Essential for the Development of Ring-Closing Metathesis Catalysts

In our CM studies, we observed that 50% conversion took place upon treatment of allylbenzene with cis-2-butene-1,4-diol in the presence of 5 mol% **Ru4b** (Scheme 3.6.1-1; *cf.* Scheme 3.5.1-1). The relatively lower efficiency was attributed to the generation of **Ru4b_{Me}** during the course of reaction, which is highly unstable and readily decomposes. Consistently with our proposal, we also showed that the use of terminal alkene-based allyl alcohol (vs internal alkene cis-2-butene-1,4-diol), which leads to the immediate generation of **Ru4b_{Me}**, is detrimental to the reaction (<2% conv). With these observations in mind, we became concerned with their implications on ring-closing metathesis (RCM), which represents an intramolecular version of the CM between two terminal alkenes, catalyzed by **Ru4b**. Furthermore, *Z*-selective macrocyclic RCM has been used as an

important strategy in total synthesis,^{7b} and developments in this area will significantly enhance the impact of **Ru4b** related carbenes. Our suspicion materialized as the subjection of triene **3.56a** to 5 mol% **Ru4b** led to full decomposition of the carbene⁵⁷ without the generation of **3.57**.

Scheme 3.6.1-1. Correlation of Low Reaction Efficiency With Ru=CH₂ Generation



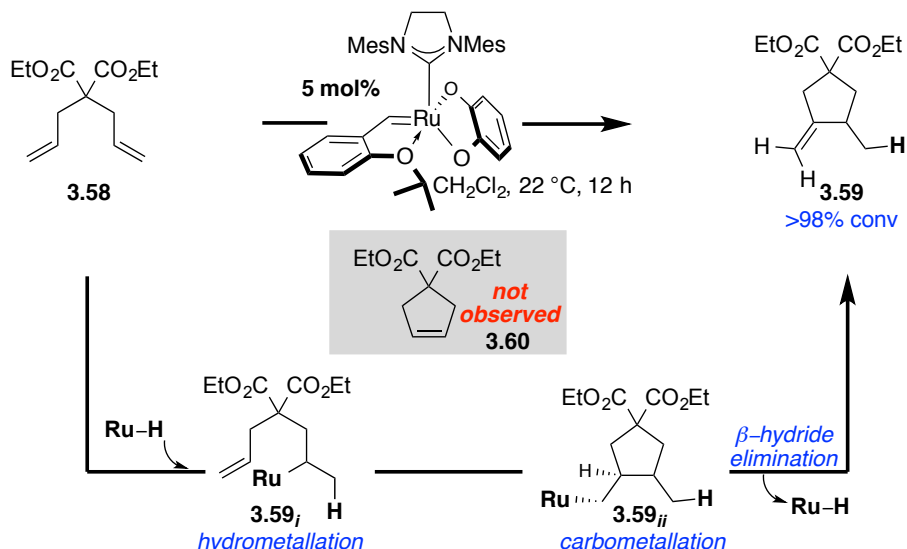
At this point, we hypothesized that triene **3.56b** would serve as an ideal RCM substrate to demonstrate that high efficiency could be achieved in the absence of diminutive Ru=CH₂. More specifically, we surmised that the catalytic establishment of Ru carbene at the alkene terminus of **3.56b** would be followed by a ring-opening event involving strained cyclopentene ring (vs homocoupling with another **3.56b** molecule),

(57) An aliquot of the reaction was checked in CD₂Cl₂ by ¹H NMR spectroscopy.

hence avoiding the generation of **Ru4b_{Me}** altogether. In line with our proposition, we were pleased to find that CM of **3.56b** takes place with >98% conversion at ambient temperature. It is worthy of note that the aforementioned ring-opening/ring-closing transformation (vs RCM) is an example, in addition to the CM involving two internal alkenes (*cf.* Scheme 3.5.3-1), in which high efficiency is attained without the generation of ethylene waste.

Whereas ROM/RCM rearrangement can be a useful tool in the elaboration of alkenes, broad-spectrum use of RCM in organic synthesis motivates us to develop efficient catalysts in this area. In conjunction with our investigations listed above, we wondered if **Ru4a** (vs **Ru4b**) could be employed in effective promotion of RCM. However, our investigations revealed that <2% conversion is observed in CM with **Ru4a**. These results are in contrast with a previous report by Fogg,^{34a} in which RCM of diethyl diallylmalonate is effectively promoted within 15 minutes by a related **Ru4a** analogue. Since the example involved the use of CDCl₃ as solvent at refluxing temperature, which is sufficient to form dichloride **Ru3** (*cf.* Scheme 3.4.1.2-1), we decided to investigate this transformation in CH₂Cl₂ at 22 °C.

Scheme 3.6.1-2. Correlation of Low Reaction Efficiency With Ru=CH₂ Generation



Interestingly, the RCM of diene **3.58** does not lead to the formation of **3.60** (Scheme 3.6.1-2). Instead, >98% conversion is observed to a cycloisomerized exocyclic alkene product **3.59**. Based on the literature precedents, we put forth a plausible pathway

for the generation of **3.59** catalyzed by a putative Ru–hydride species.⁵⁸ Our proposal deals with an initial hydrometallation step involving substrate to give **3.59_i** intermediate followed by the intramolecular carbometallation of the terminal alkene to generate **3.59_{ii}**. The latter intermediate is prone to undergo β -hydride elimination, which provides access to the observed product. The results described herein, once again point to the importance of tracking the identity of the catalytically active species in Ru-catalyzed OM as a critical tool in catalyst development. Furthermore, the above results indicate that efforts to minimize the formation of Ru-hydride could help improve the catalyst efficiency. On this basis, research is underway to develop catalysts that discourage the formation of Ru–H and readily perform RCM.

3.6.2 Development of Highly Active Catalysts for Z-Selective OM with Hindered and/or Stabilizing Alkenes

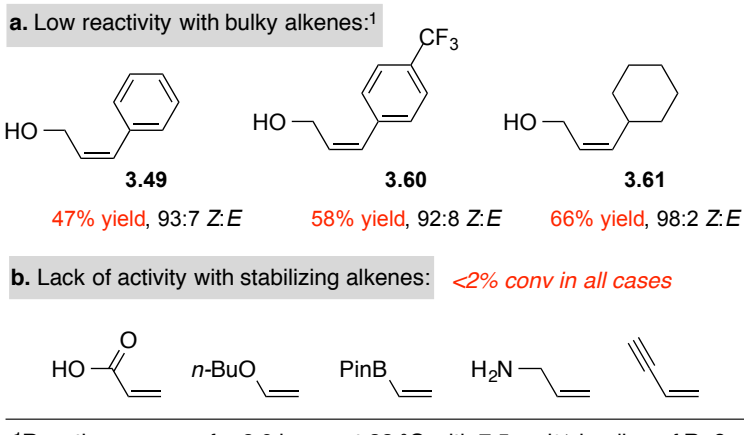
Our efforts with bulky alkenes (e.g., styrene and vinyl cyclohexane) were first showcased in the context of Z-selective ROCM promoted by **Ru4b**.¹⁹ However, in the area of Z-selective CM, wherein a more active **Ru9** variant provides higher efficiency (*cf.* Scheme 3.5.1-2), the transformations with sterically congested alkenes suffer from relatively low reaction yields. For instance, CM with large styrene proceeds to give 47% yield of the desired **3.49** at 7.5 mol% loading of **Ru9** after eight hours at ambient temperature (Scheme 3.6.2a). Although other examples with hindered alkenes (**3.60–3.61**) exhibit slightly improved reaction efficiencies (e.g., up to 66% yield in case of **3.61**), the relatively higher catalyst loading (7.5 mol%) required underlines the importance of developing more active catalysts. It is also noteworthy that these transformations are still more efficient than the reactivity levels promoted by **Ru1** (*cf.* Scheme 3.5.1-3).

As shown in Scheme 3.6.2b, the scenario with alkenes that lead to the generation of stabilized carbenes (i.e. either through resonance or coordination of a strongly binding group) is more problematic. In all cases, <2% conversion is observed. Currently, we look

(58) For a representative study showing that Ru-carbenes are capable of decomposing to Ru–hydride species, which catalyzes cycloisomerization of the diene substrate, see: Mallagaray, Á, Mohammadiannejad-Abbasabadi, K.; Medina, S.; Domínguez, G.; Pérez-Castells, J. *Org. Biomol. Chem.*, **2012**, *10*, 6665–6672.

forward to developing catalysts that avoid the attenuation in reactivity through carbene stabilization and promote efficient reactions.

Scheme 3.6.2. Alkenes Exhibiting Diminution in Reactivity



3.7 Conclusions

Our efforts described herein demonstrate that developing a deeper understanding of the mechanistic principles (e.g., the critical role of donor-donor repulsions and trans influence in OM and non-OM rearrangements, Sections 1.4 and 1.5, Chapter 1) led us to rationally design a new class of Ru carbenes (e.g., **Ru4b**, **Ru5**, and **Ru9**) for Z-selective OM. The newly developed stereogenic-at-Ru complexes **Ru4b** and **Ru5** demonstrate superior activity and selectivity in ROMP reactions of norbornene and cyclooctene (vs another Z-selective complex **Ru1** developed recently; *cf.* Section 3.3.1). Furthermore, **Ru4b** is highly efficient and Z-selective in promoting ROCM with an unprecedented scope of alkenes of large and small steric sizes and broad array of functional groups (e.g., alcohols, enol ethers, vinyl sulfides, amides, heterocycles, and conjugated 1,3-dienes; *cf.* Section 3.3). More importantly, we discovered that not only **Ru4b** tolerates alcohols, but it also exhibits increased activity due to H–bonding with thiolate anions (vs protected alcohols, *cf.* Scheme 3.3.2.4a). To reveal this interaction, we disclosed the first examples of highly Z- (up to >98%) and diastereoselective (up to >98% d. r.) ROCM of an enantiomerically enriched allylic alcohol **3.36a** (*cf.* Scheme 3.3.2.4b).

We then explained the origins of the differences in reactivity, selectivity, and stability of catecholate and catechothiolate Ru complexes (**Ru4a** and **Ru4b**, respectively;

cf. Section 3.4) in OM. In these efforts, we showed that while **Ru4a** readily decomposes in the presence of alcohols, **Ru4b** shows no sign of decomposition (*cf.* Scheme 3.4.1.1). Most notably, we uncovered a remarkable decomposition of **Ru4a** to **Ru3** in commonly used solvents (CDCl_3 at 22 °C; CD_2Cl_2 at 50 °C; *cf.* Table 3.4.1.2, Scheme 3.4.1.2-1), which has broader implications for future catalyst development. Furthermore, computational investigations revealed that the low selectivity with **Ru4a** (e.g., 58% Z in ROMP of **3.16** vs >98% Z with **Ru4b**, *cf.* Table 3.3.1) is due to the change in rate limiting step to alkene association (vs ruthenacyclobutane formation for **Ru4b**, *cf.* Scheme 3.4.2-1).

On the basis of newly gained experimental and computational insights, **Ru9** was developed to promote highly Z-selective CM to access a broad range of functionalized Z-allyl alcohols (*cf.* Section 3.5). The aforementioned complex performs efficiently and selectively even in the presence of carboxylic acid and carboxaldehyde moieties, which is a clear advantage over **Ru1** and Mo/W-based alkylidene catalysts (*cf.* Scheme 3.5.1-3). Furthermore, the above methodology has been successfully employed to access an anti tumor agent precursor (i.e. neopeltolide, *cf.* Scheme 3.5.2b). Finally, applications in readily functionalizing naturally occurring plant oils to form highly useful fatty acids and alcohols are also notable (*cf.* Section 3.5.3). For instance, Z-selective OM of Oleic acid catalyzed by **Ru9** readily provides one-step access to an antifungal molecule **3.53a** and fatty oil **3.53b** (*cf.* Scheme 3.5.3-2).

Finally, we have listed the challenges and opportunities with catechothiolate Ru carbenes (*cf.* Section 3.6). Currently, efforts are underway to identify more active catalyst based on these considerations. Overall, we have developed a new class of rationally designed Ru carbene catalysts for Z-selective olefin metathesis with a remarkable range of alkenes; these complexes not only outperform the existing Ru/Mo/W-based catalysts in many instances, but also have found useful applications in organic synthesis.

3.8 Experimental

■ General:

Unless otherwise noted, all reactions were performed with distilled and degassed solvents under an atmosphere of dry N₂ in oven- (135 °C) or flame-dried glassware with standard dry box or vacuum line techniques. Infrared (IR) spectra were recorded on a Bruker FTIR Alpha (ATR Mode) spectrometer, ν_{max} in cm⁻¹. Bands are characterized as broad (br), strong (s), medium (m), or weak (w). ¹H NMR spectra were recorded on a Varian Unity INOVA 400 (400 MHz) or a Varian Unity INOVA 500 (500 MHz) spectrometer. Chemical shifts are reported in ppm from tetramethylsilane with the solvent resonance resulting from incomplete deuterium incorporation as the internal standard (CDCl₃: δ 7.26 ppm, C₆D₆: δ 7.16 ppm, CD₂Cl₂: δ 5.32 ppm). Data are reported as follows: chemical shift, integration, multiplicity (s = singlet, d = doublet, t = triplet, q = quartet, br = broad, m = multiplet), and coupling constants (Hz). ¹³C NMR spectra were recorded on a Varian Unity INOVA 400 (100 MHz) or Varian Unity INOVA 500 (125 MHz) spectrometer with complete proton decoupling. Chemical shifts are reported in ppm from tetramethylsilane with the solvent resonance as the internal standard (CDCl₃: δ 77.16 ppm, CD₂Cl₂: δ 54.00 ppm). High-resolution mass spectrometry was performed on a Micromass LCT ESI-MS and JEOL Accu TOF Dart (positive mode) at the Boston College Mass Spectrometry Facility. Values for Z:E ratios of products were determined by analysis of ¹H NMR spectra or ¹³C NMR spectra of the unpurified material.

X-Ray Data Collection

Selected single crystals suitable for X-ray crystallographic analysis were used for structural determination. The X-ray intensity data were measured at 100(2) K (Oxford Cryostream 700) on a Bruker Kappa APEX Duo diffractometer system equipped with a sealed Mo-target X-ray tube (λ = 0.71073 Å) and a high brightness I μ S copper source (λ = 1.54178 Å). The crystals were mounted on a goniometer head with paratone oil. The detector was placed at a distance of 5.000 or 6.000 cm from the crystal. For each experiment, data collection strategy was determined by APEX software package and all frames were collected with a scan width of 0.5° in ω and ϕ with an exposure time of 10 or

20 s/frame. The frames were integrated with the Bruker SAINT Software package using a narrow-frame integration algorithm to a maximum 2θ angle of 56.54° (0.75 \AA resolution) for Mo data and of 134° (0.84 \AA resolution) for Cu data. The final cell constants are based upon the refinement of the XYZ-centroids of several thousand reflections above $20 \sigma(I)$. Analysis of the data showed negligible decay during data collection. Data were corrected for absorption effects using the empirical method (SADABS). The structures were solved and refined by full-matrix least squares procedures on $|F^2|$ using the Bruker SHELXTL (version 6.12) software package. All hydrogen atoms were included in idealized positions for structure factor calculations except for those forming hydrogen bonds or on a chiral center. Anisotropic displacement parameters were assigned to all non-hydrogen atoms, except those disordered.

Solvents

Solvents (CH_2Cl_2 , pentane, benzene) were purified under a positive pressure of dry Ar by a modified Innovative Technologies purification system. Unless otherwise noted, chlorinated solvents (CH_2Cl_2 , CD_2Cl_2 , CDCl_3 , CHCl_3) were freshly passed twice through a plug of basic alumina before each use. Tetrahydrofuran was distilled under a nitrogen atmosphere from Na/benzophenone. Methanol was distilled from CaH_2 under nitrogen atmosphere. Work-up of Ru complexes was performed in a glove box filled with nitrogen using dry and degassed solvents. All other purification procedures of ROMP, ROCM, CM, RO/RCM, cycloisomerization products were carried out with reagent grade solvents (purchased from Fisher) under bench-top conditions.

Deuterated solvents

CDCl_3 , CD_2Cl_2 , C_6D_6 were purchased from Cambridge Isotope Laboratories and freshly passed twice through a plug of basic alumina before each use.

Reagents

Complex **Ru3** (Aldrich), sodium maleonitriledithiolate **3.14** (TCI America), 1,2-dihydroxybenzene (Aldrich) and benzene-1,2-dithiol (Aldrich) were used as received. Bispyridyl Ru-dichloride (**Ru6**) was prepared as described in the literature.⁵⁹ 3,4,5,6-

(59) Sanford, M. S.; Love, J. A.; Grubbs, R. H. *Organometallics* **2001**, *20*, 5314–5318.

Tetrafluorobenzene-1,2-diol was also purchased (Matrix Scientific) and used as received. Styrene (Aldrich), vinylcyclohexane (Aldrich), allyl alcohol (Aldrich), homoallyl alcohol (Aldrich), 1,5-cyclooctadiene **3.18** (Aldrich), *p*-methoxystyrene (Aldrich) and 3-fluorostyrene (Aldrich) were passed through a plug of basic alumina prior to the experiment. Unless otherwise indicated, norbornene **3.16** (Aldrich) was used without purification but purified for polymerization experiments with low catalyst loading (see below). 5-Norbornene-2-*exo*,3-*exo*-dimethanol **3.22** (Aldrich) was used as received. Cyclobutene **3.24**⁶⁰ and cyclopropene **3.26**⁶¹ were prepared in analogy to previously reported procedures. Strained alkene **3.35_{pre}** was prepared by *N*-tosylation of a precursor previously reported in the literature.⁶² 3,6-Dichloro-1,2-benzenedithiol (Aldrich), 2,5-dimethylbenzenethiol (Aldrich), 2-bromo-5-chlorobenzenethiol (Oakwood), 1,2,3,4-tetrafluorobenzene (Oakwood), 2,5-dibromoaniline (Aldrich), allylbenzene (Aldrich), allyl butyl ether (Aldrich), 1-dodecene (Aldrich), 4-phenyl-1-buten-4-ol (Aldrich), 5-hexenoic acid (Aldrich), 2,2-dimethyl-4-pentenoic acid (Acros), undecylenic aldehyde (Aldrich), (*E*)-1-methoxy-1,3-butadiene (Aldrich), were either distilled (from CaH₂ or CaCl₂) under vacuum or dried by azeotropic distillation (with C₆H₆) prior to use. (*E*)-Deca-1,3-diene,⁶³ (*Z*)-nona-1,3-diene,⁶⁴ 2-(5-hexenyl)isoindoline-1,3-dione⁶⁵ were prepared according to literature procedures. Z-2-butene-1,4-diol (Fluka), 3'-Allyl-4'-hydroxyacetophenone (Aldrich), oleic acid (Aldrich) and oleyl alcohol (Aldrich) were used as received.

■ Synthesis of Ligands and Related Ru Carbene Complexes:

Preparation of Ligands

Synthesis of i. Zinc dithiolate **i** was prepared by using a previously reported procedure in the literature.⁶⁶

(60) Khan, R. K. M.; Zhugralin, A. R.; Torker, S.; O'Brien, R. V.; Lombardi, P. J.; Hoveyda, A. H. *J. Am. Chem. Soc.* **2012**, *134*, 12438–12441.

(61) M. Rubin, V. Gevorgyan, *Synthesis* **2004**, 796–800.

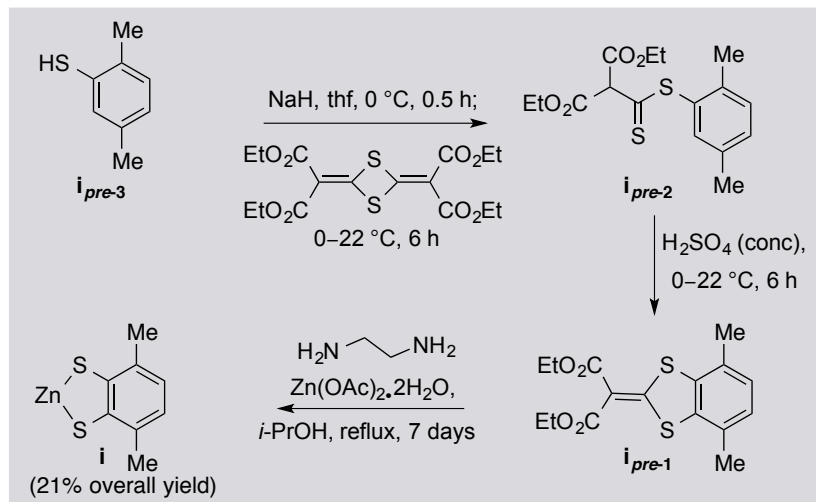
(62) L. A. Carpino, D. E. Barr, *J. Org. Chem.* **1966**, *31*, 764–767.

(63) E. M. Townsend, R. R. Schrock, A. H. Hoveyda, *J. Am. Chem. Soc.* **2012**, *134*, 11334–11337.

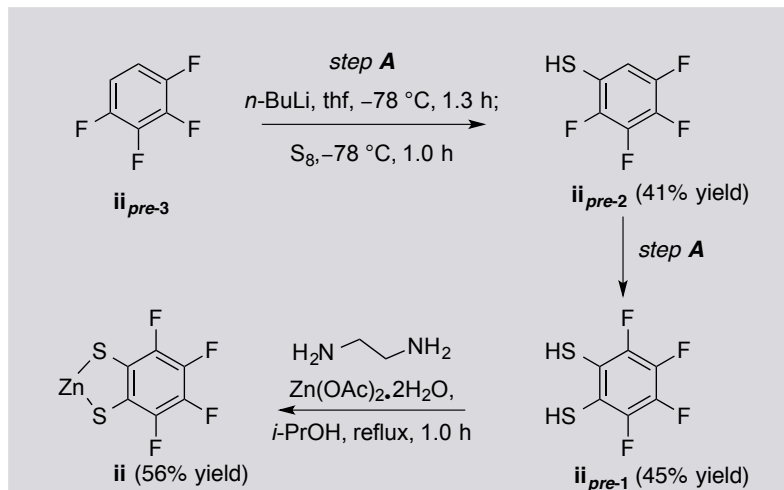
(64) Kliman, L. T.; Mlynarski, S. N.; Ferris, G. E.; Morken, J. P. *Angew. Chem. Int. Ed.* **2012**, *51*, 521–524.

(65) Smith, B. J.; Sulikowski, G. A. *Angew. Chem. Int. Ed.* **2010**, *49*, 1599–1602.

(66) Yeung, C. M.; Klein, L. L. *Tetrahedron Lett.* **1990**, *31*, 2121–2124.

Chart 1. Preparation of Ligand Precursor i

Synthesis of ii. Following steps were performed to prepare the Zinc salt:

Chart 2. Preparation of Ligand Precursor ii

Synthesis of ii_{pre-2}. To a stirred solution of *n*-BuLi (0.69 mL, 1.10 mmol, 1.10 equiv) in tetrahydrofuran (2 mL) at -78 °C was added 1,2,3,4-tetrafluorobenzene (150 mg, 1.00 mmol, 1.00 equiv) over 30 minutes. The solution was allowed to stir for a further 45 minutes at -78 °C, after which dry, powdered sulfur (35.3 mg, 1.10 mmol, 1.10 equiv) was added in portions over 30 minutes. The solution was allowed to stir for a further 30 minutes at -78 °C. The reaction was quenched with 6M HCl (1.5 mL) and extracted with Et₂O (3 x 5.0 mL). The combined organic layers were washed with water (10 mL), dried over anhydrous MgSO₄, filtered and concentrated in *vacuo* to afford ii_{pre-2} (75.0 mg, 0.41

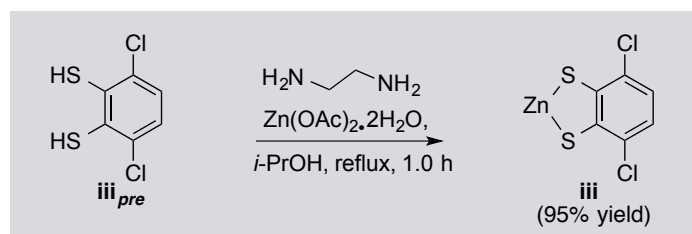
mmol, 41% yield) as yellow oil, which was used in the next step without further purification.

Synthesis of $\text{ii}_{\text{pre-1}}$. To a stirred solution of *n*-BuLi (0.28 mL, 0.45 mmol, 1.10 equiv) in tetrahydrofuran (1 mL) at -78 °C was added $\text{ii}_{\text{pre-2}}$ (75.0 mg, 0.41 mmol, 1.00 equiv) in tetrahydrofuran (1 mL) over 30 minutes. The solution was allowed to stir for a further 45 minutes at -78 °C, after which dry, powdered sulfur (14.4 mg, 0.45 mmol, 1.10 equiv) was added in portions over 30 minutes. The solution was allowed to stir for a further 30 minutes at -78 °C. The reaction was quenched with 6M HCl (0.6 mL) and extracted with Et₂O (3 x 3.0 mL). The combined organic layers were washed with water (5.0 mL), dried over anhydrous MgSO₄, filtered and concentrated in *vacuo* to afford $\text{ii}_{\text{pre-1}}$ (39.5 mg, 0.18 mmol, 45% yield) as brown oil, which was used in the next step without further purification.

Synthesis of ii . A mixture of $\text{ii}_{\text{pre-1}}$ (214 mg, 1.00 mmol, 1.00 equiv), Zn(OAc)₂.2H₂O (878 mg, 4.00 mmol, 4.00 equiv) and ethylenediamine (0.40 mL, 6.00 mmol, 6.00 equiv) in *i*-PrOH (8 mL) was allowed to stir for one hour at 22 °C. The precipitated solid was filtered, washed with methanol (5.0 mL) and hot chloroform (5.0 mL), and dried in a vacuum desiccator overnight to afford ii (155 mg, 0.56 mmol, 56% yield) as white solid.

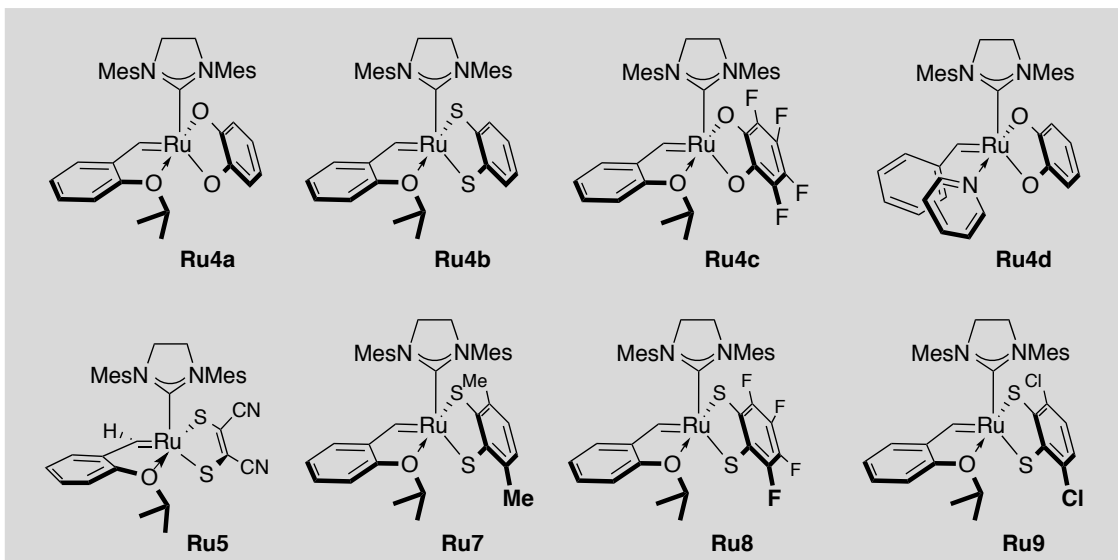
Synthesis of iii . A mixture of 3,6-dichlorobenzene-1,2-dithiol iii_{pre} (211 mg, 1.00 mmol, 1.00 equiv), Zn(OAc)₂.2H₂O (878 mg, 4.00 mmol, 4.00 equiv) and ethylenediamine (0.40 mL, 6.00 mmol, 6.00 equiv) in *i*-PrOH (8 mL) was allowed to stir for one hour at 22 °C. The precipitated solid was filtered, washed with methanol (5.0 mL) and hot chloroform (5.0 mL), and dried in a vacuum desiccator overnight to afford iii (261 mg, 0.95 mmol, 95% yield) as white solid.

Chart 3. Preparation of Ligand Precursor iii



Preparation of Ru Carbenes

Chart 4. New Class of Stereogenic-at-Ru Carbenes for Z-Selective OM



Synthesis of 4a. To a 2-dram vial charged with a stir bar and disodium catecholate **3.13** (37.0 mg, 0.240 mmol, 1.50 equiv) under N₂ atmosphere, a solution of complex **Ru3** (100 mg, 0.160 mmol, 1.00 equiv) in tetrahydrofuran (2.0 mL) is added. The resulting mixture is allowed to stir at 22 °C for three hours, at which time the solvent is evaporated under vacuum. Residual tetrahydrofuran is removed through co-evaporation with pentane (2 x 4 mL). The resulting solid is dissolved in dichloromethane and passed through a short column of Celite (4 cm in height), placed in a pipette (~0.5 cm diameter), with dichloromethane (10 mL). The filtrate is adsorbed onto fresh Celite and subjected to vacuum until complete dryness. The adsorbed material is loaded onto a second short column of Celite (4 cm in height) and washed with Et₂O (20 mL), after which complex **Ru4a** is collected upon elution with dichloromethane. After removal of solvents and co-evaporation with pentane, Ru-based catecholate **Ru4a** is isolated as an orange-brown solid (68.9 mg, 0.104 mmol, 65% yield). **¹H NMR (400 MHz, CD₂Cl₂):** δ 16.03 (1H, s), 7.32 (1H, td, *J* = 7.8, 1.6 Hz), 7.07 (2H, s), 6.97 (1H, d, *J* = 8.4 Hz), 6.87 (1H, t, *J* = 7.4 Hz), 6.73 (1H, dd, *J* = 7.2, 1.6 Hz), 6.59 (2H, br s), 6.51 (1H, dd, *J* = 7.6, 1.6 Hz), 6.37 (1H, dd, *J* = 7.6, 1.6 Hz), 6.30 (1H, td, *J* = 7.4, 1.6 Hz), 6.16 (1H, td, *J* = 7.4, 1.6 Hz), 4.86–4.76 (1H, m), 3.99 (4H, apparent br s), 2.51 (6H, s), 2.30 (6H, s), 1.80 (6H, br s),

1.41 (3H, d, $J = 6.4$ Hz), 1.24 (3H, d, $J = 6.4$ Hz); **^{13}C NMR (100 MHz, CD_2Cl_2):** δ 265.6, 222.8, 164.6, 161.1, 157.2, 143.7, 138.9, 138.2 (very br), 137.8, 136.3 (br), 130.2, 129.8, 127.1, 123.7, 122.4, 116.4, 115.8, 114.1, 114.0, 113.8, 82.4, 51.6, 23.2, 21.4, 20.8, 18.9, 17.5.

Synthesis of Ru4b. To a 2-dram vial equipped with a stir bar and charged with disodium benzenedithiolate **3.15** (44.6 mg, 0.240 mmol, 1.50 equiv) under N_2 atmosphere, a solution of complex **Ru3** (100 mg, 0.160 mmol, 1.00 equiv) in tetrahydrofuran (2.0 mL) is added. The resulting mixture is allowed to stir at 22 °C for three hours, at which time the solvent is evaporated under vacuum. Residual tetrahydrofuran is removed through co-evaporation with pentane (2 x 4 mL). The obtained solid is dissolved in dichloromethane and passed through a short column of Celite (4 cm in height) in a pipette (~0.5 cm diameter) with dichloromethane (10 mL). The filtrate is adsorbed onto fresh Celite and subjected to vacuum until complete dryness. The adsorbed material is loaded onto another short column of Celite (4 cm in height) and washed with diethyl ether (20 mL), after which complex **Ru4b** is collected upon elution with dichloromethane. After removal of solvents and co-evaporation with pentane, **Ru4b** is isolated as an orange-brown solid (75.6 mg, 0.109 mmol, 68% yield). **^1H NMR (400 MHz, CD_2Cl_2):** δ 14.36 (1H, s), 7.45 (1H, dd, $J = 7.2, 1.6$ Hz), 7.31-7.26 (2H, m), 7.09 (1H, d, $J = 8.8$ Hz), 6.99 (2H, s), 6.9-6.4 (1H, very br s, overlapping), 6.80 (1H, td, $J = 7.4, 0.8$ Hz), 6.75 (1H, ddd, $J = 8.0, 7.2, 1.6$ Hz), 6.68 (1H, ddd, $J = 7.6, 6.8, 1.6$ Hz), 6.62 (1H, dd, $J = 7.6, 1.6$ Hz), 6.4-5.9 (1H, very br s), 5.25-5.17 (1H, m), 3.90 (4H, apparent br s), 2.53 (6H, br s), 2.5-2.0 (3H, very br s), 2.24 (6H, s), 1.9-1.5 (3H, very br s), 1.67 (3H, d, $J = 6.8$ Hz), 1.48 (3H, d, $J = 6.4$ Hz); **^{13}C NMR (100 MHz, CD_2Cl_2):** δ 250.7, 219.4, 154.9, 153.2, 142.3, 141.6, 138.5 (very br), 136.7 (br), 135.6 (very br), 130.0 (br), 129.6 (br), 128.6, 127.48, 127.45, 124.7, 122.6, 121.7, 120.8, 115.9, 82.0, 51.9, 24.4, 21.8, 21.3, 19.6 (very br), 17.8 (very br).

Synthesis of Ru4c. To a 2-dram vial charged with a stir bar and 3,4,5,6-tetrafluorobenzene-1,2-diol (28.1 mg, 0.154 mmol, 1.50 equiv) under N_2 atmosphere, a solution of complex **Ru4a** (68.6 mg, 0.103 mmol, 1.00 equiv) in tetrahydrofuran (1.0 mL) is added. The resulting mixture is allowed to stir at 22 °C for 30 minutes, at which

time the solvent is evaporated under vacuum. Residual tetrahydrofuran is removed through co-evaporation with pentane (3 x 4 mL). The resulting solid is stirred with (1:1) mixture of pentane/diethyl ether (2 mL) for five minutes followed by loading onto a Celite column. The residue is washed with (1:1) pentane/diethyl ether (6 mL) and then collected with tetrahydrofuran (3 mL). After removal of solvents and co-evaporation with pentane (3 x 2 mL), Ru complex **Ru4c** is isolated as light green solid (60.6 mg, 0.082 mmol, 80% yield). **¹H NMR (400 MHz, CD₂Cl₂)**: δ 16.31 (1H, s), 7.35 (1H, ddd, *J* = 8.7, 5.8, 1.7 Hz), 7.07 (2H, d, *J* = 2.2 Hz), 7.00 (1H, d, *J* = 8.4 Hz), 6.90 (1H, dd, *J* = 7.8, 7.0 Hz), 6.77 (1H, dd, *J* = 7.6, 1.7 Hz), 6.55 (2H, s), 4.84 (1H, m), 4.12 – 3.90 (4H, m), 2.48 (6H, s), 2.28 (6H, s), 1.81 (6H, br. s), 1.46 (3H, d, *J* = 6.6 Hz), 1.22 (3H, d, *J* = 6.4 Hz); **¹³C NMR (150 MHz, CD₂Cl₂)** δ 270.9, 220.4, 157.5, 149.6, 146.6, 143.9, 139.4, 138.5, 137.7, 136.9, 136.1, 134.5, 133.1, 131.4, 130.3, 129.9, 129.7, 127.9, 124.1, 122.6, 121.3, 121.2, 120.9, 116.4, 51.6, 30.3, 23.4, 21.4, 21.2, 20.6, 18.8, 17.5.

Synthesis of Ru4d. Under an atmosphere of dry N₂, a suspension of complex **Ru6** (73.4 mg, 0.101 mmol, 1.00 equiv) and disodium catecholate **3.13** (31.1 mg, 0.202 mmol, 2.00 equiv) is allowed to stir in tetrahydrofuran (1.3 mL) for five hours. The solvent is evaporated and the residual tetrahydrofuran is removed through co-evaporation with pentane (3 x 3 mL). The residue is taken up in dichloromethane and the solution filtered through a plug of Celite. After removal of solvents and co-evaporation with pentane (3 x 2 mL), Ru complex **Ru4d** is isolated as dark brown solid (61.7 mg, 0.090 mmol, 89% yield). **¹H NMR (400 MHz, CD₂Cl₂)** δ 16.81 (1H, s), 8.26 (2H, dt, *J* = 5.1, 1.5 Hz), 7.54 (1H, tt, *J* = 7.6, 1.6 Hz), 7.17 (1H, tt, *J* = 7.3, 1.3 Hz), 7.11 – 6.98 (4H, m), 6.94 – 6.82 (4H, m), 6.67 (2H, s), 6.55 (1H, dd, *J* = 7.6, 1.6 Hz), 6.40 (1H, dd, *J* = 7.5, 1.6 Hz), 6.32 (1H, td, *J* = 7.5, 1.7 Hz), 6.17 (1H, td, *J* = 7.4, 1.6 Hz), 4.15 – 3.93 (4H, m), 2.34 (6H, s), 2.25 (6H, s), 2.04 (6H, s); **¹³C NMR (100 MHz, CD₂Cl₂)**: δ 221.9, 164.6, 161.4, 155.6, 152.9, 139.1, 138.6, 135.4, 130.0, 129.9, 128.4, 127.3, 127.2, 124.5, 116.4, 115.0, 113.98, 113.89, 52.0, 21.3, 18.1.

Synthesis of Ru5. Under an atmosphere of dry N₂, a suspension of complex **Ru3** (100 mg, 0.160 mmol, 1.00 equiv) and sodium maleonitriledithiolate **3.14** (38.7 mg, 0.208 mmol, 1.30 equiv) is allowed to stir in tetrahydrofuran (1.5 mL) for 3 hours, during which a color change from green to reddish brown is observed. The solvent is evaporated

and the residual tetrahydrofuran is removed through co-evaporation with pentane. The residue is taken up in dichloromethane and the solution filtered through a glass microfiber filter (WhatmanTM). After removal of the solvent in vacuo, dichloromethane (1.0 mL) is added and the complex precipitated while stirring by slow addition of diethyl ether (10 mL). The resulting suspension is transferred onto a short column of Celite (4 cm in height) placed in a pipette (~0.5 cm diameter) and washed with a 1:10 mixture of dichloromethane/diethyl ether (5.5 mL). The first filtrate is collected and left for crystallization (see below). The complex is then eluted with dichloromethane until the second filtrate is colorless. After removal of the solvent and co-evaporation of dichloromethane with pentane, complex **Ru5** is obtained as an orange-brown solid (75.0 mg, 0.109 mmol, 68% yield). After two days, the crystals from the first filtrate were collected and washed with diethyl ether to give an overall yield of **Ru5** of 82% (90.0 mg, 0.131 mmol). **¹H NMR (500 MHz, CD₂Cl₂)**: δ 14.28 (1H, s), 7.34 (1H, td, *J* = 7.8, 1.6 Hz), 7.16 (1H, d, *J* = 8.4 Hz), 7.0-6.4 (1H, very br s), 6.97 (2H, s), 6.85 (1H, t, *J* = 7.4 Hz), 6.60 (1H, dd, *J* = 7.6, 1.6 Hz), 6.4-5.9 (1H, br s), 5.38 (1H, m), 3.95 (4H, apparent br s), 2.5-1.9 (3H, very br s), 2.45 (6H, s), 2.25 (6H, br s), 1.9-1.4 (3H, very br s), 1.78 (3H, d, *J* = 6.7 Hz), 1.49 (3H, d, *J* = 6.6 Hz). **¹³C NMR (100 MHz, CD₂Cl₂)**: ¹³C spectrum shows many carbene-¹H peaks, which is due to the coagulation at high concentration of **Ru5** in the NMR sample (see X-ray of **Ru5** below for detailed structural information).

Synthesis of Ru7. Ru complex was made by using the same procedure as for **Ru4a** (61% yield).

Synthesis of Ru8. To a 2-dram vial charged with a stir bar and zinc dithiolate **ii** (27.2 mg, 0.098 mmol, 2.00 equiv) under N₂ atmosphere, a solution of **Ru3** (30.7 mg, 0.049 mmol, 1.00 equiv) in tetrahydrofuran (610 μL) is added. The resulting mixture is allowed to stir for five hours at 22 °C, at which time the solvent is evaporated under vacuum. Residual tetrahydrofuran is removed through co-evaporation with pentane (2 x 2 mL). The obtained solid is dissolved in dichloromethane and passed through a short column of Celite (4 cm in height) in a pipette (~0.5 cm diameter) with dichloromethane (10 mL). After removal of dichloromethane from the filtrate and co-evaporation with pentane, **Ru8**

is isolated as brown solid (30.7 mg, 0.040 mmol, 82% yield); **¹H NMR (400 MHz, CD₂Cl₂):** δ 14.43 (1H, s), 7.32–7.26 (1H, m), 7.12 (1H, d, *J* = 8.4 Hz), 6.95 (2H, s), 6.80 (1H, t, *J* = 7.4 Hz), 6.70–6.50 (1H, br s), 6.60 (1H, dd, *J* = 7.5, 1.6 Hz), 6.11 (1H, br s), 5.32–5.29 (1H, m), 3.92 (4H, br s), 2.49 (6H, br s), 2.37–2.15 (3H, br s), 2.18 (6H, s), 1.73 (3H, d, *J* = 6.7 Hz), 1.62 (3H, br s), 1.47 (3H, d, *J* = 6.6 Hz); **¹³C NMR (100 MHz, CD₂Cl₂):** δ 255.2 (d, *J* = 28.3 Hz), 216.8, 144.5 (ddd, 236.0, 43.8, 10.5 Hz), 141.9, 139.9–137.6 (m), 138.9 (d, *J* = 17.6 Hz), 138.6 (br), 136.6 (br), 134.9 (dt, *J* = 129.0, 18.0 Hz), 130.0, 129.7, 129.7, 128.9, 128.2, 126.9 (d, *J* = 18.1 Hz), 124.8, 122.8, 116.3, 83.3, 52.0, 24.8, 21.5, 21.2, 19.8 (br), 19.0 (br).

Synthesis of Ru9. To a 2-dram vial charged with a stir bar and zinc dithiolate **iii** (26.9 mg, 0.098 mmol, 2.00 equiv) under N₂ atmosphere, a solution of **Ru3** (30.7 mg, 0.049 mmol, 1.00 equiv) in tetrahydrofuran (610 μL) is added. The resulting mixture is allowed to stir for five hours at 22 °C, at which time the solvent is evaporated under vacuum. Residual tetrahydrofuran is removed through co-evaporation with pentane (2 × 2 mL). The obtained solid is dissolved in dichloromethane and passed through a short column of Celite (4 cm in height) in a pipette (~0.5 cm diameter) with dichloromethane (10 mL). After removal of dichloromethane from the filtrate and co-evaporation with pentane, **Ru9** is isolated as brown solid (31.9 mg, 0.042 mmol, 85% yield); **¹H NMR (400 MHz, CD₂Cl₂):** δ 14.30 (1H, s), 7.32–7.26 (1H, m), 7.10 (1H, d, *J* = 8.1 Hz), 6.96 (2H, s), 6.87 (1H, dd, *J* = 8.1, 0.6 Hz), 6.82–6.76 (2H, m), 6.61 (1H, dd, *J* = 7.5, 1.6 Hz), 6.45–6.00 (2H, br s), 5.29–5.25 (1H, m), 3.92 (4H, br s), 2.52 (6H, br s), 2.30–2.10 (3H, br s), 2.20 (6H, s), 1.75–1.55 (3H, br s), 1.68 (3H, d, *J* = 6.6 Hz), 1.50 (3H, d, *J* = 6.6 Hz); **¹³C NMR (100 MHz, CD₂Cl₂):** δ 253.9 (d, *J* = 13.6 Hz), 218.0, 154.9, 154.2, 142.4, 141.9, 138.8 (br), 136.6 (br), 136.3 (br), 131.6, 130.0, 130.0, 129.7, 128.0, 124.7, 123.4, 122.6, 121.9, 115.9, 82.2, 52.0, 24.5, 21.6, 21.3, 19.4 (br), 18.0 (br).

■ **Highly Z-Selective Ring-Opening Metathesis Polymerization (ROMP) Reactions:**
Representative procedure for polymerization of norbornene (3.16) at 0.1 mol % catalyst loading of Ru5. In an N₂ filled glove box, norbornene (**3.16**; 94.2 mg, 1.00 mmol, not rigorously purified) is dissolved in CH₂Cl₂ (1.8 mL) upon which a solution of **Ru5** (0.70 mg, 0.0010 mmol) in CH₂Cl₂ (0.2 mL) is added. The resulting solution is allowed to stir at 22 °C for one hour, after which the polymer is precipitated by addition

of MeOH (4.0 mL). The polymer is washed again with MeOH (2.0 mL) and dried under high vacuum (1.0×10^{-1} torr) to yield poly-norbornene **3.17** in 90% yield (85.0 mg). A 30 mg sample of the polymer is dissolved in an NMR tube for 12 hours in CDCl_3 . **IR (neat):** 2996 (m), 2939 (s), 2861 (m), 1710 (w), 1652 (w), 1463 (w), 1445 (m), 1404 (w), 1296 (w), 1265 (w), 1040 (w), 954 (w), 731 (s); **$^1\text{H NMR}$ (500 MHz, CDCl_3):** δ 5.25-5.19 (2H, m), 2.87-2.75 (2H, m), 1.95-1.87 (1H, m) 1.86-1.76 (2H, m), 1.42-1.33 (2H, m), 1.07-0.98 (1H, m); **$^{13}\text{C NMR}$ (125 MHz, CDCl_3):** δ 134.0, 42.9, 38.7, 33.4.

Representative procedure for polymerization of cyclooctadiene (3.18**) at 0.1 mol catalyst loading of **Ru5**.** In an N_2 filled glove box, a solution of **Ru5** (0.70 mg, 0.0010 mmol) in CH_2Cl_2 (0.2 mL) is added to 1,5-cyclooctadiene (**3.18**; 108 mg, 1.00 mmol, after purification by passing through a plug of basic alumina). The resulting solution is allowed to stir at 22 °C for 24 hours, after which the polymer is precipitated by the addition of MeOH (2.0 mL). The polymer is washed again with MeOH (2.0 mL) and dried under high vacuum (1.0×10^{-1} torr) to yield polycyclooctadiene **3.19** in 75% yield (80.0 mg). A 30 mg sample of the polymer is dissolved in a common NMR tube for 12 hours in CDCl_3 . **IR (neat):** 3005 (m), 2939 (m), 2852 (m), 1655 (w), 1450 (m), 1433 (m), 1404 (w), 1308 (w), 1239 (w), 994 (w), 733 (s); **$^1\text{H NMR}$ (500 MHz, CDCl_3):** δ 5.41-5.37 (4H, m), 2.11-2.06 (8H, m); **$^{13}\text{C NMR}$ (125 MHz, CDCl_3):** δ 129.7, 27.6.

Procedures for polymerization reactions at < 0.1 mol% catalyst loading of **Ru5 (cf. Table 3.3.1 entries 7–10).** Polymerizations at reduced catalyst loading are performed at a 5.0 mmol scale of substrate (**3.16** or **3.18**), which has been purified by passing a corresponding sample over a plug of basic alumina (either neat in case of **3.18** or as a solution in CH_2Cl_2 in case of **3.16**). The amount of solvent is increased accordingly to maintain the monomer concentration from the experiments at 0.1 mol % loading. A corresponding aliquot (0.40 or 0.08 mL) of a solution of complex **Ru5** (2.0 mg, 2.9 mmol in 2.3 mL dichloromethane) is added to initiate the polymerization.

■ Highly Z-Selective Ring-Opening Cross/Metathesis (ROCM) Reactions:

General Procedure for Transformations in Table 3.3.2.1

In an N₂-filled glove box, an oven-dried 4 mL vial equipped with a magnetic stir bar is charged with strained alkene substrate (1.0 equiv) and terminal olefin cross partner (10-20 equiv). To this vial, a solution of Ru complex **4b** (1.0-3.0 mol %) in tetrahydrofuran is added. The resulting mixture is allowed to stir for 1-12 hours at 22-40 °C, after which the reaction is quenched by addition of wet diethyl ether and concentrated *in vacuo* (percent conversion determined by 400 MHz ¹H NMR analysis). Purification is performed through silica gel chromatography.

((Z)-2-((1*S*,3*R*)-3-Vinylcyclopentyl)vinyl)benzene (**3.21a**).

Following the general procedure above, a solution of **Ru4b** (1.1 mg, 1.5 mmol, 1.0 mol %) in tetrahydrofuran (320 μL) is transferred by syringe to a vial containing norbornene **3.16** (15.0 mg, 0.159 mmol, 1.00 equiv) and styrene (332 mg, 3.19 mmol, 20.0 equiv). The resulting mixture is allowed to stir for one hour at 22 °C. Analysis of the ¹H NMR (400 MHz) spectrum reveals >98% conv of norbornene, and the corresponding ROCM product **3.21a** is obtained as a mixture of 98:2 *Z:E* isomers. The resulting brown oil is purified by silica gel chromatography (100% hexanes) to afford **3.21a** (23.7 mg, 0.119 mmol, 75% yield) as colorless oil. **IR (neat)**: 3079 (w), 3024 (w), 3002 (w), 2944 (s), 2863 (m), 1639 (s), 1600 (w), 1492 (w), 1464 (m), 1446 (m), 1409 (m), 1299 (w), 1074 (w), 1028 (m), 993 (m), 964 (m), 909 (s), 768 (s), 732 (m), 698 (s), 664 (w), 553 (w), 500 (w), 422 (w); **¹H NMR (400 MHz, CDCl₃)**: δ 7.36-7.32 (2H, m), 7.28-7.21 (3H, m), 6.38 (1H, d, *J* = 11.2 Hz)⁶⁷, 5.88-5.79 (1H, m), 5.59 (1H, dd, *J* = 11.6, 10.4 Hz), 5.03-4.98 (1H, m), 4.92-4.89 (1H, m), 3.12-3.02 (1H, m), 2.60-2.50 (1H, m), 2.07-2.00 (1H, m), 1.97-1.80 (2H, m), 1.58-1.45 (2H, m), 1.29-1.22 (1H, m); **¹³C NMR (100 MHz, CDCl₃)**: δ 143.2, 138.1, 138.0, 128.8, 128.3, 127.8, 126.6, 112.7, 44.7, 41.6, 38.8, 33.2, 32.1; **HRMS [M+H]⁺** calcd for C₁₅H₁₉: 199.1487; found: 199.1479.

((Z)-2-((1*S*,3*R*)-3-Vinylcyclopentyl)vinyl)cyclohexane (**3.21b**).

Following the general procedure above, a solution of **Ru4b** (1.1 mg, 1.5 mmol, 1.0 mol %) in tetrahydrofuran (320 μL) is transferred by syringe to a vial containing

(67) The coupling constants (*J* = 11.2 and 11.6 Hz, respectively) of the signals at δ 6.38 and 5.59 ppm are indicative of *Z* isomer of **3.21a**.

norbornene **7** (15.0 mg, 0.159 mmol, 1.00 equiv) and vinyl cyclohexane (351 mg, 3.19 mmol, 20.0 equiv). The resulting mixture is allowed to stir for two hours at 22 °C. Analysis of the ¹H NMR (400 MHz) spectrum reveals >98% conv of norbornene, and the corresponding ROCM product **3.21b** is obtained as >98% Z-isomer. The resulting brown oil is purified by silica gel chromatography (100% hexanes) to afford **3.21b** (19.2 mg, 0.0940 mmol, 59% yield) as colorless oil. **IR (neat)**: 3077 (w), 2994 (w), 2921 (s), 2849 (s), 1640 (m), 1447 (s), 1407 (w), 1269 (w), 1029 (s), 992 (w), 951 (s), 907 (s), 889 (w), 742 (s), 666 (w); **¹H NMR (500 MHz, CDCl₃)**: δ 5.84-5.77 (1H, m), 5.18 (1H, apparent t with strong roof effect, *J* = 10.0 Hz)⁶⁸, 5.13 (1H, apparent t with strong roof effect, 9.8 Hz), 4.98 (1H, d, *J* = 17.0 Hz), 4.88 (1H, d, *J* = 10.5 Hz), 2.85-2.76 (1H, m), 2.56-2.49 (1H, m), 2.29-2.22 (1H, m), 1.94-1.84 (3H, m), 1.71-1.59 (4H, m), 1.49-1.24 (4H, m), 1.21-1.04 (4H, m), 0.89-0.84 (1H, m); **¹³C NMR (100 MHz, CDCl₃)**: δ 143.5, 135.1, 133.2, 112.4, 44.7, 41.6, 38.6, 36.8, 36.7, 33.9, 33.1, 31.9, 26.2; **HRMS [M+H]⁺** calcd for C₁₅H₂₅: 205.1956; found: 205.1953.

(Z)-3-((1*R*,3*S*)-3-Vinylcyclopentyl)prop-2-en-1-ol (3.21c).

Following the general procedure, a solution of **Ru4b** (5.5 mg, 8.0 mmol, 5.0 mol %) in dichloromethane (320 μL) was transferred by syringe to a vial containing norbornene **3.16** (15.0 mg, 0.159 mmol, 1.00 equiv) and allyl alcohol (93.0 mg, 1.59 mmol, 10.0 equiv). The resulting solution was allowed to stir for 2 hours at 22 °C. Analysis of the unpurified mixture revealed >98% consumption of **3.16**, and the ROCM product was obtained in 88:12 *Z:E* ratio. The resulting oil was purified by silica gel chromatography (10% Et₂O in hexanes to 30% Et₂O in hexanes) to afford **3.21c** (16.4 mg, 0.108 mmol, 68% yield) as colorless oil; **IR (CH₂Cl₂)**: 3319 (br), 2943 (m), 2864 (m), 1639 (w), 1447 (w), 1012 (s), 993 (s), 907 (s); **¹H NMR (400 MHz, CDCl₃)**: Z-isomer (major): δ 5.79 (1H, ddd, *J* = 17.4, 10.2, 7.5 Hz), 5.53 (1H, dt, *J* = 10.8, 6.8 Hz)⁶⁹, 5.43 (1H, dd, *J* = 10.6, 9.4 Hz), 4.98 (1H, ddd, *J* = 17.1, 1.9, 1.2 Hz), 4.88 (1H, ddd, *J* = 10.2, 1.9, 1.0 Hz), 4.20 (2H, d, *J* = 5.6 Hz), 2.89-2.76 (1H, m), 2.61-2.46 (1H, m), 1.96-

(68) The coupling constants (*J* = 10.0 and 9.8 Hz, respectively) of the signals at δ 5.18 and 5.13 ppm are indicative of *Z* isomer of **3.21b**.

(69) Coupling constants (*J* = 10.8 and *J* = 10.6 Hz) of the signals at δ 5.53 and 5.43 ppm indicate the predominance of *Z*-isomer **3.21c**.

1.89 (1H, m), 1.87–1.77 (2H, m), 1.51–1.32 (3H, m), 1.12 (1H, dt, $J = 12.4, 10.5$ Hz); ^{13}C NMR (100 MHz, C_6D_6): δ 142.7, 136.7, 128.0, 112.3, 58.4, 44.4, 41.0, 38.0, 32.4, 31.6; HRMS [M+H-H₂O]⁺ calcd for C₁₀H₁₅: 135.1174, found: 135.1179.

(Z)-4-((1*R*,3*S*)-3-Vinylcyclopentyl)but-3-en-1-ol (3.21e).

Following the general procedure, a solution of **Ru4b** (5.5 mg, 8.0 mmol, 5.0 mol %) in dichloromethane (320 μL) was transferred by syringe to a vial containing norbornene **3.16** (15.0 mg, 0.159 mmol, 1.00 equiv) and 3-buten-1-ol (115 mg, 1.59 mmol, 10.0 equiv). The resulting solution was allowed to stir for 2 hours at 22 °C. Analysis of the unpurified mixture revealed >98% consumption of **3.16**, and the product was obtained in 87:13 Z:E ratio. The resulting oil was purified by silica gel chromatography (5% Et₂O in hexanes to 10% Et₂O in hexanes) to afford **3.21e** (23.3 mg, 0.140 mmol, 88% yield) as colorless oil; IR (CH₂Cl₂): 3334 (br), 2944 (s), 2864 (m), 1639 (w), 1447 (w), 1045 (s), 907 (s); ^1H NMR (400 MHz, CDCl₃): Z-isomer (major): δ 5.80 (1H, ddd, $J = 17.3, 10.1, 7.5$ Hz), 5.50 (1H, t, $J = 10.1$ Hz)⁷⁰, 5.29 (1H, dt, $J = 10.8, 7.5$ Hz), 4.97 (1H, dd, $J = 17.1, 1.1$ Hz), 4.91–4.83 (1H, m), 3.63 (2H, t, $J = 6.3$ Hz), 2.90–2.76 (1H, m), 2.62–2.47 (1H, m), 2.34 (2H, qd, $J = 6.5, 1.3$ Hz), 1.99–1.87 (1H, m), 1.86–1.78 (2H, m), 1.52–1.32 (2H, m), 1.18–1.04 (1H, m), 0.92–0.79 (1H, m); ^{13}C NMR (100 MHz, CDCl₃): δ 143.1, 138.6, 123.7, 112.4, 62.3, 44.4, 41.1, 38.1, 32.6, 31.7, 31.0; HRMS [M+H]⁺ calcd for C₁₁H₁₉O: 167.1436, found: 167.1431.

(1*R*,3*S*)-1-((Z)-4-butoxybut-1-en-1-yl)-3-vinylcyclopentane (3.21f).

The compound is prepared following the procedure for **3.21e**.

3-((Z)-Styryl)-5-vinylcyclopentane-1,2-diyl)dimethanol (3.23a).

Following the general procedure above, a solution of **Ru4b** (0.70 mg, 1.0 mmol, 1.0 mol %) in tetrahydrofuran (195 μL) is transferred by syringe to a vial containing 5-norbornene-2-*exo*,3-*exo*-dimethanol **3.22** (15.0 mg, 0.0970 mmol, 1.00 equiv) and styrene (202 mg, 1.94 mmol, 20.0 equiv). The resulting mixture is allowed to stir for one hour at 22 °C. Analysis of the ^1H NMR (400 MHz) spectrum reveals >98% conv of **3.22**, and the

(70) Coupling constants ($J = 10.8$ and $J = 10.1$ Hz) of the signals at δ 5.50 and 5.29 ppm indicate Z-isomer **3.21e**.

corresponding ROCM product **3.23a** is obtained as a mixture of 97:3 *Z:E* isomers. The resulting brown oil is purified by silica gel chromatography (100% hexanes followed by 30-70% Et₂O in hexanes) to afford **3.23a** (23.2 mg, 0.0890 mmol, 92% yield) as colorless oil. **IR (neat)**: 3263 (br), 3078 (m), 3023 (m), 3002 (m), 2018 (m), 1639 (s), 1600 (s), 1493 (s), 1447 (m), 1413 (m), 1318 (br), 1252 (m), 1209 (m), 1180 (m), 1132 (m), 1066 (s), 1047 (s), 1027 (s), 993 (s), 913 (s), 875 (s), 809 (s), 770 (s), 736 (s), 700 (s), 673 (s), 563 (s), 494 (m), 449 (m); **¹H NMR (400 MHz, CDCl₃)**: δ 7.34-7.30 (2H, m), 7.24-7.21 (3H, m), 6.48 (1H, d, *J* = 11.6 Hz)⁷¹, 5.79-5.70 (1H, m), 5.52 (1H, dd, *J* = 11.6, 10.4 Hz), 5.04-4.99 (1H, m), 4.98-4.95 (1H, m), 3.66-3.52 (5H, m), 3.31 (1H, br s), 2.78-2.69 (1H, m), 2.21-2.07 (3H, m), 2.03-1.97 (1H, m), 1.41-1.32 (1H, m); **¹³C NMR (100 MHz, CDCl₃)**: δ 141.5, 137.6, 135.9, 129.9, 128.6, 128.4, 126.9, 114.6, 62.05, 62.03, 50.6, 48.6, 46.4, 40.3, 39.9; **HRMS [M+H]⁺** calcd for C₁₇H₂₃O₂: 259.1698; found: 259.1694.

3-((*Z*)-3-Fluorostyryl)-5-vinylcyclopentane-1,2-diyldimethanol (**3.23b**).

Following the general procedure, a solution of **Ru4b** (0.70 mg, 1.0 mmol, 1.0 mol %) in tetrahydrofuran (195 μL) is transferred by syringe to a vial containing 5-norbornene-2-*exo,3-exo*-dimethanol **3.22** (15.0 mg, 0.0970 mmol, 1.00 equiv) and 4-methoxystyrene (237 mg, 1.94 mmol, 20.0 equiv). The resulting mixture is allowed to stir for one hour at 22 °C. Analysis of the ¹H NMR (400 MHz) spectrum reveals >98% conv of **3.22**, and the corresponding ROCM product **3.23b** is obtained as a mixture of 96:4 *Z:E* isomers. The resulting brown oil is purified by silica gel chromatography (100% hexanes followed by 30-70% diethyl ether in hexanes) to afford **3.23b** (24.9 mg, 0.0900 mmol, 93% yield) as colorless oil. **IR (neat)**: 3285 (br), 3075 (m), 3004 (m), 2919 (m), 1640 (s), 1611 (s), 1580 (s), 1485 (s), 1441 (s), 1375 (m), 1282 (m), 1245 (s), 1136 (s), 1066 (s), 1047 (s), 1024 (s), 994 (s), 914 (s), 875 (s), 795 (s), 756 (s), 697 (s), 673 (s), 604 (m), 522 (s), 443 (w), 424 (w); **¹H NMR (400 MHz, CDCl₃)**: δ 7.29-7.24 (1H, m), 7.00-6.98 (1H, m), 6.94-6.89 (2H, m), 6.42 (1H, d, *J* = 11.2 Hz)⁷², 5.78-5.69 (1H, m), 5.56 (1H, dd, *J* = 11.2, 10.0 Hz), 5.05-4.99 (1H, m), 4.98-4.96 (1H, m), 3.68-3.52 (4H, m), 3.37 (2H, br s),

(71) The coupling constants (*J* = 11.6 and 11.6 Hz, respectively) of the signals at δ 6.48 and 5.52 ppm are indicative of *Z* isomer of **3.23a**.

(72) The coupling constants (*J* = 11.2 and 11.2 Hz, respectively) of the signals at δ 6.42 and 5.56 ppm are indicative of *Z* isomer of **3.23b**.

2.75-2.66 (1H, m), 2.22-2.10 (3H, m), 2.02-1.96 (1H, m), 1.40-1.31 (1H, m); **¹³C NMR (100 MHz, CDCl₃)**: δ 162.8 (d, *J*_{C,F} = 244.4 Hz), 141.3, 139.7 (d, *J*_{C,F} = 7.6 Hz), 137.0, 129.9 (d, *J*_{C,F} = 8.3 Hz), 128.8 (d, *J*_{C,F} = 2.3 Hz), 124.4 (d, *J*_{C,F} = 3.0 Hz), 115.4 (d, *J*_{C,F} = 21.2 Hz), 114.8, 113.7 (d, *J*_{C,F} = 21.2 Hz), 62.01, 61.99, 50.5, 48.6, 46.4, 40.3, 39.8; **HRMS [M+NH₄]⁺** calcd for C₁₇H₂₂FO₂: 277.1604; found: 277.1591.

3-((Z)-4-Methoxystyryl)-5-vinylcyclopentane-1,2-diyldimethanol (3.23c).

Following the general procedure, a solution of **Ru4b** (0.70 mg, 1.0 mmol, 1.0 mol %) in tetrahydrofuran (195 μL) is transferred by syringe to a vial containing 5-norbornene-2-*exo*,3-*exo*-dimethanol **3.22** (15.0 mg, 0.0970 mmol, 1.00 equiv) and 4-methoxystyrene (260 mg, 1.94 mmol, 20.0 equiv). The resulting mixture is allowed to stir for one hour at 22 °C. Analysis of the **¹H NMR (400 MHz)** spectrum reveals >98% conv of **3.22**, and the corresponding ROCM product **3.23c** is obtained as a mixture of 98:2 *Z:E* isomers. The resulting brown oil is purified by silica gel chromatography (100% hexanes followed by 20-70% diethyl ether in hexanes) to afford **3.23c** (23.2 mg, 0.0800 mmol, 82% yield) as colorless oil. **IR (neat)**: 3271 (br), 3074 (m), 2999 (m), 2917 (m), 1639 (s), 1607 (s), 1574 (s), 1509 (s), 1460 (m), 1405 (m), 1300 (m), 1245 (s), 1174 (s), 1108 (m), 1065 (m), 1031 (s), 994 (m), 913 (s), 842 (s), 817 (m), 746 (m), 710 (m), 669 (m), 631 (m), 564 (m), 517 (m), 443 (m); **¹H NMR (400 MHz, CDCl₃)**: δ 7.19-7.15 (2H, m), 6.87-6.84 (2H, m), 6.41 (1H, d, *J* = 11.6 Hz)⁷³, 5.79-5.71 (1H, m), 5.44 (1H, dd, *J* = 11.6, 10.0 Hz), 5.04-4.99 (1H, m), 4.98-4.95 (1H, m), 3.80 (3H, s), 3.68-3.54 (4H, m), 3.45 (1H, br s), 3.18 (1H, br s), 2.79-2.70 (1H, m), 2.27-2.08 (3H, m), 2.03-1.97 (1H, m), 1.39-1.31 (1H, m); **¹³C NMR (100 MHz, CDCl₃)**: δ 158.5, 141.6, 134.6, 130.1, 129.8, 129.4, 114.6, 113.8, 62.09, 62.08, 55.4, 50.7, 48.6, 46.4, 40.3, 39.9; **HRMS [M+H]⁺** calcd for C₁₈H₂₅O₃: 289.1804; found: 289.1809.

3-((Z)-2-Cyclohexylvinyl)-5-vinylcyclopentane-1,2-diyldimethanol (3.23d).

Following the general procedure, a solution of **Ru4b** (0.70 mg, 1.0 mmol, 1.0 mol %) in tetrahydrofuran (195 μL) is transferred by syringe to a vial containing 5-norbornene-2-*exo*,3-*exo*-dimethanol **3.22** (15.0 mg, 0.0970 mmol, 1.00 equiv) and vinyl

(73) The coupling constants (*J* = 11.6 and 11.6 Hz, respectively) of the signals at δ 6.41 and 5.44 ppm are indicative of *Z* isomer of **3.23c**.

cyclohexane (214 mg, 1.94 mmol, 20.0 equiv). The resulting mixture is allowed to stir for 8 hours at 22 °C. Analysis of the ¹H NMR (400 MHz) spectrum reveals >98% conv of **3.22**, and the corresponding ROCM product **3.23d** is obtained as >98% Z isomer. The resulting brown oil is purified by silica gel chromatography (100% hexanes followed by 30-50% diethyl ether in hexanes) to afford **3.23d** (15.8 mg, 0.0590 mmol, 61% yield) as colorless oil. **IR (neat)**: 3284 (br), 3076 (w), 2990 (w), 2920 (s), 2849 (s), 1639 (m), 1448 (s), 1349 (w), 1258 (w), 1072 (m), 1044 (m), 1028 (m), 993 (m), 947 (s), 911 (s), 890 (w), 748 (m), 675 (w); **¹H NMR (400 MHz, CDCl₃)**: δ 5.78-5.69 (1H, m), 5.23 (1H, apparent t with roof effect, *J* = 10.8 Hz)⁷⁴, 5.11 (1H, apparent t with roof effect, *J* = 10.8 Hz), 5.03-4.98 (1H, m), 4.97-4.94 (1H, m), 3.76-3.60 (4H, m), 3.28 (2H, br s), 2.51-2.42 (1H, m), 2.29-1.98 (4H, m), 1.88-1.82 (1H, m), 1.72-1.53 (5H, m), 1.32-0.99 (6H, m); **¹³C NMR (100 MHz, CDCl₃)**: δ 141.7, 137.0, 131.0, 114.5, 62.35, 62.26, 50.0, 48.6, 46.6, 40.3, 40.1, 36.8, 35.0, 33.9, 33.7, 26.1, 26.0; **HRMS [M+H]⁺** calcd for C₁₇H₂₉O₂: 265.2168; found: 265.2178.

(Z)-(((1-Phenylhexa-1,5-diene-3,4-diyl)bis(oxy))bis(methylene))dibenzene (3.25).

Following the general procedure, a solution of **Ru4b** (1.8 mg, 2.5 mmol, 3.0 mol %) in tetrahydrofuran (170 μL) is transferred by syringe to a vial containing cyclobutene **3.24** (22.4 mg, 0.0840 mmol, 1.00 equiv) and styrene (88.0 mg, 0.845 mmol, 10.0 equiv). The resulting mixture is allowed to stir for 12 hours at 40 °C. Analysis of the ¹H NMR (400 MHz) spectrum reveals 94% conv of **3.24**, and the corresponding ROCM product **3.25** is obtained as a mixture of 93:7 Z:E isomers. The resulting brown oil is purified by silica gel chromatography (100% hexanes to 2% diethyl ether in hexanes) followed by passing through a plug of activated charcoal with 100% dichloromethane to afford **3.25** (20.9 mg, 0.0560 mmol, 63% yield) as colorless oil. **IR (neat)**: 3062 (w), 3028 (m), 2863 (m), 1641 (m), 1600 (m), 1495 (w), 1454 (w), 1422 (w), 1388 (w), 1368 (w), 1332 (w), 1246 (w), 1205 (w), 1090 (s), 1069 (s), 1028 (s), 991 (m), 928 (m), 804 (w), 779 (w), 736 (s), 697 (s), 606 (w), 459 (w); **¹H NMR (400 MHz, CDCl₃)**: δ 7.36-7.12 (13H, m), 7.15-7.12 (s), 606 (w), 459 (w); **¹³C NMR (100 MHz, CDCl₃)**: δ 141.7, 137.0, 131.0, 114.5, 62.35, 62.26, 50.0, 48.6, 46.6, 40.3, 40.1, 36.8, 35.0, 33.9, 33.7, 26.1, 26.0; **HRMS [M+H]⁺** calcd for C₂₇H₃₈O₂: 406.2820; found: 406.2820.

(74) The coupling constants (*J* = 10.8 and 10.8 Hz, respectively) of the signals at δ 5.23 and 5.11 ppm are indicative of Z isomer of **3.23d**.

(2H, m), 6.80 (1H, d, J = 12.0 Hz)⁷⁵, 5.96-5.87 (1H, m), 5.68 (1H, dd, J = 12.0, 10.0 Hz), 5.37-5.29 (2H, m), 4.68 (1H, d, J = 12.4 Hz), 4.52 (1H, d, J = 12.0 Hz), 4.48-4.44 (2H, m), 4.27 (1H, d, J = 11.6 Hz), 3.94-3.90 (1H, m); **^{13}C NMR (100 MHz, CDCl₃)**: δ 138.8, 138.5, 136.8, 135.8, 133.9, 130.1, 128.9, 128.4, 128.3, 128.2, 128.0, 127.8, 127.5, 127.4, 127.3, 119.2, 82.3, 76.2, 70.4, 70.3; **HRMS [M+NH₄]⁺** calcd for C₂₆H₃₀NO₂: 388.2277; found: 388.2278.

(R,Z)-(3-Methylpenta-1,4-diene-1,3-diyl)dibenzene (3.27).

Following the general procedure, a solution of **Ru4b** (1.6 mg, 2.3 mmol, 2.0 mol %) in dichloromethane (230 μL) was transferred by syringe to a vial containing cyclopropene **3.26** (15.0 mg, 0.115 mmol, 1.00 equiv) and styrene (120 mg, 1.15 mmol, 10.0 equiv). The resulting solution was allowed to stir for two hours at 22 °C. Analysis of the unpurified mixture revealed >98% consumption of **3.26**, and the ROCM product was obtained in >98:2 Z:E ratio. The resulting oil was purified by silica gel chromatography (100% hexanes) to afford **3.27** (18.6 mg, 0.0794 mmol, 69% yield) as colorless oil; **IR (CH₂Cl₂)**: 2960 (w), 2924 (m), 2851 (w), 1599 (w), 1492 (m), 1445 (m), 915 (m); **^1H NMR (400 MHz, CDCl₃)**: Z-isomer (major): δ 7.34–7.30 (2H, m), 7.24–7.19 (2H, m), 7.15–7.06 (4H, m), 7.01–6.69 (2H, m), 6.62 (1H, d, J = 12.7 Hz)⁷⁶, 6.15 (1H, dd, J = 17.4, 10.6 Hz), 5.89 (1H, d, J = 12.7 Hz), 5.08 (1H, dd, J = 12.1, 1.2 Hz), 5.04 (1H, dd, J = 5.2, 1.2 Hz), 1.45 (3H, s); **^{13}C NMR (100 MHz, CDCl₃)**: δ 147.4, 145.2, 138.2, 137.6, 129.8, 129.0, 128.0, 127.3, 126.9, 126.3, 125.8, 112.3, 48.0, 28.6; **HRMS [M+H]⁺** calcd for C₁₈H₁₉: 235.1487, found: 235.1482.

General Procedure for Transformations in Schemes (3.3.2.2, 3.3.2.3, 3.3.2.4a, and 3.3.2.4a).

In an N₂-filled glove box, an oven-dried 4 mL vial equipped with a magnetic stir bar is charged with strained alkene substrate (1.0 equiv) and terminal olefin cross partner (10 equiv). To this vial, a solution of Ru complex **4b** (2.0-5.0 mol %) in dichloromethane is added. The resulting solution is allowed to stir for 2-12 hours at 22-40 °C, after which

(75) The coupling constants (J = 12.0 and 12.0 Hz, respectively) of the signals at δ 6.80 and 5.68 ppm are indicative of Z isomer of **3.25**.

(76) Coupling constants (J = 12.7 Hz and J = 12.7 Hz) for the signals at δ 6.62 and 5.89 ppm indicate the predominance of **3.27**.

the reaction is quenched by addition of wet diethyl ether and concentrated *in vacuo* (percent conversion determined by 400 MHz or 500 MHz ¹H NMR analysis). Purification is performed through silica gel chromatography.

((1*S*,2*R*,3*R*,5*S*)-3-((*Z*)-3-(Trimethylsilyl)prop-1-enyl)-5-vinylcyclopentane-1,2-diyldimethanol (3.28a).

Following the general procedure, a solution of **Ru4b** (3.4 mg, 4.9 mmol, 5.0 mol %) in dichloromethane (195 μ L) was transferred by syringe to a vial containing 5-norbornene-2-*exo*,3-*exo*-dimethanol **3.22** (15.0 mg, 0.0973 mmol, 1.00 equiv) and allyltrimethylsilane (111 mg, 0.973 mmol, 10.0 equiv). The resulting solution was allowed to stir for 8 hours at 22 °C. Analysis of the unpurified mixture revealed >98% consumption of **3.22**, and the ROCM product was obtained in >98:2 *Z:E* ratio. The resulting oil was purified by silica gel chromatography (10% EtOAc in hexanes to 30% EtOAc in hexanes) to afford **3.28a** (23.2 mg, 0.0864 mmol, 89% yield) as colorless oil; **IR (CH₂Cl₂)**: 3274 (br), 2951 (w), 2918 (w), 1640 (w), 1398 (w), 1048 (w), 993 (w), 850 (s), 837 (s), 663 (m); **¹H NMR (400 MHz, CDCl₃)**: *Z*-isomer (major): δ 5.74 (1H, ddd, *J* = 17.1, 10.1, 7.9 Hz), 5.48–5.31 (1H, m), 5.15 (1H, dd, *J* = 12.0, 10.8 Hz)⁷⁷, 5.00 (1H, ddd, *J* = 17.0, 1.8, 0.9 Hz), 4.95 (1H, dd, *J* = 10.1, 1.3 Hz), 3.75–3.62 (4H, m), 3.32 (2H, s), 2.42 (1H, ddd, *J* = 20.5, 12.7, 7.8 Hz), 2.21–1.98 (3H, m), 1.85 (1H, dt, *J* = 12.3, 6.1 Hz), 1.53 (1H, ddd, *J* = 13.6, 9.7, 1.3 Hz), 1.36 (1H, ddd, *J* = 13.6, 7.5, 1.5 Hz), 1.22 (1H, t, *J* = 12.0 Hz), 0.00 (9H, s); **¹³C NMR (100 MHz, CDCl₃)**: δ 141.8, 130.9, 126.4, 114.4, 62.3, 62.3, 50.3, 48.6, 46.6, 39.9, 39.5, 18.8, -1.7; **HRMS [M+H-H₂O]⁺** calcd for C₁₅H₂₇OSi: 251.1831, found: 251.1837.

((1*S*,2*R*,3*R*,5*S*)-3-((*Z*)-3-(4-Methoxyphenyl)prop-1-enyl)-5-vinylcyclopentane-1,2-diyldimethanol (3.28b).

Following the general procedure, a solution of **Ru4b** (3.4 mg, 4.9 mmol, 5.0 mol %) in dichloromethane (195 μ L) was transferred by syringe to a vial containing 5-norbornene-2-*exo*,3-*exo*-dimethanol **3.22** (15.0 mg, 0.0973 mmol, 1.00 equiv) and 4-allylanisole (144 mg, 0.973 mmol, 10.0 equiv). The resulting solution was allowed to stir

(77) Coupling constant (*J* = 12.0 Hz) of the signal at δ 5.15 ppm indicates the predominance of *Z*-isomer **3.28a**.

for 8 hours at 22 °C. Analysis of the unpurified mixture revealed >98% consumption of **3.22**, and the ROCM product was obtained in >98:2 Z:E ratio. The resulting oil was purified by silica gel chromatography (10% EtOAc in hexanes to 40% EtOAc in hexanes) to afford **3.28b** (24.4 mg, 0.0807 mmol, 83% yield) as yellow oil; **IR** (CH_2Cl_2): 3286 (br), 2917 (m), 1610 (w), 1509 (s), 1463 (w), 1243 (s), 1175 (m), 1033 (s), 995 (m), 911 (m), 816 (m); **$^1\text{H NMR}$** (400 MHz, CDCl_3): Z-isomer (major): δ 7.09 (2H, d, J = 8.7 Hz), 6.83 (2H, d, J = 8.6 Hz), 5.75 (1H, ddd, J = 16.0, 12.0, 8.0 Hz), 5.57 (1H, dt, J = 10.7, 7.5 Hz)⁷⁸, 5.37 (1H, t, J = 10.2 Hz), 5.05–4.99 (1H, m), 4.98–4.95 (1H, m), 3.78 (3H, s), 3.75–3.64 (4H, m), 3.34 (1H, dd, J = 10.9, 7.6 Hz), 3.29–3.26 (2H, m), 2.69–2.56 (1H, m), 2.27–2.19 (1H, m), 2.16–2.03 (2H, m), 1.93 (1H, dt, J = 12.3, 6.2 Hz), 1.28 (2H, m); **$^{13}\text{C NMR}$** (100 MHz, C_6D_6): δ 158.3, 141.7, 133.7, 132.8, 129.2, 129.1, 113.9, 113.9, 61.4, 54.4, 49.9, 48.5, 46.1, 39.7, 39.27, 32.9; **HRMS** [$\text{M}+\text{H}]^+$ calcd for $\text{C}_{19}\text{H}_{27}\text{O}_3$: 303.1960, found: 303.1955.

(Z)-5-((1*R*,2*R*,3*S*,4*S*)-2,3-Bis(hydroxymethyl)-4-vinylcyclopentyl)-*N*-phenylpent-4-enamide (3.28c).

Following the general procedure, a solution of **Ru4b** (3.4 mg, 4.9 mmol, 5.0 mol %) in dichloromethane (195 μL) was transferred by syringe to a vial containing 5-norbornene-2-*exo*,3-*exo*-dimethanol **3.22** (15.0 mg, 0.0973 mmol, 1.00 equiv) and *N*-phenylpent-4-enamide (320 mg, 0.973 mmol, 10.0 equiv). The resulting solution was allowed to stir for 4 hours at 22 °C. Analysis of the unpurified mixture revealed >98% conv of **3.22**, and the ROCM product was obtained in >98:02 Z/E ratio. The resulting oil was purified by silica gel chromatography (10% EtOAc in hexanes to 50% EtOAc in hexanes) to afford **3.28c** (20.8 mg, 0.0631 mmol, 65% yield) as colorless oil; **IR** (CH_2Cl_2): 3299 (br), 2920 (m), 2853 (m), 1663 (m), 1599 (m), 1545 (m), 1443 (s), 1027 (m); **$^1\text{H NMR}$** (400 MHz, CDCl_3): Z-isomer (major): δ 7.61 (1H, s), 7.50 (2H, d, J = 7.7 Hz), 7.31 (2H, t, J = 7.9 Hz), 7.10 (1H, t, J = 7.4 Hz), 5.75 (1H, ddd, J = 17.1, 10.1, 8.1 Hz), 5.45–5.36 (1H, m), 5.25 (1H, t, J = 10.2 Hz)⁷⁹, 5.02 (1H, ddd, J = 17.1, 1.8, 1.0 Hz),

(78) Coupling constants (J = 10.7 Hz and J = 10.2 Hz) of the signals at δ 5.57 and 5.37 ppm indicate the predominance Z-isomer **3.28b**.

(79) Coupling constant (J = 10.2 Hz) of the signal at δ 5.25 ppm indicates the predominance of Z-isomer **3.28c**.

4.94 (1H, ddd, $J = 10.1, 1.8, 0.5$ Hz), 3.79 (1H, dd, $J = 11.6, 2.7$ Hz), 3.71 (1H, dd, $J = 12.0, 2.5$ Hz), 3.67–3.61 (2H, m), 2.92–2.80 (1H, m), 2.75–2.65 (1H, m), 2.57–2.43 (2H, m), 2.36–2.28 (2H, m), 2.03–1.81 (4H, m), 1.23–1.16 (2H, m); **^{13}C NMR (100 MHz, CDCl_3)**: δ 171.4, 142.1, 138.0, 135.1, 129.2, 128.5, 124.5, 119.9, 114.1, 61.8, 60.4, 50.1, 48.7, 45.6, 39.8, 39.2, 38.0, 23.9; **HRMS [M+H]⁺** calcd for $\text{C}_{20}\text{H}_{28}\text{NO}_3$: 330.2069, found: 330.2076.

((1*S*,2*R*,3*R*,5*S*)-3-((*Z*)-4-(*tert*-Butyldimethylsilyloxy)but-1-enyl)-5-vinylcyclopentane-1,2-diyl)dimethanol (3.28d).

Following the general procedure, a solution of **Ru4b** (3.4 mg, 4.9 mmol, 5.0 mol %) in dichloromethane (195 μL) was transferred by syringe to a vial containing 5-norbornene-2-*exo*,3-*exo*-dimethanol **3.22** (15.0 mg, 0.0973 mmol, 1.00 equiv) and 1-(*tert*-butyldimethylsilyloxy)-3-butene (181 mg, 0.973 mmol, 10.0 equiv). The resulting solution was allowed to stir for 8 hours at 22 °C. Analysis of the unpurified mixture revealed 89% consumption of **3.22**, and the ROCM product was obtained in >98:2 *Z:E* ratio. The resulting oil was purified by silica gel chromatography (10% EtOAc in hexanes to 30% EtOAc in hexanes) to afford **3.28d** (22.5 mg, 0.0661 mmol, 68% yield) as yellow oil; **IR (CH₂Cl₂)**: 3299 (br), 2926 (s), 2856 (m), 1639 (w), 1463 (w), 1095 (m), 1046 (m), 836 (s); **^1H NMR (500 MHz, CDCl_3)**: *Z*-isomer (major): δ 5.76 (1H, ddd, $J = 17.8, 10.3, 8.3$ Hz), 5.43–5.36 (1H, m), 5.30 (1H, t, $J = 10.3$ Hz)⁸⁰, 5.04–4.98 (1H, m), 4.94 (1H, ddd, $J = 10.1, 1.7, 0.8$ Hz), 3.75–3.71 (1H, m), 3.69 (1H, d, $J = 10.6$ Hz), 3.67–3.58 (4H, m), 2.67–2.57 (1H, m), 2.42–2.28 (2H, m), 2.25–2.16 (2H, m), 2.08–2.00 (1H, m), 1.95 (1H, tdd, $J = 10.3, 7.7, 2.8$ Hz), 1.89 (1H, dt, $J = 12.3, 6.3$ Hz), 1.27–1.19 (2H, m), 0.90 (9H, d, $J = 0.7$ Hz), 0.07 (6H, s); **^{13}C NMR (125 MHz, CDCl_3)**: δ 142.1, 134.8, 127.2, 114.1, 63.4, 62.3, 61.3, 50.1, 48.6, 46.1, 39.8, 39.7, 31.5, 26.2, –5.1, –5.1; **HRMS [M+Na]⁺** calcd for $\text{C}_{19}\text{H}_{36}\text{O}_3\text{NaSi}$: 363.2326, found: 363.2330.

((1*S*,2*R*,3*R*,5*S*)-3-((*Z*)-Dec-1-enyl)-5-vinylcyclopentane-1,2-diyl)dimethanol (3.28e).

Following the general procedure, a solution of **Ru4b** (3.4 mg, 4.9 mmol, 5.0 mol %) in dichloromethane (195 μL) was transferred by syringe to a vial containing 5-

(80) Coupling constant ($J = 10.3$ Hz) of the signal at δ 5.30 ppm indicates the predominance of *Z*-isomer **3.28d**.

norbornene-2-*exo*,3-*exo*-dimethanol **3.22** (15.0 mg, 0.0973 mmol, 1.00 equiv) and 1-decene (136 mg, 0.973 mmol, 10.0 equiv). The resulting solution was allowed to stir for 8 hours at 22 °C. Analysis of the unpurified mixture revealed 91% consumption of **3.22**, and the ROCM product was obtained in 92:8 *Z:E* ratio. The resulting oil was purified by silica gel chromatography (10% EtOAc in hexanes to 30% EtOAc in hexanes) to afford **3.28e** (16.6 mg, 0.0564 mmol, 58% yield) as colorless oil; **IR** (CH_2Cl_2): 3274 (br), 2921 (s), 2853 (m), 1640 (w), 1458 (w), 1029 (m), 993 (m), 911 (m); **$^1\text{H NMR}$** (**400 MHz**, CDCl_3): *Z*-isomer (major): δ 5.74 (1H, ddd, $J = 17.2, 10.1, 7.9$ Hz), 5.39 (1H, dt, $J = 10.8, 7.3$ Hz)⁸¹, 5.22 (1H, dd, $J = 10.8, 9.5$ Hz), 5.01 (1H, dd, $J = 17.0, 1.8, 0.9$ Hz), 4.96 (1H, ddd, $J = 10.1, 1.8, 0.6$ Hz), 3.79–3.58 (4H, m), 2.84 (2H, s), 2.54–2.41 (1H, m), 2.19–1.97 (5H, m), 1.86 (1H, dt, $J = 12.3, 6.1$, Hz), 1.34–1.19 (13H, m), 0.88 (3H, t, $J = 6.8$ Hz); **$^{13}\text{C NMR}$** (**100 MHz**, CDCl_3): δ 141.7, 132.9, 131.0, 114.5, 62.3, 62.3, 50.1, 48.6, 46.6, 40.0, 39.8, 32.1, 30.1, 29.7, 29.5, 29.5, 27.8, 22.8, 14.3; **HRMS** [$\text{M}+\text{H}]^+$ calcd for $\text{C}_{19}\text{H}_{35}\text{O}_2$: 295.2637, found: 295.2634.

(*3S,4R,Z*)-7-Phenylhepta-1,5-diene-3,4-diyloxybis(methylene)dibenzene (3.29).

Following the general procedure, a solution of **Ru4b** (1.9 mg, 2.8 mmol, 5.0 mol %) in dichloromethane (113 μL) was transferred by syringe to a vial containing cyclobutene **3.24** (15.0 mg, 0.0563 mmol, 1.00 equiv) and allylbenzene (67.0 mg, 0.563 mmol, 10.0 equiv). The resulting solution was allowed to stir for 12 hours at 40 °C. Analysis of the unpurified mixture revealed 75% consumption of **3.24**, and the ROCM product was obtained in >98:2 *Z:E* ratio. The resulting oil was purified by silica gel chromatography (100% hexanes to 10% Et_2O in hexanes) followed by passing through a plug of activated charcoal with 50% Et_2O in pentane to afford **3.29** (12.6 mg, 0.0328 mmol, 58% yield) as colorless oil; **IR** (CH_2Cl_2): 3027 (w), 2918 (w), 2860 (w), 1602 (w), 1495 (w), 1453 (m), 1088 (s), 1069 (s), 1028 (m), 927 (w); **$^1\text{H NMR}$** (**400 MHz**, CDCl_3): *Z*-isomer (major): δ 7.36–7.27 (10H, m), 7.25–7.17 (3H, m), 7.12 (2H, d, $J = 7.3$ Hz), 5.96–5.83 (2H, m), 5.56 (1H, ddt, $J = 11.0, 9.4, 1.7$ Hz)⁸², 5.35–5.29 (2H, m), 4.67 (2H,

(81) Coupling constants ($J = 10.3$ and $J = 10.3$ Hz) of the signals at δ 5.39 and 5.22 ppm indicate a predominance of *Z*-isomer **3.28e**.

(82) Coupling constant ($J = 11.0$ Hz) of the signal at δ 5.56 ppm indicates a predominance of *Z*-isomer **3.29**.

d, $J = 12.2$ Hz), 4.46 (2H, dd, $J = 12.2, 8.2$ Hz), 4.36 (1H, ddd, $J = 9.4, 4.7, 1.0$ Hz), 3.92–3.85 (1H, m), 3.33 (2H, t, $J = 6.9$ Hz); ^{13}C NMR (100 MHz, CDCl_3): δ 140.2, 138.6, 135.5, 133.3, 128.4, 128.4, 128.2, 128.2, 128.1, 127.6, 127.6, 127.4, 127.3, 126.0, 118.9, 82.5, 76.1, 70.5, 70.2, 34.1; HRMS [M+NH₄]⁺ calcd for C₂₇H₃₂NO₂: 402.2433, found: 402.2443.

((1*S*,2*R*,3*R*,5*S*)-3-((*Z*)-2-(1-Tosyl-1*H*-indol-3-yl)vinyl)-5-vinylcyclopentane-1,2-diyldimethanol (3.30a).

Following the general procedure, a solution of **Ru4b** (3.4 mg, 4.9 mmol, 5.0 mol %) in dichloromethane (195 μL) was transferred by syringe to a vial containing 5-norbornene-2-*exo*,3-*exo*-dimethanol **3.22** (15.0 mg, 0.0973 mmol, 1.00 equiv) and 1-tosyl-3-vinyl-1*H*-indole (289 mg, 0.973 mmol, 10.0 equiv). The resulting solution was allowed to stir for 2 hours at 22 °C. Analysis of the unpurified mixture revealed >98% consumption of **3.22**, and the ROCM product was obtained in 93:7 *Z:E* ratio. The resulting oil was purified by silica gel chromatography (10% EtOAc in hexanes to 40% EtOAc in hexanes) to afford **3.30a** (40.9 mg, 0.0906 mmol, 93% yield) as off-white wax; IR (CH_2Cl_2): 3308 (br), 3076 (w), 2922 (m), 1639 (w), 1597 (w), 1447 (m), 1370 (m), 1173 (s), 965 (m); ^1H NMR (400 MHz, CDCl_3): *Z*-isomer (major): δ 7.99 (1H, d, $J = 8.3$ Hz), 7.76 (2H, d, $J = 8.4$ Hz), 7.59 (1H, s), 7.47 (1H, d, $J = 7.8$ Hz), 7.35–7.30 (1H, m), 7.22 (3H, t, $J = 7.2$ Hz), 6.38 (1H, d, $J = 11.3$ Hz)⁸³, 5.76 (1H, ddd, $J = 17.1, 10.1, 8.1$ Hz), 5.68 (1H, dd, $J = 11.3, 10.1$ Hz), 5.09–5.02 (1H, m), 5.00 (1H, dd, $J = 10.1, 1.3$ Hz), 3.73–3.68 (2H, m), 3.61–3.59 (2H, m), 3.10 (2H, s), 2.82–2.73 (1H, m), 2.33 (3H, s), 2.32–2.22 (1H, m), 2.17–2.12 (2H, m), 2.00 (1H, dt, $J = 12.5, 6.3$ Hz), 0.90–0.83 (1H, m); ^{13}C NMR (100 MHz, CDCl_3): δ 145.1, 141.4, 138.0, 135.2, 134.9, 131.0, 130.0, 126.9, 125.1, 123.5, 123.3, 119.6, 119.1, 118.5, 114.8, 113.8, 61.9, 61.9, 50.2, 48.6, 46.3, 41.3, 39.7, 21.7; HRMS [M+H]⁺ calcd for C₂₆H₃₀NO₄S: 452.1896, found: 452.1887.

(83) Coupling constants ($J = 11.3$ and $J = 11.3$ Hz) of the signals at δ 6.38 and 5.68 ppm indicate the predominance of *Z*-isomer **3.30a**.

((1*S*,2*R*,3*R*,5*S*)-3-((*Z*)-2-(Benzo[β]thiophen-2-yl)-5-vinylcyclopentane-1,2-diyil)dimethanol (3.30b).

Following the general procedure, a solution of **Ru4b** (3.4 mg, 4.9 mmol, 5.0 mol %) in dichloromethane (195 μ L) was transferred by syringe to a vial containing 5-norbornene-2-*exo*,3-*exo*-dimethanol **3.22** (15.0 mg, 0.0973 mmol, 1.00 equiv) and 2-vinylbenzo[β]thiophene (156 mg, 0.973 mmol, 10.0 equiv). The resulting solution was allowed to stir for 2 hours at 22 °C. Analysis of the unpurified mixture revealed >98% consumption of **3.22**, and the ROCM product was obtained in >98:2 *Z:E* ratio. The resulting oil was purified by silica gel chromatography (10% EtOAc in hexanes to 40% EtOAc in hexanes) to afford **3.30b** (29.6 mg, 0.0941 mmol, 97% yield) as yellow oil; **IR** (CH_2Cl_2): 3275 (br), 3070 (w), 2917 (m), 2850 (w), 1638 (w), 1456 (w), 1015 (m), 993 (m); **^1H NMR** (400 MHz, CDCl_3): *Z*-isomer (major): δ 7.77 (1H, dd, J = 7.6, 0.8 Hz), 7.73–7.68 (1H, m), 7.38–7.26 (2H, m), 7.16 (1H, s), 6.61 (1H, dd, J = 11.5, 0.6 Hz), 5.77 (1H, ddd, J = 17.4, 10.0, 8.0 Hz), 5.56 (1H, t, J = 10.8 Hz)⁸⁴, 5.11–5.02 (1H, m), 5.00 (1H, dd, J = 10.1, 1.7 Hz), 3.82–3.76 (2H, m), 3.73–3.65 (2H, m), 3.26–2.97 (3H, m), 2.37–2.29 (1H, m), 2.21–2.17 (2H, m), 2.11 (1H, dt, J = 12.4, 6.3 Hz), 1.39–1.31 (1H, m); **^{13}C NMR** (100 MHz, CDCl_3): δ 141.4, 140.0, 139.8, 139.3, 136.4, 124.7, 124.7, 123.5, 123.0, 122.1, 122.1, 114.8, 62.3, 62.2, 50.8, 48.7, 46.6, 41.6, 39.5; **HRMS** [$\text{M}+\text{H}]^+$ calcd for $\text{C}_{19}\text{H}_{23}\text{O}_2\text{S}$: 315.1419, found: 315.1410.

((1*S*,2*R*,3*R*,5*S*)-3-((1*Z*,3*E*)-4-Methoxybuta-1,3-dienyl)-5-vinylcyclopentane-1,2-diyil)dimethanol (3.30c).

Following the general procedure, a solution of **Ru4b** (1.4 mg, 1.9 mmol, 2.0 mol %) in dichloromethane (195 μ L) was transferred by syringe to a vial containing 5-norbornene-2-*exo*,3-*exo*-dimethanol **3.22** (15.0 mg, 0.0973 mmol, 1.00 equiv) and (*E*)-1-methoxy-1,3-butadiene (82.0 mg, 0.973 mmol, 10.0 equiv). The resulting solution was allowed to stir for 2 hours at 22 °C. Analysis of the ^1H NMR (400 MHz) spectrum revealed >98% consumption of **3.22**, and the ROCM product was obtained in 91:9 *Z:E* ratio. The resulting oil was purified by silica gel chromatography (10% EtOAc in hexanes

(84) Coupling constant (J = 10.8 Hz) of the signal at δ 5.56 ppm indicates the predominance of *Z*-isomer **3.30b**.

to 40% EtOAc in hexanes) to afford **3.30c** (19.5 mg, 0.0818 mmol, 84% yield) as colorless oil; **IR** (CH_2Cl_2): 3305 (br), 2920 (m), 1648 (m), 1608 (m), 1452 (w), 1210 (s), 1027 (s), 993 (s), 912 (s); **^1H NMR** (400 MHz, CDCl_3): Z-isomer (major): δ 6.56 (1H, d, J = 12.3 Hz), 5.88 (1H, t, J = 11.0 Hz)⁸⁵, 5.80–5.66 (2H, m), 5.09–4.98 (2H, m), 4.96 (1H, dd, J = 10.1, 1.7 Hz), 3.76–3.63 (4H, m), 3.60 (3H, s), 3.28 (2H, s), 2.64–2.52 (1H, m), 2.28–2.19 (1H, m), 2.15–1.99 (2H, m), 1.93 (1H, dt, J = 12.4, 6.2 Hz), 1.24 (1H, d, J = 11.2 Hz); **^{13}C NMR** (100 MHz, CDCl_3): δ 152.1, 141.7, 129.9, 125.3, 114.5, 101.7, 62.2, 62.0, 56.9, 50.3, 48.5, 46.5, 40.3, 39.9; **HRMS** $[\text{M}+\text{H}-\text{H}_2\text{O}]^+$ calcd for $\text{C}_{14}\text{H}_{21}\text{O}_2$: 221.1542, found: 221.1545.

((1*S*,2*R*,3*R*,5*S*)-3-((1*Z*,3*E*)-Deca-1,3-dienyl)-5-vinylcyclopentane-1,2-diyl)dimethanol (3.30d).

Following the general procedure, a solution of **Ru4b** (3.4 mg, 4.9 mmol, 5.0 mol %) in dichloromethane (195 μL) was transferred by syringe to a vial containing 5-norbornene-2-*exo*,3-*exo*-dimethanol **3.22** (15.0 mg, 0.0973 mmol, 1.00 equiv) and (*E*)-deca-1,3-diene (134 mg, 0.973 mmol, 10.0 equiv). The resulting solution was allowed to stir for 2 hours at 22 °C. Analysis of the **^1H NMR** (400 MHz) spectrum revealed >98% consumption of **3.22**, and the ROCM product was obtained in >98:2 *Z:E* ratio. The resulting oil was purified by silica gel chromatography (10% EtOAc in hexanes to 30% EtOAc in hexanes) to afford **3.30d** (22.8 mg, 0.0780 mmol, 80% yield) as colorless oil; **IR** (CH_2Cl_2): 3276 (br), 2922 (s), 2854 (m), 1639 (w), 1455 (m), 1027 (s), 983 (s), 946 (s), 910 (s); **^1H NMR** (400 MHz, CDCl_3): Z-isomer (major): δ 6.25 (1H, ddd, J = 13.6, 11.5, 6.0 Hz), 5.97 (1H, t, J = 10.9 Hz)⁸⁶, 5.82–5.61 (2H, m), 5.16 (1H, t, J = 10.2 Hz), 5.04–4.98 (1H, m), 4.96 (1H, dd, J = 10.1, 1.8, Hz), 3.77–3.61 (4H, m), 3.22 (2H, s), 2.70–2.61 (1H, m), 2.28–2.16 (1H, m), 2.15–1.99 (4H, m), 1.93 (1H, dt, J = 12.3, 6.2 Hz), 1.42–1.24 (9H, m), 0.88 (3H, t, J = 6.8 Hz); **^{13}C NMR** (100 MHz, CDCl_3): δ 141.5, 135.8, 132.4, 129.4, 125.3, 114.4, 62.0, 61.9, 50.0, 48.4, 46.3, 40.0, 39.8, 32.9, 31.7, 29.3, 28.9, 22.6, 14.1; **HRMS** $[\text{M}+\text{H}]^+$ calcd for $\text{C}_{19}\text{H}_{33}\text{O}_2$: 293.2481, found: 293.2473.

(85) Coupling constant (J = 11.0 Hz) of the signal at δ 5.88 ppm indicates the predominance of Z-isomer **3.30c**.

(86) Coupling constants (J = 10.9 and 10.2 Hz) of the signals at δ 5.97 and 5.16 ppm indicate the predominance of Z-isomer **3.30d**.

((3*S*,4*R*,5*Z*,7*E*)-8-Methoxyocta-1,5,7-triene-3,4-diyl)bis(oxy)bis(methylene)dibenzene (3.31a).

Following the general procedure, a solution of **Ru4b** (1.9 mg, 2.8 mmol, 5.0 mol %) in dichloromethane (113 μ L) was transferred by syringe to a vial containing cyclobutene **3.24** (15.0 mg, 0.0563 mmol, 1.00 equiv) and (*E*)-1-methoxy-1,3-butadiene (47.0 mg, 0.563 mmol, 10.0 equiv). The resulting solution was allowed to stir for 12 hours at 40 °C. Analysis of the unpurified mixture revealed >98% consumption of **3.24**, and the ROCM product was obtained in >98:2 *Z:E* ratio. The resulting oil was purified by silica gel chromatography (100% hexanes to 10% Et₂O in hexanes) to afford **3.31a** (17.4 mg, 0.0497 mmol, 88% yield) as colorless oil; **IR** (CH₂Cl₂): 2918 (w), 2850 (w), 1649 (m), 1608 (w), 1453 (w), 1335 (w), 1210 (s), 1168 (m), 1087 (s), 1065 (s), 925 (m); **¹H NMR** (400 MHz, CDCl₃): *Z*-isomer (major): δ 7.38–7.29 (8H, m), 7.27–7.23 (2H, m), 6.63 (1H, d, *J* = 12.3 Hz), 6.16 (1H, t, *J* = 11.2 Hz), 5.89 (1H, ddd, *J* = 17.3, 10.4, 7.7 Hz), 5.56 (1H, t, *J* = 12.1 Hz), 5.35–5.25 (2H, m), 5.21 (1H, t, *J* = 10.3 Hz)⁸⁷, 4.66 (2H, d, *J* = 12.3 Hz), 4.45 (2H, dd, *J* = 12.3, 5.5, Hz), 4.31–4.24 (1H, m), 3.87 (1H, dd, *J* = 7.7, 4.5 Hz), 3.49 (3H, s); **¹³C NMR** (100 MHz, CDCl₃): δ 153.1, 138.7, 138.7, 135.5, 129.5, 128.2, 128.1, 127.8, 127.6, 127.27, 127.3, 122.8, 118.8, 101.3, 82.7, 76.3, 70.4, 69.7, 56.4; **HRMS** [M+NH₄]⁺ calcd for C₂₃H₃₀NO₃: 368.2226, found: 368.2243.

(3*S*,4*R*,5*Z*,7*E*)-Tetradeca-1,5,7-triene-3,4-diylbis(oxy)bis(methylene)dibenzene (3.31b).

Following the general procedure, a solution of **Ru4b** (1.9 mg, 2.8 mmol, 5.0 mol %) in dichloromethane (113 μ L) was transferred by syringe to a vial containing cyclobutene **3.24** (15.0 mg, 0.0563 mmol, 1.00 equiv) and (*E*)-deca-1,3-diene (78.0 mg, 0.563 mmol, 10.0 equiv). The resulting solution was allowed to stir for 12 hours at 40 °C. Analysis of the unpurified mixture revealed 73% consumption of **3.24**, and the ROCM product was obtained in >98:2 *Z:E* ratio. The resulting oil was purified by silica gel chromatography (100% hexanes to 5% Et₂O in hexanes) followed by passing through a plug of activated charcoal with 50% Et₂O in pentane to afford **3.31b** (13.7 mg, 0.0339

(87) Coupling constant (*J* = 10.3 Hz) of the signal at δ 5.21 ppm indicates the predominance of *Z*-isomer **3.31a**.

mmol, 60% yield) as colorless oil; **IR (CH₂Cl₂)**: 3028 (w), 2955 (m), 2925 (s), 2855 (m), 1653 (w), 1496 (w), 1455 (m), 1090 (s), 1070 (s), 1028 (w), 988 (w); **¹H NMR (400 MHz, CDCl₃)**: Z-isomer (major): δ 7.37–7.27 (10H, m), 6.24 (1H, t, J = 11.0 Hz)⁸⁸, 6.18–6.07 (1H, m), 5.87 (1H, ddd, J = 16.0, 12.0, 8.0 Hz), 5.74 (1H, dt, J = 14.2, 6.9 Hz), 5.34–5.25 (3H, m), 4.64 (2H, dd, J = 12.3, 2.2 Hz), 4.44 (2H, dd, J = 12.2, 9.0 Hz), 4.35 (1H, dd, J = 9.3, 4.6 Hz), 3.86 (1H, dd, J = 7.7, 4.6 Hz), 2.05 (2H, q, J = 7.0 Hz), 1.41–1.24 (8H, m), 0.89 (3H, t, J = 6.7 Hz); **¹³C NMR (100 MHz, CDCl₃)**: δ 138.6, 138.6, 137.6, 135.4, 133.4, 128.1, 128.1, 127.8, 127.5, 127.3, 127.3, 125.8, 125.4, 118.8, 82.6, 76.1, 70.4, 69.9, 32.8, 31.7, 29.1, 28.9, 22.6, 14.1; **HRMS [M+NH₄]⁺** calcd for C₂₈H₄₀NO₂: 422.3059, found: 422.3072.

((1*S*,2*R*,3*S*,5*S*)-3-((*Z*)-2-Butoxyvinyl)-5-vinylcyclopentane-1,2-diyl)dimethanol (3.32a).

Following the general procedure, a solution of **Ru4b** (1.4 mg, 1.9 mmol, 2.0 mol %) in dichloromethane (195 μ L) was transferred by syringe to a vial containing 5-norbornene-2-*exo*,3-*exo*-dimethanol **3.22** (15.0 mg, 0.0973 mmol, 1.00 equiv) and butylvinyl ether (97.0 mg, 0.973 mmol, 10.0 equiv). The resulting solution was allowed to stir for 2 hours at 22 °C. Analysis of the unpurified mixture revealed >98% consumption of **3.22**, and the ROCM product was obtained in >98:2 *Z:E* ratio. The resulting oil was purified by silica gel chromatography (10% EtOAc in hexanes to 40% EtOAc in hexanes) to afford **3.32a** (23.5 mg, 0.0924 mmol, 95% yield) as colorless oil; **IR (CH₂Cl₂)**: 3414 (br), 2920 (m), 2987 (m), 1639 (w), 1455 (w), 1367 (w), 1135 (m), 1038 (s), 907 (m); **¹H NMR (400 MHz, CDCl₃)**: Z-isomer (major): δ 6.00 (1H, dd, J = 6.2, 0.8 Hz)⁸⁹, 5.76 (1H, ddd, J = 17.2, 10.1, 8.1 Hz), 5.00 (1H, ddd, J = 17.0, 1.8, 1.0 Hz), 4.94–4.89 (1H, m), 4.27 (1H, dd, J = 9.1, 6.2 Hz), 3.77–3.70 (5H, m), 3.60 (1H, dd, J = 11.9, 6.7 Hz), 2.79–2.70 (1H, m), 2.42 (1H, dq, J = 11.2, 7.9 Hz), 2.03–1.90 (2H, m), 1.87–1.76 (1H, m), 1.64–1.53 (3H, m), 1.43–1.31 (2H, m), 1.28–1.15 (2H, m), 0.93 (3H, t, J = 7.4 Hz); **¹³C NMR (100 MHz, CDCl₃)**: δ 145.5, 142.3, 113.6, 109.4, 72.3, 62.0,

(88) Coupling constant (J = 11.0 Hz) of the signal at δ 6.24 ppm indicates the predominance of Z-isomer **3.31b**.

(89) Coupling constants (J = 6.2 and J = 6.2 Hz) of the signal at δ 6.00 and 4.27 ppm indicate the predominance of Z-isomer **3.32a**.

60.9, 50.0, 48.4, 45.4, 39.4, 36.3, 31.7, 18.9, 13.8; **HRMS** [M+H-H₂O]⁺ calcd for C₁₅H₂₅O₂: 237.1860, found: 237.1855.

((1*S*,2*R*,3*R*,5*S*)-3-((*Z*)-2-(Ethylthio)vinyl)-5-vinylcyclopentane-1,2-diyl)dimethanol (3.32b).

Following the general procedure, a solution of **Ru4b** (3.4 mg, 4.9 mmol, 5.0 mol %) in dichloromethane (195 μL) was transferred by syringe to a vial containing 5-norbornene-2-*exo*,3-*exo*-dimethanol **3.22** (15.0 mg, 0.0973 mmol, 1.00 equiv) and ethyl vinyl sulfide (86.0 mg, 0.973 mmol, 10.0 equiv). The resulting solution was allowed to stir for 12 hours at 40 °C. Analysis of the unpurified mixture revealed 85% consumption of **3.22**, and the ROCM product was obtained in 92:8 *Z:E* ratio. The resulting oil was purified by silica gel chromatography (10% EtOAc in hexanes to 40% EtOAc in hexanes) to afford **3.32b** (18.9 mg, 0.0780 mmol, 80% yield) as colorless oil; **IR** (CH₂Cl₂): 3284 (br), 2919 (m), 2871 (w), 1639 (w), 1450 (m), 1047 (s), 1029 (s), 993 (s), 912 (s); **¹H NMR** (400 MHz, CDCl₃): *Z*-isomer (major): δ 5.95 (1H, d, *J* = 9.4 Hz)⁹⁰, 5.75 (1H, ddd, *J* = 17.1, 10.1, 8.1 Hz), 5.46 (1H, t, *J* = 9.4 Hz), 5.02 (1H, dd, *J* = 17.1, 1.0 Hz), 4.98–4.92 (1H, m), 3.76–3.66 (4H, m), 3.27 (1H, s), 2.72–2.54 (3H, m), 2.37–2.26 (1H, m), 2.11–1.95 (3H, m), 1.31–1.25 (5H, m); **¹³C NMR** (100 MHz, CDCl₃): δ 141.6, 132.6, 125.2, 114.2, 61.9, 61.5, 49.9, 49.9, 48.5, 45.8, 41.5, 38.8, 27.9, 15.4; **HRMS** [M+H-H₂O]⁺ calcd for C₁₃H₂₁OS: 225.1313, found: 225.1324.

((3*R*,4*S*,*Z*)-1-Butoxyhexa-1,5-diene-3,4-diyl)bis(oxy)bis(methylene)dibenzene (3.33).

Following the general procedure, a solution of **Ru4b** (1.9 mg, 2.8 mmol, 5.0 mol %) in dichloromethane (113 μL) was transferred by syringe to a vial containing cyclobutene **3.24** (15.0 mg, 0.0563 mmol, 1.00 equiv) and butyl vinyl ether (56.0 mg, 0.563 mmol, 10.0 equiv). The resulting solution was allowed to stir for 12 hours at 40 °C. Analysis of the unpurified mixture revealed >98% consumption of **3.24**, and the ROCM product was obtained in 88:12 *Z:E* ratio. The resulting oil was purified by silica gel chromatography (100% hexanes to 10% Et₂O in hexanes) followed by passing through a plug of activated charcoal with 100% Et₂O to afford **3.33** (16.7 mg, 0.0456 mmol, 81%

(90) Coupling constants (*J* = 9.4 and *J* = 9.4 Hz) of the signals at δ 5.95 and 5.46 ppm indicate indicates the predominance of *Z*-isomer **3.32b**.

yield) as a colorless oil; **IR (CH₂Cl₂)**: 2957 (w), 2926 (m), 2858 (w), 1659 (m), 1454 (w), 1377 (m), 1085 (s), 1068 (s), 1028 (m); **¹H NMR (400 MHz, CDCl₃)**: Z-isomer (major): δ 7.37–7.29 (8H, m), 7.25–7.22 (2H, m), 6.20 (1H, d, J = 6.2 Hz)⁹¹, 5.87 (1H, ddd, J = 17.1, 10.7, 7.5 Hz), 5.29–5.28 (1H, m), 5.27–5.22 (1H, m), 4.65 (2H, dd, J = 12.3, 4.6 Hz), 4.55 (1H, dd, J = 9.4, 3.7 Hz), 4.51–4.45 (3H, m), 3.91–3.87 (1H, m), 3.74 (2H, t, J = 6.5 Hz), 1.60–1.52 (2H, m), 1.41–1.30 (2H, m), 0.91 (3H, t, J = 7.4 Hz); **¹³C NMR (100 MHz, CDCl₃)**: δ 148.8, 139.3, 138.9, 135.6, 128.1, 128.0, 127.6, 127.5, 127.1, 127.0, 118.3, 103.1, 82.5, 74.3, 72.3, 70.3, 70.1, 31.8, 18.9, 13.8; **HRMS [M+NH₄]⁺** calcd for C₂₄H₃₄NO₃: 384.2539, found: 384.2544.

(R,Z)-(1-Butoxy-3-methylpenta-1,4-dien-1,3-diyl)dibenzene (3.34).

Following the general procedure, a solution of **Ru4b** (1.6 mg, 2.3 mmol, 2.0 mol %) in dichloromethane (230 μ L) was transferred by syringe to a vial containing cyclopropene **3.26** (15.0 mg, 0.115 mmol, 1.00 equiv) and butylvinyl ether (115 mg, 1.15 mmol, 10.0 equiv). The resulting solution was allowed to stir for 2 hours at 22 °C. Analysis of the unpurified mixture revealed >98% consumption of **3.26**, and the ROCM product was obtained in 88:12 Z:E ratio. The resulting oil was purified by silica gel chromatography (5% Et₂O in hexanes to 10% Et₂O in hexanes) to afford **3.34** (20.9 mg, 0.0907 mmol, 79% yield) as colorless oil; **IR (CH₂Cl₂)**: 2960 (w), 2932 (w), 2872 (w), 1655 (m), 1372 (w), 1095 (s), 909 (m); **¹H NMR (400 MHz, CDCl₃)**: Z-isomer (major): δ 7.42–7.37 (2H, m), 7.30–7.25 (2H, m), 7.19–7.14 (1H, m), 6.29 (1H, ddd, J = 17.7, 10.2, 1.3 Hz), 5.95 (1H, dd, J = 6.8, 1.3 Hz)⁹², 5.09–5.08 (1H, m), 5.05 (1H, dt, J = 4.8, 1.4 Hz), 4.49 (1H, dd, J = 6.8, 1.2 Hz), 3.66–3.60 (2H, m), 1.58 (3H, d, J = 1.2 Hz), 1.47 (1H, d, J = 6.9 Hz), 1.44–1.42 (1H, m), 1.29–1.19 (2H, m), 0.86 (3H, td, J = 7.2, 1.0 Hz); **¹³C NMR (100 MHz, CDCl₃)**: δ 148.6, 145.9, 145.2, 127.8, 126.6, 125.5, 112.0, 110.6, 72.2, 45.8, 31.8, 27.2, 18.9, 13.7; **HRMS [M+H]⁺** calcd for C₁₆H₂₃O: 231.1749, found: 231.1752.

(91) Coupling constant (J = 6.2 Hz) of the signal at δ 6.20 ppm indicates indicates the predominance of Z-isomer **3.33**.

(92) Coupling constants (J = 6.8 and J = 6.8 Hz) of the signals at δ 5.95 and 4.49 ppm indicate the predominance of Z-isomer **3.34**.

(1*R*,3*S*)-1-((*Z*)-2-Butoxyvinyl)-2-tosyl-3-vinylisoindoline (3.35).

Following the general procedure, a solution of **Ru4b** (0.70 mg, 1.0 mmol, 2.0 mol %) in dichloromethane (100 μ L) was transferred by syringe to a vial containing 7-azanorbornene **3.35_{pre}** (15.0 mg, 0.0504 mmol, 1.00 equiv) and butylvinyl ether (51.0 mg, 0.504 mmol, 10.0 equiv). The resulting solution was allowed to stir for 2 hours at 22 °C. Analysis of the unpurified mixture revealed >98% consumption of **3.35_{pre}**, and the ROCM product was obtained in >98:2 *Z:E* ratio. The resulting oil was purified by silica gel chromatography (10% Et₂O in hexanes to 40% Et₂O in hexanes) to afford **3.35** (16.6 mg, 0.0418 mmol, 83% yield) as colorless oil; **IR** (CH₂Cl₂): 2957 (w), 2928 (m), 1661 (m), 1460 (w), 1352 (m), 1164 (s), 1095 (s), 1039 (s), 578 (s), 551 (s); **¹H NMR** (400 MHz, CDCl₃): *Z*-isomer (major): δ 7.80 (2H, d, *J* = 8.3 Hz), 7.26–7.19 (4H, m), 7.17–7.00 (2H, m), 6.14 (1H, dd, *J* = 6.1, 1.1 Hz)⁹³, 5.99–5.90 (1H, m), 5.88 (1H, d, *J* = 9.8 Hz), 5.42 (1H, dt, *J* = 17.0, 1.0 Hz), 5.28 (1H, d, *J* = 7.5 Hz), 5.22 (1H, dt, *J* = 10.1, 1.0 Hz), 4.56 (1H, dd, *J* = 8.9, 6.1 Hz), 3.97–3.81 (2H, m), 2.38 (3H, s), 1.75–1.68 (2H, m), 1.49 (2H, q, *J* = 8.0 Hz), 1.00 (3H, t, *J* = 7.4 Hz); **¹³C NMR** (100 MHz, CDCl₃): δ 148.9, 139.3, 138.9, 135.6, 128.1, 128.0, 127.6, 127.5, 127.1, 127.0, 118.3, 103.1, 82.5, 74.3, 72.3, 70.3, 70.1, 31.8, 18.9, 13.8; **HRMS** [M+H]⁺ calcd for C₂₃H₂₈NO₃S: 398.1784, found: 398.1792.

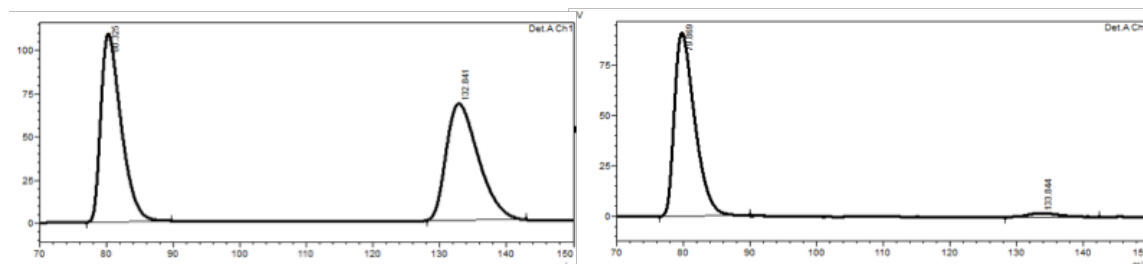
((1*S*,2*R*,3*R*,5*S*)-3-((*R,Z*)-3-Hydroxy-3-phenylprop-1-enyl)-5-vinylcyclopentane-1,2-diyldimethanol (3.37a).

Following the general procedure, a solution of **Ru4a** (3.4 mg, 4.9 mmol, 5.0 mol %) in dichloromethane (195 μ L) was transferred by syringe to a vial containing 5-norbornene-2-*exo*,3-*exo*-dimethanol **3.22** (15.0 mg, 0.0973 mmol, 1.00 equiv) and (*R*)-1-phenyl-2-propen-1-ol **3.36a** (65.2 mg, 0.486 mmol, 5.0 equiv). The resulting solution was allowed to stir for 8 hours at 22 °C. Analysis of the unpurified mixture revealed >98% consumption of **3.22**, and the ROCM product was obtained in >98:2 *Z:E* ratio. The resulting oil was purified by silica gel chromatography (20% EtOAc in hexanes to 80% EtOAc in hexanes) to afford **3.37a** (18.8 mg, 0.0652 mmol, 67% yield) as colorless oil;

(93) Coupling constants (*J* = 6.1 and *J* = 6.1 Hz) of the signals at δ 6.14 and 4.56 ppm indicate the predominance of *Z*-isomer **3.35**.

IR (CH_2Cl_2): 3299 (br), 2961 (w), 2921 (m), 2856 (m), 1639 (w), 1492 (m), 1021 (m), 913 (m); **$^1\text{H NMR}$ (400 MHz, CDCl_3):** Z-isomer (major): δ 7.42–7.33 (4H, m), 7.31–7.26 (1H, m), 5.78 (1H, ddd, $J = 17.6, 10.2, 8.2$ Hz), 5.72 (1H, dd, $J = 10.8, 8.4$ Hz)⁹⁴, 5.55 (1H, d, $J = 7.9$ Hz), 5.43 (1H, t, $J = 10.5$ Hz), 5.04 (1H, ddt, $J = 17.1, 1.8, 1.0$ Hz), 4.99–4.92 (1H, m), 4.20 (1H, s), 3.82 (3H, s); 3.69–3.52 (2H, m), 3.14–3.03 (2H, m), 2.62–2.52 (1H, m), 2.03–1.94 (2H, m), 1.33–1.23 (2H, m); **$^{13}\text{C NMR}$ (100 MHz, CDCl_3):** δ 143.7, 142.0, 136.6, 132.9, 128.7, 127.7, 126.1, 114.2, 69.7, 61.9, 60.1, 50.1, 48.4, 45.6, 39.9, 39.5; **HRMS [M+H-H₂O]⁺** calcd for $\text{C}_{18}\text{H}_{23}\text{O}_2$: 271.1698, found: 271.1701; diastereomeric ratio was established by HPLC analysis in comparison with authentic racemic material prepared from **3.22** and *rac*-1-phenyl-2-propen-1-ol (*+/−***3.36a**) under standard conditions; Daicel Chiralpak OD-H column (97:3 hexanes:*i*-PrOH, 0.5 mL/min, 220 nm) was used.

Chart 5. HPLC Trace Shows High Stereoselectivity



Peak #	Retention time (min)	Area	Area %	Peak #	Retention time (min)	Area	Area %
1	80.33	23060079	50.39	1	79.87	19429049	97.06
2	132.84	22706960	49.61	2	133.84	588688	2.94

Stereochemical Proof for **3.37a**:

(R,Z)-1-Phenyl-3-((5aR,6R,8S,8aS)-3-phenyl-8-vinylhexahydro-1*H*-cyclopenta[*e*][1,3,2]dioxaborepin-6-yl)prop-2-en-1-ol (3.37b).

A previously reported procedure was adopted.⁹⁵ A flame-dried round-bottom flask, equipped with a stir bar and reflux condenser, was charged with **3.37a** (20.0 mg, 0.069 mmol, 1.00 equiv), phenylboronic acid (20.0 mg, 0.069 mmol, 1.00 equiv) and

(94) Coupling constants ($J = 10.8$ and $J = 10.5$ Hz) of the signals at δ 5.72 and 5.43 ppm indicate Z-isomer of **3.37a**.

(95) J. M. Sugihara, C. M. Bowman, *J. Am. Chem. Soc.* **1958**, *80*, 2443–2446.

acetone (0.5 mL). The solution was allowed to stir at reflux for 12 hours. The resulting mixture was concentrated *in vacuo* to afford **3.37b** as yellow solid, which was recrystallized from hexane, affording colorless crystals (24.4 mg, 0.0652 mmol, 94% yield); mp: 84–86 °C; **IR (CH₂Cl₂)**: 3386 (br), 3075 (w), 2919 (w), 1640 (w), 1599 (w), 1479 (m), 1439 (m), 1141 (m), 1030 (m), 915 (w); **¹H NMR (400 MHz, CDCl₃)**: Z-isomer (major): δ 7.84–7.79 (2H, m), 7.44–7.37 (1H, m), 7.36–7.32 (2H, m), 7.32–7.28 (3H, m), 7.26–7.25 (2H, m), 5.80–5.69 (2H, m), 5.52–5.47 (1H, m), 5.43 (1H, t, J = 10.3 Hz)⁹⁶, 5.08 (1H, ddd, J = 17.1, 1.7, 1.0 Hz), 5.01 (1H, ddd, J = 10.1, 1.7, 0.6 Hz), 4.42 (1H, d, J = 12.2 Hz), 4.37 (1H, d, J = 12.1 Hz), 4.30–4.22 (1H, m), 4.20–4.13 (1H, m), 2.98–2.84 (1H, m), 2.58–2.44 (1H, m), 2.27 (2H, s), 2.15–2.09 (1H, m), 1.86 (1H, dt, J = 11.6, 5.7 Hz), 1.34 (1H, q, J = 12.0 Hz); **¹³C NMR (100 MHz, CDCl₃)**: δ 143.7, 140.6, 134.4, 134.0, 133.7, 130.7, 128.7, 127.7, 127.6, 126.1, 115.3, 69.9, 64.3, 64.1, 49.6, 48.4, 46.3, 40.3, 39.9; **HRMS [M+H-H₂O]⁺** calcd for C₂₄H₂₆BO₂: 357.2026, found: 357.2021.

X-ray of **3.37b**:

Chart 6. Absolute Stereochemical Proof

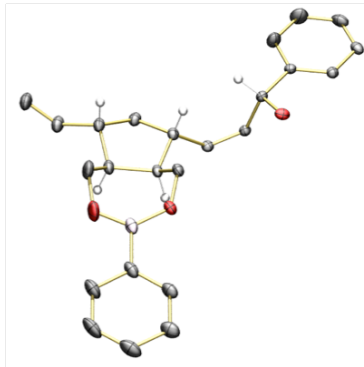


Table 1. Crystal data and structure refinement for **3.37b**

Identification code	C ₂₄ H ₂₇ BO ₃
Empirical formula	C ₂₄ H ₂₇ BO ₃
Formula weight	374.26
Temperature	100(2) K
Wavelength	1.54178 Å

(96) Coupling constant (J = 10.3 Hz) of the signal at δ 5.43 ppm indicate the predominance of Z-isomer **3.37b**.

Crystal system	Orthorhombic	
Space group	C 2 2 21	
Unit cell dimensions	$a = 21.808(2) \text{ \AA}$	$\alpha = 90^\circ$
	$b = 24.164(2) \text{ \AA}$	$\beta = 90^\circ$
	$c = 9.1450(8) \text{ \AA}$	$\gamma = 90^\circ$
Volume	$4819.2(8) \text{ \AA}^3$	
Z	8	
Density (calculated)	1.032 Mg/m^3	
Absorption coefficient	0.519 mm^{-1}	
F(000)	1600	
Crystal size	$0.420 \times 0.040 \times 0.020 \text{ mm}^3$	
Theta range for data collection	2.729 to 68.517°	
Index ranges	$-26 \leq h \leq 25, -29 \leq k \leq 27, -10 \leq l \leq 10$	
Reflections collected	21415	
Independent reflections	4309 [$R(\text{int}) = 0.0431$]	
Completeness to theta = 67.679°	99.3 %	
Absorption correction	Semi-empirical from equivalents	
Max. and min. transmission	0.7533 and 0.6403	
Refinement method	Full-matrix least-squares on F^2	
Data / restraints / parameters	4309 / 2 / 261	
Goodness-of-fit on F^2	1.051	
Final R indices [$I > 2\sigma(I)$]	$R_1 = 0.0292, wR_2 = 0.0732$	
R indices (all data)	$R_1 = 0.0326, wR_2 = 0.0748$	
Absolute structure parameter	0.17(8)	
Extinction coefficient	na	
Largest diff. peak and hole	$0.103 \text{ and } -0.101 \text{ e.\AA}^{-3}$	

Table 2. Atomic coordinates ($\times 10^4$) and equivalent isotropic displacement parameters ($\text{\AA}^2 \times 10^3$) for **3.37b**. $U(\text{eq})$ is defined as one third of the trace of the orthogonalized U_{ij} tensor

	x	y	z	U(eq)
B(1)	7034(1)	-263(1)	7775(2)	48(1)
O(1)	7640(1)	-270(1)	7432(2)	44(1)
O(2)	6703(1)	181(1)	8166(2)	80(1)
O(3)	9774(1)	358(1)	6136(2)	40(1)
C(1)	6691(1)	-834(1)	7722(2)	53(1)
C(2)	6088(1)	-883(1)	8223(3)	71(1)
C(3)	5789(1)	-1390(1)	8215(3)	84(1)
C(4)	6078(1)	-1852(1)	7699(3)	80(1)
C(5)	6675(1)	-1818(1)	7194(3)	68(1)
C(6)	6975(1)	-1313(1)	7228(2)	56(1)
C(7)	8043(1)	200(1)	7344(2)	41(1)
C(8)	7794(1)	670(1)	6428(2)	37(1)
C(9)	8301(1)	1116(1)	6197(2)	38(1)
C(10)	7959(1)	1669(1)	6316(2)	47(1)
C(11)	7466(1)	1568(1)	7469(2)	46(1)
C(12)	7238(1)	980(1)	7110(2)	46(1)
C(13)	6966(1)	716(1)	8457(3)	67(1)
C(14)	8634(1)	1049(1)	4772(2)	36(1)
C(15)	9229(1)	972(1)	4552(2)	34(1)
C(16)	9703(1)	927(1)	5742(2)	32(1)
C(17)	10304(1)	1188(1)	5277(2)	33(1)
C(18)	10791(1)	880(1)	4763(2)	36(1)
C(19)	11330(1)	1130(1)	4301(2)	46(1)
C(20)	11385(1)	1689(1)	4342(3)	60(1)
C(21)	10911(1)	2003(1)	4861(3)	79(1)
C(22)	10369(1)	1756(1)	5330(3)	64(1)
C(23)	6965(1)	1989(1)	7485(3)	59(1)
C(24)	6766(1)	2253(1)	8645(3)	68(1)

Table 3. Bond lengths [Å] and angles [°] for **3.37b**

B(1)-O(2)	1.342(3)
B(1)-O(1)	1.360(2)
B(1)-C(1)	1.570(3)
O(1)-C(7)	1.439(2)
O(2)-C(13)	1.439(3)
O(3)-C(16)	1.429(2)
O(3)-H(3O)	0.81(2)
O(3)-H(3OA)	0.81(2)
C(1)-C(6)	1.388(3)
C(1)-C(2)	1.398(3)
C(2)-C(3)	1.387(4)
C(2)-H(2)	0.9500
C(3)-C(4)	1.364(4)
C(3)-H(3)	0.9500
C(4)-C(5)	1.385(4)
C(4)-H(4)	0.9500
C(5)-C(6)	1.385(3)
C(5)-H(5)	0.9500
C(6)-H(6)	0.9500
C(7)-C(8)	1.510(2)
C(7)-H(7A)	0.9900
C(7)-H(7B)	0.9900
C(8)-C(12)	1.557(2)
C(8)-C(9)	1.559(3)
C(8)-H(8)	1.0000
C(9)-C(14)	1.500(2)
C(9)-C(10)	1.534(2)
C(9)-H(9)	1.0000
C(10)-C(11)	1.525(3)
C(10)-H(10A)	0.9900

C(10)-H(10B)	0.9900
C(11)-C(23)	1.494(3)
C(11)-C(12)	1.541(3)
C(11)-H(11)	1.0000
C(12)-C(13)	1.508(3)
C(12)-H(12)	1.0000
C(13)-H(13A)	0.9900
C(13)-H(13B)	0.9900
C(14)-C(15)	1.326(2)
C(14)-H(14)	0.9500
C(15)-C(16)	1.505(2)
C(15)-H(15)	0.9500
C(16)-C(17)	1.517(2)
C(16)-H(16)	1.0000
C(17)-C(22)	1.380(3)
C(17)-C(18)	1.380(2)
C(18)-C(19)	1.389(3)
C(18)-H(18)	0.9500
C(19)-C(20)	1.356(3)
C(19)-H(19)	0.9500
C(20)-C(21)	1.366(4)
C(20)-H(20)	0.9500
C(21)-C(22)	1.392(3)
C(21)-H(21)	0.9500
C(22)-H(22)	0.9500
C(23)-C(24)	1.311(3)
C(23)-H(23)	0.9500
C(24)-H(24A)	0.9500
C(24)-H(24B)	0.9500
O(2)-B(1)-O(1)	126.5(2)
O(2)-B(1)-C(1)	117.08(17)

O(1)-B(1)-C(1)	116.42(19)
B(1)-O(1)-C(7)	126.56(16)
B(1)-O(2)-C(13)	123.61(17)
C(16)-O(3)-H(3O)	118(3)
C(16)-O(3)-H(3OA)	110(4)
H(3O)-O(3)-H(3OA)	126(4)
C(6)-C(1)-C(2)	117.1(2)
C(6)-C(1)-B(1)	122.03(17)
C(2)-C(1)-B(1)	120.9(2)
C(3)-C(2)-C(1)	121.0(3)
C(3)-C(2)-H(2)	119.5
C(1)-C(2)-H(2)	119.5
C(4)-C(3)-C(2)	120.5(2)
C(4)-C(3)-H(3)	119.7
C(2)-C(3)-H(3)	119.7
C(3)-C(4)-C(5)	120.0(3)
C(3)-C(4)-H(4)	120.0
C(5)-C(4)-H(4)	120.0
C(4)-C(5)-C(6)	119.2(3)
C(4)-C(5)-H(5)	120.4
C(6)-C(5)-H(5)	120.4
C(5)-C(6)-C(1)	122.1(2)
C(5)-C(6)-H(6)	118.9
C(1)-C(6)-H(6)	118.9
O(1)-C(7)-C(8)	113.96(14)
O(1)-C(7)-H(7A)	108.8
C(8)-C(7)-H(7A)	108.8
O(1)-C(7)-H(7B)	108.8
C(8)-C(7)-H(7B)	108.8
H(7A)-C(7)-H(7B)	107.7
C(7)-C(8)-C(12)	114.79(15)

C(7)-C(8)-C(9)	109.92(13)
C(12)-C(8)-C(9)	105.89(14)
C(7)-C(8)-H(8)	108.7
C(12)-C(8)-H(8)	108.7
C(9)-C(8)-H(8)	108.7
C(14)-C(9)-C(10)	112.99(15)
C(14)-C(9)-C(8)	112.72(14)
C(10)-C(9)-C(8)	104.34(14)
C(14)-C(9)-H(9)	108.9
C(10)-C(9)-H(9)	108.9
C(8)-C(9)-H(9)	108.9
C(11)-C(10)-C(9)	104.64(15)
C(11)-C(10)-H(10A)	110.8
C(9)-C(10)-H(10A)	110.8
C(11)-C(10)-H(10B)	110.8
C(9)-C(10)-H(10B)	110.8
H(10A)-C(10)-H(10B)	108.9
C(23)-C(11)-C(10)	114.47(17)
C(23)-C(11)-C(12)	113.19(16)
C(10)-C(11)-C(12)	103.18(15)
C(23)-C(11)-H(11)	108.6
C(10)-C(11)-H(11)	108.6
C(12)-C(11)-H(11)	108.6
C(13)-C(12)-C(11)	110.07(17)
C(13)-C(12)-C(8)	115.42(16)
C(11)-C(12)-C(8)	106.11(15)
C(13)-C(12)-H(12)	108.3
C(11)-C(12)-H(12)	108.3
C(8)-C(12)-H(12)	108.3
O(2)-C(13)-C(12)	112.69(19)
O(2)-C(13)-H(13A)	109.1

C(12)-C(13)-H(13A)	109.1
O(2)-C(13)-H(13B)	109.1
C(12)-C(13)-H(13B)	109.1
H(13A)-C(13)-H(13B)	107.8
C(15)-C(14)-C(9)	128.33(16)
C(15)-C(14)-H(14)	115.8
C(9)-C(14)-H(14)	115.8
C(14)-C(15)-C(16)	124.90(16)
C(14)-C(15)-H(15)	117.5
C(16)-C(15)-H(15)	117.5
O(3)-C(16)-C(15)	109.14(13)
O(3)-C(16)-C(17)	112.17(13)
C(15)-C(16)-C(17)	111.13(13)
O(3)-C(16)-H(16)	108.1
C(15)-C(16)-H(16)	108.1
C(17)-C(16)-H(16)	108.1
C(22)-C(17)-C(18)	118.06(18)
C(22)-C(17)-C(16)	119.50(17)
C(18)-C(17)-C(16)	122.42(15)
C(17)-C(18)-C(19)	121.31(17)
C(17)-C(18)-H(18)	119.3
C(19)-C(18)-H(18)	119.3
C(20)-C(19)-C(18)	120.00(19)
C(20)-C(19)-H(19)	120.0
C(18)-C(19)-H(19)	120.0
C(19)-C(20)-C(21)	119.73(19)
C(19)-C(20)-H(20)	120.1
C(21)-C(20)-H(20)	120.1
C(20)-C(21)-C(22)	120.8(2)
C(20)-C(21)-H(21)	119.6
C(22)-C(21)-H(21)	119.6

C(17)-C(22)-C(21)	120.1(2)
C(17)-C(22)-H(22)	119.9
C(21)-C(22)-H(22)	119.9
C(24)-C(23)-C(11)	125.6(2)
C(24)-C(23)-H(23)	117.2
C(11)-C(23)-H(23)	117.2
C(23)-C(24)-H(24A)	120.0
C(23)-C(24)-H(24B)	120.0
H(24A)-C(24)-H(24B)	120.0

Symmetry transformations used to generate equivalent atoms:

Table 4. Anisotropic displacement parameters ($\text{\AA}^2 \times 10^3$) for **3.37b**. The anisotropic displacement factor exponent takes the form: $-2\pi^2 [h^2 a^* U_{11} + \dots + 2 h k a^* b^* U_{12}]$

	U ¹¹	U ²²	U ³³	U ²³	U ¹³	U ¹²
B(1)	38(1)	68(1)	36(1)	9(1)	6(1)	3(1)
O(1)	32(1)	53(1)	48(1)	5(1)	1(1)	-2(1)
O(2)	53(1)	75(1)	111(2)	1(1)	43(1)	4(1)
O(3)	46(1)	34(1)	40(1)	10(1)	-10(1)	-7(1)
C(1)	36(1)	79(2)	46(1)	14(1)	3(1)	-5(1)
C(2)	39(1)	98(2)	77(2)	20(1)	8(1)	-7(1)
C(3)	40(1)	120(2)	91(2)	34(2)	3(1)	-21(2)
C(4)	60(1)	98(2)	84(2)	28(2)	-5(1)	-35(2)
C(5)	63(1)	76(2)	65(1)	16(1)	5(1)	-24(1)
C(6)	44(1)	73(1)	51(1)	12(1)	6(1)	-16(1)
C(7)	31(1)	49(1)	43(1)	1(1)	-1(1)	2(1)
C(8)	31(1)	50(1)	30(1)	-2(1)	-2(1)	7(1)
C(9)	35(1)	45(1)	33(1)	1(1)	-3(1)	6(1)
C(10)	50(1)	47(1)	43(1)	-2(1)	-2(1)	10(1)
C(11)	43(1)	57(1)	40(1)	-4(1)	-4(1)	15(1)

C(12)	34(1)	62(1)	43(1)	-4(1)	-1(1)	14(1)
C(13)	60(1)	68(2)	72(2)	-5(1)	32(1)	12(1)
C(14)	39(1)	38(1)	30(1)	3(1)	-4(1)	1(1)
C(15)	39(1)	33(1)	31(1)	0(1)	0(1)	-2(1)
C(16)	37(1)	30(1)	31(1)	-1(1)	0(1)	-1(1)
C(17)	36(1)	33(1)	31(1)	-2(1)	-3(1)	-4(1)
C(18)	38(1)	38(1)	34(1)	1(1)	-3(1)	1(1)
C(19)	36(1)	67(1)	36(1)	1(1)	-2(1)	-4(1)
C(20)	51(1)	73(2)	57(1)	4(1)	1(1)	-28(1)
C(21)	84(2)	44(1)	109(2)	-2(1)	20(2)	-28(1)
C(22)	62(1)	35(1)	94(2)	-9(1)	18(1)	-8(1)
C(23)	58(1)	66(1)	54(1)	-4(1)	-1(1)	24(1)
C(24)	62(1)	69(1)	71(2)	-12(1)	6(1)	25(1)

Table 5. Hydrogen coordinates (x 10⁴) and isotropic displacement parameters (Å²x 10³) for **3.37b**

	x	y	z	U(eq)
H(3O)	9950(20)	289(15)	6890(30)	48(12)
H(3OA)	9780(20)	168(17)	5410(40)	56(15)
H(2)	5879	-565	8575	86
H(3)	5381	-1416	8571	100
H(4)	5868	-2196	7687	97
H(5)	6877	-2138	6829	82
H(6)	7388	-1294	6902	67
H(7A)	8440	80	6928	49
H(7B)	8122	339	8345	49
H(8)	7670	520	5453	44
H(9)	8604	1090	7015	45
H(10A)	8240	1968	6625	56

H(10B)	7772	1771	5367	56
H(11)	7665	1562	8453	56
H(12)	6909	1009	6352	56
H(13A)	7291	677	9207	80
H(13B)	6645	963	8859	80
H(14)	8386	1063	3918	43
H(15)	9366	944	3569	41
H(16)	9548	1132	6617	39
H(18)	10757	488	4725	44
H(19)	11661	910	3956	55
H(20)	11751	1862	4011	72
H(21)	10952	2394	4903	95
H(22)	10043	1979	5687	76
H(23)	6774	2073	6578	71
H(24A)	6944	2182	9574	81
H(24B)	6443	2515	8556	81

Table 6. Torsion angles [°] for **3.37b**

O(2)-B(1)-O(1)-C(7)	-3.5(3)
C(1)-B(1)-O(1)-C(7)	177.20(17)
O(1)-B(1)-O(2)-C(13)	-8.0(4)
C(1)-B(1)-O(2)-C(13)	171.3(2)
O(2)-B(1)-C(1)-C(6)	175.1(2)
O(1)-B(1)-C(1)-C(6)	-5.5(3)
O(2)-B(1)-C(1)-C(2)	-7.1(3)
O(1)-B(1)-C(1)-C(2)	172.3(2)
C(6)-C(1)-C(2)-C(3)	-0.3(3)
B(1)-C(1)-C(2)-C(3)	-178.2(2)
C(1)-C(2)-C(3)-C(4)	-0.8(4)
C(2)-C(3)-C(4)-C(5)	0.8(4)
C(3)-C(4)-C(5)-C(6)	0.3(4)

C(4)-C(5)-C(6)-C(1)	-1.5(4)
C(2)-C(1)-C(6)-C(5)	1.4(3)
B(1)-C(1)-C(6)-C(5)	179.3(2)
B(1)-O(1)-C(7)-C(8)	-50.0(2)
O(1)-C(7)-C(8)-C(12)	69.8(2)
O(1)-C(7)-C(8)-C(9)	-171.01(14)
C(7)-C(8)-C(9)-C(14)	96.35(17)
C(12)-C(8)-C(9)-C(14)	-139.12(15)
C(7)-C(8)-C(9)-C(10)	-140.68(15)
C(12)-C(8)-C(9)-C(10)	-16.16(17)
C(14)-C(9)-C(10)-C(11)	157.90(15)
C(8)-C(9)-C(10)-C(11)	35.11(18)
C(9)-C(10)-C(11)-C(23)	-163.74(17)
C(9)-C(10)-C(11)-C(12)	-40.31(18)
C(23)-C(11)-C(12)-C(13)	-80.5(2)
C(10)-C(11)-C(12)-C(13)	155.25(16)
C(23)-C(11)-C(12)-C(8)	153.98(17)
C(10)-C(11)-C(12)-C(8)	29.71(18)
C(7)-C(8)-C(12)-C(13)	-9.1(2)
C(9)-C(8)-C(12)-C(13)	-130.52(18)
C(7)-C(8)-C(12)-C(11)	113.11(17)
C(9)-C(8)-C(12)-C(11)	-8.33(18)
B(1)-O(2)-C(13)-C(12)	66.7(3)
C(11)-C(12)-C(13)-O(2)	175.64(16)
C(8)-C(12)-C(13)-O(2)	-64.3(2)
C(10)-C(9)-C(14)-C(15)	120.5(2)
C(8)-C(9)-C(14)-C(15)	-121.53(19)
C(9)-C(14)-C(15)-C(16)	1.1(3)
C(14)-C(15)-C(16)-O(3)	91.07(19)
C(14)-C(15)-C(16)-C(17)	-144.72(17)
O(3)-C(16)-C(17)-C(22)	-158.52(19)

C(15)-C(16)-C(17)-C(22)	79.0(2)
O(3)-C(16)-C(17)-C(18)	23.0(2)
C(15)-C(16)-C(17)-C(18)	-99.44(17)
C(22)-C(17)-C(18)-C(19)	-0.5(3)
C(16)-C(17)-C(18)-C(19)	177.95(16)
C(17)-C(18)-C(19)-C(20)	-0.3(3)
C(18)-C(19)-C(20)-C(21)	1.0(3)
C(19)-C(20)-C(21)-C(22)	-0.9(4)
C(18)-C(17)-C(22)-C(21)	0.6(4)
C(16)-C(17)-C(22)-C(21)	-177.9(2)
C(20)-C(21)-C(22)-C(17)	0.1(5)
C(10)-C(11)-C(23)-C(24)	-129.8(3)
C(12)-C(11)-C(23)-C(24)	112.3(3)

Symmetry transformations used to generate equivalent atoms:

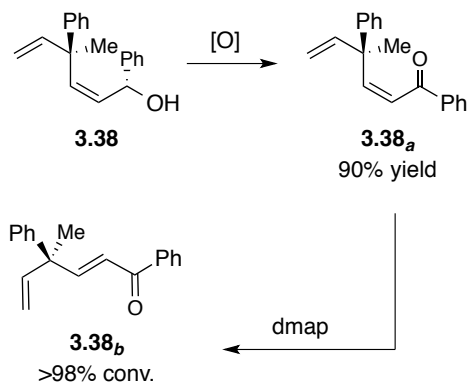
(1*R*,4*R*,*Z*)-4-Methyl-1,4-diphenylhexa-2,5-dien-1-ol (3.38).

Following the general procedure, a solution of **Ru4b** (3.9 mg, 5.6 mmol, 5.0 mol %) in dichloromethane (224 mL) was transferred by syringe to a vial containing (*R*)-1-phenyl-2-propen-1-ol **3.36a** (15.0 mg, 0.112 mmol, 1.00 equiv) and cyclopropene **3.26** (29.0 mg, 0.224 mmol, 2.00 equiv). The resulting solution was allowed to stir for 4 hours at 22 °C. Analysis of the unpurified mixture revealed >98% consumption of **3.26**, and the product was obtained in 91:9 *Z:E* ratio. The resulting oil was purified by silica gel chromatography (10% Et₂O in hexanes to 20% Et₂O in hexanes) after which it was passed through a plug of activated charcoal with 50% Et₂O in pentane to afford **3.38** (23.1 mg, 0.0870 mmol, 78% yield) as colorless oil; **IR** (CH₂Cl₂): 3408 (br), 2961 (w), 2924 (m), 2852 (w), 1616 (w), 1579 (w), 1491 (w), 1446 (w), 1005 (w), 914 (w); **¹H NMR** (400 MHz, CDCl₃): *Z*-isomer (major): δ 7.37 (2H, dd, *J* = 8.1, 1.0 Hz), 7.34–7.26 (3H, m), 7.26–7.17 (4H, m), 7.06–7.04 (2H, m), 6.34 (1H, dd, *J* = 17.3, 10.5 Hz), 5.90

(1H, dd, $J = 11.5, 0.8$ Hz)⁹⁷, 5.68 (1H, dd, $J = 11.5, 9.9$ Hz), 5.16 (2H, ddd, $J = 18.4, 13.9, 1.0$ Hz), 5.08 (1H, d, $J = 9.8$ Hz), 1.58 (3H, s); **^{13}C NMR (100 MHz, CDCl_3)**: δ 147.8, 146.0, 142.7, 138.9, 132.9, 128.4, 128.3, 127.4, 127.1, 126.3, 126.1, 112.7, 69.1, 47.3, 29.1; **HRMS [M+H-H₂O]⁺** calcd for $\text{C}_{19}\text{H}_{19}$: 247.1487, found: 247.1485.

Stereochemical Proof for 3.38:

Chart 7. Stereochemical Proof of Compound 3.38



(R,Z)-4-Methyl-1,4-diphenylhexa-2,5-dien-1-one (3.38_a).

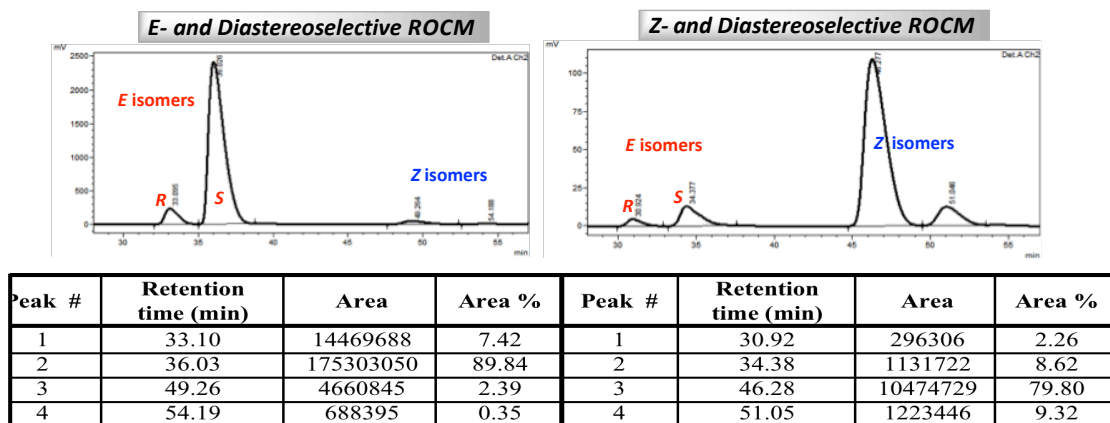
A previously reported procedure was adopted.⁹⁸ An oven-dried vial equipped with a stir bar was charged with **3.38** (16.0 mg, 0.0610 mmol, 1.00 equiv). Diethyl ether (1.8 mL) was added through a syringe followed by manganese dioxide (160 mg, 10 mg/mg of substrate, ~30 equiv). The resulting suspension was allowed to stir vigorously until the reaction was determined to be complete according to TLC analysis (30 min). The mixture was filtered through a short pad of celite, which was then washed with diethyl ether (3 x 5.0 mL). The volatiles were removed *in vacuo*, affording yellow oil, which was purified by silica gel chromatography (5% Et₂O in hexanes). The product **3.38_a** was obtained in 91:09 Z/E ratio and as colorless oil (14.3 mg, 0.0550 mmol, 90% yield); **IR (CH₂Cl₂)**: 2965 (w), 2926 (w), 1670 (s), 1580 (w), 1492 (w), 1448 (m), 1007 (m), 919 (w); **^1H NMR (400 MHz, CDCl_3)**: Z-isomer (major): δ 7.84–7.79 (2H, m), 7.55–7.49 (1H, m), 7.40 (2H, t, $J = 7.7$ Hz), 7.33–7.28 (2H, m), 7.17 (2H, t, $J = 7.6$ Hz), 7.12–7.05 (1H, m),

(97) Coupling constants ($J = 11.5$ and $J = 11.5$ Hz) of the signals at δ 5.90 and 5.68 ppm indicate the predominance of Z-isomer **3.38**.

(98) A. H. Hoveyda, P. J. Lombardi, R. V. O'Brien, A. R. Zhugralin, *J. Am. Chem. Soc.* **2009**, *131*, 8378–8379.

6.49 (1H, d, $J = 13.2$ Hz)⁹⁹, 6.23 (1H, d, $J = 12.8$ Hz), 6.20 (1H, dd, $J = 17.2, 10.8$ Hz), 5.09 (1H, d, $J = 10.6$ Hz), 5.05 (1H, d, $J = 17.4$ Hz), 1.55 (s, 3H); **^{13}C NMR (100 MHz, CDCl_3)**: δ 194.7, 146.0, 145.8, 144.2, 137.3, 133.0, 128.7, 128.3, 128.0, 127.0, 126.7, 126.2, 113.5, 48.7, 26.7; **HRMS [M+H]⁺** calcd for $\text{C}_{19}\text{H}_{19}\text{O}$: 263.1436, found: 263.1438; diastereomeric ratio was established by HPLC analysis (shown below) in comparison with authentic material prepared according to a previously reported procedure³³ where the absolute stereochemistry of the major *E*-enone isomers³³ had been formerly established [89.5:10.5 e.r. shown for **3.38_a**; after correction for 96:4 e.r. of the starting material, diastereoselectivity is measured to be 93:7 d.r.; Daicel Chiraldapak OD-H column (99.5:0.5 hexanes:*i*-PrOH, 0.7 mL/min, 254 nm) was used].

Chart 8. Comparison of Stereochemistry of *E*- and *Z*-Selective ROCM Products



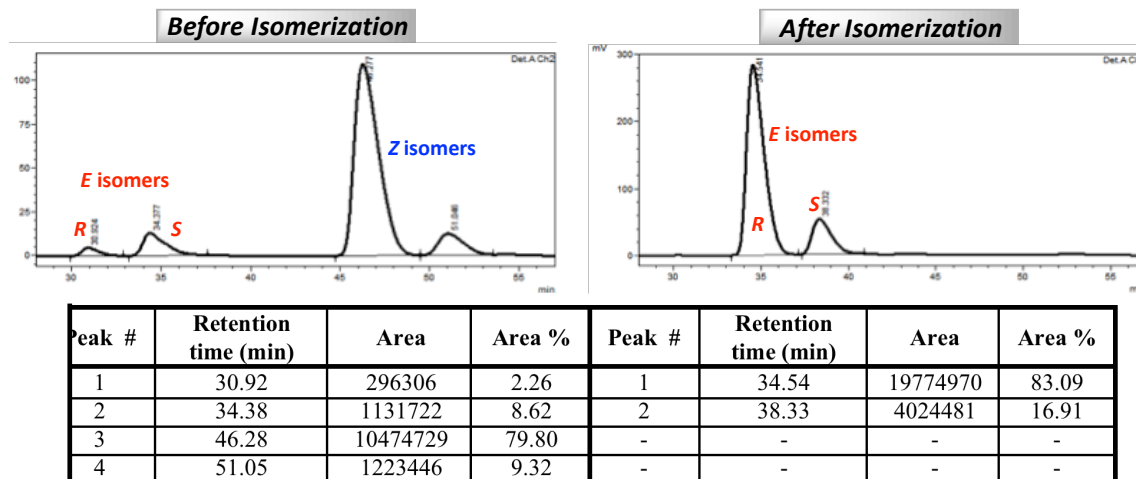
To ascertain the absolute stereochemistry of the diastereoselective ROCM product, *Z*-enone **3.38_a** was isomerized to its corresponding *E* isomer **3.38_b** through a modified reported procedure.¹⁰⁰ An oven-dried vial equipped with a stir bar was charged with **3.38_a** (12.0 mg, 0.046 mmol, 1.00 equiv, 91:09 *Z/E*). Dry MeCN (0.2 mL) was added through syringe followed by *N,N*-dimethylaminopyridine (1.1 mg, 5.6 mmol, 20 mol %). The resulting solution was allowed to reflux for 24 hours in a sealed vial. After addition of H_2O , the mixture was washed with Et_2O (3 x 2.0 mL). The combined organic layers were dried over anhydrous MgSO_4 , filtered and concentrated *in vacuo* to afford **3.38_b** in >98:2 *E/Z* as yellow oil, which was purified by silica gel chromatography (5% Et_2O in hexanes) to afford colorless oil (11.3 mg, 0.0430 mmol, 94% yield). Comparison

(99) Coupling constants ($J = 13.2$ and $J = 12.8$ Hz) of the signals at δ 6.49 and 6.23 ppm indicate the predominance of **3.38_a**.

(100) D. Könning, W. Hiller, M. Christmann, *Org. Lett.* **2012**, *14*, 5258–5261.

of the HPLC retention times for the *E* isomers before and after isomerization, allowing us to establish the absolute configuration at the all-carbon quaternary stereogenic center of the product [Daicel Chiralpak OD-H column (99.5:0.5 hexanes:*i*-PrOH, 0.7 mL/min, 254 nm) was used].

Chart 9. Absolute Stereochemistry of 3.38



■ Highly *Z*-Selective Cross/Metathesis (ROCM) Reactions

General Procedure for Transformations in Table 3.5.1-1, 3.5.1-2, 3.5.1-3, 3.5.2, and 3.5.3-2

An oven-dried 8 mL vial equipped with a magnetic stir bar is charged with alkene substrate (1.0 equiv) and *Z*-2-butene-1,4-diol (2.0–5.0 equiv) *outside the glove box*. The vial is then sealed, evacuated and purged with N₂. To this vial, a solution of **Ru9** (5.0 mol %) in tetrahydrofuran is added. The resulting solution is allowed to stir for 4–12 hours at 22°C, after which the reaction is quenched by addition of wet diethyl ether and concentrated *in vacuo* (percent conversion determined by 400 MHz or 500 MHz ¹H NMR analysis). Purification is performed through silica gel chromatography and/or Kugelrohr distillation.

(*Z*)-4-phenyl-2-butene-1-ol (3.43).

Following the general procedure, a solution of **Ru9** (4.9 mg, 6.3 mmol, 5.0 mol %) in tetrahydrofuran (255 µL) was transferred by syringe to a vial charged with allylbenzene (15.0 mg, 0.127 mmol, 1.00 equiv) and *Z*-2-butene-1,4-diol (22.4 mg, 0.254

mmol, 2.00 equiv). The resulting solution was allowed to stir for 4 hours at 22 °C. Analysis of the unpurified mixture revealed 84% consumption of allylbenzene. The resulting brown oil was purified by silica gel chromatography (10% Et₂O in hexanes to 40% Et₂O in hexanes) to afford **3.43** (13.4 mg, 0.0904 mmol, 71% yield) as pale yellow oil in 96:04 Z/E ratio. The spectral data for this compound were identical to those reported in the literature.¹⁰¹

(Z)-7-hydroxy-5-heptenoic acid (3.44).

Following the general procedure, a solution of **Ru9** (4.9 mg, 6.3 mmol, 5.0 mol %) in tetrahydrofuran (255 µL) was transferred by syringe to a vial charged with 5-hexenoic acid (14.5 mg, 0.127 mmol, 1.00 equiv) and Z-2-butene-1,4-diol (24.2 mg, 0.254 mmol, 2.00 equiv). The resulting solution was allowed to stir for 4 hours at 22 °C. Analysis of the unpurified mixture revealed 85% consumption of 5-hexenoic acid. The resulting brown oil was purified by silica gel chromatography (100% CH₂Cl₂ to 5% CH₂Cl₂ in MeOH) to afford **3.44** (12.8 mg, 0.0890 mmol, 70% yield) as pale yellow oil in 96:04 Z/E ratio. The spectral data for this compound were identical to those reported in the literature.¹⁰²

(Z)-6-hydroxy-2,2-dimethyl-4-hexenoic acid (3.45).

Following the general procedure, a solution of **Ru9** (4.9 mg, 6.3 mmol, 5.0 mol %) in tetrahydrofuran (255 µL) was transferred by syringe to a vial charged with 2,2-dimethyl-4-pentenoic acid (16.3 mg, 0.127 mmol, 1.00 equiv) and Z-2-butene-1,4-diol (24.2 mg, 0.254 mmol, 2.00 equiv). The resulting solution was allowed to stir for 4 hours at 22 °C. Analysis of the unpurified mixture revealed 66% consumption of 2,2-dimethyl-4-pentenoic acid. The resulting brown oil was purified by silica gel chromatography (100% CH₂Cl₂ to 5% CH₂Cl₂ in MeOH) to afford **3.45** (12.3 mg, 0.0778 mmol, 61% yield) as pale yellow oil in 98:02 Z/E ratio; **IR (CH₂Cl₂)**: 3316 (br), 3021 (w), 2963 (w), 2923 (m), 2854 (w), 1698 (s), 1473 (m), 1389 (w), 1366 (w), 1197 (m), 1146 (m), 1021 (m), 866 (w); **¹H NMR (400 MHz, CDCl₃)**: Z-isomer (major): δ 6.42 (1H, br s), 5.80–

(101) Ely, R. J.; Morken, J. P. *J. Am. Chem. Soc.* **2010**, *132*, 2534–2535.

(102) Taber, D. F.; Herr, R. J.; Gleave, D. M. *J. Org. Chem.* **1997**, *62*, 194–198.

5.70 (1H, m), 5.56 (1H, dtt, $J = 12.0, 8.0, 1.2$ Hz),¹⁰³ 4.19 (2H, d, $J = 6.8$ Hz), 2.33 (2H, d, $J = 7.9$ Hz), 1.29 (1H, s), 1.23 (6H, s); ^{13}C NMR (100 MHz, CDCl₃): δ 183.0, 131.4, 127.9, 58.4, 42.8, 37.9, 24.5; HRMS [M+H]⁺ calcd for C₈H₁₅O₃: 159.1021, found: 159.1029.

(Z)-12-hydroxy-10-dodecenal (3.46):

Following the general procedure, a solution of **Ru9** (4.9 mg, 6.3 mmol, 5.0 mol %) in tetrahydrofuran (255 μL) was transferred by syringe to a vial charged with undecylenic aldehyde (21.4 mg, 0.127 mmol, 1.00 equiv) and Z-2-butene-1,4-diol (24.2 mg, 0.254 mmol, 2.00 equiv). The resulting solution was allowed to stir for 4 hours at 22 °C. Analysis of the unpurified mixture revealed 86% consumption of undecylenic aldehyde. The resulting brown oil was purified by silica gel chromatography (10% Et₂O in hexanes to 40% Et₂O in hexanes) to afford **3.46** (20.1 mg, 0.101 mmol, 80% yield) as pale yellow oil in 94:06 Z/E ratio; IR (CH₂Cl₂): 3408 (br), 2924 (s), 2854 (s), 1725 (m), 1558 (m), 1462 (m), 1265 (w), 1027 (w); ^1H NMR (400 MHz, C₆D₆): Z-isomer (major): δ 9.33 (1H, s), 5.58 (1H, dt, $J = 11.4, 6.3$ Hz),¹⁰⁴ 5.56–5.36 (1H, m), 4.01 (2H, d, $J = 6.4$ Hz), 1.98–1.89 (2H, m), 1.87–1.78 (2H, m), 1.33–1.05 (13H, m); ^{13}C NMR (100 MHz, CDCl₃): δ 203.1, 133.3, 128.5, 58.8, 44.1, 29.7, 29.4, 29.4, 29.3, 29.2, 27.5, 22.2; HRMS [M+H-H₂O]⁺ calcd for C₁₂H₂₁O: 181.1592, found: 181.1598.

(Z)-1-(4-hydroxy-3-(4-hydroxy-2-butenyl)phenyl)ethanone (3.47).

Following the general procedure, a solution of **Ru9** (4.9 mg, 6.3 mmol, 5.0 mol %) in tetrahydrofuran (255 μL) was transferred by syringe to a vial charged with 3'-allyl-4'-hydroxyacetophenone (22.4 mg, 0.127 mmol, 1.00 equiv) and Z-2-butene-1,4-diol (24.2 mg, 0.254 mmol, 2.00 equiv). The resulting solution was allowed to stir for 4 hours at 22 °C. Analysis of the unpurified mixture revealed 77% consumption of 3'-allyl-4'-hydroxyacetophenone. The resulting brown residue was purified by silica gel chromatography (10% Et₂O in hexanes to 60% Et₂O in hexanes) to afford **3.47** (17.8 mg, 0.0863 mmol, 68% yield) as off-white solid in 98:02 Z/E ratio; mp: 97–99 °C; IR (CH₂Cl₂): 3251 (br), 3018 (w), 2962 (m), 2925 (m), 1656 (s), 1592 (s), 1509 (w), 1426

(103) Coupling constant ($J = 12.0$ Hz) of the signal at δ 5.56 ppm is indicative of Z-isomer **3.45**.

(104) Coupling constant ($J = 11.4$ Hz) of the signal at δ 5.58 ppm is indicative of Z-isomer **3.46**.

(w), 1360 (m), 1281 (s), 1120 (w), 1020 (w), 824 (w); **¹H NMR (400 MHz, CDCl₃)**: Z-isomer (major): δ 7.80 (1H, d, J = 2.2 Hz), 7.77 (1H, dd, J = 8.4, 2.3 Hz), 6.86 (1H, d, J = 8.4 Hz), 5.79 (1H, dt, J = 10.9, 6.2 Hz),¹⁰⁵ 5.69 (1H, dt, J = 10.8, 7.6 Hz),¹⁸ 4.42 (2H, d, J = 6.2 Hz), 3.56 (2H, d, J = 7.8 Hz), 2.55 (3H, s), 1.25 (2H, br s); **¹³C NMR (100 MHz, CDCl₃)**: δ 159.9, 132.6, 131.5, 130.1, 129.6, 127.1, 127.1, 125.5, 116.3, 58.7, 30.3, 26.5; **HRMS [M+H]⁺** calcd for C₁₂H₁₅O₃: 207.1021, found: 207.1015.

(2Z,4E)-undeca-2,4-dien-1-ol (3.48).

Following the general procedure, a solution of **Ru9** (4.9 mg, 6.3 mmol, 5.0 mol %) in tetrahydrofuran (255 μ L) was transferred by syringe to a vial charged with deca-1,3-diene (17.6 mg, 0.127 mmol, 1.00 equiv) and Z-2-butene-1,4-diol (24.2 mg, 0.254 mmol, 2.00 equiv). The resulting solution was allowed to stir for 8 hours at 22 °C. Analysis of the unpurified mixture revealed 88% consumption of deca-1,3-diene. The resulting brown oil was purified by silica gel chromatography (10% Et₂O in hexanes to 40% Et₂O in hexanes) to afford **3.48** (14.1 mg, 0.0838 mmol, 66% yield) as colorless oil in 95:05 Z/E ratio; **IR (CH₂Cl₂)**: 3320 (br), 3023 (w), 2956 (m), 2924 (s), 2854 (m), 1653 (w), 1459 (m), 1264 (m), 1027 (m), 985 (m), 952 (m); **¹H NMR (400 MHz, CDCl₃)**: Z-isomer (major): δ 6.35–6.25 (1H, m), 6.07 (1H, t, J = 11.0 Hz),¹⁰⁶ 5.76 (1H, dt, J = 14.5, 7.0 Hz), 5.49 (1H, dt, J = 10.9, 7.0 Hz),²⁶ 4.30 (2H, d, J = 7.0 Hz), 2.15–2.06 (2H, m), 1.42–1.34 (2H, m), 1.32–1.25 (7H, m), 0.88 (3H, t, J = 6.8 Hz); **¹³C NMR (100 MHz, CDCl₃)**: δ 137.8, 131.5, 127.2, 124.9, 59.0, 33.0, 31.9, 29.3, 29.1, 22.8, 14.2; **HRMS [M+H-H₂O]⁺** calcd for C₁₁H₁₉: 151.1487, found: 151.1487.

(Z)-3-phenyl-2-propene-1-ol (3.49).

Following the general procedure, a solution of **Ru9** (7.50 mol %) in tetrahydrofuran (255 μ L) was transferred by syringe to a vial charged with styrene (13.2 mg, 0.127 mmol, 1.00 equiv) and Z-2-butene-1,4-diol (56.0 mg, 0.635 mmol, 5.00 equiv). The resulting solution was allowed to stir for 8 hours at 22 °C. Analysis of the unpurified mixture revealed 57% consumption of styrene. The resulting brown oil was purified by

(105) Coupling constants (J = 10.9 Hz and J = 10.8 Hz) of the signals at δ 5.79 and 5.69 ppm are indicative of Z-isomer **3.47**.

(106) Coupling constants (J = 11.0 Hz and J = 10.9 Hz) of the signals at δ 6.07 and 5.49 ppm are indicative of Z-isomer **3.48**.

silica gel chromatography (10% Et₂O in hexanes to 40% Et₂O in hexanes) to afford **3.49** (9.0 mg, 0.0671 mmol, 47% yield) as pale yellow oil in 93:07 Z/E ratio; The spectral data for this compound were identical to those reported in the literature.¹⁰⁷

Syntheses of Natural Product Precursors

(Z)-2-tridecene-1-ol (3.50).

Following the general procedure, a solution of **Ru9** (4.9 mg, 6.3 mmol, 5.0 mol %) in tetrahydrofuran (255 µL) was transferred by syringe to a vial charged with 1-dodecene (21.4 mg, 0.127 mmol, 1.00 equiv) and Z-2-butene-1,4-diol (24.2 mg, 0.254 mmol, 2.00 equiv). The resulting solution was allowed to stir for 4 hours at 22 °C. Analysis of the unpurified mixture revealed 81% consumption of 1-dodecene. The resulting brown oil was purified by silica gel chromatography (10% Et₂O in hexanes to 40% Et₂O in hexanes) to afford **3.50** (18.1 mg, 0.091 mmol, 72% yield) as pale yellow oil in 96:04 Z/E ratio The spectral data for this compound were identical to those reported in the literature.¹⁰⁸

Methyl (Z)-(3-(4,4,5,5-tetramethyl-1,3,2-dioxaborolan-2-yl)allyl)carbamate (3.52).

In a N₂-filled glove box, a 25 mL flask with a magnetic stir bar was charged with diene **3.51**¹⁰⁹ (160 mg, 0.672 mmol) and Z-2-butene-1,4-diol (178 mg, 2.02 mmol) and THF (6.7 mL). A catalyst solution of **Ru9** (10 mg/mL in THF, 2.57 mL, 25.7 mg, 0.034 mmol, 5 mol %) was added and the mixture was allowed to stir at 22 °C for two hours under 100 torr vacuum. Additional catalyst (10 mg/mL in THF, 2.57 mL, 25.7 mg, 0.034 mmol, 5 mol %) was added and the mixture was allowed to stir for another 10 hours. The reaction mixture was taken out of the glove box and filtered through a thin pad of silica gel (EtOAc). The filtrate was concentrated by vacuum and the resulting brown oil was purified by silica gel chromatography (1:2 hexanes: ethyl acetate) to afford **3.52** as colorless oil (128 mg, 0.478 mmol, 71% yield). **IR (neat)**: 3329 (br), 2920 (m), 2850 (m), 1701 (s), 1589 (w), 1521 (s), 1462 (m), 1261 (s), 1193 (w), 1023 (s), 778 (m); **¹H NMR**

(107) Reed, S. A.; White, M. C. *J. Am. Chem. Soc.* **2008**, *130*, 3316–3318.

(108) Wang, Z.; Zheng, J.; Huang, P. *Chin. J. Chem.* **2012**, *30*, 23–28.

(109) Diene **3.51** was prepared based on the procedure reported here: Yu, M.; Hoveyda, A. H. *Angew. Chem. Int. Ed.* **2014**, submitted.

(400 MHz, CDCl₃): Z-isomer (major): δ 7.34 (1H, s), 6.28 (1H, dt, J = 11.6, 1.6 Hz),¹¹⁰ 6.10–6.04 (1H, m), 5.68–5.62 (1H, m), 5.60 (1H, br, s), 5.55–5.49 (1H, m), 4.32 (2H, t, J = 5.6 Hz), 4.15 (2H, d, J = 6.8 Hz), 3.68 (3H, s), 2.62 (2H, t, J = 7.2 Hz), 2.48 (2H, q, J = 7.2 Hz), 1.97 (1H, br, s); **¹³C NMR (100 MHz, CDCl₃):** δ 160.2, 157.3, 141.2, 136.4, 134.1, 131.6, 129.7, 116.7, 58.4, 52.3, 39.5, 26.0, 25.9; **HRMS [M+H]⁺** calcd for C₁₃H₁₉N₂O₄: 267.1345, found: 267.1341.

Gram-Scale Cross-Metathesis (CM) Reactions

An oven-dried 40 mL vial equipped with a magnetic stir bar is charged with alkene substrate (1.0 equiv) and Z-2-butene-1,4-diol (2.0 equiv) *outside the glove box*. The vial is then sealed, evacuated and purged with N₂. To this vial, a solution of **Ru9** (5.0 mol %) in tetrahydrofuran is added. The resulting solution is allowed to stir for 4 or 6 hours at 22°C, after which the reaction is quenched by addition of wet diethyl ether and concentrated *in vacuo* (percent conversion determined by 400 MHz or 500 MHz ¹H NMR analysis). Purification is performed through silica gel chromatography and/or Kugelrohr distillation.

(Z)-2-(7-hydroxy-5-heptenyl)isoindoline-1,3-dione (**3.49a**).

Following the general procedure, a solution of **Ru9** (167 mg, 0.218 mmol, 5.0 mol %) in tetrahydrofuran (8.7 mL) was transferred by syringe to a vial charged with 2-(hex-5-enyl)isoindoline-1,3-dione (1.00 g, 4.36 mmol, 1.00 equiv) and Z-2-butene-1,4-diol (0.769 g, 8.72 mmol, 2.00 equiv). The resulting solution was allowed to stir for 4 hours at 22 °C. Analysis of the unpurified mixture revealed 73% consumption of 2-(hex-5-enyl)isoindoline-1,3-dione. The resulting brown oil was purified by silica gel chromatography (10% Et₂O in hexanes to 40% Et₂O in hexanes) to afford **3.49a** (0.724 g, 2.79 mmol, 64% yield) as yellow oil in 98:02 Z/E ratio. The spectral data for this compound were identical to those reported in the literature.¹¹²

(Z)-11-hydroxy-9-undecenoic acid (**3.53a**) and **3.53b**.

Following the general procedure, a solution of **Ru9** (135 mg, 0.177 mmol, 5.0 mol %) in tetrahydrofuran (7.1 mL) was transferred by syringe to a vial charged with

(110) Coupling constant (J = 11.6 Hz) of the signal at δ 6.28 is indicative of Z-isomer **3.52**.

oleic acid (1.00 g, 3.54 mmol, 1.00 equiv) and Z-2-butene-1,4-diol (0.624 g, 7.08 mmol, 2.00 equiv). The resulting solution was allowed to stir for 6 hours at 22 °C. Analysis of the unpurified mixture revealed 68% consumption of oleic acid. The resulting brown oil was purified by silica gel chromatography (10% EtOAc in hexanes to 60% EtOAc in hexanes) to afford an inseparable mixture of unreacted oleic acid and **3.52b**, as well as **3.53a** (0.461 g, 2.30 mmol, 66% yield) as yellow oil in 94:06 Z/E ratio. The spectral data for **3.53a** were identical to those reported in the literature.¹¹¹ The mixture of oleic acid and **3.53b** was further purified by Kugelrohr distillation to afford **3.53b** (0.362 g, 2.13 mmol, 60% yield) as colorless oil in 94:06 Z/E ratio. The spectral data for **3.53b** were identical to those reported in the literature.¹¹²

(Z)-2-undecene-1,11-diol (**3.54**) and **3.53b**.

Following the general procedure, a solution of **Ru9** (142 mg, 0.186 mmol, 5.0 mol %) in tetrahydrofuran (7.4 mL) was transferred by syringe to a vial charged with oleyl alcohol (1.00 g, 3.72 mmol, 1.00 equiv) and Z-2-butene-1,4-diol (0.656 g, 7.45 mmol, 2.00 equiv). The resulting solution was allowed to stir for 6 hours at 22 °C. Analysis of the unpurified mixture revealed 65% consumption of oleyl alcohol. The resulting brown oil was purified by silica gel chromatography (10% EtOAc in hexanes to 60% EtOAc in hexanes) to afford an inseparable mixture of unreacted oleyl alcohol and **3.53b**, as well as **3.54** (0.431 g, 2.31 mmol, 64% yield) as yellow oil in 96:04 Z/E ratio; **IR (CH₂Cl₂)**: 3331 (br), 3054 (w), 2926 (m), 2854 (m), 1684 (w), 1458 (w), 1264 (m), 1021 (m), 909 (m); **¹H NMR (400 MHz, CDCl₃)**: Z-isomer (major): δ 5.60 (1H, dt, J = 11.2, 6.4 Hz),¹¹³ 5.56–5.49 (1H, m), 4.19 (2H, d, J = 6.3 Hz), 3.63 (2H, t, J = 6.6 Hz), 2.10–2.02 (2H, m), 1.59–1.50 (2H, m), 1.38–1.27 (12H, m); **¹³C NMR (100 MHz, CDCl₃)**: δ 133.3, 128.5, 63.2, 58.8, 32.9, 29.7, 29.5, 29.5, 29.2, 27.5, 25.8; **HRMS [M+H-H₂O]⁺** calcd for C₁₁H₂₁O: 169.1592, found: 169.1585. The mixture of oleyl alcohol and **3.53b** was further purified by Kugelrohr distillation to afford **3.53b** (0.374 g,

(111) Suzuki, Y.; Kurita, O.; Kono, Y.; Hyakutake, H.; Sakurai, A. *Biosci. Biotech. Biochem.* **1995**, *59*, 2049–2051.

(112) Kiesewetter, E. T.; O'Brien, R. V.; Yu, E. C.; Meek, S. J.; Schrock, R. R.; Hoveyda, A. H. *J. Am. Chem. Soc.* **2013**, *135*, 6026–6029.

(113) Coupling constant (J = 11.2 Hz) of the signal at δ 5.60 ppm is indicative of Z-isomer **3.54**.

2.20 mmol, 60% yield) as colorless oil in 94:06 Z/E ratio. The spectral data for **3.53b** were identical to those reported in the literature.¹¹²

(Z)-3-(4-(trifluoromethyl)phenyl)-2-propene-1-ol (3.60).

Following the general procedure, a solution of **Ru9** (7.50 mol %) in tetrahydrofuran (255 μ L) was transferred by syringe to a vial charged with 4-(trifluoromethyl)styrene (21.9 mg, 0.127 mmol, 1.00 equiv) and *Z*-2-butene-1,4-diol (56.0 mg, 0.635 mmol, 5.00 equiv). The resulting solution was allowed to stir for 8 hours at 22 °C. Analysis of the unpurified mixture revealed 66% consumption of 4-(trifluoromethyl)styrene. The resulting brown oil was purified by silica gel chromatography (10% Et₂O in hexanes to 40% Et₂O in hexanes) to afford **3.60** (15.4 mg, 0.0762 mmol, 60% yield) as pale yellow oil in 93:07 Z/E ratio; **IR** (CH_2Cl_2): 3334 (br), 3022 (w), 2924 (m), 1617 (m), 1403 (w), 1322 (s), 1163 (m), 1111 (s), 1066 (s), 1014 (m), 851 (m); **¹H NMR** (400 MHz, CDCl_3): *Z*-isomer (major): δ 7.60 (2H, d, J = 8.0 Hz), 7.32 (2H, d, J = 8.0 Hz), 6.60 (1H, d, J = 11.8 Hz),¹¹⁴ 6.00 (1H, dt, J = 12.4, 6.4 Hz), 4.42 (2H, s), 1.50 (1H, s); **¹³C NMR** (100 MHz, CDCl_3): δ 171.9, 133.3, 130.0, 129.1, 125.4, 125.3, 125.3, 59.6; **HRMS** [$\text{M}+\text{H}-\text{H}_2\text{O}$]⁺ calcd for $\text{C}_{10}\text{H}_8\text{F}_3$: 185.0578, found: 185.0580.

(Z)-3-cyclohexyl-2-propene-1-ol (3.61).

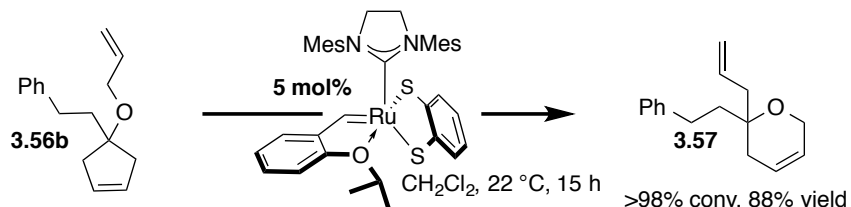
Following the general procedure, a solution of **Ru9** (7.50 mol %) in tetrahydrofuran (255 μ L) was transferred by syringe to a vial charged with vinylcyclohexane (14.0 mg, 0.127 mmol, 1.00 equiv) and *Z*-2-butene-1,4-diol (56.0 mg, 0.635 mmol, 5.00 equiv). The resulting solution was allowed to stir for 8 hours at 22 °C. Analysis of the unpurified mixture revealed 65% consumption of vinylcyclohexane. The resulting brown oil was purified by silica gel chromatography (10% Et₂O in hexanes to 40% Et₂O in hexanes) to afford **3.61** (10.5 mg, 0.075 mmol, 59% yield) as pale yellow oil in 98:02 Z/E ratio. The spectral data for this compound were identical to those reported in the literature.¹¹⁵

(114) Coupling constant (J = 11.8 Hz) of the signal at δ 6.60 ppm is indicative of *Z*-isomer **3.60**.

(115) Reed, S. A.; White, M. C. *J. Am. Chem. Soc.* **2008**, *130*, 3316–3318.

■ Ru-Catalyzed Ring-Opening/Ring-Closing Metathesis (RO/RCM):

Chart 10. Efficient RO/RCM to Access 3.57

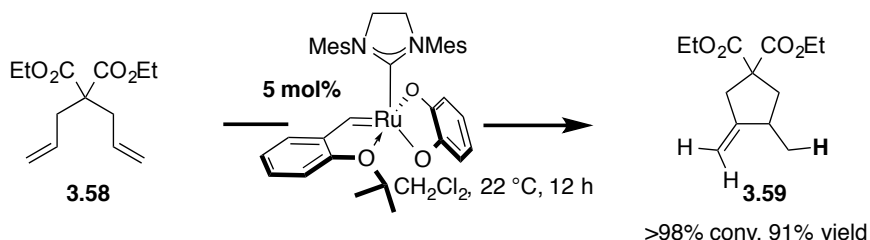


2-Allyl-2-phenethyl-3,6-dihydro-2H-pyran (3.57).

A solution of **Ru4b** (2.0 mg, 2.9 μ mol, 5.0 mol %) in dichloromethane (575 μ L, 0.1 M) was transferred by syringe to a vial containing **13.56b** (13.1 mg, 0.0575 mmol, 1.00 equiv). The resulting mixture was allowed to stir for 15 hours at 22 °C. Analysis of the ^1H NMR (400 MHz) spectrum revealed >98% conv of the substrate, and the resulting mixture was purified by silica gel chromatography (2% Et₂O in hexanes to 4% Et₂O in hexanes) to afford product **3.57** (11.5 mg, 0.0504 mmol, 88% yield) as a colorless oil; ^1H NMR (400 MHz, CDCl₃): δ 7.31–7.17 (5H, m), 5.94–5.83 (1H, m), 5.80–5.72 (2H, m), 5.19–5.38 (2H, m), 4.19 (2H, dd, J = 2.0, 2.0 Hz), 2.68 (2H, t, J = 8.0), 2.46 (1H, dd, J = 13.6, 6.8 Hz), 2.34 (1H, dd, J = 14.0, 6.8 Hz), 2.13–2.00 (2H, m), 1.97–1.89 (1H, m), 1.80–1.72 (1H, m). All characterization data for **3.57** matched with the literature reported values.¹¹⁶

■ Ru-Catalyzed Cycloisomerization Reaction:

(116) La, D. S.; Ford, J. G.; Sattley, E. S.; Bonitatebus, P. J.; Schrock, R. R.; Hoveyda, A. H. *J. Am. Chem. Soc.* **2000**, *122*, 1828–1829.

Chart 11. Cycloisomerization to Access 3.59

Diethyl 3-methyl-4-methylenecyclopentane-1,1-dicarboxylate (3.59)

A solution of **Ru4a** (2.0 mg, 2.9 μ mol, 5.0 mol %) in dichloromethane (575 μ L, 0.1 M) was transferred by syringe to a vial containing **3.58** (13.9 mg, 0.0580 mmol, 1.00 equiv). The resulting mixture was allowed to stir for 12 hours at 22 °C. Analysis of the ^1H NMR (400 MHz) spectrum revealed >98% conv of the substrate, and the resulting mixture was purified by silica gel chromatography (2% Et₂O in hexanes to 4% Et₂O in hexanes) to afford product **3.59** (12.7 mg, 0.0529 mmol, 91% yield) as a colorless oil; all characterization data of which matched with the literature reported values.¹¹⁷

■ NMR Spectra:

Detailed ^1H and ^{13}C NMR spectra of compounds listed above have been reported in the literature.¹¹⁸

■ Decomposition of Ru Complexes:

General Procedure:

In an N₂-filled glove box, an NMR tube is charged with the Ru complex (0.009 mmol, 1.00 equiv) and 9-methylanthracene (0.014 mmol, 1.55 equiv) as internal standard. To this tube, *d*-solvent¹¹⁹ (860 μ L, 0.01 M) is added at 22 °C and the sample is analyzed by ^1H NMR spectroscopy.

(117) Mallagaray, Á., Mohammadiannejad-Abbasabadi, K.; Medina, S.; Domínguez, G.; Pérez-Castells, J. *Org. Biomol. Chem.*, **2012**, *10*, 6665–6672.

(118) (a) Khan, R. K. M.; Torker, S.; Hoveyda, A. H. *J. Am. Chem. Soc.* **2013**, *135*, 10258–10261. (b) Koh, M. J.; Khan, R. K. M.; Torker, S.; Hoveyda, A. H. *Angew. Chem., Int. Ed.* **2014**, *53*, 1968–1972. (c) Khan, R. K. M.; Torker, S.; Hoveyda, A. H. *J. Am. Chem. Soc.* **2014**, *136*, 14337–14340. (d) Koh, M. J.; Khan, R. K. M.; Torker, S.; Yu, M.; Mikus, M. S. and Hoveyda, A. H., manuscript submitted.

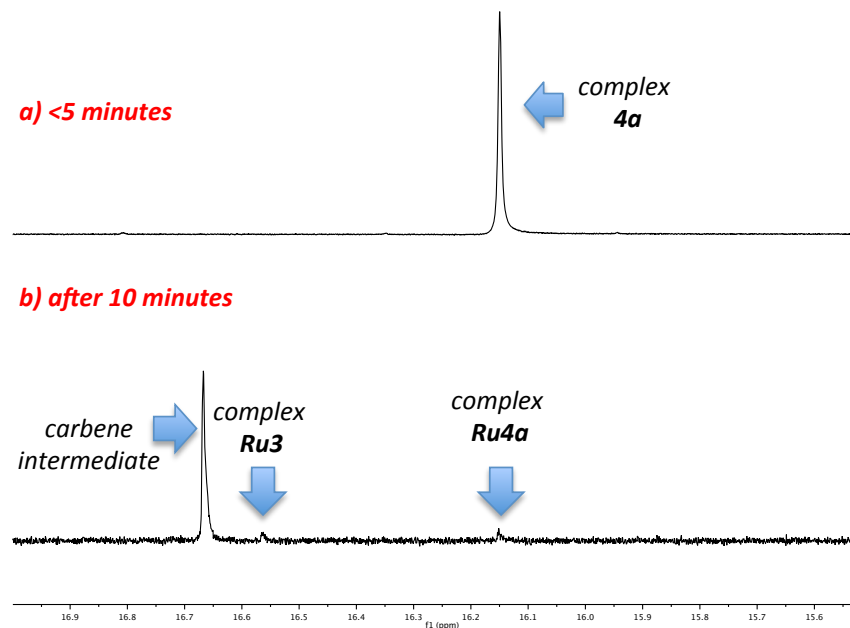
(119) Halogenated solvents (CDCl₃ or CD₂Cl₂) are freshly passed twice through short columns of basic alumina, and C₆D₆ is distilled over Na under N₂.

I. Reactions in CDCl_3 :

a. Stability of **Ru4a**:

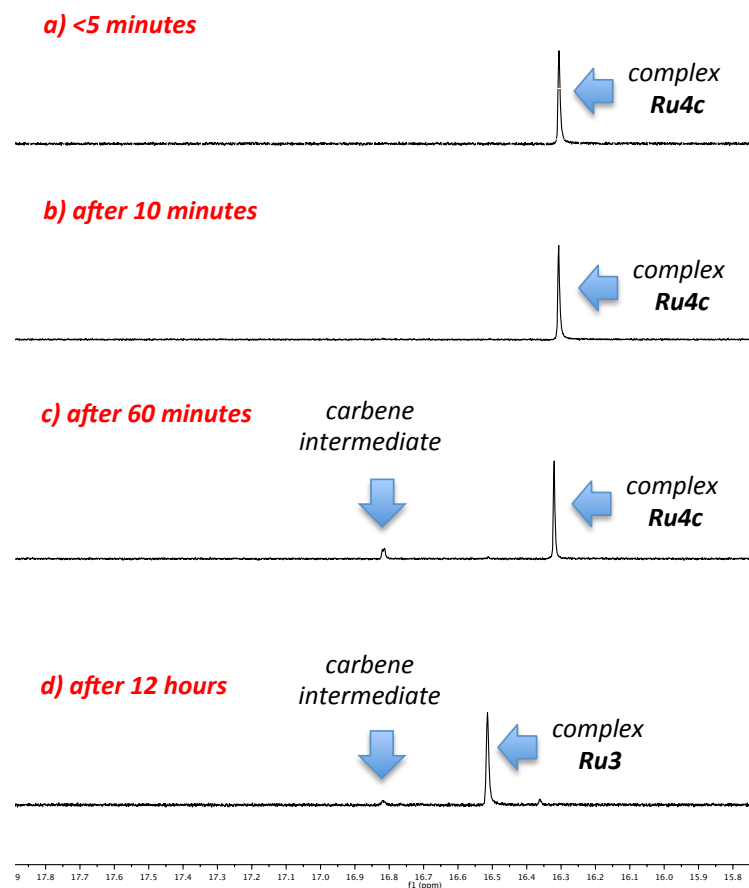
Following the general procedure listed above, an NMR tube was charged with **Ru4a** (6.00 mg, 0.009 mmol, 1.00 equiv) and 9-methylanthracene (2.70 mg, 0.014 mmol, 1.55 equiv) followed by the addition of CDCl_3 (860 μL , 0.01 M) at 22 °C. Analysis of the sample after 10 minutes revealed that 97% conversion of **Ru4a** took place to generate a new carbene complex (Chart 11).

Chart 12. Decomposition of complex Ru4a in CDCl_3 at 22 °C

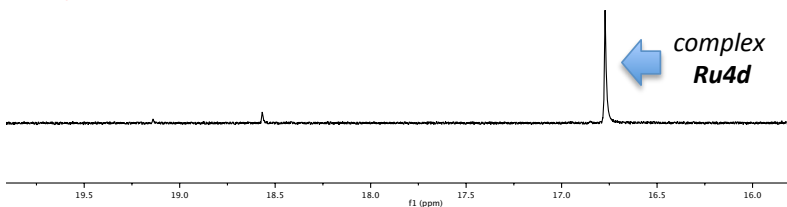


b. Stability of **Ru4c**:

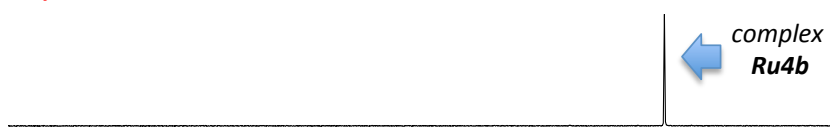
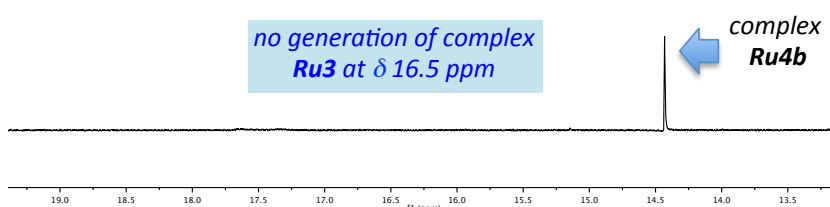
Following the general procedure listed above, an NMR tube was charged with **Ru4c** (6.60 mg, 0.009 mmol, 1.00 equiv) and 9-methylanthracene (2.70 mg, 0.014 mmol, 1.55 equiv) followed by the addition of CDCl_3 (860 μL , 0.01 M) at 22 °C. Analysis of the sample after 10 minutes revealed that 16% conversion of **Ru4c** took place, however, no new carbene complex was detected (Chart 12b). The conversion of **Ru4c** increased with time (i.e. 40% after one hour and >98% conversions after 12 hours) to generate complex **Ru3** through the intermediacy of a carbene intermediate (Charts 12c and 12d).

Chart 13. Decomposition of complex Ru4c in CDCl_3 at 22 °C**c. Stability of Ru 4d:**

Following the general procedure listed above, an NMR tube was charged with **Ru4d** (6.20 mg, 0.009 mmol, 1.00 equiv) and 9-methylanthracene (2.70 mg, 0.014 mmol, 1.55 equiv) followed by the addition of CDCl_3 (860 μL , 0.01 M) at 22 °C. Analysis of the sample after 12 hours revealed that 11% conversion of **Ru4d** took place (Chart 13b).

Chart 14. Decomposition of complex Ru4d in CDCl₃ at 22 °C**a) <5 minutes****b) after 12 hours****d. Stability of Ru4b:**

Following the general procedure listed above, an NMR tube was charged with **Ru4b** (6.30 mg, 0.009 mmol, 1.00 equiv) and 9-methylanthracene (2.70 mg, 0.014 mmol, 1.55 equiv) followed by the addition of CDCl₃ (860 μL, 0.01 M) at 22 °C. Analysis of the sample after one hour revealed that 45% conversion of **Ru4b** took place (Chart 14b), however, no dichloride complex **Ru3** was generated (vs **Ru4a**, see Chart 11b).

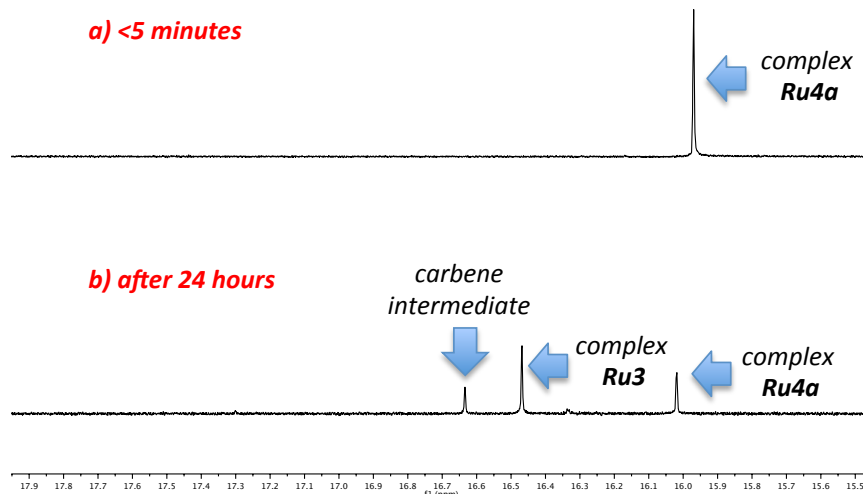
Chart 15. Decomposition of complex Ru4b in CDCl₃ at 22 °C**a) <5 minutes****b) after 60 minutes**

II. Reactions in CD₂Cl₂:

a. Stability of Ru4a:

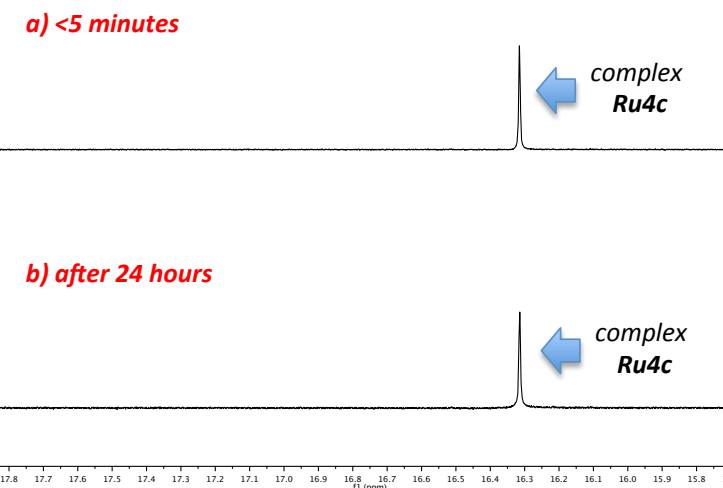
Following the general procedure listed above, an NMR tube was charged with **Ru4a** (6.00 mg, 0.009 mmol, 1.00 equiv) and 9-methylanthracene (2.70 mg, 0.014 mmol, 1.55 equiv) followed by the addition of CD₂Cl₂ (860 μL, 0.01 M) at 50 °C. Analysis of the sample after 24 hours revealed that 82% conversion of **Ru4a** took place to generate the carbene intermediate and **Ru3** (Chart 15b).

Chart 16. Decomposition of complex Ru4a in CD₂Cl₂ at 50 °C

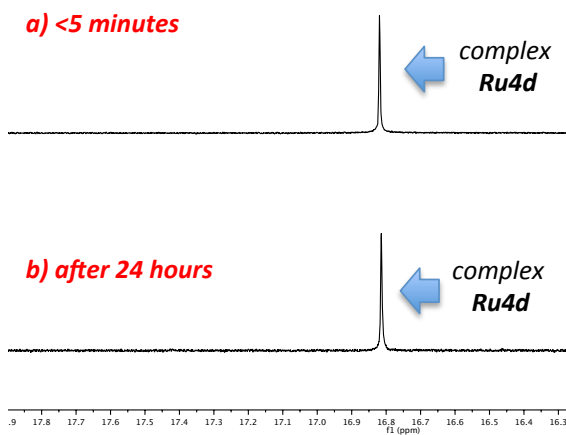


b. Stability of Ru4c:

Following the general procedure listed above, an NMR tube was charged with **Ru4c** (6.60 mg, 0.009 mmol, 1.00 equiv) and 9-methylanthracene (2.70 mg, 0.014 mmol, 1.55 equiv) followed by the addition of CD₂Cl₂ (860 μL, 0.01 M) at 50 °C. Analysis of the sample after 24 hours revealed that 29% conversion of **Ru4c** took place, however, no new carbene signals were detected (Chart 16b).

Chart 17. Decomposition of complex Ru4c in CD₂Cl₂ at 50 °C**c. Stability of Ru4d:**

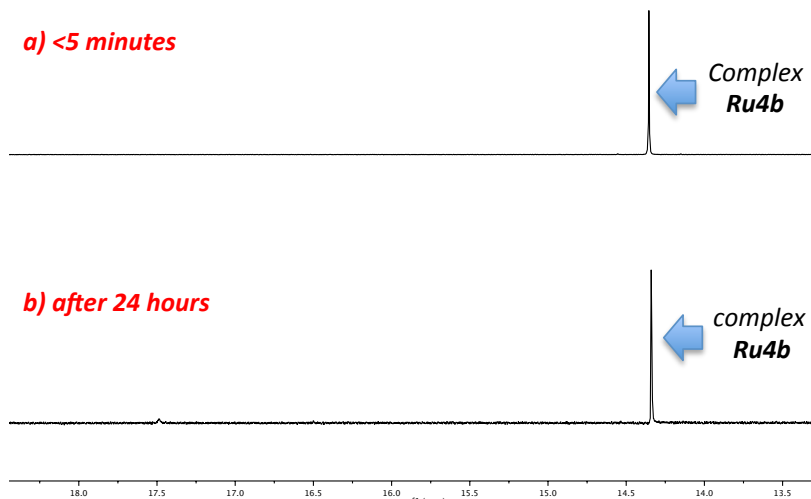
Following the general procedure listed above, an NMR tube was charged with **Ru4d** (6.20 mg, 0.009 mmol, 1.00 equiv) and 9-methylanthracene (2.70 mg, 0.014 mmol, 1.55 equiv) followed by the addition of CD₂Cl₂ (860 μL, 0.01 M) at 50 °C. Analysis of the sample after 24 hours revealed that 24% conversion of **Ru4d** took place, however, no new carbene signals were detected (Chart 17b).

Chart 18. Decomposition of complex Ru4d in CD₂Cl₂ at 50 °C**d. Stability of Ru4b:**

Following the general procedure listed above, an NMR tube was charged with **Ru4b** (6.30 mg, 0.009 mmol, 1.00 equiv) and 9-methylanthracene (2.70 mg, 0.014 mmol, 1.55 equiv) followed by the addition of CD₂Cl₂ (860 μL, 0.01 M) at 50 °C. Analysis of

the sample after 24 hours revealed that 9% conversion of **Ru4b** took place whereas no generation of **Ru3** was observed (Chart 18b).

Chart 19. Decomposition of complex Ru4b in CD₂Cl₂ at 50 °C



III. Reactions in C₆D₆:

All Ru complexes (**Ru4a-d**) showed <2% conversions after 24 hours in C₆D₆.

■ X-ray Crystallographic Data:

X-ray structure of Ru4a:

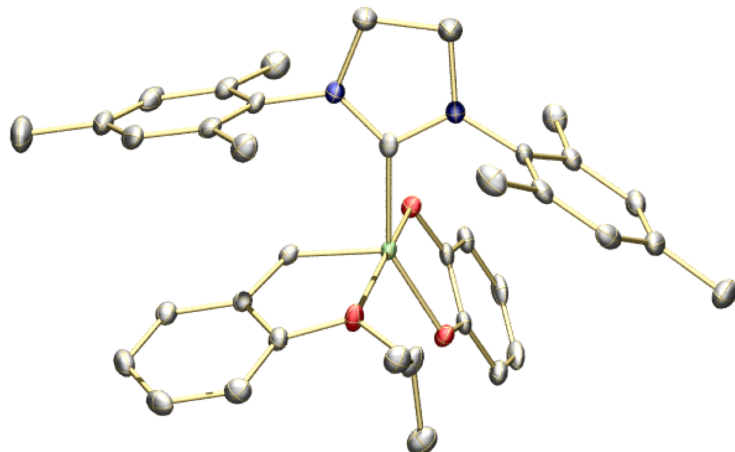


Table 1. Crystal data and structure refinement for complex Ru4a

Empirical formula	$C_{37}H_{42}N_2O_3Ru \bullet CH_2Cl_2 \bullet 1/2(C_6H_6)$		
Formula weight	787.78		
Temperature	100(2) K		
Wavelength	1.54178 Å		
Crystal system	Monoclinic		
Space group	P 2(1)/n		
Unit cell dimensions	$a = 8.6694(3)$ Å	$\alpha = 90^\circ$	
	$b = 21.5135(7)$ Å	$\beta = 101.4020(10)^\circ$	
	$c = 20.3017(7)$ Å	$\gamma = 90^\circ$	
Volume	$3711.7(2)$ Å ³		
Z	4		
Density (calculated)	1.410 Mg/m ³		
Absorption coefficient	5.060 mm ⁻¹		
F(000)	1636		
Crystal size	0.48 x 0.22 x 0.10 mm ³		
Theta range for data collection	3.02 to 66.58°		
Index ranges	$-10 \leq h \leq 10, -24 \leq k \leq 25, -24 \leq l \leq 21$		
Reflections collected	42474		

Independent reflections	6532 [R(int) = 0.0282]
Completeness to theta = 66.58°	99.5 %
Absorption correction	Semi-empirical from equivalents
Max. and min. transmission	0.6316 and 0.1950
Refinement method	Full-matrix least-squares on F ²
Data / restraints / parameters	6532 / 0 / 448
Goodness-of-fit on F ²	1.109
Final R indices [I>2sigma(I)]	R1 = 0.0277, wR2 = 0.0699
R indices (all data)	R1 = 0.0277, wR2 = 0.0700
Extinction coefficient	na
Largest diff. peak and hole	0.621 and -0.671 e.Å ⁻³

Table 2. Atomic coordinates (x 10⁴) and equivalent isotropic displacement parameters (Å²x 10³) for complex Ru4a. U(eq) is defined as one third of the trace of the orthogonalized U^{ij} tensor

	x	y	z	U(eq)
Ru(1)	768(1)	1913(1)	2267(1)	11(1)
O(1)	112(2)	1468(1)	1380(1)	15(1)
O(2)	2124(2)	2397(1)	1763(1)	17(1)
O(3)	1929(2)	2355(1)	3208(1)	18(1)
N(1)	-2592(2)	2096(1)	2171(1)	17(1)
N(2)	-1982(2)	1259(1)	2760(1)	17(1)
C(1)	-1384(2)	1732(1)	2455(1)	14(1)
C(2)	-4137(3)	1840(1)	2217(1)	28(1)
C(3)	-3688(2)	1329(1)	2736(1)	22(1)
C(4)	-2356(2)	2688(1)	1880(1)	15(1)
C(5)	-2478(2)	2749(1)	1189(1)	17(1)
C(6)	-2173(2)	3332(1)	940(1)	20(1)
C(7)	-1772(2)	3840(1)	1356(1)	22(1)
C(8)	-1722(2)	3768(1)	2042(1)	21(1)
C(9)	-2028(2)	3202(1)	2313(1)	17(1)
C(10)	-2931(3)	2209(1)	718(1)	23(1)
C(11)	-1402(3)	4462(1)	1078(1)	32(1)
C(12)	-2045(3)	3136(1)	3050(1)	26(1)
C(13)	-1113(2)	767(1)	3137(1)	16(1)
C(14)	-490(2)	853(1)	3821(1)	19(1)

C(15)	339(3)	363(1)	4174(1)	23(1)
C(16)	564(3)	-197(1)	3864(1)	25(1)
C(17)	-73(3)	-265(1)	3183(1)	24(1)
C(18)	-925(2)	208(1)	2810(1)	20(1)
C(19)	-651(3)	1467(1)	4157(1)	24(1)
C(20)	1484(3)	-720(1)	4251(2)	40(1)
C(21)	-1579(3)	136(1)	2074(1)	26(1)
C(22)	915(2)	1691(1)	928(1)	16(1)
C(23)	721(3)	1454(1)	280(1)	19(1)
C(24)	1610(3)	1694(1)	-165(1)	24(1)
C(25)	2678(3)	2167(1)	34(1)	25(1)
C(26)	2876(3)	2412(1)	682(1)	22(1)
C(27)	1998(2)	2180(1)	1132(1)	16(1)
C(28)	1734(2)	1238(1)	2715(1)	14(1)
C(29)	2795(2)	1334(1)	3354(1)	14(1)
C(30)	3675(2)	862(1)	3721(1)	18(1)
C(31)	4723(2)	994(1)	4314(1)	22(1)
C(32)	4892(3)	1605(1)	4539(1)	23(1)
C(33)	4006(3)	2086(1)	4192(1)	21(1)
C(34)	2947(2)	1944(1)	3603(1)	16(1)
C(35)	2089(3)	3041(1)	3251(1)	22(1)
C(36)	1804(3)	3291(1)	3915(1)	21(1)
C(37)	3606(3)	3245(1)	3070(1)	26(1)
C(1S)	2610(3)	10260(1)	1284(1)	28(1)
Cl(1)	3647(1)	9877(1)	2017(1)	32(1)
Cl(2)	1016(1)	9809(1)	868(1)	28(1)
C(2S)	5127(3)	9360(1)	46(1)	29(1)
C(3S)	6342(3)	9734(1)	373(1)	31(1)
C(4S)	6215(3)	10377(1)	328(1)	28(1)

Table 3. Bond lengths [Å] and angles [°] for complex Ru4a

Ru(1)-C(28)	1.828(2)
Ru(1)-O(2)	1.9956(14)
Ru(1)-C(1)	2.015(2)
Ru(1)-O(1)	2.0196(13)
Ru(1)-O(3)	2.1922(14)
O(1)-C(22)	1.345(2)
O(2)-C(27)	1.349(2)
O(3)-C(34)	1.388(2)
O(3)-C(35)	1.482(2)
N(1)-C(1)	1.344(3)
N(1)-C(4)	1.436(3)
N(1)-C(2)	1.468(3)
N(2)-C(1)	1.347(3)
N(2)-C(13)	1.431(3)
N(2)-C(3)	1.478(3)
C(2)-C(3)	1.520(3)
C(2)-H(2A)	0.9900
C(2)-H(2B)	0.9900
C(3)-H(3A)	0.9900
C(3)-H(3B)	0.9900
C(4)-C(5)	1.392(3)
C(4)-C(9)	1.405(3)
C(5)-C(6)	1.397(3)
C(5)-C(10)	1.506(3)
C(6)-C(7)	1.382(3)
C(6)-H(6A)	0.9500
C(7)-C(8)	1.393(3)
C(7)-C(11)	1.511(3)
C(8)-C(9)	1.384(3)
C(8)-H(8A)	0.9500
C(9)-C(12)	1.505(3)
C(10)-H(10A)	0.9800
C(10)-H(10B)	0.9800
C(10)-H(10C)	0.9800
C(11)-H(11A)	0.9800

C(11)-H(11B)	0.9800
C(11)-H(11C)	0.9800
C(12)-H(12A)	0.9800
C(12)-H(12B)	0.9800
C(12)-H(12C)	0.9800
C(13)-C(18)	1.398(3)
C(13)-C(14)	1.398(3)
C(14)-C(15)	1.393(3)
C(14)-C(19)	1.507(3)
C(15)-C(16)	1.390(3)
C(15)-H(15A)	0.9500
C(16)-C(17)	1.390(3)
C(16)-C(20)	1.508(3)
C(17)-C(18)	1.390(3)
C(17)-H(17A)	0.9500
C(18)-C(21)	1.500(3)
C(19)-H(19A)	0.9800
C(19)-H(19B)	0.9800
C(19)-H(19C)	0.9800
C(20)-H(20A)	0.9800
C(20)-H(20B)	0.9800
C(20)-H(20C)	0.9800
C(21)-H(21A)	0.9800
C(21)-H(21B)	0.9800
C(21)-H(21C)	0.9800
C(22)-C(23)	1.389(3)
C(22)-C(27)	1.417(3)
C(23)-C(24)	1.397(3)
C(23)-H(23A)	0.9500
C(24)-C(25)	1.383(4)
C(24)-H(24A)	0.9500
C(25)-C(26)	1.396(3)
C(25)-H(25A)	0.9500
C(26)-C(27)	1.391(3)
C(26)-H(26A)	0.9500
C(28)-C(29)	1.449(3)
C(28)-H(28A)	0.9500

C(29)-C(30)	1.394(3)
C(29)-C(34)	1.403(3)
C(30)-C(31)	1.387(3)
C(30)-H(30A)	0.9500
C(31)-C(32)	1.391(3)
C(31)-H(31A)	0.9500
C(32)-C(33)	1.394(3)
C(32)-H(32A)	0.9500
C(33)-C(34)	1.389(3)
C(33)-H(33A)	0.9500
C(35)-C(37)	1.499(3)
C(35)-C(36)	1.516(3)
C(35)-H(35A)	1.0000
C(36)-H(36A)	0.9800
C(36)-H(36B)	0.9800
C(36)-H(36C)	0.9800
C(37)-H(37A)	0.9800
C(37)-H(37B)	0.9800
C(37)-H(37C)	0.9800
C(1S)-Cl(2)	1.762(2)
C(1S)-Cl(1)	1.781(2)
C(1S)-H(1S1)	0.9900
C(1S)-H(1S2)	0.9900
C(2S)-C(4S)#1	1.379(4)
C(2S)-C(3S)	1.386(4)
C(2S)-H(2S)	0.9500
C(3S)-C(4S)	1.390(3)
C(3S)-H(3S)	0.9500
C(4S)-C(2S)#1	1.379(4)
C(4S)-H(4S)	0.9500
C(28)-Ru(1)-O(2)	114.28(7)
C(28)-Ru(1)-C(1)	95.82(8)
O(2)-Ru(1)-C(1)	149.24(7)
C(28)-Ru(1)-O(1)	95.04(7)
O(2)-Ru(1)-O(1)	83.17(5)
C(1)-Ru(1)-O(1)	88.24(7)
C(28)-Ru(1)-O(3)	79.89(7)

O(2)-Ru(1)-O(3)	90.26(6)
C(1)-Ru(1)-O(3)	101.63(7)
O(1)-Ru(1)-O(3)	169.26(6)
C(22)-O(1)-Ru(1)	110.30(12)
C(27)-O(2)-Ru(1)	111.20(12)
C(34)-O(3)-C(35)	123.94(16)
C(34)-O(3)-Ru(1)	110.94(11)
C(35)-O(3)-Ru(1)	120.32(12)
C(1)-N(1)-C(4)	122.10(17)
C(1)-N(1)-C(2)	113.43(17)
C(4)-N(1)-C(2)	124.41(17)
C(1)-N(2)-C(13)	126.54(17)
C(1)-N(2)-C(3)	112.48(17)
C(13)-N(2)-C(3)	120.66(16)
N(1)-C(1)-N(2)	107.42(17)
N(1)-C(1)-Ru(1)	118.55(14)
N(2)-C(1)-Ru(1)	133.54(15)
N(1)-C(2)-C(3)	101.75(17)
N(1)-C(2)-H(2A)	111.4
C(3)-C(2)-H(2A)	111.4
N(1)-C(2)-H(2B)	111.4
C(3)-C(2)-H(2B)	111.4
H(2A)-C(2)-H(2B)	109.3
N(2)-C(3)-C(2)	102.35(17)
N(2)-C(3)-H(3A)	111.3
C(2)-C(3)-H(3A)	111.3
N(2)-C(3)-H(3B)	111.3
C(2)-C(3)-H(3B)	111.3
H(3A)-C(3)-H(3B)	109.2
C(5)-C(4)-C(9)	121.50(19)
C(5)-C(4)-N(1)	120.56(18)
C(9)-C(4)-N(1)	117.93(18)
C(4)-C(5)-C(6)	117.74(19)
C(4)-C(5)-C(10)	121.75(19)
C(6)-C(5)-C(10)	120.51(19)
C(7)-C(6)-C(5)	122.2(2)
C(7)-C(6)-H(6A)	118.9

C(5)-C(6)-H(6A)	118.9
C(6)-C(7)-C(8)	118.5(2)
C(6)-C(7)-C(11)	121.2(2)
C(8)-C(7)-C(11)	120.3(2)
C(9)-C(8)-C(7)	121.6(2)
C(9)-C(8)-H(8A)	119.2
C(7)-C(8)-H(8A)	119.2
C(8)-C(9)-C(4)	118.36(19)
C(8)-C(9)-C(12)	121.2(2)
C(4)-C(9)-C(12)	120.47(19)
C(5)-C(10)-H(10A)	109.5
C(5)-C(10)-H(10B)	109.5
H(10A)-C(10)-H(10B)	109.5
C(5)-C(10)-H(10C)	109.5
H(10A)-C(10)-H(10C)	109.5
H(10B)-C(10)-H(10C)	109.5
C(7)-C(11)-H(11A)	109.5
C(7)-C(11)-H(11B)	109.5
H(11A)-C(11)-H(11B)	109.5
C(7)-C(11)-H(11C)	109.5
H(11A)-C(11)-H(11C)	109.5
H(11B)-C(11)-H(11C)	109.5
C(9)-C(12)-H(12A)	109.5
C(9)-C(12)-H(12B)	109.5
H(12A)-C(12)-H(12B)	109.5
C(9)-C(12)-H(12C)	109.5
H(12A)-C(12)-H(12C)	109.5
H(12B)-C(12)-H(12C)	109.5
C(18)-C(13)-C(14)	121.77(19)
C(18)-C(13)-N(2)	118.79(19)
C(14)-C(13)-N(2)	119.44(19)
C(15)-C(14)-C(13)	118.0(2)
C(15)-C(14)-C(19)	121.0(2)
C(13)-C(14)-C(19)	120.95(19)
C(16)-C(15)-C(14)	121.8(2)
C(16)-C(15)-H(15A)	119.1
C(14)-C(15)-H(15A)	119.1

C(15)-C(16)-C(17)	118.6(2)
C(15)-C(16)-C(20)	121.2(2)
C(17)-C(16)-C(20)	120.3(2)
C(18)-C(17)-C(16)	121.8(2)
C(18)-C(17)-H(17A)	119.1
C(16)-C(17)-H(17A)	119.1
C(17)-C(18)-C(13)	118.1(2)
C(17)-C(18)-C(21)	121.5(2)
C(13)-C(18)-C(21)	120.3(2)
C(14)-C(19)-H(19A)	109.5
C(14)-C(19)-H(19B)	109.5
H(19A)-C(19)-H(19B)	109.5
C(14)-C(19)-H(19C)	109.5
H(19A)-C(19)-H(19C)	109.5
H(19B)-C(19)-H(19C)	109.5
C(16)-C(20)-H(20A)	109.5
C(16)-C(20)-H(20B)	109.5
H(20A)-C(20)-H(20B)	109.5
C(16)-C(20)-H(20C)	109.5
H(20A)-C(20)-H(20C)	109.5
H(20B)-C(20)-H(20C)	109.5
C(18)-C(21)-H(21A)	109.5
C(18)-C(21)-H(21B)	109.5
H(21A)-C(21)-H(21B)	109.5
C(18)-C(21)-H(21C)	109.5
H(21A)-C(21)-H(21C)	109.5
H(21B)-C(21)-H(21C)	109.5
O(1)-C(22)-C(23)	122.17(19)
O(1)-C(22)-C(27)	117.90(18)
C(23)-C(22)-C(27)	119.93(19)
C(22)-C(23)-C(24)	119.8(2)
C(22)-C(23)-H(23A)	120.1
C(24)-C(23)-H(23A)	120.1
C(25)-C(24)-C(23)	120.5(2)
C(25)-C(24)-H(24A)	119.8
C(23)-C(24)-H(24A)	119.8
C(24)-C(25)-C(26)	120.3(2)

C(24)-C(25)-H(25A)	119.9
C(26)-C(25)-H(25A)	119.9
C(27)-C(26)-C(25)	120.1(2)
C(27)-C(26)-H(26A)	119.9
C(25)-C(26)-H(26A)	119.9
O(2)-C(27)-C(26)	123.22(19)
O(2)-C(27)-C(22)	117.33(17)
C(26)-C(27)-C(22)	119.46(19)
C(29)-C(28)-Ru(1)	118.69(14)
C(29)-C(28)-H(28A)	120.7
Ru(1)-C(28)-H(28A)	120.7
C(30)-C(29)-C(34)	119.12(19)
C(30)-C(29)-C(28)	123.92(19)
C(34)-C(29)-C(28)	116.96(18)
C(31)-C(30)-C(29)	120.6(2)
C(31)-C(30)-H(30A)	119.7
C(29)-C(30)-H(30A)	119.7
C(30)-C(31)-C(32)	119.2(2)
C(30)-C(31)-H(31A)	120.4
C(32)-C(31)-H(31A)	120.4
C(31)-C(32)-C(33)	121.6(2)
C(31)-C(32)-H(32A)	119.2
C(33)-C(32)-H(32A)	119.2
C(34)-C(33)-C(32)	118.4(2)
C(34)-C(33)-H(33A)	120.8
C(32)-C(33)-H(33A)	120.8
O(3)-C(34)-C(33)	126.41(18)
O(3)-C(34)-C(29)	112.60(17)
C(33)-C(34)-C(29)	120.98(19)
O(3)-C(35)-C(37)	110.68(18)
O(3)-C(35)-C(36)	112.12(17)
C(37)-C(35)-C(36)	114.73(19)
O(3)-C(35)-H(35A)	106.2
C(37)-C(35)-H(35A)	106.2
C(36)-C(35)-H(35A)	106.2
C(35)-C(36)-H(36A)	109.5
C(35)-C(36)-H(36B)	109.5

H(36A)-C(36)-H(36B)	109.5
C(35)-C(36)-H(36C)	109.5
H(36A)-C(36)-H(36C)	109.5
H(36B)-C(36)-H(36C)	109.5
C(35)-C(37)-H(37A)	109.5
C(35)-C(37)-H(37B)	109.5
H(37A)-C(37)-H(37B)	109.5
C(35)-C(37)-H(37C)	109.5
H(37A)-C(37)-H(37C)	109.5
H(37B)-C(37)-H(37C)	109.5
Cl(2)-C(1S)-Cl(1)	111.35(13)
Cl(2)-C(1S)-H(1S1)	109.4
Cl(1)-C(1S)-H(1S1)	109.4
Cl(2)-C(1S)-H(1S2)	109.4
Cl(1)-C(1S)-H(1S2)	109.4
H(1S1)-C(1S)-H(1S2)	108.0
C(4S)#1-C(2S)-C(3S)	120.2(2)
C(4S)#1-C(2S)-H(2S)	119.9
C(3S)-C(2S)-H(2S)	119.9
C(2S)-C(3S)-C(4S)	120.3(2)
C(2S)-C(3S)-H(3S)	119.9
C(4S)-C(3S)-H(3S)	119.9
C(2S)#1-C(4S)-C(3S)	119.5(2)
C(2S)#1-C(4S)-H(4S)	120.3
C(3S)-C(4S)-H(4S)	120.3

Symmetry transformations used to generate equivalent atoms:

#1 -x+1,-y+2,-z

Table 4. Anisotropic displacement parameters ($\text{\AA}^2 \times 10^3$) for complex Ru4a. The anisotropic displacement factor exponent takes the form: $-2\pi^2 [h^2 a^{*2} U^{11} + \dots + 2 h k a^* b^* U^{12}]$

	U ¹¹	U ²²	U ³³	U ²³	U ¹³	U ¹²
Ru(1)	15(1)	9(1)	9(1)	1(1)	1(1)	0(1)
O(1)	20(1)	14(1)	11(1)	-1(1)	3(1)	-2(1)
O(2)	21(1)	15(1)	14(1)	2(1)	2(1)	-3(1)
O(3)	28(1)	10(1)	14(1)	-1(1)	-2(1)	-1(1)
N(1)	16(1)	16(1)	18(1)	4(1)	2(1)	2(1)
N(2)	17(1)	17(1)	18(1)	5(1)	4(1)	1(1)
C(1)	21(1)	13(1)	8(1)	-2(1)	1(1)	1(1)
C(2)	19(1)	28(1)	35(1)	12(1)	4(1)	1(1)
C(3)	18(1)	24(1)	26(1)	5(1)	5(1)	1(1)
C(4)	14(1)	13(1)	16(1)	3(1)	0(1)	3(1)
C(5)	15(1)	18(1)	17(1)	0(1)	1(1)	4(1)
C(6)	21(1)	24(1)	16(1)	6(1)	3(1)	4(1)
C(7)	18(1)	18(1)	30(1)	6(1)	4(1)	4(1)
C(8)	18(1)	17(1)	26(1)	-6(1)	-1(1)	2(1)
C(9)	14(1)	20(1)	16(1)	-1(1)	0(1)	6(1)
C(10)	28(1)	23(1)	16(1)	-3(1)	1(1)	2(1)
C(11)	32(1)	21(1)	44(2)	10(1)	9(1)	0(1)
C(12)	26(1)	35(1)	16(1)	-5(1)	2(1)	4(1)
C(13)	18(1)	14(1)	18(1)	6(1)	5(1)	-1(1)
C(14)	18(1)	19(1)	19(1)	4(1)	5(1)	-5(1)
C(15)	22(1)	28(1)	18(1)	9(1)	2(1)	-4(1)
C(16)	22(1)	23(1)	30(1)	13(1)	6(1)	0(1)
C(17)	26(1)	14(1)	35(1)	3(1)	13(1)	0(1)
C(18)	22(1)	18(1)	21(1)	2(1)	8(1)	-4(1)
C(19)	30(1)	24(1)	18(1)	0(1)	3(1)	-4(1)
C(20)	40(2)	34(1)	45(2)	21(1)	9(1)	12(1)
C(21)	32(1)	25(1)	23(1)	-4(1)	8(1)	-3(1)
C(22)	18(1)	15(1)	14(1)	5(1)	1(1)	6(1)
C(23)	23(1)	19(1)	14(1)	2(1)	-1(1)	6(1)
C(24)	32(1)	28(1)	11(1)	6(1)	2(1)	12(1)
C(25)	27(1)	30(1)	19(1)	13(1)	8(1)	9(1)
C(26)	23(1)	21(1)	22(1)	9(1)	4(1)	2(1)

C(27)	18(1)	16(1)	14(1)	5(1)	0(1)	4(1)
C(28)	18(1)	12(1)	14(1)	0(1)	4(1)	-2(1)
C(29)	15(1)	16(1)	12(1)	2(1)	3(1)	-2(1)
C(30)	20(1)	18(1)	18(1)	3(1)	5(1)	0(1)
C(31)	20(1)	28(1)	17(1)	7(1)	1(1)	4(1)
C(32)	20(1)	34(1)	14(1)	1(1)	-1(1)	-2(1)
C(33)	25(1)	21(1)	17(1)	-4(1)	2(1)	-4(1)
C(34)	19(1)	16(1)	13(1)	3(1)	3(1)	0(1)
C(35)	36(1)	11(1)	19(1)	0(1)	6(1)	-2(1)
C(36)	27(1)	18(1)	18(1)	-3(1)	4(1)	-2(1)
C(37)	32(1)	22(1)	27(1)	-4(1)	7(1)	-4(1)
C(1S)	40(1)	23(1)	18(1)	0(1)	-1(1)	-3(1)
Cl(1)	41(1)	25(1)	25(1)	-4(1)	-8(1)	8(1)
Cl(2)	30(1)	28(1)	23(1)	-2(1)	-2(1)	1(1)
C(2S)	44(1)	20(1)	26(1)	3(1)	11(1)	2(1)
C(3S)	33(1)	31(1)	26(1)	2(1)	2(1)	7(1)
C(4S)	34(1)	28(1)	23(1)	-2(1)	7(1)	-3(1)

Table 5. Hydrogen coordinates ($\times 10^4$) and isotropic displacement parameters ($\text{\AA}^2 \times 10^3$) for complex 5

	x	y	z	U(eq)
H(2A)	-4688	1670	1781	33
H(2B)	-4811	2158	2373	33
H(3A)	-3901	1454	3179	27
H(3B)	-4260	938	2591	27
H(6A)	-2244	3381	470	24
H(8A)	-1472	4117	2331	25
H(10A)	-2268	1850	880	34
H(10B)	-2780	2323	268	34
H(10C)	-4038	2103	700	34
H(11A)	-288	4560	1241	48
H(11B)	-2054	4784	1228	48

H(11C)	-1623	4444	586	48
H(12A)	-1725	3530	3279	39
H(12B)	-1312	2808	3243	39
H(12C)	-3109	3029	3106	39
H(15A)	763	412	4639	28
H(17A)	79	-645	2967	29
H(19A)	-40	1458	4618	36
H(19B)	-1761	1543	4166	36
H(19C)	-257	1801	3906	36
H(20A)	1905	-584	4712	60
H(20B)	2354	-838	4033	60
H(20C)	790	-1078	4259	60
H(21A)	-1325	-279	1927	40
H(21B)	-1116	452	1823	40
H(21C)	-2724	189	1989	40
H(23A)	-15	1129	140	23
H(24A)	1480	1530	-607	29
H(25A)	3278	2327	-272	30
H(26A)	3612	2737	817	26
H(28A)	1544	832	2533	17
H(30A)	3555	445	3563	22
H(31A)	5319	671	4563	26
H(32A)	5629	1698	4939	28
H(33A)	4122	2501	4354	25
H(35A)	1230	3213	2896	26
H(36A)	792	3137	3994	32
H(36B)	1786	3746	3901	32
H(36C)	2650	3151	4279	32
H(37A)	3693	3066	2635	40
H(37B)	4490	3102	3416	40
H(37C)	3626	3699	3042	40
H(1S1)	2214	10665	1413	33
H(1S2)	3338	10342	975	33
H(2S)	5219	8920	81	35
H(3S)	7265	9550	629	37
H(4S)	7046	10634	553	34

Table 6. Torsion angles [°] for complex Ru4a

C(28)-Ru(1)-O(1)-C(22)	-111.65(13)
O(2)-Ru(1)-O(1)-C(22)	2.25(12)
C(1)-Ru(1)-O(1)-C(22)	152.66(13)
O(3)-Ru(1)-O(1)-C(22)	-50.4(3)
C(28)-Ru(1)-O(2)-C(27)	89.54(14)
C(1)-Ru(1)-O(2)-C(27)	-77.75(18)
O(1)-Ru(1)-O(2)-C(27)	-2.92(12)
O(3)-Ru(1)-O(2)-C(27)	168.56(12)
C(28)-Ru(1)-O(3)-C(34)	8.80(13)
O(2)-Ru(1)-O(3)-C(34)	-105.84(13)
C(1)-Ru(1)-O(3)-C(34)	102.73(13)
O(1)-Ru(1)-O(3)-C(34)	-53.7(3)
C(28)-Ru(1)-O(3)-C(35)	165.22(16)
O(2)-Ru(1)-O(3)-C(35)	50.58(15)
C(1)-Ru(1)-O(3)-C(35)	-100.86(15)
O(1)-Ru(1)-O(3)-C(35)	102.7(3)
C(4)-N(1)-C(1)-N(2)	171.42(17)
C(2)-N(1)-C(1)-N(2)	-6.0(2)
C(4)-N(1)-C(1)-Ru(1)	-15.6(2)
C(2)-N(1)-C(1)-Ru(1)	167.01(15)
C(13)-N(2)-C(1)-N(1)	-178.72(18)
C(3)-N(2)-C(1)-N(1)	-5.2(2)
C(13)-N(2)-C(1)-Ru(1)	9.7(3)
C(3)-N(2)-C(1)-Ru(1)	-176.74(16)
C(28)-Ru(1)-C(1)-N(1)	-175.08(16)
O(2)-Ru(1)-C(1)-N(1)	-6.7(2)
O(1)-Ru(1)-C(1)-N(1)	-80.20(15)
O(3)-Ru(1)-C(1)-N(1)	104.08(15)
C(28)-Ru(1)-C(1)-N(2)	-4.3(2)
O(2)-Ru(1)-C(1)-N(2)	164.09(15)
O(1)-Ru(1)-C(1)-N(2)	90.61(19)
O(3)-Ru(1)-C(1)-N(2)	-85.1(2)
C(1)-N(1)-C(2)-C(3)	13.9(2)
C(4)-N(1)-C(2)-C(3)	-163.49(19)
C(1)-N(2)-C(3)-C(2)	13.4(2)

C(13)-N(2)-C(3)-C(2)	-172.67(19)
N(1)-C(2)-C(3)-N(2)	-15.1(2)
C(1)-N(1)-C(4)-C(5)	99.0(2)
C(2)-N(1)-C(4)-C(5)	-83.8(3)
C(1)-N(1)-C(4)-C(9)	-82.1(2)
C(2)-N(1)-C(4)-C(9)	95.0(2)
C(9)-C(4)-C(5)-C(6)	3.7(3)
N(1)-C(4)-C(5)-C(6)	-177.52(18)
C(9)-C(4)-C(5)-C(10)	-176.01(19)
N(1)-C(4)-C(5)-C(10)	2.8(3)
C(4)-C(5)-C(6)-C(7)	-0.4(3)
C(10)-C(5)-C(6)-C(7)	179.25(19)
C(5)-C(6)-C(7)-C(8)	-2.1(3)
C(5)-C(6)-C(7)-C(11)	178.2(2)
C(6)-C(7)-C(8)-C(9)	1.4(3)
C(11)-C(7)-C(8)-C(9)	-178.8(2)
C(7)-C(8)-C(9)-C(4)	1.7(3)
C(7)-C(8)-C(9)-C(12)	-177.1(2)
C(5)-C(4)-C(9)-C(8)	-4.3(3)
N(1)-C(4)-C(9)-C(8)	176.87(18)
C(5)-C(4)-C(9)-C(12)	174.52(19)
N(1)-C(4)-C(9)-C(12)	-4.3(3)
C(1)-N(2)-C(13)-C(18)	-94.2(2)
C(3)-N(2)-C(13)-C(18)	92.7(2)
C(1)-N(2)-C(13)-C(14)	86.4(3)
C(3)-N(2)-C(13)-C(14)	-86.7(2)
C(18)-C(13)-C(14)-C(15)	0.2(3)
N(2)-C(13)-C(14)-C(15)	179.56(18)
C(18)-C(13)-C(14)-C(19)	177.53(19)
N(2)-C(13)-C(14)-C(19)	-3.1(3)
C(13)-C(14)-C(15)-C(16)	0.5(3)
C(19)-C(14)-C(15)-C(16)	-176.9(2)
C(14)-C(15)-C(16)-C(17)	-0.5(3)
C(14)-C(15)-C(16)-C(20)	179.2(2)
C(15)-C(16)-C(17)-C(18)	-0.3(3)
C(20)-C(16)-C(17)-C(18)	-179.9(2)
C(16)-C(17)-C(18)-C(13)	0.9(3)

C(16)-C(17)-C(18)-C(21)	178.7(2)
C(14)-C(13)-C(18)-C(17)	-0.8(3)
N(2)-C(13)-C(18)-C(17)	179.75(18)
C(14)-C(13)-C(18)-C(21)	-178.69(19)
N(2)-C(13)-C(18)-C(21)	1.9(3)
Ru(1)-O(1)-C(22)-C(23)	178.24(15)
Ru(1)-O(1)-C(22)-C(27)	-1.2(2)
O(1)-C(22)-C(23)-C(24)	-178.64(18)
C(27)-C(22)-C(23)-C(24)	0.8(3)
C(22)-C(23)-C(24)-C(25)	-0.3(3)
C(23)-C(24)-C(25)-C(26)	-0.1(3)
C(24)-C(25)-C(26)-C(27)	-0.1(3)
Ru(1)-O(2)-C(27)-C(26)	-176.67(16)
Ru(1)-O(2)-C(27)-C(22)	3.1(2)
C(25)-C(26)-C(27)-O(2)	-179.61(19)
C(25)-C(26)-C(27)-C(22)	0.6(3)
O(1)-C(22)-C(27)-O(2)	-1.3(3)
C(23)-C(22)-C(27)-O(2)	179.22(17)
O(1)-C(22)-C(27)-C(26)	178.51(18)
C(23)-C(22)-C(27)-C(26)	-1.0(3)
O(2)-Ru(1)-C(28)-C(29)	79.38(16)
C(1)-Ru(1)-C(28)-C(29)	-107.11(15)
O(1)-Ru(1)-C(28)-C(29)	164.15(15)
O(3)-Ru(1)-C(28)-C(29)	-6.30(14)
Ru(1)-C(28)-C(29)-C(30)	-175.69(15)
Ru(1)-C(28)-C(29)-C(34)	3.1(2)
C(34)-C(29)-C(30)-C(31)	-1.9(3)
C(28)-C(29)-C(30)-C(31)	176.91(19)
C(29)-C(30)-C(31)-C(32)	-0.2(3)
C(30)-C(31)-C(32)-C(33)	1.6(3)
C(31)-C(32)-C(33)-C(34)	-0.8(3)
C(35)-O(3)-C(34)-C(33)	16.6(3)
Ru(1)-O(3)-C(34)-C(33)	171.98(18)
C(35)-O(3)-C(34)-C(29)	-164.66(18)
Ru(1)-O(3)-C(34)-C(29)	-9.3(2)
C(32)-C(33)-C(34)-O(3)	177.31(19)
C(32)-C(33)-C(34)-C(29)	-1.4(3)

C(30)-C(29)-C(34)-O(3)	-176.15(17)
C(28)-C(29)-C(34)-O(3)	5.0(3)
C(30)-C(29)-C(34)-C(33)	2.7(3)
C(28)-C(29)-C(34)-C(33)	-176.20(19)
C(34)-O(3)-C(35)-C(37)	62.6(2)
Ru(1)-O(3)-C(35)-C(37)	-90.67(19)
C(34)-O(3)-C(35)-C(36)	-66.9(3)
Ru(1)-O(3)-C(35)-C(36)	139.84(15)
C(4S)#1-C(2S)-C(3S)-C(4S)	0.2(4)
C(2S)-C(3S)-C(4S)-C(2S)#1	-0.2(4)

Symmetry transformations used to generate equivalent atoms:

#1 -x+1,-y+2,-z

X-ray structure of Ru4b:

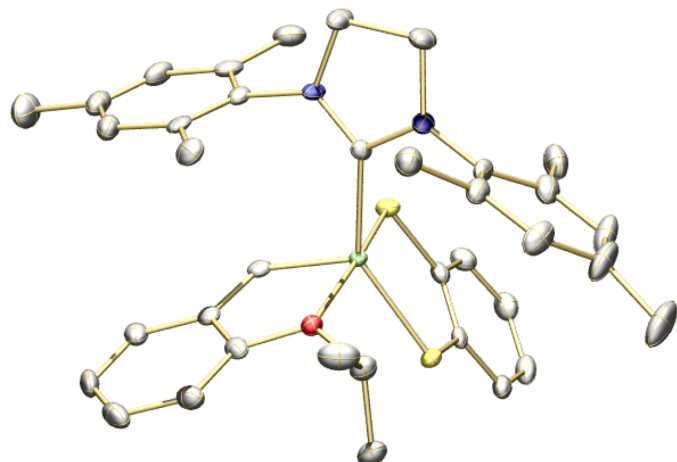


Table 1. Crystal data and structure refinement for complex Ru4b

Empirical formula	$\text{C}_{37}\text{H}_{42}\text{N}_2\text{ORuS}_2 \bullet \text{CH}_2\text{Cl}_2$	
Formula weight	780.84	
Temperature	100(2) K	
Wavelength	1.54178 Å	
Crystal system	Orthorhombic	
Space group	P2(1)2(1)2(1)	
Unit cell dimensions	$a = 12.3030(8)$ Å	$\alpha = 90^\circ$
	$b = 16.4866(11)$ Å	$\beta = 90^\circ$

	$c = 17.9428(13) \text{ \AA}$	$\gamma = 90^\circ$
Volume	$3639.4(4) \text{ \AA}^3$	
Z	4	
Density (calculated)	1.425 Mg/m^3	
Absorption coefficient	6.156 mm^{-1}	
F(000)	1616	
Crystal size	$0.20 \times 0.16 \times 0.05 \text{ mm}^3$	
Theta range for data collection	3.64 to 68.21°	
Index ranges	$-10 \leq h \leq 14, -19 \leq k \leq 19, -21 \leq l \leq 21$	
Reflections collected	24903	
Independent reflections	6395 [$R(\text{int}) = 0.0514$]	
Completeness to theta = 68.21°	98.3 %	
Absorption correction	Semi-empirical from equivalents	
Max. and min. transmission	0.7483 and 0.3723	
Refinement method	Full-matrix least-squares on F^2	
Data / restraints / parameters	6395 / 398 / 426	
Goodness-of-fit on F^2	1.045	
Final R indices [$I > 2\sigma(I)$]	$R_1 = 0.0276, wR_2 = 0.0689$	
R indices (all data)	$R_1 = 0.0283, wR_2 = 0.0694$	
Absolute structure parameter	0.023(6)	
Largest diff. peak and hole	0.697 and $-0.309 \text{ e.\AA}^{-3}$	

Table 2. Atomic coordinates ($x \times 10^4$) and equivalent isotropic displacement parameters ($\text{\AA}^2 \times 10^3$) for complex Ru4b. U(eq) is defined as one third of the trace of the orthogonalized U^{ij} tensor

	x	y	z	U(eq)
Ru(1)	5175(1)	958(1)	7818(1)	11(1)
S(1)	6677(1)	1763(1)	7662(1)	15(1)
S(2)	5298(1)	1200(1)	9068(1)	17(1)
O(1)	4923(1)	940(1)	6561(1)	15(1)
N(1)	5384(2)	-819(1)	8082(1)	18(1)
N(2)	3748(2)	-463(1)	8394(1)	16(1)
C(1)	3875(2)	1499(1)	7733(2)	15(1)
C(2)	3465(2)	1706(2)	6997(2)	16(1)
C(3)	2560(2)	2200(2)	6878(2)	22(1)
C(4)	2231(2)	2407(2)	6161(2)	26(1)

C(5)	2811(3)	2105(2)	5554(2)	27(1)
C(6)	3710(2)	1609(2)	5654(2)	23(1)
C(7)	4041(2)	1419(2)	6371(2)	18(1)
C(8)	5810(2)	761(2)	6032(2)	20(1)
C(9)	5448(3)	174(2)	5425(2)	31(1)
C(10)	6341(2)	1526(2)	5736(2)	23(1)
C(11)	6988(2)	2141(2)	8558(1)	15(1)
C(12)	7867(2)	2678(2)	8654(2)	19(1)
C(13)	8157(2)	2942(2)	9359(2)	24(1)
C(14)	7543(3)	2690(2)	9971(2)	24(1)
C(15)	6652(3)	2187(2)	9880(2)	23(1)
C(16)	6380(2)	1891(2)	9170(2)	16(1)
C(17)	4681(2)	-200(1)	8089(1)	14(1)
C(18)	4956(2)	-1552(2)	8452(2)	25(1)
C(19)	3759(2)	-1343(2)	8548(2)	24(1)
C(20)	6403(2)	-822(1)	7697(2)	18(1)
C(21)	6422(2)	-1126(2)	6968(2)	21(1)
C(22)	7406(3)	-1139(2)	6591(2)	29(1)
C(23)	8367(2)	-875(2)	6933(2)	35(1)
C(24)	8324(2)	-617(2)	7666(2)	33(1)
C(25)	7351(2)	-593(2)	8063(2)	24(1)
C(26)	5406(2)	-1457(2)	6604(2)	24(1)
C(27)	9477(12)	-998(13)	6570(13)	43(4)
C(27X)	9373(16)	-779(15)	6452(16)	43(4)
C(28)	7361(3)	-340(2)	8870(2)	30(1)
C(29)	2740(2)	-30(2)	8442(2)	16(1)
C(30)	2386(2)	230(2)	9145(2)	20(1)
C(31)	1406(2)	656(2)	9172(2)	25(1)
C(32)	786(2)	814(2)	8540(2)	26(1)
C(33)	1152(2)	517(2)	7862(2)	23(1)
C(34)	2127(2)	89(1)	7798(2)	18(1)
C(35)	3018(3)	62(2)	9844(2)	27(1)
C(36)	-231(3)	1305(2)	8591(2)	41(1)
C(37)	2494(2)	-233(2)	7055(2)	23(1)
C(1S)	9365(3)	2027(3)	6585(2)	49(1)
Cl(1)	9177(1)	3085(1)	6448(1)	51(1)
Cl(2)	9512(1)	1505(1)	5733(1)	60(1)

Table 3. Bond lengths [\AA] and angles [$^\circ$] for complex Ru4b

Ru(1)-C(1)	1.838(3)
Ru(1)-C(17)	2.061(2)
Ru(1)-O(1)	2.2769(17)
Ru(1)-S(2)	2.2830(6)
Ru(1)-S(1)	2.2933(6)
S(1)-C(11)	1.766(3)
S(2)-C(16)	1.761(3)
O(1)-C(7)	1.385(3)
O(1)-C(8)	1.476(3)
N(1)-C(17)	1.337(3)
N(1)-C(20)	1.432(3)
N(1)-C(18)	1.476(3)
N(2)-C(17)	1.344(4)
N(2)-C(29)	1.433(3)
N(2)-C(19)	1.476(3)
C(1)-C(2)	1.455(4)
C(1)-H(1)	0.9500
C(2)-C(3)	1.396(4)
C(2)-C(7)	1.410(4)
C(3)-C(4)	1.391(4)
C(3)-H(3)	0.9500
C(4)-C(5)	1.394(5)
C(4)-H(4)	0.9500
C(5)-C(6)	1.388(5)
C(5)-H(5)	0.9500
C(6)-C(7)	1.384(4)
C(6)-H(6)	0.9500
C(8)-C(10)	1.517(4)
C(8)-C(9)	1.523(4)
C(8)-H(8)	1.0000
C(9)-H(9A)	0.9800
C(9)-H(9B)	0.9800
C(9)-H(9C)	0.9800

C(10)-H(10A)	0.9800
C(10)-H(10B)	0.9800
C(10)-H(10C)	0.9800
C(11)-C(16)	1.391(4)
C(11)-C(12)	1.408(4)
C(12)-C(13)	1.385(4)
C(12)-H(12)	0.9500
C(13)-C(14)	1.396(5)
C(13)-H(13)	0.9500
C(14)-C(15)	1.385(5)
C(14)-H(14)	0.9500
C(15)-C(16)	1.405(4)
C(15)-H(15)	0.9500
C(18)-C(19)	1.522(4)
C(18)-H(18A)	0.9900
C(18)-H(18B)	0.9900
C(19)-H(19A)	0.9900
C(19)-H(19B)	0.9900
C(20)-C(25)	1.390(4)
C(20)-C(21)	1.402(4)
C(21)-C(22)	1.388(4)
C(21)-C(26)	1.512(4)
C(22)-C(23)	1.401(5)
C(22)-H(22)	0.9500
C(23)-C(24)	1.384(5)
C(23)-C(27X)	1.517(12)
C(23)-C(27)	1.526(9)
C(24)-C(25)	1.394(5)
C(24)-H(24)	0.9500
C(25)-C(28)	1.507(4)
C(26)-H(26A)	0.9800
C(26)-H(26B)	0.9800
C(26)-H(26C)	0.9800
C(27)-H(27A)	0.9800
C(27)-H(27B)	0.9800
C(27)-H(27C)	0.9800
C(27X)-H(27D)	0.9800

C(27X)-H(27E)	0.9800
C(27X)-H(27F)	0.9800
C(28)-H(28A)	0.9800
C(28)-H(28B)	0.9800
C(28)-H(28C)	0.9800
C(29)-C(34)	1.395(4)
C(29)-C(30)	1.401(4)
C(30)-C(31)	1.396(4)
C(30)-C(35)	1.501(4)
C(31)-C(32)	1.391(5)
C(31)-H(31)	0.9500
C(32)-C(33)	1.385(4)
C(32)-C(36)	1.494(4)
C(33)-C(34)	1.397(4)
C(33)-H(33)	0.9500
C(34)-C(37)	1.504(4)
C(35)-H(35A)	0.9800
C(35)-H(35B)	0.9800
C(35)-H(35C)	0.9800
C(36)-H(36A)	0.9800
C(36)-H(36B)	0.9800
C(36)-H(36C)	0.9800
C(37)-H(37A)	0.9800
C(37)-H(37B)	0.9800
C(37)-H(37C)	0.9800
C(1S)-Cl(2)	1.763(5)
C(1S)-Cl(1)	1.777(5)
C(1S)-H(1S1)	0.9900
C(1S)-H(1S2)	0.9900
C(1)-Ru(1)-C(17)	102.30(10)
C(1)-Ru(1)-O(1)	78.79(9)
C(17)-Ru(1)-O(1)	100.46(8)
C(1)-Ru(1)-S(2)	93.11(8)
C(17)-Ru(1)-S(2)	87.16(7)
O(1)-Ru(1)-S(2)	169.84(5)
C(1)-Ru(1)-S(1)	114.18(7)
C(17)-Ru(1)-S(1)	143.40(8)

O(1)-Ru(1)-S(1)	89.77(5)
S(2)-Ru(1)-S(1)	87.98(2)
C(11)-S(1)-Ru(1)	105.51(9)
C(16)-S(2)-Ru(1)	105.40(9)
C(7)-O(1)-C(8)	122.34(19)
C(7)-O(1)-Ru(1)	110.09(15)
C(8)-O(1)-Ru(1)	122.59(15)
C(17)-N(1)-C(20)	125.0(2)
C(17)-N(1)-C(18)	112.9(2)
C(20)-N(1)-C(18)	121.8(2)
C(17)-N(2)-C(29)	127.1(2)
C(17)-N(2)-C(19)	112.6(2)
C(29)-N(2)-C(19)	119.1(2)
C(2)-C(1)-Ru(1)	119.41(19)
C(2)-C(1)-H(1)	120.3
Ru(1)-C(1)-H(1)	120.3
C(3)-C(2)-C(7)	118.4(3)
C(3)-C(2)-C(1)	123.5(2)
C(7)-C(2)-C(1)	118.1(2)
C(4)-C(3)-C(2)	121.0(3)
C(4)-C(3)-H(3)	119.5
C(2)-C(3)-H(3)	119.5
C(3)-C(4)-C(5)	119.2(3)
C(3)-C(4)-H(4)	120.4
C(5)-C(4)-H(4)	120.4
C(6)-C(5)-C(4)	121.1(3)
C(6)-C(5)-H(5)	119.4
C(4)-C(5)-H(5)	119.4
C(7)-C(6)-C(5)	119.2(3)
C(7)-C(6)-H(6)	120.4
C(5)-C(6)-H(6)	120.4
C(6)-C(7)-O(1)	126.0(2)
C(6)-C(7)-C(2)	121.1(3)
O(1)-C(7)-C(2)	112.9(2)
O(1)-C(8)-C(10)	112.2(2)
O(1)-C(8)-C(9)	111.7(2)
C(10)-C(8)-C(9)	113.8(2)

O(1)-C(8)-H(8)	106.2
C(10)-C(8)-H(8)	106.2
C(9)-C(8)-H(8)	106.2
C(8)-C(9)-H(9A)	109.5
C(8)-C(9)-H(9B)	109.5
H(9A)-C(9)-H(9B)	109.5
C(8)-C(9)-H(9C)	109.5
H(9A)-C(9)-H(9C)	109.5
H(9B)-C(9)-H(9C)	109.5
C(8)-C(10)-H(10A)	109.5
C(8)-C(10)-H(10B)	109.5
H(10A)-C(10)-H(10B)	109.5
C(8)-C(10)-H(10C)	109.5
H(10A)-C(10)-H(10C)	109.5
H(10B)-C(10)-H(10C)	109.5
C(16)-C(11)-C(12)	120.2(2)
C(16)-C(11)-S(1)	119.8(2)
C(12)-C(11)-S(1)	119.9(2)
C(13)-C(12)-C(11)	120.5(3)
C(13)-C(12)-H(12)	119.8
C(11)-C(12)-H(12)	119.8
C(12)-C(13)-C(14)	119.1(3)
C(12)-C(13)-H(13)	120.5
C(14)-C(13)-H(13)	120.5
C(15)-C(14)-C(13)	120.9(3)
C(15)-C(14)-H(14)	119.5
C(13)-C(14)-H(14)	119.5
C(14)-C(15)-C(16)	120.2(3)
C(14)-C(15)-H(15)	119.9
C(16)-C(15)-H(15)	119.9
C(11)-C(16)-C(15)	119.0(3)
C(11)-C(16)-S(2)	121.1(2)
C(15)-C(16)-S(2)	119.9(2)
N(1)-C(17)-N(2)	108.1(2)
N(1)-C(17)-Ru(1)	120.89(19)
N(2)-C(17)-Ru(1)	130.29(18)
N(1)-C(18)-C(19)	102.2(2)

N(1)-C(18)-H(18A)	111.3
C(19)-C(18)-H(18A)	111.3
N(1)-C(18)-H(18B)	111.3
C(19)-C(18)-H(18B)	111.3
H(18A)-C(18)-H(18B)	109.2
N(2)-C(19)-C(18)	102.2(2)
N(2)-C(19)-H(19A)	111.3
C(18)-C(19)-H(19A)	111.3
N(2)-C(19)-H(19B)	111.3
C(18)-C(19)-H(19B)	111.3
H(19A)-C(19)-H(19B)	109.2
C(25)-C(20)-C(21)	121.6(2)
C(25)-C(20)-N(1)	120.4(2)
C(21)-C(20)-N(1)	117.7(2)
C(22)-C(21)-C(20)	118.3(3)
C(22)-C(21)-C(26)	120.4(3)
C(20)-C(21)-C(26)	121.3(2)
C(21)-C(22)-C(23)	121.2(3)
C(21)-C(22)-H(22)	119.4
C(23)-C(22)-H(22)	119.4
C(24)-C(23)-C(22)	118.7(3)
C(24)-C(23)-C(27X)	122.7(12)
C(22)-C(23)-C(27X)	118.1(13)
C(24)-C(23)-C(27)	118.7(10)
C(22)-C(23)-C(27)	121.8(9)
C(27X)-C(23)-C(27)	16.5(13)
C(23)-C(24)-C(25)	121.8(3)
C(23)-C(24)-H(24)	119.1
C(25)-C(24)-H(24)	119.1
C(20)-C(25)-C(24)	118.1(3)
C(20)-C(25)-C(28)	122.4(3)
C(24)-C(25)-C(28)	119.5(3)
C(21)-C(26)-H(26A)	109.5
C(21)-C(26)-H(26B)	109.5
H(26A)-C(26)-H(26B)	109.5
C(21)-C(26)-H(26C)	109.5
H(26A)-C(26)-H(26C)	109.5

H(26B)-C(26)-H(26C)	109.5
C(23)-C(27)-H(27A)	109.5
C(23)-C(27)-H(27B)	109.5
C(23)-C(27)-H(27C)	109.5
C(23)-C(27X)-H(27D)	109.5
C(23)-C(27X)-H(27E)	109.5
H(27D)-C(27X)-H(27E)	109.5
C(23)-C(27X)-H(27F)	109.5
H(27D)-C(27X)-H(27F)	109.5
H(27E)-C(27X)-H(27F)	109.5
C(25)-C(28)-H(28A)	109.5
C(25)-C(28)-H(28B)	109.5
H(28A)-C(28)-H(28B)	109.5
C(25)-C(28)-H(28C)	109.5
H(28A)-C(28)-H(28C)	109.5
H(28B)-C(28)-H(28C)	109.5
C(34)-C(29)-C(30)	122.3(2)
C(34)-C(29)-N(2)	119.2(2)
C(30)-C(29)-N(2)	118.4(2)
C(31)-C(30)-C(29)	117.1(3)
C(31)-C(30)-C(35)	120.7(3)
C(29)-C(30)-C(35)	122.2(3)
C(32)-C(31)-C(30)	122.5(3)
C(32)-C(31)-H(31)	118.7
C(30)-C(31)-H(31)	118.7
C(33)-C(32)-C(31)	118.2(3)
C(33)-C(32)-C(36)	121.1(3)
C(31)-C(32)-C(36)	120.7(3)
C(32)-C(33)-C(34)	122.0(3)
C(32)-C(33)-H(33)	119.0
C(34)-C(33)-H(33)	119.0
C(29)-C(34)-C(33)	117.8(3)
C(29)-C(34)-C(37)	121.5(2)
C(33)-C(34)-C(37)	120.6(3)
C(30)-C(35)-H(35A)	109.5
C(30)-C(35)-H(35B)	109.5
H(35A)-C(35)-H(35B)	109.5

C(30)-C(35)-H(35C)	109.5
H(35A)-C(35)-H(35C)	109.5
H(35B)-C(35)-H(35C)	109.5
C(32)-C(36)-H(36A)	109.5
C(32)-C(36)-H(36B)	109.5
H(36A)-C(36)-H(36B)	109.5
C(32)-C(36)-H(36C)	109.5
H(36A)-C(36)-H(36C)	109.5
H(36B)-C(36)-H(36C)	109.5
C(34)-C(37)-H(37A)	109.5
C(34)-C(37)-H(37B)	109.5
H(37A)-C(37)-H(37B)	109.5
C(34)-C(37)-H(37C)	109.5
H(37A)-C(37)-H(37C)	109.5
H(37B)-C(37)-H(37C)	109.5
Cl(2)-C(1S)-Cl(1)	111.8(2)
Cl(2)-C(1S)-H(1S1)	109.2
Cl(1)-C(1S)-H(1S1)	109.2
Cl(2)-C(1S)-H(1S2)	109.2
Cl(1)-C(1S)-H(1S2)	109.2
H(1S1)-C(1S)-H(1S2)	107.9

Symmetry transformations used to generate equivalent atoms:

Table 4. Anisotropic displacement parameters ($\text{\AA}^2 \times 10^3$) for complex Ru4b. The anisotropic displacement factor exponent takes the form: $-2\pi^2 [h^2 a^{*2} U^{11} + \dots + 2 h k a^* b^* U^{12}]$

	U ¹¹	U ²²	U ³³	U ²³	U ¹³	U ¹²
Ru(1)	11(1)	10(1)	13(1)	1(1)	0(1)	-2(1)
S(1)	13(1)	15(1)	17(1)	0(1)	0(1)	-3(1)
S(2)	20(1)	16(1)	14(1)	0(1)	1(1)	-4(1)
O(1)	14(1)	17(1)	15(1)	1(1)	2(1)	0(1)
N(1)	16(1)	11(1)	26(1)	0(1)	1(1)	0(1)
N(2)	17(1)	8(1)	23(1)	2(1)	5(1)	0(1)
C(1)	17(1)	10(1)	19(1)	0(1)	2(1)	-5(1)
C(2)	15(1)	12(1)	22(1)	1(1)	-1(1)	-6(1)

C(3)	19(1)	15(1)	33(2)	4(1)	-3(1)	-3(1)
C(4)	16(1)	22(1)	40(2)	8(1)	-10(1)	0(1)
C(5)	32(2)	22(1)	28(2)	7(1)	-14(1)	-5(1)
C(6)	25(2)	24(1)	20(1)	4(1)	-3(1)	-5(1)
C(7)	19(1)	13(1)	22(1)	1(1)	-6(1)	-5(1)
C(8)	21(1)	22(1)	18(1)	-1(1)	3(1)	-1(1)
C(9)	48(2)	24(1)	21(1)	-4(1)	7(1)	-5(1)
C(10)	22(1)	25(1)	22(1)	0(1)	5(1)	-4(1)
C(11)	12(1)	11(1)	21(1)	-1(1)	-4(1)	2(1)
C(12)	15(1)	15(1)	27(1)	0(1)	-2(1)	2(1)
C(13)	19(1)	18(1)	35(2)	-9(1)	-7(1)	1(1)
C(14)	27(2)	21(1)	24(1)	-6(1)	-7(1)	1(1)
C(15)	29(2)	18(1)	21(1)	0(1)	-2(1)	0(1)
C(16)	17(1)	12(1)	20(1)	0(1)	-4(1)	2(1)
C(17)	15(1)	12(1)	14(1)	-1(1)	2(1)	2(1)
C(18)	26(2)	14(1)	34(2)	6(1)	5(1)	2(1)
C(19)	20(1)	10(1)	40(2)	2(1)	9(1)	1(1)
C(20)	12(1)	12(1)	30(1)	1(1)	4(1)	3(1)
C(21)	17(1)	13(1)	32(1)	-3(1)	1(1)	1(1)
C(22)	24(2)	24(2)	39(2)	-12(1)	10(1)	-1(1)
C(23)	16(1)	34(2)	54(2)	-18(2)	10(1)	-3(1)
C(24)	15(1)	28(1)	56(2)	-18(1)	-1(1)	0(1)
C(25)	22(1)	17(1)	35(2)	-4(1)	-2(1)	3(1)
C(26)	22(2)	23(1)	28(1)	-2(1)	0(1)	0(1)
C(27)	19(3)	42(9)	69(6)	-24(6)	14(4)	-1(4)
C(27X)	19(3)	42(9)	69(6)	-24(6)	14(4)	-1(4)
C(28)	26(2)	31(2)	35(2)	-5(1)	-11(1)	4(1)
C(29)	14(1)	10(1)	24(1)	0(1)	3(1)	-3(1)
C(30)	25(1)	12(1)	25(1)	1(1)	9(1)	-5(1)
C(31)	21(1)	20(1)	34(2)	-4(1)	13(1)	-2(1)
C(32)	17(1)	18(1)	43(2)	1(1)	6(1)	0(1)
C(33)	17(1)	19(1)	34(2)	1(1)	-1(1)	0(1)
C(34)	15(1)	11(1)	30(1)	2(1)	5(1)	-6(1)
C(35)	35(2)	22(1)	24(1)	2(1)	8(1)	-6(1)
C(36)	28(2)	35(2)	61(2)	1(2)	7(2)	10(2)
C(37)	22(1)	23(1)	25(2)	-5(1)	-1(1)	-6(1)
C(1S)	31(2)	67(2)	49(2)	16(2)	-1(2)	-3(2)

Cl(1)	37(1)	64(1)	51(1)	9(1)	4(1)	8(1)
Cl(2)	42(1)	73(1)	66(1)	-6(1)	1(1)	2(1)

Table 5. Hydrogen coordinates ($\times 10^4$) and isotropic displacement parameters ($\text{\AA}^2 \times 10^3$) for complex Ru4b

	x	y	z	U(eq)
H(1)	3475	1643	8166	19
H(3)	2162	2398	7294	27
H(4)	1620	2749	6087	31
H(5)	2586	2242	5063	33
H(6)	4095	1402	5236	27
H(8)	6383	471	6325	25
H(9A)	5118	-306	5655	46
H(9B)	6078	10	5128	46
H(9C)	4914	441	5103	46
H(10A)	6560	1872	6154	35
H(10B)	5824	1820	5420	35
H(10C)	6984	1381	5442	35
H(12)	8264	2859	8231	23
H(13)	8764	3291	9425	28
H(14)	7740	2866	10457	29
H(15)	6223	2041	10299	27
H(18A)	5312	-1644	8939	30
H(18B)	5051	-2039	8136	30
H(19A)	3301	-1643	8188	28
H(19B)	3507	-1461	9060	28
H(22)	7429	-1329	6091	35
H(24)	8976	-450	7905	40
H(26A)	5545	-1553	6074	36
H(26B)	4814	-1064	6658	36
H(26C)	5201	-1968	6844	36
H(27A)	10047	-806	6908	65
H(27B)	9510	-691	6103	65

H(27C)	9586	-1576	6466	65
H(27D)	9746	-274	6583	65
H(27E)	9161	-763	5926	65
H(27F)	9863	-1239	6536	65
H(28A)	7148	231	8910	46
H(28B)	8094	-411	9074	46
H(28C)	6848	-676	9152	46
H(31)	1152	846	9641	30
H(33)	726	608	7428	28
H(35A)	2960	-515	9969	40
H(35B)	2723	388	10253	40
H(35C)	3783	203	9765	40
H(36A)	-78	1865	8440	62
H(36B)	-498	1299	9105	62
H(36C)	-784	1073	8260	62
H(37A)	3151	55	6896	35
H(37B)	1917	-151	6685	35
H(37C)	2652	-814	7099	35
H(1S1)	10021	1938	6894	59
H(1S2)	8733	1805	6858	59

Table 6. Torsion angles [°] for complex Ru4b

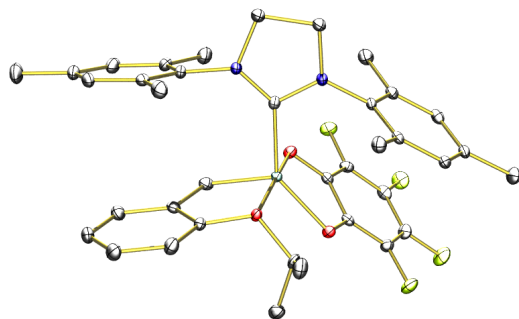
C(1)-Ru(1)-S(1)-C(11)	88.86(13)
C(17)-Ru(1)-S(1)-C(11)	-86.14(14)
O(1)-Ru(1)-S(1)-C(11)	166.45(10)
S(2)-Ru(1)-S(1)-C(11)	-3.64(9)
C(1)-Ru(1)-S(2)-C(16)	-110.49(11)
C(17)-Ru(1)-S(2)-C(16)	147.34(12)
O(1)-Ru(1)-S(2)-C(16)	-73.7(3)
S(1)-Ru(1)-S(2)-C(16)	3.62(9)
C(1)-Ru(1)-O(1)-C(7)	7.89(16)
C(17)-Ru(1)-O(1)-C(7)	108.50(16)
S(2)-Ru(1)-O(1)-C(7)	-29.7(4)
S(1)-Ru(1)-O(1)-C(7)	-106.84(14)
C(1)-Ru(1)-O(1)-C(8)	163.39(18)
C(17)-Ru(1)-O(1)-C(8)	-95.99(18)

S(2)-Ru(1)-O(1)-C(8)	125.8(3)
S(1)-Ru(1)-O(1)-C(8)	48.66(16)
C(17)-Ru(1)-C(1)-C(2)	-105.29(19)
O(1)-Ru(1)-C(1)-C(2)	-6.88(18)
S(2)-Ru(1)-C(1)-C(2)	166.94(18)
S(1)-Ru(1)-C(1)-C(2)	77.76(19)
Ru(1)-C(1)-C(2)-C(3)	-171.9(2)
Ru(1)-C(1)-C(2)-C(7)	5.4(3)
C(7)-C(2)-C(3)-C(4)	-0.1(4)
C(1)-C(2)-C(3)-C(4)	177.2(3)
C(2)-C(3)-C(4)-C(5)	0.8(4)
C(3)-C(4)-C(5)-C(6)	-0.4(5)
C(4)-C(5)-C(6)-C(7)	-0.7(4)
C(5)-C(6)-C(7)-O(1)	-179.5(2)
C(5)-C(6)-C(7)-C(2)	1.5(4)
C(8)-O(1)-C(7)-C(6)	18.2(4)
Ru(1)-O(1)-C(7)-C(6)	173.8(2)
C(8)-O(1)-C(7)-C(2)	-162.6(2)
Ru(1)-O(1)-C(7)-C(2)	-7.1(2)
C(3)-C(2)-C(7)-C(6)	-1.1(4)
C(1)-C(2)-C(7)-C(6)	-178.5(2)
C(3)-C(2)-C(7)-O(1)	179.7(2)
C(1)-C(2)-C(7)-O(1)	2.3(3)
C(7)-O(1)-C(8)-C(10)	57.1(3)
Ru(1)-O(1)-C(8)-C(10)	-95.5(2)
C(7)-O(1)-C(8)-C(9)	-72.1(3)
Ru(1)-O(1)-C(8)-C(9)	135.36(19)
Ru(1)-S(1)-C(11)-C(16)	3.0(2)
Ru(1)-S(1)-C(11)-C(12)	-178.65(18)
C(16)-C(11)-C(12)-C(13)	2.0(4)
S(1)-C(11)-C(12)-C(13)	-176.3(2)
C(11)-C(12)-C(13)-C(14)	-2.0(4)
C(12)-C(13)-C(14)-C(15)	-0.4(4)
C(13)-C(14)-C(15)-C(16)	2.9(4)
C(12)-C(11)-C(16)-C(15)	0.5(4)
S(1)-C(11)-C(16)-C(15)	178.8(2)
C(12)-C(11)-C(16)-S(2)	-178.33(19)

S(1)-C(11)-C(16)-S(2)	0.0(3)
C(14)-C(15)-C(16)-C(11)	-2.9(4)
C(14)-C(15)-C(16)-S(2)	175.9(2)
Ru(1)-S(2)-C(16)-C(11)	-3.0(2)
Ru(1)-S(2)-C(16)-C(15)	178.2(2)
C(20)-N(1)-C(17)-N(2)	169.6(2)
C(18)-N(1)-C(17)-N(2)	-4.2(3)
C(20)-N(1)-C(17)-Ru(1)	-19.4(3)
C(18)-N(1)-C(17)-Ru(1)	166.82(18)
C(29)-N(2)-C(17)-N(1)	-173.0(2)
C(19)-N(2)-C(17)-N(1)	-5.8(3)
C(29)-N(2)-C(17)-Ru(1)	17.1(4)
C(19)-N(2)-C(17)-Ru(1)	-175.7(2)
C(1)-Ru(1)-C(17)-N(1)	169.1(2)
O(1)-Ru(1)-C(17)-N(1)	88.39(19)
S(2)-Ru(1)-C(17)-N(1)	-98.37(19)
S(1)-Ru(1)-C(17)-N(1)	-15.6(3)
C(1)-Ru(1)-C(17)-N(2)	-22.1(3)
O(1)-Ru(1)-C(17)-N(2)	-102.8(2)
S(2)-Ru(1)-C(17)-N(2)	70.4(2)
S(1)-Ru(1)-C(17)-N(2)	153.19(18)
C(17)-N(1)-C(18)-C(19)	11.7(3)
C(20)-N(1)-C(18)-C(19)	-162.3(2)
C(17)-N(2)-C(19)-C(18)	12.6(3)
C(29)-N(2)-C(19)-C(18)	-179.0(2)
N(1)-C(18)-C(19)-N(2)	-13.5(3)
C(17)-N(1)-C(20)-C(25)	93.4(3)
C(18)-N(1)-C(20)-C(25)	-93.3(3)
C(17)-N(1)-C(20)-C(21)	-92.0(3)
C(18)-N(1)-C(20)-C(21)	81.3(3)
C(25)-C(20)-C(21)-C(22)	-4.9(4)
N(1)-C(20)-C(21)-C(22)	-179.4(2)
C(25)-C(20)-C(21)-C(26)	173.3(3)
N(1)-C(20)-C(21)-C(26)	-1.3(4)
C(20)-C(21)-C(22)-C(23)	1.7(4)
C(26)-C(21)-C(22)-C(23)	-176.5(3)
C(21)-C(22)-C(23)-C(24)	1.4(5)

C(21)-C(22)-C(23)-C(27X)	-170.4(11)
C(21)-C(22)-C(23)-C(27)	171.0(12)
C(22)-C(23)-C(24)-C(25)	-1.6(5)
C(27X)-C(23)-C(24)-C(25)	169.9(12)
C(27)-C(23)-C(24)-C(25)	-171.4(11)
C(21)-C(20)-C(25)-C(24)	4.7(4)
N(1)-C(20)-C(25)-C(24)	179.2(2)
C(21)-C(20)-C(25)-C(28)	-174.0(3)
N(1)-C(20)-C(25)-C(28)	0.4(4)
C(23)-C(24)-C(25)-C(20)	-1.4(5)
C(23)-C(24)-C(25)-C(28)	177.4(3)
C(17)-N(2)-C(29)-C(34)	71.9(3)
C(19)-N(2)-C(29)-C(34)	-94.6(3)
C(17)-N(2)-C(29)-C(30)	-110.6(3)
C(19)-N(2)-C(29)-C(30)	82.9(3)
C(34)-C(29)-C(30)-C(31)	-3.1(4)
N(2)-C(29)-C(30)-C(31)	179.5(2)
C(34)-C(29)-C(30)-C(35)	176.6(2)
N(2)-C(29)-C(30)-C(35)	-0.8(4)
C(29)-C(30)-C(31)-C(32)	0.8(4)
C(35)-C(30)-C(31)-C(32)	-178.9(3)
C(30)-C(31)-C(32)-C(33)	1.5(4)
C(30)-C(31)-C(32)-C(36)	-177.1(3)
C(31)-C(32)-C(33)-C(34)	-1.7(4)
C(36)-C(32)-C(33)-C(34)	177.0(3)
C(30)-C(29)-C(34)-C(33)	3.0(4)
N(2)-C(29)-C(34)-C(33)	-179.6(2)
C(30)-C(29)-C(34)-C(37)	-176.7(2)
N(2)-C(29)-C(34)-C(37)	0.7(4)
C(32)-C(33)-C(34)-C(29)	-0.5(4)
C(32)-C(33)-C(34)-C(37)	179.2(3)

Symmetry transformations used to generate equivalent atoms:

X-ray structure of Ru4c:**Table 1.** Crystal data and structure refinement for Ru4c.

Identification code	C37H38F4N2O3Ru		
Empirical formula	C37 H38 F4 N2 O3 Ru		
Formula weight	735.76		
Temperature	100(2) K		
Wavelength	1.54178 \approx		
Crystal system	Triclinic		
Space group	P -1		
Unit cell dimensions	$a = 10.272(2) \approx$	$\alpha = 92.947(6)\infty.$	
	$b = 10.655(2) \approx$	$\beta = 101.171(6)\infty.$	
	$c = 17.385(4) \approx$	$\gamma = 117.538(5)\infty.$	
Volume	$1633.2(6) \approx^3$		
Z	2		
Density (calculated)	1.496 Mg/m ³		
Absorption coefficient	4.421 mm ⁻¹		
F(000)	756		
Crystal size	0.420 x 0.200 x 0.120 mm ³		
Theta range for data collection	2.625 to 68.282 ∞ .		
Index ranges	-9 <= h <= 12, -12 <= k <= 12, -20 <= l <= 20		
Reflections collected	31065		
Independent reflections	5668 [R(int) = 0.0236]		
Completeness to theta = 66.500 ∞	97.4 %		
Absorption correction	Semi-empirical from equivalents		
Max. and min. transmission	0.7531 and 0.5606		
Refinement method	Full-matrix least-squares on F ²		
Data / restraints / parameters	5668 / 0 / 432		

Goodness-of-fit on F ²	1.053
Final R indices [I>2sigma(I)]	R1 = 0.0208, wR2 = 0.0508
R indices (all data)	R1 = 0.0209, wR2 = 0.0509
Extinction coefficient	na
Largest diff. peak and hole	0.347 and -0.426 e. \AA^{-3}

Table 2. Atomic coordinates (x 10⁴) and equivalent isotropic displacement parameters ($\text{\AA}^2 \times 10^3$) for Ru4c. U(eq) is defined as one third of the trace of the orthogonalized U^{ij} tensor.

	x	y	z	U(eq)
Ru(1)	1341(1)	4791(1)	2285(1)	11(1)
F(1)	6572(1)	6634(1)	3605(1)	24(1)
F(2)	8180(1)	9529(1)	3994(1)	30(1)
F(3)	6844(1)	11177(1)	3547(1)	26(1)
F(4)	3897(1)	9917(1)	2743(1)	22(1)
O(1)	563(1)	2475(1)	2107(1)	13(1)
O(2)	3525(1)	5315(1)	2758(1)	14(1)
O(3)	2223(1)	6938(1)	2346(1)	15(1)
N(1)	-1939(2)	4133(2)	2279(1)	14(1)
N(2)	-262(2)	4979(2)	3414(1)	16(1)
C(1)	-477(2)	4599(2)	2631(1)	12(1)
C(2)	-2816(2)	4198(2)	2845(1)	22(1)
C(3)	-1658(2)	4705(2)	3649(1)	17(1)
C(4)	-2600(2)	3920(2)	1445(1)	15(1)
C(5)	-2295(2)	5122(2)	1067(1)	18(1)
C(6)	-3015(2)	4889(2)	266(1)	22(1)
C(7)	-4029(2)	3518(2)	-151(1)	22(1)
C(8)	-4305(2)	2360(2)	247(1)	21(1)
C(9)	-3601(2)	2531(2)	1046(1)	17(1)
C(10)	-1234(2)	6623(2)	1511(1)	23(1)
C(11)	-4798(3)	3300(3)	-1020(1)	33(1)
C(12)	-3906(2)	1246(2)	1455(1)	23(1)
C(13)	1175(2)	5550(2)	3978(1)	14(1)
C(14)	1656(2)	4619(2)	4306(1)	14(1)
C(15)	3080(2)	5218(2)	4833(1)	16(1)
C(16)	3983(2)	6692(2)	5059(1)	18(1)
C(17)	3435(2)	7583(2)	4749(1)	18(1)

C(18)	2040(2)	7044(2)	4208(1)	16(1)
C(19)	622(2)	3019(2)	4147(1)	19(1)
C(20)	5496(2)	7322(2)	5648(1)	27(1)
C(21)	1485(2)	8039(2)	3883(1)	22(1)
C(22)	459(2)	4345(2)	1220(1)	16(1)
C(23)	-253(2)	2863(2)	830(1)	15(1)
C(24)	-1022(2)	2367(2)	30(1)	20(1)
C(25)	-1715(2)	923(2)	-277(1)	22(1)
C(26)	-1659(2)	-41(2)	216(1)	23(1)
C(27)	-909(2)	421(2)	1018(1)	20(1)
C(28)	-203(2)	1870(2)	1311(1)	14(1)
C(29)	1716(2)	2070(2)	2497(1)	16(1)
C(30)	980(2)	609(2)	2752(1)	23(1)
C(31)	2790(2)	2228(2)	1983(1)	22(1)
C(32)	4380(2)	6748(2)	2950(1)	14(1)
C(33)	5882(2)	7424(2)	3369(1)	17(1)
C(34)	6719(2)	8904(2)	3576(1)	20(1)
C(35)	6042(2)	9726(2)	3356(1)	19(1)
C(36)	4541(2)	9074(2)	2940(1)	16(1)
C(37)	3681(2)	7596(2)	2731(1)	14(1)

Table 3. Bond lengths [\AA] and angles [$^\circ$] for Ru4c.

Ru(1)-C(22)	1.8274(18)
Ru(1)-C(1)	1.9962(18)
Ru(1)-O(3)	2.0217(12)
Ru(1)-O(2)	2.0247(13)
Ru(1)-O(1)	2.1968(12)
F(1)-C(33)	1.362(2)
F(2)-C(34)	1.352(2)
F(3)-C(35)	1.357(2)
F(4)-C(36)	1.362(2)
O(1)-C(28)	1.403(2)
O(1)-C(29)	1.497(2)
O(2)-C(32)	1.344(2)
O(3)-C(37)	1.333(2)
N(1)-C(1)	1.341(2)

N(1)-C(4)	1.435(2)
N(1)-C(2)	1.477(2)
N(2)-C(1)	1.344(2)
N(2)-C(13)	1.434(2)
N(2)-C(3)	1.471(2)
C(2)-C(3)	1.531(2)
C(2)-H(2A)	0.9900
C(2)-H(2B)	0.9900
C(3)-H(3A)	0.9900
C(3)-H(3B)	0.9900
C(4)-C(9)	1.393(3)
C(4)-C(5)	1.402(3)
C(5)-C(6)	1.394(3)
C(5)-C(10)	1.508(3)
C(6)-C(7)	1.391(3)
C(6)-H(6)	0.9500
C(7)-C(8)	1.387(3)
C(7)-C(11)	1.513(3)
C(8)-C(9)	1.396(3)
C(8)-H(8)	0.9500
C(9)-C(12)	1.505(3)
C(10)-H(10A)	0.9800
C(10)-H(10B)	0.9800
C(10)-H(10C)	0.9800
C(11)-H(11A)	0.9800
C(11)-H(11B)	0.9800
C(11)-H(11C)	0.9800
C(12)-H(12A)	0.9800
C(12)-H(12B)	0.9800
C(12)-H(12C)	0.9800
C(13)-C(14)	1.398(3)
C(13)-C(18)	1.404(3)
C(14)-C(15)	1.394(3)
C(14)-C(19)	1.509(2)
C(15)-C(16)	1.389(3)
C(15)-H(15)	0.9500
C(16)-C(17)	1.391(3)

C(16)-C(20)	1.505(3)
C(17)-C(18)	1.389(3)
C(17)-H(17)	0.9500
C(18)-C(21)	1.505(3)
C(19)-H(19A)	0.9800
C(19)-H(19B)	0.9800
C(19)-H(19C)	0.9800
C(20)-H(20A)	0.9800
C(20)-H(20B)	0.9800
C(20)-H(20C)	0.9800
C(21)-H(21A)	0.9800
C(21)-H(21B)	0.9800
C(21)-H(21C)	0.9800
C(22)-C(23)	1.455(2)
C(22)-H(22)	0.9500
C(23)-C(28)	1.394(3)
C(23)-C(24)	1.397(3)
C(24)-C(25)	1.383(3)
C(24)-H(24)	0.9500
C(25)-C(26)	1.386(3)
C(25)-H(25)	0.9500
C(26)-C(27)	1.394(3)
C(26)-H(26)	0.9500
C(27)-C(28)	1.382(3)
C(27)-H(27)	0.9500
C(29)-C(31)	1.507(3)
C(29)-C(30)	1.517(3)
C(29)-H(29)	1.0000
C(30)-H(30A)	0.9800
C(30)-H(30B)	0.9800
C(30)-H(30C)	0.9800
C(31)-H(31A)	0.9800
C(31)-H(31B)	0.9800
C(31)-H(31C)	0.9800
C(32)-C(33)	1.382(3)
C(32)-C(37)	1.416(3)
C(33)-C(34)	1.387(3)

C(34)-C(35)	1.375(3)
C(35)-C(36)	1.382(3)
C(36)-C(37)	1.387(2)
C(22)-Ru(1)-C(1)	96.16(8)
C(22)-Ru(1)-O(3)	95.94(7)
C(1)-Ru(1)-O(3)	92.45(6)
C(22)-Ru(1)-O(2)	124.02(7)
C(1)-Ru(1)-O(2)	139.80(6)
O(3)-Ru(1)-O(2)	82.98(5)
C(22)-Ru(1)-O(1)	80.26(6)
C(1)-Ru(1)-O(1)	94.49(6)
O(3)-Ru(1)-O(1)	172.41(5)
O(2)-Ru(1)-O(1)	93.66(5)
C(28)-O(1)-C(29)	117.97(13)
C(28)-O(1)-Ru(1)	110.24(10)
C(29)-O(1)-Ru(1)	114.35(9)
C(32)-O(2)-Ru(1)	109.97(10)
C(37)-O(3)-Ru(1)	109.99(10)
C(1)-N(1)-C(4)	127.10(15)
C(1)-N(1)-C(2)	112.66(14)
C(4)-N(1)-C(2)	118.52(15)
C(1)-N(2)-C(13)	123.91(15)
C(1)-N(2)-C(3)	113.59(14)
C(13)-N(2)-C(3)	122.46(14)
N(1)-C(1)-N(2)	108.28(15)
N(1)-C(1)-Ru(1)	136.05(13)
N(2)-C(1)-Ru(1)	115.63(12)
N(1)-C(2)-C(3)	103.12(15)
N(1)-C(2)-H(2A)	111.1
C(3)-C(2)-H(2A)	111.1
N(1)-C(2)-H(2B)	111.1
C(3)-C(2)-H(2B)	111.1
H(2A)-C(2)-H(2B)	109.1
N(2)-C(3)-C(2)	102.06(14)
N(2)-C(3)-H(3A)	111.4
C(2)-C(3)-H(3A)	111.4

N(2)-C(3)-H(3B)	111.4
C(2)-C(3)-H(3B)	111.4
H(3A)-C(3)-H(3B)	109.2
C(9)-C(4)-C(5)	121.94(16)
C(9)-C(4)-N(1)	119.00(16)
C(5)-C(4)-N(1)	118.93(15)
C(6)-C(5)-C(4)	117.81(17)
C(6)-C(5)-C(10)	120.81(17)
C(4)-C(5)-C(10)	121.37(16)
C(7)-C(6)-C(5)	121.89(18)
C(7)-C(6)-H(6)	119.1
C(5)-C(6)-H(6)	119.1
C(8)-C(7)-C(6)	118.36(17)
C(8)-C(7)-C(11)	120.98(18)
C(6)-C(7)-C(11)	120.66(19)
C(7)-C(8)-C(9)	122.13(17)
C(7)-C(8)-H(8)	118.9
C(9)-C(8)-H(8)	118.9
C(4)-C(9)-C(8)	117.85(17)
C(4)-C(9)-C(12)	121.49(16)
C(8)-C(9)-C(12)	120.65(17)
C(5)-C(10)-H(10A)	109.5
C(5)-C(10)-H(10B)	109.5
H(10A)-C(10)-H(10B)	109.5
C(5)-C(10)-H(10C)	109.5
H(10A)-C(10)-H(10C)	109.5
H(10B)-C(10)-H(10C)	109.5
C(7)-C(11)-H(11A)	109.5
C(7)-C(11)-H(11B)	109.5
H(11A)-C(11)-H(11B)	109.5
C(7)-C(11)-H(11C)	109.5
H(11A)-C(11)-H(11C)	109.5
H(11B)-C(11)-H(11C)	109.5
C(9)-C(12)-H(12A)	109.5
C(9)-C(12)-H(12B)	109.5
H(12A)-C(12)-H(12B)	109.5
C(9)-C(12)-H(12C)	109.5

H(12A)-C(12)-H(12C)	109.5
H(12B)-C(12)-H(12C)	109.5
C(14)-C(13)-C(18)	121.65(16)
C(14)-C(13)-N(2)	119.82(15)
C(18)-C(13)-N(2)	118.49(16)
C(15)-C(14)-C(13)	118.04(16)
C(15)-C(14)-C(19)	120.65(16)
C(13)-C(14)-C(19)	121.14(16)
C(16)-C(15)-C(14)	121.76(17)
C(16)-C(15)-H(15)	119.1
C(14)-C(15)-H(15)	119.1
C(15)-C(16)-C(17)	118.55(17)
C(15)-C(16)-C(20)	121.19(17)
C(17)-C(16)-C(20)	120.22(17)
C(18)-C(17)-C(16)	122.01(17)
C(18)-C(17)-H(17)	119.0
C(16)-C(17)-H(17)	119.0
C(17)-C(18)-C(13)	117.86(16)
C(17)-C(18)-C(21)	120.60(16)
C(13)-C(18)-C(21)	121.54(16)
C(14)-C(19)-H(19A)	109.5
C(14)-C(19)-H(19B)	109.5
H(19A)-C(19)-H(19B)	109.5
C(14)-C(19)-H(19C)	109.5
H(19A)-C(19)-H(19C)	109.5
H(19B)-C(19)-H(19C)	109.5
C(16)-C(20)-H(20A)	109.5
C(16)-C(20)-H(20B)	109.5
H(20A)-C(20)-H(20B)	109.5
C(16)-C(20)-H(20C)	109.5
H(20A)-C(20)-H(20C)	109.5
H(20B)-C(20)-H(20C)	109.5
C(18)-C(21)-H(21A)	109.5
C(18)-C(21)-H(21B)	109.5
H(21A)-C(21)-H(21B)	109.5
C(18)-C(21)-H(21C)	109.5
H(21A)-C(21)-H(21C)	109.5

H(21B)-C(21)-H(21C)	109.5
C(23)-C(22)-Ru(1)	119.19(13)
C(23)-C(22)-H(22)	120.4
Ru(1)-C(22)-H(22)	120.4
C(28)-C(23)-C(24)	118.47(16)
C(28)-C(23)-C(22)	116.46(16)
C(24)-C(23)-C(22)	125.01(17)
C(25)-C(24)-C(23)	120.59(17)
C(25)-C(24)-H(24)	119.7
C(23)-C(24)-H(24)	119.7
C(24)-C(25)-C(26)	119.67(17)
C(24)-C(25)-H(25)	120.2
C(26)-C(25)-H(25)	120.2
C(25)-C(26)-C(27)	121.04(17)
C(25)-C(26)-H(26)	119.5
C(27)-C(26)-H(26)	119.5
C(28)-C(27)-C(26)	118.40(17)
C(28)-C(27)-H(27)	120.8
C(26)-C(27)-H(27)	120.8
C(27)-C(28)-C(23)	121.80(16)
C(27)-C(28)-O(1)	124.33(16)
C(23)-C(28)-O(1)	113.82(15)
O(1)-C(29)-C(31)	110.47(14)
O(1)-C(29)-C(30)	111.71(15)
C(31)-C(29)-C(30)	114.26(16)
O(1)-C(29)-H(29)	106.6
C(31)-C(29)-H(29)	106.6
C(30)-C(29)-H(29)	106.6
C(29)-C(30)-H(30A)	109.5
C(29)-C(30)-H(30B)	109.5
H(30A)-C(30)-H(30B)	109.5
C(29)-C(30)-H(30C)	109.5
H(30A)-C(30)-H(30C)	109.5
H(30B)-C(30)-H(30C)	109.5
C(29)-C(31)-H(31A)	109.5
C(29)-C(31)-H(31B)	109.5
H(31A)-C(31)-H(31B)	109.5

C(29)-C(31)-H(31C)	109.5
H(31A)-C(31)-H(31C)	109.5
H(31B)-C(31)-H(31C)	109.5
O(2)-C(32)-C(33)	123.46(16)
O(2)-C(32)-C(37)	117.71(16)
C(33)-C(32)-C(37)	118.80(16)
F(1)-C(33)-C(32)	120.07(16)
F(1)-C(33)-C(34)	118.02(16)
C(32)-C(33)-C(34)	121.89(17)
F(2)-C(34)-C(35)	120.49(16)
F(2)-C(34)-C(33)	120.30(17)
C(35)-C(34)-C(33)	119.21(17)
F(3)-C(35)-C(34)	120.20(17)
F(3)-C(35)-C(36)	119.83(17)
C(34)-C(35)-C(36)	119.97(16)
F(4)-C(36)-C(35)	118.50(15)
F(4)-C(36)-C(37)	119.76(16)
C(35)-C(36)-C(37)	121.73(17)
O(3)-C(37)-C(36)	122.95(16)
O(3)-C(37)-C(32)	118.66(15)
C(36)-C(37)-C(32)	118.39(17)

Symmetry transformations used to generate equivalent atoms:

Table 4. Anisotropic displacement parameters ($\approx 2 \times 10^3$) for Ru4c. The anisotropic displacement factor exponent takes the form: $-2\pi^2 [h^2 a^{*2} U^{11} + \dots + 2 h k a^{*} b^{*} U^{12}]$

	U ¹¹	U ²²	U ³³	U ²³	U ¹³	U ¹²
Ru(1)	11(1)	8(1)	12(1)	1(1)	2(1)	5(1)
F(1)	18(1)	18(1)	34(1)	2(1)	-2(1)	11(1)
F(2)	16(1)	20(1)	41(1)	-3(1)	-6(1)	3(1)
F(3)	24(1)	9(1)	36(1)	-2(1)	3(1)	2(1)
F(4)	25(1)	12(1)	32(1)	5(1)	7(1)	11(1)
O(1)	14(1)	11(1)	14(1)	-1(1)	-1(1)	7(1)
O(2)	14(1)	9(1)	18(1)	1(1)	2(1)	6(1)
O(3)	14(1)	11(1)	20(1)	2(1)	2(1)	6(1)

N(1)	12(1)	17(1)	12(1)	0(1)	1(1)	7(1)
N(2)	14(1)	20(1)	12(1)	-1(1)	1(1)	8(1)
C(1)	16(1)	7(1)	13(1)	1(1)	0(1)	6(1)
C(2)	17(1)	30(1)	17(1)	-3(1)	3(1)	12(1)
C(3)	15(1)	21(1)	15(1)	0(1)	4(1)	8(1)
C(4)	14(1)	19(1)	12(1)	0(1)	1(1)	9(1)
C(5)	16(1)	20(1)	18(1)	0(1)	0(1)	11(1)
C(6)	22(1)	27(1)	19(1)	7(1)	3(1)	14(1)
C(7)	18(1)	34(1)	14(1)	0(1)	1(1)	14(1)
C(8)	16(1)	24(1)	17(1)	-6(1)	1(1)	6(1)
C(9)	13(1)	20(1)	17(1)	-1(1)	3(1)	9(1)
C(10)	26(1)	18(1)	24(1)	2(1)	-1(1)	12(1)
C(11)	31(1)	48(1)	15(1)	1(1)	0(1)	16(1)
C(12)	22(1)	18(1)	24(1)	-1(1)	4(1)	6(1)
C(13)	13(1)	17(1)	9(1)	0(1)	2(1)	7(1)
C(14)	16(1)	16(1)	11(1)	1(1)	5(1)	7(1)
C(15)	18(1)	21(1)	12(1)	2(1)	4(1)	12(1)
C(16)	15(1)	23(1)	11(1)	-1(1)	2(1)	8(1)
C(17)	18(1)	14(1)	15(1)	-1(1)	4(1)	4(1)
C(18)	20(1)	17(1)	13(1)	3(1)	6(1)	9(1)
C(19)	21(1)	15(1)	19(1)	2(1)	3(1)	8(1)
C(20)	19(1)	31(1)	23(1)	-7(1)	-3(1)	10(1)
C(21)	28(1)	17(1)	21(1)	4(1)	5(1)	12(1)
C(22)	21(1)	15(1)	17(1)	6(1)	7(1)	11(1)
C(23)	16(1)	17(1)	16(1)	2(1)	6(1)	9(1)
C(24)	24(1)	23(1)	16(1)	3(1)	5(1)	14(1)
C(25)	21(1)	26(1)	16(1)	-4(1)	-1(1)	12(1)
C(26)	22(1)	16(1)	25(1)	-5(1)	-2(1)	9(1)
C(27)	20(1)	14(1)	23(1)	1(1)	-1(1)	8(1)
C(28)	12(1)	16(1)	14(1)	-1(1)	1(1)	7(1)
C(29)	16(1)	13(1)	17(1)	1(1)	-4(1)	10(1)
C(30)	28(1)	14(1)	22(1)	3(1)	-4(1)	9(1)
C(31)	19(1)	18(1)	27(1)	-3(1)	1(1)	10(1)
C(32)	17(1)	12(1)	13(1)	2(1)	6(1)	7(1)
C(33)	17(1)	16(1)	19(1)	2(1)	3(1)	10(1)
C(34)	14(1)	16(1)	22(1)	-1(1)	1(1)	3(1)
C(35)	21(1)	9(1)	21(1)	-1(1)	6(1)	3(1)

C(36)	21(1)	12(1)	19(1)	4(1)	8(1)	10(1)
C(37)	17(1)	13(1)	12(1)	2(1)	5(1)	7(1)

Table 5. Hydrogen coordinates ($\times 10^4$) and isotropic displacement parameters ($\approx 2 \times 10^{-3}$) for Ru4c.

	x	y	z	U(eq)
H(2A)	-3685	3243	2829	26
H(2B)	-3194	4888	2731	26
H(3A)	-1556	5588	3931	21
H(3B)	-1936	3953	3991	21
H(6)	-2808	5689	-3	26
H(8)	-4996	1420	-33	25
H(10A)	-1622	6805	1952	35
H(10B)	-1164	7315	1149	35
H(10C)	-228	6722	1719	35
H(11A)	-5661	2329	-1176	50
H(11B)	-4075	3428	-1343	50
H(11C)	-5155	4003	-1102	50
H(12A)	-2975	1422	1833	35
H(12B)	-4249	400	1058	35
H(12C)	-4693	1080	1739	35
H(15)	3442	4601	5044	19
H(17)	4034	8591	4912	21
H(19A)	1219	2531	4299	29
H(19B)	114	2710	3580	29
H(19C)	-138	2775	4459	29
H(20A)	6306	7767	5372	41
H(20B)	5592	6560	5904	41
H(20C)	5576	8048	6051	41
H(21A)	544	7835	4035	33
H(21B)	1295	7896	3303	33
H(21C)	2254	9034	4101	33
H(22)	464	5071	923	19
H(24)	-1070	3027	-307	24

H(25)	-2227	595	-823	26
H(26)	-2138	-1032	4	27
H(27)	-884	-245	1356	24
H(29)	2331	2784	2994	19
H(30A)	710	-138	2307	35
H(30B)	63	462	2914	35
H(30C)	1690	560	3200	35
H(31A)	3587	2039	2267	33
H(31B)	3248	3206	1861	33
H(31C)	2234	1542	1488	33

Table 6. Torsion angles [\circ] for Ru4c.

C(4)-N(1)-C(1)-N(2)	165.33(16)
C(2)-N(1)-C(1)-N(2)	0.6(2)
C(4)-N(1)-C(1)-Ru(1)	-17.0(3)
C(2)-N(1)-C(1)-Ru(1)	178.31(14)
C(13)-N(2)-C(1)-N(1)	-178.99(15)
C(3)-N(2)-C(1)-N(1)	3.1(2)
C(13)-N(2)-C(1)-Ru(1)	2.8(2)
C(3)-N(2)-C(1)-Ru(1)	-175.13(11)
C(1)-N(1)-C(2)-C(3)	-3.7(2)
C(4)-N(1)-C(2)-C(3)	-169.88(15)
C(1)-N(2)-C(3)-C(2)	-5.2(2)
C(13)-N(2)-C(3)-C(2)	176.85(16)
N(1)-C(2)-C(3)-N(2)	4.95(18)
C(1)-N(1)-C(4)-C(9)	112.9(2)
C(2)-N(1)-C(4)-C(9)	-83.2(2)
C(1)-N(1)-C(4)-C(5)	-71.2(2)
C(2)-N(1)-C(4)-C(5)	92.7(2)
C(9)-C(4)-C(5)-C(6)	-0.8(3)
N(1)-C(4)-C(5)-C(6)	-176.63(16)
C(9)-C(4)-C(5)-C(10)	178.62(17)
N(1)-C(4)-C(5)-C(10)	2.8(3)
C(4)-C(5)-C(6)-C(7)	1.2(3)
C(10)-C(5)-C(6)-C(7)	-178.24(18)
C(5)-C(6)-C(7)-C(8)	-0.8(3)

C(5)-C(6)-C(7)-C(11)	179.75(19)
C(6)-C(7)-C(8)-C(9)	0.0(3)
C(11)-C(7)-C(8)-C(9)	179.45(19)
C(5)-C(4)-C(9)-C(8)	0.1(3)
N(1)-C(4)-C(9)-C(8)	175.88(16)
C(5)-C(4)-C(9)-C(12)	179.23(18)
N(1)-C(4)-C(9)-C(12)	-4.9(3)
C(7)-C(8)-C(9)-C(4)	0.4(3)
C(7)-C(8)-C(9)-C(12)	-178.82(18)
C(1)-N(2)-C(13)-C(14)	-84.7(2)
C(3)-N(2)-C(13)-C(14)	93.1(2)
C(1)-N(2)-C(13)-C(18)	97.5(2)
C(3)-N(2)-C(13)-C(18)	-84.8(2)
C(18)-C(13)-C(14)-C(15)	-4.3(3)
N(2)-C(13)-C(14)-C(15)	177.98(15)
C(18)-C(13)-C(14)-C(19)	171.00(16)
N(2)-C(13)-C(14)-C(19)	-6.8(2)
C(13)-C(14)-C(15)-C(16)	2.6(3)
C(19)-C(14)-C(15)-C(16)	-172.63(16)
C(14)-C(15)-C(16)-C(17)	0.3(3)
C(14)-C(15)-C(16)-C(20)	178.04(17)
C(15)-C(16)-C(17)-C(18)	-1.8(3)
C(20)-C(16)-C(17)-C(18)	-179.58(17)
C(16)-C(17)-C(18)-C(13)	0.3(3)
C(16)-C(17)-C(18)-C(21)	-179.89(17)
C(14)-C(13)-C(18)-C(17)	2.8(3)
N(2)-C(13)-C(18)-C(17)	-179.38(16)
C(14)-C(13)-C(18)-C(21)	-176.99(17)
N(2)-C(13)-C(18)-C(21)	0.8(3)
C(1)-Ru(1)-C(22)-C(23)	-92.69(15)
O(3)-Ru(1)-C(22)-C(23)	174.18(14)
O(2)-Ru(1)-C(22)-C(23)	88.66(15)
O(1)-Ru(1)-C(22)-C(23)	0.82(14)
Ru(1)-C(22)-C(23)-C(28)	-0.2(2)
Ru(1)-C(22)-C(23)-C(24)	177.05(15)
C(28)-C(23)-C(24)-C(25)	-0.1(3)
C(22)-C(23)-C(24)-C(25)	-177.30(18)

C(23)-C(24)-C(25)-C(26)	0.7(3)
C(24)-C(25)-C(26)-C(27)	-0.2(3)
C(25)-C(26)-C(27)-C(28)	-0.8(3)
C(26)-C(27)-C(28)-C(23)	1.4(3)
C(26)-C(27)-C(28)-O(1)	178.65(17)
C(24)-C(23)-C(28)-C(27)	-1.0(3)
C(22)-C(23)-C(28)-C(27)	176.47(17)
C(24)-C(23)-C(28)-O(1)	-178.46(16)
C(22)-C(23)-C(28)-O(1)	-1.0(2)
C(29)-O(1)-C(28)-C(27)	50.2(2)
Ru(1)-O(1)-C(28)-C(27)	-175.87(15)
C(29)-O(1)-C(28)-C(23)	-132.34(16)
Ru(1)-O(1)-C(28)-C(23)	1.56(18)
C(28)-O(1)-C(29)-C(31)	49.37(19)
Ru(1)-O(1)-C(29)-C(31)	-82.72(14)
C(28)-O(1)-C(29)-C(30)	-79.00(19)
Ru(1)-O(1)-C(29)-C(30)	148.91(12)
Ru(1)-O(2)-C(32)-C(33)	172.15(14)
Ru(1)-O(2)-C(32)-C(37)	-5.72(18)
O(2)-C(32)-C(33)-F(1)	0.4(3)
C(37)-C(32)-C(33)-F(1)	178.21(15)
O(2)-C(32)-C(33)-C(34)	-178.21(16)
C(37)-C(32)-C(33)-C(34)	-0.4(3)
F(1)-C(33)-C(34)-F(2)	0.5(3)
C(32)-C(33)-C(34)-F(2)	179.14(17)
F(1)-C(33)-C(34)-C(35)	-178.85(17)
C(32)-C(33)-C(34)-C(35)	-0.2(3)
F(2)-C(34)-C(35)-F(3)	1.2(3)
C(33)-C(34)-C(35)-F(3)	-179.45(16)
F(2)-C(34)-C(35)-C(36)	-178.93(17)
C(33)-C(34)-C(35)-C(36)	0.5(3)
F(3)-C(35)-C(36)-F(4)	-1.1(3)
C(34)-C(35)-C(36)-F(4)	178.96(16)
F(3)-C(35)-C(36)-C(37)	179.85(16)
C(34)-C(35)-C(36)-C(37)	0.0(3)
Ru(1)-O(3)-C(37)-C(36)	-172.80(14)
Ru(1)-O(3)-C(37)-C(32)	6.20(19)

F(4)-C(36)-C(37)-O(3)	-0.5(3)
C(35)-C(36)-C(37)-O(3)	178.45(16)
F(4)-C(36)-C(37)-C(32)	-179.55(15)
C(35)-C(36)-C(37)-C(32)	-0.6(3)
O(2)-C(32)-C(37)-O(3)	-0.3(2)
C(33)-C(32)-C(37)-O(3)	-178.30(15)
O(2)-C(32)-C(37)-C(36)	178.72(15)
C(33)-C(32)-C(37)-C(36)	0.7(3)

Symmetry transformations used to generate equivalent atoms:

X-ray structure of Ru4d:

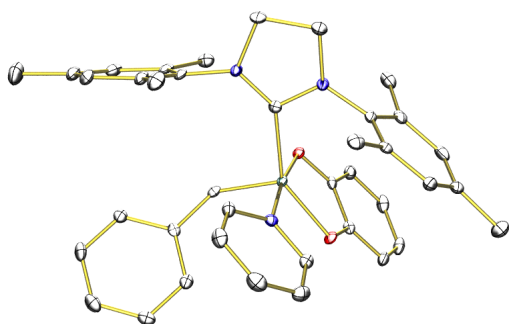


Table 1. Crystal data and structure refinement for Ru4d.

Identification code	C39H41N3O2Ru(C6H6)		
Empirical formula	C45 H47 N3 O2 Ru		
Formula weight	762.92		
Temperature	100(2) K		
Wavelength	0.71073 \approx		
Crystal system	Monoclinic		
Space group	P 21/n		
Unit cell dimensions	a = 15.5758(8) \approx	$\alpha = 90^\circ$.	
	b = 15.5050(8) \approx	$\beta = 98.722(3)^\circ$.	
	c = 15.5858(8) \approx	$\gamma = 90^\circ$.	
Volume	3720.5(3) Å^3		
Z	4		
Density (calculated)	1.362 Mg/m ³		
Absorption coefficient	0.463 mm ⁻¹		
F(000)	1592		
Crystal size	0.300 x 0.150 x 0.060 mm ³		

Theta range for data collection	1.722 to 28.372°.
Index ranges	-20≤h≤20, -20≤k≤20, -19≤l≤20
Reflections collected	63599
Independent reflections	9104 [R(int) = 0.0961]
Completeness to theta = 25.242°	99.6 %
Absorption correction	Semi-empirical from equivalents
Max. and min. transmission	0.7457 and 0.6709
Refinement method	Full-matrix least-squares on F ²
Data / restraints / parameters	9104 / 0 / 466
Goodness-of-fit on F ²	1.008
Final R indices [I>2sigma(I)]	R1 = 0.0430, wR2 = 0.0766
R indices (all data)	R1 = 0.0859, wR2 = 0.0891
Extinction coefficient	na
Largest diff. peak and hole	0.587 and -0.619 e.Å ⁻³

Table 2. Atomic coordinates (x 10⁴) and equivalent isotropic displacement parameters (≈ x 10³) for Ru4d. U(eq) is defined as one third of the trace of the orthogonalized U^{ij} tensor.

	x	y	z	U(eq)
Ru(1)	2490(1)	9680(1)	1925(1)	11(1)
O(1)	1332(1)	9340(1)	1272(1)	15(1)
O(2)	1956(1)	9178(1)	2951(1)	14(1)
N(1)	2717(1)	11294(1)	2802(2)	16(1)
N(2)	3993(1)	10706(1)	3102(2)	16(1)
N(3)	2868(1)	10142(1)	790(1)	13(1)
C(1)	3183(2)	10587(2)	2674(2)	13(1)
C(2)	3206(2)	11966(2)	3331(2)	22(1)
C(3)	4087(2)	11534(2)	3585(2)	24(1)
C(4)	1868(2)	11408(2)	2309(2)	15(1)
C(5)	1145(2)	11140(2)	2682(2)	19(1)
C(6)	339(2)	11163(2)	2146(2)	24(1)
C(7)	242(2)	11465(2)	1301(2)	23(1)
C(8)	963(2)	11794(2)	991(2)	21(1)
C(9)	1786(2)	11777(2)	1486(2)	18(1)
C(10)	1233(2)	10860(2)	3610(2)	24(1)
C(11)	-629(2)	11419(2)	727(2)	36(1)
C(12)	2555(2)	12168(2)	1142(2)	20(1)

C(13)	4695(2)	10098(2)	3222(2)	16(1)
C(14)	5422(2)	10256(2)	2824(2)	18(1)
C(15)	6134(2)	9701(2)	3008(2)	21(1)
C(16)	6126(2)	9003(2)	3555(2)	21(1)
C(17)	5384(2)	8866(2)	3944(2)	20(1)
C(18)	4674(2)	9415(2)	3809(2)	17(1)
C(19)	5478(2)	11018(2)	2233(2)	24(1)
C(20)	6900(2)	8407(2)	3728(2)	36(1)
C(21)	3917(2)	9295(2)	4300(2)	20(1)
C(22)	3296(2)	8805(2)	2033(2)	13(1)
C(23)	3761(2)	8397(2)	1390(2)	13(1)
C(24)	4602(2)	8066(2)	1651(2)	16(1)
C(25)	5060(2)	7680(2)	1059(2)	21(1)
C(26)	4692(2)	7599(2)	197(2)	23(1)
C(27)	3854(2)	7900(2)	-69(2)	20(1)
C(28)	3393(2)	8295(2)	519(2)	17(1)
C(29)	797(2)	9008(2)	1796(2)	14(1)
C(30)	1134(2)	8928(2)	2688(2)	14(1)
C(31)	597(2)	8596(2)	3250(2)	17(1)
C(32)	-253(2)	8342(2)	2934(2)	21(1)
C(33)	-570(2)	8421(2)	2063(2)	21(1)
C(34)	-54(2)	8761(2)	1487(2)	18(1)
C(35)	2260(2)	10275(2)	83(2)	16(1)
C(36)	2469(2)	10550(2)	-702(2)	21(1)
C(37)	3328(2)	10724(2)	-776(2)	25(1)
C(38)	3953(2)	10598(2)	-59(2)	21(1)
C(39)	3704(2)	10298(2)	700(2)	17(1)
C(1S)	7522(2)	1604(2)	3985(3)	40(1)
C(2S)	7611(2)	1638(2)	3129(3)	37(1)
C(3S)	8098(2)	1032(2)	2787(2)	38(1)
C(4S)	8510(2)	392(2)	3297(3)	40(1)
C(5S)	8441(2)	366(3)	4166(3)	45(1)
C(6S)	7931(2)	961(3)	4508(3)	47(1)

Table 3. Bond lengths [\AA] and angles [$^\circ$] for Ru4d.

Ru(1)-C(22)	1.839(3)
Ru(1)-O(1)	2.0029(16)
Ru(1)-C(1)	2.031(3)
Ru(1)-O(2)	2.0639(18)
Ru(1)-N(3)	2.074(2)
O(1)-C(29)	1.354(3)
O(2)-C(30)	1.341(3)
N(1)-C(1)	1.347(3)
N(1)-C(4)	1.436(3)
N(1)-C(2)	1.468(3)
N(2)-C(1)	1.347(3)
N(2)-C(13)	1.435(3)
N(2)-C(3)	1.484(3)
N(3)-C(39)	1.353(3)
N(3)-C(35)	1.354(3)
C(2)-C(3)	1.523(4)
C(2)-H(2A)	0.9900
C(2)-H(2B)	0.9900
C(3)-H(3A)	0.9900
C(3)-H(3B)	0.9900
C(4)-C(9)	1.394(4)
C(4)-C(5)	1.405(4)
C(5)-C(6)	1.399(4)
C(5)-C(10)	1.496(4)
C(6)-C(7)	1.385(4)
C(6)-H(6)	0.9500
C(7)-C(8)	1.386(4)
C(7)-C(11)	1.508(4)
C(8)-C(9)	1.392(4)
C(8)-H(8)	0.9500
C(9)-C(12)	1.511(4)
C(10)-H(10A)	0.9800
C(10)-H(10B)	0.9800
C(10)-H(10C)	0.9800
C(11)-H(11A)	0.9800

C(11)-H(11B)	0.9800
C(11)-H(11C)	0.9800
C(12)-H(12A)	0.9800
C(12)-H(12B)	0.9800
C(12)-H(12C)	0.9800
C(13)-C(14)	1.394(4)
C(13)-C(18)	1.403(4)
C(14)-C(15)	1.397(4)
C(14)-C(19)	1.509(4)
C(15)-C(16)	1.379(4)
C(15)-H(15)	0.9500
C(16)-C(17)	1.400(4)
C(16)-C(20)	1.510(4)
C(17)-C(18)	1.386(4)
C(17)-H(17)	0.9500
C(18)-C(21)	1.511(4)
C(19)-H(19A)	0.9800
C(19)-H(19B)	0.9800
C(19)-H(19C)	0.9800
C(20)-H(20A)	0.9800
C(20)-H(20B)	0.9800
C(20)-H(20C)	0.9800
C(21)-H(21A)	0.9800
C(21)-H(21B)	0.9800
C(21)-H(21C)	0.9800
C(22)-C(23)	1.466(4)
C(22)-H(22)	0.9500
C(23)-C(28)	1.400(4)
C(23)-C(24)	1.407(3)
C(24)-C(25)	1.386(4)
C(24)-H(24)	0.9500
C(25)-C(26)	1.383(4)
C(25)-H(25)	0.9500
C(26)-C(27)	1.389(4)
C(26)-H(26)	0.9500
C(27)-C(28)	1.389(4)
C(27)-H(27)	0.9500

C(28)-H(28)	0.9500
C(29)-C(34)	1.394(3)
C(29)-C(30)	1.414(4)
C(30)-C(31)	1.399(4)
C(31)-C(32)	1.396(4)
C(31)-H(31)	0.9500
C(32)-C(33)	1.377(4)
C(32)-H(32)	0.9500
C(33)-C(34)	1.396(4)
C(33)-H(33)	0.9500
C(34)-H(34)	0.9500
C(35)-C(36)	1.381(4)
C(35)-H(35)	0.9500
C(36)-C(37)	1.386(4)
C(36)-H(36)	0.9500
C(37)-C(38)	1.381(4)
C(37)-H(37)	0.9500
C(38)-C(39)	1.380(4)
C(38)-H(38)	0.9500
C(39)-H(39)	0.9500
C(1S)-C(2S)	1.364(5)
C(1S)-C(6S)	1.381(5)
C(1S)-H(1S)	0.9500
C(2S)-C(3S)	1.365(5)
C(2S)-H(2S)	0.9500
C(3S)-C(4S)	1.369(5)
C(3S)-H(3S)	0.9500
C(4S)-C(5S)	1.376(5)
C(4S)-H(4S)	0.9500
C(5S)-C(6S)	1.377(5)
C(5S)-H(5S)	0.9500
C(6S)-H(6S)	0.9500
C(22)-Ru(1)-O(1)	113.73(9)
C(22)-Ru(1)-C(1)	99.32(10)
O(1)-Ru(1)-C(1)	146.49(9)
C(22)-Ru(1)-O(2)	90.08(10)

O(1)-Ru(1)-O(2)	81.77(7)
C(1)-Ru(1)-O(2)	93.25(9)
C(22)-Ru(1)-N(3)	93.17(10)
O(1)-Ru(1)-N(3)	90.43(8)
C(1)-Ru(1)-N(3)	93.22(9)
O(2)-Ru(1)-N(3)	172.20(7)
C(29)-O(1)-Ru(1)	112.49(16)
C(30)-O(2)-Ru(1)	110.46(15)
C(1)-N(1)-C(4)	119.6(2)
C(1)-N(1)-C(2)	114.5(2)
C(4)-N(1)-C(2)	124.9(2)
C(1)-N(2)-C(13)	127.8(2)
C(1)-N(2)-C(3)	112.5(2)
C(13)-N(2)-C(3)	119.2(2)
C(39)-N(3)-C(35)	116.9(2)
C(39)-N(3)-Ru(1)	123.51(18)
C(35)-N(3)-Ru(1)	119.54(17)
N(1)-C(1)-N(2)	107.5(2)
N(1)-C(1)-Ru(1)	113.42(17)
N(2)-C(1)-Ru(1)	139.11(19)
N(1)-C(2)-C(3)	101.8(2)
N(1)-C(2)-H(2A)	111.4
C(3)-C(2)-H(2A)	111.4
N(1)-C(2)-H(2B)	111.4
C(3)-C(2)-H(2B)	111.4
H(2A)-C(2)-H(2B)	109.3
N(2)-C(3)-C(2)	103.5(2)
N(2)-C(3)-H(3A)	111.1
C(2)-C(3)-H(3A)	111.1
N(2)-C(3)-H(3B)	111.1
C(2)-C(3)-H(3B)	111.1
H(3A)-C(3)-H(3B)	109.0
C(9)-C(4)-C(5)	122.4(2)
C(9)-C(4)-N(1)	119.4(2)
C(5)-C(4)-N(1)	118.3(2)
C(6)-C(5)-C(4)	116.6(3)
C(6)-C(5)-C(10)	121.8(3)

C(4)-C(5)-C(10)	121.6(2)
C(7)-C(6)-C(5)	122.4(3)
C(7)-C(6)-H(6)	118.8
C(5)-C(6)-H(6)	118.8
C(6)-C(7)-C(8)	118.5(3)
C(6)-C(7)-C(11)	120.5(3)
C(8)-C(7)-C(11)	121.0(3)
C(7)-C(8)-C(9)	121.9(3)
C(7)-C(8)-H(8)	119.1
C(9)-C(8)-H(8)	119.1
C(8)-C(9)-C(4)	117.7(3)
C(8)-C(9)-C(12)	120.6(3)
C(4)-C(9)-C(12)	121.7(2)
C(5)-C(10)-H(10A)	109.5
C(5)-C(10)-H(10B)	109.5
H(10A)-C(10)-H(10B)	109.5
C(5)-C(10)-H(10C)	109.5
H(10A)-C(10)-H(10C)	109.5
H(10B)-C(10)-H(10C)	109.5
C(7)-C(11)-H(11A)	109.5
C(7)-C(11)-H(11B)	109.5
H(11A)-C(11)-H(11B)	109.5
C(7)-C(11)-H(11C)	109.5
H(11A)-C(11)-H(11C)	109.5
H(11B)-C(11)-H(11C)	109.5
C(9)-C(12)-H(12A)	109.5
C(9)-C(12)-H(12B)	109.5
H(12A)-C(12)-H(12B)	109.5
C(9)-C(12)-H(12C)	109.5
H(12A)-C(12)-H(12C)	109.5
H(12B)-C(12)-H(12C)	109.5
C(14)-C(13)-C(18)	121.6(2)
C(14)-C(13)-N(2)	118.8(2)
C(18)-C(13)-N(2)	119.2(2)
C(13)-C(14)-C(15)	118.2(3)
C(13)-C(14)-C(19)	122.3(2)
C(15)-C(14)-C(19)	119.4(2)

C(16)-C(15)-C(14)	122.0(3)
C(16)-C(15)-H(15)	119.0
C(14)-C(15)-H(15)	119.0
C(15)-C(16)-C(17)	118.1(3)
C(15)-C(16)-C(20)	120.6(3)
C(17)-C(16)-C(20)	121.3(3)
C(18)-C(17)-C(16)	122.3(3)
C(18)-C(17)-H(17)	118.9
C(16)-C(17)-H(17)	118.9
C(17)-C(18)-C(13)	117.7(3)
C(17)-C(18)-C(21)	120.9(3)
C(13)-C(18)-C(21)	121.4(2)
C(14)-C(19)-H(19A)	109.5
C(14)-C(19)-H(19B)	109.5
H(19A)-C(19)-H(19B)	109.5
C(14)-C(19)-H(19C)	109.5
H(19A)-C(19)-H(19C)	109.5
H(19B)-C(19)-H(19C)	109.5
C(16)-C(20)-H(20A)	109.5
C(16)-C(20)-H(20B)	109.5
H(20A)-C(20)-H(20B)	109.5
C(16)-C(20)-H(20C)	109.5
H(20A)-C(20)-H(20C)	109.5
H(20B)-C(20)-H(20C)	109.5
C(18)-C(21)-H(21A)	109.5
C(18)-C(21)-H(21B)	109.5
H(21A)-C(21)-H(21B)	109.5
C(18)-C(21)-H(21C)	109.5
H(21A)-C(21)-H(21C)	109.5
H(21B)-C(21)-H(21C)	109.5
C(23)-C(22)-Ru(1)	131.1(2)
C(23)-C(22)-H(22)	114.5
Ru(1)-C(22)-H(22)	114.5
C(28)-C(23)-C(24)	117.7(2)
C(28)-C(23)-C(22)	122.7(2)
C(24)-C(23)-C(22)	119.6(2)
C(25)-C(24)-C(23)	121.0(3)

C(25)-C(24)-H(24)	119.5
C(23)-C(24)-H(24)	119.5
C(26)-C(25)-C(24)	120.4(3)
C(26)-C(25)-H(25)	119.8
C(24)-C(25)-H(25)	119.8
C(25)-C(26)-C(27)	119.5(3)
C(25)-C(26)-H(26)	120.3
C(27)-C(26)-H(26)	120.3
C(28)-C(27)-C(26)	120.4(3)
C(28)-C(27)-H(27)	119.8
C(26)-C(27)-H(27)	119.8
C(27)-C(28)-C(23)	120.9(2)
C(27)-C(28)-H(28)	119.6
C(23)-C(28)-H(28)	119.6
O(1)-C(29)-C(34)	122.4(2)
O(1)-C(29)-C(30)	117.1(2)
C(34)-C(29)-C(30)	120.5(2)
O(2)-C(30)-C(31)	123.3(2)
O(2)-C(30)-C(29)	118.1(2)
C(31)-C(30)-C(29)	118.6(2)
C(32)-C(31)-C(30)	120.5(3)
C(32)-C(31)-H(31)	119.7
C(30)-C(31)-H(31)	119.7
C(33)-C(32)-C(31)	120.2(3)
C(33)-C(32)-H(32)	119.9
C(31)-C(32)-H(32)	119.9
C(32)-C(33)-C(34)	120.7(3)
C(32)-C(33)-H(33)	119.6
C(34)-C(33)-H(33)	119.6
C(29)-C(34)-C(33)	119.5(3)
C(29)-C(34)-H(34)	120.3
C(33)-C(34)-H(34)	120.3
N(3)-C(35)-C(36)	122.6(2)
N(3)-C(35)-H(35)	118.7
C(36)-C(35)-H(35)	118.7
C(35)-C(36)-C(37)	119.6(3)
C(35)-C(36)-H(36)	120.2

C(37)-C(36)-H(36)	120.2
C(38)-C(37)-C(36)	118.4(3)
C(38)-C(37)-H(37)	120.8
C(36)-C(37)-H(37)	120.8
C(39)-C(38)-C(37)	119.1(3)
C(39)-C(38)-H(38)	120.5
C(37)-C(38)-H(38)	120.5
N(3)-C(39)-C(38)	123.4(3)
N(3)-C(39)-H(39)	118.3
C(38)-C(39)-H(39)	118.3
C(2S)-C(1S)-C(6S)	120.0(4)
C(2S)-C(1S)-H(1S)	120.0
C(6S)-C(1S)-H(1S)	120.0
C(1S)-C(2S)-C(3S)	120.0(4)
C(1S)-C(2S)-H(2S)	120.0
C(3S)-C(2S)-H(2S)	120.0
C(2S)-C(3S)-C(4S)	120.8(4)
C(2S)-C(3S)-H(3S)	119.6
C(4S)-C(3S)-H(3S)	119.6
C(3S)-C(4S)-C(5S)	119.5(4)
C(3S)-C(4S)-H(4S)	120.2
C(5S)-C(4S)-H(4S)	120.2
C(4S)-C(5S)-C(6S)	119.8(4)
C(4S)-C(5S)-H(5S)	120.1
C(6S)-C(5S)-H(5S)	120.1
C(5S)-C(6S)-C(1S)	119.7(4)
C(5S)-C(6S)-H(6S)	120.1
C(1S)-C(6S)-H(6S)	120.1

Symmetry transformations used to generate equivalent atoms:

Table 4. Anisotropic displacement parameters ($\approx 2 \times 10^3$) for Ru4d. The anisotropic displacement factor exponent takes the form: $-2\pi^2 [h^2 a^*{}^2 U^{11} + \dots + 2 h k a^* b^* U^{12}]$

	U ¹¹	U ²²	U ³³	U ²³	U ¹³	U ¹²
Ru(1)	8(1)	11(1)	12(1)	-1(1)	0(1)	-1(1)

O(1)	9(1)	19(1)	16(1)	-1(1)	0(1)	-4(1)
O(2)	10(1)	17(1)	14(1)	-1(1)	1(1)	-2(1)
N(1)	12(1)	10(1)	24(1)	-4(1)	-2(1)	-1(1)
N(2)	12(1)	11(1)	21(1)	-4(1)	-3(1)	0(1)
N(3)	15(1)	10(1)	14(1)	-1(1)	2(1)	0(1)
C(1)	14(1)	13(1)	13(1)	0(1)	4(1)	-2(1)
C(2)	22(2)	17(2)	26(2)	-8(1)	-1(1)	0(1)
C(3)	23(2)	16(2)	31(2)	-12(1)	-5(1)	-2(1)
C(4)	14(1)	10(1)	20(2)	-4(1)	0(1)	1(1)
C(5)	19(1)	12(1)	26(2)	-6(1)	4(1)	0(1)
C(6)	17(1)	20(2)	36(2)	-14(1)	10(1)	-3(1)
C(7)	18(1)	20(2)	29(2)	-14(1)	-4(1)	3(1)
C(8)	21(1)	17(2)	21(2)	-4(1)	-3(1)	3(1)
C(9)	20(1)	11(1)	21(2)	-7(1)	0(1)	2(1)
C(10)	24(2)	20(2)	30(2)	-4(1)	11(1)	0(1)
C(11)	19(2)	45(2)	41(2)	-17(2)	-7(2)	1(2)
C(12)	25(2)	13(1)	22(2)	-1(1)	2(1)	-2(1)
C(13)	11(1)	15(1)	18(2)	-4(1)	-5(1)	-2(1)
C(14)	13(1)	19(1)	21(2)	-2(1)	-3(1)	-2(1)
C(15)	12(1)	25(2)	27(2)	-4(1)	1(1)	-3(1)
C(16)	16(1)	20(2)	26(2)	-5(1)	-5(1)	1(1)
C(17)	22(1)	16(1)	18(2)	0(1)	-5(1)	-2(1)
C(18)	15(1)	19(1)	16(2)	-5(1)	-4(1)	-5(1)
C(19)	19(1)	24(2)	30(2)	2(1)	1(1)	-6(1)
C(20)	23(2)	34(2)	48(2)	4(2)	-2(2)	8(1)
C(21)	22(1)	22(2)	17(2)	-1(1)	3(1)	-4(1)
C(22)	10(1)	14(1)	14(1)	1(1)	-1(1)	-4(1)
C(23)	15(1)	6(1)	17(1)	1(1)	4(1)	-1(1)
C(24)	17(1)	14(1)	18(2)	0(1)	2(1)	-1(1)
C(25)	12(1)	20(2)	31(2)	2(1)	7(1)	1(1)
C(26)	24(2)	23(2)	26(2)	-1(1)	14(1)	-1(1)
C(27)	26(2)	17(2)	16(2)	-1(1)	6(1)	-3(1)
C(28)	15(1)	14(1)	21(2)	1(1)	1(1)	-1(1)
C(29)	12(1)	10(1)	19(2)	0(1)	4(1)	-2(1)
C(30)	12(1)	9(1)	21(2)	-1(1)	3(1)	2(1)
C(31)	16(1)	19(2)	17(2)	3(1)	3(1)	2(1)
C(32)	16(1)	18(2)	31(2)	5(1)	9(1)	0(1)

C(33)	10(1)	19(2)	33(2)	3(1)	1(1)	-1(1)
C(34)	13(1)	17(1)	22(2)	0(1)	-2(1)	2(1)
C(35)	16(1)	14(1)	18(1)	1(1)	1(1)	-1(1)
C(36)	28(2)	19(2)	16(2)	4(1)	0(1)	0(1)
C(37)	33(2)	24(2)	21(2)	4(1)	12(1)	-1(1)
C(38)	18(1)	20(2)	27(2)	3(1)	9(1)	-2(1)
C(39)	14(1)	15(1)	22(2)	0(1)	3(1)	1(1)
C(1S)	26(2)	47(2)	47(2)	-17(2)	6(2)	-4(2)
C(2S)	21(2)	43(2)	47(2)	1(2)	3(2)	-8(2)
C(3S)	22(2)	54(2)	38(2)	-2(2)	9(2)	-10(2)
C(4S)	28(2)	37(2)	59(3)	-8(2)	20(2)	-6(2)
C(5S)	28(2)	50(2)	53(3)	7(2)	-2(2)	-6(2)
C(6S)	25(2)	82(3)	34(2)	-6(2)	5(2)	-10(2)

Table 5. Hydrogen coordinates ($\times 10^4$) and isotropic displacement parameters ($\approx 2 \times 10^{-3}$) for Ru4d.

	x	y	z	U(eq)
H(2A)	2935	12107	3848	27
H(2B)	3256	12497	2990	27
H(3A)	4558	11889	3407	29
H(3B)	4210	11433	4219	29
H(6)	-159	10965	2371	28
H(8)	895	12038	426	25
H(10A)	1419	11350	3989	36
H(10B)	1665	10398	3715	36
H(10C)	672	10648	3733	36
H(11A)	-679	10869	414	54
H(11B)	-680	11896	309	54
H(11C)	-1093	11463	1085	54
H(12A)	2608	12778	1307	30
H(12B)	2469	12119	508	30
H(12C)	3085	11861	1387	30
H(15)	6637	9808	2749	26
H(17)	5366	8380	4312	24
H(19A)	4890	11207	1990	36

H(19B)	5793	10851	1760	36
H(19C)	5786	11491	2564	36
H(20A)	7414	8697	3573	54
H(20B)	6784	7882	3379	54
H(20C)	7005	8253	4345	54
H(21A)	3988	8754	4627	31
H(21B)	3375	9276	3888	31
H(21C)	3896	9778	4702	31
H(22)	3436	8579	2604	16
H(24)	4859	8109	2243	19
H(25)	5630	7470	1245	25
H(26)	5010	7340	-209	28
H(27)	3594	7835	-658	24
H(28)	2821	8498	328	20
H(31)	811	8544	3852	21
H(32)	-612	8115	3320	25
H(33)	-1147	8241	1853	25
H(34)	-282	8824	890	21
H(35)	1668	10174	129	19
H(36)	2027	10619	-1189	25
H(37)	3483	10925	-1308	30
H(38)	4547	10716	-87	25
H(39)	4142	10195	1183	20
H(1S)	7179	2022	4221	48
H(2S)	7335	2084	2770	45
H(3S)	8152	1056	2189	45
H(4S)	8840	-32	3051	48
H(5S)	8746	-61	4530	54
H(6S)	7859	929	5102	56

Table 6. Torsion angles [\circ] for Ru4d.

C(4)-N(1)-C(1)-N(2)	170.0(2)
C(2)-N(1)-C(1)-N(2)	1.0(3)
C(4)-N(1)-C(1)-Ru(1)	-10.1(3)
C(2)-N(1)-C(1)-Ru(1)	-179.12(19)

C(13)-N(2)-C(1)-N(1)	173.6(3)
C(3)-N(2)-C(1)-N(1)	2.4(3)
C(13)-N(2)-C(1)-Ru(1)	-6.1(5)
C(3)-N(2)-C(1)-Ru(1)	-177.4(2)
C(1)-N(1)-C(2)-C(3)	-3.7(3)
C(4)-N(1)-C(2)-C(3)	-172.1(3)
C(1)-N(2)-C(3)-C(2)	-4.6(3)
C(13)-N(2)-C(3)-C(2)	-176.7(2)
N(1)-C(2)-C(3)-N(2)	4.6(3)
C(1)-N(1)-C(4)-C(9)	-84.9(3)
C(2)-N(1)-C(4)-C(9)	83.0(3)
C(1)-N(1)-C(4)-C(5)	95.2(3)
C(2)-N(1)-C(4)-C(5)	-97.0(3)
C(9)-C(4)-C(5)-C(6)	7.5(4)
N(1)-C(4)-C(5)-C(6)	-172.6(2)
C(9)-C(4)-C(5)-C(10)	-171.3(2)
N(1)-C(4)-C(5)-C(10)	8.6(4)
C(4)-C(5)-C(6)-C(7)	-2.4(4)
C(10)-C(5)-C(6)-C(7)	176.4(3)
C(5)-C(6)-C(7)-C(8)	-3.2(4)
C(5)-C(6)-C(7)-C(11)	175.6(3)
C(6)-C(7)-C(8)-C(9)	4.2(4)
C(11)-C(7)-C(8)-C(9)	-174.6(3)
C(7)-C(8)-C(9)-C(4)	0.6(4)
C(7)-C(8)-C(9)-C(12)	-177.9(2)
C(5)-C(4)-C(9)-C(8)	-6.7(4)
N(1)-C(4)-C(9)-C(8)	173.4(2)
C(5)-C(4)-C(9)-C(12)	171.8(2)
N(1)-C(4)-C(9)-C(12)	-8.1(4)
C(1)-N(2)-C(13)-C(14)	113.1(3)
C(3)-N(2)-C(13)-C(14)	-76.1(3)
C(1)-N(2)-C(13)-C(18)	-73.7(4)
C(3)-N(2)-C(13)-C(18)	97.1(3)
C(18)-C(13)-C(14)-C(15)	1.4(4)
N(2)-C(13)-C(14)-C(15)	174.4(2)
C(18)-C(13)-C(14)-C(19)	-176.2(3)
N(2)-C(13)-C(14)-C(19)	-3.2(4)

C(13)-C(14)-C(15)-C(16)	1.2(4)
C(19)-C(14)-C(15)-C(16)	178.8(3)
C(14)-C(15)-C(16)-C(17)	-1.2(4)
C(14)-C(15)-C(16)-C(20)	178.9(3)
C(15)-C(16)-C(17)-C(18)	-1.4(4)
C(20)-C(16)-C(17)-C(18)	178.6(3)
C(16)-C(17)-C(18)-C(13)	3.8(4)
C(16)-C(17)-C(18)-C(21)	-174.5(3)
C(14)-C(13)-C(18)-C(17)	-3.8(4)
N(2)-C(13)-C(18)-C(17)	-176.7(2)
C(14)-C(13)-C(18)-C(21)	174.5(3)
N(2)-C(13)-C(18)-C(21)	1.6(4)
O(1)-Ru(1)-C(22)-C(23)	70.9(2)
C(1)-Ru(1)-C(22)-C(23)	-114.7(2)
O(2)-Ru(1)-C(22)-C(23)	152.0(2)
N(3)-Ru(1)-C(22)-C(23)	-20.9(2)
Ru(1)-C(22)-C(23)-C(28)	-32.8(4)
Ru(1)-C(22)-C(23)-C(24)	149.2(2)
C(28)-C(23)-C(24)-C(25)	2.2(4)
C(22)-C(23)-C(24)-C(25)	-179.7(2)
C(23)-C(24)-C(25)-C(26)	-1.1(4)
C(24)-C(25)-C(26)-C(27)	-0.7(4)
C(25)-C(26)-C(27)-C(28)	1.3(4)
C(26)-C(27)-C(28)-C(23)	-0.1(4)
C(24)-C(23)-C(28)-C(27)	-1.6(4)
C(22)-C(23)-C(28)-C(27)	-179.6(2)
Ru(1)-O(1)-C(29)-C(34)	177.3(2)
Ru(1)-O(1)-C(29)-C(30)	-2.0(3)
Ru(1)-O(2)-C(30)-C(31)	-177.2(2)
Ru(1)-O(2)-C(30)-C(29)	2.5(3)
O(1)-C(29)-C(30)-O(2)	-0.4(3)
C(34)-C(29)-C(30)-O(2)	-179.7(2)
O(1)-C(29)-C(30)-C(31)	179.3(2)
C(34)-C(29)-C(30)-C(31)	0.0(4)
O(2)-C(30)-C(31)-C(32)	-179.7(2)
C(29)-C(30)-C(31)-C(32)	0.6(4)
C(30)-C(31)-C(32)-C(33)	-0.4(4)

C(31)-C(32)-C(33)-C(34)	-0.6(4)
O(1)-C(29)-C(34)-C(33)	179.8(2)
C(30)-C(29)-C(34)-C(33)	-1.0(4)
C(32)-C(33)-C(34)-C(29)	1.3(4)
C(39)-N(3)-C(35)-C(36)	0.4(4)
Ru(1)-N(3)-C(35)-C(36)	-177.5(2)
N(3)-C(35)-C(36)-C(37)	-1.9(4)
C(35)-C(36)-C(37)-C(38)	1.3(4)
C(36)-C(37)-C(38)-C(39)	0.6(4)
C(35)-N(3)-C(39)-C(38)	1.6(4)
Ru(1)-N(3)-C(39)-C(38)	179.4(2)
C(37)-C(38)-C(39)-N(3)	-2.1(4)
C(6S)-C(1S)-C(2S)-C(3S)	0.6(5)
C(1S)-C(2S)-C(3S)-C(4S)	-0.7(5)
C(2S)-C(3S)-C(4S)-C(5S)	-0.9(5)
C(3S)-C(4S)-C(5S)-C(6S)	2.8(5)
C(4S)-C(5S)-C(6S)-C(1S)	-3.0(5)
C(2S)-C(1S)-C(6S)-C(5S)	1.3(5)

Symmetry transformations used to generate equivalent atoms:

X-ray structure of Ru8:

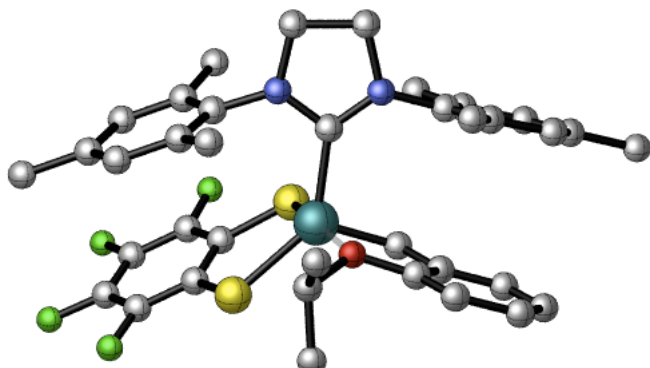


Table 1. Crystal data and structure refinement for Ru8.

Identification code	C37H38F4N2ORuS2
Empirical formula	C37 H38 F4 N2 O Ru S2
Formula weight	767.88
Temperature	100(2) K
Wavelength	0.71073 ≈
Crystal system	Triclinic
Space group	P -1

Unit cell dimensions	$a = 10.1440(5) \approx$	$\alpha = 92.458(3)\infty.$
	$b = 10.9170(5) \approx$	$\beta = 102.025(3)\infty.$
	$c = 17.5734(8) \approx$	$\gamma = 116.998(2)\infty.$
Volume	$1674.75(14) \approx^3$	
Z	2	
Density (calculated)	1.523 Mg/m^3	
Absorption coefficient	0.649 mm^{-1}	
F(000)	788	
Crystal size	$0.400 \times 0.120 \times 0.060 \text{ mm}^3$	
Theta range for data collection	2.120 to 28.416 ∞ .	
Index ranges	$-13 \leq h \leq 13, -14 \leq k \leq 14, -23 \leq l \leq 23$	
Reflections collected	62314	
Independent reflections	8397 [$R(\text{int}) = 0.0461$]	
Completeness to theta = 25.242 ∞	100.0 %	
Absorption correction	Semi-empirical from equivalents	
Max. and min. transmission	0.7533 and 0.6403	
Refinement method	Full-matrix least-squares on F^2	
Data / restraints / parameters	8397 / 0 / 436	
Goodness-of-fit on F^2	1.026	
Final R indices [$I > 2\sigma(I)$]	$R_1 = 0.0267, wR_2 = 0.0582$	
R indices (all data)	$R_1 = 0.0359, wR_2 = 0.0613$	
Extinction coefficient	na	
Largest diff. peak and hole	0.419 and -0.522 e. \approx^{-3}	

Table 2. Atomic coordinates ($\times 10^4$) and equivalent isotropic displacement parameters ($\approx 2 \times 10^{-3}$) for Ru8. U(eq) is defined as one third of the trace of the orthogonalized U^{ij} tensor.

	x	y	z	U(eq)
Ru(1)	3624(1)	276(1)	2741(1)	12(1)
S(1)	1141(1)	-138(1)	2214(1)	16(1)
S(2)	2717(1)	-2060(1)	2700(1)	16(1)
F(1)	620(1)	-5042(1)	2066(1)	24(1)
F(2)	-2298(1)	-6213(1)	1205(1)	31(1)
F(3)	-3649(1)	-4590(1)	773(1)	32(1)
F(4)	-2106(1)	-1828(1)	1280(1)	27(1)
O(1)	4501(1)	2617(1)	2966(1)	15(1)
N(1)	6917(2)	943(2)	2672(1)	16(1)
N(2)	5188(2)	49(2)	1557(1)	16(1)
C(1)	5416(2)	434(2)	2330(1)	13(1)
C(2)	7806(2)	925(2)	2108(1)	23(1)
C(3)	6604(2)	380(2)	1318(1)	17(1)
C(4)	7637(2)	1219(2)	3499(1)	17(1)
C(5)	8553(2)	2596(2)	3872(1)	17(1)
C(6)	9304(2)	2836(2)	4665(1)	20(1)
C(7)	9166(2)	1758(2)	5087(1)	22(1)
C(8)	8261(2)	398(2)	4694(1)	24(1)
C(9)	7506(2)	103(2)	3899(1)	20(1)
C(10)	8735(2)	3800(2)	3435(1)	22(1)
C(11)	9952(2)	2046(2)	5954(1)	31(1)
C(12)	6596(2)	-1384(2)	3485(1)	29(1)
C(13)	3732(2)	-602(2)	985(1)	14(1)
C(14)	2972(2)	-2049(2)	771(1)	16(1)
C(15)	1537(2)	-2654(2)	240(1)	18(1)
C(16)	874(2)	-1863(2)	-87(1)	17(1)
C(17)	1699(2)	-426(2)	105(1)	16(1)
C(18)	3144(2)	229(2)	630(1)	14(1)
C(19)	3663(2)	-2957(2)	1077(1)	22(1)
C(20)	-690(2)	-2561(2)	-654(1)	25(1)
C(21)	4082(2)	1788(2)	772(1)	20(1)
C(22)	4518(2)	686(2)	3805(1)	21(1)

C(23)	5237(2)	2108(2)	4209(1)	18(1)
C(24)	5989(2)	2518(2)	5012(1)	25(1)
C(25)	6693(2)	3895(2)	5355(1)	24(1)
C(26)	6657(2)	4887(2)	4900(1)	23(1)
C(27)	5921(2)	4520(2)	4101(1)	20(1)
C(28)	5222(2)	3131(2)	3762(1)	16(1)
C(29)	3627(2)	3246(2)	2514(1)	22(1)
C(30)	4672(3)	4581(2)	2256(1)	38(1)
C(31)	2546(2)	3373(2)	2949(1)	31(1)
C(32)	108(2)	-1958(2)	1950(1)	15(1)
C(33)	812(2)	-2787(2)	2156(1)	15(1)
C(34)	-35(2)	-4212(2)	1895(1)	18(1)
C(35)	-1518(2)	-4824(2)	1446(1)	21(1)
C(36)	-2206(2)	-4007(2)	1237(1)	21(1)
C(37)	-1400(2)	-2599(2)	1500(1)	19(1)

Table 3. Bond lengths [\approx] and angles [∞] for Ru8.

Ru(1)-C(22)	1.836(2)
Ru(1)-C(1)	2.0317(17)
Ru(1)-S(2)	2.2759(5)
Ru(1)-O(1)	2.2770(12)
Ru(1)-S(1)	2.3160(5)
S(1)-C(32)	1.7571(18)
S(2)-C(33)	1.7464(18)
F(1)-C(34)	1.356(2)
F(2)-C(35)	1.349(2)
F(3)-C(36)	1.351(2)
F(4)-C(37)	1.353(2)
O(1)-C(28)	1.392(2)
O(1)-C(29)	1.481(2)
N(1)-C(1)	1.346(2)
N(1)-C(4)	1.435(2)
N(1)-C(2)	1.477(2)
N(2)-C(1)	1.344(2)
N(2)-C(13)	1.437(2)
N(2)-C(3)	1.471(2)

C(2)-C(3)	1.528(2)
C(2)-H(2A)	0.9900
C(2)-H(2B)	0.9900
C(3)-H(3A)	0.9900
C(3)-H(3B)	0.9900
C(4)-C(5)	1.395(2)
C(4)-C(9)	1.401(3)
C(5)-C(6)	1.391(3)
C(5)-C(10)	1.509(3)
C(6)-C(7)	1.386(3)
C(6)-H(6)	0.9500
C(7)-C(8)	1.391(3)
C(7)-C(11)	1.511(3)
C(8)-C(9)	1.390(3)
C(8)-H(8)	0.9500
C(9)-C(12)	1.509(3)
C(10)-H(10A)	0.9800
C(10)-H(10B)	0.9800
C(10)-H(10C)	0.9800
C(11)-H(11A)	0.9800
C(11)-H(11B)	0.9800
C(11)-H(11C)	0.9800
C(12)-H(12A)	0.9800
C(12)-H(12B)	0.9800
C(12)-H(12C)	0.9800
C(13)-C(14)	1.397(2)
C(13)-C(18)	1.398(2)
C(14)-C(15)	1.391(2)
C(14)-C(19)	1.511(3)
C(15)-C(16)	1.391(3)
C(15)-H(15)	0.9500
C(16)-C(17)	1.386(2)
C(16)-C(20)	1.506(2)
C(17)-C(18)	1.393(2)
C(17)-H(17)	0.9500
C(18)-C(21)	1.503(2)
C(19)-H(19A)	0.9800

C(19)-H(19B)	0.9800
C(19)-H(19C)	0.9800
C(20)-H(20A)	0.9800
C(20)-H(20B)	0.9800
C(20)-H(20C)	0.9800
C(21)-H(21A)	0.9800
C(21)-H(21B)	0.9800
C(21)-H(21C)	0.9800
C(22)-C(23)	1.452(3)
C(22)-H(22)	0.93(3)
C(23)-C(28)	1.397(3)
C(23)-C(24)	1.400(3)
C(24)-C(25)	1.379(3)
C(24)-H(24)	0.9500
C(25)-C(26)	1.382(3)
C(25)-H(25)	0.9500
C(26)-C(27)	1.391(3)
C(26)-H(26)	0.9500
C(27)-C(28)	1.388(2)
C(27)-H(27)	0.9500
C(29)-C(31)	1.512(3)
C(29)-C(30)	1.519(3)
C(29)-H(29)	1.0000
C(30)-H(30A)	0.9800
C(30)-H(30B)	0.9800
C(30)-H(30C)	0.9800
C(31)-H(31A)	0.9800
C(31)-H(31B)	0.9800
C(31)-H(31C)	0.9800
C(32)-C(37)	1.390(2)
C(32)-C(33)	1.403(2)
C(33)-C(34)	1.389(2)
C(34)-C(35)	1.371(3)
C(35)-C(36)	1.380(3)
C(36)-C(37)	1.373(3)
C(22)-Ru(1)-C(1)	99.88(8)

C(22)-Ru(1)-S(2)	94.10(6)
C(1)-Ru(1)-S(2)	90.93(5)
C(22)-Ru(1)-O(1)	78.62(7)
C(1)-Ru(1)-O(1)	94.29(5)
S(2)-Ru(1)-O(1)	171.66(3)
C(22)-Ru(1)-S(1)	122.85(6)
C(1)-Ru(1)-S(1)	137.19(5)
S(2)-Ru(1)-S(1)	88.740(16)
O(1)-Ru(1)-S(1)	91.82(3)
C(32)-S(1)-Ru(1)	103.47(6)
C(33)-S(2)-Ru(1)	104.34(6)
C(28)-O(1)-C(29)	119.61(13)
C(28)-O(1)-Ru(1)	109.90(10)
C(29)-O(1)-Ru(1)	120.27(10)
C(1)-N(1)-C(4)	127.19(15)
C(1)-N(1)-C(2)	113.04(14)
C(4)-N(1)-C(2)	118.52(14)
C(1)-N(2)-C(13)	125.59(14)
C(1)-N(2)-C(3)	113.84(14)
C(13)-N(2)-C(3)	120.56(14)
N(2)-C(1)-N(1)	107.71(15)
N(2)-C(1)-Ru(1)	119.18(12)
N(1)-C(1)-Ru(1)	133.00(13)
N(1)-C(2)-C(3)	102.90(13)
N(1)-C(2)-H(2A)	111.2
C(3)-C(2)-H(2A)	111.2
N(1)-C(2)-H(2B)	111.2
C(3)-C(2)-H(2B)	111.2
H(2A)-C(2)-H(2B)	109.1
N(2)-C(3)-C(2)	102.18(14)
N(2)-C(3)-H(3A)	111.3
C(2)-C(3)-H(3A)	111.3
N(2)-C(3)-H(3B)	111.3
C(2)-C(3)-H(3B)	111.3
H(3A)-C(3)-H(3B)	109.2
C(5)-C(4)-C(9)	121.42(17)
C(5)-C(4)-N(1)	119.18(16)

C(9)-C(4)-N(1)	119.20(16)
C(6)-C(5)-C(4)	118.09(17)
C(6)-C(5)-C(10)	120.40(17)
C(4)-C(5)-C(10)	121.51(16)
C(7)-C(6)-C(5)	122.16(18)
C(7)-C(6)-H(6)	118.9
C(5)-C(6)-H(6)	118.9
C(6)-C(7)-C(8)	118.26(18)
C(6)-C(7)-C(11)	121.10(18)
C(8)-C(7)-C(11)	120.63(19)
C(9)-C(8)-C(7)	121.79(18)
C(9)-C(8)-H(8)	119.1
C(7)-C(8)-H(8)	119.1
C(8)-C(9)-C(4)	118.23(17)
C(8)-C(9)-C(12)	120.21(18)
C(4)-C(9)-C(12)	121.55(17)
C(5)-C(10)-H(10A)	109.5
C(5)-C(10)-H(10B)	109.5
H(10A)-C(10)-H(10B)	109.5
C(5)-C(10)-H(10C)	109.5
H(10A)-C(10)-H(10C)	109.5
H(10B)-C(10)-H(10C)	109.5
C(7)-C(11)-H(11A)	109.5
C(7)-C(11)-H(11B)	109.5
H(11A)-C(11)-H(11B)	109.5
C(7)-C(11)-H(11C)	109.5
H(11A)-C(11)-H(11C)	109.5
H(11B)-C(11)-H(11C)	109.5
C(9)-C(12)-H(12A)	109.5
C(9)-C(12)-H(12B)	109.5
H(12A)-C(12)-H(12B)	109.5
C(9)-C(12)-H(12C)	109.5
H(12A)-C(12)-H(12C)	109.5
H(12B)-C(12)-H(12C)	109.5
C(14)-C(13)-C(18)	121.60(15)
C(14)-C(13)-N(2)	119.06(16)
C(18)-C(13)-N(2)	119.27(15)

C(15)-C(14)-C(13)	117.71(16)
C(15)-C(14)-C(19)	119.59(16)
C(13)-C(14)-C(19)	122.68(16)
C(16)-C(15)-C(14)	122.08(16)
C(16)-C(15)-H(15)	119.0
C(14)-C(15)-H(15)	119.0
C(17)-C(16)-C(15)	118.56(16)
C(17)-C(16)-C(20)	121.03(17)
C(15)-C(16)-C(20)	120.39(17)
C(16)-C(17)-C(18)	121.52(17)
C(16)-C(17)-H(17)	119.2
C(18)-C(17)-H(17)	119.2
C(17)-C(18)-C(13)	118.26(16)
C(17)-C(18)-C(21)	120.67(16)
C(13)-C(18)-C(21)	120.97(15)
C(14)-C(19)-H(19A)	109.5
C(14)-C(19)-H(19B)	109.5
H(19A)-C(19)-H(19B)	109.5
C(14)-C(19)-H(19C)	109.5
H(19A)-C(19)-H(19C)	109.5
H(19B)-C(19)-H(19C)	109.5
C(16)-C(20)-H(20A)	109.5
C(16)-C(20)-H(20B)	109.5
H(20A)-C(20)-H(20B)	109.5
C(16)-C(20)-H(20C)	109.5
H(20A)-C(20)-H(20C)	109.5
H(20B)-C(20)-H(20C)	109.5
C(18)-C(21)-H(21A)	109.5
C(18)-C(21)-H(21B)	109.5
H(21A)-C(21)-H(21B)	109.5
C(18)-C(21)-H(21C)	109.5
H(21A)-C(21)-H(21C)	109.5
H(21B)-C(21)-H(21C)	109.5
C(23)-C(22)-Ru(1)	120.21(14)
C(23)-C(22)-H(22)	113.5(15)
Ru(1)-C(22)-H(22)	125.9(16)
C(28)-C(23)-C(24)	118.32(17)

C(28)-C(23)-C(22)	117.77(17)
C(24)-C(23)-C(22)	123.88(17)
C(25)-C(24)-C(23)	121.05(19)
C(25)-C(24)-H(24)	119.5
C(23)-C(24)-H(24)	119.5
C(24)-C(25)-C(26)	119.52(18)
C(24)-C(25)-H(25)	120.2
C(26)-C(25)-H(25)	120.2
C(25)-C(26)-C(27)	121.11(18)
C(25)-C(26)-H(26)	119.4
C(27)-C(26)-H(26)	119.4
C(28)-C(27)-C(26)	118.81(18)
C(28)-C(27)-H(27)	120.6
C(26)-C(27)-H(27)	120.6
C(27)-C(28)-O(1)	125.27(16)
C(27)-C(28)-C(23)	121.20(17)
O(1)-C(28)-C(23)	113.49(15)
O(1)-C(29)-C(31)	110.92(16)
O(1)-C(29)-C(30)	111.74(17)
C(31)-C(29)-C(30)	114.88(18)
O(1)-C(29)-H(29)	106.2
C(31)-C(29)-H(29)	106.2
C(30)-C(29)-H(29)	106.2
C(29)-C(30)-H(30A)	109.5
C(29)-C(30)-H(30B)	109.5
H(30A)-C(30)-H(30B)	109.5
C(29)-C(30)-H(30C)	109.5
H(30A)-C(30)-H(30C)	109.5
H(30B)-C(30)-H(30C)	109.5
C(29)-C(31)-H(31A)	109.5
C(29)-C(31)-H(31B)	109.5
H(31A)-C(31)-H(31B)	109.5
C(29)-C(31)-H(31C)	109.5
H(31A)-C(31)-H(31C)	109.5
H(31B)-C(31)-H(31C)	109.5
C(37)-C(32)-C(33)	118.61(16)
C(37)-C(32)-S(1)	120.69(14)

C(33)-C(32)-S(1)	120.63(13)
C(34)-C(33)-C(32)	118.15(16)
C(34)-C(33)-S(2)	120.30(14)
C(32)-C(33)-S(2)	121.52(13)
F(1)-C(34)-C(35)	117.79(16)
F(1)-C(34)-C(33)	119.80(16)
C(35)-C(34)-C(33)	122.40(17)
F(2)-C(35)-C(34)	120.38(17)
F(2)-C(35)-C(36)	120.14(17)
C(34)-C(35)-C(36)	119.48(16)
F(3)-C(36)-C(37)	120.75(17)
F(3)-C(36)-C(35)	120.10(17)
C(37)-C(36)-C(35)	119.15(17)
F(4)-C(37)-C(36)	117.60(16)
F(4)-C(37)-C(32)	120.16(16)
C(36)-C(37)-C(32)	122.18(17)

Symmetry transformations used to generate equivalent atoms:

Table 4. Anisotropic displacement parameters ($\approx^2 \times 10^3$) for Ru8. The anisotropic displacement factor exponent takes the form: $-2\pi^2 [h^2 a^* b^* U^{11} + \dots + 2 h k a^* b^* U^{12}]$

	U ¹¹	U ²²	U ³³	U ²³	U ¹³	U ¹²
Ru(1)	13(1)	12(1)	13(1)	2(1)	4(1)	7(1)
S(1)	15(1)	13(1)	21(1)	4(1)	4(1)	8(1)
S(2)	16(1)	13(1)	20(1)	4(1)	4(1)	9(1)
F(1)	27(1)	14(1)	37(1)	6(1)	11(1)	12(1)
F(2)	26(1)	14(1)	44(1)	-4(1)	6(1)	2(1)
F(3)	18(1)	28(1)	36(1)	-1(1)	-3(1)	4(1)
F(4)	20(1)	25(1)	36(1)	6(1)	-1(1)	14(1)
O(1)	18(1)	13(1)	14(1)	2(1)	1(1)	9(1)
N(1)	12(1)	21(1)	13(1)	-2(1)	0(1)	8(1)
N(2)	12(1)	22(1)	12(1)	-2(1)	2(1)	8(1)
C(1)	13(1)	11(1)	15(1)	1(1)	2(1)	6(1)
C(2)	14(1)	34(1)	19(1)	-5(1)	2(1)	11(1)
C(3)	14(1)	22(1)	17(1)	0(1)	4(1)	9(1)
C(4)	14(1)	22(1)	14(1)	-1(1)	0(1)	10(1)

C(5)	16(1)	20(1)	16(1)	1(1)	2(1)	9(1)
C(6)	17(1)	23(1)	16(1)	-3(1)	2(1)	8(1)
C(7)	17(1)	32(1)	15(1)	2(1)	0(1)	11(1)
C(8)	21(1)	26(1)	24(1)	8(1)	1(1)	13(1)
C(9)	16(1)	20(1)	22(1)	1(1)	0(1)	9(1)
C(10)	23(1)	21(1)	20(1)	1(1)	2(1)	9(1)
C(11)	26(1)	44(1)	17(1)	3(1)	0(1)	15(1)
C(12)	26(1)	19(1)	35(1)	1(1)	-5(1)	11(1)
C(13)	12(1)	19(1)	11(1)	0(1)	2(1)	6(1)
C(14)	18(1)	18(1)	13(1)	4(1)	5(1)	9(1)
C(15)	18(1)	15(1)	15(1)	-2(1)	3(1)	4(1)
C(16)	14(1)	22(1)	11(1)	0(1)	2(1)	6(1)
C(17)	15(1)	22(1)	13(1)	3(1)	4(1)	11(1)
C(18)	15(1)	17(1)	12(1)	0(1)	5(1)	7(1)
C(19)	25(1)	22(1)	22(1)	3(1)	4(1)	14(1)
C(20)	16(1)	29(1)	20(1)	-3(1)	-3(1)	8(1)
C(21)	21(1)	16(1)	22(1)	2(1)	4(1)	9(1)
C(22)	33(1)	18(1)	17(1)	5(1)	7(1)	16(1)
C(23)	25(1)	19(1)	15(1)	2(1)	7(1)	13(1)
C(24)	40(1)	27(1)	15(1)	4(1)	6(1)	22(1)
C(25)	29(1)	28(1)	17(1)	-5(1)	1(1)	17(1)
C(26)	20(1)	20(1)	24(1)	-5(1)	1(1)	9(1)
C(27)	20(1)	16(1)	21(1)	2(1)	2(1)	8(1)
C(28)	15(1)	17(1)	15(1)	0(1)	3(1)	9(1)
C(29)	32(1)	19(1)	16(1)	2(1)	-2(1)	17(1)
C(30)	66(2)	17(1)	20(1)	5(1)	2(1)	15(1)
C(31)	34(1)	39(1)	27(1)	-8(1)	-5(1)	29(1)
C(32)	16(1)	15(1)	16(1)	4(1)	6(1)	7(1)
C(33)	15(1)	15(1)	15(1)	3(1)	6(1)	7(1)
C(34)	22(1)	15(1)	22(1)	6(1)	10(1)	11(1)
C(35)	22(1)	13(1)	24(1)	-1(1)	7(1)	3(1)
C(36)	14(1)	22(1)	21(1)	1(1)	2(1)	4(1)
C(37)	19(1)	20(1)	22(1)	7(1)	6(1)	11(1)

Table 5. Hydrogen coordinates ($\times 10^4$) and isotropic displacement parameters ($\approx 2 \times 10^{-3}$) for Ru8.

	x	y	z	U(eq)
H(2A)	8255	296	2228	28
H(2B)	8635	1870	2114	28
H(3A)	6818	1101	970	21
H(3B)	6552	-459	1045	21
H(6)	9932	3769	4926	24
H(8)	8157	-351	4976	29
H(10A)	8896	4588	3800	34
H(10B)	7810	3519	3010	34
H(10C)	9619	4075	3212	34
H(11A)	9342	2234	6261	46
H(11B)	10969	2858	6058	46
H(11C)	10055	1235	6106	46
H(12A)	6629	-2011	3862	43
H(12B)	7037	-1509	3060	43
H(12C)	5532	-1597	3262	43
H(15)	993	-3637	95	21
H(17)	1270	124	-127	19
H(19A)	2853	-3849	1143	33
H(19B)	4409	-2489	1585	33
H(19C)	4176	-3122	700	33
H(20A)	-767	-3300	-1026	37
H(20B)	-850	-1873	-944	37
H(20C)	-1472	-2964	-361	37
H(21A)	4616	2111	1331	30
H(21B)	3409	2204	620	30
H(21C)	4834	2066	456	30
H(22)	4460(30)	40(30)	4143(15)	40(7)
H(24)	6016	1838	5325	30
H(25)	7199	4160	5901	29
H(26)	7143	5835	5138	27
H(27)	5898	5207	3793	24
H(29)	2970	2569	2020	26

H(30A)	5005	5373	2665	57
H(30B)	4116	4707	1764	57
H(30C)	5568	4524	2170	57
H(31A)	1955	2482	3117	47
H(31B)	1846	3621	2600	47
H(31C)	3135	4098	3413	47

Table 6. Torsion angles [\circ] for Ru8.

C(13)-N(2)-C(1)-N(1)	177.18(16)
C(3)-N(2)-C(1)-N(1)	-4.1(2)
C(13)-N(2)-C(1)-Ru(1)	-6.2(2)
C(3)-N(2)-C(1)-Ru(1)	172.54(12)
C(4)-N(1)-C(1)-N(2)	-166.60(16)
C(2)-N(1)-C(1)-N(2)	0.3(2)
C(4)-N(1)-C(1)-Ru(1)	17.4(3)
C(2)-N(1)-C(1)-Ru(1)	-175.67(14)
C(1)-N(1)-C(2)-C(3)	3.2(2)
C(4)-N(1)-C(2)-C(3)	171.38(15)
C(1)-N(2)-C(3)-C(2)	5.9(2)
C(13)-N(2)-C(3)-C(2)	-175.33(16)
N(1)-C(2)-C(3)-N(2)	-5.02(19)
C(1)-N(1)-C(4)-C(5)	-109.7(2)
C(2)-N(1)-C(4)-C(5)	84.1(2)
C(1)-N(1)-C(4)-C(9)	75.5(2)
C(2)-N(1)-C(4)-C(9)	-90.8(2)
C(9)-C(4)-C(5)-C(6)	-1.9(3)
N(1)-C(4)-C(5)-C(6)	-176.64(16)
C(9)-C(4)-C(5)-C(10)	178.03(17)
N(1)-C(4)-C(5)-C(10)	3.3(3)
C(4)-C(5)-C(6)-C(7)	-0.1(3)
C(10)-C(5)-C(6)-C(7)	179.99(17)
C(5)-C(6)-C(7)-C(8)	1.0(3)
C(5)-C(6)-C(7)-C(11)	-177.93(18)
C(6)-C(7)-C(8)-C(9)	0.0(3)
C(11)-C(7)-C(8)-C(9)	178.94(19)

C(7)-C(8)-C(9)-C(4)	-1.9(3)
C(7)-C(8)-C(9)-C(12)	177.12(18)
C(5)-C(4)-C(9)-C(8)	2.8(3)
N(1)-C(4)-C(9)-C(8)	177.59(16)
C(5)-C(4)-C(9)-C(12)	-176.13(17)
N(1)-C(4)-C(9)-C(12)	-1.4(3)
C(1)-N(2)-C(13)-C(14)	-97.4(2)
C(3)-N(2)-C(13)-C(14)	83.9(2)
C(1)-N(2)-C(13)-C(18)	85.3(2)
C(3)-N(2)-C(13)-C(18)	-93.3(2)
C(18)-C(13)-C(14)-C(15)	-5.4(3)
N(2)-C(13)-C(14)-C(15)	177.45(16)
C(18)-C(13)-C(14)-C(19)	172.92(17)
N(2)-C(13)-C(14)-C(19)	-4.2(3)
C(13)-C(14)-C(15)-C(16)	1.2(3)
C(19)-C(14)-C(15)-C(16)	-177.16(17)
C(14)-C(15)-C(16)-C(17)	2.3(3)
C(14)-C(15)-C(16)-C(20)	-179.33(17)
C(15)-C(16)-C(17)-C(18)	-1.8(3)
C(20)-C(16)-C(17)-C(18)	179.83(17)
C(16)-C(17)-C(18)-C(13)	-2.2(3)
C(16)-C(17)-C(18)-C(21)	174.20(16)
C(14)-C(13)-C(18)-C(17)	5.9(3)
N(2)-C(13)-C(18)-C(17)	-176.97(15)
C(14)-C(13)-C(18)-C(21)	-170.46(16)
N(2)-C(13)-C(18)-C(21)	6.7(2)
C(1)-Ru(1)-C(22)-C(23)	92.70(16)
S(2)-Ru(1)-C(22)-C(23)	-175.64(15)
O(1)-Ru(1)-C(22)-C(23)	0.27(15)
S(1)-Ru(1)-C(22)-C(23)	-84.49(16)
Ru(1)-C(22)-C(23)-C(28)	-0.1(2)
Ru(1)-C(22)-C(23)-C(24)	-177.66(16)
C(28)-C(23)-C(24)-C(25)	0.3(3)
C(22)-C(23)-C(24)-C(25)	177.90(19)
C(23)-C(24)-C(25)-C(26)	-0.1(3)
C(24)-C(25)-C(26)-C(27)	0.1(3)
C(25)-C(26)-C(27)-C(28)	-0.3(3)

C(26)-C(27)-C(28)-O(1)	-177.16(16)
C(26)-C(27)-C(28)-C(23)	0.5(3)
C(29)-O(1)-C(28)-C(27)	-36.4(2)
Ru(1)-O(1)-C(28)-C(27)	178.31(14)
C(29)-O(1)-C(28)-C(23)	145.84(16)
Ru(1)-O(1)-C(28)-C(23)	0.51(17)
C(24)-C(23)-C(28)-C(27)	-0.5(3)
C(22)-C(23)-C(28)-C(27)	-178.25(17)
C(24)-C(23)-C(28)-O(1)	177.39(16)
C(22)-C(23)-C(28)-O(1)	-0.3(2)
C(28)-O(1)-C(29)-C(31)	-48.8(2)
Ru(1)-O(1)-C(29)-C(31)	92.92(16)
C(28)-O(1)-C(29)-C(30)	80.8(2)
Ru(1)-O(1)-C(29)-C(30)	-137.50(14)
Ru(1)-S(1)-C(32)-C(37)	-170.09(14)
Ru(1)-S(1)-C(32)-C(33)	6.90(16)
C(37)-C(32)-C(33)-C(34)	0.5(3)
S(1)-C(32)-C(33)-C(34)	-176.52(13)
C(37)-C(32)-C(33)-S(2)	178.45(14)
S(1)-C(32)-C(33)-S(2)	1.4(2)
Ru(1)-S(2)-C(33)-C(34)	168.84(13)
Ru(1)-S(2)-C(33)-C(32)	-9.04(16)
C(32)-C(33)-C(34)-F(1)	178.37(16)
S(2)-C(33)-C(34)-F(1)	0.4(2)
C(32)-C(33)-C(34)-C(35)	0.0(3)
S(2)-C(33)-C(34)-C(35)	-177.99(15)
F(1)-C(34)-C(35)-F(2)	1.6(3)
C(33)-C(34)-C(35)-F(2)	180.00(17)
F(1)-C(34)-C(35)-C(36)	-177.83(17)
C(33)-C(34)-C(35)-C(36)	0.6(3)
F(2)-C(35)-C(36)-F(3)	-1.7(3)
C(34)-C(35)-C(36)-F(3)	177.68(17)
F(2)-C(35)-C(36)-C(37)	178.94(17)
C(34)-C(35)-C(36)-C(37)	-1.7(3)
F(3)-C(36)-C(37)-F(4)	0.3(3)
C(35)-C(36)-C(37)-F(4)	179.62(17)
F(3)-C(36)-C(37)-C(32)	-177.12(17)

C(35)-C(36)-C(37)-C(32)	2.2(3)
C(33)-C(32)-C(37)-F(4)	-178.98(16)
S(1)-C(32)-C(37)-F(4)	-1.9(2)
C(33)-C(32)-C(37)-C(36)	-1.7(3)
S(1)-C(32)-C(37)-C(36)	175.40(15)

Symmetry transformations used to generate equivalent atoms:

X-ray structure of Ru9:

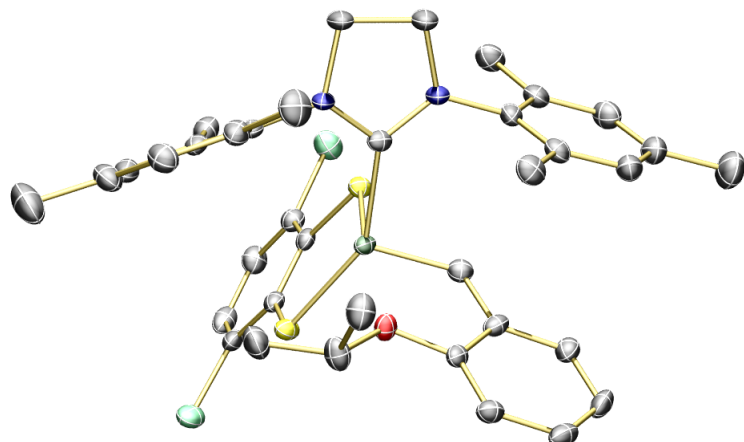


Table 1. Crystal data and structure refinement for Ru9

Identification code	<chem>C37H40Cl2N2ORuS2(CH2Cl2)</chem>		
Empirical formula	<chem>C38H42Cl4N2ORuS2</chem>		
Formula weight	849.72		
Temperature	100(2) K		
Wavelength	0.71073 Å		
Crystal system	Orthorhombic		
Space group	P b c a		
Unit cell dimensions	$a = 19.3211(8)$ Å	$\alpha = 90^\circ$.	
	$b = 17.4846(7)$ Å	$\beta = 90^\circ$.	
	$c = 22.8338(8)$ Å	$\gamma = 90^\circ$.	
Volume	$7713.8(5)$ Å ³		
Z	8		
Density (calculated)	1.463 Mg/m ³		
Absorption coefficient	0.825 mm ⁻¹		
F(000)	3488		
Crystal size	0.200 x 0.100 x 0.080 mm ³		

Theta range for data collection	1.784 to 28.364°.
Index ranges	-25≤h≤24, -23≤k≤23, -27≤l≤30
Reflections collected	100010
Independent reflections	9598 [R(int) = 0.1107]
Completeness to theta = 25.242°	100.0 %
Absorption correction	Semi-empirical from equivalents
Max. and min. transmission	0.7531 and 0.6187
Refinement method	Full-matrix least-squares on F ²
Data / restraints / parameters	9598 / 0 / 441
Goodness-of-fit on F ²	1.021
Final R indices [I>2sigma(I)]	R1 = 0.0477, wR2 = 0.1060
R indices (all data)	R1 = 0.0922, wR2 = 0.1259
Extinction coefficient	na
Largest diff. peak and hole	1.166 and -0.999 e.Å ⁻³

Table 2. Atomic coordinates (x 10⁴) and equivalent isotropic displacement parameters (Å² x 10³) for Ru9. U(eq) is defined as one third of the trace of the orthogonalized U^{ij} tensor.

	x	y	z	U(eq)
Ru(1)	1991(1)	9678(1)	3053(1)	16(1)
Cl(1)	658(1)	12215(1)	2281(1)	31(1)
Cl(2)	-329(1)	10112(1)	4309(1)	32(1)
S(1)	1058(1)	9697(1)	3658(1)	19(1)
S(2)	1560(1)	10755(1)	2609(1)	22(1)
O(1)	3018(1)	9899(1)	2555(1)	21(1)
N(1)	1667(2)	8035(2)	2740(1)	20(1)
N(2)	2085(2)	8075(2)	3622(1)	20(1)
C(1)	1956(2)	8500(2)	3144(2)	18(1)
C(2)	1505(2)	7269(2)	2973(2)	27(1)
C(3)	1935(2)	7251(2)	3529(2)	27(1)
C(4)	1506(2)	8221(2)	2144(2)	18(1)
C(5)	1922(2)	7899(2)	1701(2)	24(1)
C(6)	1749(2)	8055(2)	1120(2)	29(1)
C(7)	1183(2)	8506(2)	970(2)	29(1)
C(8)	783(2)	8793(2)	1414(2)	25(1)
C(9)	915(2)	8644(2)	2003(2)	19(1)
C(10)	2518(2)	7379(3)	1835(2)	35(1)

C(11)	997(3)	8653(3)	338(2)	49(1)
C(12)	394(2)	8894(2)	2451(2)	26(1)
C(13)	2481(2)	8294(2)	4126(2)	20(1)
C(14)	3205(2)	8332(2)	4069(2)	22(1)
C(15)	3590(2)	8526(2)	4561(2)	27(1)
C(16)	3278(2)	8673(2)	5100(2)	30(1)
C(17)	2566(2)	8616(2)	5140(2)	30(1)
C(18)	2155(2)	8421(2)	4659(2)	25(1)
C(19)	3562(2)	8165(2)	3499(2)	28(1)
C(20)	3715(3)	8884(3)	5625(2)	45(1)
C(21)	1382(2)	8359(2)	4734(2)	30(1)
C(22)	2580(2)	9917(2)	3654(2)	21(1)
C(23)	3284(2)	10142(2)	3529(2)	20(1)
C(24)	3746(2)	10367(2)	3966(2)	23(1)
C(25)	4414(2)	10581(2)	3832(2)	26(1)
C(26)	4630(2)	10568(2)	3254(2)	26(1)
C(27)	4187(2)	10347(2)	2809(2)	22(1)
C(28)	3517(2)	10132(2)	2948(2)	18(1)
C(29)	3214(2)	9835(2)	1928(2)	28(1)
C(30)	2573(2)	9908(3)	1570(2)	34(1)
C(31)	3601(2)	9095(2)	1835(2)	32(1)
C(32)	587(2)	10507(2)	3456(2)	18(1)
C(33)	-31(2)	10704(2)	3751(2)	23(1)
C(34)	-404(2)	11356(2)	3618(2)	28(1)
C(35)	-177(2)	11829(2)	3170(2)	28(1)
C(36)	408(2)	11639(2)	2862(2)	22(1)
C(37)	809(2)	10986(2)	2998(2)	20(1)
C(1S)	1214(3)	1426(3)	4697(2)	53(2)
Cl(1S)	2013(1)	1328(1)	5028(1)	92(1)
Cl(2S)	592(1)	1816(1)	5163(1)	78(1)

Table 3. Bond lengths [Å] and angles [°] for Ru9.

Ru(1)-C(22)	1.830(4)
Ru(1)-C(1)	2.071(3)
Ru(1)-S(1)	2.2706(10)

Ru(1)-S(2)	2.2954(9)
Ru(1)-O(1)	2.319(3)
Cl(1)-C(36)	1.734(4)
Cl(2)-C(33)	1.739(4)
S(1)-C(32)	1.747(4)
S(2)-C(37)	1.749(4)
O(1)-C(28)	1.380(4)
O(1)-C(29)	1.484(5)
N(1)-C(1)	1.352(5)
N(1)-C(4)	1.433(5)
N(1)-C(2)	1.475(4)
N(2)-C(1)	1.344(5)
N(2)-C(13)	1.434(5)
N(2)-C(3)	1.484(4)
C(2)-C(3)	1.517(5)
C(4)-C(9)	1.399(5)
C(4)-C(5)	1.410(5)
C(5)-C(6)	1.394(6)
C(5)-C(10)	1.498(5)
C(6)-C(7)	1.391(6)
C(7)-C(8)	1.370(6)
C(7)-C(11)	1.509(6)
C(8)-C(9)	1.393(5)
C(9)-C(12)	1.500(5)
C(13)-C(18)	1.390(5)
C(13)-C(14)	1.406(5)
C(14)-C(15)	1.389(5)
C(14)-C(19)	1.503(5)
C(15)-C(16)	1.393(6)
C(16)-C(17)	1.382(6)
C(16)-C(20)	1.513(6)
C(17)-C(18)	1.398(6)
C(18)-C(21)	1.508(6)
C(22)-C(23)	1.445(5)
C(23)-C(24)	1.395(5)
C(23)-C(28)	1.399(5)
C(24)-C(25)	1.377(6)

C(25)-C(26)	1.385(6)
C(26)-C(27)	1.384(6)
C(27)-C(28)	1.386(5)
C(29)-C(30)	1.489(6)
C(29)-C(31)	1.511(6)
C(32)-C(37)	1.407(5)
C(32)-C(33)	1.413(5)
C(33)-C(34)	1.382(5)
C(34)-C(35)	1.388(6)
C(35)-C(36)	1.371(6)
C(36)-C(37)	1.414(5)
C(1S)-Cl(1S)	1.726(6)
C(1S)-Cl(2S)	1.745(6)
C(22)-Ru(1)-C(1)	99.91(15)
C(22)-Ru(1)-S(1)	91.98(13)
C(1)-Ru(1)-S(1)	85.87(10)
C(22)-Ru(1)-S(2)	111.69(11)
C(1)-Ru(1)-S(2)	148.03(11)
S(1)-Ru(1)-S(2)	88.23(3)
C(22)-Ru(1)-O(1)	78.36(14)
C(1)-Ru(1)-O(1)	104.03(12)
S(1)-Ru(1)-O(1)	167.13(7)
S(2)-Ru(1)-O(1)	87.49(7)
C(32)-S(1)-Ru(1)	105.37(13)
C(37)-S(2)-Ru(1)	105.43(13)
C(28)-O(1)-C(29)	118.1(3)
C(28)-O(1)-Ru(1)	109.1(2)
C(29)-O(1)-Ru(1)	132.8(2)
C(1)-N(1)-C(4)	127.0(3)
C(1)-N(1)-C(2)	112.8(3)
C(4)-N(1)-C(2)	120.2(3)
C(1)-N(2)-C(13)	127.0(3)
C(1)-N(2)-C(3)	112.6(3)
C(13)-N(2)-C(3)	118.6(3)
N(2)-C(1)-N(1)	107.3(3)
N(2)-C(1)-Ru(1)	128.7(3)

N(1)-C(1)-Ru(1)	122.9(3)
N(1)-C(2)-C(3)	101.8(3)
N(2)-C(3)-C(2)	101.9(3)
C(9)-C(4)-C(5)	120.8(3)
C(9)-C(4)-N(1)	121.1(3)
C(5)-C(4)-N(1)	117.8(3)
C(6)-C(5)-C(4)	117.8(4)
C(6)-C(5)-C(10)	119.9(4)
C(4)-C(5)-C(10)	122.2(4)
C(7)-C(6)-C(5)	122.3(4)
C(8)-C(7)-C(6)	118.0(4)
C(8)-C(7)-C(11)	120.7(4)
C(6)-C(7)-C(11)	121.2(4)
C(7)-C(8)-C(9)	122.8(4)
C(8)-C(9)-C(4)	118.1(4)
C(8)-C(9)-C(12)	118.7(3)
C(4)-C(9)-C(12)	123.0(3)
C(18)-C(13)-C(14)	121.6(4)
C(18)-C(13)-N(2)	120.2(3)
C(14)-C(13)-N(2)	118.1(3)
C(15)-C(14)-C(13)	118.1(4)
C(15)-C(14)-C(19)	120.2(4)
C(13)-C(14)-C(19)	121.7(3)
C(14)-C(15)-C(16)	121.7(4)
C(17)-C(16)-C(15)	118.5(4)
C(17)-C(16)-C(20)	121.3(4)
C(15)-C(16)-C(20)	120.2(4)
C(16)-C(17)-C(18)	122.1(4)
C(13)-C(18)-C(17)	118.0(4)
C(13)-C(18)-C(21)	122.5(4)
C(17)-C(18)-C(21)	119.5(4)
C(23)-C(22)-Ru(1)	120.0(3)
C(24)-C(23)-C(28)	118.4(4)
C(24)-C(23)-C(22)	122.5(4)
C(28)-C(23)-C(22)	119.1(3)
C(25)-C(24)-C(23)	121.2(4)
C(24)-C(25)-C(26)	119.2(4)

C(27)-C(26)-C(25)	121.2(4)
C(26)-C(27)-C(28)	119.1(4)
O(1)-C(28)-C(27)	125.7(3)
O(1)-C(28)-C(23)	113.4(3)
C(27)-C(28)-C(23)	120.9(3)
O(1)-C(29)-C(30)	108.1(3)
O(1)-C(29)-C(31)	109.0(3)
C(30)-C(29)-C(31)	114.1(4)
C(37)-C(32)-C(33)	117.9(3)
C(37)-C(32)-S(1)	121.3(3)
C(33)-C(32)-S(1)	120.8(3)
C(34)-C(33)-C(32)	122.4(4)
C(34)-C(33)-Cl(2)	118.6(3)
C(32)-C(33)-Cl(2)	119.0(3)
C(33)-C(34)-C(35)	119.2(4)
C(36)-C(35)-C(34)	119.7(4)
C(35)-C(36)-C(37)	122.3(4)
C(35)-C(36)-Cl(1)	118.7(3)
C(37)-C(36)-Cl(1)	119.0(3)
C(32)-C(37)-C(36)	118.5(4)
C(32)-C(37)-S(2)	119.6(3)
C(36)-C(37)-S(2)	122.0(3)
Cl(1S)-C(1S)-Cl(2S)	112.8(3)

Symmetry transformations used to generate equivalent atoms:

Table 4. Anisotropic displacement parameters ($\text{\AA}^2 \times 10^3$) for Ru9. The anisotropic displacement factor exponent takes the form: $-2\pi^2 [h^2 a^{*2} U^{11} + \dots + 2 h k a^{*} b^{*} U^{12}]$

	U^{11}	U^{22}	U^{33}	U^{23}	U^{13}	U^{12}
Ru(1)	14(1)	14(1)	21(1)	1(1)	-1(1)	-1(1)
Cl(1)	28(1)	21(1)	43(1)	9(1)	-5(1)	0(1)
Cl(2)	26(1)	39(1)	30(1)	6(1)	6(1)	4(1)
S(1)	17(1)	17(1)	23(1)	2(1)	1(1)	1(1)
S(2)	17(1)	18(1)	30(1)	5(1)	-1(1)	0(1)
O(1)	16(1)	28(1)	21(1)	0(1)	-1(1)	0(1)

N(1)	24(2)	11(1)	26(2)	4(1)	-7(1)	-3(1)
N(2)	24(2)	14(1)	23(2)	2(1)	-3(1)	-3(1)
C(1)	15(2)	15(2)	24(2)	1(1)	2(2)	1(1)
C(2)	37(2)	16(2)	29(2)	5(2)	-8(2)	-8(2)
C(3)	35(2)	17(2)	30(2)	4(2)	-8(2)	-5(2)
C(4)	22(2)	11(2)	22(2)	1(1)	-4(2)	-3(1)
C(5)	24(2)	18(2)	29(2)	0(2)	-4(2)	2(2)
C(6)	34(2)	26(2)	27(2)	1(2)	2(2)	2(2)
C(7)	39(3)	22(2)	25(2)	4(2)	-2(2)	2(2)
C(8)	29(2)	17(2)	30(2)	2(2)	-9(2)	-2(2)
C(9)	21(2)	14(2)	22(2)	-3(1)	-4(2)	-3(1)
C(10)	29(2)	37(2)	39(3)	-2(2)	0(2)	10(2)
C(11)	68(4)	45(3)	32(3)	7(2)	-7(3)	12(3)
C(12)	23(2)	26(2)	31(2)	-4(2)	-4(2)	-1(2)
C(13)	23(2)	17(2)	21(2)	2(2)	-4(2)	0(2)
C(14)	26(2)	19(2)	22(2)	3(2)	0(2)	4(2)
C(15)	25(2)	28(2)	26(2)	3(2)	-2(2)	-3(2)
C(16)	32(2)	31(2)	26(2)	2(2)	-5(2)	-5(2)
C(17)	37(3)	30(2)	22(2)	0(2)	2(2)	-1(2)
C(18)	28(2)	21(2)	25(2)	6(2)	-1(2)	0(2)
C(19)	24(2)	28(2)	31(2)	2(2)	3(2)	7(2)
C(20)	45(3)	57(3)	34(3)	-4(2)	-10(2)	-8(3)
C(21)	26(2)	34(2)	29(2)	7(2)	6(2)	-1(2)
C(22)	22(2)	18(2)	23(2)	0(2)	2(2)	1(2)
C(23)	16(2)	16(2)	29(2)	-2(2)	0(2)	-1(1)
C(24)	25(2)	20(2)	25(2)	-2(2)	-4(2)	-1(2)
C(25)	19(2)	26(2)	34(2)	-5(2)	-9(2)	-3(2)
C(26)	17(2)	19(2)	41(2)	1(2)	-1(2)	-2(2)
C(27)	20(2)	21(2)	27(2)	3(2)	2(2)	-2(2)
C(28)	16(2)	16(2)	23(2)	2(1)	-2(2)	2(1)
C(29)	26(2)	37(2)	20(2)	1(2)	2(2)	6(2)
C(30)	37(3)	38(2)	27(2)	7(2)	-6(2)	3(2)
C(31)	28(2)	37(2)	30(2)	-6(2)	-2(2)	7(2)
C(32)	17(2)	17(2)	19(2)	-5(1)	-4(2)	0(1)
C(33)	22(2)	21(2)	25(2)	-2(2)	-1(2)	-1(2)
C(34)	25(2)	28(2)	30(2)	-4(2)	-1(2)	6(2)
C(35)	24(2)	19(2)	41(3)	-6(2)	-10(2)	6(2)

C(36)	19(2)	20(2)	27(2)	1(2)	-7(2)	-4(2)
C(37)	20(2)	15(2)	25(2)	-1(2)	-6(2)	-2(1)
C(1S)	77(4)	43(3)	40(3)	0(2)	-15(3)	-7(3)
Cl(1S)	63(1)	115(2)	97(1)	-28(1)	-21(1)	-11(1)
Cl(2S)	79(1)	54(1)	102(1)	14(1)	20(1)	-16(1)

Table 5. Hydrogen coordinates ($\times 10^4$) and isotropic displacement parameters ($\text{\AA}^2 \times 10^3$) for Ru9.

	x	y	z	U(eq)
H(2A)	1648	6861	2697	33
H(2B)	1006	7215	3059	33
H(3A)	1670	7033	3860	33
H(3B)	2366	6953	3474	33
H(6)	2027	7847	817	35
H(8)	399	9107	1316	30
H(10A)	2727	7529	2209	52
H(10B)	2864	7418	1523	52
H(10C)	2352	6851	1862	52
H(11A)	648	8282	211	73
H(11B)	1412	8601	94	73
H(11C)	811	9172	298	73
H(12A)	443	9445	2520	40
H(12B)	474	8617	2818	40
H(12C)	-74	8785	2308	40
H(15)	4080	8560	4529	32
H(17)	2350	8712	5506	36
H(19A)	3448	7645	3372	41
H(19B)	4064	8210	3551	41
H(19C)	3407	8532	3202	41
H(20A)	4149	8596	5615	68
H(20B)	3462	8761	5985	68
H(20C)	3816	9433	5616	68
H(21A)	1178	8133	4381	45
H(21B)	1186	8870	4797	45
H(21C)	1278	8034	5073	45

H(22)	2423	9893	4048	25
H(24)	3598	10372	4362	28
H(25)	4723	10735	4134	31
H(26)	5091	10713	3161	31
H(27)	4340	10343	2414	27
H(29)	3530	10270	1829	33
H(30A)	2242	9512	1686	51
H(30B)	2689	9847	1154	51
H(30C)	2368	10414	1633	51
H(31A)	4028	9099	2068	48
H(31B)	3717	9039	1420	48
H(31C)	3310	8665	1959	48
H(34)	-810	11480	3832	33
H(35)	-425	12281	3076	34
H(1S1)	1054	917	4563	64
H(1S2)	1263	1758	4349	64

Table 6. Torsion angles [°] for Ru9.

C(13)-N(2)-C(1)-N(1)	169.9(3)
C(3)-N(2)-C(1)-N(1)	5.4(4)
C(13)-N(2)-C(1)-Ru(1)	-21.5(6)
C(3)-N(2)-C(1)-Ru(1)	174.1(3)
C(4)-N(1)-C(1)-N(2)	-173.4(3)
C(2)-N(1)-C(1)-N(2)	7.6(4)
C(4)-N(1)-C(1)-Ru(1)	17.1(5)
C(2)-N(1)-C(1)-Ru(1)	-161.9(3)
C(1)-N(1)-C(2)-C(3)	-16.5(4)
C(4)-N(1)-C(2)-C(3)	164.4(3)
C(1)-N(2)-C(3)-C(2)	-15.2(4)
C(13)-N(2)-C(3)-C(2)	178.9(3)
N(1)-C(2)-C(3)-N(2)	17.5(4)
C(1)-N(1)-C(4)-C(9)	-78.8(5)
C(2)-N(1)-C(4)-C(9)	100.1(4)
C(1)-N(1)-C(4)-C(5)	107.7(4)
C(2)-N(1)-C(4)-C(5)	-73.4(5)
C(9)-C(4)-C(5)-C(6)	4.0(5)

N(1)-C(4)-C(5)-C(6)	177.5(3)
C(9)-C(4)-C(5)-C(10)	-173.7(4)
N(1)-C(4)-C(5)-C(10)	-0.2(5)
C(4)-C(5)-C(6)-C(7)	-0.7(6)
C(10)-C(5)-C(6)-C(7)	177.1(4)
C(5)-C(6)-C(7)-C(8)	-0.8(6)
C(5)-C(6)-C(7)-C(11)	-178.7(4)
C(6)-C(7)-C(8)-C(9)	-0.9(6)
C(11)-C(7)-C(8)-C(9)	177.0(4)
C(7)-C(8)-C(9)-C(4)	4.0(6)
C(7)-C(8)-C(9)-C(12)	-171.9(4)
C(5)-C(4)-C(9)-C(8)	-5.6(5)
N(1)-C(4)-C(9)-C(8)	-178.9(3)
C(5)-C(4)-C(9)-C(12)	170.1(3)
N(1)-C(4)-C(9)-C(12)	-3.2(5)
C(1)-N(2)-C(13)-C(18)	110.1(4)
C(3)-N(2)-C(13)-C(18)	-86.3(4)
C(1)-N(2)-C(13)-C(14)	-73.6(5)
C(3)-N(2)-C(13)-C(14)	90.1(4)
C(18)-C(13)-C(14)-C(15)	-2.1(5)
N(2)-C(13)-C(14)-C(15)	-178.4(3)
C(18)-C(13)-C(14)-C(19)	177.5(3)
N(2)-C(13)-C(14)-C(19)	1.3(5)
C(13)-C(14)-C(15)-C(16)	0.7(6)
C(19)-C(14)-C(15)-C(16)	-178.9(4)
C(14)-C(15)-C(16)-C(17)	0.5(6)
C(14)-C(15)-C(16)-C(20)	-179.9(4)
C(15)-C(16)-C(17)-C(18)	-0.3(6)
C(20)-C(16)-C(17)-C(18)	180.0(4)
C(14)-C(13)-C(18)-C(17)	2.2(5)
N(2)-C(13)-C(18)-C(17)	178.4(3)
C(14)-C(13)-C(18)-C(21)	-178.0(3)
N(2)-C(13)-C(18)-C(21)	-1.8(5)
C(16)-C(17)-C(18)-C(13)	-1.0(6)
C(16)-C(17)-C(18)-C(21)	179.3(4)
C(1)-Ru(1)-C(22)-C(23)	106.0(3)
S(1)-Ru(1)-C(22)-C(23)	-167.9(3)

S(2)-Ru(1)-C(22)-C(23)	-79.0(3)
O(1)-Ru(1)-C(22)-C(23)	3.6(3)
Ru(1)-C(22)-C(23)-C(24)	176.7(3)
Ru(1)-C(22)-C(23)-C(28)	-3.6(5)
C(28)-C(23)-C(24)-C(25)	0.5(5)
C(22)-C(23)-C(24)-C(25)	-179.8(3)
C(23)-C(24)-C(25)-C(26)	-0.4(6)
C(24)-C(25)-C(26)-C(27)	0.3(6)
C(25)-C(26)-C(27)-C(28)	-0.4(6)
C(29)-O(1)-C(28)-C(27)	3.0(5)
Ru(1)-O(1)-C(28)-C(27)	-177.1(3)
C(29)-O(1)-C(28)-C(23)	-177.5(3)
Ru(1)-O(1)-C(28)-C(23)	2.4(3)
C(26)-C(27)-C(28)-O(1)	180.0(3)
C(26)-C(27)-C(28)-C(23)	0.6(5)
C(24)-C(23)-C(28)-O(1)	179.9(3)
C(22)-C(23)-C(28)-O(1)	0.2(5)
C(24)-C(23)-C(28)-C(27)	-0.6(5)
C(22)-C(23)-C(28)-C(27)	179.7(3)
C(28)-O(1)-C(29)-C(30)	-156.2(3)
Ru(1)-O(1)-C(29)-C(30)	23.9(5)
C(28)-O(1)-C(29)-C(31)	79.2(4)
Ru(1)-O(1)-C(29)-C(31)	-100.7(3)
Ru(1)-S(1)-C(32)-C(37)	0.5(3)
Ru(1)-S(1)-C(32)-C(33)	-179.2(3)
C(37)-C(32)-C(33)-C(34)	-2.3(5)
S(1)-C(32)-C(33)-C(34)	177.4(3)
C(37)-C(32)-C(33)-Cl(2)	178.7(3)
S(1)-C(32)-C(33)-Cl(2)	-1.6(4)
C(32)-C(33)-C(34)-C(35)	1.8(6)
Cl(2)-C(33)-C(34)-C(35)	-179.2(3)
C(33)-C(34)-C(35)-C(36)	0.6(6)
C(34)-C(35)-C(36)-C(37)	-2.4(6)
C(34)-C(35)-C(36)-Cl(1)	177.0(3)
C(33)-C(32)-C(37)-C(36)	0.5(5)
S(1)-C(32)-C(37)-C(36)	-179.2(3)
C(33)-C(32)-C(37)-S(2)	-178.6(3)

S(1)-C(32)-C(37)-S(2)	1.8(4)
C(35)-C(36)-C(37)-C(32)	1.8(5)
Cl(1)-C(36)-C(37)-C(32)	-177.6(3)
C(35)-C(36)-C(37)-S(2)	-179.2(3)
Cl(1)-C(36)-C(37)-S(2)	1.4(4)
Ru(1)-S(2)-C(37)-C(32)	-3.0(3)
Ru(1)-S(2)-C(37)-C(36)	178.0(3)

Symmetry transformations used to generate equivalent atoms:

■ DFT Computational Data:

DFT¹²⁰ computations were performed with the Gaussian 09 suite of programs¹²¹ by application of the generalized gradient approximation (GGA) functional BP86.¹²² The following basis set (termed “basis1”) was used for geometry optimizations, calculation of dipole moments and evaluation of thermal corrections to the Gibbs free energy at standard conditions (298.15 K, 1 atm): 6-31G(d,p) basis set for hydrogen and carbon atoms, including additional diffuse functions (+) on heteroatoms (oxygen, nitrogen, sulfur and chloride). A quasi-relativistic effective core potential (ECP) of the Stuttgart-Dresden type¹²³ was used for ruthenium (MWB28 keyword in Gaussian for basis set and ECP). The nature of all stationary points was checked through vibrational analysis. Single point electronic energies of metallacyclobutanes **Z-A**, **Z-B**, **E-A** and **E-B** in solution (tetrahydrofuran) were performed on the gas phase geometries obtained with basis1 through application of an integral equation formalism variant of the polarizable

(120) For a recent review on the application of DFT to complexes containing transition metals, see: Cramer, C. J.; Truhlar, D. G. *Phys. Chem. Chem. Phys.* **2009**, *11*, 10757.

(121) Frisch, M. J.; Trucks, G. W.; Schlegel, H. B.; Scuseria, G. E.; Robb, M. A.; Cheeseman, J. R.; Scalmani, G.; Barone, V.; Mennucci, B.; Petersson, G. A.; Nakatsuji, H.; Caricato, M.; Li, X.; Hratchian, H. P.; Izmaylov, A. F.; Bloino, J.; Zheng, G.; Sonnenberg, J. L.; Hada, M.; Ehara, M.; Toyota, K.; Fukuda, R.; Hasegawa, J.; Ishida, M.; Nakajima, T.; Honda, Y.; Kitao, O.; Nakai, H.; Vreven, T.; Montgomery, Jr., J. A.; Peralta, J. E.; Ogliaro, F.; Bearpark, M.; Heyd, J. J.; Brothers, E.; Kudin, K. N.; Staroverov, V. N.; Kobayashi, R.; Normand, J.; Raghavachari, K.; Rendell, A.; Burant, J. C.; Iyengar, S. S.; Tomasi, J.; Cossi, M.; Rega, N.; Millam, J. M.; Klene, M.; Knox, J. E.; Cross, J. B.; Bakken, V.; Adamo, C.; Jaramillo, J.; Gomperts, R.; Stratmann, R. E.; Yazyev, O.; Austin, A. J.; Cammi, R.; Pomelli, C.; Ochterski, J. W.; Martin, R. L.; Morokuma, K.; Zakrzewski, V. G.; Voth, G. A.; Salvador, P.; Dannenberg, J. J.; Dapprich, S.; Daniels, A. D.; Farkas, Ö.; Foresman, J. B.; Ortiz, J. V.; Cioslowski, J.; Fox, D. J. *Gaussian 09, Revision A.1*, Gaussian, Inc., Wallingford CT, 2009.

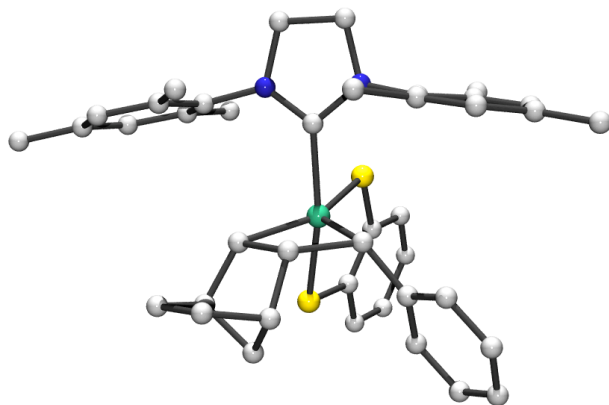
(122) (a) Becke, A. D. *Phys. Rev. A* **1988**, *38*, 3098. (b) Perdew, J. P.; Yue, W. *Phys. Rev. B* **1986**, *33*, 8800.

(123) Andrae, D.; Haeussermann, U.; Dolg, M.; Stoll, H.; Preuss, H. *Theor. Chim. Acta* **1990**, *77*, 123.

continuum model (IEFPCM)¹²⁴ and the larger basis set termed “basis2”: 6-311+G(2df,2pd) on H, C, N, S and MWB28 on ruthenium. The single point electronic energies at the BP86/basis2 level were corrected by addition of thermal corrections to the Gibbs free energy obtained at the BP86/basis1 level.

Geometries and Energies of Computed Structures for Scheme 3.3.3

(124) Scalmani, G.; Frisch, M. J. *J. Chem. Phys.* **2010**, *132*, 114110.

Ruthenacyclobutane Z-A

Gas phase electronic energy (basis 1):

-2591.06281055 hartree

Gas phase thermal correction to free energy (basis 1):

0.665857 hartree

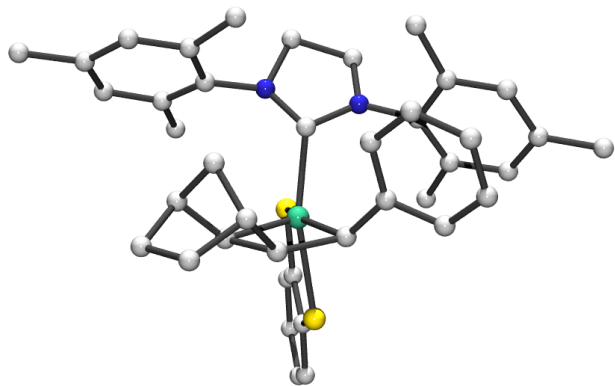
Single point electronic energy in thf (basis 2):

-2591.62434465 hartree

S	0.035816	1.353116	-1.996672
C	0.478050	-1.274346	-0.970569
Ru	0.176262	0.517660	0.101254
C	1.352181	0.003788	1.696219
C	-1.376405	-0.217386	1.161335
S	0.495073	2.832867	0.734581
N	-0.431609	-1.961768	-1.752025
N	1.721557	-1.712115	-1.373751
C	-1.851391	-2.136878	-1.546356
C	0.191309	-2.887342	-2.735224
C	1.694826	-2.668759	-2.509329
C	3.016444	-1.445619	-0.793916
H	2.234962	-3.595276	-2.244936
H	2.198952	-2.224088	-3.386092
H	-0.129011	-3.926217	-2.535364
C	-4.617479	-2.668426	-1.215730
C	-2.791531	-1.486741	-2.381010
C	-2.279015	-3.107018	-0.596969
C	-3.654578	-3.344587	-0.442063
C	-4.161055	-1.761884	-2.183967
H	-3.981703	-4.088487	0.294939
H	-4.890696	-1.249316	-2.822970
C	5.619393	-1.110803	0.273935
C	3.484412	-2.327988	0.217274
C	3.859290	-0.435532	-1.318708
C	5.144481	-0.286279	-0.759250
C	4.775802	-2.136771	0.738425
C	2.619495	-3.452555	0.745956
C	3.437650	0.481040	-2.442961
H	5.796345	0.499903	-1.159566
H	5.133850	-2.814410	1.523220
C	6.993953	-0.899297	0.871354
H	7.400818	-1.833031	1.293460
H	4.321757	0.863898	-2.978553
H	-0.132938	-2.627931	-3.757979
H	6.960434	-0.156538	1.689483
H	2.275028	-4.129751	-0.055610
H	1.713035	-3.067183	1.244532
H	7.707548	-0.521854	0.120259

H	2.867714	1.342696	-2.056100
H	2.776092	-0.016763	-3.169033
H	3.175071	-4.057944	1.479571
C	-2.398184	-0.529110	-3.482562
H	-3.012903	-0.707957	-4.381437
H	-2.555640	0.516346	-3.166687
H	-1.335960	-0.612910	-3.752517
C	-6.096139	-2.909069	-1.002357
H	-6.295266	-3.940145	-0.665425
H	-6.498022	-2.228385	-0.229647
H	-6.672741	-2.731281	-1.924910
C	-1.284311	-3.893734	0.230015
H	-0.637752	-3.234625	0.833251
H	-1.804532	-4.580708	0.916032
H	-0.609791	-4.499981	-0.401385
C	0.005554	3.127208	-1.958471
C	-0.186793	3.868516	-3.145045
C	0.216335	3.782560	-0.722868
C	-0.180675	5.268076	-3.102103
H	-0.339823	3.339806	-4.093211
C	0.231887	5.199060	-0.699620
C	0.032048	5.930694	-1.875279
H	-0.337139	5.842767	-4.020933
H	0.397845	5.711578	0.254384
H	0.039505	7.025495	-1.838840
C	1.776920	0.830631	2.924148
H	2.531036	1.602234	2.705809
H	2.082999	-0.779271	1.455519
C	-0.085037	-0.582501	2.102813
H	-0.014787	-1.678980	2.026775
H	-1.756664	-1.179404	0.794531
C	-0.193044	-0.090175	3.580851
H	-1.220422	-0.154477	3.971579
C	2.219788	-0.218889	3.994234
H	2.955144	-0.939928	3.597677
H	2.687004	0.291115	4.855469
C	0.862362	-0.888482	4.402363
H	0.662858	-0.770872	5.481442
H	0.832574	-1.970897	4.183411
C	0.441425	1.311667	3.539658
H	-0.110278	2.025218	2.914655
H	0.568344	1.746991	4.546846
C	-2.541222	0.526148	1.758377
C	-2.640348	1.928718	1.902734
C	-3.642876	-0.259318	2.185578
C	-3.780804	2.514247	2.472817
H	-1.819989	2.556556	1.537196
C	-4.781194	0.325237	2.758727
H	-3.598156	-1.347899	2.061672
C	-4.853817	1.719665	2.907730
H	-3.833023	3.604544	2.565827
H	-5.613493	-0.308774	3.084150
H	-5.743814	2.183063	3.347076

Ruthenacyclobutane Z-B



Gas phase electronic energy (basis 1):

-2591.04519743 hartree

Gas phase thermal correction to free energy (basis 1):

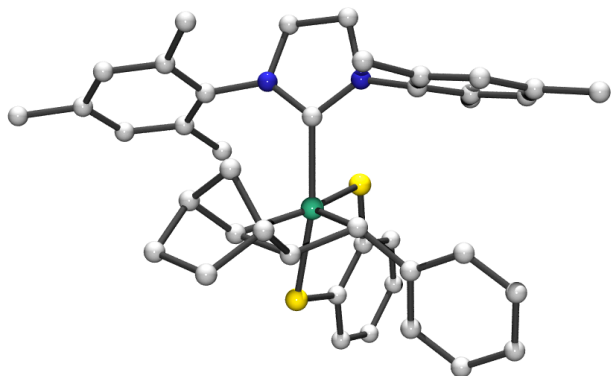
0.669445 hartree

Single point electronic energy in thf (basis 2):

-2591.60424425 hartree

C	0.156966	-0.468622	-1.135592
Ru	0.212217	0.798636	0.546329
C	1.569503	0.200421	1.857536
N	-0.949983	-0.442046	-1.977370
N	1.215540	-0.893052	-1.935047
C	-2.364127	-0.317772	-1.680428
C	-0.578669	-0.575223	-3.408670
C	0.806339	-1.215512	-3.327070
C	2.482237	-1.454377	-1.514888
H	0.774322	-2.313004	-3.473185
H	1.525796	-0.791421	-4.046619
H	-1.314299	-1.186986	-3.953573
C	-5.181444	-0.234071	-1.286079
C	-3.017379	0.932512	-1.529842
C	-3.132397	-1.517903	-1.718992
C	-4.519252	-1.452554	-1.513710
C	-4.412077	0.936612	-1.313983
H	-5.096248	-2.384869	-1.532480
H	-4.909451	1.906149	-1.186726
C	4.972340	-2.644152	-0.821033
C	2.541882	-2.829302	-1.154376
C	3.681640	-0.702092	-1.629618
C	4.897509	-1.312772	-1.262824
C	3.781399	-3.388745	-0.794663
C	1.331374	-3.738129	-1.198077
C	3.720537	0.712527	-2.155873
H	5.819224	-0.723587	-1.345152
H	3.813916	-4.445005	-0.499428
C	6.290121	-3.256099	-0.396616
H	6.300435	-4.347054	-0.556112
H	4.706226	0.925994	-2.601175
H	-0.548522	0.429861	-3.872117
H	6.483081	-3.080979	0.677849
H	0.390427	-3.185022	-1.062142
H	1.390640	-4.511662	-0.415252
H	7.136136	-2.819477	-0.952923
H	3.537158	1.443255	-1.350345
H	2.942209	0.895968	-2.912254
H	1.267649	-4.265601	-2.168485
C	-2.325627	2.272089	-1.627047
H	-1.449626	2.246187	-2.291060
H	-3.032715	3.031114	-2.001967
H	-1.961867	2.615864	-0.641476
C	-6.670314	-0.194664	-1.021204
H	-7.221468	-0.873021	-1.695037

H	-6.892541	-0.515884	0.013063
H	-7.078212	0.821248	-1.148339
C	-2.513155	-2.860438	-2.039773
H	-2.355243	-2.986400	-3.128267
H	-1.537127	-2.994322	-1.551207
H	-3.173150	-3.678120	-1.711221
C	0.935142	3.882409	-0.423865
C	1.375730	4.945497	-1.243276
C	0.485531	4.129078	0.897683
C	1.394261	6.254107	-0.745456
H	1.704379	4.732153	-2.267226
C	0.510912	5.458788	1.385055
C	0.961508	6.505336	0.572696
H	1.741034	7.075791	-1.380392
H	0.169920	5.656001	2.407131
H	0.974540	7.527080	0.967440
C	0.549023	-1.704481	3.012676
H	-0.327761	-2.320977	3.263795
C	0.162847	-0.255036	2.593923
C	-1.229420	-0.013044	1.842854
C	2.450048	-1.052833	1.943785
H	3.277730	-1.060219	1.218318
S	0.973578	2.218472	-1.049617
S	-0.145225	2.799395	1.863268
C	1.586427	-1.585191	4.167481
H	1.267127	-0.863679	4.939483
H	1.704978	-2.563079	4.665363
C	2.902475	-1.155312	3.434388
H	3.690864	-1.920995	3.542627
H	3.313373	-0.203119	3.812249
C	1.434145	-2.203171	1.851161
H	0.915976	-2.197260	0.883136
H	1.871681	-3.199897	2.035046
C	-2.226896	-1.111427	1.721173
C	-1.963203	-2.435048	1.289725
C	-3.548327	-0.827692	2.157756
C	-2.950318	-3.429441	1.342782
H	-0.971248	-2.687333	0.910947
C	-4.542434	-1.813390	2.190908
H	-3.783072	0.188893	2.493861
C	-4.244894	-3.128280	1.796049
H	-2.705603	-4.448489	1.023048
H	-5.547112	-1.558260	2.545285
H	-5.011956	-3.908592	1.840758
H	-1.729996	0.835260	2.331855
H	2.016743	1.072524	2.363165
H	0.101776	0.435175	3.451692

Ruthenacyclobutane E-A

Gas phase electronic energy (basis 1):

-2591.06329315 hartree

Gas phase thermal correction to free energy (basis 1):

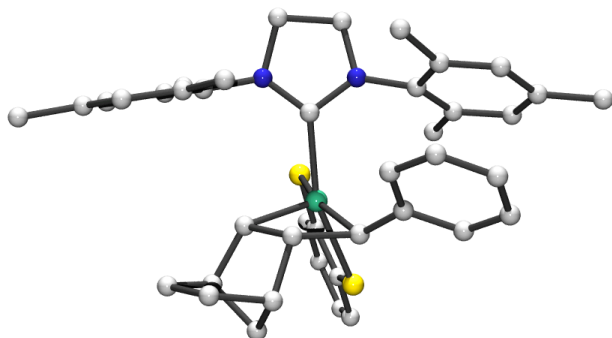
0.667798 hartree

Single point electronic energy in thf (basis 2):

-2591.62280483 hartree

C	1.441403	0.361966	1.853994
C	-1.204160	-0.373467	1.427864
S	0.139067	2.902381	1.143708
Ru	0.128164	0.641693	0.298508
C	0.600928	-0.937411	-0.979878
S	-0.491056	1.597289	-1.667668
N	-0.271060	-1.663536	-1.783969
N	1.851288	-1.096576	-1.563844
C	-1.619370	-2.114402	-1.511917
C	0.406685	-2.375467	-2.898254
C	1.785743	-1.716881	-2.910713
C	3.164259	-0.760376	-1.065005
H	2.610006	-2.431558	-3.060443
H	1.867803	-0.926966	-3.682383
H	0.452031	-3.461853	-2.683284
C	-4.228680	-3.204215	-1.184512
C	-2.710079	-1.576907	-2.247850
C	-1.819628	-3.251015	-0.680399
C	-3.121904	-3.763476	-0.525009
C	-3.992128	-2.123828	-2.049509
H	-3.265703	-4.642295	0.116343
H	-4.830621	-1.697038	-2.613487
C	5.817761	-0.264105	-0.169878
C	3.974781	-1.834850	-0.598199
C	3.702404	0.549874	-1.152470
C	5.013411	0.766652	-0.681765
C	5.281803	-1.563619	-0.156010
C	3.487237	-3.268294	-0.583036
C	2.955139	1.719061	-1.746053
H	5.421465	1.783158	-0.742801
H	5.895838	-2.395533	0.210799
C	7.211159	0.015120	0.351167
H	7.857143	-0.875455	0.278866
H	3.663392	2.420383	-2.218598
H	-0.150361	-2.237579	-3.839521
H	7.185393	0.316231	1.414657
H	2.413115	-3.337353	-0.353157
H	4.037671	-3.859181	0.166581
H	7.693706	0.835628	-0.205547
H	2.399330	2.274182	-0.968174
H	2.210668	1.406562	-2.492749

H	3.646387	-3.764284	-1.559662
C	-2.563529	-0.467652	-3.264628
H	-3.253136	-0.634590	-4.109279
H	-2.804458	0.509889	-2.813901
H	-1.538574	-0.381221	-3.653004
C	-5.624549	-3.752509	-0.981887
H	-5.603633	-4.804567	-0.652981
H	-6.168134	-3.177162	-0.210228
H	-6.220462	-3.692905	-1.907912
C	-0.688407	-3.964160	0.029557
H	0.288052	-3.780868	-0.443107
H	-0.602087	-3.643255	1.082874
H	-0.866780	-5.052421	0.036793
C	-0.756140	3.338327	-1.416942
C	-1.207060	4.141056	-2.488285
C	-0.511528	3.910970	-0.144637
C	-1.438863	5.507764	-2.291515
H	-1.375826	3.682409	-3.469595
C	-0.742916	5.296403	0.035578
C	-1.204845	6.082877	-1.025575
H	-1.796832	6.125537	-3.121591
H	-0.554581	5.742365	1.018271
H	-1.383284	7.152116	-0.868300
C	0.430998	-1.451051	3.143922
H	-0.433736	-2.098176	3.365733
C	0.001736	-0.113321	2.447870
C	2.399366	-0.768756	2.243427
H	3.326276	-0.788818	1.653871
C	1.273789	-1.075964	4.393954
H	0.789549	-0.288297	4.996109
H	1.392274	-1.959426	5.045198
C	2.641825	-0.629150	3.780995
H	3.461412	-1.297125	4.100933
H	2.924052	0.399240	4.064215
C	1.501283	-2.019993	2.188682
H	1.114122	-2.206059	1.176285
H	1.980556	-2.935087	2.579032
C	-2.554868	0.131760	1.828301
C	-2.805281	1.435601	2.318645
C	-3.647352	-0.763417	1.732045
C	-4.094648	1.819098	2.707616
H	-1.982046	2.158451	2.356264
C	-4.940289	-0.374353	2.113551
H	3.474946	-1.775463	1.349165
C	-5.170347	0.918783	2.606963
H	-4.263376	2.834791	3.081576
H	-5.768223	-1.087264	2.031120
H	-6.178137	1.225803	2.906618
H	-1.268788	-1.446000	1.186879
H	1.759758	1.327350	2.279118
H	-0.346111	0.655245	3.154888

Ruthenacyclobutane E-B

Gas phase electronic energy (basis 1):

-2591.05806998 hartree

Gas phase thermal correction to free energy (basis 1):

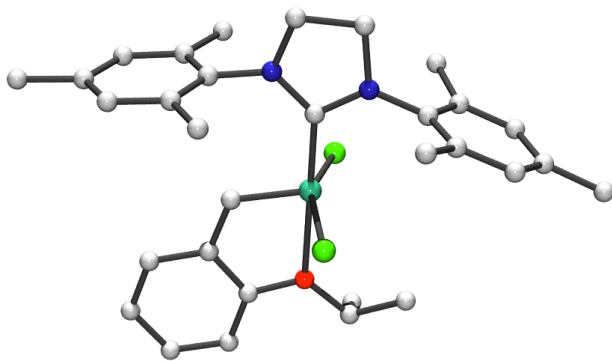
0.666349 hartree

Single point electronic energy in thf (basis 2):

-2591.61843404 hartree

C	0.089940	-0.650775	-1.231459
Ru	0.248807	0.637627	0.408485
C	1.640759	-0.338125	1.430258
N	-1.022251	-0.631362	-2.053040
N	1.107798	-1.199463	-2.001356
C	-2.410456	-0.374717	-1.740466
C	-0.708339	-0.971202	-3.464178
C	0.651888	-1.657889	-3.339322
C	2.369483	-1.729663	-1.548157
H	0.574840	-2.763181	-3.354758
H	1.365740	-1.349669	-4.119974
H	-1.488212	-1.618893	-3.894597
C	-5.199099	-0.036182	-1.352718
C	-2.967486	0.927118	-1.781171
C	-3.248551	-1.512657	-1.569498
C	-4.624048	-1.319923	-1.372488
C	-4.355568	1.062841	-1.567361
H	-5.263022	-2.198885	-1.227311
H	-4.786423	2.071478	-1.591747
C	4.846860	-2.864120	-0.758688
C	2.387770	-2.928508	-0.785916
C	3.582135	-1.136403	-1.982760
C	4.796832	-1.712900	-1.562709
C	3.627796	-3.464756	-0.394234
C	1.108953	-3.651833	-0.424380
C	3.607749	0.053645	-2.914432
H	5.734480	-1.243671	-1.884883
H	3.638542	-4.384509	0.203566
C	6.169385	-3.434260	-0.292515
H	6.104586	-4.521770	-0.122500
H	3.461429	-0.261232	-3.965635
H	-0.658915	-0.042832	-4.065355
H	6.487873	-2.972594	0.660214
H	0.363035	-2.967587	0.011171
H	1.305737	-4.462016	0.295745
H	6.970726	-3.248619	-1.026779
H	4.581786	0.566259	-2.864145
H	2.818456	0.780273	-2.667438
H	0.640059	-4.109115	-1.315254
C	-2.163241	2.173929	-2.067965
H	-1.265291	1.968829	-2.668882
H	-2.786383	2.912768	-2.599534

H	-1.809918	2.646176	-1.133744
C	-6.680496	0.144315	-1.104440
H	-7.281202	-0.569063	-1.694883
H	-6.924116	-0.031948	-0.040722
H	-7.013521	1.164035	-1.357275
C	-2.702040	-2.921670	-1.652313
H	-1.746299	-3.023774	-1.116838
H	-3.415748	-3.638556	-1.217735
H	-2.526633	-3.230165	-2.701088
C	1.231963	3.651339	-0.593173
C	1.805000	4.666072	-1.394824
C	0.685981	3.962509	0.680172
C	1.860555	5.981927	-0.924886
H	2.206660	4.407603	-2.381351
C	0.743049	5.304311	1.134745
C	1.326602	6.297796	0.343461
H	2.314226	6.763597	-1.542910
H	0.325775	5.548346	2.117626
H	1.367668	7.328287	0.712589
C	2.520891	0.149634	2.599459
H	3.287606	0.879145	2.294084
H	2.143296	-1.133026	0.859830
C	0.278629	-0.881911	2.157752
H	0.163710	-1.936955	1.872254
C	-1.074572	-0.145422	1.878580
C	0.721559	-0.724210	3.663216
H	-0.139692	-0.797557	4.346851
S	1.150177	1.986356	-1.183086
S	-0.094527	2.700179	1.619566
C	3.096437	-1.153970	3.240393
H	3.550745	-1.824966	2.491608
H	3.875960	-0.903159	3.981195
C	1.835112	-1.777611	3.931868
H	1.984753	-1.890631	5.019533
H	1.574246	-2.774792	3.535798
C	1.522441	0.591723	3.687206
H	0.942018	1.484184	3.410464
H	2.003798	0.764814	4.666429
C	-2.321806	-0.955920	1.853804
C	-2.384331	-2.357524	1.663936
C	-3.536718	-0.288519	2.163461
C	-3.592966	-3.057475	1.792575
H	-1.472703	-2.922191	1.443524
C	-4.744804	-0.983624	2.282893
H	-3.512298	0.795418	2.323382
C	-4.781318	-2.377887	2.103567
H	-3.601275	-4.145616	1.663429
H	-5.659873	-0.437709	2.537507
H	-5.720707	-2.928660	2.218742
H	-1.223862	0.682728	2.589766

Complex Ru3

Gas phase electronic energy (basis I):

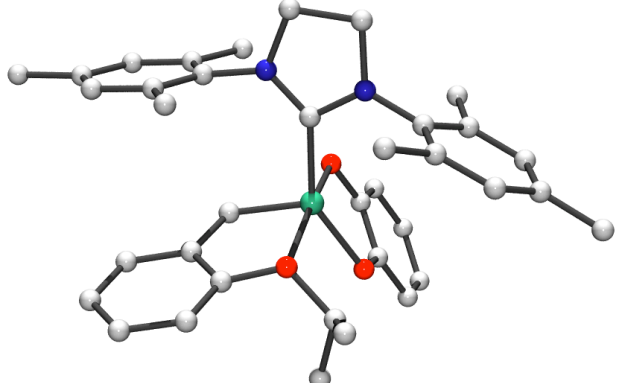
-2404.50152636 hartree

Dipole moment:

1.9702 Debye

C	0.268656	-1.451340	0.034342
Ru	0.154935	0.506897	-0.022181
C	-1.668877	0.782116	-0.079054
N	1.485245	-2.114118	0.008449
N	-0.694532	-2.431926	0.139111
C	2.802124	-1.527905	-0.029516
C	1.361485	-3.564336	0.270403
C	-0.139543	-3.803532	0.064005
C	-2.123945	-2.298411	0.107385
H	-0.362126	-4.253232	-0.923190
H	-0.589241	-4.442629	0.842039
H	1.992416	-4.140567	-0.426558
C	5.415320	-0.453502	-0.146324
C	3.481348	-1.214360	1.176058
C	3.461898	-1.425487	-1.285758
C	4.752881	-0.871850	-1.316552
C	4.772423	-0.656415	1.085539
H	5.260796	-0.779861	-2.284326
H	5.294604	-0.394036	2.014078
C	-4.938520	-2.145308	0.076873
C	-2.801041	-2.298914	-1.137331
C	-2.825102	-2.226333	1.335611
C	-4.229396	-2.145429	1.292985
C	-4.206255	-2.218458	-1.123529
C	-2.040202	-2.322456	-2.444679
C	-2.081986	-2.189592	2.652208
H	-4.782402	-2.077909	2.237816
H	-4.741860	-2.206495	-2.080828
C	-6.452054	-2.097896	0.060540
H	-6.881712	-3.116517	0.086970
H	-2.786878	-2.134631	3.497010
H	1.685353	-3.794316	1.304055
H	-6.832181	-1.608849	-0.851615
H	-1.319922	-1.487053	-2.503961
H	-2.731797	-2.243946	-3.298369
H	-6.850090	-1.554763	0.933592
H	-1.405514	-1.317376	2.703422
H	-1.456176	-3.089289	2.793915
H	-1.463553	-3.256721	-2.571036
H	-2.418577	-0.021330	-0.051756
C	2.920903	-1.555443	2.538959
H	3.343210	-2.516988	2.889994
H	3.192096	-0.787113	3.280111
H	1.825288	-1.628448	2.534683

C	6.787265	0.182254	-0.217459
H	7.324982	0.094318	0.740843
H	7.407514	-0.280452	-1.003745
H	6.713509	1.259261	-0.456028
C	2.829006	-1.948827	-2.554363
H	1.907264	-1.394353	-2.796855
H	3.526377	-1.850750	-3.401666
H	2.563867	-3.017869	-2.460063
Cl	0.631940	0.690848	-2.327958
Cl	0.557351	0.779053	2.291137
C	-2.204842	2.125357	-0.188553
C	-1.311109	3.234934	-0.193178
C	-3.593771	2.377882	-0.308901
C	-1.788260	4.547998	-0.317302
C	-4.078599	3.684081	-0.435807
H	4.277888	1.522049	-0.304957
C	-3.173274	4.759828	-0.441473
H	-1.108388	5.402480	-0.319758
H	-5.152983	3.868425	-0.530261
H	-3.543410	5.785596	-0.540892
O	0.008309	2.866921	-0.080619
C	1.056910	3.897797	0.063961
H	0.832244	4.673152	-0.692580
C	2.384656	3.232903	-0.281781
H	2.351976	2.781164	-1.284977
H	3.181154	3.996451	-0.257331
H	2.633553	2.451811	0.455942
C	1.022932	4.473884	1.481019
H	0.043811	4.916861	1.722892
H	1.231375	3.673499	2.208845
H	1.790587	5.260752	1.578507

Complex Ru4a

Gas phase electronic energy (basis I):

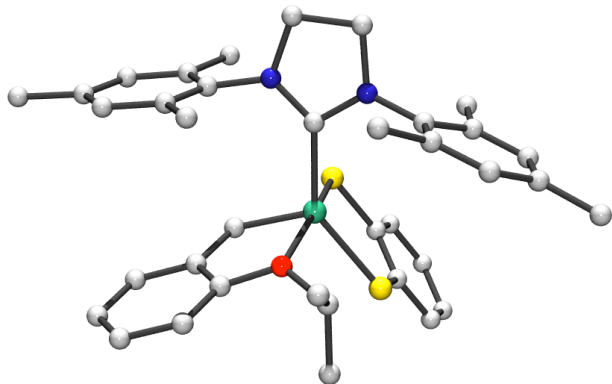
-1865.48358042 hartree

Dipole moment:

7.8511 Debye

C	-0.202196	-0.634074	-1.310126
Ru	0.262974	-0.020816	0.543847
C	-1.446597	0.186978	1.201379
N	0.803804	-0.799427	-2.232952
N	-1.343082	-1.147778	-1.869581
C	2.155473	-0.338902	-2.058001
C	0.394576	-1.618380	-3.394839
C	-1.139737	-1.597445	-3.269707
C	-2.657519	-1.214017	-1.295355
H	-1.610384	-0.883984	-3.974206

H	-1.597098	-2.588069	-3.425824		C	1.492149	4.231697	-0.110834
H	0.758823	-1.171560	-4.334822		H	0.866639	5.096436	0.163994
C	4.805733	0.597263	-1.809794		H	2.545141	4.550538	-0.022098
C	3.152464	-1.212919	-1.556090		H	1.304578	3.975214	-1.164457
C	2.472837	0.977099	-2.482924					
C	3.797512	1.423804	-2.344259					
C	4.463878	-0.713804	-1.435318					
H	4.052033	2.439316	-2.672453					
H	5.239582	-1.376228	-1.032677					
C	-5.286945	-1.417167	-0.296630					
C	-3.560664	-0.144288	-1.500187					
C	-3.043716	-2.387508	-0.601149					
C	-4.359909	-2.460071	-0.109070					
C	-4.865553	-0.266657	-0.988583					
C	-3.131163	1.108400	-2.230759					
C	-2.062143	3.512620	-0.372356					
H	-4.667939	-3.361549	0.434751					
H	-5.569172	0.561647	-1.136084					
C	-6.709519	-1.545022	0.206621					
H	-7.165910	-0.557989	0.388134					
H	-2.537844	-4.337962	0.181333					
H	0.804885	-2.642959	-3.312165					
H	-6.756864	-2.123073	1.144560					
H	-2.216527	1.533711	-1.783812					
H	-3.921121	1.874636	-2.191885					
H	-7.346816	-2.069025	-0.529828					
H	-1.182843	-3.158210	0.198526					
H	-1.684334	-3.924529	-1.326481					
H	-2.911261	0.909763	-3.295806					
H	-2.029643	-0.647252	1.633214					
C	2.833550	-2.639368	-1.172328					
H	2.691535	-3.273587	-2.068007					
H	3.657340	-3.077113	-0.587686					
H	1.913019	-2.692695	-0.564517					
C	6.217549	1.113369	-1.629730					
H	6.959699	0.303751	-1.725823					
H	6.461847	1.893807	-2.369583					
H	6.351036	1.558702	-0.626596					
C	1.408833	1.866620	-3.087479					
H	0.578095	2.031928	-2.379859					
H	1.829714	2.844869	-3.371048					
H	0.970176	1.417114	-3.996715					
C	1.342620	-2.110841	2.097446					
C	1.613117	-3.348737	2.710371					
C	1.998225	-0.937568	2.559093					
C	2.520076	-3.408527	3.784390					
H	1.104729	-4.247348	2.343440					
C	2.901556	-1.004234	3.632386					
C	3.160998	-2.244779	4.244959					
H	2.721404	-4.371989	4.265463					
H	3.393222	-0.085519	3.971082					
H	3.863601	-2.298589	5.083402					
O	0.482438	-1.979418	1.048735					
O	1.711694	0.225396	1.896359					
C	-2.015703	1.526580	1.304761					
C	-3.323152	1.802057	1.773625					
C	-1.210554	2.618442	0.882813					
C	-3.808284	3.115447	1.815714					
H	-3.948166	0.963201	2.097551					
C	-1.689999	3.933316	0.908807					
C	-2.993158	4.175389	1.383191					
H	-4.819928	3.316247	2.182677					
H	-1.073947	4.763846	0.560694					
H	-3.368047	5.203736	1.407693					
O	0.051303	2.240412	0.401008					
C	1.277394	3.022276	0.802257					
H	2.057895	2.271939	0.604435					
C	1.271567	3.348283	2.291617					
H	0.475990	4.062892	2.559426					
H	1.163878	2.424217	2.878722					
H	2.242024	3.806383	2.549505					

Complex Ru4b*Gas phase electronic energy (basis 1):*

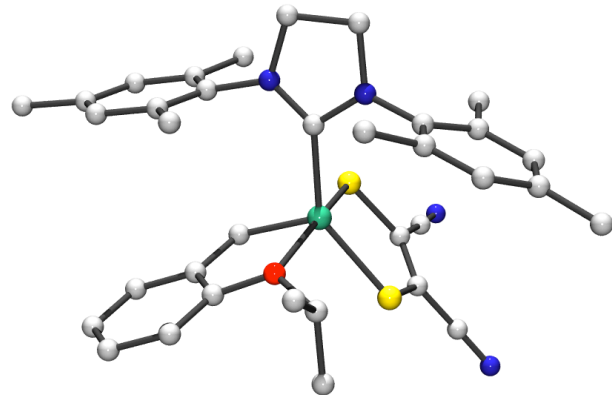
-2511.50014885 hartree

Dipole moment:

7.7302 Debye

S	-1.994843	-0.052354	-1.924227
Ru	-0.200776	-0.171944	-0.485674
S	-0.589809	-2.436463	-0.348664
C	1.460092	-0.385127	-1.284043
O	0.389199	2.070839	-1.082553
C	0.220647	-0.238576	1.508765
N	1.328004	-0.694257	2.180731
N	-0.758668	-0.026455	2.447423
C	-2.044005	0.577699	2.206720
C	-0.371786	-0.488689	3.801260
C	1.148116	-0.663418	3.655774
C	2.657388	-0.893998	1.666114
H	1.716449	0.183414	4.088309
H	1.520051	-1.595541	4.110607
H	-0.652664	0.259372	4.561036
C	-4.539960	1.835935	1.803729
C	-3.205554	-0.220870	2.064450
C	-2.125835	1.993803	2.230826
C	-3.375110	2.598955	2.015320
C	-4.433574	0.435667	1.853172
H	-3.443538	3.693986	2.030196
H	-5.334418	-0.175270	1.720344
C	5.324203	-1.291896	0.826081
C	3.487355	0.229170	1.427394
C	3.146474	-2.214431	1.515039
C	4.477561	-2.383559	1.088888
C	4.807934	0.005453	1.000121
C	2.970773	1.637367	1.616441
C	2.275394	-3.418545	1.792571
H	4.860909	-3.403285	0.960617
H	5.450190	0.871837	0.800976
C	6.762141	-1.505821	0.402565
H	7.112866	-0.697745	-0.260652
H	2.823620	-4.350297	1.580555
H	-0.881447	-1.440941	4.041468
H	6.889171	-2.464145	-0.127476
H	2.104805	1.830966	0.961489

H	3.753252	2.375711	1.381015
H	7.437697	-1.524879	1.278015
H	1.361771	-3.405813	1.173274
H	1.951011	-3.459071	2.848585
H	2.639361	1.817870	2.655314
H	1.909556	-1.377299	-1.464576
C	-3.152557	-1.726551	2.156057
H	-2.987064	-2.060887	3.197792
H	-4.101090	-2.170808	1.815897
H	-2.334459	-2.137202	1.535968
C	-5.868406	2.506255	1.525971
H	-6.712956	1.897295	1.888546
H	-5.930178	3.498880	2.002589
H	-6.016278	2.653641	0.440269
C	-0.903307	2.831372	2.533761
H	-0.074585	2.606294	1.842140
H	-1.136985	3.905717	2.465619
H	-0.527230	2.638675	3.555719
C	-1.882934	-2.787765	-1.520275
C	-2.501225	-1.733127	-2.231688
C	2.157327	0.741265	-1.887980
C	3.394100	0.600988	-2.564887
C	1.584570	2.040813	-1.797520
C	4.040184	1.706496	-3.129769
H	3.831350	-0.400606	-2.638821
C	2.229728	3.154888	-2.353018
C	3.455381	2.979210	-3.021489
H	4.992048	1.580404	-3.655287
H	1.802464	4.154479	-2.271213
H	3.950497	3.852578	-3.458440
C	-0.652476	3.107944	-1.340684
H	-1.502470	2.655569	-0.804942
C	-1.000098	3.223403	-2.824982
H	-0.178571	3.659660	-3.415034
H	-1.263162	2.239756	-3.242797
H	-1.878458	3.884400	-2.924535
C	-0.311388	4.449376	-0.677719
H	0.351529	5.080164	-1.291018
H	-1.248367	5.012874	-0.527040
H	0.156424	4.300459	0.306891
C	-3.522137	-2.020491	-3.163919
C	-2.307617	-4.117853	-1.740146
C	-3.324532	-4.392193	-2.662646
C	-3.933577	-3.342295	-3.378560
H	-1.827534	-4.931331	-1.183553
H	-3.641305	-5.427680	-2.828015
H	-4.724957	-3.555675	-4.104855
H	-3.987389	-1.195768	-3.715903



Gas phase electronic energy (basis 1):

-2542.34928152 hartree

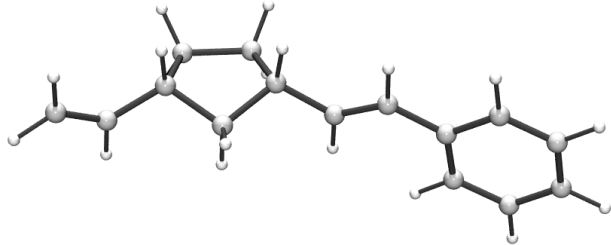
Dipole moment:

17.2896 Debye

C	-0.209289	-0.731430	-1.331262
Ru	0.214363	-0.020156	0.544753
C	-1.468455	0.097575	1.322148
N	0.784326	-0.868303	-2.264634
N	-1.328911	-1.338425	-1.834580
C	2.104705	-0.295872	-2.172657
C	0.386571	-1.722778	-3.409344
C	-1.139339	-1.796940	-3.237240
C	-2.664179	-1.327039	-1.296346
H	-1.679423	-1.121154	-3.928228
H	-1.538923	-2.814955	-3.368232
H	0.694886	-1.262436	-4.362228
C	4.661402	0.894377	-2.033433
C	3.206205	-1.074195	-1.736560
C	2.281934	1.034562	-2.632428
C	3.559833	1.611090	-2.540491
C	4.465310	-0.447370	-1.662959
H	3.702854	2.641363	-2.889431
H	5.318465	-1.033552	-1.301671
C	-5.336759	-1.358487	-0.387182
C	-3.463148	-0.167115	-1.446134
C	-3.187427	-2.513952	-0.726042
C	-4.519829	-2.498418	-0.273508
C	-4.788240	-0.204833	-0.976276
C	-2.913347	1.087530	-2.087318
C	-2.354946	-3.770211	-0.599935
H	-4.929630	-3.409775	0.178608
H	-5.408613	0.693516	-1.079184
C	-6.777563	-1.387080	0.076907
H	-7.144108	-0.376896	0.321986
H	-2.919971	-4.559139	-0.079235
H	0.866778	-2.715426	-3.327293
H	-6.902680	-2.024035	0.968228
H	-2.063399	1.489911	-1.510475
H	-3.688244	1.867909	-2.143988
H	-7.440459	-1.794776	-0.708637
H	-1.424593	-3.588537	-0.036234
H	-2.062806	-4.172433	-1.587380
H	-2.550467	0.899862	-3.114096
H	-1.968803	-0.762938	1.797864
C	3.071503	-2.540822	-1.401617
H	3.022084	-3.154447	-2.320979
H	3.940769	-2.891251	-0.823596
H	2.164362	-2.743423	-0.807790
C	6.017562	1.549820	-1.889783
H	6.835410	0.828189	-2.049830
H	6.145381	2.380329	-2.603631

Complex Ru5

H	6.146026	1.965154	-0.873522
C	1.136689	1.792420	-3.266982
C	0.243474	1.804950	-2.621231
H	1.427204	2.831965	-3.486080
H	0.833683	1.328449	-4.224086
C	1.810058	-2.157061	2.384472
C	2.438384	-0.968804	2.724195
S	0.526442	-2.189440	1.167873
S	1.975719	0.543682	1.916498
C	-2.121944	1.383330	1.503455
C	-3.366603	1.518130	2.166931
C	-1.494113	2.555294	0.997360
C	-3.968005	2.771430	2.323231
H	-3.844895	0.614476	2.559422
C	-2.094753	3.813653	1.142572
C	-3.329295	3.912753	1.809752
H	-4.925811	2.863296	2.844290
H	-1.627288	4.713746	0.744382
H	-3.789792	4.899296	1.924603
O	-0.295076	2.298439	0.338088
C	0.769095	3.342071	0.208690
H	1.602699	2.715219	-0.146589
C	1.142432	3.956017	1.557933
H	0.341949	4.592507	1.966813
H	1.391455	3.176609	2.293824
H	2.036469	4.586924	1.414484
C	0.438024	4.378780	-0.873698
H	-0.181407	5.210269	-0.502598
H	1.383770	4.816640	-1.236426
H	-0.070830	3.915626	-1.732289
C	3.472459	-0.885866	3.695617
C	2.156460	-3.414440	2.956105
N	4.337711	-0.768465	4.491624
N	2.411183	-4.481418	3.392969

E isomer of ROCM product 3.21a*Gas phase electronic energy (basis 1):*

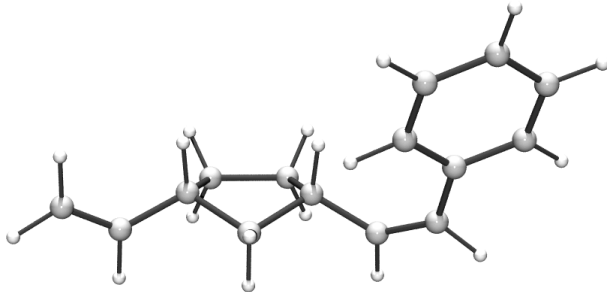
-582.390941560 hartree

Sum of electronic and thermal Free Energies (basis 1):

-582.156194 hartree

C	3.639796	-0.026792	-0.235526
C	3.476051	1.300749	0.569784
C	1.959863	1.658888	0.519960
C	1.261827	0.512218	-0.284112
C	2.239589	-0.679803	-0.109679
C	4.771529	-0.893522	0.243826
C	-0.144490	0.229244	0.159022
C	-1.237481	0.300827	-0.636000
C	5.811428	-1.305500	-0.500793
C	-2.638322	0.036056	-0.270339
C	-3.642141	0.192329	-1.256435
C	-4.992932	-0.045219	-0.967047
C	-5.376215	-0.447425	0.321833

C	-4.392954	-0.608860	1.314816
C	-3.044754	-0.371540	1.024655
H	5.907791	-1.022151	-1.555744
H	6.602880	-1.939000	-0.087758
H	4.714030	-1.199754	1.300467
H	3.807832	0.219531	-1.302557
H	1.248436	0.786665	-1.357277
H	2.070166	-1.488226	-0.840230
H	2.120831	-1.116992	0.902209
H	4.120300	2.096996	0.161352
H	3.800331	1.140692	1.614198
H	1.765408	2.640202	0.056209
H	1.538374	1.706747	1.540214
H	-0.253528	-0.052877	1.217586
H	-1.084089	0.591681	-1.686060
H	-3.348663	0.506237	-2.265240
H	-5.747516	0.084081	-1.750365
H	-6.429932	-0.634655	0.552996
H	-4.681349	-0.923340	2.323751
H	-2.296072	-0.505734	1.812452

Z isomer of ROCM product 3.21a*Gas phase electronic energy (basis 1):*

-582.386301883 hartree

Sum of electronic and thermal Free Energies (basis 1):

-582.149981 hartree

C	2.937795	0.370512	0.221880
C	3.081542	-0.889118	1.132148
C	1.710883	-1.629232	1.074597
C	0.807598	-0.812180	0.094440
C	1.841255	-0.058082	-0.785712
C	4.226111	0.810482	-0.417555
C	-0.154489	-1.673774	-0.675876
C	-1.490047	-1.519874	-0.855717
C	4.793896	2.020728	-0.281412
C	-2.377731	-0.434551	-0.393463
C	-3.718074	-0.748869	-0.058255
C	-4.605847	0.236493	0.392059
C	-4.180988	1.571192	0.503017
C	-2.865091	1.908200	0.146383
C	-1.975785	0.920712	-0.301702
H	4.334398	2.802410	0.335313
H	5.735202	2.276604	-0.778208
H	4.722209	0.053101	-1.045143
H	2.537658	1.207284	0.827794
H	0.244987	-0.061222	0.678574
H	1.405677	0.792918	-1.338221
H	2.270236	-0.751447	-1.536539
H	3.378101	-0.609831	2.156716
H	3.885950	-1.536966	0.738456
H	1.234010	-1.721560	2.064443

H	1.841758	-2.658408	0.693494
H	0.299700	-2.574214	-1.117799
H	-2.010097	-2.330068	-1.386349
H	-4.055513	-1.788467	-0.143055
H	-5.633929	-0.036343	0.653594
H	-4.874350	2.344561	0.849569
H	-2.531893	2.950190	0.202650
H	-0.970274	1.206523	-0.624272

Geometries and Energies of Computed Structures for Schemes 3.4.2-1 and 3.4.2-2

DFT calculations related to Scheme 3.4.2-2 are recently reported.¹²⁵

(125) Khan, R. K. M.; Torker, S.; Hoveyda, A. H. *J. Am. Chem. Soc.* **2014**, *136*, 14337–14340.